IAEA
International Atomic Energy Agency

IAEA TECDOC SERIES

No. 2079

Analysis and Modelling of Severe Accidents for Liquid Metal Fast Reactors

Proceedings of a Technical Meeting

IAEA SAFETY STANDARDS AND RELATED PUBLICATIONS

IAEA SAFETY STANDARDS

Under the terms of Article III of its Statute, the IAEA is authorized to establish or adopt standards of safety for protection of health and minimization of danger to life and property, and to provide for the application of these standards.

The publications by means of which the IAEA establishes standards are issued in the **IAEA Safety Standards Series**. This series covers nuclear safety, radiation safety, transport safety and waste safety. The publication categories in the series are **Safety Fundamentals**, **Safety Requirements** and **Safety Guides**.

Information on the IAEA's safety standards programme is available at the IAEA Internet site

www.iaea.org/resources/safety-standards

The site provides the texts in English of published and draft safety standards. The texts of safety standards issued in Arabic, Chinese, French, Russian and Spanish, the IAEA Safety Glossary and a status report for safety standards under development are also available. For further information, please contact the IAEA at: Vienna International Centre, PO Box 100, 1400 Vienna, Austria.

All users of IAEA safety standards are invited to inform the IAEA of experience in their use (e.g. as a basis for national regulations, for safety reviews and for training courses) for the purpose of ensuring that they continue to meet users' needs. Information may be provided via the IAEA Internet site or by post, as above, or by email to Official.Mail@iaea.org.

RELATED PUBLICATIONS

The IAEA provides for the application of the standards and, under the terms of Articles III and VIII.C of its Statute, makes available and fosters the exchange of information relating to peaceful nuclear activities and serves as an intermediary among its Member States for this purpose.

Reports on safety in nuclear activities are issued as **Safety Reports**, which provide practical examples and detailed methods that can be used in support of the safety standards.

Other safety related IAEA publications are issued as **Emergency Preparedness and Response** publications, **Radiological Assessment Reports**, the International Nuclear Safety Group's **INSAG Reports**, **Technical Reports** and **TECDOCs**. The IAEA also issues reports on radiological accidents, training manuals and practical manuals, and other special safety related publications.

Security related publications are issued in the **IAEA Nuclear Security Series**.

The **IAEA Nuclear Energy Series** comprises informational publications to encourage and assist research on, and the development and practical application of, nuclear energy for peaceful purposes. It includes reports and guides on the status of and advances in technology, and on experience, good practices and practical examples in the areas of nuclear power, the nuclear fuel cycle, radioactive waste management and decommissioning.

ANALYSIS AND MODELLING OF SEVERE ACCIDENTS FOR LIQUID METAL FAST REACTORS

The following States are Members of the International Atomic Energy Agency:

AFGHANISTAN
ALBANIA
ALGERIA
ANGOLA
ANTIGUA AND BARBUDA
ARGENTINA
ARMENIA
AUSTRALIA
AUSTRIA
AZERBAIJAN
BAHAMAS
BAHRAIN
BANGLADESH
BARBADOS
BELARUS
BELGIUM
BELIZE
BENIN
BOLIVIA, PLURINATIONAL STATE OF
BOSNIA AND HERZEGOVINA
BOTSWANA
BRAZIL
BRUNEI DARUSSALAM
BULGARIA
BURKINA FASO
BURUNDI
CABO VERDE
CAMBODIA
CAMEROON
CANADA
CENTRAL AFRICAN REPUBLIC
CHAD
CHILE
CHINA
COLOMBIA
COMOROS
CONGO
COOK ISLANDS
COSTA RICA
CÔTE D'IVOIRE
CROATIA
CUBA
CYPRUS
CZECH REPUBLIC
DEMOCRATIC REPUBLIC OF THE CONGO
DENMARK
DJIBOUTI
DOMINICA
DOMINICAN REPUBLIC
ECUADOR
EGYPT
EL SALVADOR
ERITREA
ESTONIA
ESWATINI
ETHIOPIA
FIJI
FINLAND
FRANCE
GABON
GAMBIA, THE
GEORGIA
GERMANY
GHANA
GREECE
GRENADA
GUATEMALA
GUINEA
GUYANA
HAITI
HOLY SEE
HONDURAS
HUNGARY
ICELAND
INDIA
INDONESIA
IRAN, ISLAMIC REPUBLIC OF
IRAQ
IRELAND
ISRAEL
ITALY
JAMAICA
JAPAN
JORDAN
KAZAKHSTAN
KENYA
KOREA, REPUBLIC OF
KUWAIT
KYRGYZSTAN
LAO PEOPLE'S DEMOCRATIC REPUBLIC
LATVIA
LEBANON
LESOTHO
LIBERIA
LIBYA
LIECHTENSTEIN
LITHUANIA
LUXEMBOURG
MADAGASCAR
MALAWI
MALAYSIA
MALI
MALTA
MARSHALL ISLANDS
MAURITANIA
MAURITIUS
MEXICO
MONACO
MONGOLIA
MONTENEGRO
MOROCCO
MOZAMBIQUE
MYANMAR
NAMIBIA
NEPAL
NETHERLANDS, KINGDOM OF THE
NEW ZEALAND
NICARAGUA
NIGER
NIGERIA
NORTH MACEDONIA
NORWAY
OMAN
PAKISTAN
PALAU
PANAMA
PAPUA NEW GUINEA
PARAGUAY
PERU
PHILIPPINES
POLAND
PORTUGAL
QATAR
REPUBLIC OF MOLDOVA
ROMANIA
RUSSIAN FEDERATION
RWANDA
SAINT KITTS AND NEVIS
SAINT LUCIA
SAINT VINCENT AND THE GRENADINES
SAMOA
SAN MARINO
SAUDI ARABIA
SENEGAL
SERBIA
SEYCHELLES
SIERRA LEONE
SINGAPORE
SLOVAKIA
SLOVENIA
SOMALIA
SOUTH AFRICA
SPAIN
SRI LANKA
SUDAN
SWEDEN
SWITZERLAND
SYRIAN ARAB REPUBLIC
TAJIKISTAN
THAILAND
TOGO
TONGA
TRINIDAD AND TOBAGO
TUNISIA
TÜRKİYE
TURKMENISTAN
UGANDA
UKRAINE
UNITED ARAB EMIRATES
UNITED KINGDOM OF GREAT BRITAIN AND NORTHERN IRELAND
UNITED REPUBLIC OF TANZANIA
UNITED STATES OF AMERICA
URUGUAY
UZBEKISTAN
VANUATU
VENEZUELA, BOLIVARIAN REPUBLIC OF
VIET NAM
YEMEN
ZAMBIA
ZIMBABWE

The Agency's Statute was approved on 23 October 1956 by the Conference on the Statute of the IAEA held at United Nations Headquarters, New York; it entered into force on 29 July 1957. The Headquarters of the Agency are situated in Vienna. Its principal objective is "to accelerate and enlarge the contribution of atomic energy to peace, health and prosperity throughout the world''.

IAEA-TECDOC-2079

ANALYSIS AND MODELLING OF SEVERE ACCIDENTS FOR LIQUID METAL FAST REACTORS

PROCEEDINGS OF A TECHNICAL MEETING

INTERNATIONAL ATOMIC ENERGY AGENCY
VIENNA, 2025

COPYRIGHT NOTICE

For further information on this publication, please contact:

Safety Assessment Section
International Atomic Energy Agency
Vienna International Centre
PO Box 100
1400 Vienna, Austria
Email: Official.Mail@iaea.org

Printed by the IAEA in Austria
January 2025
https://doi.org/10.61092/iaea.xpz1-gu7q

IAEA Library Cataloguing in Publication Data

Names: International Atomic Energy Agency.
Title: Analysis and modelling of severe accidents for liquid metal fast reactors / International Atomic Energy Agency.
Description: Vienna : International Atomic Energy Agency, 2025. | Series: IAEA TECDOC series, ISSN 1011-4289 ; no. 2079 | Includes bibliographical references.
Identifiers: IAEAL 25-01733 | ISBN 978-92-0-100125-2 (paperback : alk. paper) | ISBN 978-92-0-100025-5 (pdf)
Subjects: LCSH: Liquid metal cooled reactors. | Liquid metal cooled reactors — Accidents. | Nuclear accidents. | Nuclear industry — Safety measures. | Sodium cooled reactors.

FOREWORD

Design safety and safety assessment of liquid metal cooled fast reactors — comprising sodium cooled fast reactors and lead cooled fast reactors — require tailored approaches that consider the specifics of these technologies. One fundamental safety related aspect concerns the notion of ‘severe accident’, which involves different scenarios or phenomena in liquid metal cooled fast reactors compared with water cooled reactors as well as adapted analysis tools.

In this framework, the IAEA organized a technical meeting in March 2023 to provide a platform for Member States to exchange information on the design of liquid metal cooled fast reactors relating to the general safety approach and the consideration of severe accidents in the design and safety assessment, with an emphasis on the deterministic analysis and modelling of severe accidents and their consequences. This publication summarizes the material presented at that technical meeting.

The IAEA wishes to thank the experts from Member States involved in the drafting and review for their valuable contributions to this publication. The IAEA officers responsible for the preparation of this publication were S. Massara and V. Tiberi of the Division of Nuclear Installation Safety and V. Kriventsev of the Division of Nuclear Power.

EDITORIAL NOTE

This publication has been prepared from the original material as submitted by the contributors and has not been edited by the editorial staff of the IAEA. The views expressed remain the responsibility of the contributors and do not necessarily represent the views of the IAEA or its Member States.

Guidance and recommendations provided here in relation to identified good practices represent expert opinion but are not made on the basis of a consensus of all Member States.

Neither the IAEA nor its Member States assume any responsibility for consequences which may arise from the use of this publication. This publication does not address questions of responsibility, legal or otherwise, for acts or omissions on the part of any person.

The use of particular designations of countries or territories does not imply any judgement by the publisher, the IAEA, as to the legal status of such countries or territories, of their authorities and institutions or of the delimitation of their boundaries.

The mention of names of specific companies or products (whether or not indicated as registered) does not imply any intention to infringe proprietary rights, nor should it be construed as an endorsement or recommendation on the part of the IAEA.

The authors are responsible for having obtained the necessary permission for the IAEA to reproduce, translate or use material from sources already protected by copyrights.

The IAEA has no responsibility for the persistence or accuracy of URLs for external or third party Internet web sites referred to in this publication and does not guarantee that any content on such web sites is, or will remain, accurate or appropriate.

CONTENTS

1 INTRODUCTION

1.1 BACKGROUND

Over the past several years, there has been an increased interest among Member States in commercial deployment of reactors with coolants other than water, including small and medium sized or modular reactors (SMRs). These technologies present specific design features (e.g. different nuclear fuels, neutron spectra, types of coolant) needing dedicated safety approaches.

One of the aspects of the safety approach that raises concerns relates to the fourth level of defence in depth. Paragraph 2.13 of IAEA Safety Standards Series No. SSR-2/1 (Rev. 1), Safety of Nuclear Power Plants: Design [1] — which refers primarily to land based stationary nuclear power plants with water cooled reactors — states:

> "The purpose of the fourth level of defence is to mitigate the consequences of accidents that result from failure of the third level of defence in depth. This is achieved by preventing the progression of such accidents and mitigating the consequences of a severe accident."

The concept of 'severe accident'[1] [2] (and also 'damage to the reactor core', as stated in in para. 2.13 of SSR-2/1 (Rev. 1) [1] in relation to the third level of defence) may apply in a different way or involve different scenarios/physical phenomena for reactors with coolants other than water. Reference [3] investigates the areas of novelty for these technologies and provides general insights on the scope and definition of the plant states that are considered in their design, in particular severe accident conditions. Follow up activities to ensure that, in due course, the IAEA safety standards fully apply to all reactor types, include the collection of available knowledge on these technologies to fill existing gaps.

In this context, the IAEA organized a Technical Meeting on "The Safety Approach for Liquid Metal Cooled Fast Reactors (LMFRs) and the Analysis and Modelling of Severe Accidents" in March 2023 (jointly by the Department of Nuclear Safety and Security and the Department of Nuclear Energy) to provide a platform for Member States to exchange information on the design of LMFRs, with regard to the general approach to design safety and safety assessment of these technologies, with an emphasis on the consideration of severe accidents, including their analysis and modelling.

LMFRs comprise of:

- Sodium cooled fast reactors (SFRs), for which the total operational experience recently achieved 500 reactor-years, mainly with pure sodium as coolant;
- Lead cooled fast reactors (LFRs), cooled with either lead-bismuth eutectic (accounting for about 70 reactor-years of operational experience) or pure lead (which was never previously adopted as reactor coolant and for which the operational experience is absent).

[1] The IAEA safety glossary [2] defines severe accidents as "accidents more severe than design basis accidents and involving significant core degradation". The SFR studies presented in this TECDOC consider a core melt as severe accident to mitigate.

Specific features to mitigate the consequences of potential severe accidents are being considered at the design stage of SFRs in many Member States, with the aim of demonstrating, with a high degree of confidence, that such sequences do not jeopardize the integrity of the third confinement barrier, including the reactor containment, hence ensuring the confinement of radioactive material. The ultimate purposes of mitigation features implemented at the fourth level of defence in depth, are to:

- Minimize the mechanical energy releases generated through core re-criticality and/or fuel–coolant interaction (e.g. devices to enhance the discharge of the molten fuel towards a core catcher);

- Maintaining the integrity of the containment to ensure the capability to manage accident conditions where a significant amount of radioactive material in the containment is involved (e.g. implementation of a core catcher to collect, spread and cool the corium);

- Minimizing radiological releases (e.g. limitation by design of containment leakages) ensuring the fulfilment of radiological acceptance criteria (i.e. ensuring that only emergency countermeasures that are of limited scope in terms of area and time are necessary).

In this framework, severe accidents are currently being analysed as an integral part of the safety demonstration of SFRs by using a methodology that integrates deterministic safety analyses and probabilistic safety assessment, with the ultimate goals of strengthening the safety of SFR design and enhancing the robustness of the safety demonstration of these reactors.

In parallel, stakeholders involved in the development or regulation of LFRs have initiated research and development (R&D) to develop tools and methodologies suitable for analysing severe accident sequences for this technology type, within the framework of the development of a safety approach for new reactor designs.

For both SFRs and LFRs, the validation of tools involves an experimental database covering the wide range of phenomena described by individual models, obtained through in-pile and out-of-pile experiments with prototypical and simulant materials in the framework of separate effect tests and semi-integral configurations.

1.2 OBJECTIVES

This TECDOC summarizes the material presented at the technical meeting on “The Safety Approach for Liquid Metal Cooled Fast Reactors and the Analysis and Modelling of Severe Accidents” organized by the IAEA in March 2023, in relation to analysis and modelling of severe accidents for LMFRs[2] [4], as follows:

- Twenty-two technical papers, associated with oral presentations in four technical sessions, which were submitted and peer-reviewed before the technical meeting by an Advisory Committee constituted for this purpose;

[2] The consideration of severe accident conditions in the safety approach for LMFRs is addressed in a separate publication currently in preparation [4].

- Two panel discussions, the first one focusing on the status of knowledge and challenges for the consideration of severe accidents for SFRs, the second one on the status of development and challenges for the development of LFR technology.

This TECDOC aims to illustrate the status of knowledge of physical phenomena, development of models and numerical tools, and validation through experimental data, in relation to the progression of severe accidents in LMFRs.

For SFRs, the status of knowledge discussed at the technical meeting can be considered as being the state of the art in the field, considering that the attendees included a large majority of the key parties from design organizations, regulatory bodies, technical support organizations and R&D organizations, including both modellers of numerical codes and experimenters.

1.3 SCOPE

This TECDOC considers severe accident sequences that are not 'practically eliminated'[3] for LMFRs, including deterministic modelling and analysis of severe accident progression, numerical codes development and validation, and related experimental programmes for SFRs and, as applicable, LFRs, with due account taken of the lower level of knowledge associated with this technology, in relation to severe accidents.

This TECDOC covers the following topics related to LMFR mechanistic models for core degradation under severe accident conditions:

- Fuel pin behaviour (fuel–cladding interaction, in-pin fuel movement, reactivity effects);
- Initiation/primary phase (including two-phase thermohydraulics);
- Event termination or transition/secondary phase (assembly hexagonal can failure, fuel-coolant interaction, melt propagation and material movement and associated reactivity effects, potential secondary power excursions due to re-criticality effects);
- Expansion phase (expansion of sodium vapour bubble, pressure increase and release of mechanical energy, sodium ejection);
- Material relocation (debris formation, thermochemistry effects, jet impingement);
- Long term behaviour (ability to cool the core material, re-criticality).

This TECDOC also covers topics related to: i) radioactive material release and transport in-vessel and ex-vessel[4] [5]; ii) conservative simplified/parametric fast running models during the core degradation phases; iii) code development and performance optimization, multiphysics approaches and platform architecture; and iv) experimental programmes, code validation and uncertainty analyses.

---

[3] Paragraph 5.13 of SSR-2/1 (Rev. 1) [1], states that "The design shall be such that the possibility of conditions arising that could lead to an early radioactive release or a large radioactive release is 'practically eliminated'" and "The possibility of certain conditions arising may be considered to have been 'practically eliminated' if it would be physically impossible for the conditions to arise or if these conditions could be considered with a high level of confidence to be extremely unlikely to arise".

[4] Further information is provided in Ref. [5].

1.4 STRUCTURE

The TECDOC consists of seven sections:

- Section 1 describes the background, objectives, scope and structure of the publication.
- Section 2 describes the main phenomena and challenges to be addressed for severe accident consequences mitigation in LMFRs.
- Section 3 describes national programmes and activities related to the development of models and tools for SFRs, as well as experimental programmes for validation purposes.
- Section 4 focuses on new or expanded capabilities of existing software tools to model phenomena associated with the initiation and transition phases of severe accidents for SFRs.
- Section 5 presents the research on the characterization of the physical phenomena involved during the expansion phase of the accident and during the long term behaviour of SFRs.
- Section 6 gathers contributions illustrating progress in the understanding of basic phenomena and associated modelling capabilities of accidental conditions for LFRs. This section also focuses on ongoing experimental programmes aiming at accumulating experimental data necessary both for increasing the phenomenological knowledge as well as for validation of numerical tools.
- Section 7 presents the conclusions and highlights gaps which might be the focus of future activities.

The technical papers submitted and reviewed prior the technical meeting are included at the end of this TECDOC.

2 PHENOMENOLOGY OF SEVERE ACCIDENTS IN LIQUID METAL FAST REACTORS

2.1 PHENOMENOLOGY OF SEVERE ACCIDENT PROGRESSION IN SODIUM COOLED FAST REACTORS

Sequences leading to severe accidents (which involve significant core damage) in SFRs, and which need to be mitigated, are caused by a reactor power and heat removal mismatch and failure of the reactor shutdown mechanism. Such accident sequences, potentially leading to core damage, are typically categorized as unprotected transients, such as unprotected loss of flow (ULOF) and unprotected transient over power (UTOP). A local fault inside a fuel assembly is also assessed as a potential cause of core damage. The severe accident studies described in this TECDOC mainly focus on ULOF because of its wide spectrum of phenomenology, starting from the intact state of the reactor core to the termination of the accident.

Other sequences may lead to a severe accident such as a loss of decay heat removal. Nevertheless, they cannot be mitigated by design, and have to be 'practically eliminated'.

Although the progression of a severe accident is affected by the specific nature of the materials used for the nuclear fuel and coolant, and by the reactor power, the general event progression is usually divided into the primary (or initiating) phase, the transition (or secondary) phase, the expansion phase, and the long term (post-accident) phase – in accordance with the degree of core damage progression and the type of phenomena involved in the accident, as shown in Fig. 1. These phases are as follows:

- The primary (or initiating) phase deals with the fuel damage process starting from the intact state of the core. Coolant boiling, fuel pin failure and subsequent material motion inside each fuel assembly cause a change in reactor power due to the reactivity effects associated with density variations of reactor materials (e.g. fuel, cladding, hexagonal can, sodium). This phase ends with the failure of the fuel assembly duct, or hexagonal can.

- The transition (or secondary) phase deals with the core damage progression and relocation of the core materials after the fuel assembly hexagonal can failure. Depending on the core state at the end of the primary phase, a large core melt may happen, associated with a significant reactivity effect (which can be positive or negative) due to the motion of the molten core materials. Various phenomena induce material motion, such as gravity, fuel–coolant interaction (FCI), boiling, fission gas release. The discharge of molten material from the core through the steel duct structures, such as control rod guide tubes (CRGT) or dedicated duct channels, is an important phenomenon that allows reaching a subcritical state. Depending on the specific design, molten material jet impingement on the structure surrounding the core (including the core catcher) may be a challenge which may necessitate the design of specific features.

- The expansion phase deals with sequences encountered in the case of an extreme mechanical energy release occurring during the accident phases described above. In this phase, the thermal energy accumulated in the core might be converted to mechanical energy, which impacts the reactor structure. A large release of core material into the sodium pool might additionally cause intensive FCI and sodium vaporization, which represents a pressure source capable of accelerating the liquid sodium slug outwards. The pressure propagation from the core and the impact of the sodium slug, may cause a

dynamic deformation of the reactor structure such as the reactor roof. As a result of the molten material discharge from the core, the molten material jet may be injected into the sodium plenum. The mechanical energy release may degrade the integrity of the reactor system and lead to release of sodium and cover gas into the containment, which results in several 'in-containment' phenomena including sodium chemical reactions, aerosol generation, and aerosol mass evolution (e.g. agglomeration, wall plating, gravitational sedimentation).

- The long term (post-accident) phase deals with the ability to cool the degraded core, including core material relocated on the core catcher, if any. If a core catcher is needed, it may be implemented inside or outside the primary system. The ability to cool the core material requires coolant circulation between core material and the available heat sink. In this context, the material relocation process leading to a stable long term coolable subcritical state is another topic under investigation. Criticality of the relocated core materials is also a subject of study.

Radioactive material transport and release is an important aspect of severe accident evaluation. According to the accident progression described above, fission products transport and retention are assessed.

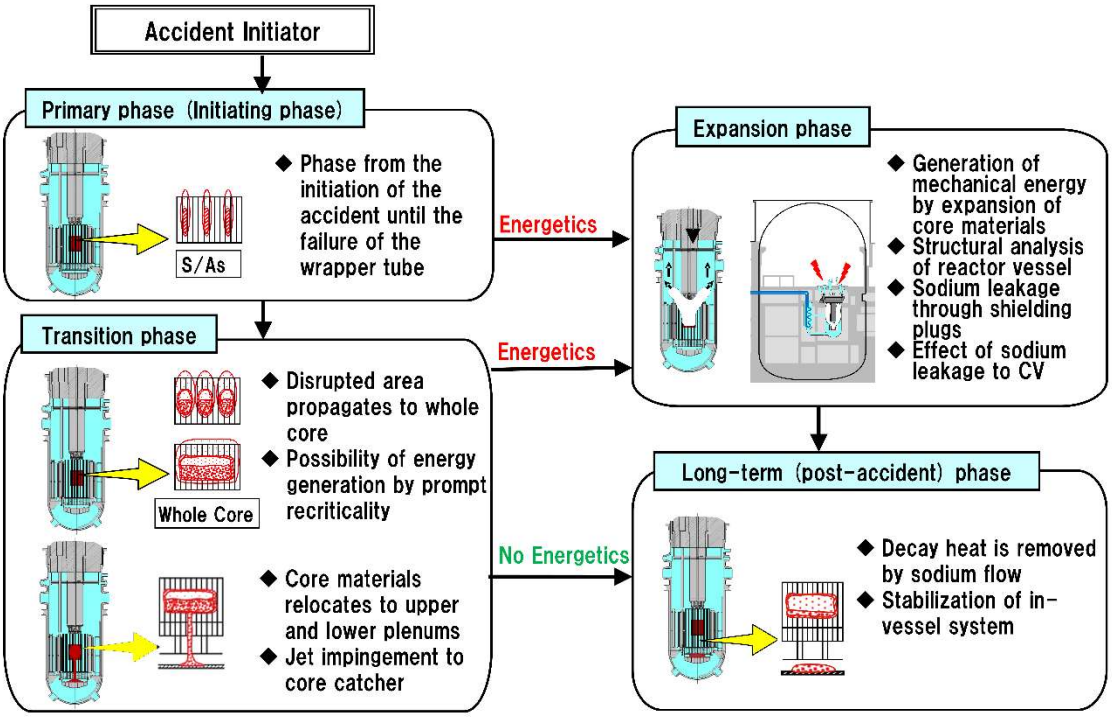

FIG. 1. Event progression of severe accidents in an SFR (courtesy of Yoshiharu Tobita, Japan Atomic Energy Agency (JAEA), Japan).

Each of the accident phases or phenomena described above is analysed by dedicated analysis tools, for instance, SAS4A/SASSYS-1 [6] for the primary phase, SIMMER [7] for the global fuel degradation including the transition phase, EUROPLEXUS [8] and AUTODYN [9] for the dynamic structural response in the expansion phase, CONTAIN-LMR [10] for fission products transport and SUPER-COPD [11] for the long term (post-accident) phase.

Depending on the reactor design and on the specific framework adopted by each regulatory body, the analysis of the progression of accident sequences might not include all the above-mentioned phases. For example, in some Member States, such as the United States of America, considering a risk informed, performance based approach and the adoption of metallic fuel, the focus may be on the initiating phase.

For more information on regulatory frameworks and safety approaches adopted by Member States for the safety assessment of LMFR, with an emphasis on accident sequences leading to severe accidents, see Ref. [4].

2.2 SPECIFIC FEATURES OF LEAD COOLED FAST REACTORS

The physical and chemical properties of lead differ considerably from those of sodium. These properties may significantly influence phenomena that play a crucial role in the accident analysis. Important examples are described hereinafter.

The high melting point of lead (328°C vs 98°C for sodium and 124°C for 45/55 LBE alloy) increases the possibility of coolant solidification during normal and transient conditions, constituting a potential safety issue and a possible initiator of core degradation.

Lead has a boiling temperature (1740°C for lead and 1670°C for LBE) much higher than the melting temperature of the structural materials of the core and the vessel. This prevents void effects and fuel melting caused by the coolant vaporization. This is an advantageous property for the prevention of core degradation.

In certain conditions, lead may be corrosive and/or erosive, and then, this may initiate core degradation. One of the possible solutions to cope with corrosion is a controlled injection of oxygen to form a protective oxide layer on structures. Indeed, the performance of steels in lead strongly depends on the presence of oxygen dissolved in the liquid metal phase. If the oxygen content exceeds a certain threshold, a continuous scale consisting of oxides of the steel constituents may form on the steel surface separating the steel from the lead coolant [5]. Consequently, the dissolution of steel constituents in lead or LBE can occur only after diffusion through the oxide scale, i.e. at a potentially lower rate. The efficiency of the structure protection by the oxide layer also depends on the control of the coolant temperature. However, feedback from experience has demonstrated that the interaction of lead with oxygen could lead to the excessive formation of lead oxides that could cause a degradation of the fuel cooling. The risk of erosion leads to limiting the coolant velocity by design. In any case, the corrosion and erosion of the structural materials of the core by lead is not modelled in numerical codes developed for the simulation of severe accidents in SFRs, such as SIMMER [7], and would need to be developed for LFRs.

The absence of a chemical interaction between oxide fuel and lead coolant intrinsically reduces the propagation beyond the fuel cladding failure of a single fuel pin failure to the neighbouring fuel pins inside a fuel assembly. Another advantage of lead and LBE over sodium, for both the prevention and mitigation of severe accidents, is the absence of a violent exothermal chemical reaction between the coolant and other substances that in accident conditions could enter into contact with the coolant, such as water in the case of a loss of integrity of the reactor barrier. Nevertheless, the risk of steam explosion has to be assessed.

The small density difference between the fuel and lead coolant, which can be positive or negative depending on fuel burn up and lead coolant temperature, could significantly influence

the core degradation behaviour, hampering the simulation of fuel relocation. Fuel could relocate to the top surface of the coolant as well as to the bottom of the vessel, or even an oscillatory behaviour is possible. Hence, very high uncertainties will be associated with the modelling of fuel relocation in the vessel.

Lead is expected to feature important retention properties for many radioactive isotopes produced in the coolant (polonium) and in the fuel pin (fission products). The retention rate of volatile fission products such as iodine and caesium, major contributors to the source term, is expected to be high for both lead and sodium.

Caution is necessary, however, because the chemistry of these elements in lead could be strongly influenced by other impurities in the coolant that are not present in current and programmed experiments.

3 SEVERE ACCIDENT ANALYSIS AND EXPERIMENTAL VALIDATION FOR SODIUM COOLED FAST REACTORS

3.1 OVERVIEW

Nine papers were presented in the related session of the technical meeting, describing the development and experimental validation of computer codes used to analyse the progression of severe accidents in SFRs.

Contributions from France covered a wide range of software tools, including the SCONE [12] code dedicated to FCI phenomena, physical model developments in the SIMMER code [7], an integral approach by chaining/coupling existing computer codes, and design-oriented fast running tools for uncertainty propagation studies. A future roadmap of an experimental programme to validate these software tools was also presented. A paper from Japan illustrated the development of an integrated code system for severe accident analysis that can be applied to the safety assessment for licensing procedures in Japan. A paper from the United States of America provided an overview of the integral SFR radionuclide transport analysis tool named Simplified Radionuclide Transport (SRT) and the result of statistical analyses obtained with this code. A paper from the Russian Federation reported on the development and application of the integral safety analysis code SOCRAT-BN [13] designed for numerical and statistical simulation of thermohydraulic, neutron physics, thermo-mechanical processes, and transport of radionuclides under anticipated operational occurrences (AOO), design basis accidents (DBA) and beyond design basis accidents (BDBA).

3.2 CONTRIBUTIONS PROVIDED AT THE TECHNICAL MEETING

3.2.1 TOWARDS AN INTEGRATED FRENCH SOFTWARE PLATFORM FOR SEVERE ACCIDENT SIMULATION IN SFRS[5]

Pierre Gubernatis (CEA, France) introduced three important objectives assigned to simulation tools to describe the severe accident sequence for SFRs, i.e.:

- The assessment of the consequences resulting from the initiating event of an accident;
- The improvement of the design of mitigation devices;
- The evaluation of the safety margins associated with the safety demonstration.

France has engaged in the development of an efficient integrated simulation platform allowing a global approach while ensuring the perenniality and ease of validation of existing numerical codes. Two classes of codes can be identified, both dedicated to the assessment of the behaviour of SFRs during severe accidents:

- Mechanistic tools contribute to carry out best estimate calculation for a limited set of scenarios. The SIMMER code [7], coupled with SEASON, is used as a mechanistic tool.

[5] The French SFR concept is based on a pool-type reactor with an in-vessel retention strategy.

- Physico-statistical tools produce a wide range of low cost and highly parameter-dependent simulations. The PROCOR platform [14] is under development to perform fast running simulations of the behaviour of the corium in SFRs.

Both types of tool (mechanistic and fast running) rely on their own verification and validation (V&V) policy, which may present common features. Both classes of tools are needed and used in a complementary way in France, given that both a deterministic and a probabilistic safety demonstration are required by the regulatory body.

The following knowledge gaps were illustrated:

- The mechanistic description of FCI in the lower plenum, with the development of the SCONE [12] simulation tool currently ongoing;

- The development of physico-statistical models to describe the behaviour of a corium pool on the core catcher [15], which is the object of preliminary evaluations.

3.2.2 3D THERMOHYDRAULICS–NEUTRONICS SIMULATION OF SFR CORE DEGRADATION WITH THE SEASON FRENCH PLATFORM

Emmanuelle Dufour (CEA, France) illustrated the French SEASON platform, dedicated to the simulation of SFR core degradation — from the initiating phase, followed by the generalized degradation phase, until the relocation phase of the corium on the core catcher — using the SIMMER-V [16] code (by considering respectively a multichannel model of the core and a full core model).

SEASON is based on a multichannel model of the SIMMER-V thermohydraulics and core degradation code. It involves the chaining of SIMMER-V with a fuel performance code (GERMINAL [17] or SAS-SFR [18]) as well as couplings of SIMMER-V with a spatial neutronics code (PARIS [19], which uses a flux solver that can be SNATCH [20], PARTISN [21] or IDT [22]) and a code modelling the primary circuit (CATHARE [23], in preparation).

An example of reactor application was provided on an ULOF transient in a simplified SFR design core in 3D cartesian geometry.

3.2.3 SFR SEVERE ACCIDENT TRANSIENT STUDY WITH NEW PARTICLE FLOW MODEL IN SIMMER-V

Andrea Bachrata (CEA, France) illustrated a new model of solid debris dynamics developed in SIMMER-V, with analysis focused on the mitigation scenario involving the controlled discharge of degraded core materials through the mitigation transfer tubes. The developed models are inspired by granular theories and are numerically implemented into the SIMMER-V code environment [16].

The study is devoted to assessing the impact of developed models on the numerical prediction of the discharge performance and the experimental comparison for the ULOF transient realized in SIMMER-V [24] with the coupled thermohydraulic–neutronics model for the reference core with a low void effect (CFV) at the beginning of life conditions (i.e. fresh fuel) [25].

The SIMMER-V results align with the SIMMER-III reference calculations concerning the primary safety criterion, which aims to prevent additional re-criticalities. Notably, SIMMER-V introduces an enhanced particle flow model that offers a more detailed depiction of particle

dynamics. This model realistically considers the hindrance caused by particle concentration and incorporates interactions at the particle level.

3.2.4 DESIGN-ORIENTED SIMULATION TOOLS IN FRENCH SFR PROJECTS

Design safety requirements established in France for SFR reactors guide the designer towards intrinsically safe concepts. Complementing other mechanistic methods and tools, several design-oriented tools are used in France and were introduced by Nathalie Seiler (CEA, France). These fast running tools were developed as a complement to more complex mechanistic tools which require high computational costs. These tools allow a large number of simulations in a reasonable computational time and enable uncertainty propagation studies and sensitivity analyses essential to achieving a satisfactory reactor design. Design-oriented physical tools are devoted to analysing unprotected accidental sequences, as opposed to mechanistic tools which encompass the physical models enabling the simulation of any type of accidental sequence.

Design-oriented tools developed for SFR French safety studies allow modelling of:

- The primary phase of each accidental sequence: ULOF, UTOP and unprotected sub-assembly failure (USAF);
- The eventual sequence involving progression of core melt and relocation;
- The vapour (fuel, steel, fission gas) expansion and related FCI causing vessel mechanical degradation and debris bed cooling.

An application result was presented, highlighting the relevant contribution of these fast running tools in the design process of the French Advanced Sodium Technology Reactor for Industrial Demonstration (ASTRID) project. The integration of those tools into the PROCOR platform is in progress.

3.2.5 ARDECO CEA-KIT COOPERATION ON ASTRID SAFETY STUDIES AND RELATED CODE DEVELOPMENTS

Andrei Rineiski (Karlsruhe Institute of Technology (KIT), Germany) presented recent modifications to the SIMMER code made at KIT, in the frame of ARDECo CEA-KIT cooperation on ASTRID 1500 MW(th) safety studies and related code developments. These developments aim at modelling reactivity feedback due to thermal expansion of the core and control rod drive lines, starting from steady state conditions up to molten core configurations. In addition, a new SIMMER calculation option allows the use of data for 72 energy groups without a significant increase in the calculation time as compared to the 11 group case, due to new SIMMER cross-section libraries, extended cross-section generation procedures, and additional reactivity feedback models. The preliminary results show a favourable impact in terms of accounting additional reactivity feedback on the ULOF accident evolution with an expected delay in power excursions that may lead to a lower extent of core degradation.

Moreover, due to new SIMMER capabilities developed at KIT, the impact of the movement of absorber material into the core during the transient was also analysed. The results provide insights into the impact of a B_4C insertion into the core at different timing of the progression of the ULOF transient.

As a conclusion, the computed mechanical energy release is very limited in the most conservative case. The discharge tubes appear to be effective for all considered simulation

options. Also, passive absorber introduction into the core after sodium flow rate reduction or sodium outlet temperature increase appears to be effective to stop the nuclear chain reaction.

3.2.6 CEA EXPERIMENTAL ROADMAP FOR SFR SEVERE ACCIDENT R&D

In support of SFR severe accident modelling and expertise, an experimental roadmap is being developed, including in-pile integral tests, out-of-pile integral and separate effects experiments with prototypic or simulant materials. This was illustrated by Christophe Journeau (CEA, France). The main issues being studied are the efficiency of corium transfer tubes to mitigate energetic power surges in the core region, interactions between materials, FCI, and short and long term behaviour of an in-vessel core catcher. Some experiments were presented which are operated by France with its partners:

- The SAIGA [26, 27], in-pile experiment, to study the degradation of two 16-fuel pin bundles having different power densities and the propagation of a molten pool from one fuel assembly to its neighbouring ones in a ULOF transient;

- The SERUA [28] facility, to study the film boiling regime, for which a sodium quenching facility has to be built;

- The SAFeTY [28], (former PLINIUS-2) facility, to run experiments with 100 kg scale prototypic corium mixture (depleted uranium oxide based melts with, if needed, metallic melt) in a sodium environment;

- Jet Ablation experiments with HAnSoLO [29, 30] (simulant material with water jet on ice at the University of Lorraine) and JIMEC [31] experiments (prototypical material with stainless jet on stainless block at KIT);

- A thermochemistry experimental programme to study the UO_2-Fe-B_4C system with heat treatments carried out at CEA/Paris-Saclay in a high temperature tungsten furnace and B_4C introduced in an UO_2-CeO_2 molten pool performed in the VITI [32, 33], facility at Cadarache.

3.2.7 DEVELOPMENT OF ANALYSIS METHODS FOR SFR SEVERE ACCIDENTS IN JAEA AND ASSESSMENT OF APPLICABILITY TO SAFETY ANALYSIS

Yoshiharu Tobita (JAEA, Japan) illustrated the set of computer codes developed at JAEA for the analysis of the event progression and the energy generation in anticipated transients without scram (ATWS) of SFRs. The analysis is performed by partitioning the entire accident progression into several stages, since the physical phenomena to be analysed and the required level of precision change as the event progresses. The codes SAS4A/SASSYS-1 [6], SIMMER-IV [7], AUTODYN [9], PLUG, CONTAIN-LMR [10] and FLUENT [34] are used to analyse the event progression at each stage.

The procedure for confirming the applicability of the methodology for analysing a core disruptive accident (CDA) in SFRs is described, with a focus on the SIMMER code, which plays a dominant role in the methodology. The procedure involves highlighting important phenomena based on the magnitude of their impact on the event progression during the CDA transition phase. Subsequently, validation analyses were performed on the SIMMER code for these important phenomena to confirm its applicability and to identify uncertainties. The

influence of uncertainties on the analytical results of SIMMER has to be evaluated in the safety analysis of the LMFR plant.

The applicability of the methodology was confirmed not only for SIMMER, but also for other analysis codes that contribute to the comprehensive analysis methodology of event progressions in CDA. The analytical methodology described in this paper provides a basis for conducting safety assessments of LMFR plants during the licensing phase under the new regulatory standards in Japan.

3.2.8 THE SIMPLIFIED RADIONUCLIDE TRANSPORT CODE FOR THE SOURCE TERM ASSESSMENT OF POOL-TYPE METAL FUEL SFR SEVERE ACCIDENTS

Matthew Bucknor (Argonne National Laboratory (ANL), United States of America) presented the SRT code, an integral SFR radionuclide transport analysis tool that assesses radionuclide movement from the reactor fuel to the environment, developed by the Argonne National Laboratory to aid mechanistic source term assessments, and to support the design and licensing efforts for pool-type, metal fuel SFR designs.

SRT relies on the output of system analysis codes, such as SAS4A/SASSYS-1 [6], or user's input, including the fuel conditions (temperature, cladding status, molten fraction) and sodium pool temperature over the transient time, which is then utilized to perform the transport calculation of a total of 770 isotopes (32 elements). SRT utilizes a data-driven approach to assess the radionuclide migration within the fuel pin during irradiation, such as radionuclide movement to the fission gas plenum and sodium bond, along with radionuclide release from the fuel during cladding failure events.

An example of SRT analysis was illustrated to demonstrate the capabilities of the code. The postulated transient scenario is a rapid heat-up of the core fuel resulting in fuel melting and cladding failure. Many radionuclide transport characteristics were treated as uncertainties by the code, including the cover gas and containment leakage rates, in-pin migration fractions, fuel pin release fractions, bubble characteristics, and aerosol deposition options. To assess these uncertainties, 250 iterations of SRT were performed. The cumulative distribution function of the total effective dose estimate, the time-dependent radionuclide inventory in the cover gas region, and the fractional release plot illustrating the inventory of the radionuclides available at each stage of the transport process, were presented as an example of SRT calculation capabilities.

3.2.9 MODERN APPROACHES TO DETERMINISTIC SAFETY ANALYSIS FOR SFRS

Within the framework of the modern requirements of the Russian Federation safety regulatory document (NP-001-15 [35]), Ruslan Chalyy (Nuclear Safety Institute, Russian Academy of Sciences, Russian Federation) illustrated the development and certification of the SOCRAT-BN code, as well as the methodology of error estimation and uncertainty analysis associated with the calculations with this code.

The SOCRAT-BN code is designed for numerical simulation of thermohydraulic, neutron physics and thermomechanical processes, and transport of radionuclides released after failure of the fuel elements in SFR power plants under AOO, DBA and BDBA with core degradation.

Examples of the use of the SOCRAT-BN code for the analysis of total instantaneous blockage (TIB), loss of flow (LOF) and ULOF were provided, complemented with Monte Carlo calculations based on the modelling errors of the main parameters evaluated by the modified ASME V&V 20 approach through the validation study of the SOCRAT-BN code:

- The analysis of TIB showed that the accident terminates with the blockage of 7 assemblies in the most penalizing configuration and confirmed the conservatism of the deterministic analysis of the safety criteria for TIB;

- The uncertainty analysis of LOF indicated the relative activity of fission products (FP) release from the reactor as the most representative results of the hydro-seal opening, which was predicted in 55 Monte Carlo calculations out of 100 performed;

- The uncertainty analysis of the ULOF accident is performed to estimate the time corresponding to the beginning of fuel cladding melting.

This study has shown that, due to the complexity of the phenomena to be simulated, the calculation time needed for modelling a SFR scenario (and especially for uncertainty analysis) considerably exceeds the one needed for modelling BDBA for VVER-type reactors. In this regard, it is necessary to adopt a very balanced approach to the selection of representative scenarios and the parameters to be analysed.

4 PRIMARY AND TRANSITION PHASES OF SEVERE ACCIDENTS FOR SODIUM COOLED FAST REACTORS

4.1 OVERVIEW

Four papers were presented in the related session of the technical meeting, which focused on new or expanded capabilities of existing software tools to model phenomena associated with the primary and transition phases of severe accidents in SFRs. With the introduction of these newly developed or updated models, it was shown that it is possible to analyse certain phenomena in more detail, which would allow for improving the designs of components and systems.

Papers from the USA and Japan focused on developments in the SAS4A/SASSYS-1 code [6], while the papers from India focused on recently developed modules in PREDIS and a new tool named TRAN-SCORE [36]. The importance of being able to model more phenomena or expand capabilities of each of the software tools was noted as a driver for software development. In most cases, where additional phenomena were included or models were refined, less conservative results were obtained.

4.2 CONTRIBUTIONS PROVIDED AT THE TECHNICAL MEETING

4.2.1 STATUS OF THE SAS4A/SASSYS-1 CODE METALLIC FUEL MODELS FOR THE SIMULATION OF POSTULATED SEVERE ACCIDENTS IN LMFRS

SAS4A/SASSYS-1 [6] is a reactor dynamics and safety analysis code developed at ANL for the safety analysis of SFRs. As part of the collaboration with the Korea Atomic Energy Research Institute on the Prototype Gen-IV SFR, a significant metal fuel model development and validation effort was undertaken at ANL. Adrian Tentner (ANL, United States of America) described recent extensions implemented in a research version of the SAS4A/SASSYS-1 code, SAS-RES, that includes changes to the metal fuel relocation module LEVITATE-M to allow the simulation of inter-assembly interactions, including inter-assembly heat transfer (IAHT) and post-assembly failure, inter-assembly material contact and physical interactions. These are unlikely events, with extremely low probability well below the beyond design basis limits. The SAS4A/SASSYS-1 code was developed initially for the analysis of the initiating phase of postulated fuel relocation events in LMFRs, that is, of the sequence of events that occur before the failure of an assembly wall, or before the initiation of the transition phase of an accident. The implementation of the post-assembly failure LEVITATE-M models significantly extends the ability of the SAS4A/SASSYS-1 code to analyse extended fuel relocation sequences.

The SAS-RES metal–fuel models address significant phenomena specific to metal fuel pins, which are absent in oxide fuel pins. These phenomena include the migration of U-Zr and U-Pu-Zr fuel components during irradiation, leading to the formation of radial fuel regions with varying compositions. To accurately describe local fuel composition, the new metal fuel modules track multiple constituents, such as uranium, plutonium, actinides, fission products, lanthanides, zirconium, and iron. Changes in local composition can strongly impact thermophysical properties, including melting and freezing temperatures. These variations can influence the timing and magnitude of cladding failure, fuel relocation events, and the related reactivity feedback. Mechanistic models for these metal fuel phenomena are included in the SAS-RES modules SSCOMP-A, DEFORM-5A, PINACLE-M, and LEVITATE-M.

The paper focused on the ability of the model to study post-assembly failure events. The failure of the assembly wall leads to local expansion of the assembly and direct contact of the molten fuel and other components in the coolant channel of the failed assembly with the outer surface of the neighbouring assembly wall. The sodium in the inter-assembly gap is displaced by the walls of the failed assembly and does not contact the coolant channel materials. The expanding assembly walls and/or local freezing of the molten fuel/steel mixture due to contact with the colder neighbouring assembly prevent the axial relocation of the molten fuel and other components in the inter-assembly space.

The SAS-RES channels which represent assemblies were assumed to be thermally isolated from their neighbours prior to assembly wall failure and an adiabatic boundary condition was applied at the outer surface of the assembly walls. It was recognized that the inter-assembly heat transfer can play a significant role during certain accidents, transferring heat from the hotter assemblies to the colder neighbouring assemblies and mitigating the accident consequences. The sides of the neighbouring assemblies that face the lead assembly are also identified, and their temperature is tracked independently of the other sidewalls. These initial results of the assembly blockage simulation show that IAHT can significantly affect the accident outcome providing an effective path for removing heat from the blocked assembly in the absence of sodium coolant flow, to reach a stable coolable configuration. Additional verification and benchmarking of these models will be completed prior to formal release.

4.2.2 STATUS OF NUMERICAL TOOL DEVELOPMENT FOR INITIATING PHASE IN SEVERE ACCIDENTS OF SFR IN JAPAN

The paper by Yoshitaka Fukano (JAEA, Japan) described the phenomena identification and ranking table (PIRT) method to identify important phenomena to be verified for ULOF and UTOP scenarios in a medium-sized SFR. Through these studies, 16 and 14 physical phenomena were identified for ULOF and UTOP scenarios, respectively. Then 10 and 8 respective key important phenomena were identified through the ranking of originally identified phenomena. Furthermore, a validation test matrix was created for the important phenomena, and validation was conducted according to the matrix. These studies further improved the validity and reliability of the SAS4A/SASSYS-1 code. The 16 and 14 identified physical phenomena for ULOF and UTOP scenarios were ranked in terms of importance. These ranks were defined as High (H), Medium (M), and Low (L) in descending order of importance.

Since the reactivity of the reactor, the energy release, and the average core fuel temperature are highly related, the importance of each physical phenomenon was determined and ranked by examining its influence on these parameters.

An evaluation matrix was created for the important phenomena identified by ranking the physical phenomena. The evaluation matrix describes the analytical models corresponding to the important phenomena and the validation methods of the models in a matrix form and confirms that the physical phenomena required for the evaluation of the targeted accident scenario have been modelled without any deficiencies. These studies further improved the validity and reliability of the SAS4A/SASSYS-1 code. As an example, the evaluation of a ULOF event for a medium-sized SFR using SAS4A/SASSYS-1 showed that the prompt criticality during the initiating phase may be avoided even under conservative conditions due to the reduced excess uncertainty.

4.2.3 RECENT DEVELOPMENTS IN MODELLING OF SEVERE ACCIDENT ANALYSIS CODE PREDIS

In this paper by Anuraj Vijayan Leela (Indira Ghandi Center for Atomic Research, India), the severe accident analysis is carried out in three stages, namely: 1) pre-disassembly phase, 2) disassembly phase, and 3) mechanical energy release phase. An in-house accident analysis code PREDIS was used to study the pre-disassembly part of the accident analysis. To improve the accident analysis capability of the code, a clad relocation model and an in-pin fuel motion model were incorporated into the code and the effect of those phenomena on severe accident evolution was studied. The clad relocation model was based on Ishii's model [37, 38] and in the analysis, it was assumed that the coolant channel was voided prior to the initiation of the molten clad motion. The molten clad was assumed to be moving as a film under the influence of gravity, the channel pressure gradient, the frictional drag due to streaming sodium vapour, and friction between the molten cladding and the fuel pin. A new subroutine RELOCS was developed and integrated into the PREDIS code to perform the calculation.

Similarly, to improve the analysis methodology of unprotected transients, an in-pin fuel motion module called MITRA was incorporated into PREDIS. In fast reactors, the use of an annular oxide fuel pin is expected to provide an inherent shutdown mechanism during accidents by providing a pathway for molten fuel to be ejected from the active core region to the top and bottom blankets. The reactivity feedback due to in-pin fuel motion and its effect on the transient progression were studied. UTOP analyses were carried out with the in-pin fuel motion module. From the analyses it was shown that, considering in-pin fuel motion feedback not only reduces the power at the end of the transient, but also reduces the hot spot clad and coolant temperatures as well as the number of radial channels that undergo melting.

At the end of disassembly (i.e. when the neutronic excursion ends), the core is left at a very high temperature and pressure. This is the beginning of core disintegration. A time-dependent module, FEXPAN, was introduced to study the hydrodynamic expansion of a homogeneous fluid medium in spherical geometry. Post disassembly hydrodynamic expansion of Fast Flux Test Facility (FFTF) benchmarks were performed to validate FEXPAN. With these changes to PREDIS, the code simulates accidents more realistically by modelling important phenomena instead of utilizing conservative assumptions.

4.2.4 DEVELOPMENT OF A FUEL DEFORMATION MODULE IN THE TRAN-SCORE CODE TO EVALUATE POWER AND FLOW TRANSIENT IN SFRS

In the paper by Amandeep Singh (Atomic Energy Regulatory Board (AERB), India), a computer code TRAN-SCORE, was developed specifically to evaluate the pre-disassembly phase of sodium cooled fast breeder reactors that uses mixed oxide (MOX) fuel. The code includes the modelling of neutronic, thermal hydrodynamic, and simplified fuel deformation behaviour. The capability of the code was demonstrated by simulating a few test problems and comparing against results from SAS1A. A newly developed fuel deformation module was added to TRAN-SCORE to estimate fuel pin stresses and deformations occurring during transients, and it considers both elastic and plastic deformation of the cladding. Mechanical deformations of the fuel and cladding were estimated in the elastic as well as in plastic regime. The fuel–clad gap width was calculated as a function of time. Thermoelastic deformation of the fuel and the elastic-plastic deformation of the cladding was estimated using the fuel and cladding temperature profiles obtained from the heat transfer module. Fuel and clad stresses and deformations were calculated by assuming a stress free configuration at normal operating

conditions. With the inclusion of the deformation model, transient analysis was carried out for a reactivity transient, and the results were compared to benchmark results from SAS1A [39].

5 EXPANSION PHASE AND LONG TERM BEHAVIOUR FOR SODIUM COOLED FAST REACTORS

5.1 OVERVIEW

This session included four papers reporting recent research on the characterization of the physical phenomena involved during the expansion phase of the accident and the long term behaviour of the corium.

The expansion phase involves a large variety of phenomena: in-core re-criticality, CDA bubble expansion and conversion of thermal energy to mechanical energy, damage to reactor structures, sodium leaks, relocation of core materials through CRGT or specific mitigation devices such as FAIDUS [40] or Transfer-Tube, and FCI.

The long term behaviour of the corium also involves many different phenomena which have been addressed in this technical meeting: the cooling of the fuel remaining in the core, corium jet impingement, debris sedimentation (addressed in earlier fundamental studies [41, 42]), the behaviour of debris beds and the liquid pool on the core catcher, and long term cooling by the decay heat removal system (addressed in past studies [43]).

5.2 CONTRIBUTIONS PROVIDED AT THE TECHNICAL MEETING

5.2.1 ANALYSIS OF THE REMAINING CORE MATERIAL COOLABILITY IN AN SFR CORE

Joji Sogabe (JAEA, Japan) illustrated the evolution of a ULOF scenario, focusing on the core conditions after material relocation.

The experimental case considered was the EAGLE ID3 [44] test at IGR, with similar masses of fuel and steel in the molten mixture after a power pulse. Analyses of thermal conductivity of the fuel–steel mixture were performed. The estimated effective thermal conductivity was about five times higher than that of molten steel; one of proposed explanations is that this could be due to steel convection effects.

5.2.2 JAEA ANALYSIS METHODOLOGIES FOR THE EVALUATION OF AN ATWS ACCIDENT AT AN SFR – MECHANICAL CONSEQUENCES DURING THE EXPANSION PHASE OF THE ACCIDENT

The paper presented by Yuichi Onoda (JAEA, Japan) focused on simulations for the expansion phase. Three codes are used at JAEA: SIMMER, AUTODYN and PLUG. The JAEA modelling approach to evaluating the mechanical energy release and radioactivity release to the out-of-vessel space was presented. Examples were given for the Prototype Fast Breeder Reactor (PFBR) and the prototype sodium cooled fast reactor (Monju) designs.

5.2.3 FRENCH RESEARCH PROGRAMMES RELATED TO SEVERE ACCIDENT PHENOMENOLOGY IN THE LOWER PLENUM OF AN SFR

A review of experimental and code development activities was presented by Rémi Clavier (CEA, France). Topics include the SCONE code development and application for FCI simulations, SERUA experiments on FCI, debris-bed behaviour studies and simulations of liquid corium pools on the core catcher.

Regarding this last point, depending on the heat transfer between sodium and core debris during their transfer from the core area, their accumulation on the core catcher may involve a combination of solidified particles (making a debris bed) and molten materials:

- The solid debris bed behaviour involves in particular: sedimentation of particles, self-levelling, neutron reactivity, the ability to cool the core melt and possible re-melting. A new OpenFoam solver is under development to simulate the self-levelling of the debris bed [45]. A comparison with previous work on self-levelling [43, 46] with SIMMER and other codes could be done in the future. The neutron reactivity of the debris bed may be evaluated using the TRIPOLI-4 [47] code on static configurations.

- Fuel re-melting and strong liquid jet impacts may lead to the formation of liquid molten pools on the core catcher. Experimental databases include past experiments (BALI [48]) and have been recently extended with the LIVE-ESFR programme [49] with representative geometry in the framework of the European ESFR-SMART research project. A new simulation tool based on the TRUST numerical platform has been developed to represent such molten pools and will be validated against LIVE-ESFR experiments and used to provide new a closure law for simplified tools like PROCOR.

A new numerical platform called TRUST [50] is now used instead of DUNE [51] as a basic numerical service provider for SCONE. Experiments have been performed with simulant materials (water/ice) and prototype materials (steel), and progress was reported concerning their numerical simulation. Codes show promising results but still require further developments.

5.2.4 DEVELOPMENT OF AN EVALUATION METHOD FOR IN-PLACE COOLING OF A DEGRADED CORE IN SEVERE ACCIDENTS OF SODIUM COOLED FAST REACTORS

Yuya Imaizumi (JAEA, Japan) presented a paper illustrating a partial fuel discharge. Some materials remain in place and their cooling has to be considered, in particular by sodium in CRGTs. The phenomenology was discussed; it provides a basis for establishing a PIRT.

An out-of-pile experimental test was reported, performed as part of cooperation between experts from Japan and Kazakhstan. A particular issue is related to simulation of inert gas and sodium vapour above the fuel. Code extensions in SIMMER, which is currently used with single velocity field for gas, are being considered for addressing this issue.

6 ACCIDENT ANALYSIS AND EXPERIMENTAL PROGRAMMES FOR LEAD COOLED FAST REACTORS

6.1 OVERVIEW

Lead cooled fast reactor technology has gained important interest in the last decade from different developers ranging from newly created companies such as NEWCLEO (LFR-AS-200) up to well established nuclear companies such as Westinghouse (Westinghouse LFR) and ANSALDO (ALFRED) and research institutes such as ENEA (ALFRED) and SCK-CEN (MYRRHA), to name only those that contributed to the Technical Meeting. The developer that is most advanced in LFR technology is Rosatom, which started the construction of the BREST-OD-300 reactor and related reprocessing plant in 2021.

However, LFR technology is still in an early development phase compared to SFR technology that benefits from a long operating experience (500 reactor-years achieved in 2023) and a history of safety analysis of severe accidents. This is reflected in the relatively low number of LFR contributions to this TECDOC (6 papers) compared to SFR (16 papers). Moreover, some of the contributions do not deal with severe accidents in LFR technology.

Although most technology developers claim to consider mitigation of severe accidents in the safety approach for their LFR design, there is insufficient information on which severe accident sequences are being considered. Nor is there information on a basis for selecting severe accidents sequences that have to be mitigated. Furthermore, the concept of 'practical elimination' is insufficiently elaborated. The Generation IV International Forum suggested limiting the severe accident conditions to be considered for LFRs to partial core damage conditions [52].

Developers of LFR technology claim that it features intrinsic properties favourable for severe accident prevention and mitigation. However, quantitative safety analyses that support these claims are needed. This requires the development of new tools or the extension of the currently available SFR codes to the peculiarities of the lead coolant and the LFR systems. While development progresses, the need for validation campaigns and facilities may constitute a challenge, in particular for severe accidents.

In the following subsections, the six contributing papers for LFR technology are discussed with respect to their relevance for severe accident modelling and analysis.

6.2 CONTRIBUTIONS PROVIDED AT THE TECHNICAL MEETING

6.2.1 DEVELOPMENT OF EXPERIMENTAL INFRASTRUCTURE FOR SEVERE ACCIDENTS INVESTIGATIONS IN SUPPORT OF THE ALFRED LICENSING PROCESS IN ROMANIA

Marin Constantin (RATEN ICN, Romania) illustrated activities related to LFR technology, which is considered a key option in Romania, and the demonstrator of this technology, the Advanced Lead Fast Reactor European Demonstrator (ALFRED), which is programmed to be built in the country. ALFRED is a lead cooled, pool type configuration reactor with steam generators directly installed inside the reactor vessel.

Several phenomena were identified in the pre-licensing process regarding potential severe accidents in ALFRED, which need experimental study, as follows:

- Fuel fragmentation due to interaction with the lead coolant and fuel dispersion and relocation in a severe accident scenario;
- Retention, deposition and transport of fission products in lead and/or migration to the cover gas;
- Chemistry of fission products in the lead pool and cover gas;
- Polonium formation in the large pure lead pool and its transport to cover gas;
- The interaction between steam and lead.

An important experimental effort is planned for supporting the safety analysis of ALFRED, and a suitable infrastructure to support the R&D efforts, also addressing the challenges of the lead fast reactor technology is needed. The nuclear platform Mioveni is the designated site for the ALFRED reactor, as well as for the research facilities.

The experimental infrastructure will consist of the following facilities:

- ATHENA, test pool for the main components in different thermohydraulic regimes;
- ChemLab, coupled with ATHENA to investigate lead and cover gas chemistry;
- HELENA2, loop facility to test equipment in relevant conditions for ALFRED;
- ELF, large pool facility to test endurance and reliability under forced and natural circulation regimes;
- HandsOn, pool facility to demonstrate fuel assemblies handling;
- Meltin'Pot, a set of facilities to investigate the phenomena associated with severe accidents.

Meltin'Pot, which is expected to be operational by 2026, is designed to accommodate four experimental modules aimed at conducting the following experimental programmes:

- Module 1: FCI, which will be used to investigate the chemical interaction between fuel and lead and the fuel/cladding microstructure status after interaction with the molten lead.
- Module 2: Fuel fragmentation and relocation, to investigate the fragments distribution in lead of fresh and irradiated MOX fuel for possible re-criticality and the influence of heat removal under core damaged conditions.
- Module 3: Fission product transport and retention, to study the retention of fission products and activation products in lead, migration of volatile products in the cover gas, and the solubility and chemistry of the different species formed in lead.

- Module 4: Polonium retention and dispersion, to assess the retention and the chemistry of polonium in lead and its volatilization in the cover gas.

Meltin'Pot will offer significant possibilities to improve the existing knowledge on some phenomena associated with severe accident conditions in a pure lead environment.

6.2.2 MODELLING OF THE LEAD COOLED FAST REACTOR ACCIDENTS WITH THE EUCLID/V2 MULTIPHYSICS CODE

The paper by Dmitry Veprev (Nuclear Safety Institute, Russian Academy of Sciences, Russian Federation) discussed the analysis of a loss of heat sink accident for the BREST-OD-300 reactor. Although the accident scenario represents design extension condition, it does not lead to fuel pin failure or degraded core conditions.

The code used for modelling the transient is a new version of the EUCLID code. EUCLID is a platform code, integrating different subcodes that model different phenomena involved in the safety analysis of LFR and SFR in Russia. Version 1 of the code (EUCLID/V1) was reported in Ref. [53]. This paper refers to a new version of the code, EUCLID/V2 [54, 55], which has been supplemented with many models that simulate phenomena during degraded core conditions, such as a model for 'secondary criticality', for 'corium in-vessel retention', and for 'in/ex-vessel phenomena'.

6.2.3 MODELLING OF SEVERE ACCIDENTS FOR SFRS AND LFRS

The paper by Stanislava Senatorova (Scientific and Engineering Centre for Nuclear and Radiation Safety, Russian Federation) discussed the impact of possible degraded core conditions in the BN-800 SFR and the BREST-OD-300 LFR.

The SFR related scenarios are modelled with the aid of SOCRAT-BN, a multiphysics code that also manages degraded core conditions with fuel displacement. These results are not relevant for LFR technology.

The LFR (BREST-OD-300) related scenarios concern the assessment of the reactivity impact of selected hypothetical design extension conditions.

The first condition is a hypothetical loss of coolant scenario for which the reactivity impact is calculated with SERPENT [56]. No fuel displacement is considered in the scenario. The analysis concluded that coolant removal has a negative impact on reactivity and will (by itself, without fuel displacement) not lead to criticality.

The second condition concerns the hypothetical removal of the clad material from the active core region, a possible phenomenon during core degradation in case of unprotected transients. No fuel displacement is considered. The analysis, performed with the SERPENT code, concluded that the disappearance of the clad injects a large amount of reactivity, much higher than the delayed neutron fraction. Although not fully mechanistic analyses of core degradation scenarios, these simplified analyses of possible phenomena during design extension conditions are very valuable to explore which phenomena could be relevant for degraded core conditions.

6.2.4 DEVELOPMENT OF DRIFT-FLUX CORRELATIONS FOR VERTICAL FORWARD BUBBLE COLUMN-TYPE GAS-LIQUID LEAD-BISMUTH TWO-PHASE FLOW

The presentation by Di Wang (China Nuclear Power Technology Research Institute Co., Ltd., China) introduced new correlations for the drift flux parameters (distribution parameter, gas drift velocity, etc.) for two-phase, vertical forward bubble column flow, relevant in case of steam generator tube rupture (SGTR) accidents in LFR.

A comprehensive literature review of existing correlations for similar fluid configurations was reported. Many steam/nitrogen/air–water two-phase flow tests have been performed in the past, but there have been much fewer tests for gas–liquid metal systems. For this reason, lead-bismuth eutectic (LBE), gallium and water systems are reported and compared with the developed correlations. The deviation of the suggested correlations from the experimental data for both gas–LBE and gas–gallium systems is low, especially for the LBE system, where it gives the best results.

6.2.5 OVERVIEW OF ENEA EXPERIMENTAL CAMPAIGN CONCERNING LFR PROJECTS

In this presentation, ENEA's activities related to the LFR technology were reported by Alessandro Bellomo (ENEA, Italy). ENEA is a partner in the FALCON Consortium, supporting the efforts for the development of the ALFRED reactor.

Several experimental facilities are available to support the validation of codes simulating lead systems. The LBE loop facility CIRCE [57] provided experimental data for the validation of the SIMMER-IV code for simulating SGTR. The LIFUS5/mod2 [58] facility, designed to perform heavy metal–water interaction experiments provided data for SIMMER-III, SIMMER-IV and RELAP5 codes. The NACIE-UP [59] facility is available for simulation of the transition from forced to natural circulation with heavy metal systems.

The preliminary results of the LEad-to-Water INteraction (LEWIN) facility were also reported, with steam bubble computation performed with the SIMMER-III code.

ENEA plans to constitute a working group specifically dedicated to the assessment of severe accidents in LFRs.

6.2.6 HEAT TRANSFER CHARACTERISTICS OF LMFRS

The paper by Abdelfattah Ali (Egyptian Atomic Energy Authority, Egypt) discussed the results of computational fluid dynamics (CFD) calculations for a five-pin fuel bundle cooled by liquid lead, in a geometry typical for the normal operation conditions of an LFR.

The CFD is a Reynolds Averaged Navier-Stokes (RANS) type calculation with standard turbulence models. The bundle is wire-spaced, and heat transfer efficiency is calculated for different wire pitch lengths.

The paper concludes that the wire is beneficial for heat transport in the coolant by increasing transverse momentum and turbulence transport. The smaller the wire pitch the better and faster the heat transport in the coolant.

7 CONCLUSIONS AND PERSPECTIVES FROM THE TECHNICAL MEETING

7.1 SODIUM COOLED FAST REACTORS

7.1.1 CONCLUSIONS

Severe accident analysis methodologies for SFRs have been developed in Member States. One of the objectives of the methodologies is to evaluate the effectiveness of design measures put in place to cope with the potential severe accident conditions considered. To achieve this, it is essential to simulate all potential phenomena that may occur during the severe accidents under consideration, along with their corresponding interrelations. These phenomena are largely influenced by the specific characteristics inherent in SFR designs.

One important aspect of severe accident analysis for SFRs is to evaluate the mechanical energy releases that might damage the containment structures, including the features implemented to maintain subcriticality and to cool the core debris. The mechanical energy releases may result from FCI and power excursion. The power excursion occurs due to significant reactivity insertions, which may be triggered initially by the sodium voiding effect at the start of the accident and later by the concentration of fuel material during the more advanced phases when the core is molten. Minimizing and mitigating such effects are crucial aspects of safety design for SFRs. For that purpose, a series of accident sequences, from intact core state to fully degraded core and termination of the accident, have to be analysed, evaluating the resulting mechanical and thermal consequences, and the effectiveness of design measures to cope with them. Other phenomena likely to damage the containment measures such as sodium fire and sodium–concrete interaction need to be evaluated (i.e. as well as fission products release and transport) for source term quantification.

Contributions at the technical meeting showed the progress in the development and improvement of simulation tools for severe accidents analysis to model additional phenomena (some of them may be due to new reactor designs) and to account for mitigation systems in SFR designs to achieve higher levels of confidence in safety assessments. Ongoing experimental programmes support verification and validation of the physical and mathematical models.

There are several ongoing efforts towards the development/improvement of models and tools, simulating a wide set of physical phenomena and their respective related fields (e.g. thermohydraulic, neutronic, mechanic, chemistry) for the accident conditions addressed during the SFR design process:

- Simulation tools for modelling the initiation/primary and transition/secondary phases have been developed and/or expanded to include modelling of additional phenomena to reduce the number of conservative assumptions often made in severe accident analysis. In simulations where additional phenomena are modelled, more favourable accident results can be obtained for both metal fuel and MOX fuel. The calculation results of these improved simulation tools can be used to help facility, system, and component design efforts.
- Tools for the simulation of the expansion phase and long term behaviour have reached a high level of complexity and address the most important phenomena of interest. They are being extended on the basis of past and recent experiments to better describe particular phenomena such as fluid–structure interaction, FCI, fuel behaviour in a

degraded core and on the core catcher. Fluid–structure interaction studies are based on a combined use of core degradation codes to describe the bubble formation and specialized codes to address the mechanical aspects. FCI is generally addressed by existing simulation codes but new FCI-focused tools with enhanced simulation are under development.

- The complexity of the phenomena to be simulated can lead to long calculation times, which is motivating the development of fast running codes such as SRT in USA and design-oriented simulation tools in France. These fast running tools allow performing large number of simulations in a reasonable computational time and sensitivity analyses using parameters of interest. Nevertheless, a validation of these tools against experiments (and/or a comparison with mechanistic tools) is necessary to increase confidence in the numerical results obtained with these simplified methods and codes.
- In addition, efforts are also being devoted towards high performance communication among these simulation tools, to manage large amounts of exchanged data. The communication and the interface between calculation tools relies on specific procedures and methodologies to provide accurate safety assessments for SFR applications.

A large spectrum of potential severe accidents needs to be covered through a large experimental database. As a result of international efforts in the past decades, a rich experimental matrix has been created. However, additional experimental tests are needed to progress in the validation of physical correlations and of calculation tools for specific SFR designs. The definition of some of these experimental programmes — in-pile and out-of-pile with prototypical and simulant materials in the frame of separate effect tests or semi-integral configurations — is in progress, for example, the EAGLE and SAIGA in-pile programmes in the IGR reactor in Kazakhstan, and out-of-pile programmes in the SAFeTY facility in France and in the MELT facility in Japan.

7.1.2 PERSPECTIVES FOR FUTURE ACTIVITIES

The perspectives for future activities are mainly focused on the knowledge and simulation of phenomena likely to damage the reactor structure. Through a great amount of R&D work, severe accidents analysis methodologies have gained a good maturity level to assess various severe accident sequences and the effectiveness of severe accident mitigation measures. Analysis tools for the primary phase (initiating phase), such as SAS4A/SASSYS-1, have been developed and applied to the reactor designs in many countries. In-pile experiments in CABRI (for oxide fuel) and TREAT (for metallic and oxide fuels) have been performed to provide a database for understanding the phenomenology of fuel pin behaviour under severe accident conditions. Such databases can be used for analysis code validation. For the transition/secondary phase, the SIMMER code family for oxide fuel has been developed with support of international collaboration. The focus of R&D is now mainly moving into the later phases of accidents.

In accordance with the pace of progress of analysis tool developments for individual accident phases or phenomena, integral code system development is underway for the systematic analysis of various accident sequences. The computational platform developed by CEA to provide an interface between various codes is one example and indicates a future trend of development.

In terms of phenomenological knowledge, analytical models, and experimental data, the R&D needs identified in the Member States are listed below. The importance or priority of the listed

items is largely dependent on the characteristics of the SFR design under consideration (e.g. oxide or metal fuel).

- Primary and transition/secondary phase:
    - Molten fuel discharge through the steel duct. Experimental activities, EAGLE and SAIGA, will provide first results for developing the corresponding models in SIMMER and PROCOR.
    - Jet impingement. Additional experiments on water/ice system and prototypic material will improve the knowledge of phenomena. Then, adapted CFD codes could be extended and validated.
    - New in-pile tests for addressing the degradation of MOX fuel in the pin and/or within the fuel assemblies (with sodium circulation outside) to validate simulation models (e.g. in the TREAT facility or in the IGR reactor).
    - Continued development of PREDIS and TRAN-SCORE to model more phenomena and reduce conservatisms.
    - Assembly-to-assembly physical interaction and potential radial geometry changes.
    - Fuel relocation, including in-pin axial fuel relocation and pin disruption.
    - For metal fuel:
        - Dynamic changes in the metal–fuel–iron mixture (eutectic reaction) during transients;
        - Behaviour of novel metal fuel types such as annular fuel and metal fuel without a sodium bond;
        - Additional experimental validation regarding fuel behaviour during fuel blockage or severe loss of flow events (e.g. in the TREAT facility), including assembly-to-assembly heat transfer and post-assembly failure phenomena (e.g. material contact and physical interactions);
        - Development of SAS4A/SASSYS-1 models.
- FCI:
    - An experimental programme is planned to perform experiments supporting the validation of FCI with large masses of corium in the new SAFeTY facility for SCONE development.
    - Separate-effect experimental programme to improve the validation of SCONE (for metallic and MOX fuel) is planned in the SERUA facility.
- Expansion phase:
    - Expansion phase and fluid–structure interaction (a coupling between SIMMER-V and EUROPLEXUS is planned).

- Long term material relocation and cooling:
    - Debris bed behaviour: EAGLE-3 in-pile test and experiments in MELT facility, in addition to CFD application for heat removal from the debris bed.
    - Molten material behaviour and crust formation in the core catcher: LIVE-ESFR experiments and specific developments on the TRUST platform to address the question of the protection of the core catcher.
    - Coupling of thermohydraulic and neutronic models of the debris bed.
- FP release, transport, and retention under severe accident sequences (both for MOX and metal fuel) to assess the importance and ability to transport fission products outside the reactor system[6] [60]: the evaluation of these items needs to be improved both for in-vessel and out-of-vessel conditions over all severe accident sequences. A PIRT process may be the starting point for this improvement as function of the reactor design (PIRT efforts have already been performed such as the one developed in the framework of the European R&D project); then, more predictive tools may be developed and qualified with experience of the calculation domain under consideration.

In addition, the following areas of improvement were also identified:

- Enhance and facilitate the coupling and chaining of simulation tools (in terms of integration of new capability, acceleration of calculation time, flexibility, etc.) and develop global numerical platforms to gather different types of calculation tool (both mechanistic and parametric) addressing different accidental phases. As an example, the global numerical platform SEASON aims to simulate the primary phase and the generalized degradation phase which will be interfaced with the SIMMER-V code and other codes.
- Addressing various types of sequence initiating the severe accident (including ULOF, UTOP, etc.) in a comprehensive manner for the safety demonstration.
- A methodology needs to be established to present the appropriate outputs (interpretation, summary) from complex analyses of severe accident sequences in the safety documentation.

Participants in the technical meeting encouraged IAEA to support effective multilateral cooperation to address some of the abovementioned challenges, including through providing a platform for discussions at technical meetings, which may cover tasks such as:

- Additional benchmarking activities for MOX fuel (such as those already performed in past or ongoing CRPs, such as EBR-II, FFTF and PFBR);
- Benchmarking activities aiming at assessing the behaviour of MOX and metal fuel in unprotected accidents;

[6] For example, see Ref. [60] for a recent assessment of knowledge gaps regarding the release and transport of fission products for metal fuel.

- Developing a validation matrix of experimental data needed for the validation of models and tools.

7.2 LEAD COOLED FAST REACTORS

7.2.1 CONCLUSIONS

The information provided on modelling of severe accidents in LFRs in the six papers contributing to this TECDOC and during the technical meeting in March 2023 is limited. The same observation holds for publicly available literature on the subject, despite an apparent consensus among LFR developers that the technology may provide beneficial characteristics in preventing severe accidents and even in mitigating degraded core conditions. A clear assessment with validated tools is not yet available or at least not provided in open literature.

More information was provided at the technical meeting on the research facilities that are being set up to investigate physical and chemical phenomena that play an important role in the normal operation and in accident conditions in LFR. Nevertheless, a clear link between the researched phenomena and the severe accident scenarios they relate to is mostly absent.

Although the development of tools for severe accident modelling is ongoing — often based on the adaptation of SFR codes such as SIMMER and SAS4A/SASSYS-1 — publicly available examples of the application of the tools adapted to LFR designs are at an early stage, and little information is available on validation efforts for these adapted codes.

There seems to be lack of consensus on which accidental sequences leading to a degraded core are required to be mitigated. The possibility of the ‘practical elimination’ of some sequences is often put forward, but the related design measures, and even examples of the demonstration, were not presented at the meeting.

7.2.2 PERSPECTIVES AND FUTURE ACTIVITIES

The concepts of severe accident sequences needing to be mitigated by design, and severe accident needing to be ‘practically eliminated’ are very important for developing the safety approach associated with the development of new reactor technologies. With regard to LFR technology, guidance is necessary to contribute to the definition of a safety approach that allows the identification of sequences that might lead to degraded core conditions, and which need to be mitigated by the design (this topic is discussed with more detail in Ref. [4]).

For SFR and water cooled reactor technologies, models and codes for the assessment of severe accidents that require mitigation have been developed and continually improved through a collaborative effort of the whole community, including regulatory bodies. The development of large multiphysics mechanistic codes, many of which already exist for SFR technology (e.g. SIMMER and SAS4A/SASSYS-1), may start with simplified models studying the importance of the separate phenomena involved in the degradation of an LFR core. A good example of this simplified approach for LFRs is the paper discussed under subsection 6.2.3 that presents the reactivity impact of a hypothetical full relocation of clad from the active core region in an LFR. Such simplified analysis helps to identify the most relevant phenomena to be considered in more comprehensive modelling.

As it is the case for SFRs, the tools for assessing fission product release, transport and retention during severe accident sequences need to be developed and qualified with experiences in the

calculation domain under consideration. For that, a PIRT process may be a starting point as a function of the LFR design.

For LFR technology, the intensive cooperation on model and code development is still in its early stages. The significant financial cost and the expertise that is needed to develop and validate models and codes for the analysis of severe accidents cannot be provided by single developers. Instead, it is suggested that this endeavour be undertaken as a joint effort by the entire community. Increased cooperation within the community, whose development and coordination may be supported by the IAEA, would be beneficial to address the considerable challenges associated with the development of LFR technology.

REFERENCES

[1] INTERNATIONAL ATOMIC ENERGY AGENCY, Safety of Nuclear Power Plants: Design, IAEA Safety Standards Series No. SSR-2/1 (Rev. 1), IAEA, Vienna (2016).

[2] INTERNATIONAL ATOMIC ENERGY AGENCY, IAEA Nuclear Safety and Security Glossary, Non-serial Publications, IAEA, Vienna (2022), https://doi.org/10.61092/iaea.rrxi-t56z.

[3] INTERNATIONAL ATOMIC ENERGY AGENCY, Applicability of IAEA Safety Standards to Non-Water-Cooled Reactors and Small Modular Reactors, IAEA Safety Report Series No. 123, IAEA, Vienna (2023).

[4] INTERNATIONAL ATOMIC ENERGY AGENCY, Considerations on the Safety of Liquid Metal Cooled Fast Reactors, IAEA, Vienna (in preparation).

[5] INTERNATIONAL ATOMIC ENERGY AGENCY, Modelling and Simulation of the Source Term for a Sodium Cooled Fast Reactor Under Hypothetical Severe Accident Conditions, IAEA-TECDOC-2006, IAEA, Vienna (2022).

[6] TENTNER, A. M., et al., The SAS4A LMFR Whole Core Accident Analysis Code, Proc. International Meeting on Fast Reactor Safety, pp.989-998, Knoxville, TN (1985).

[7] TOBITA, Y., et al., The Development of SIMMER-III, An Advanced Computer Program for LMFR Safety Analysis and its Application to Sodium Experiments, Nuclear Technology, Vol. 153, No. 3, pp. 245-255 (2006).

[8] BECCANTINI, A., BLIARD, F., BOUDA, P., DE LAMBERT, S., DRUI, F., et al., EUROPLEXUS : un code de référence pour la dynamique rapide et l'interaction fluide-structure, CSMA 2022 – 15ème Colloque National en Calcul des Structures, Giens, France (2022).

[9] ANSYS, Inc., ANSYS AUTODYN user's manual: release 15.0, Pennsylvania, USA (2013).

[10] MURATA, K. K., et al., CONTAIN LMR/1B-Mod.1, A Computer Code for Containment Analysis of Accidents in Liquid-Metal-Cooled Nuclear Reactors, SAND91-1490・UC-610 (1993).

[11] YAMADA, F., et al., Development of Natural Circulation Analytical Model in Super-COPD Code and Evaluation of Core Cooling Capability in Monju During a Station Blackout, Nuclear Technology, Vol.188, No. 3, pp. 292-321 (2014).

[12] ZABIEGO, M., FOCHESATO, C., Corium-sodium interaction the development of the SCONE software, Proceedings of NURETH-17 Conference, Xi'an, Shaanxi, China (2017).

[13] CHALYY R.V., et al., SOCRAT-BN integral code for safety analyses of NPPs with sodium cooled fast reactors: development and plant applications, Proc. International Conference on Fast Reactors and Related Fuel Cycles: Next Generation Nuclear Systems for Sustainable Development (FR17), Yekaterinburg, 2017, Paper CN245_281, IAEA, Vienna (2018).

[14] VIOT, L., Couplage et synchronisation de modèles dans un code scénario d'accidents graves dans les réacteurs nucléaires, Ph.D. Thesis, Université Paris–Saclay (2018).

[15] CLAVIER, R., JOHNSON, M., BIGOT, B., Corium pool behaviour in the core catcher of a sodium-cooled fast reactor, Nucl. Eng. Des., 412, 112439 (2023).

[16] BACHRATA, A., TROTIGNON, L., SCIORA, P., SAEZ, M., A three-dimensional neutronics-thermal hydraulics Unprotected Loss of Flow simulation in Sodium-cooled Fast Reactor with mitigation devices, Nucl. Eng. Des. 346, 1-9 (2019).

[17] LAINET, M., MICHEL, B., DUMAS, J.-C., PELLETIER, M., RAMIERE, I., GERMINAL, a fuel performance code of the PLEIADES platform to simulate the in-pile behaviour of mixed oxide fuel pins for sodium-cooled fast reactors, J. Nucl. Mater. 516, 30-53 (2019).

[18] BUBELIS, E., TOSELLO, A., PFRANG, W., SCHIKORR, M., MIKITYUK, K., PANADERO, A.-L., MARTORELL, S., ORDONEZ, J., SEUBERT, A., LERCHL, G., STEMPNIEWICZ, M., ALCARO, F., DE GEUS, E., DELMAERE, T., POUMEROULY, S., WALLENIUS, J., System codes benchmarking on a low sodium void effect SFR heterogeneous core under ULOF conditions, Nucl. Eng. Des. 320, 325-345 (2017).

[19] GASTALDO, L., LE TELLIER, R., SUTEAU, C., FOURNIER, D., RUGGIERI, J.-M., High-order discrete ordinate transport in non-conforming 2d cartesian meshes, International Conference on Mathematics, Computational Methods & Reactor Physics (M&C 2009), Proc. Int. Conf. Saratoga Springs, New York (2009).

[20] LE TELLIER, R., FOURNIER, D., SUTEAU, C., Reactivity perturbation formulation for a discontinuous Galerkin-based transport solver and its use with adaptive mesh refinement, Nucl. Sci. Eng. 167, 209–220 (2011).

[21] RSICC Computer Code Collection, PARTISN 5.97, Multi-Dimensional, Time-Independent or Time-Dependent, Multigroup, Discrete Ordinates Transport Code System, RSICC Code Package CCC-760, ORNL (2009).

[22] LENAIN, R., MASIELLO, E., DAMIAN, F., SANCHEZ, R., Domain decomposition method for 2D and 3D transport calculations using hybrid MPI/OPENMP parallelism, ANS MC2015, Joint International Conference on Mathematics and Computation (M&C), Supercomputing in Nuclear Applications (SNA) and the Monte Carlo (MC) Method, Proc. Int. Conf. Nashville, TN (2015).

[23] TENCHINE, D., BAVIERE, R., BAZIN, P., DUCROS, F., GEFFRAYE, G., KADRI, D., PERDU, F., PIALLA, D., RAMEAU, B., TAUVERON, N., Status of CATHARE code for sodium cooled fast reactors, Nucl. Eng. Des. 245, 140-152 (2012).

[24] BACHRATA, A., et al., Severe accident studies on the efficiency of mitigation devices in a SFR core with SIMMER code, Nucl. Eng. Des., 373, 111037 (2021).

[25] BERTRAND, F., et al., Comparison of the behaviour of two core designs for ASTRID in case of severe accidents, Nucl. Eng. Des. ,297, 327–342 (2016).

[26] PAYOT, F., et al., The SAIGA in-pile experimental program to qualify the SIMMER calculation tool in SFR severe accident conditions, International Conference on Fast Reactors and Related Fuel Cycles: Next Generation Nuclear Systems for Sustainable Development FR22, Proc. Int. Conf. Vienna, Austria, 19–22 April, IAEA, Vienna (2022).

[27] PAYOT, F., CHAROLLAIS F., DUFOUR, E., LEJEAIL, Y., BLEVIN, G., TROTIGNON, L., DE IZARRA, G., MICHEL, F., DUPONT, V., CHIKHI, N., CLAVIER, R., The SAIGA in-pile experimental test to study the degradation of a SFR core with mitigation devices in Severe Accident Conditions, NURETH, Washington DC, USA (2023).

[28] JOURNEAU, C., AUFORE, L., BERGE, L., BRAYER, C., CASSIAUT-LOUIS, N., ESTRE, N., PAYOT, F., PILUSO, P., PRELE, J.-C., SINGH, S., ZABIEGO, M., PLUYETTE, E., SERRE, F., TEISSEIRE, B., Corium-Sodium and Corium-Water Fuel-Coolant-Interaction Experimental Programs for the PLINIUS2 Prototypic Corium Platform, Nucl. Technol. 205, 239-247 (2019).

[29] LECOANET, A., PAYOT, F., JOURNEAU, C., RIMBERT, N., GRADECK, M., Study of the ablation consecutive to jet impingement on a meltable solid – Application to SFR core-catcher, Nucl. Eng. Des. 377, 111147 (2021).

[30] LECOANET, A., PAYOT, F., JOURNEAU, C., RIMBERT, N., GRADECK, M., Classification of ablation mode during impact of hot liquid jet on a solid, Int. J. Heat Mass Transf., 181, 121883 (2021).

[31] TROMM.W., GAUS-LIU, X., KIT-JIMEC Experiments to Investigate Jet Impingement on the Ablation of Core Catcher Bottom, Proc. Nucl. Ener. New Europe, Bled, Slovenia (2021).

[32] DELACROIX, J., JOURNEAU, C., PILUSO, P., High-Temperature Characterization of Melted Nuclear Core Materials: Investigating Corium Properties through the Case Studies of In-Vessel and Ex-Vessel Retention, Front. Energy Res. 10, 883972 (2022).

[33] JOURNEAU, C., BOUYER, V., CHAROLLAIS, F., CHIKHI, N., DELACROIX, J., DENOIX, A., LAFFOLLEY, H., MATTASSOGLIO, C., MOLINA, D., PILUSO, P., SAUVECANE, P., THILLIEZ, S., TURQUAIS, B., SUTEAU, C., Upgrading the PLINIUS platform toward smarter prototypic-corium experimental R&D, Nucl. Eng. Des. 386, 111511 (2022).

[34] ANSYS, Inc. ANSYS Fluent User's Guide, Release 17.2 (2016).

[35] FEDERAL ENVIRONMENTAL, INDUSTRIAL AND NUCLEAR SUPERVISION SERVICE (ROSTECHNADZOR), Federal rules and regulations in the area of atomic energy use: General Safety Provisions for Nuclear Power Plants, NP-001-15, Moscow (2015).

[36] AMANDEEP, S.¸ OBAIDURRAHMAN, K., GUPTA, H. P., Development of a Power and Flow Transient Model for Sodium Cooled Fast Reactor Core, Proceedings of Advances in Reactor Physics 2022, Mumbai, 18 – 21 May (2022).

[37] ISHII, M., CHEN, W. L., GROLMES M. A., Molten Clad Motion for Fast Reactor Loss-of-Flow Accidents, Nucl. Sci. Eng. 60, 435–451 (1976).

[38] ISHII, M., CHEN, W. L., GROLMES M. A., Multichannel model for relocation of molten fuel cladding in unprotected loss-of-flow accidents in liquid-metal fast breeder reactors, Nucl. Sci. Eng. 69, 297-318 (1979).

[39] CARTER, G. C., FISCHER, G. J., HEAMES, T. J., MacFARLANE, D.R., McNEAL, N.A., SHA, W. T., SANTHANAN, C. K., YOUNGDAHL, SAS1A, A computer code

for the analysis of Fast Reactor power and flow transients, Argonne National Laboratory (1970).

[40] SATO, I., TOBITA, Y., KONISHI, K., KAMIYAMA, K., TOYOOKA, J., NAKAI, R., KUBO, S., KOTAKE, S., KOYAMA, K., VASSILIEV, Y., VURIM, A., ZUEV, V., and KOLODESHNIKOV, A., Safety Strategy of JSFR Eliminating Severe Recriticality Events and Establishing In-Vessel Retention in the Core Disruptive Accident, Journal of Nuclear Science and Technology, Vol. 48, No. 4, p. 556–566 (2011).

[41] TAGAMI, H., Model for particle behavior in debris bed, Nucl. Eng. Des. 328, 95-106 (2018).

[42] SHEIKH, M.A.R., Numerical simulation of the solid particle sedimentation and bed formation behaviours using a hybrid method, Energies, 13(19) (2020).

[43] CHENG, S., An investigation on debris bed self-leveling behavior with non-spherical particles, J. Nucl. Sci. Technol. 51(9), 1096-1106 (2014).

[44] KAMIYAMA, K., KONISHI, K., SATO, I., TOYOOKA, J., MATSUBA, K., SUZUKI, T., TOBITA, Y., PAKHNITS, A. V., VITYUK, V. A., VURIM, D. A., GAIDAICHUK, V. A., KOLODESHNIKOV, A. A., VASSILIEV, Y. S., An Experimental Study on Heat Transfer from a Mixture of Solid-Fuel and Liquid-Steel during Core Disruptive Accidents in Sodium-Cooled Fast Reactors, Proceedings of the 10th international topical meeting on nuclear thermal hydraulics, operation and safety (NUTHOS-10), Okinawa, NUTHOS10-1050, 8p. (2017).

[45] TREOL, C., CLAVIER, R., SEILER, N., GOYEAU, B., Three-Phase Flow Simulation of Debris Bed Self-Leveling in case of SFR Severe Accident, NURETH-20, Washington D.C., United States (2023).

[46] GUO, L., Numerical simulations on self-leveling behaviors with cylindrical debris bed, Nucl. Eng. Des., 315, 61-68 (2017).

[47] BRUN, E., DAMIAN, F., DIOP, C.M., DUMONTEIL, E., HUGOT, F.X., JOUANNE, C., LEE, Y.K., MALVAGI, F., MAZZOLO, A., PETIT, O., TRAMA, J.C., VISONNEAU, T., ZOIA, A., TRIPOLI-4®, CEA, EDF and AREVA reference Monte Carlo code, Annals of Nuclear Energy, Volume 82, https://doi.org/10.1016/j.anucene.2014.07.053 (2015).

[48] BONNET, J.M., Thermal hydraulic phenomena in corium pools: the BALI experiment (JAERI-Conf--99-005), Sugimoto, Jun (Ed.), Japan (1999).

[49] BIGOT, B., GAUS-LIU, X., CLAVIER, R., JOURNEAU, C., PAYOT, F., CRON, T., ANGELI, P.E., PEYBERNES, M., FLUHRER, B., Experimental and Numerical Simulations on the SFR Core-Catcher Safety Analysis After Relocation of Corium, Proceedings of the 10th European Review Meeting on Severe Accident Research (ERMSAR) (2022).

[50] TrioCFD homepage https://triocfd.cea.fr/

[51] Dune numerics homepage https://www.dune-project.org/

[52] GENERATION IV INTERNATIONAL FORUM, Safety Design Criteria for Generation IV Lead-cooled Fast Reactor System (2021).

[53] AVVAKUMOV, A., et al., Coupled calculations for the fast reactors safety justification with the EUCLID/V1 integrated computer code, International Conference on Fast Reactors and Related Fuel Cycles: Next Generation Nuclear Systems for Sustainable Development FR17, Proc. Int. Conf. Yekaterinburg, Russian Federation, 26–29 June 2017, IAEA, Vienna (2018).

[54] ALIPCHENKOV, V., et al., Models of the integral EUCLID/V2 code for numerical modeling of different regimes of lead-cooled fast reactor, International Conference on Fast Reactors and Related Fuel Cycles: Next Generation Nuclear Systems for Sustainable Development FR22, Proc. Int. Conf. Vienna, Austria, 19–22 April, IAEA, Vienna (2022).

[55] ALIPCHENKOV, V., et al., Models of the integral EUCLID/V2 code for numerical simulation of severe accidents in a sodium-cooled fast reactor with MOX and MNUP fuels, International Conference on Fast Reactors and Related Fuel Cycles: Next Generation Nuclear Systems for Sustainable Development FR22, Proc. Int. Conf. Vienna, Austria, 19–22 April, IAEA Vienna (2022).

[56] LEPPÄNEN, J., et al., The Serpent Monte Carlo code: Status, development and applications in 2013, Annals of Nuclear Energy 82, 142–150 (2015).

[57] PESETTI, A., TARANTINO, M., GAGGINI, P., POLAZZI, G., FORGIONE, N., Commissioning of CIRCE Facility for SGTR Experimental Investigation for HLMRS and Pre-Test Analysis by SIMMER-IV Code, International Conference on Nuclear Engineering, paper ICONE25-67419, Shanghai, China (2017).

[58] PESETTI, A., DEL NEVO, A., FORGIONE, N., Experimental investigation and SIMMER-III code modelling of LBE–water interaction in LIFUS5/Mod2 facility, Nucl. Eng. Des. 290, 119–126 (2015).

[59] LORUSSO P., DI PIAZZA I., MARTELLI D., MUSOLESI A., TARANTINO M., NACIE-UP: An Heavy Liquid Metal Loop for Mixed Convection Experiments with Instrumented Pin Bundle, in HLMC-2013, IPPE, Obninsk, Russian Federation (2013).

[60] GRABASKAS, D., et al., Regulatory Technology Development Plan – Sodium Fast Reactor: Mechanistic Source Term – Trial Calculation, Argonne National Laboratory, ANL-ART-49 (2016).

ABBREVIATIONS

ANL	Argonne National Laboratory, United States of America
ASME	American Society of Mechanical Engineers
ASTRID	Advanced sodium technology reactor for industrial demonstration
AOO	Anticipated operational occurrences
ATWS	Anticipated transient without scram
BDBA	Beyond design basis accidents
CDA	Core disruptive accident
CEA	French Alternative Energies and Atomic Energy Commission, France
CFD	Computational fluid dynamics
CFV	Core with a low void effect
CRGT	Control rod guide tube
CRP	Coordinated Research Project
DBA	Design basis accident
ENEA	Italian National Agency for New Technologies, Energy and Sustainable Economic Development, Italy
ESFR	European sodium fast reactor
ESFR-SMART	European sodium fast reactor safety measures assessment and research tools
FCI	Fuel–coolant interaction
FFTF	Fast flux test facility
IAHT	Inter-assembly heat transfer
JAEA	Japan Atomic Energy Agency
KIT	Kalrsuhe Institute of Technology, Germany
LBE	Lead-bismuth eutectic
LFR	Lead cooled fast reactor
LMFR	Liquid metal cooled fast reactor
LOF	Loss of flow
MOX	Mixed oxide fuel
MYRRHA	Multipurpose hybrid research reactor for high-tech applications
PFBR	Prototype fast breeder reactor
PIRT	Phenomena identification and ranking table
RANS	Reynolds Averaged Navier-Stokes
RATEN	Technologies for Nuclear Energy State owned company, Romania

SFR	Sodium cooled fast reactor
SGTR	Steam generator tube rupture
SMR	Small and medium sized or modular reactors
SRT	Simplified radionuclide transport
TIB	Total instantaneous blockage
ULOF	Unprotected loss of flow
USAF	Unprotected sub-assembly failure
UTOP	Unprotected transient over power
V&V	Verification and validation
VVER	Water cooled water-moderated energy reactor

PAPERS PRESENTED AT THE MEETING

SESSION I

SEVERE ACCIDENT ANALYSIS AND EXPERIMENTAL VALIDATION OF SODIUM COOLED FAST REACTORS

Chairpersons

F. PAYOT
France

D. ZHANG
China

Y. TOBITA
Japan

TOWARDS AN INTEGRATED FRENCH SOFTWARE PLATFORM FOR SEVERE ACCIDENT SIMULATION IN SFRs

P. GUBERNATIS, R. CLAVIER
CEA, DES, IRESNE, DTN
Saint-Paul-lez-Durance, France

Abstract

During the last decades, development efforts for the simulation of severe accidents in sodium fast reactors (SFRs) have resulted in two classes of calculation tools. On the one side, mechanistic tools implementing the most detailed and precise physical models perform “best estimate” but very time consuming calculations, while on the other side physico-statistical tools relying on parametric models perform fast running evaluations approaching the “best estimate” results. Owing to its positive results, this methodology motivates a more global approach leading to the development of an integrated platform for severe accident simulation in SFRs. The paper first justifies the interest of such a platform around the PROCOR tool, which comes from the need of consistent simulations of SFR degradation scenarios. Even the most adapted existing tools are unable to treat some specific phases of the scenario, and there is a great variability of events and associated phenomenology, which may occur or not during the simulation, in an unpredictable manner. This characteristic is very specific to severe accidents and implies that the platform needs to support dynamic modifications (during the scenario) of the physical and numerical models and couplings. Then, the paper details the objectives and constraints that need to be met for this platform, which go far beyond those conventionally considered in the context of normal operation or a 'weakly' accidental state of the system. The severe accident platform needs to simulate an installation in its nominal state, possibly with a moderate level of accuracy but nevertheless with global consistency, and also the accidental sequence, up to the most advanced phases of the degradation. Due to the magnitude of this task, the efforts have to be spread out over a long period, which notably implies adaptability to evolutions of computing capabilities, code architectures and human resources. Finally, the paper presents current and recent developments performed at CEA to initiate the future platform management module as a part of the PROCOR platform.

1. INTRODUCTION

The French safety requirements for the fourth generation sodium fast reactors (SFR) comply with the WENRA "Safety Objectives for New Nuclear Power Plants" [1] that recalled, among the important safety objectives, to increase the robustness of the demonstration by means of a combined deterministic and probabilistic approach that integrates the prevention and mitigation systems [2]. Combining both deterministic and probabilistic approaches requires enhanced consistency between the calculation tools involved. Furthermore, accounting for the innovative mitigation devices in accident scenario simulations requires considerable improvements of the performance and precision of the severe accident simulation tools, in particular multiphysics and multiscale descriptions (in both time and space), and inter-operability of the calculation tools.

For several years, and particularly since the beginning of the ASTRID project, the CEA has invested many efforts in this objective. This paper starts by giving a non-exhaustive presentation of the calculation tools devoted to the severe accident studies on SFRs, and then focuses on the analysis of needs in order to design an efficient coupling platform in the near future. In a second step, the identified needs are declined into preliminary requirements for the future platform. Finally, examples of recent technical realizations are given to illustrate the progress of CEA in this subject.

The emphasis is put on how to assemble the computational components and how to organize their interoperability by using the computer tools being developed in parallel. Conversely, the physical specifications of the components are not described.

2. OVERVIEW OF THE EXISTING CEA SIMULATION TOOLS FOR SEVERE ACCIDENTS IN SFR

The simulation tools for severe accidents in an SFR contribute to three important objectives:

- The assessment of the range of consequences of an accident initiator;
- The improvement of the design of the mitigation devices;
- The evaluation of the safety margins as input to the safety demonstration.

There are many types of code that can contribute to these goals and many ways to categorize them. This paper concentrates on two classes of codes, both dedicated to the assessment of the behaviour of the system of interest during a severe accident sequence: the mechanistic tools contribute to the best estimation of a limited set of scenarios, with the most precise and detailed description of the system and its physics; and the physico-statistical tools produce a wide range of low-cost and highly parameterizable simulations, both classes relying on their own V&V policy, which are possibly common. Both classes are necessary and complementary as the French safety policy relies both on a deterministic and a probabilistic demonstration. A brief overview of the existing tools at CEA for these two classes is presented below.

2.1 Mechanistic tools

The SIMMER family tools started in the late 1980s with the development of SIMMER-III at JAEA [3]. SIMMER-III is a two-dimensional multivelocity field, multiphase, multicomponent, Eulerian fluid dynamics code, coupled with a dedicated structure model to represent the fuel pins and the vertical plates of a typical SFR. It describes most of the heat and mass transfers that occur during the disruption of the core (vaporization/condensation and melting/freezing of the structures). Moreover, the code is equipped with an internal S_N neutron kinetics model. Since then, a 3D (SIMMER-IV) version has been developed by JAEA in 2010, and more recently, the ASTRID programme in France has led to a France–Japan collaboration in order to develop a thoroughly improved version SIMMER-V (dynamic allocation, hybrid parallelism, object-oriented programming, boundary coupling, etc.). As an example, Fig. 1 and Fig. 2 show typical results: a vertical cut of the nominal temperature in ASTRID; and a disrupted state during a ULOF sequence.

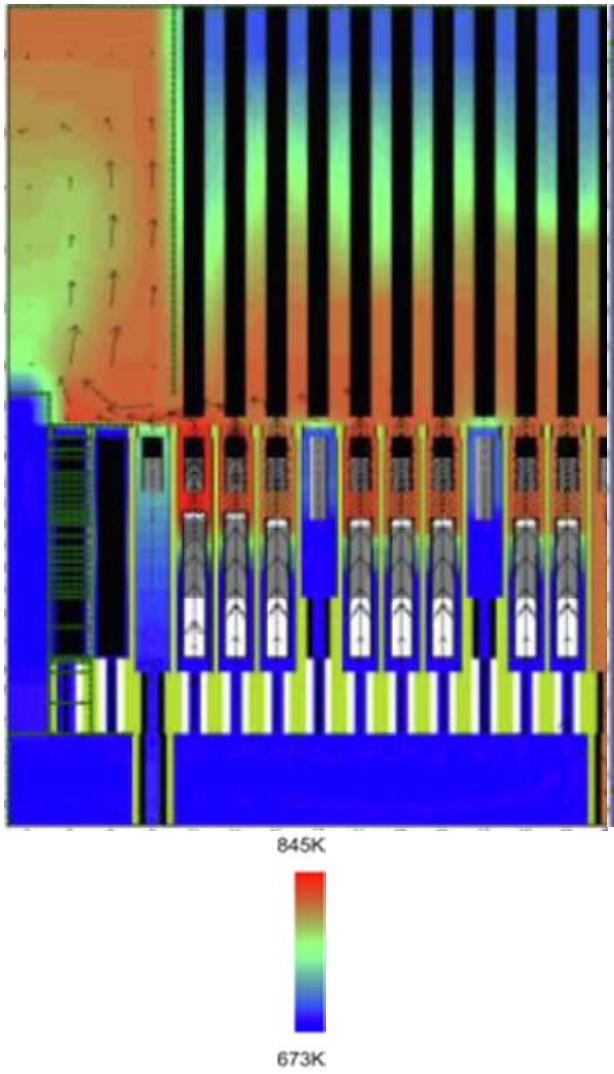

FIG. 1. Vertical cut of the sodium temperature.

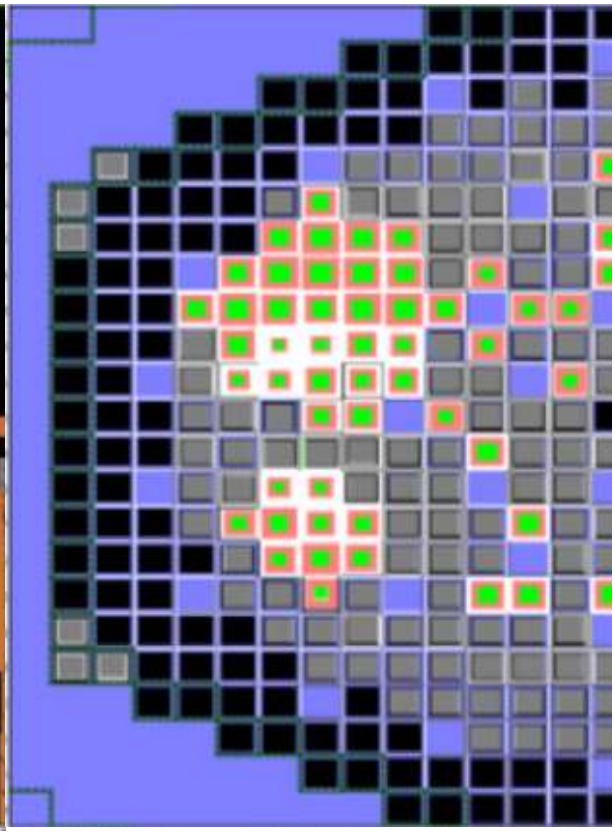

FIG. 2. Radial cut of a typical disrupted state.

Still within the same project framework, CEA has started the development of a SEvere Accident SimulatiON platform (SEASON). This platform aims at managing the process of definition of a core, setting its initial irradiated state and offering various modes of computation. The platform allows to compute the nominal state of a core and its disruption, either in a global 3D approach or with a multichannel concept which is an extension of the one used by SAS4A [4]. It offers a graphical user interface for modelling the initial core and setting up the SIMMER-V computation, and it ensures a tight coupling with an external neutronics parallel computation. In addition, it makes it possible to compute the early phase of the degradation (sodium boiling, up to the first clad melting) with the channel-wise modelling, and next, to switch to a complete 3D description of the core-wide disruption.

SEASON confers various possibilities of interoperability to SIMMER-V which are summarized in Table 1.

TABLE 1. SEASON POSSIBILITIES OF INTEROPERABILITY TO SIMMER-V

INTEROPERABILITY	CODE	TECHNICS
Upstream chaining of SIMMER-V with a fuel performance code	GERMINAL V2 [5]	SQL queries to a DB containing a set of various irradiated states for the core pins
In time coupling of SIMMER-V with an external 3D neutronics spatial code	PARIS (ERANOS)	• Initial macroscopic cross-sections, feedback coefficients for the counter-reactions • MPI exchange is used to set PCQM or IQM kinetics schemes
Tight thermohydraulic boundary coupling of SIMMER-V with itself	SIMMER-V	Exact SIMMER-V-SIMMER-V coupling based on an extension of the domain decomposition
Loose thermohydraulic boundary coupling (coupling with the complete circuit)	CATHARE [6]	Use of C3PO, ICoCo [7], MedCoupling (currently under development)

Currently, SEASON is limited to these interactions but, as will be seen later, it is important to enlarge its interoperability in order to account for many other phases of the scenarios: the transfer of the corium to the core catcher; the long term cooling of the debris; the sodium-corium interactions with their mechanical consequences; the evaluation of the fission products transported in the circuit; etc.. Consequently, the list of the mechanistic tools that are likely to be used by the SEASON platform is far from being complete. As an example, the CEA codes TRUST for the multiphase CFD modelling, and EUROPLEXUS [8] for the high rate dynamic mechanics, should be integrated in the global simulation process.

2.2 Physico-statistical tools

Physico-statistical tools are generally devoted to a specific part of the scenario sequence or a particular initiator event, and they simulate the main associated physical phenomena to perform fast running simulations of the treated sub-problem. These evaluations provide many types of interesting information for the design process and longer term R&D: rapid feedback on the proposed design choices, exploratory assessment of new accidental scenarios, and sensitivity analyses when they are coupled to uncertainty propagation tools. In the framework of the ASTRID project, a set of seven design-oriented simulation tools have been developed to describe the phenomenology associated with core degradation following three main initiator events (USAF, ULOF, UTOP), and later phases of the degradation (corium relocation in the lower plenum, FCI, debris bed cooling and fuel explosion). Figure 3 gives an overview of these tools and their perimeter. Ad hoc chaining of these tools has been proposed to describe specific sequences from the nominal state to the post-accidental cooling, e.g. the ULOF sequence.

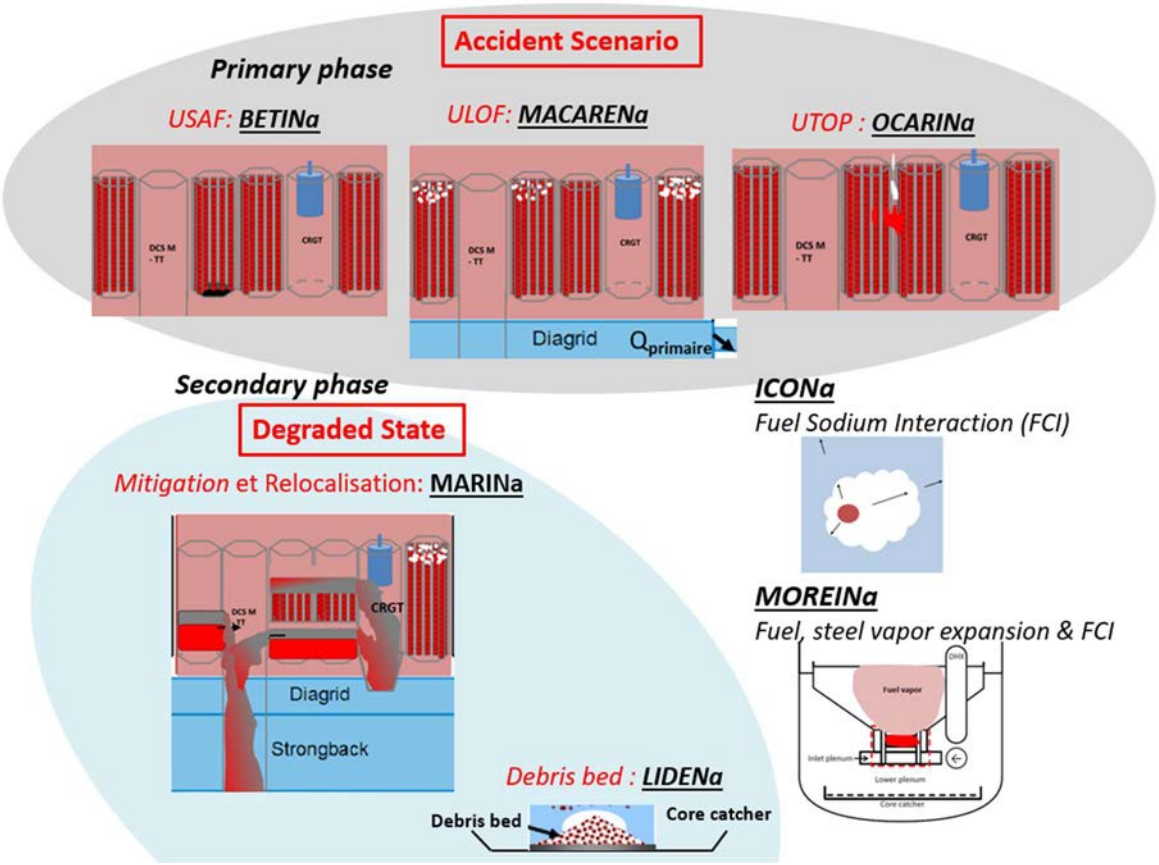

FIG. 3. Illustration of designed-oriented tools devoted to SFR.

In parallel, the PROCOR platform has been developed to perform fast running simulations of the behaviour of the corium, originally in a PWR pressure vessel [9]. The implementation of an increasing number of diverse coupled physical models has led to new questions about the best way to describe a physical model from the computer code point of view, to exchange information between those models and to manage their coupling, which has resulted in the construction of a new coupling architecture for physical models with a high level of genericity [10]. Consequently, the PROCOR platform has been re-structured particularly in order to separate the model coupling functionalities from the physical model themselves. At the same time, the integration of the physical models implemented into the previously described fast running calculation tools have started, and the models have been categorized as 'specialized' (PWR or SFR) or 'generic' (common to both types of reactor).

2.3 Need for an integrated platform

The separate approach described in Sections 2.1 and 2.2 has produced many positive results concerning the safety evaluation of the new SFR designs, and it needs to be completed. Some advanced phases of the accidental sequence are not covered by the existing tools, for example the mechanistic description of the fuel–coolant interaction in the lower plenum, whose developments on the SCONE simulation tool are under progress, or the physico-statistical models to describe a corium pool on the core catcher, which is the subject of preliminary evaluations [11]. Beyond these gaps that need to be filled, the separate approach presents some inherent weaknesses that need to be addressed:

- The diversity of the tools implies a difficult avoidable redundancy, implying risks of inconsistency in the descriptive data, the material properties and even the physical models.
- Regardless of the software methodology for assembling the computations, the validation of the tools will remain a delicate point, in particular when every tool undergoes a separate validation process.
- The results obtained by a serial chaining of codes, for a given scenario study, strongly depend on how the final state of a computation is transferred to the initial state of the next. Furthermore, the chaining needs to be adapted to each type of scenario sequence, while a scenario tool is expected to determine by itself the path to follow in the event tree based on particular events.
- Severe accidents involve strong phenomenological couplings that might require more than an instantaneous chaining while making a serial computation. For example, the expansion phase of the fuel explosion may be influenced by what happens in the core area, implying a strong coupling between the core module and the bubble expansion code, which may require regular exchange of information or even an implicit coupling scheme. On a more general level (scenario), the transfer of corium through the transfer tubes may occur in several phases, implying more than a single chaining between the core degradation code and the corium transfer code.
- Full scale mechanistic simulations, when they are technically possible, imply very important calculation costs because the whole reactor has to be described with an equivalent level of detail, while some less important parts could be described more roughly without undermining the quality of the simulation.

These considerations militate for the construction of a common platform able to manage both axes of calculation (mechanistic/physico-statistical), reduce their weaknesses while making the best possible use of the knowledge acquired so far.

3. REQUIREMENTS FOR THE FUTURE SOFTWARE INTEGRATION PLATFORM

It is important to specify the technical requirements for the future severe accident platform at the earliest stage. Considering the identified gaps in the separate approach, reported in Section 2.3, and the specifics of the existing and anticipated calculation tools, a list of requirements has been proposed and is still under discussion at CEA. Two main types of requirement have been identified: “technical requirements” refer to the functionalities, from the point of view of informatics code development and platform architecture, while “quality requirements” refer to the implications of the technical functionalities in terms of project management and organization.

The present paper does not concentrate on the physical requirements of the various components. In short, the physical specifications that have guided developments to date will be retained and completed in the future. The construction process will therefore have to be flexible enough so that these specifications can be progressively enriched, without questioning the architectural choices.

3.1 Technical requirements

Consistency between mechanistic and physico-statistical approaches**:** We need to strengthen the consistency between the simplified approach and the detailed approach. Despite their differences in precision or scale, their respective physical modelling should be consistent with each other, and should have input and output data that remain as coherent as possible. Some

organisational aspect of the platform development may promote this consistency on the long term (see 3.2), as well as the centralization of the data.

Centralization of the data: Redundancies between the different computing tools need to be reduced. It seems important to centralize the technological data in a unique data model, as well as the physical properties of materials. Having a unique data model for describing the technological objects (geometries and material) is a simple idea but which proves to be very challenging when dealing with a large panel of varied existing codes. This centralization cannot be satisfied easily, but it is important that the development process reduce the redundancies as developments unfold.

Dynamic coupling graph and scenario events: The necessary couplings are of several kinds: they can be a coupling at the boundaries of two codes (including immersed boundaries and domain embedding), or the coupling of two phenomenologies that affect at the same time a given object (e.g. the neutronics and the thermohydraulics of the core), or the temporal chaining of two different models for the same object (e.g. the preliminary irradiation of the core and its degradation during the primary phase).

Beyond these classic couplings, the specific nature of the scenario studies leads us to have to manage the occurrence of particular events, likely to generate significant changes in the calculation configuration. The platform has to therefore facilitate this event management. This includes the possibility to dynamically reconfigure the calculation scheme, the internal model structure of the codes during the calculation, or the coupling algorithm itself.

Hybrid mechanistic/simplified coupling scheme: Rather than having two separate calculation chains, simplified and best estimate, the platform should allow us a better use by hybridizing the two approaches. The counterpart of this requirement is the necessity of a good consistency between the simplified models and the detailed models, as mentioned above, and a particular effort to standardize the interface. There are several important advantages that would inherit from this flexibility.

The first advantage is to make it possible to adjust the level of precision in the description of a component, spatially or temporally. In the limit of the consistency of the simplified and the detailed approach, it becomes possible to build a computing scheme where the first stages of the accident (initiating phase) are treated with a large precision, and the rest of the scenario (generalized core degradation and corium transfer) will be treated with a lower precision (this is important in terms of uncertainty reductions). Alternatively, for a same phase of the scenario, the user will be able to make a spatial (boundary) coupling between a very detailed component and a simplified one, which can help to match performance objectives.

A second advantage is the possibility to build a validation process which is common to every scale, as long as the experiments cover the phase and the phenomenology that need to be validated.

A third advantage lies in the fact that this allows a complete replacement of a given tool by a new upgraded one, provided that this new tool wrapping adopts the interface of the previous one.

Enhanced user interactivity**:** In terms of exploitation, it would be interesting to offer the possibility of a simulator-type operating mode. This interactive mode allows the user to intervene in the sequence of the scenario by generating an event of the type interruption/restart, by change of an option or an element of configuration of the application, or by extraction of

simple or complex data, etc. This type of operation would clearly not aim at the real-time management of the scenario. It is equally clear that it cannot be compatible with a safety analysis type study. But on the other hand it is a very effective and educational exploratory approach to consolidate a collective expertise on the behaviour of scenarios.

To conclude this technical requirement part, the platform we aim for has to therefore support all the flexibilities we have listed above and make it as simple as possible for the user who has to build a complex application and operate it. Without entering into the technical details of the architecture, it seems clear that the platform should provide the user with a framework that allows the assembly of the codes that constitute the application, but also to control their initial configurations, manage the general transient, orchestrate the exchanges of data and the various processes of coupling. Obviously, the technical elements that permit to match these needs already exist and will be summarized in Section 4.1.

3.2 Quality requirements

State-of-the-art code quality management: this includes in particular the use of a version control system and a complete test policy including unitary functionality tests and verification tests using reference analytical results, and automatic testing machine.

Validation and qualification: code benchmarking and comparison with experimental data require an adequate reference database which may be used by all the components of the platform. This requirement echoes the need for consistency between all the tools incorporated into the platform that has been underlined in Section 3.1. Furthermore, this justifies a more global approach to promote all experimental results (past and future) into a new consistent information system.

Uncertainty evaluation: this point is essential to complete the validation process and then to perform safety studies. It is also useful to identify missing or sensitive phenomena and models that need to be enhanced or upgraded (see technical requirements “Hybrid mechanistic/simplified coupling scheme” above). Specific external tools will have to be incorporated into the platform to perform these studies.

Documentation and formation: these points are essential to ensure knowledge transmission over long time periods, typically a few decades, which will be necessary given the amount of work required to develop the described platform. However obvious those aspects might seem in a development process, we want to underline them because they often appear to be discarded, despite their fundamental nature, when the budget constraints require choices in the development effort.

Versatility and long term maintenance: long development period will necessarily lead to evolutions of development environments (IDE, OS) and even code languages. Furthermore the incorporated tools will evolve and even be replaced by new ones (see technical requirements “Hybrid mechanistic/simplified coupling scheme” above). The platform has to be robust to this kind of profound evolutions.

4. CURRENT STATE OF PROGRESS

4.1 Available technical elements

Since the early 2000s, CEA and EDF have commonly developed the platform SALOME [12] which is a very complete environment platform that brings numerus services for CAD

modelling, meshing and partitioning, coupling and supervision of the codes, visualisation, and uncertainties. Based on this experience, the tools dedicated to interoperability (supervision and coupling) have recently been the subject of special efforts to make these coupling techniques accessible to platforms other than SALOME. In particular, C3PO (ICoCo, MedCoupling) has been developed. Other similar initiatives have emerged in various CEA research units such as the PROCOR platform. These tools, C3PO (with ICoCo and MedCoupling) and PROCOR, are briefly presented hereafter.

C3PO: The paradigm of C3PO (Collaborative Code Coupling PlatfOrm, open source) relies on the principle of encapsulation of the computational codes into an API which implements the ICoCo (*Interface for Coupling of Code*) standard interface. In this paradigm, a computation code is an object-oriented code with a C++ or Python API that allows a user to pilot a calculation process through its ICoCo interface. This standard interface bears all the common services that a user may need to control the computational process. Moreover, it also provides a set of methods devoted to the exchange of standard data (MedCoupling objects).

For such codes, C3PO offers a Python set of classes that allow to construct several standardizations facilitating the coupling of codes for complex applications. We give hereafter the four main ones. The first one is the *PhysicsDriver* which coincides with the ICoCo interface of the code. The second one is the *DataManager* that is devoted to the manipulation of the exchanged data (MedCoupling fields). The third one is the *Exchanger* that handles all the specific treatments to a given coupling (for example, it may contain specific methods that make a field conform to another given code). The fourth one is the *Coupler* that is the standardization of the coupling strategy and that provides an extendable set of coupling algorithms (fixed-point, Anderson, Jacobian-Free-Newton-Krylov, etc.). In addition, these tools (C3PO, ICoCo, MedCoupling) handle the MPI parallelism of the codes.

PROCOR [9] is a similar ongoing development at CEA since 2013. This is a platform initially dedicated to the simulation of the relocated corium onto the core catcher (or the vessel) but which has proven to be extendable. PROCOR offers two levels of services: a first one devoted to the rapid prototyping of simplified models, and a second one which is the integration of these models in a complex (multiphysics) coupled application [10]. It is a java-based tool, except some classes devoted to the coupling with specific external C++ codes. It integrates the ICoCo interface definition and can be used to produce an ICoCo compliant component. In terms of coupling algorithms, PROCOR is very versatile and it is particularly adapted to the event driven scenario studies.

Both platforms, PROCOR and C3PO are in progress. Even though they are not equivalent and originate from different needs, they can feed each other with their most interesting functionalities to eventually converge.

In parallel to these integration tools, CEA has also developed the statistical toolbox URANIE (ROOT based open software) that is designed for data analysis, statistical modelling, sensitivity analysis and uncertainty analysis. It is briefly mentioned here because of its great transversality. Several examples of application of URANIE to various simulation codes have been done at CEA and a future SFR severe accident platform would take a large advantage of it.

4.2 Implementation examples

The CEA-JAEA co-development currently underway on the SIMMER-V code is typical of the work of adapting a relatively old code to the modern platform context described above. The

initial code underwent an important first phase of modernization: FORTRAN update, dynamic memory management, introduction of hybrid parallelism, use of powerful libraries, etc. More recently, a second phase of adaptation consisted in producing an object formulation of the code (API C++ and Python) capable of receiving ICoCo/MedCoupling coupling technologies. The component resulting from this re-engineering is fully compatible with the supervision methodology (with C3PO/ICoCo) described above. It can be activated in a complex application and exchange MedCoupling fields with other codes.

Boundary coupling: As a typical example of realization, SIMMER-V has been equipped with a boundary coupling technique based on an extension of the domain decomposition formulation [13], which offers an exact method to couple several SIMMER-V computations for representing a loop geometry (Fig. 4). This functionality is being expanded to allow for domain embedding (with immersed boundaries). This will facilitate modelling the pool geometry of the primary circuit by the mixing of differently meshed SIMMER-V components (Fig. 5).

In addition, the C3PO hybrid coupling of CATHARE [14] and SIMMER-V is in progress (not shown here) and will be soon benchmarked with the previous SIMMER-V coupling.

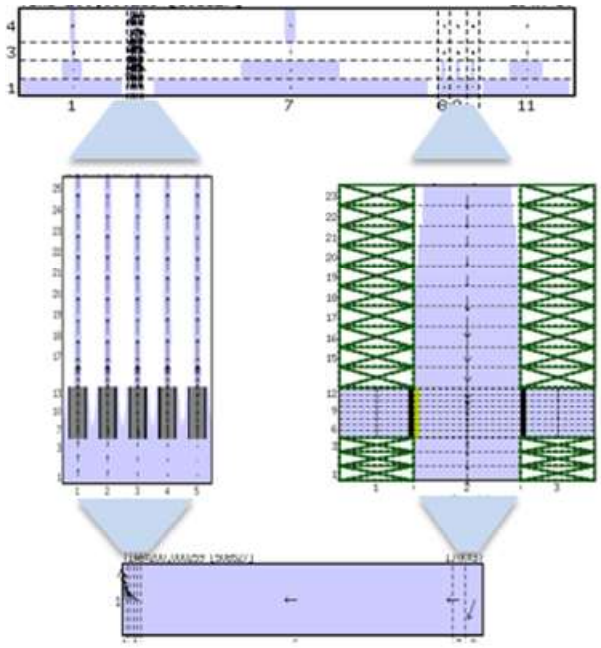

FIG. 4. Application of the boundary coupling in SIMMER-V to a loop computation.

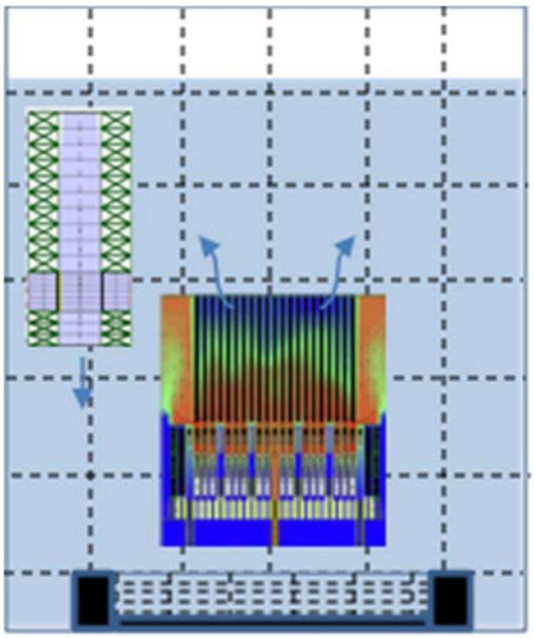

FIG. 5. Idealization of a pool geometry modelled with nonconforming domain embedding.

Multiphysical coupling: Figure 6 shows a view of the early degradation of a SFR core obtained within SEASON with the coupling of SIMMER-V and the external neutronics computation PARIS.

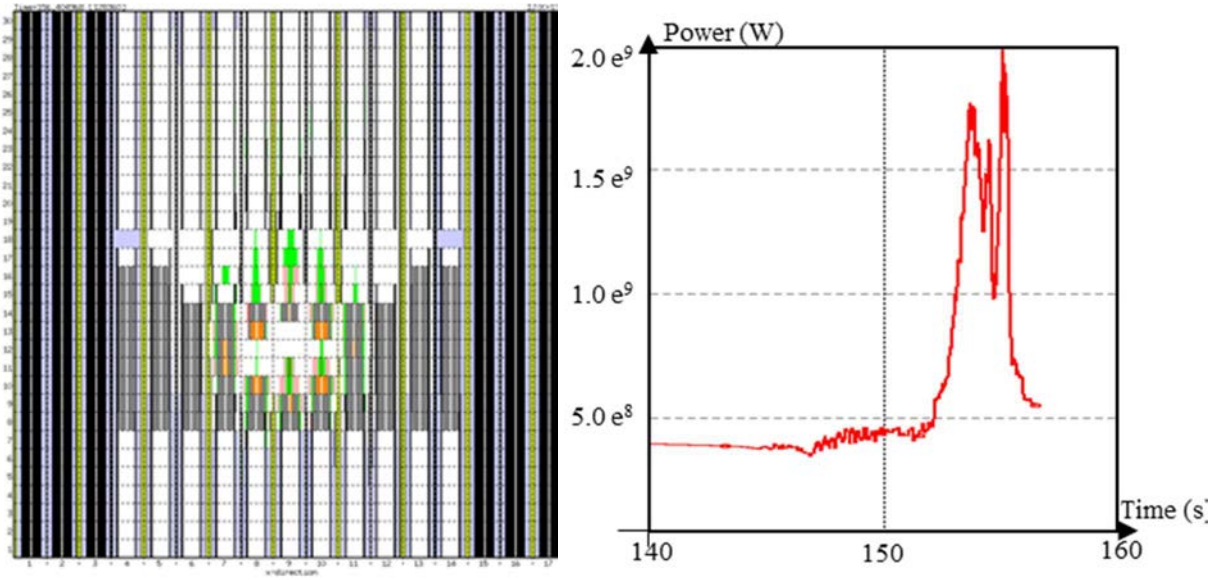

FIG. 6. View of the early degradation of a SFR core (left) and the corresponding nuclear power (right).

Figure 7 shows an example of a PROCOR computation. Even though a PWR application is shown, it also indicates how the compound application describes the pool stratification of the corium in the lower plenum of the vessel, the crust formation, the heat transfer to the vessel and its breaking.

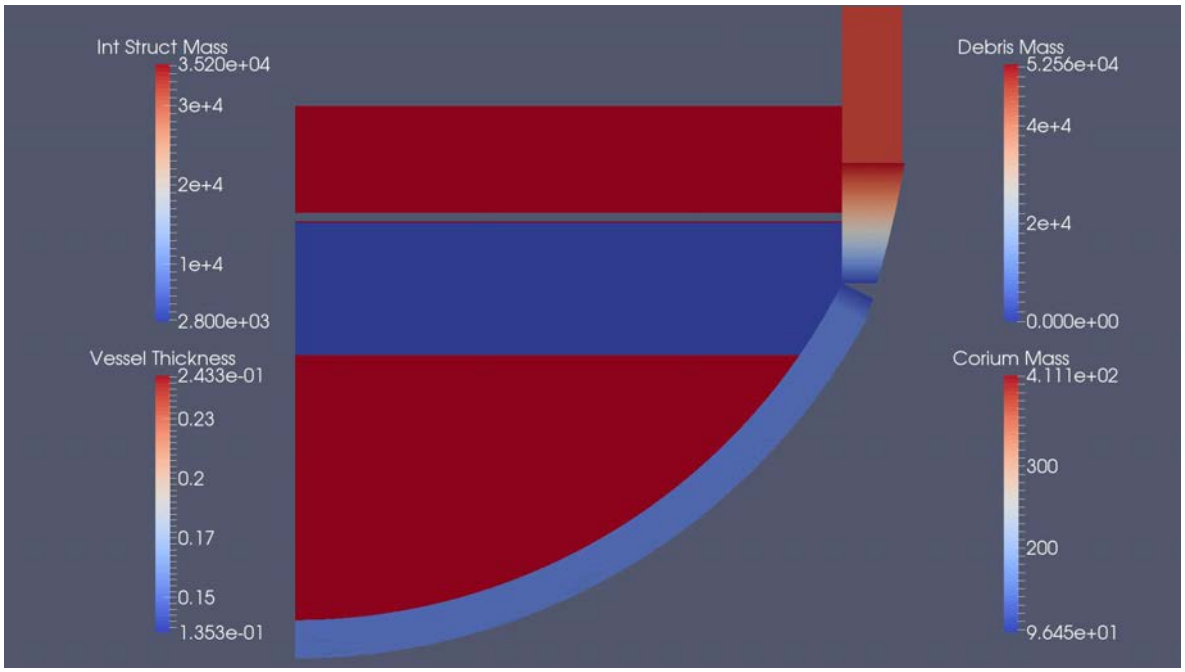

FIG. 7. Visualization of a multilayer corium pool in the reactor vessel as simulated by PROCOR-FDC application.

The example in Fig. 8 extracted from Ref. [8] is the result of a coupled computation of EPX (EUROPLEXUS) and APOLLO3 where a reactivity event (APOLLO3) produces a shock wave and the plastic deformation of the surrounding vessel.

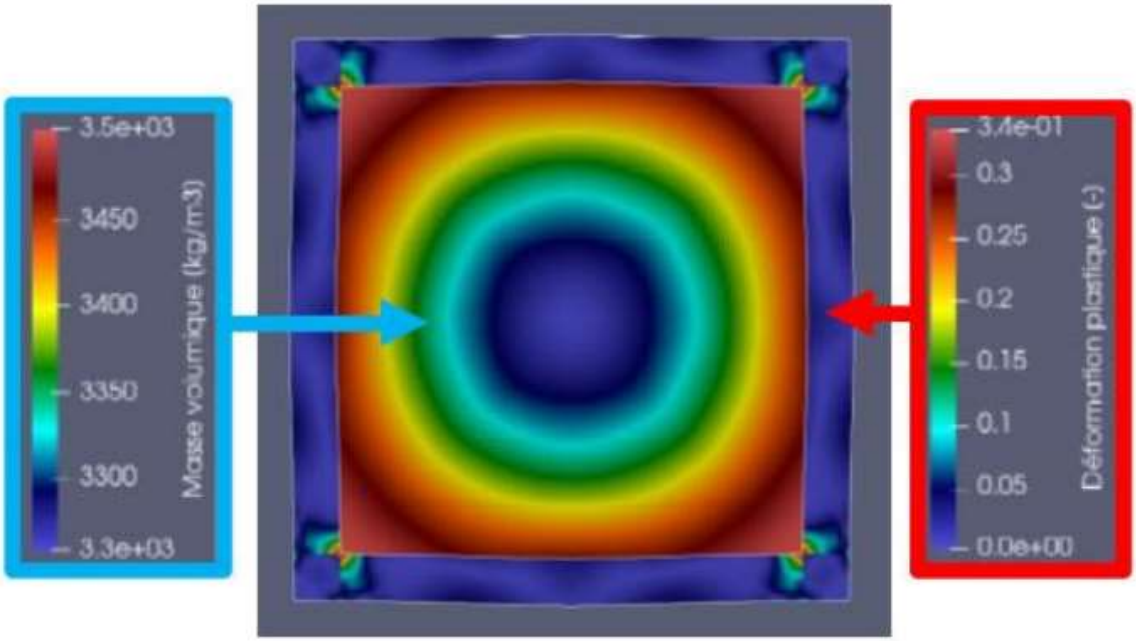

FIG. 8. Impact of the contact wave in the fluid (iso-density values on the left) on the vessel (iso-strain values on the right).

5. CONCLUSIONS

The simulation of severe accidents on a SFR is an area that we have invested in many aspects for many years, both in terms of phenomenology but also in terms of the structure and functionality required for our design and safety objectives. This maturity allows us to consider the construction of an efficient platform in which we best preserve and modernize existing codes with their validation, and we gradually bring all the interoperability features between these components.

Among the objectives we have identified, the ones which consist in designing a system that coherently supports the two-calculation level (mechanistic and physico-statistical), and which offer sufficient versatility to calculate complex sequences, promise significant progress in simulation.

This construction, more evolutionary than revolutionary, deserves a long term research programme, ideally in the framework of an international collaboration. In the meantime, we intend to progressively demonstrate its relevance, with a first application treated with both mechanistic and physico-statistical approaches.

ACKNOWLEDGEMENTS

The authors would like to thank the Generation IV programme of the industrial nuclear support and innovation Division of CEA which supports this work as well as the SFR R&D Project. The SIMMER calculations were granted access to the HPC resources of the CEA's Very Large Computing Centre (TGCC) under the allocation 2022 A0092A07691 made by GENCI.

REFERENCES

[1] WENRA, Western European Nuclear Regulator's Association (2010): Statement on safety objectives for new NPP, November 2010

[2] COMMISSARIAT À L'ÉNERGIE ATOMIQUE ET AUX ÉNERGIES ALTERNATIVES, 4th Generation Sodium-Cooled Fast Reactors: The ASTRID Technological Demonstrator, internal report, CEA Nuclear Energy Division., 2012.

[3] TOBITA, Y., KONDO, S., et al., The development of SIMMER-III, an advanced computer program for LMFR safety analysis and its application to sodium experiments, *Nucl. Technol.* 153 3 (2006), 245–255.

[4] TENTNER, A. M., MILES, K. J., KALIMULLAH and HILL, D. J., "Fuel relocation modeling in the SAS4A accident analysis code system", Proc. Int. Conf. on Science and Technology of Fast Reactor Safety, Guernsey (1986).

[5] LAINET, M., MICHEL, B., DUMAS, J.C., PELLETIER, M., RAMIÈRE, I., GERMINAL, a fuel performance code of the PLEIADES platform to simulate the in-pile behaviour of mixed oxide fuel pins for sodium-cooled fast reactors, J. Nucl. Mater. 516 (2019) 30 – 53.

[6] BRUN, B., COURTAUD, M., HOUDAYER, G., Le code Cathare et son support expérimental thermohydraulique, RGN N° 4 Juillet-Août 1982 p. 329–337, https://cathare.cea.fr.

[7] DEVILLE, E., PERDU, F., Documentation of the interface for Code Coupling: ICoCo, internal report, CEA, 2012.

[8] BECCANTINI, A., BLIARD, F., BOUDA, P., DE LAMBERT, S., DRUI, F., et al., "EUROPLEXUS: un code de référence pour la dynamique rapide et l'interaction fluide-structure", CSMA 2022 – 15ème Colloque National en Calcul des Structures", Giens, France, 2022.

[9] LE TELLIER, R., SAAS, L., BAJARD, S., Transient stratification modelling of a corium pool in a LWR vessel lower head, Nucl. Eng. Des. 287 (2015) 68–77.

[10] VIOT, L., Couplage et synchronisation de modèles dans un code scénario d'accidents graves dans les réacteurs nucléaires Ph.D. Thesis, Université Paris–Saclay, 2018.

[11] CLAVIER, R., JOHNSON, M., BIGOT, B., Corium pool behaviour in the core catcher of a sodium-cooled fast reactor. Submitted to Nucl. Eng. Des., 2023.

[12] SALOME PLATFORM, website: https://www.salome-platform.org.

[13] KEDZIERSKA, B., GUBERNATIS, P., MÉDALE, M., Implementation of multi-domains in SIMMER-V thermohydraulic code, Ann. Nucl. Energy 178 (2022).

[14] BRUN, B., COURTAUD, M., HOUDAYER, G., Le code Cathare et son support expérimental thermohydraulique, RGN N° 4 Juillet-Août 1982 p. 329–337, https://cathare.cea.fr.

ABBREVIATIONS

API	Application programming interface
C3PO	Collaborative code coupling
CFD	Computational fluid dynamics
ICoCo	Interface for code coupling
IQM	Improved quasi static method
JAEA	Japan Atomic Energy Agency
MPI	Message passing interface
PCQM	Predictor-corrector quasistatic method
SFR	Sodium fast reactor
SIMMER	Sn implicit multifield multicomponent eulerian recriticality
SQL	Structured query language
ULOF	Unprotected loss of flow
USAF	Unprotected sub-assembly failure
UTOP	Unprotected transient of power

MODERN APPROACHES TO DETERMINISTIC SAFETY ANALYSIS FOR SODIUM FAST REACTORS

R.V. CHALYY, N.I. RYZHOV, V.N. SEMENOV, A.E. TARASOV
Nuclear Safety Institute of the Russian Academy of Sciences
Moscow, Russian Federation

A.M. ANFIMOV
Joint Stock Company "Afrikantov OKB Mechanical Engineering"
Nizhniy Novgorod, Russian Federation

Abstract

At present, there is a steady interest in the world in the technology of fast reactors cooled with liquid metal coolant. It is determined by such factors as the possibility of effective implementation of a closed nuclear fuel cycle, as well as the high level of safety of such facilities. Russia has accumulated extensive experience in operating sodium cooled fast reactors (SFRs). Two power reactors BN-600 (in operation since 1980) and BN-800 (since 2016) are currently in operation. In addition, an innovative design of the BN-1200 reactor with improved technical and economic characteristics and high level of self-protection is being developed. Modern requirements of the Russian safety regulatory document (NP-001-15) regulate the use of certified codes when performing safety justifications calculations and accompany the calculation results with estimates of errors and uncertainties. Within the framework of these requirements, work on the development and certification of the SOCRAT-BN programme [1] was carried out and the methodology of error estimation and uncertainty analysis for calculations was proposed.

1. INTRODUCTION

In 2020, as a result of joint work by specialists from leading Russian scientific institutes and organizations, as well as the Russian regulatory body, recommendations on assessment of errors and uncertainties in the results of safety analyses of nuclear plants (RB-166-20) [2] were developed. This document includes recommended methods on uncertainty analysis for design basis accidents (DBA) and beyond design basis accidents (BDBA), and on accounting for uncertainties obtained during validation. For the design basis accidents the proposed algorithm is based on the Gesellschaft für Anlagen- und Reaktorsicherheit mbH (GRS) approach [3]. This method is based on a conservative approach and a search for the worst case result by means of uncertainty analysis and sensitivity assessment. The result is compared with an established safety limit. For BDBA there is the methodology based on the ASME V&V 20 approach [4]. The result of the uncertainty analysis is the best estimate value of the parameter and its dispersion. It is important to note that initially the proposed methodologies were developed on the basis of the experience of justification of safety of VVER type reactors. In this regard, in 2022 comprehensive work was carried out to adapt these recommendations to SFRs. To demonstrate the possibility of application of the developed methods, calculations of a DBA with flow blockage of one fuel assembly and a BDBA with station blackout of the sample model of a power unit with an SFR.

2. DESCRIPTION OF THE SOCRAT-BN CODE

SOCRAT-BN code is designed for numerical simulation of thermohydraulic, neutron-physical, thermomechanical processes, evolution of nuclide composition of fuel and transport of radionuclides released after failure of the fuel elements in SFR power plants under anticipated operational occurrences (AOO), DBA and BDBA with core degradation. The final version of the SOCRAT-BN code was certified in 2019. The code currently has the following basic modules:

- SOFAR-TH - one-dimensional thermohydraulics with a two-phase, heterogeneous, two-speed model of coolant flow, r-z model of heat transfer in solid structures.

- BONUS-BN - module for calculation of fission products accumulation in the fuel.
- RTOP-BNO - determining geometric and thermomechanical parameters of the fuel rod before the accident (the time interval corresponds to the duration of the fuel micro campaign).
- TVEL-BN - calculates stresses and strains of fuel rod claddings under transient and emergency conditions.
- TRANS-FP is a module for calculating the transport and deposition of fission products in the primary circuit, the primary circuit gas system, and the main rooms of the power unit of an SFR.
- SYNTES - neutron-physical calculations of the SFR core based on the solution of the direct, conjugate, nonuniform and nonstationary problem of neutron transport in 2D geometry in the diffusion multigroup approximation. For solving unsteady task use quasi-steady approximation. Also, there is option using point kinetic approximation.
- MELT-BN - modelling processes of melting of fuel rods, formation of blockages in the assemblies, melt movement in the core.

A discussion of the validation matrix was presented in Ref. [1]. A summary of the matrix is presented in Ref. [5] and is shown in Table 1.

TABLE 1. INFORMATION ABOUT VALIDATION OF THE SOCRAT-BN CODE

Module	Example of the validation
Thermal-hydraulic module SOFAR-TH	Local phenomena experiments, BN-600, PHENIX and EBR-II [6].
Thermomechanical modules RTOP-BNO and TVEL-BN	Analytical tests, experimental data provided by JSC "INM" [7], cross-validation with finite element 3-D codes COMSOL and Z88, cross-validation with certified fuel behaviour code [8]
Module for calculating the transport TRANS-FP	Loop [9, 10] and capsular [11] experiments, reactor experimental data provided by BN-600
Module BONUS-BN	Capsular experiments, cross-validation with ORIGEN2 [12]
Module MELT-BN	TREAT reactor [13] experiments
Module SYNTES	reactor experimental data provided by BN-600, analytical tests

During the validation of SOCRAT-BN the modified ASME V&V 20 approach was used for the first time to estimate the code modelling errors. As a result, the modelling errors estimation of the main calculated parameters takes into account the uncertainties of measurement of the parameters in experiments and the uncertainties of calculations of these parameters by the code. The modelling error is presented as. $\pm\delta$:

$$\delta = \max\left(|\bar{E} - 2 \cdot u_{val}|; |\bar{E} + 2 \cdot u_{val}|\right),$$

where $\bar{E}$ is the comparison error of the calculation result in relation to the measurement, and u_{val} is the validation uncertainty. Errors of some of the calculated parameters are shown in Table 2.

TABLE 2. ERRORS OF THE MAIN PARAMETERS OF THE SOCRAT-BN

Parameter	Validation range	$\pm\delta$
Coolant temperature		
In conditions of AOO	473 to 823 K	± 40 K
Under DBA and BDBA conditions	800 to 1250 K	± 70 K
Pressure losses in equipment elements in sodium circuits		
single-phase flow	120 to 138 kPa	± 31 %
two-phase flow	139 to 468 kPa	± 47 %
Temperatures of fuel rods cladding		
cooling with single-phase flow	473 to 823 K	± 50 K
cooling with two-phase flow	1173 to 1300 K	± 80 K
Mass rate (mass flow rate)		
Mass velocity for forced flow regime (mass flow rate)	1800 to 6000 kg/(m^2 c)	± 10 %
Mass velocity for natural convection (mass flow rate for single-phase flow)	0 to 1800 kg/(m^2 c)	± 30 %
Failure time of fuel rod cladding	-	± 30 %
Neutron power	-	± 10 %

The model composition of the code allows to simulate a wide range of DBA and BDBA related to violation of heat removal from the core and input of positive reactivity. The code is used for safety justification for operation of the BN-600 and BN-800 reactors, as well as in the design of the BN-1200 reactor.

3. DESCRIPTION OF APPROACH FOR ANALYSIS OF DESIGN BASIS ACCIDENTS

In accordance with the Russian regulatory requirements, deterministic analyses of DBA should be performed with a conservative approach (clause 1.2.9 of NP-001-15). These requirements are consistent with the recommendations presented in the IAEA Safety Guide SSG-2 (Rev. 1) [14]. Note that the conservative approach means the choice of a combination of parameters of a simulated facility, which provides the most unfavourable result in accident analysis. SSG-2 (Rev. 1) [14] offers 3 ways (options) of obtaining such a result. Option 1, called "conservative", recommends application of conservative code, conservative assumptions about systems availability and conservative initial and boundary conditions. Option 2, "combined", allows the use of a best estimate code and recommends performing a sensitivity analysis to confirm conservatism in the input parameters. Option 3 recommends the use of best estimate code in the conservative calculation and suggests using a combination of conservative and realistic values as initial and boundary conditions. Since SOCRAT-BN is a best estimate code, the first option is excluded from consideration. Option 2 allows the use of the improved estimation programme but involves a lot of preliminary calculations to find the values of input parameters that would give the worst result. In addition, at different stages of the accident the conservative value of input parameters do not always give the worst result [15]. Thus, option 3 is the most reasonable choice for the DBA analysis for an SFR reactor using the SOCRAT-BN code.

Implementation of option 3 assumes the following algorithm of actions. In the first stage, an analysis of accident phenomenology is performed, in which the analysis of the key phenomena determining the progression of the accident is performed. Also, the analysis of design and construction characteristics of the plant is performed. In the second stage, conservative

parameters are determined, which are used as initial and boundary conditions, and realistic parameters, for which ranges of values and probability distribution functions are determined. In the third stage, Monte Carlo calculations are performed and a tolerance interval is obtained for the calculated parameters for which acceptance criteria are established. The programme error is added to the obtained tolerance limits, and the obtained results are compared with the acceptance criteria.

To demonstrate the described algorithm, we consider an accident with a total instantaneous blockage (TIB) of a sample model of an SFR type reactor. The choice of this accident is interesting because it creates conditions for fuel rod melting, but, in accordance with the requirements for the safety justification report (NP-018-05), the initial events for this accident refer to design accidents: complete blocking of the cross-section of one assembly.

3.1 Features of the nodalization scheme

To model this accident, the standard reactor design scheme presented in Ref. [1] was used. A more detailed analysis was performed to simulate the blocked and surrounding assemblies. A more detailed analysis was performed for 19 fuel assemblies: one central blocked fuel assembly (FA) and two rows of adjacent FA (6 and 12 fuel assemblies). The detailed scheme is shown in Fig. 1. The detail of the scheme was determined by the one-dimensional approximation of the thermohydraulic model. The scheme consists of parallel channels (CH) in which the coolant flows. The channel pos.1 simulates the central FA. The heat elements simulating fuel pins (HE) (pos. 8), absorbing rods (HP) (pos. 9) and shroud FA (HS) (pos. 10) are connected with the channel. The next channel simulates the space between the fuel assembly shrouds (pos. 2). The next row of FAs is simulated by two channels (pos. 3. and pos. 4). The first channel simulates the part of the FA that is closer to the central FA. This channel includes part of shroud FA (pos. 11), fuel pins (pos. 12) and absorbing rods (pos. 13), which are adjacent to the central fuel assembly. The second channel (Pos. 4) simulates the part of FA, including shroud FA (Pos. 16), fuel pins (Pos. 14) and absorbing rods (Pos. 15), facing the next row of FA The next row is modelled like to the previous row.

In the radial direction, the heat transfer is from the channel pos. 1 to the shroud FA pos. 10, from shroud FA to channel pos. 2, from channel to shroud FA pos. 11, from shroud FA to channel pos. 3. Channels pos. 3 and pos. 4 conservatively do not exchange heat. Exchange of heat between the channels pos. 4–6 are implemented according to the same scheme. Melt relocation in a radial direction is modelled mechanistically (between fuel pins and shroud, between shrouds): the possibility of melt contact between adjacent elements is calculated geometrically and, when contact conditions are reached, a model of convective heat transfer between adjacent elements is considered. At the melt penetration through surface the adjacent shroud FA towards the first and second adjacent rows, a complete blockage of their cross-sections are postulated.

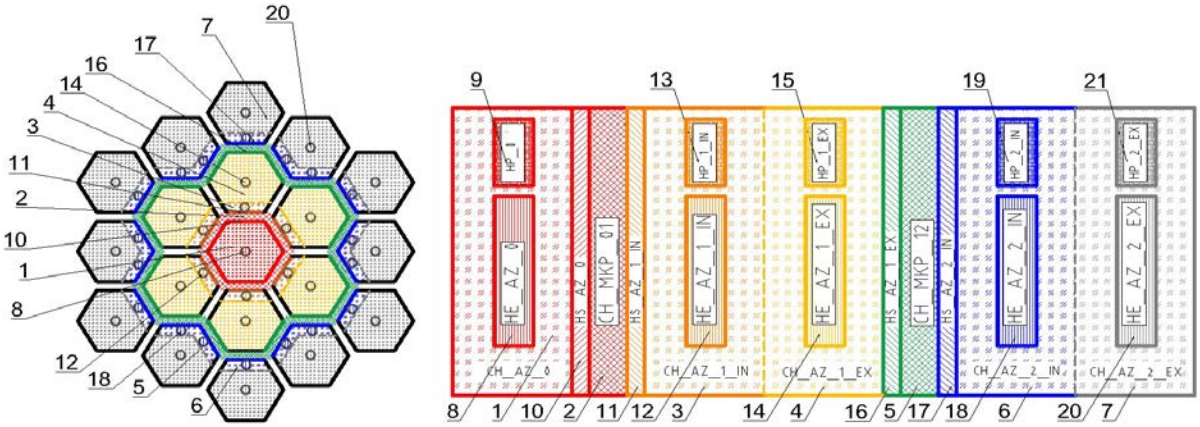

FIG. 1. Core partitioning scheme for a TIB accident.

3.2 Analysis of the accident phenomenology

The results of preliminary calculations of the TIB accident showed that, after the initial event, the heat removal from the fuel rods inside the blocked fuel assembly is disturbed, resulting in rapid sodium boiling and melting of the fuel and claddings in the assembly. In the process of movement, the melt touches the blocked fuel assembly shroud, which leads to its melting (we use a simplified mechanism: the sheath collapses when heated to solidus temperature) and release of the melt into the space between shrouds and then into the upper mixing chamber of the reactor. Together with the fuel melt, the precursors of delayed neutrons escape into the upper mixing chamber and are carried by a sodium flow to the inlet of the intermediate heat exchangers (IHX). As the concentration of delayed neutron precursors grows at the inlet windows of the IHX, the readings of the ionization chambers of the containment leakage monitoring system increase and the scram signal is generated. Part of the melt that has released into the space between assemblies' shrouds contacts with the shrouds of neighbouring fuel assemblies, which leads to their melting. After the melting of the shrouds of neighbouring assemblies, partial blockages of the cross-sections are formed inside them, preventing the normal heat removal from the fuel rods. Due to the disruption of heat removal inside the neighbouring fuel assemblies, the fuel rods start melting. As a result of introducing absorbing rods into the core by the reactor scram signal, the reactor power is reduced, and the melting inside the neighbouring fuel rods stops spreading.

For the conservative scenario we had the following times: lockout 0 s, fuel cladding melting 3.6 s, start of melting of the emergency assembly shroud 8 s, start of melting of the neighbour assembly shroud 11 s, start of the shutdown system 21 s.

Taking into account the scenario described above, an analysis of the key phenomena for this accident was performed. Table 3 presents some of the most important phenomena.

TABLE 3. KEY PHENOMENA FOR THE TIB ACCIDENT

Phenomena	Impact on the accident
Pressure losses at local resistances and friction	Influences the value of the coolant flow rate
Sodium boiling in individual fuel assemblies	Influences the heat exchange in blocked fuel assemblies
Heat exchange in the partially uncovered core	Determines the time of melt occurrence
Release of gaseous fission products from the fuel rod	Determines the radiation situation
Fuel and cladding melting	Determines the extent of damage in the core
Forced circulation	Determines the heat exchange conditions before triggering an emergency protection
Natural circulation	Determines the heat transfer conditions after the emergency protection has been triggered
Heat transfer processes from fuel elements	Defines fuel rod cooling conditions
Fuel and cladding properties	Affects the growth rate of fuel rod temperature
The properties of the assembly shroud	Influences the conditions of melt propagation
Reactivity effects when triggering scram signal	Affects the rate of power reduction during reactor shutdown

3.3 Determination of the list of realistic and conservative parameters

Under option 3, conservative assumptions and realistic parameters are selected.

The conservative assumptions are selected based on preliminary estimates and expert analysis of their impact on the calculation result. The main conservative assumptions are presented in Table 4.

TABLE 4. CONSERVATIVE ASSUMPTIONS

№	Assumption	Expected effect
1	Maximum capacity of emergency fuel assemblies, fuel assemblies of the first and second adjacent row	Increasing the temperature in fuel assemblies and reducing their damage time
2	Instantaneous blockage of one fuel assembly cross-section	Reducing the time of the beginning of the failure of the fuel assembly
3	Minimum thickness of fuel assembly shroud	Reduced penetration time
4	Instantaneous blockage of the cross-section of the first adjacent row of fuel assemblies (when their shrouds are melted)	Reducing the heating and melting time of fuel rods in neighbouring assemblies
5	Minimum distance between fuel assemblies	Reduced heating time
6	Minimum heat transfer surface between fuel assemblies, taking into account the partitioning in the calculation scheme	Reducing the effective heat transfer surface
7	Loss of heat exchange between the channels simulating the fuel assemblies of the adjacent row	Loss of additional cooling
8	Loss of heat exchange between the channels simulating the fuel assemblies of the two adjacent rows	Loss of additional cooling
9	Blocking at the input of the space between shroud	Loss of additional cooling

№	Assumption	Expected effect
10	Release of delayed neutron precursors into the primary circuit after the melting of the cladding of a blocked fuel assembly	Additional delay in triggering of scram signals
12	Maximum time delay for registration of delayed neutron precursors and the time of formation and passage of scram signals	Additional delay in triggering of scram signals

The realistic parameters are selected based on an analysis of the design and technological uncertainties of the reactor, and validation experience is also taken into account. The list of basic realistic parameters is presented in Table 5. Normal truncated distribution law is assumed for the parameters monitored during manufacturing or operation of the equipment, and uniform distribution law is assumed for other parameters.

TABLE 5. LIST OF THE MAIN RELISTIC PARAMETERS

Parameter name
Geometric characteristics of fuel rods and fuel assemblies
Thermal conductivity of materials and fuel
Heat transfer coefficient from sodium to the fuel assembly shroud
Multiplier for the coefficient of friction in the assembly
Multiplier for the coefficient of interphase friction
Reactivity of the element of the reactor PCS
Proportion of delayed neutron precursors
Reactivity coefficients for the point kinetics model

3.4 Choice of acceptance criteria and peculiarities of Monte Carlo calculations

For a TIB-type accident, two main criteria are usually established in SFR designs: as a result of an accident, the number of fuel assemblies with molten fuel rods has to not exceed 7 (the remaining assemblies' temperatures has to not exceed the design limit), doses at the border of the sanitary protection zone have to be such to exclude any measures to protect the public. The demonstration calculations consider two acceptance criteria: 1) the temperature of the internal surface of the shrouds of fuel assemblies of the second adjacent row has to not exceed the melting temperature (thus, the localization of melting in 7 fuel assemblies is confirmed); 2) the fuel rod cladding temperature in assemblies of the second adjacent row has to not exceed the design limit (thus, the exclusion of fuel rod damage outside the boundary of 7 damaged assemblies is confirmed).

The realistic input parameters are generated by simple random sampling. In this analysis, it is necessary to obtain two tolerance limits so that the resulting semi-constrained space contains at least 95% of possible values from the population with at given confidence level. In accordance with regulatory document RB-166-20, it is recommended to choose a value of confidence level of not less than 95%. The minimum number of calculations (sample size) n required to meet these conditions is calculated using the formula [16]:

$$a \leq 1 - I(b, n - p + 1, p)$$

where $b \cdot 100\%$ is the fraction of the population that is bounded by the tolerance limits; $a \cdot 100\%$ is the confidence level; p is the number of tolerance limits, in this case 2; I is the

non-complete β-function. The numerical solution of this inequality gives $n \geq 93$. In engineering practice, generally, 100 Monte Carlo calculations are performed.

3.5 Comparison with acceptance criteria

The uncertainty analysis when using the conservative approach in deterministic safety analysis consists of estimating the distribution functions of the input uncertain parameters, transforming their distributions by the Monte Carlo method and obtaining the corresponding tolerance limit. When comparing the tolerance limit with the acceptance criterion, it is necessary to take into account the modelling errors of the code.

During the validation of the SOCRAT-BN code an estimate of the modelling error and uncertainties was made directly to the experimental data. Since in the certificate of SOCRAT-BN code there is a modelling error estimate for the analysed parameter important for safety, in order to take into account this error, the obtained tolerance limit should be corrected by the corresponding error from the certificate. And the corrected value is a conservative result of the analysis and is compared to the acceptance criterion. The procedure for calculating the tolerance limit and its correction for the code modelling error is presented below.

The upper and lower tolerance limits at each time point are calculated using the formulas:

$$S_{max}(t) = \max\left(S_1(t), \dots, S_N(t)\right) \text{ and } S_{min}(t) = \min\left(S_1(t), \dots, S_N(t)\right),$$

where $S_{max}(t)$ is the upper tolerance limit at time t; $S_{min}(t)$ is the lower tolerance limit; $S_1(t), \dots, S_N(t)$ are Monte Carlo results; N is the number of Monte Carlo calculations.

The tolerance limits corrected for the program modelling error are calculated by the formulas:

$$\tilde{S}_{max}(t) = S_{max}(t) + \delta \text{ and } \tilde{S}_{min}(t) = S_{min}(t) - \delta.$$

The tolerance limit thus obtained will contain at least 95% of the population.

For calculation parameters without estimated modelling error (in this case, the temperature of the fuel assembly shroud), the correction of the tolerance limit by expert judgment is assumed to be equal to twice the value of the standard deviation, which additionally ensures the conservativeness of the calculation results.

Figure 2 shows a scheme comparing the tolerance limit with the acceptance criterion. The figure shows that the safety margin before breaking the safety barrier will be larger than the margin to acceptance criterion estimated based on the conservative approach. Additional conservatism can be introduced by setting an acceptance criterion more stringent than the safety limit.

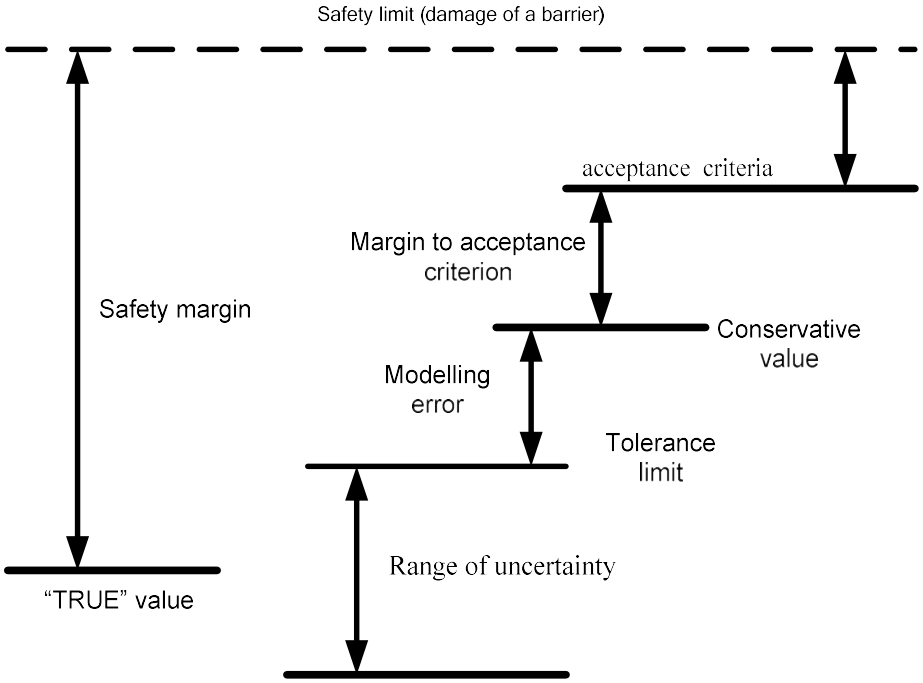

FIG. 2. To the description of the methodology.

The results of the demonstration calculations have shown that the TIB accident scenario can proceed with a melting of one blocked assembly (21 of 100 variants) or seven assemblies (79 of 100 variants). Since the values of the acceptance criteria for these cases are fundamentally different, their statistical processing is performed separately. Figure 3 shows the results of the demonstration calculations for the most representative case with fuel rod melting in seven assemblies. Figure 3 shows that for the considered model of the SFR, the accepted acceptance criteria are fulfilled.

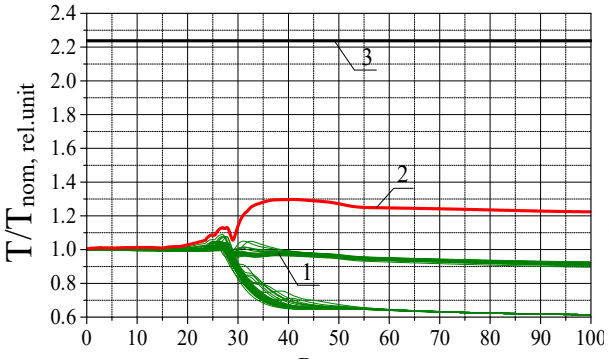

a) Temperature of the inner surface of the shroud of the second adjacent row.

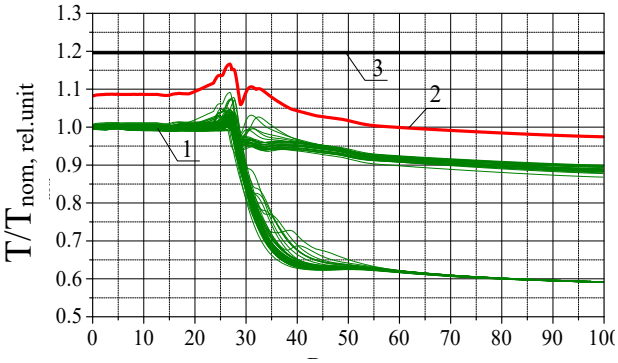

b) Temperature of the fuel rod cladding in the second adjacent row.

FIG. 3. Results of demonstration calculations of the TIB accident.

4. DESCRIPTION OF APPROACH FOR ANALYSIS OF BEYOND DESIGN BASIS ACCIDENTS

Unlike DBA, in accordance with the requirements, deterministic calculations of BDBA are performed using a realistic (non-conservative) approach (Clause 1.2.16 of NP-001-15). The analysis of BDBA is the basis for making plans for protection of public and personnel in case of an accident and development of instructions for severe accident management guidelines. In RB-166-20, an approach based on the ASME V&V20-2009 method is presented for uncertainty analysis of DBDA. For SFRs, application of this methodology does not require additional modification. A general description of the technique is given Ref. [17]. According to RB-166-20, the purpose of uncertainty analysis of the calculation result of DBDA analysis is to determine the expected value of the parameter important for safety, as well as statistical characteristics of its variation. Thus, deterministic analysis of BDBA with uncertainty quantification will have the following algorithm:

- An analysis of the phenomenology of the accident;
- Definition of the list of uncertain parameters;
- Selection of parameters important for safety and Monte Carlo calculations;
- Analysis of the obtained results.

To demonstrate the uncertainty analysis methodology for BDBA, we consider two accident scenarios with power unit blackout and failure to activate the emergency protection. The first option considers the tripping of passive reactor shutdown rods (an LOF type accident). The second option additionally postulates the failure of all passive shutdown absorber rods (ULOF type accident).

4.1 Analysis of the LOF accident

The initial event in the LOF accident is the loss of system power supply, which results in the reduction of rotation frequency of the rotors of the main circulation pumps of the primary circuit (MCP-1). After connection of diesel generator units of reliable power supply, the rotational speed of MCP-1 is set at the reduced level. This leads to disruption of heat removal from the core. Since the accident scenario postulates the failure of rods of the control and protection system (CPS) activated by scram signal, the reactor power at the beginning of the accident decreases only due to the negative temperature effects of reactivity (mainly the Doppler effect). When the flow through the core decreases below 50% of the nominal value, passive absorber rods of CPS (PAZ) are inserted, which ensures the reduction of reactor power to the level of residual heat release. At the same time, after the insertion of PAZ rods, the temperature of the fuel rods cladding and the pressure in gas plenum of the reactor decrease. The results of calculations of the main reactor parameters are shown in Fig. 4.

Uncertainty analysis is performed for fuel rod cladding temperatures, gas plenum pressure, and fission product release activity from the reactor. The calculation results are represented by the mean value and the associated standard uncertainty. For validated parameters, the standard uncertainty includes the uncertainty of modelling (u_{val}), which is determined at the validation. For parameters without estimated modelling uncertainty, the standard uncertainty is taken to be equal to twice the value of the standard deviation. In practical problems, the number of Monte Carlo calculations is usually assumed to be 100. If necessary, the sufficiency of calculations can be specified iteratively as the variance of one or more parameters converges. For demonstration calculations, 100 Monte Carlo calculations are considered. The list of the main parameters to be varied was determined on the basis of the uncertainty analysis of the reactor

plant characteristics given in the design and operating documentation, as well as taking into account the validation experience, and is presented in Table 6 (overall, about 63 parameters were used, but only some of them have been included in the paper, as the length of the paper is limited. For this scenario, the PAZ response time has less impact than the given parameters, so we have not included it in the table). Within the framework of demonstration calculations for all runs, the accumulation of radioactive fission products in the fuel rod gap during normal operation was accepted in accordance with the upper limit of experimental data for burned fuel.

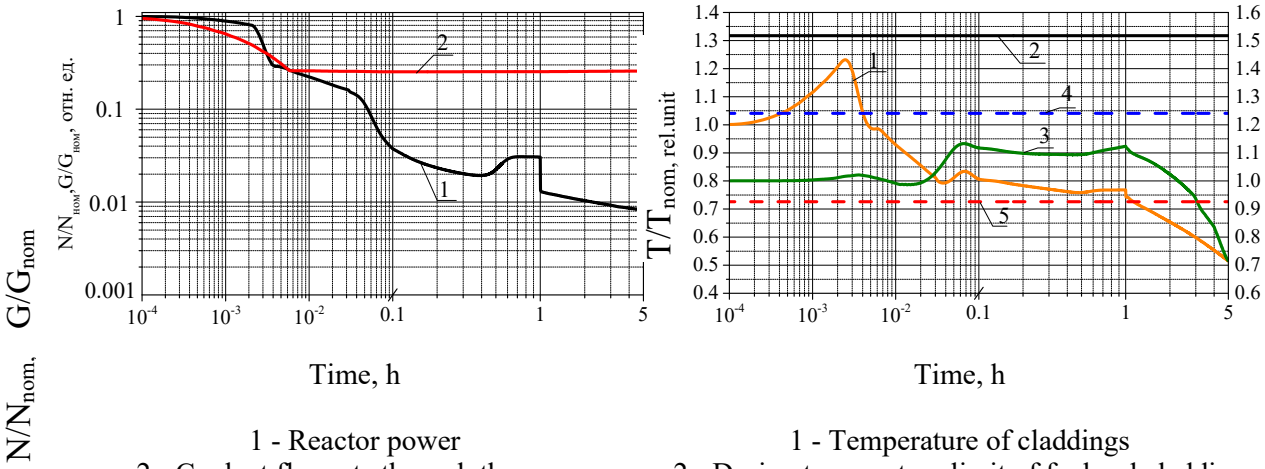

(a) Reactor power and coolant flowrate through the core.

(b) Temperature of the claddings and the pressure in the gas system of the primary circuit.

FIG. 4. Results of calculations of the main reactor parameters in a LOF accident.

TABLE 6. LIST OF MAIN UNCERTAIN PARAMETERS

Parameter name
Reactor power
Pressure loss coefficient on local resistances in the reactor plant circuits
Coefficients of pressure and flow characteristics of main circulation pumps
Dimensions of assemblies and fuel rods
Multiplier for the thermal conductivity coefficient of construction materials and fuel
Dimensions of tubes in heat exchanger
Multiplier for heat transfer coefficient in heat exchanger
Pressure and temperature in the gas system of the primary circuit
Gas system volume
Mass of gaseous fission products accumulated in fuel rods gap during normal operation
Multipliers on the activity of fission products in the fuel and gas system of the primary circuit
Reactivity of CPS rods
Proportion of delayed neutron precursors
Reactivity coefficients for the point kinetics model

Among 100 Monte Carlo calculations, the opening of the hydro seal occurred in 55 variants, and in 45 variants the hydro seal remained closed. Since the operation of the hydro seal determines the release of fission products from the reactor, the statistical processing of the calculation results for these two variants was performed separately. The main results of the

uncertainty analysis for the most representative cases (with a hydro seal) are shown in Table 7 and Fig. 5.

TABLE 7. RELATIVE ACTIVITY OF FP RELEASE FROM REACTOR (RELATIVE TO NOMINAL FUEL REACTIVITY), %

Calculation parameter	Gaseous FP	Volatile FP
Average value	0.49	1.75E-6
Standard uncertainty	0.8	3.42E-6

The results of the LOF accident uncertainty analysis showed that, taking into account the modelling error and uncertainties, the fuel rod cladding temperature can reach the design limit of about 28% of the fuel assemblies, so their depressurization can occur with the release of fission products into the primary circuit. As a result of release of gaseous fission products from damaged fuel rods, the pressure in the gas system of the primary circuit grows. In this case hydro seal can be actuated one or two times. Release of fission products from the reactor is carried out together with the gas medium of the primary circuit when the hydro seal is opened. The significantly lower release of volatile fission products, relative to gaseous fission products, is due to their effective retention in the fuel and sodium.

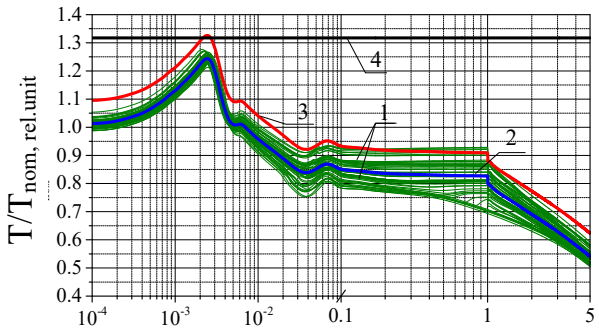

(a) Cladding temperature of the fuel rod

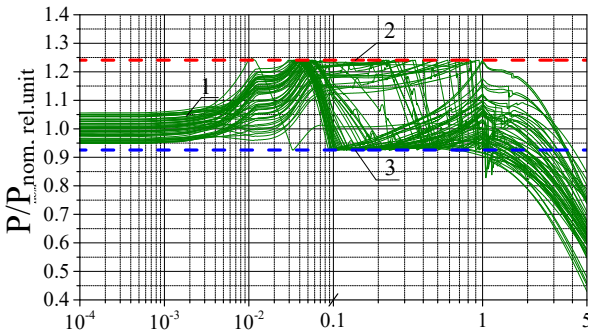

(b) Pressure in the gas system of the primary circuit

FIG. 5. Results of the LOF accident uncertainty analysis.

4.2 Analysis of the ULOF accident

In a ULOF accident, the loss of system and reliable power supply is postulated as the initial event. Unlike the LOF accident, in a ULOF accident the reactor power decreases much more slowly (since failure of the passive absorber rods are postulated), and the coolant flowrate is reduced to the level of natural circulation (due to a complete shutdown of the MCP-1). Therefore, already at the beginning of the accident, the coolant in the core heats up to the sodium boiling point. Boiling first occurs in the upper part of the fuel assembly (the sodium cavity and the upper absorbing screen), which leads to the introduction of some additional (along with the Doppler effect) negative sodium void reactivity effect. As the boiling region spreads down to

the centre of the core, the coolant flow rate through the core decreases and a crisis of heat transfer occurs, leading to melting of the fuel cladding. Since the SOCRAT-BN code certification area is limited to the beginning of fuel rods destruction, the analysis of further processes within the framework of demonstration calculations was not carried out. For the referent simulation we had the following times: Initial boiling of coolant 21 s, melting cladding 26 s., introduction of positive reactivity and power increase up to 1.7 nominal values around 30 s by movement of melted cladding. The main results of the calculations are shown in Fig. 6.

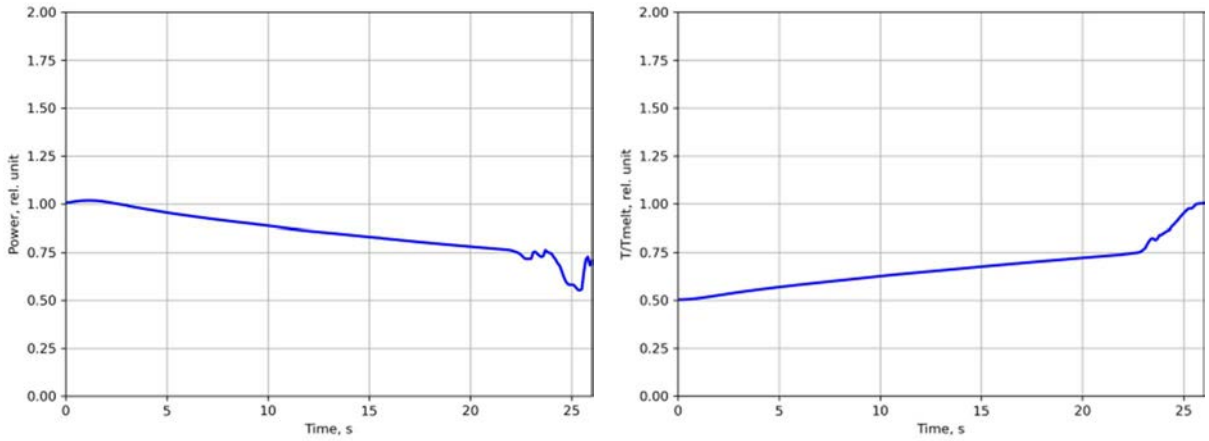

a) Reactor power *b) The temperature of the fuel cladding*

FIG. 6. Results of calculations of the main reactor parameters in an ULOF accident.

The uncertainty analysis of the ULOF accident in the demonstration calculations was performed to estimate the possible change in reactor power, as well as to estimate the expected time of the beginning of the melting of the fuel cladding. The approach to the uncertainty analysis of the ULOF accident is similar to the approach used in the LOF accident analysis. However, it should be noted that in the ULOF accident the uncertainty of the reactivity coefficients of the point kinetics model was not considered, since the spatial kinetics implemented in the SYNTES module was used.

The main results of the uncertainty analysis for ULOF are shown in Fig. 7 and Table 8.

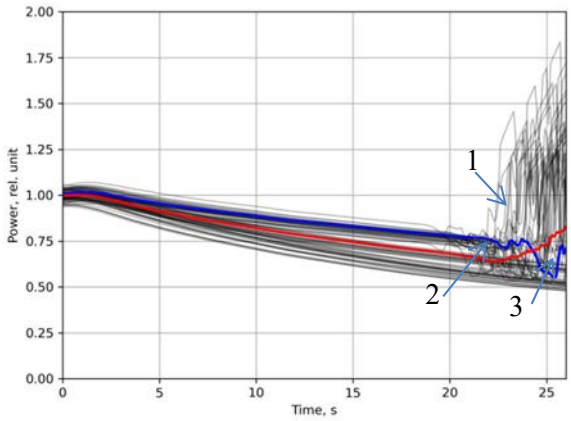

1 - Results of Monte Carlo calculations
2 - Mean value
3 - Reference calculation

a) Reactor power

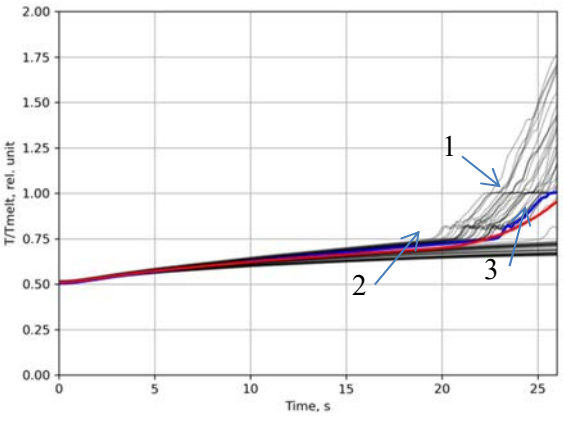

1 - Results of Monte Carlo calculations
2 - Mean value
3 - Reference calculation

b) Cladding temperature of fuel elements

FIG. 7 Results of the ULOF accident uncertainty analysis.

TABLE 8. TIME OF MELTING OF FUEL CLADDING

Calculation parameter	Value, s
Average value	36
Standard uncertainty	12,7

The obtained data on the uncertainty of the ULOF accident parameters calculation can be used by the personnel to take a decision on the beginning of its control (pressing the button of the scram signal on the unit or backup control panel to move to the active zone the regulatory (RS) and control rods (CR), which are powered for several hours by the batteries).

5. CONCLUSION

As part of this work, we developed a methodology for deterministic safety analysis of an SFR in a DBA with blockage of cross-section of one fuel assembly and BDBA (before the start of core melting). In the future, it is planned to extend the safety analysis methodology to the stage of core melting and melt retention in the reactor. For these tasks we will use the code SOCRAT-BN.

This experience can be fully extended to any modern reactors with liquid metal coolant, considering their design. It is worth noting that the experience of modelling severe accidents at fast reactors has shown that, due to the complexity of the simulated phenomena, the time costs greatly exceed the costs of modelling BDBA for VVER-type reactors. In this regard, it is necessary to take a very balanced approach to the selection of representative scenarios and parameters to be analysed.

REFERENCES

[1] CHALYY R.V., et al. "SOCRAT-BN integral code for safety analyses of NPPs with sodium cooled fast reactors: development and plant applications", International Conference on Fast Reactors and Related Fuel Cycles: Next Generation Nuclear Systems for Sustainable Development (FR17), (Proc. Int. Conf., Yekaterinburg, 2017), IAEA, Vienna (2018), Paper CN245_281.

[2] Safety Guidelines for the Use of Atomic Energy «Recommendations on Evaluation of Errors and Uncertainties of the Results of Computed Safety Analyses for Nuclear Power Plants». RB-166-20. https://docs.secnrs.ru/catalog/RB/RB_166_20/.

[3] GLAESER, H. GRS Method for Uncertainty and Sensitivity Evaluation of Code Results and Applications, Science and Technology of Nuclear Installations - 2008.

[4] Standard for verification and validation in computational fluid dynamics and heat transfer. ASME V&V20-2009. New York: ASME, 2009. 88 p.

[5] Rtishchev N.A., Chalyy R.V., et al. SOCRAT-BN integral code for safety analyses of NPP with sodium cooled fast reactors: development and plant applications. IAEA-CN245-281

[6] RTISHCHEV N.A., Chalyy R.V., Tarasov A.E., Semenov V.N., Butov A.A., Vozhakov I.S., Zhigach SA, Kudashov I.G., Usov E.V., Pribaturin N.A., Osipov S.L, Gorbunov V.S., Anfimov A.M. Development of the code SOCRAT-BN, IRTC NIKIET 2012, the collection of reports. from. 348-359.

[7] KINEV E.A. The influence of irradiation on materials of fuel elements with uranium and uranium-plutonium oxide fuel when operating in the BN-600 reactor. Abstract of diss. on competition uch. degree Ph.D. Zarechnyi 2009 (In Russian).

[8] "Performing Of Validation Simulation In Engineering Fuel Code And Analysis Of The Results." Chapter 19. Invent. no 60. 2013.

[9] GUON J. Deposition of Cesium and Barium in Sodium-Stainless Steel System. Canoga Park, Calif: Atomics International, 30 Jun 1970. 78 p. AI-AEC-12952.

[10] BORISHANSKII V.M., PALEEV I.I., AREF'EV K.M. et al. Condensation Of Cesium Vapor From Flowing Argon. Journal Of Engineering Physics. 1971, VOL. 20, 4, PP. 431-435.

[11] NISHIMURA M., NAKAGIRI T., MIYAHARA S., Evaporation Release Behaviour Of Volatile Fission Products (Iodine, Cesium, Tellurium) From Liquid Sodium Pool To The Inert Cover Gas. Japan: O-Arai Engineering Center, 1996.

[12] A.G. CROFF. ORIGEN 2, A Revised And Updated Version Of The Oak Ridge Isotope Generation And Depletion Code. ORNL-5621, JULY 1980.

[13] G. HOPPNER A.O., Treat R5 Loss-Of-Flow Experiment In Comparison With Sas Pretest Analysis, Tansao Vol.18, P.213 (1974).

[14] INTERNATIONAL ATOMIC ENERGY AGENCY, Deterministic Safety Analysis for Nuclear Power Plants, IAEA, Safety Standards Series No. SSG-2 (Rev. 1), Vienna (2019).

[15] INTERNATIONAL ATOMIC ENERGY AGENCY, Best Estimate Safety Analysis for Nuclear Power Plants: Uncertainty Evaluation, Safety Reports Series No. 52, IAEA, Vienna (2008).

[16] "SOCRAT-BN INTEGRAL CODE: development, validation and current status" authors: Chalyi R.V., et al. IAEA International Conference on Fast Reactors and Related Fuel Cycles: Sustainable Clean Energy for the Future (FR22), Beijing (China) 2022.

[17] Attila Guba, Mihaly Makai, Lenard Pal, Statistical aspects of best estimate method - I, Reliability Engineering and System Safety, Vol. 80, pp. 217-232, 2003.

DEVELOPMENT OF ANALYSIS METHODS FOR SFR SEVERE ACCIDENTS IN JAEA AND ASSESSMENT OF APPLICABILITY TO SAFETY ANALYSIS

Y. TOBITA, H. TAGAMI[1], S. ISHIDA[1], Y, ONODA[1], J. SOGABE, Y. OKANO[1]
Japan Atomic Energy Agency
Ibaraki, JAPAN

Abstract

Since the fast reactor core is not in the maximum reactivity configuration, a hypothetical core disruptive accident could lead to prompt criticality due to a change in the core material configuration, and the resulting energy generation has been one of the issues in fast reactor safety, and therefore appropriate measures are needed to mitigate and contain the effect of energy generated in the accident. In order to assess the effectiveness of these mitigative measures, a set of computer codes to analyse the event progressions and energy generation behaviour in the ATWS of fast reactors have been developed, maintained, and improved under international collaboration in JAEA. Since the important physical phenomena, which govern the event progression, vary along with the progression of the accident, the whole accident process is divided into several phases in the analysis of accident, and dedicated analysis methods for each phase are provided to analyse the event progression in each phase. The organization and overview of these analysis methods are described in the paper. As a representative example of the validation approaches in applying these analysis methods to the reactor safety assessment in licensing procedure in Japan, the validation studies to confirm the applicability to reactor analysis of the SIMMER code for analysing core material movement and reactor power, which is important to analyse the energy generation in the accident, are presented in the paper. The validation studies of the SIMMER code confirmed the applicability of SIMMER to the reactor analysis, while the critical phenomena for which the effect of their uncertainty in the reactor analysis should be checked were also recognized.

1. INTRODUCTION

In the siting and installation of nuclear reactor facilities, it is assumed that severe accidents with the potential to result in substantial releases of radioactive material may occur, and thus, adequate safety measures are implemented to mitigate such incidents. For light water reactors (LWRs), accidents such as a loss of coolant accident (LOCA) and station blackout (SBO) are considered the primary sources of risk. These risks can be effectively managed by ensuring the integrity of the containment vessel and demonstrating the efficacy of such measures through comprehensive and conservative analysis. In contrast, sodium cooled fast reactors (SFRs) are inherently stable and exhibit little deviation from their operating state, which means that there is no direct impact on the primary system boundary or containment vessel, which serve as barriers to the release of radioactive material during design basis accidents (DBAs). On the other hand, since the core of a fast reactor is not designed to maximize reactivity, there is a potential risk that fuel meltdown or relocation in core disruptive accidents (CDAs) could cause the reactivity to exceed the prompt criticality and result in a large energy release. In other words, CDAs encapsulate the unique risks associated with fast reactors, which are not covered by DBAs.

During the early stages of fast reactor development, the evaluation of the energy release associated with prompt criticality was based on conservative scenarios and hypothetical initial conditions [1, 2]. Subsequently, safety research utilizing in-pile facilities such as CABRI [3] and TREAT [4], as well as a multitude of out-of-pile tests, has advanced our understanding of accident phenomena. Furthermore, advancements in computer technology have facilitated the development of safety analysis computer codes, such as SAS4A [5] and SIMMER [6], among others. These mechanistic analysis methods have paved the way for more realistic assessments of CDA event sequences, supplanting the previously used overly conservative evaluations that relied on arbitrary initial conditions and hypothetical scenarios.

In the aftermath of the Fukushima Daiichi Nuclear Power Plant accident in Japan, new regulatory standards [7] were instituted in 2013, requiring even fast reactors in the research and development stage that possess high reactor power and the potential for significant

consequences in the event of an accident, to implement measures aimed at preventing containment failure against severe accidents and to confirm their effectiveness through safety analysis. To this end, JAEA has developed analytical methods that demonstrate the conformance of fast breeder reactors (LMFRs) to these new regulatory standards by combining existing plant dynamics codes, commercial codes, empirical formulas, and safety analysis codes, such as SIMMER, to perform safety analyses of fast reactors. This paper provides an overview of these analysis methods and evaluates the applicability of SIMMER, a crucial component of these methods, to actual LMFR plants as a representative example of other codes.

2. EVENT PROGRESSION OF CDA AND ANALYSIS METHODOLOGY

A typical scenario for a CDA in fast reactors is the failure of the emergency shutdown system during a significant departure from normal operating conditions, commonly referred to as anticipated transient without scram (ATWS). There are two common types of CDA, unprotected loss of flow (ULOF) resulting from a failure of the reactor scram during loss of primary coolant flow and unprotected transient over power (UTOP) resulting from a failure of the reactor scram during uncontrolled control rod withdrawal. This section will outline the progression of the ATWS event and the analysis methodology developed in JAEA.

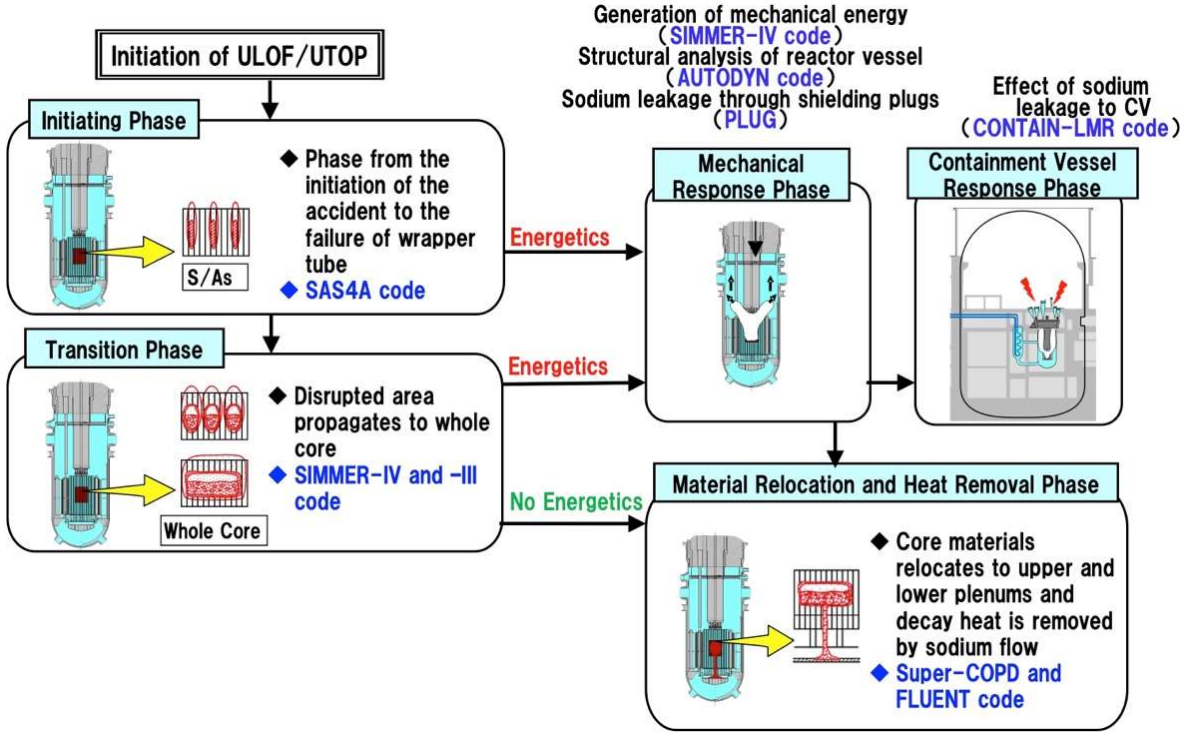

FIG. 1. Event progression of ATWS and computer codes used in safety analysis.

A schematic representation of the progression of an ATWS event is depicted in Fig. 1. As illustrated in the figure, the ATWS analysis is carried out by partitioning the entire progression into several stages, owing to the fact that the physical phenomena being analysed and the necessary level of precision alters as the event advances. The Initiating Phase (IP), which encompasses the process from the inception of the accident to the disruption of fuel resulting in wrapper tube failure, is analysed using the SAS4A code. The Transition Phase (TP), spanning from the wrapper tube failure to the full scale core meltdown, is analysed using the SIMMER code. In the event of a substantial energy release due to prompt criticality in IP or TP, so called energetics, the Mechanical Response Phase (MRP) is examined, comprising the analysis of

mechanical energy generation, structural response of the reactor vessel, response of the shielding plug, and sodium leakage. The mechanical energy generation behaviour is analysed using the SIMMER code, the structural response of the reactor vessel using the AUTODYN [8] code, and the response of the rotating plug and sodium ejection behaviour using the PLUG code. If there is sodium leakage into the containment vessel, the Containment Response Phase is analysed, comprising the examination of the containment vessel's response to the sodium leakage, utilizing the CONTAIN-LMR [9] code. The Material Relocation and Heat Removal Phase, regardless of the presence or absence of mechanical energy generation, entails the analysis of the migration and relocation of molten core materials and the subsequent long term decay heat removal by sodium flow. This process is analysed using the Super-COPD [10] and FLUENT [11] codes. An example of reactor analysis using these codes can be found in the analysis of ULOF in the Monju reactor [12]. Outlines of each code are presented below.

2.1 SAS4A

SAS4A [5] is a computational code that integrates modules analysing the various phenomena that transpire in each assembly during the IP. The entire core is simulated through about 33 SAS4A channels, each channel being hydraulically linked at the interface to the upper and lower plenum and neutronically linked through a point reactor kinetics analysis to study the progression of the accident. Each SAS channel comprises a representative single fuel element model divided by radial and axial meshes, where the fuel pellet, fuel–cladding gap, cladding, coolant, and wrapper tube are coupled through the radial heat transfer model and axially through the coolant thermohydraulic model. In voided channels, in which liquid sodium is lost by vaporization, the motion of the molten cladding due to sodium vapour flow and the subsequent fuel disintegration is calculated; in non-voided or partially voided channels, the fuel–coolant interaction (FCI) following fuel failure and axial fuel motion are calculated. The behaviour of molten fuel and other materials in the coolant channels following fuel failure is analysed by solving the axial one-dimensional conservation laws of mass, momentum, and energy.

2.2 SIMMER-IV and SIMMER-III

SIMMER-IV and SIMMER-III [6] are computational codes that perform a comprehensive analysis of the nuclear thermohydraulic behaviour of a damaged core. Both codes can simulate a reactor system in three-dimensional Cartesian and two-dimensional cylindrical coordinates, respectively. They are collectively referred to as the SIMMER code, as the physical models in both codes are identical, apart from their geometric calculation systems. The SIMMER code is employed to analyse the propagation of the disrupted area within the reactor core and the consequent reactor power changes in the TP, with a particular focus on the energy generation behaviour due to prompt criticality and the transformation of this energy into mechanical energy by core expansion. The code incorporates a fluid dynamics module to calculate the thermohydraulics of the mixture of degraded core materials, a neutron calculation module to analyse space-dependent kinetics, and a structure module that considers the melting and failure of structures. SIMMER treats core materials such as fuel, steel, sodium, and fission product gas as different components in solid, liquid, and gaseous states. The fluid dynamics module computes multivelocity field flow, multiphase. multicomponent flow, heat and mass transfer between components, and momentum exchange. Solid particles are treated as fluid but are treated separately from liquid components. The structure module calculates heat transfer and melting/solidification/failure behaviour among fuel elements, assembly walls, and fluid, while fluid convection is limited by the presence of intact assembly walls. The neutron calculation module calculates reactivity and power from macroscopic cross-sections based on mass and temperature distribution of the core material, neutron flux distribution based on multigroup

transport theory, and kinetics of the improved quasi-static approximation. In the safety analysis of LMFR, the initial condition of SIMMER is provided by automatic data transformation tool from SAS4A [13].

2.3 AUTODYN

AUTODYN [8] is a commercially available software designed specifically for the calculation of nonlinear time history responses of dynamic events, such as explosions and impacts. The software integrates a computational mesh with Eulerian elements suitable for fluid dynamics analysis of gases and liquids, and a mesh with Lagrangian and shell elements ideal for structural deformation analysis, enabling the computation of interactions between the two mesh types. The versatility of AUTODYN allows for its application to a wide range of explosion and impact scenarios, including those where a fluid pressure source drives surrounding fluid and imparts a pressure load on structural walls. Through the analysis of coupled fluid–structure behaviour, AUTODYN calculates strains and displacements in the structure, taking into account the geometry of the analysed object, structural material properties, and the properties of the applied pressure source. In the safety analysis of LMFR, the code is utilized to assess the effects of mechanical energy produced by a prompt criticality incident on the reactor vessel. The high temperature core material after prompt criticality is treated as a pressure source and its pressure-volume relation is provided to AUTODYN as an input from the preceding analysis of core expansion behaviour by SIMMER.

2.4 PLUG

PLUG serves as a computational tool for modelling the dynamics of the plugs and bolts that comprise a reactor vessel's shielding plug. It also analyses the amount of sodium that is expelled onto the containment floor through the gap between the shielding plugs due to the pressure difference between the top and bottom of the shielding assembly. The PLUG methodology characterizes the individual shielding plugs as rigid bodies and the connecting bolts as elastoplastic bodies, then solves the coupled one-dimensional equations of motion for each plug to determine their relative motion. To determine the amount of sodium ejected from the gap as a result of the relative displacement between the shielding plugs, PLUG employs Bernoulli's equation, using the pressure difference between the reactor vessel and the containment vessel. The input for PLUG is the pressure transients at lower surface of each plug and is given by the preceding analysis of core expansion behaviour by SIMMER.

2.5 CONTAIN-LMR

CONTAIN-LMR [9] performs assessments on a range of phenomena that occur within the containment vessel during a severe accident, including sodium combustion, hydrogen combustion, sodium–concrete reaction, and others, evaluating the type and quantity of radioactive material that may be leaked or released into the environment. The analysis system of CONTAIN-LMR is divided into cells, and the physical quantities within each cell, including pressure, gas temperature/composition, and aerosol concentration, are averaged and calculated. Furthermore, multiple structures within the cell, such as floors, walls, ceilings, and internal structures, can be incorporated into the analysis. As a modular code system, CONTAIN-LMR integrates separate analysis codes for sodium combustion, debris–concrete interaction, sodium-concrete reaction, and hydrogen combustion to offer a comprehensive solution for a broad spectrum of accident assessments within containment vessels.

2.6 Super-COPD

Super-COPD [10] is a general-purpose modular plant dynamics code for LMFRs, with capabilities for analysing the dynamic behaviour of LMFR plants under various transient conditions. It has functions for reactor kinetics, thermohydraulics of the cooling system, operation of dynamic components (valves, pumps, etc.) and the reactor protection system. In addition, the debris bed thermal calculation module, which is integrated into Super-COPD as an independent module, calculates the temperature in the debris bed during the material relocation and heat removal phases.

2.7 FLUENT

FLUENT [11] is a widely utilized commercial computational code that offers diverse physical models for analysing heat and fluid flow, chemical reactions, and heat transfer in various engineering problems. Its applications range from air flow around aircraft wings, combustion phenomena in combustion reactors and bubble towers, to thermohydraulics analysis in nuclear reactors and semiconductor manufacturing processes, as well as clean room design. FLUENT has also been utilized to evaluate various thermohydraulic issues in sodium cooled fast reactor plants, making it a valuable tool for safety analysis in fast reactors. Specifically, the code is employed to analyse the temperature changes of various structural materials resulting from the thermohydraulics of the coolant within the reactor vessel [14].

3. CONFIRMATION OF APPLICABILITY OF ANALYSIS METHOD TO SAFETY ANALYSIS

This section describes the confirmation of the applicability of the SIMMER code, a crucial component of the calculation codes previously discussed, to fast reactor safety analysis as an example of the similar confirmation procedures for the other codes. The applicability of the calculation codes to the safety analysis of LMFR plants is confirmed by identifying important phenomena that dominate event progressions, validating the models of the analysis codes for the important phenomena, and examining the applicability of the codes based on the validation results.

3.1 Physical phenomena in the event progression in transition phase and assessment index

In the TP of a CDA in a fast reactor, which is the focus of the SIMMER code analysis, the event progression is depicted as shown in Fig. 2, where the parenthesized numbers indicate the physical phenomena impacting the progression. First of all, the event progression is dominated by (1) the neutronic behaviour of disrupted core. In the early stages of the TP, a void reactivity is inserted by (2) sodium voiding. As the reactor power is maintained, the area of fuel pin disruption by (3) fuel pin melting and failure gradually propagates by (5) wrapper tube melting and failure, and positive reactivity is inserted as the disrupted fuel densely accumulates by gravity. The (4) fission product gas release may affect the fuel concentration behaviour. The increase of nuclear power accelerates the failure of the remaining fuel elements, eventually leading to the formation of whole core scale disruption.

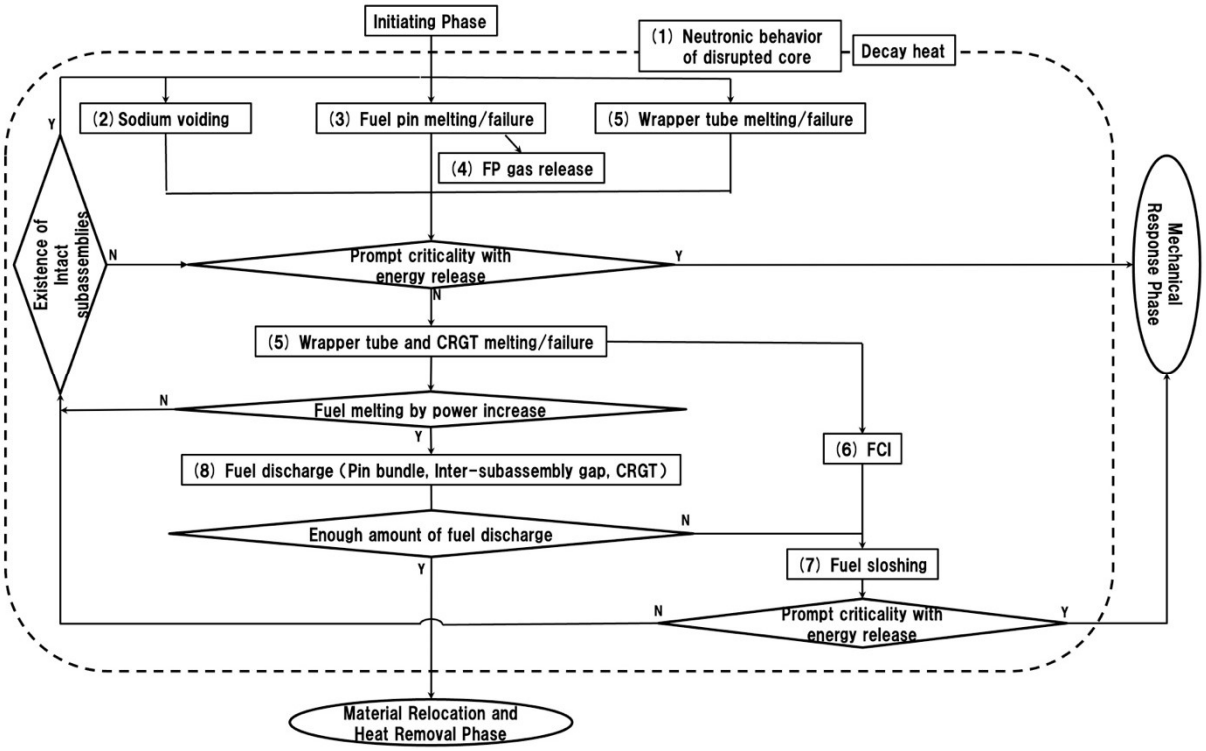

FIG. 2. Event progression in the Transition Phase and related phenomena.

Positive reactivity is inserted by the accumulation of disrupted fuel in the lower part of the core as a result of gravity settling over a wide area, forming a molten pool. In the molten pool, a fuel cohesive motion, i.e. (7) fuel sloshing, may result in a prompt criticality, leading to a large energy release. Negative reactivity is inserted due to (8) fuel discharge into the pin bundle channels above and below the core, or into the inter-assembly gap outside the core. On the other hand, positive reactivity may be inserted due to radial fuel concentration caused by sodium vapour pressure by (6) FCI when molten fuel contacts with residual coolant in the core periphery. If the negative reactivity insertion by fuel discharge from the core prevails and deep subcriticality is reached, the nuclear event progression in the TP will terminate.

If the insertion of positive reactivity due to fuel concentration prevails, it may result in an excessive level of reactivity and prompt criticality, leading to a rapid release of thermal energy through what is referred to as a power excursion and/or energetics. As a result of this very rapid power excursion, the fuel within the core experiences nearly adiabatic heating, and the rise in fuel temperature can serve as a gauge of the magnitude of released thermal energy and represent the potential for mechanical energy generation in the subsequent MRP. In other words, the core average fuel temperature can be utilized as a figure of merit in subsequent processes to identify important phenomena in the analysis of TP.

On the other hand, with respect to the thermal effects of CDA, the distribution and state of core materials are necessary for analysis in the subsequent Material Relocation and Heat Removal Phase. As the TP event progresses, a portion of the molten core fuel may flow out of the core along various flow paths, as described previously. The amount of fuel discharge from the core is a determinant of the potential for prompt criticality and the initial conditions for the Material Relocation and Heat Removal Phase, thus serving as a figure of merit in identifying the important phenomena of TP.

3.2 Extraction of important phenomena

The physical phenomena affecting the event progression discussed in the preceding section were categorized as "High" (H), "Moderate" (M) or "Low" (L) based on the definitions provided in Table 1. This classification was determined by the extent of their impact on the core average fuel temperature and the amount of fuel discharge from the core, which serve as figure of merit for TP. Phenomenon with a classification of "High" or "Moderate" for either figure of merit was considered to be important phenomenon.

TABLE 1. DEFINITION OF RANK

Rank	Definition of rank	Treatment in the confirmation of applicability of the analysis code
H	Phenomena that are considered to have a significant impact on event progressions	The uncertainty associated with physical phenomena is determined through the comparison of experimental results and sensitivity analysis. The effect of the uncertainty on figures of merit in the safety analysis of nuclear plant is evaluated accordingly.
M	Phenomena that are considered to have a moderate impact on event progressions	Although the phenomenon plays a certain role in simulating event progressions, it is a physical phenomenon whose impact on figures of merit is less pronounced than that of "H". Nevertheless, this study evaluates the impact of uncertainty on the figure of merit through sensitivity analysis similarly to the assessment of "H."
L	Phenomena that are considered to have a small impact on event progressions	Since this is a physical phenomenon that clearly has a small impact on the figures of merit, the verification/validation assessment is not needed.

The core average fuel temperature rapidly increases due to nuclear heating during prompt criticality, which occurs upon the spatial concentration of fuel. Large scale fuel concentration, resulting in a severe prompt criticality, is driven by the generation of localized pressure in whole core molten pool. The energy release by prompt criticality ends on the quantity of fuel participating in the concentration and the velocity of concentration. Hence, the ranking of physical phenomena with regards to the "core average fuel temperature", a figure of merit in the TP, can be determined by evaluating the impact of each phenomenon on fuel concentration quantity and concentration velocity during the formation of the whole core pool.

On the other hand, fuel discharge from the core during the TP occurs when the molten fuel accesses discharge paths. These paths include the CRGTs, the pin bundle channels at the top and bottom of the fuel assembly, and the gap between assemblies of the radial reflector/shielding surrounding the lateral side of the core. The physical phenomena having influence on the behaviour of the core material in the discharge paths are likely to have a substantial impact on "the quantity of fuel discharge from the core", another important metric in the TP.

The following are the outcomes of the discussion based on the above-mentioned ranking methodology for each phenomenon that affects event transition. Given the page limit, this

section presents a discussion of only three representative phenomena selected from Section 3.1, ranked as "L," "M," or "H," respectively. It should be noted that the numbers in parentheses correspond to the numbers depicted in Fig. 2.

(1) Neutronic behaviour of disrupted core.

Reactivity and reactor power exhibit dynamic variations that are contingent upon the time-dependent distribution and temperature of materials. This physical phenomenon has a certain influence in determining the core average fuel temperature, and its impact is considered moderate ("M"). Conversely, its influence on fuel discharge from the core is minimal ("L").

(2) Sodium voiding.

This physical phenomenon pertains to the rapidity of core damage progression due to the insertion of void reactivity, which arises from the expansion of the coolant boiling region and the loss of its role as a coolant. Nevertheless, upon the formation of a molten core pool that leads to extensive fuel concentration, there is no direct impact on fuel concentration as nearly all of the core's coolant has become voided. As such, the significance of this physical phenomenon is considered low ("L").

(6) FCI.

This physical phenomenon refers to the generation of coolant vapour pressure resulting from the direct heat exchange between the coolant and hot core materials, caused by the failure of structural components such as the CRGTs and assembly walls, as well as by the inflow of coolant from the lower and upper peripheries of the core. This phenomenon can induce fuel sloshing and affect the concentration of fuel, accompanying reactivity changes, and thereby impacting the core average fuel temperature significantly ("H").

Based on the results of the aforementioned ranking, the following important phenomena were extracted: (1) nuclear behaviour of the damaged core, (5) structural wall melting and failure, (6) FCI, (7) fuel sloshing, and (8) fuel discharge, where their effect on the relevant figures of merit was rated as high ("H") or moderate ("M"). The methodology for extracting important phenomena based on their impact on figures of merit is analogous to that used in the PIRT [15]. However, while PIRT incorporates not only the impact of the phenomena on figures of merit, but also the current level of knowledge, as criterion to prioritize future research needs, this methodology only employs the impact of the phenomena as the criterion, given that the current objective is to extract important phenomena to confirm the applicability of the SIMMER code.

3.3 Validation of the SIMMER code on the important phenomena

The validity of the SIMMER code was confirmed for the important phenomena identified in the previous subsection through conducting analyses of existing in- and out-of-pile experiments. Table 2 presents a list of these important phenomena and the experiments for which validation was performed. Due to page limitations, only the validation results for (6) FCI are described here as a representative example, since FCI directly affects energy generation in the TP, with the discussion on the applicability of SIMMER to the FCI in the safety analysis of an LMFR plant.

TABLE 2. LIST OF EXPERIMENTS TO VALIDATE SIMMER ON IMPORTANT PHENOMENA

Phenomena with high impact on figures of merit	Experiments for Validation Analysis
(1) Neutronic behaviour of damaged core	FCA VIII-2 experiment [16]
(5) Melting and failure of structural wall	EAGLE in-pile experiments [17]
(6) FCI	THINA experiment [18]
(7) Fuel sloshing	Sloshing behaviour experiment [19]
	High liquid–vapour density ratio two-phase flow experiment [20]
	SCARABEE BF2 experiment [21]
(8) Fuel discharge	GEYSER experiment [22], THEFIS experiment [23]

In SIMMER, the FCI coolant vapour pressure is calculated as a result of the vaporization due to heat transfer from the fuel to the coolant. The heat transfer rate is calculated from the temperature of each material, empirical heat transfer coefficient, and the interfacial contact area between them, which are determined by multiphase, multicomponent, multivelocity field hydrodynamics analysis within the framework of SIMMER. Although it is not possible to measure the interfacial area, inter-component heat transfer, nor mass transfer in the test, our focus was on the pressure transients associated with the generation of coolant vapour as a result of the integration of these physical phenomena, which is of prime importance in FCI.

3.3.1 Validation analysis using THINA experiment

THINA experiment is an out-of-pile simulation that aims to replicate FCI by introducing a high temperature melt generated through thermite reaction into a sodium pool from the bottom. As depicted in Fig. 3, the cylindrical vessel with an inner diameter of 30 cm and a height of 5 m and was filled with 150 kg of sodium at an initial temperature of 770 K. The sodium was filled with argon gas at a pressure of 0.11 MPa, and a high temperature melt, with an initial temperature of 3,270 K and a mass of 5.5 kg, simulating the molten core material, was injected into the sodium pool through a 3 cm inner diameter tube at a pressure of 2.5 MPa.

The sodium pool pressure at a height of 10 cm and cover gas pressure at a height of 4 m as evaluated by SIMMER are compared with experimental results in Fig.3. The experiment reveals that sodium vaporization, which is a result of the contact between the hot melt and the coolant, frequently gives rise to sharp time-dependent pressure peaks between 1 and 1.2 s. On the other hand, in the cover gas region, the pressure increases relatively gradually due to the generation of sodium vapour at the bottom of the pool, bubble generation and expansion in the sodium pool, sodium level rise, and compression by sodium surface. The pressure peaks after 1.6 s in the sodium pool are attributed to compression by sodium slug, as the sodium, once lifted by sodium vapour, descends due to sodium condensation.

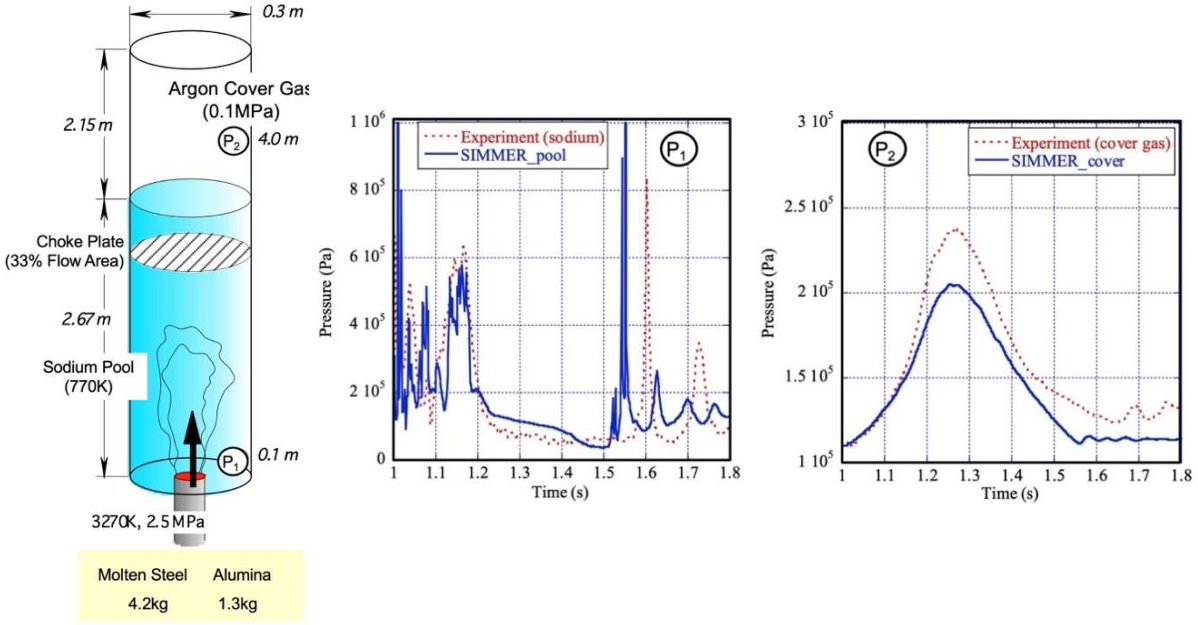

FIG. 3. Schematic of THINA experiment and the comparison of pressure transients.

The magnitude and timing of the sharp pressure peaks in the sodium pool, as observed in the experiment, in the left graph of Fig. 3, are susceptible to slight variations in the test conditions. Despite such uncertainty, the results of the test analysis accurately reproduce the onset time within an error range of the order of 10^{-2} to 10^{-3} s, with a tendency to slightly overestimate the pressure peak. The onset time of the pressure peak is also reproduced in the cover gas region, as depicted in the right graph of Fig. 3, which signifies that the motion of the sodium slug, driven by the sodium vapour generated through fluid-to-fluid heat transfer calculations, is realistically simulated. The higher experimental value of the cover gas pressure is presumed to be a result of the inflow of non-condensable gas along with the high temperature melt. If this factor is taken into account, the simulation results are within a 10% error range.

The outcome that the pressure transient in the sodium pool and the cover gas pressure are effectively replicated implies the adequacy of SIMMER's physical models associated with evaporation/condensation, liquid-to-liquid heat transfer, and multicomponent, multiphase fluid dynamics, further indicating the applicability of SIMMER to the simulation of FCI in the TP of LMFR.

3.3.2 Discussions on the uncertainty related to FCI

Although SIMMER has a tendency to slightly overestimate the pressure values generated in the sodium pool, it can approximately reproduce the order of magnitude of the pressure values based on the THEFIS simulation. On the other hand, FCI affects the core average fuel temperature by inducing fuel sloshing which may result in large fuel concentration and prompt criticality. The FCI phenomenon in the TP itself has a large uncertainty on its magnitude and occurrence timing, as the structure wall failure and the contacting geometry of fuel and coolant, which are the precondition phenomena for FCI, have also a large uncertainty. In addition, it is difficult to conduct demonstrative experiment of fuel sloshing caused by FCI around the core utilizing reactor materials. As such, the application of SIMMER to the FCI in the TP should

use conditions that conservatively encompass the uncertainty of FCI, which is discussed here, in the safety analysis of LMFR plants.

THINA experiment is also concerned with the generation of mechanical energy in the MRP. The pressure generation and cover gas compression behaviour observed in the test were properly analysed by SIMMER. In addition, the situation of FCI occurrence in THINA experiment is analogous to the FCI phenomena in the MRP, in which hot molten material is injected from the bottom of sodium pool, and therefore, it is concluded that SIMMER is applicable for the analysis of the mechanical energy generation in the MRP with small uncertainty.

4. CONCLUSION

An analytical methodology for CDA of LMFRs has been developed to conform the requirements of the Japanese new regulatory standards. The methodology encompasses the entire CDA event sequences, from initiation to termination, by integrating existing plant dynamics code, commercial code, empirical correlations, and a safety analysis code that evaluates event progression in the CDA. This methodology can demonstrate the efficacy of CDA mitigation measures, taking into account the impact of uncertainties associated with important physical phenomena governing the progression of the accident.

In this paper, the procedure for confirming the applicability of the methodology for analysing CDA in LMFR is described, with a focus on the SIMMER code, which plays a dominant role in the methodology. The procedure involves extracting important phenomena based on their magnitude of impact on event progression during the CDA transition phase. Subsequently, validation analyses were performed on the SIMMER code for these important phenomena to affirm its applicability and to identify uncertainties that their influence on the analytical results of SIMMER needs to be assessed in the safety analysis of the LMFR plant.

The applicability of the methodology was not only confirmed for SIMMER, but also for other analysis codes that make up the comprehensive analysis methodology for all event progressions in CDA. The analytical methodology described in this paper lays a foundation for conducting safety assessments of LMFR plants during the licensing procedure under the new regulatory standards in Japan.

REFERENCES

[1] OKRENT, D., On the History of the Evolution of Light Water Reactor Safety in the United States of America, US NRC/ACRS document, ML090630275 (1977).

[2] FUJII-E, Y., History of Fast Reactor Safety in Japan, Proc. the 1990 Int. Fast Reactor Safety Meeting, Snowbird, Utah, U.S.A., August 12–16 (1990).

[3] KUSSMAUL, G., et al., The CABRI Project-Overall Status and Achievements, Proc. of Science and Technology of Fast Reactor Safety, Guernsey, Vol. I., p.103 (1986).

[4] WRIGHT, A.E., et al. Fast Reactor Safety Testing in TREAT in the 1980s, Proc. Int. Fast Reactor Safety Meeting, Snowbird, Vol. II, p.233 (1990).

[5] TENTNER, A. M., et al., The SAS4A LMFR Whole Core Accident Analysis Code, Proc. International Meeting on Fast Reactor Safety, pp.989-998, Knoxville, TN (1985).

[6] TOBITA, Y. et al., The Development of SIMMER-III, An Advanced Computer Program for LMFR Safety Analysis and Its Application to Sodium Experiments, Nuclear Technology, Vol. 153, No. 3, pp. 245-255 (2006).

[7] Overview Draft New Safety Standards for Nuclear Power Stations NRA, Japan, January 2013. https://www.nra.go.jp/data/000067120.pdf

[8] ANSYS, Inc., ANSYS AUTODYN user's manual: release 15.0, Pennsylvania, USA (2013).

[9] MURATA, K. K., et al., CONTAIN LMR/1B-Mod.1, A Computer Code for Containment Analysis of Accidents in Liquid-Metal-Cooled Nuclear Reactors, SAND91-1490・UC-610, Jan. 1993.

[10] YAMADA, F. et al., Development of Natural Circulation Analytical Model in Super-COPD Code and Evaluation of Core Cooling Capability in Monju During a Station Blackout, Nuclear Technology, Vol.188, No. 3, pp. 292-321 (2014).

[11] ANSYS, Inc. ANSYS Fluent User's Guide, Release 17.2 (2016).

[12] Suzuki, T., et al., A PRELIMINARY EVALUATION OF UNPROTECTED LOSS-OF-FLOW ACCIDENT FOR A PROTOTYPE FAST-BREEDER REACTOR, Nuclear Technology, Vol. 47, pp. 240-252 (2015).

[13] Tobita, Y., et al., Development of SAME-II: A Connection Code between SAS4A and SIMMER-III, JNC TN9400 2002-018 (in Japanese), March (2002).

[14] Tanaka, M., et al., Numerical Investigation of Thermal Striping near Core Instruments Plate around Control Rod Channels in JSFR, Proc. of 13th Int. Topical Meeting. on Nuclear Reactor Thermal Hydraulics, N13P1190 (2009).

[15] Phenomena Identification and Ranking Table, OECD NEA No.7443, 2018.

[16] NAKANO, M., et al., An Experimental Study of Reactivity Changes and Flux Distortion in Simulated LMFR Meltdown Cores, Nuclear Science and Engineering, Volume 87, pp. 283-294 (1984).

[17] KONISHI, K., et al., The result of a wall failure in-pile experiment under the EAGLE project, Nuclear Engineering and Design, pp 2165-2174, Volume 237, Issue 22, November (2007).

[18] HUBER, F., et al., EXPERIMENTS TO THE BEHAVIOR OF THERMITE MELT INJECTED INTO A SODIUM POOL, Proc. Int. Fast Reactor Safety Meeting, Volume II, pp.407-416, Snowbird USA (1990).

[19] MASCHEK, W., et al., Simulation Experiments for Centralized Liquid Sloshing Motions, KfK 5090 (1992).

[20] MISHIMA, K., et al., Visualization and Measurement of Gas-Liquid Two-Phase Flow with Large Density Difference Using Thermal Neutrons as Microscopic Probes, Nuclear Instruments and Methods in Physic Research A, Vol. 424, pp.229-234 (1999).

[21] Seiler, J. M., et al., Synthesis on research on boiling pool thermal hydraulics at CEA and KFK, IAEA meeting O-Arai, Japan, June (1994).

[22] SCHWARTZ, M., et al., Interpretation of out-of-pile experiments on the propagation and freezing of molten fuel, Proc. 13th Meeting of the Liquid Metal Boiling Working Group," Winfrith, p.878, September (1988).

[23] FIEG, G., et al., Penetration and freezing phenomena of ceramic melts into pin bundles, Proc. International Fast Reactor Safety Meeting, Snowbird, Volume 3, p.387 (1990).

GLOSSARY

Energetics	Rapid release of thermal energy by prompt criticality that may affect the integrity of primary boundary
Figure of merit	Quantity used to characterize the performance of a device, system or method, relative to its alternatives
Prompt criticality	Nuclear fission event in which criticality is achieved with prompt neutrons alone
Unprotected	Failure of reactor scram

3D THERMOHYDRAULICS-NEUTRONICS SIMULATION OF SFR CORE DEGRADATION WITH THE SEASON FRENCH PLATFORM

E. DUFOUR[1], P. GUBERNATIS[1], L. TROTIGNON[1]
[1]CEA, DES, IRESNE, DTN, SMTA, LMAG, Cadarache, F-13108 Saint-Paul-lez-Durance, France

Abstract

SEASON is a new platform developed by the French Alternative Energies and Atomic Energy Commission (CEA) in order to simulate the core degradation of sodium cooled fast reactors (SFRs) during severe accident transients. It relies on a multichannel formulation of the SIMMER-V thermohydraulics and core degradation code. It involves the chaining of SIMMER-V with a fuel performance code (GERMINAL or SAS-SFR) as well as couplings of SIMMER-V with a spatial neutronics code (PARIS which uses a flux solver that can be SNATCH, PARTISN or IDT) and a code modelling the primary circuit (SIMMER-V or CATHARE). Contrary to the former computational scheme for calculating a severe accident transient, SEASON allows to calculate the initiating phase and the generalized degradation phase of the accident with the same SIMMER-V code by considering respectively a multichannel description of the core and a full core description. It manages the transition between multichannel and full core calculations, with thermohydraulics coupled to neutronics. The paper describes the architecture and the main features of the current version 4.2 of the platform. An example of calculation of an unprotected loss of flow (ULOF) transient in an SFR simplified design core is provided. Eventually, perspectives for the future development of the platform are given.

1. INTRODUCTION

In the framework of the Generation IV R&D programme on sodium cooled fast reactors (SFRs), CEA is involved with its partners — for example, the Japan Atomic Energy Agency (JAEA) — in the development of computational tools devoted to the simulation of the core degradation during severe accident transients. The objective of the paper is to present the new SEvere Accident SimulatiON (SEASON) platform whose development began in the framework of the implementing arrangement between CEA, AREVA, JAEA, MHI and MFBR (2014–2019).

The SEASON platform is dedicated to the simulation of SFR core degradation during severe accident transients, from the initial state of the irradiated core until the relocation phase of the corium towards the core catcher. It is based on a multichannel formulation of the SIMMER-V thermohydraulics and core degradation code. It involves the chaining of SIMMER-V with a fuel performance code (GERMINAL or SAS-SFR) as well as couplings of SIMMER-V with a spatial neutronics code (PARIS which uses a flux solver that can be SNATCH, PARTISN or IDT) and a code modelling the primary circuit (SIMMER-V or CATHARE in preparation).

Contrary to the former computational scheme based on the chaining of the SAS-SFR and SIMMER codes for calculating a severe accident transient (Fig. 1), SEASON allows to calculate the initiating phase and the generalized degradation phase of the accident with the same SIMMER-V code by considering respectively a multichannel description of the core (which offers a good computing performance as long as the channels evolve thermohydraulically independently) and a full core description. This allows to perform a more easily achievable transition between the multichannel calculation of the initiating phase and the full core calculation of the generalized degradation phase and offers at the same time a better coherency of the whole sequence treatment.

In the paper, the architecture and the main features of the current version 4.2 of the SEASON platform are described. Then, an example of calculation of the complete sequence of degradation (the initiating phase computed in the multichannel approximation and the transition to the core-wide degradation phase) coupled to neutronics is provided. This example is an unprotected loss of flow (ULOF) transient in an SFR simplified design core in 3D Cartesian geometry. Finally, perspectives for the future developments of the SEASON platform are given.

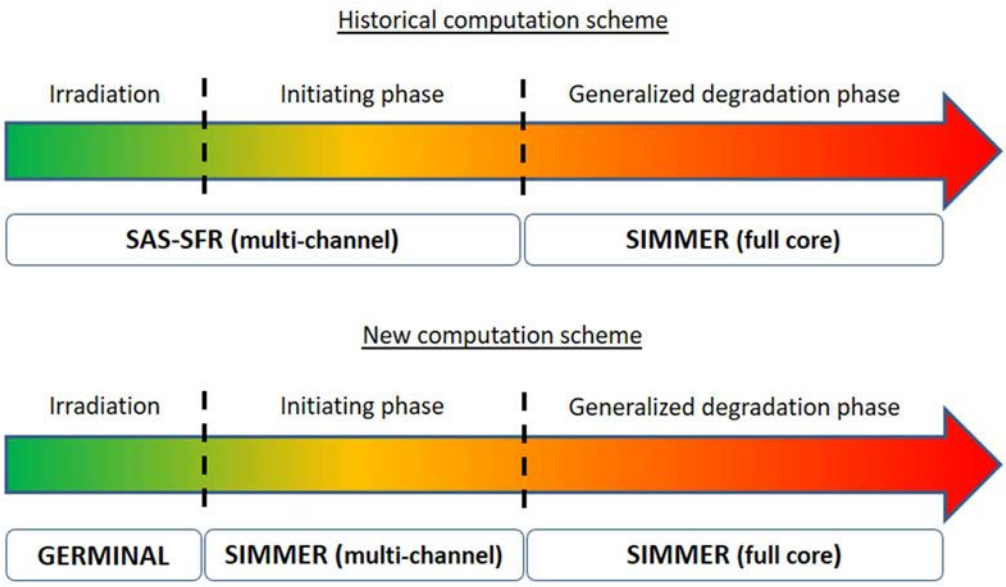

FIG. 1. Historical and new computational schemes for calculating a severe accident transient in an SFR.

2. DESCRIPTION OF THE SEASON PLATFORM (version 4.2)

The architecture of the SEASON platform is shown in Fig. 2.

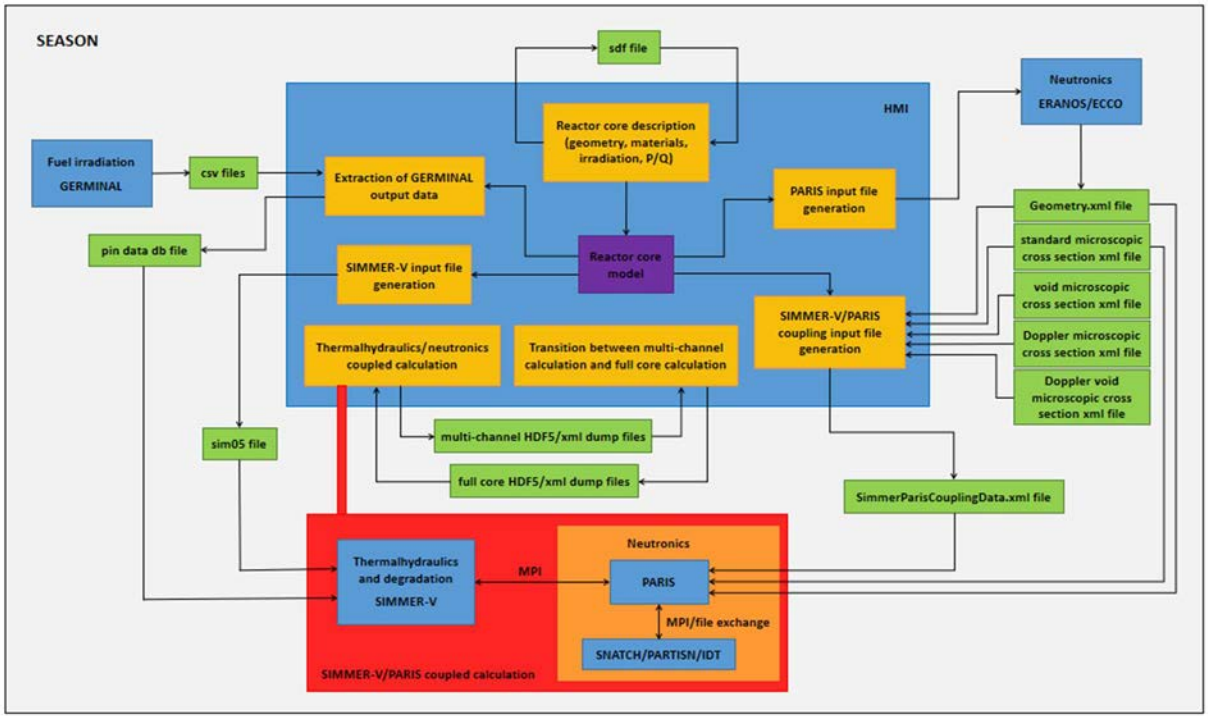

FIG. 2. Architecture of the SEASON platform.

The SIMMER-V code [1] is a fundamental component of the SEASON platform. SIMMER-V is a three-dimensional multivelocity field, multiphase, multicomponent, Eulerian, fluid dynamics code coupled with a fuel pin model and a space- and energy-dependent neutron transport kinetics model. It is co-developed by CEA and JAEA within the framework of the implementing arrangement between CEA, FRAMATOME, JAEA, MHI and MFBR (2020-2024). JAEA is owner of the SIMMER-V code. SIMMER-V was derived from

SIMMER-IV [2], a three-dimensional code based on the two-dimensional SIMMER-III [3] technology, with the objective of improving numerical performance and addressing in a more precise and consistent way the whole severe accident sequence from the initiating phase. SIMMER-V benefits from (a) an in-development detailed model of fuel pin degradation (called DPIN3) and a precise description of Pu isotope vector in order to describe irradiated fuel and in-pin fuel motion, (b) a MPI (domain decomposition) thermohydraulics parallelization, (c) an OpenMP neutronics parallelization, (d) a dynamical memory allocation, (e) in-development standardized interfacing capabilities allowing the code to dialog and get coupled with other codes. Within the SEASON platform, the SIMMER-V internal neutron kinetics and transport model is not used, but an external neutronics code (PARIS which uses a flux solver that can be SNATCH, PARTISN or IDT) is coupled to SIMMER-V.

The SEASON platform is based on a new tool that consists of a multichannel formulation of the SIMMER-V code. It allows to calculate the initiating phase of a severe accident by considering a multichannel modelling of the core. In this approach, the core is represented by a partition of the core into several thermohydraulic channels. These channels are thermally independent and each channel is computed separately by a different run of the SIMMER-V code. The geometry of a channel can correspond either to a single assembly containing an average fuel pin representative of the bundle or several fuel pins (such a channel is called a 'simple channel'), or to a group of contiguous assemblies with one or more representative fuel pins per assembly (such a channel is called an 'extended channel' and will allow the representation of a local accident — as a total instantaneous blockage (TIB) — on a group of assemblies). At this stage of development of the platform, the channels are simulated with user-imposed conditions at axial boundaries of the core. They will be connected to the primary circuit in a future version of the platform due to the ongoing development of two types of thermohydraulic boundary coupling in SIMMER-V: on the one hand, an internal and total SIMMER-V boundary coupling and, on the other hand, a hybrid boundary coupling (SIMMER-V + another code such as CATHARE [4]).

The different channel degradation calculations performed with SIMMER-V are coupled to a single spatial neutronics calculation, performed by the PARIS code [5], using an MPI environment [6–8]. PARIS initially used the SNATCH flux solver [9]. In the framework of a collaboration with KIT (ARDECO project), the parallelized neutron flux solver PARTISN [10] was implemented in SEASON as an alternative to SNATCH [11]. PARIS can drive these two flux solvers. The interface between the neutronics kinetics and the neutronics flux solver was generalized. Owing to this, the implementation of another flux solver is greatly facilitated. In addition, the introduction of the high performance parallel flux solver IDT [12] in SEASON is currently underway and a first operational version of the coupling between SIMMER-V and PARIS/IDT using a file exchange is available and being tested. The neutronics computing process was also improved. In particular, the flowchart of the neutronics process was adapted in order to be very close to the process in SIMMER-V (native computation of the neutronics in SIMMER-V by the GRIND module). At this stage of development, only the shielding process is missing in SEASON. This point is under investigation together with the question of the update of the cross-sections during the degradation. In addition, the time management for the coupling between neutronics and thermohydraulics was improved. The amplitude variation of the power between two rendezvous times was linear until now. The new scheme allows now to consider a higher order time definition of the amplitude.

The SEASON platform allows to take into account the state of irradiation of the fuel pins (as initial condition before degradation) using the GERMINAL code [13]. The irradiation phase is externally calculated by GERMINAL for each representative fuel pin of the core. The chaining

between irradiation and degradation is managed by a SEASON functionality that processes the GERMINAL results and stores in a SQL database the properties of the fuel pins for different states of irradiation. This database is then directly read by SIMMER-V to initialize the degradation phase. SEASON uses the cycle number of each assembly (as defined by the core reloading) to identify the instant in the irradiation history of its fuel pins. The extension of the irradiation–degradation chaining to the irradiation module of the SAS-SFR code [14] was done in order to possibly replace GERMINAL. The irradiation–degradation chaining will be adapted to the ongoing developments of the detailed pin degradation model DPIN3 of SIMMER-V in a future version of the platform.

The SEASON platform relies on a central module called HMI that is a graphical user interface, specifically designed for the reactor core representation constructed on a serializable specific data model. The graphical interface allows the user to define the core (geometry and materials at a given reference thermal state, irradiation, power, flow rate) and to perform the partitioning of the core into channels based on several criteria (assembly geometry, assembly cycle number, power overflow rate ratio in the assembly). The HMI module offers three other important services. First, it allows the pre-processing of the SIMMER-V/PARIS coupled calculation of the severe accident transient: (a) the creation of the irradiated fuel pin database from GERMINAL calculation results, (b) the calculation of the neutronics cross-sections for the nominal core geometry using the ECCO/ERANOS code [15], (c) the generation of large parts of the SIMMER-V input files (sim05 files) for the various channel calculations, (d) the generation of the "SimmerParisCouplingData.xml" input file for the coupling between thermohydraulics and neutronics. Then, it allows to run a multichannel or full core SIMMER-V/PARIS coupled calculation. And finally, it manages the transition between the multichannel calculation of the initiating phase of the accident and the full core calculation of the generalized degradation phase.

Fig. 3 shows the principle of the transition between multichannel and full core simulations with thermohydraulics coupled to neutronics. (1) SEASON generates the input data (sim05 and xml files) for both the full core calculation and the multichannel calculation. (2) Steady state full core and multichannel calculations, with thermohydraulics coupled to neutronics, are performed by SEASON. A HDF5 dump file of the full core calculation is generated after the initialization or later at the steady state. (3) Only the multichannel calculation of the initiating phase is performed by SEASON until the stopping criterion. Currently, the multichannel calculation is stopped as soon as one of the can walls located on the periphery of the simulated domain completely breaks up in one of the SIMMER-V channels. This stopping criterion is suitable for 'single' channels as well as for 'extended' channels. The HDF5 dump files of the different channels are generated just shortly before the first assembly can wall break-up. (4) At this point, SEASON merges the different HDF5 dump files of the multichannel calculation into the corresponding full core HDF5 dump file. The unique neutronics dump file (.xml file) of the multichannel calculation is also converted to a full core dump file. More precisely, the unique neutronics dump file of the multichannel calculation contains a multichannel description of the core and SEASON rearranges the file in order to have a description that corresponds to the full core. (5) Then, SEASON starts the full core calculation of the generalized degradation phase.

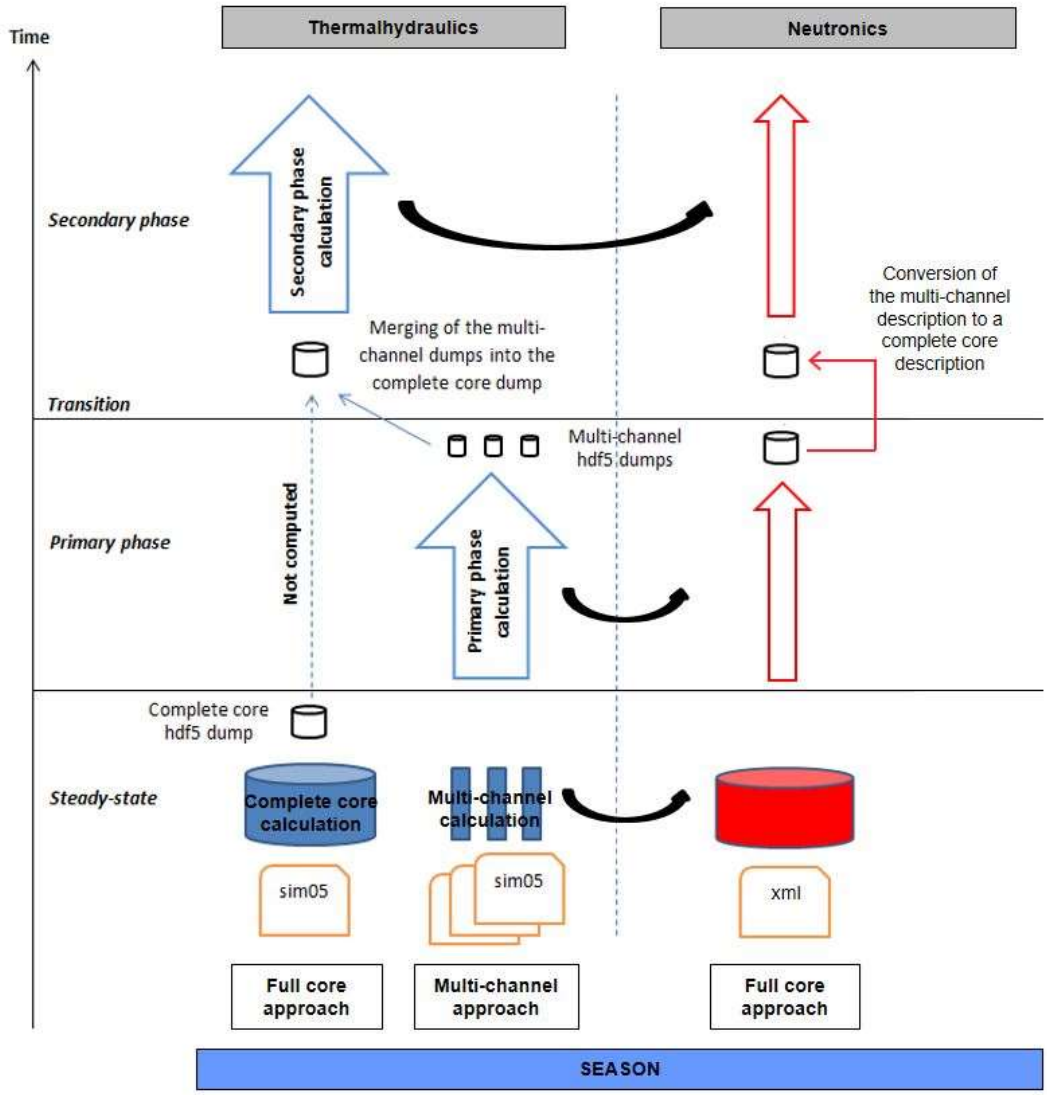

FIG. 3. Principle of the transition between the multichannel calculation of the initiating phase of the accident and the full core calculation of the generalized degradation phase, with thermohydraulics coupled to neutronics.

At this stage of development, the transition procedure is operational for 'simple' channels having meshes that match exactly the full core mesh. It is foreseen to extend the transition procedure to cases with one or several 'extended' channels and cases with different meshes for the multichannel calculation and the full core calculation.

A functionality that allows to run the full core calculation of the generalized degradation phase in a multiprocessor mode after the transition is under development. This functionality is based on the domain decomposition procedure of SIMMER-V. It generates, from the unique full core HDF5 dump file obtained by the merge of the different HDF5 dump files of the multichannel calculation, several HDF5 dump files corresponding to the decomposition of the simulated domain.

3. APPLICATION CASE: 3D CALCULATION OF AN ULOF TRANSIENT ON A SIMPLIFIED CORE

The application case presented in the paper covers the complete sequence of an ULOF transient (the initiating phase computed in the multichannel approximation and the transition to the

core-wide degradation phase) in a simplified SFR core in 3D geometry with thermohydraulics coupled to neutronics. This simplified core is a core invented to demonstrate the capabilities of the SEASON platform.

Fig. 4 (left) gives the radial cut of the simplified core built in the graphical interface. It is composed of 217 assemblies and contains 3 types of assembly: ZC1 (yellow) and ZC2 (pink) are respectively inner core and outer core fuel assemblies while ZREFL (grey) represent reflector assemblies. Fuel assemblies contain axially homogeneous fissile fuel pins, a longer fissile zone for the outer core and a sodium plenum above the fissile area. Table 1 gives the main characteristics of the core and fuel assemblies.

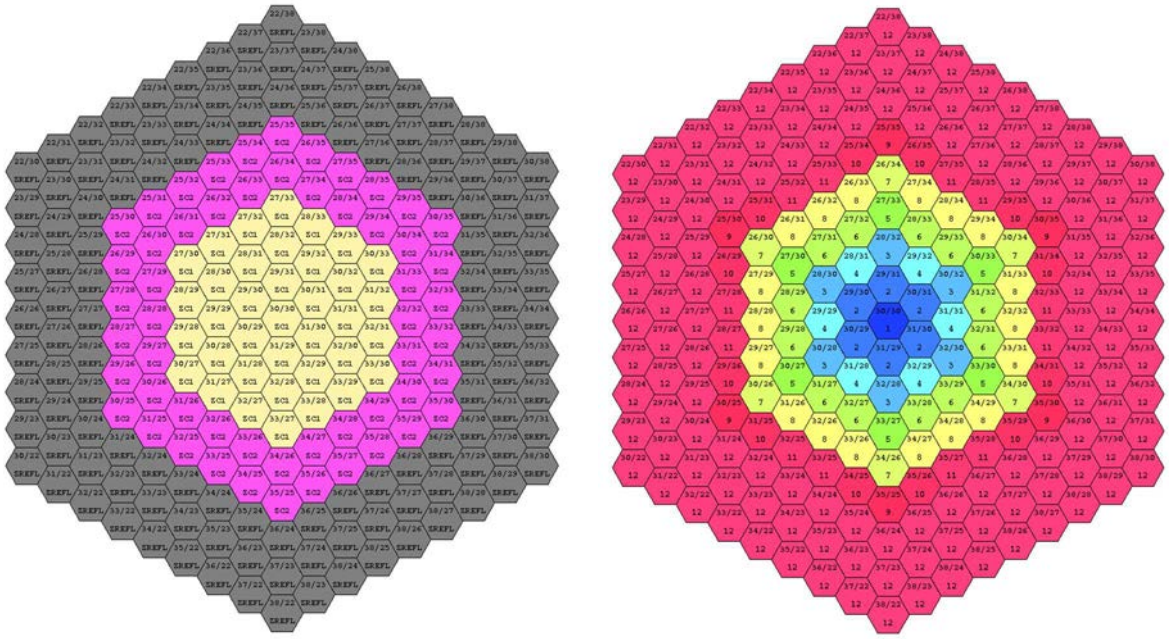

FIG. 4. Application case – Left: Radial cut of the core showing the different assembly types. Right: Partitioning of the core into 12 'simple' channels.

TABLE 1. APPLICATION CASE – MAIN CHARACTERISTICS OF THE REACTOR CORE AND THE FUEL ASSEMBLIES

Core characteristics	Valu
Nominal thermal power (MW(th))	450
Inner fissile zone height (cm)	105
Outer fissile zone height (cm)	135
Assembly pitch (cm)	17.8
Inter-assembly coolant thickness	0.6

Fuel assembly characteristics	Value
Hexagonal tube thickness (cm)	0.5
Number of fuel pin rings	8
Fuel pin pitch (cm)	1.22
Central hole diameter (cm)	0.24
Fuel pellet diameter (cm)	0.994
Fuel/cladding gap (cm)	0.0125
Cladding thickness (cm)	0.05

For the multichannel calculation, assemblies are gathered according to their geometry and their power overflow rate ratio. The core is then partitioned into 12 'simple' channels as shown in Fig. 4 (right).

The multichannel and full core SIMMER-V simulations are performed using an ortho-hexagonal approach. In this approach, the hexagonal pattern of assemblies is modelled in a Cartesian grid using staggered rectangular assemblies (Fig. 5). This approach enables to keep

consistent mass, distance and neighbourhood between the hexagonal pattern and the Cartesian grid. Each assembly is discretized with 1 mesh cell in X direction, 2 mesh cells in Y direction and 30 mesh cells in the axial direction Z. The number of computational mesh cells for the full core calculation is 17 x 34 x 30 (X, Y and Z direction respectively). Fig. 6 gives a view of the discretization of the full core (note that green dotted lines outside the core mark out mesh cells excluded from the calculation). Meshes of the different channels match exactly the full core mesh.

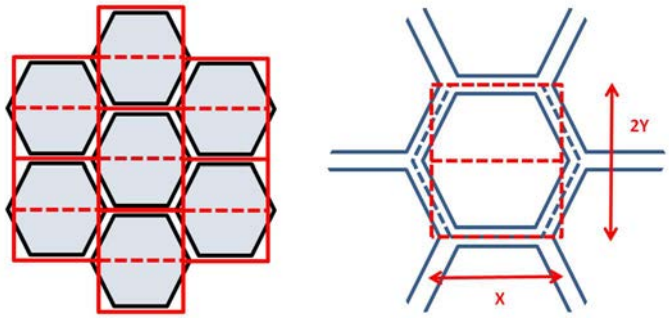

FIG. 5. Application case – X-Y-Z Cartesian geometry: ortho-hexagonal approach with two mesh cells per assembly.

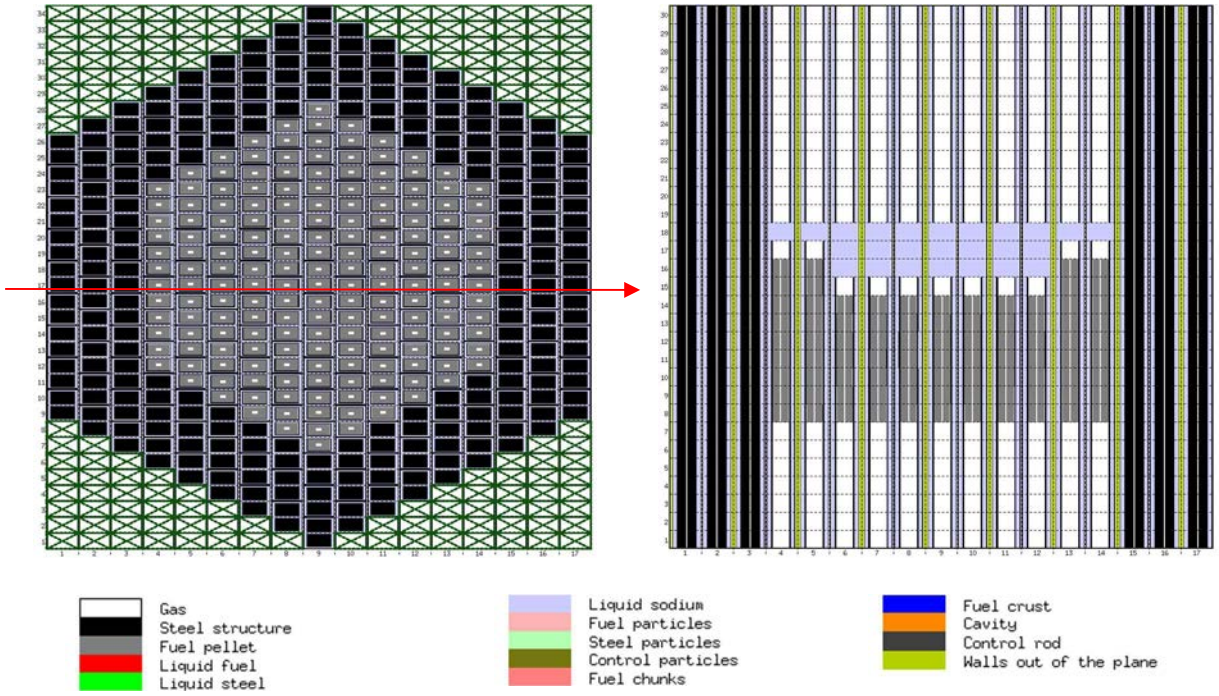

FIG. 6. Application case – Discretization of the full core with SIMMER-V: radial-azimuthal cut (left) and axial-radial cut (right). Green dotted lines outside the core mark out mesh cells excluded from the calculation.

In this application case, the state of irradiation of the fuel pins is not simulated (i.e. fresh fuel is considered). Coupling with neutronics is performed with the SNATCH flux solver.

To establish initial conditions before SIMMER-V/PARIS transient simulation, the sodium flow is piloted by the prescription of the core inlet and outlet pressures. The sodium temperature at core inlet is kept constant at 673 K during the whole sequence. A pressure of 1.1 bar is imposed

as outlet boundary condition. Coolant mass flow rate per fuel assembly is adjusted by fixing appropriate orifice coefficients at the entrance of each assembly in order to homogenize the sodium temperature at the outlet of the different fuel assemblies. After the calculation of the steady state with the constant nominal conditions of power and sodium flow, the ULOF transient is simulated by a sodium flow decrease at the core inlet with a pump halving time of 10 s.

In order to validate the procedure of transition between the multichannel calculation of the initiating phase and the full core calculation of the generalized degradation phase, two simulations of the ULOF transient are performed: (1) a full core calculation of the whole sequence of the transient, (2) a multichannel calculation of the initiating phase of the transient followed by a full core calculation of the generalized degradation phase (with a transition performed an instant before the first assembly can wall break-up that occurs in the channel n°1). Fig. 7 compares the reactor power variation during the ULOF transient for simulations (1) and (2). It can be seen that the power variation of simulation (2) is consistent with the power variation of simulation (1) and that there is no power discontinuity at the time of the transition. This validates the multichannel approach and shows that the transition between multichannel and full core calculations is well managed by SEASON.

It should be remembered that the multichannel approach has several major advantages: (a) it saves computation time as long as the channels evolve thermohydraulically independently, (b) it offers the possibility of meshing some channels more finely (i.e. representing some assemblies with several fuel pins per assembly), (c) the use of an 'extended' channel will allow to represent a local accident (as a TIB) on a group of assemblies (the damaged assembly and the ring of neighbouring assemblies).

Fig. 8 shows the core degradation state after the power peak in the simulation (2).

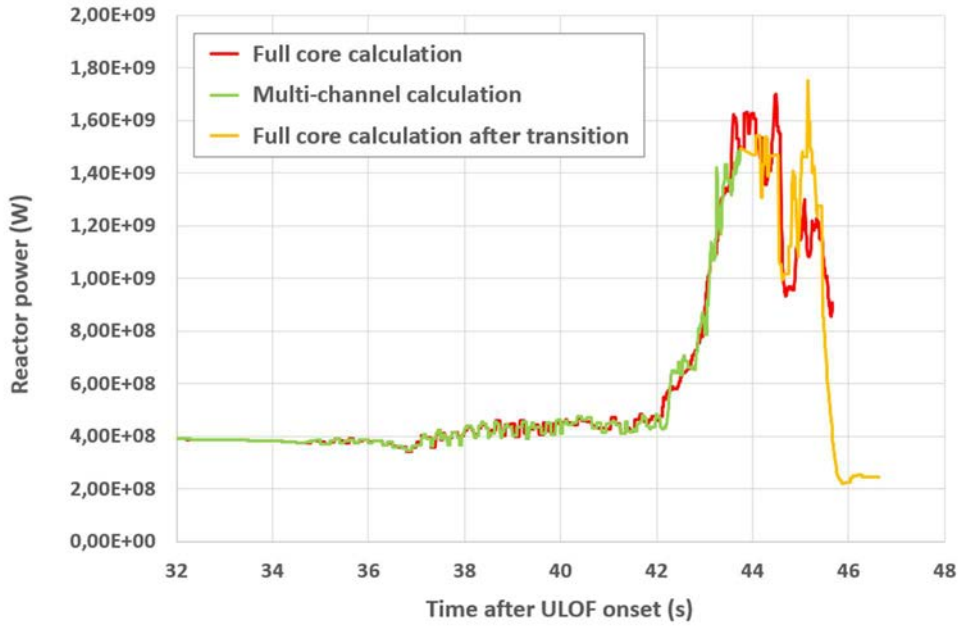

FIG. 7. Application case – Core power variation during ULOF transient – Comparison between the full core calculation of the whole sequence (red) and the multichannel calculation of the initiating phase (green) followed by the full core calculation of the generalized degradation phase (yellow). The transition between multichannel and full core calculations is performed at t = 43.75 s after ULOF onset.

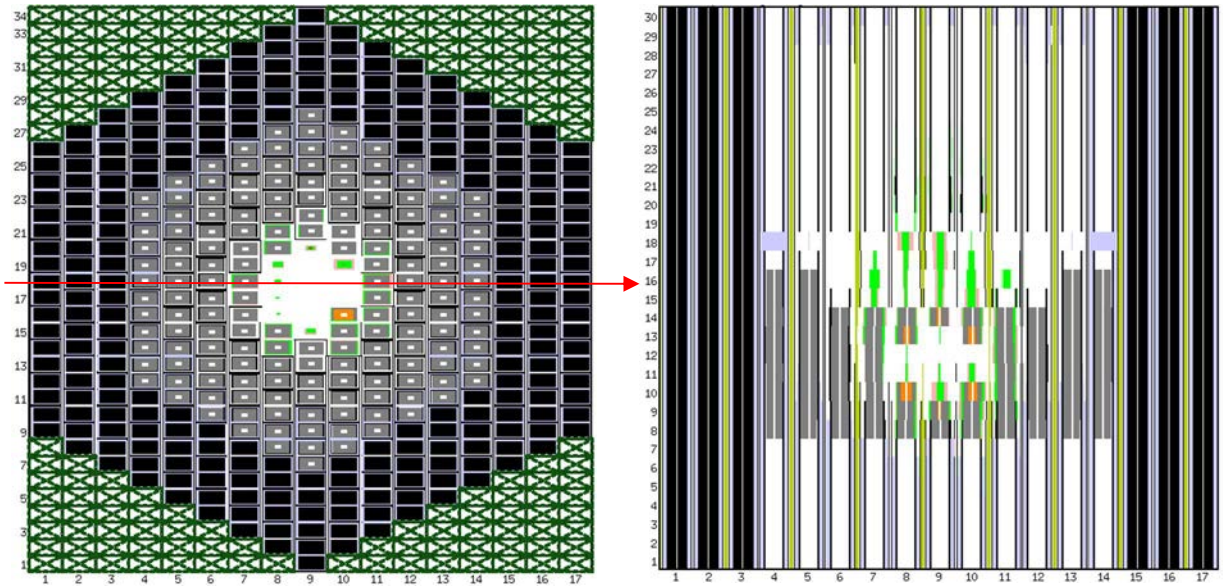

FIG. 8. Application case – Core state after the power peak (t = 46.6 s after ULOF onset) in the full core calculation of the generalized degradation phase.

4. PERSPECTIVES

Short term perspectives for the future developments of the SEASON platform are:

- Adaptation of the irradiation–degradation chaining to the detailed pin model DPIN3 of SIMMER-V.
- Implementation of the two types of thermohydraulic boundary coupling of SIMMER-V:
  - The inner (SIMMER-V/SIMMER-V) boundary coupling (using MPI exchanges and the MEDCoupling library), which will allow to embed a domain inside another one with the possibility of local mesh refining (for example, a core finely meshed into a vessel coarsely meshed);
  - The hybrid (SIMMER-V/another code) boundary coupling (using ICoCo/MEDCoupling exchanges), which will allow to couple SIMMER-V to a code modelling the primary circuit as CATHARE.
- Implementation of the on-the-fly update of the macroscopic cross-sections during the degradation.

Longer term perspectives are:

- Introduction of a simplified model describing the axial extension of the structures of the core;
- Improvement of the neutron computing by introducing a shielding module (from the neutronics platform APOLLO3 [16]) and taking into account the transport of fission products and their delayed neutrons;
- Introduction of an advanced modelling of cross-sections in case of degraded geometry (from APOLLO3).

ACKNOWLEDGEMENTS

The authors would like to thank the Generation IV programme of the industrial nuclear support and innovation Division of CEA which supports this work as well as the SFR R&D Project.

The SEASON calculations were granted access to the HPC resources of TGCC (Très Grand Centre de Calcul of CEA) under the allocation A0111007070 made by GENCI (Grand Equipment National de Calcul Intensif).

REFERENCES

[1] BACHRATA, A., TROTIGNON, L., SCIORA, P., SAEZ M., A three-dimensional neutronics –thermalhydraulics Unprotected Loss of Flow simulation in Sodium-cooled Fast Reactor with mitigation devices, Nucl. Eng. Des. **346** (2019) 1-9.

[2] Yamano, H., Tobita, Y., Fujita, S., A three-dimensional neutronics-thermohydraulics simulation of core disruptive accident in sodium-cooled fast reactor, Nucl. Eng. Des. 239 (2009) 1673-1681.

[3] Tobita, Y., Kondo, SA., Yamano, H., Morita, K., Maschek, W., Coste, P., Cadiou, T., The development of SIMMER-III, an advanced computer program for LMFR safety analysis and its application to sodium experiments, Nucl. Technol. 153 3 (2006) 245-255.

[4] TENCHINE, D., BAVIERE, R., BAZIN, P., DUCROS, F., GEFFRAYE, G., KADRI, D., PERDU, F., PIALLA, D., RAMEAU, B., TAUVERON, N., Status of CATHARE code for sodium cooled fast reactors, Nucl. Eng. Des. 245 (2012) 140-152.

[5] GASTALDO, L., LE TELLIER, R., SUTEAU, C., FOURNIER, D., RUGGIERI, J.-M., High-order discrete ordinate transport in non-conforming 2d cartesian meshes, International Conference on Mathematics, Computational Methods & Reactor Physics (M&C 2009) (Proc. Int. Conf. Saratoga Springs, New York, 2009).

[6] GUYOT, M., GUBERNATIS, P., SUTEAU, C., Development and first application of a new tool for the simulation of the initiating phase of a severe accident on SFR, Joint International Conference on Supercomputing in Nuclear Applications and Monte Carlo 2013 (SNA + MC 2013) (Proc. Int. Conf. La Cité des Sciences et de l'Industrie, Paris, France, 2013).

[7] GUYOT, M., GUBERNATIS, P., SUTEAU, C., On the multiple-pin modeling of the fuel bundle for the simulation of the initiating phase of a severe accident in a sodium fast reactor, Nucl. Sci. Eng. 178 (2014) 202-224.

[8] GUYOT, M., Neutronics and thermalhydraulics coupling: some contributions toward an improved methodology to simulate the initiating phase of a severe accident in a sodium fast reactor, PhD thesis, Université d'Aix-Marseille, France (2014).

[9] Le Tellier, R., Fournier, D., Suteau, C., Reactivity perturbation formulation for a discontinuous Galerkin-based transport solver and its use with adaptive mesh refinement, Nucl. Sci. Eng. 167 (2011) 209–220.

[10] RSICC Computer Code Collection, PARTISN 5.97 – Multi-Dimensional, Time-Independent or Time-Dependent, Multigroup, Discrete Ordinates Transport Code System, RSICC Code Package CCC-760, ORNL (2009).

[11] MARCHETTI, M., Neutronics methods for transient and safety analysis of fast reactors, PhD thesis, Fakultät für Maschinenbau, Germany (2016).

[12] Lenain, R., Masiello, E., Damian, F., Sanchez, R., Domain decomposition method for 2D and 3D transport calculations using hybrid MPI/OPENMP parallelism, ANS MC2015 – Joint International Conference on Mathematics and Computation (M&C), Supercomputing in Nuclear Applications (SNA) and the Monte Carlo (MC) Method (Proc. Int. Conf. Nashville, TN, 2015).

[13] LAINET, M., Michel, B., Dumas, J.-C., Pelletier, M., RAMIERE, I., GERMINAL, a fuel performance code of the PLEIADES platform to simulate the in-pile behaviour of mixed oxide fuel pins for sodium-cooled fast reactors, J. Nucl. Mater. 516 (2019) 30-53.

[14] Bubelis, E., Tosello, A., Pfrang, W., Schikorr, M., Mikityuk, K., Panadero, A.-L., Martorell, S., Ordóñez, J., Seubert, A., Lerchl, G., Stempniewicz, M., Alcaro, f., De Geus, E., Delmaere, T., Poumerouly, S., Wallenius, J., System codes benchmarking on a low sodium void effect SFR heterogeneous core under ULOF conditions, Nucl. Eng. Des. 320 (2017) 325-345.

[15] RIMPAULT, G., PLISSON, D., TOMMASI, J., JACQMIN, R., RIEUNIER, J.-M., VERRIER, D., BIRON, D., The ERANOS code and data system for fast reactor neutronic analyses, PHYSOR 2002 (Proc. Int. Conf. Seoul, South Korea, 2002).

[16] SCHNEIDER, D., DOLCI, F., GABRIEL, F., PALAU, J.-M., GUILLO, M., POTHET, B., APOLLO3: CEA/DEN deterministic multi-purpose code for reactor physics analysis, PHYSOR 2016 (Proc. Int. Conf. Sun Valley, Idaho, United States, 2016).

THE SIMPLIFIED RADIONUCLIDE TRANSPORT CODE FOR THE SOURCE TERM ASSESSMENT OF POOL-TYPE METAL FUEL SODIUM FAST REACTOR SEVERE ACCIDENTS

D. GRABASKS, T. STARKUS, D.H. KAM, M. BUCKNOR, S. SHAHBAZI
Argonne National Laboratory
Lemont, United States of America

Abstract

Mechanistic source term (MST) assessment, or the realistic evaluation of radionuclide transport and retention for specific transient event sequences, is central to the licensing approach for advanced reactor designs. To aid MST assessments for pool-type, metal fuel sodium fast reactor (SFR) designs, Argonne National Laboratory developed the Simplified Radionuclide Transport (SRT) code, which is an integral SFR radionuclide transport analysis tool that assesses radionuclide movement from the reactor fuel to the environment. The code includes models for phenomena associated with radionuclide behaviour within the fuel pins, release from failed fuel, migration through the sodium pool, and behaviour in the cover gas region and containment. SRT is purposefully designed to facilitate sensitivity and uncertainty analyses with off-site consequences as the metric of interest. The paper provides an overview of SRT development, including a review of the latest models and capabilities, current verification and validation status, and example analyses.

1. INTRODUCTION

A central aspect of the nuclear reactor licensing process is the evaluation of the potential release of radionuclides to the environment and the possible impact on human health. For advanced, non-light-water reactors (non-LWRs), the U.S. Nuclear Regulatory Commission (USNRC) has established an expectation for the use of mechanistic source term (MST) assessments, which realistically assess the transport and retention of radionuclides during potential accident scenarios [1–3]. To support the design and licensing efforts of metal fuel pool-type sodium fast reactors (SFRs), Argonne National Laboratory (Argonne) has developed the Simplified Radionuclide Transport (SRT) code. The code provides an integral assessment of radionuclide release and transport through the reactor system and is specifically tailored to address the phenomena associated with potential severe accidents associated with metal fuel pool-type SFRs. The paper begins with an overview of the predicted severe accident phenomena for metal fuel pool-type SFRs and is followed by an overview of the SRT, with an example analysis.

2. POOL-TYPE METAL FUEL SFR SEVERE ACCIDENT BEHAVIOUR

In the U.S., the design of SFRs has evolved based on lessons learned through extensive design and operational experience. While initial U.S. sodium reactors utilized metal fuel, they were limited in the maximum achievable burnup level due to cladding stress from fuel swelling. Subsequent SFR designs utilized oxide fuel and loop-type layouts, however, challenges were encountered regarding the potential for energetic severe accident scenarios and its impact on the licensing process. With further research regarding metal fuel, the issue of pin swelling was addressed through the inclusion of fission gas plena, which reduced cladding stress. Therefore, the U.S. shifted SFR design philosophy to leverage the inherent benefits of metal fuel and pool-type SFR designs to address the challenges encountered during the licensing of oxide fuel loop-type SFR systems.

Current U.S. SFR designs utilize passive and inherent features to both prevent and mitigate severe accidents. The large thermal inertia of the sodium pool, along with passive heat removal systems, aids in preventing accident scenarios with fuel temperatures exceeding cladding limits. Similarly, the inherent negative reactivity feedback of the core with increasing temperature can prevent fuel damage in accident scenarios that include a failure of the reactor protection system.

In addition, the behaviour of molten metal fuel during very severe accident scenarios aids in the benign termination of the events without further propagation of core damage. Further detail on these topics and reviews of past studies can be found in Refs [4–6].

Recently, an Argonne study explored the phenomena associated with two types of potential severe accident associated with metal fuel pool-type SFR designs [7]. While both scenarios are extremely unlikely event sequences that are expected to be well outside of the design basis of the reactor based on event frequency, they represent the most plausible pathways to fuel damage, in terms of the realistic behaviour of the reactor. First, a prolonged, protected loss-of-heat-removal (PLOF+)[1] scenario was analysed, which could represent extensive damage occurring at the plant due to a severe seismic event or other external hazard. The second scenario assessed a severe unprotected transient over power scenario (UTOP+). While a mechanistic initiator of such a reactivity insertion could not be identified, the event represented different fuel damage phenomena than the PLOF+. In the PLOF+ scenario, the sodium pool and fuel in the core slowly increases in temperature over a period of multiple days. Due to eutectic penetration of the cladding, fuel failure occurs at temperatures (700 – 800ºC) far below the melting temperature of the fuel (>1000ºC). With fuel failure, the contents of the fission gas plenum and bond sodium are released from the fuel pin, but the fuel matrix remains intact. In the UTOP+ case, there is a rapid increase in fuel temperatures, resulting in melting of the fuel matrix, but this is quickly (within seconds) terminated by the negative reactivity that is caused by the movement of molten fuel. For this event, the molten fuel is ejected from failed fuel pins but the temperature of the sodium pool remains near nominal. Following fuel pin failure, there are multiple barriers to the release of radionuclides and a multitude of radionuclide transport and retention phenomena, as outlined in Fig. 1. Both scenarios were explored with an early version of SRT, which indicated off-site doses well within acceptable limits, including more stringent criteria associated with the design basis level.

[1] The "+" was added to the acronym to denote that the severity of the event is beyond what is typically considered for a PLOF or UTOP analysis.

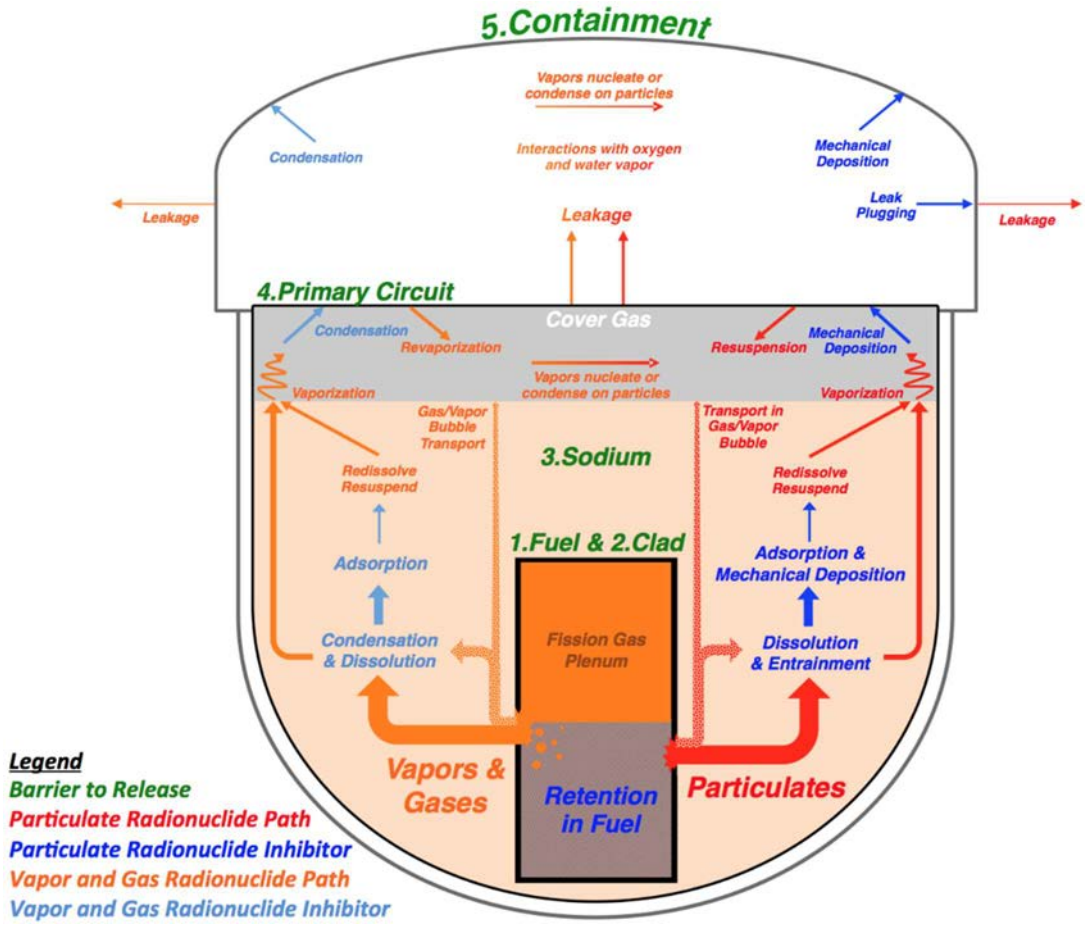

FIG. 1. Metal fuel pool-type SFR radionuclide barriers and transport and retention phenomena [8].

3. SRT OVERVIEW

The SRT code was developed to provide integral MST analyses for SFRs, with a specific focus on the phenomena relevant for metal fuel pool-type designs. In addition, the code was designed to perform rapid uncertainty and sensitivity analyses to aid in design and licensing calculations. The following sections provide an overview of the code, including a brief description of the phenomena models.

3.1 Calculation process

SRT performs a time-dependent assessment of radionuclide transport and retention, including a simple assessment of radiological consequence. As outlined in Fig. 2, SRT does not perform an analysis of the transient scenario, but relies on the output of systems analysis codes, such as SAS4A/SASSYS-1 [9], or postulated information from the user. This information includes the fuel conditions (temperature, cladding status, percent molten) and sodium pool temperature over the transient time, which is then utilized to perform the radionuclide transport calculation. The code is capable of tracking 770 isotopes of the 32 elements outlined in Table 1. This includes stable isotopes, as they may impact chemical behaviour through the radionuclide transport and retention process. SRT accounts for radioactive decay of all radionuclide isotopes and the birth of daughter products for certain short-lived noble gases.

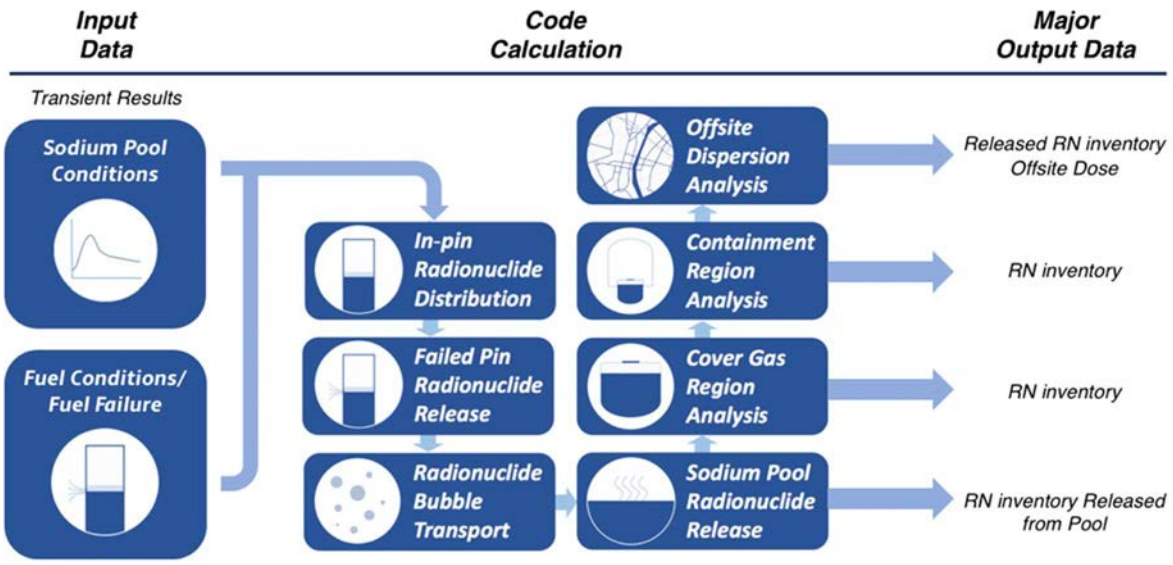

FIG. 2. Overview of SRT Input, Calculation, and Output for SFR Calculation [10].

TABLE 1. ELEMENTS TRACKED BY SRT

Elements		
Kr	Eu	Pr
Xe	Ru	Sm
I	Rh	Y
Br	Pd	Cm
Cs	Mo	Am
Rb	Tc	Ce
Te	Co	Np
Sb	La	Pu
Se	Zr	U
Ba	Nd	Na
Sr	Pm	

3.2 Uncertainty and sensitivity analysis

To facilitate uncertainty and sensitivity analyses, almost all inputs to SRT can be identified as uncertainties with specified distributions (uniform, log-uniform, normal, lognormal, and binomial). The user can then select for the code to perform multiple iterations, which are repeat calculations utilizing newly sampled values from the uncertainty distributions. Figure 3 outlines the inputs, outputs, and execution structure of SRT, including the creation of multiple iterations and outputs describing both individual iterations and summary data. As part of the summary

data, SRT conducts importance measure calculations on the input uncertainties, including Kendall and Pearson correlation coefficients. The "nominal output" folder is a new addition to the SRT output that contains a combination of output files found in both the Summary and Iteration folders. In it, a separate reference case utilizing nominal conditions (the mean value in a normal distribution for an uncertainty input) is performed before the main calculation of the code.

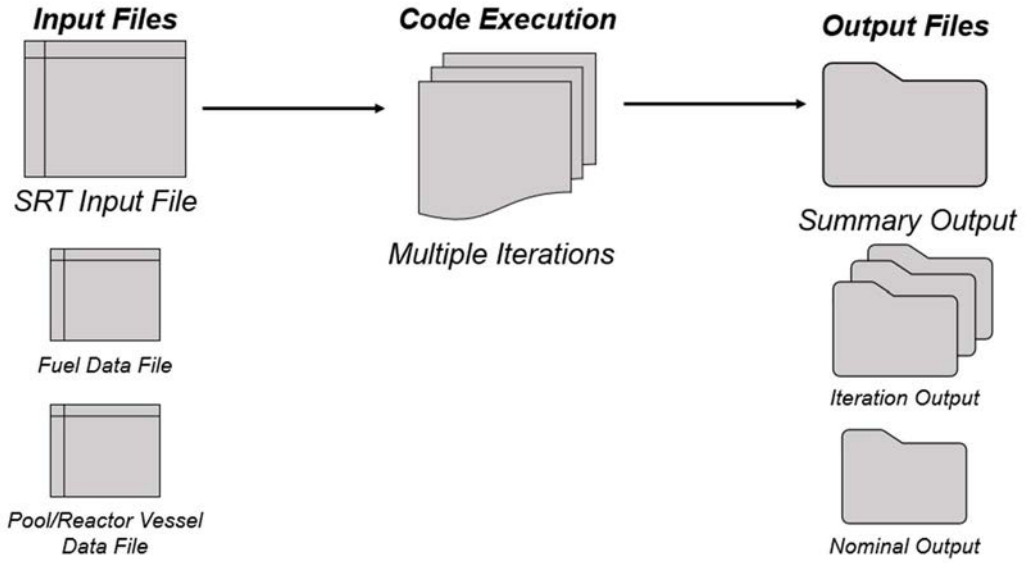

FIG. 3. SRT input, output, and code iteration structure [10].

3.3 Phenomena models

3.3.1 Radionuclide migration in-pin and release from failed fuel pins

SRT utilizes a data-driven approach to assess radionuclide migration within the fuel pin during irradiation, such as radionuclide movement to the fission gas plenum and sodium bond, along with radionuclide release from the fuel during cladding failure events. For radionuclide migration, the user supplies burnup-dependent tables for each radionuclide class of elements. Such information can be obtained from past Argonne studies regarding metal fuel behaviour [8, 11]. When fuel pin failure occurs, it is assumed that all radionuclides contained within the fission gas plenum and bond sodium are available for instantaneous release to the sodium pool. To determine additional radionuclide releases from the fuel matrix, the user supplies temperature-dependent and melt percentage-dependent tables for the code to utilize. Information to support these inputs is also available from Argonne studies [8, 11].

3.3.2 Bubble transport

The transport of radionuclides (both vapour and aerosol) within noble gas bubbles in the sodium pool is a critical calculation for the MST assessment, as it represents a mechanism to bypass the radionuclide retention properties of the sodium pool. When a metal fuel pin fails, there is a large release of noble gases given the initial pin pre-load of a noble gas, along with those noble gases produced during irradiation. SRT contains both a simplified and detailed model for the bubble transport analysis. In the simple model, the user inputs a designated decontamination factor (DF), which is the ratio of radionuclide aerosols entering the bubble versus those that reach the surface of the pool and cover gas region.

In the detailed bubble transport model, SRT performs a mechanistic calculation to determine the DF based on classical pool scrubbing theory, which includes condensation, Brownian diffusion, inertial deposition, and gravitational sedimentation. Additional information on the calculation performed by the detailed bubble model can be found in Refs [12, 13].

There have been recent improvements to the detailed bubble transport model and associated validation case based on the findings of bubble transport experiments in sodium conducted at the University of Wisconsin [14, 15]. Multiple options are now available to users of the detailed bubble model, including the possibility to conduct an internal uncertainty analysis focused on the bubble transport calculation, which is performed separately from the code's greater uncertainty iterations, described in Section 3.2. This allows the user to obtain further insight into the influence of parameters such as radionuclide aerosol diameter and density on the bubble DF, without the need to perform many iterations of the entire code.

3.3.3 Sodium pool vaporization

The vaporization models examine radionuclide vaporization from the sodium pool to the cover gas region. To develop this model, thermodynamic equilibrium calculations were performed utilizing the HSC Chemistry code [16], which resulted in release fraction response surface functions that were incorporated into SRT. Different response surface functions are utilized for each element and different temperature ranges. For each timestep of SRT, the vaporization function within the code compares the radionuclide element vapour/gas inventory in the cover gas region versus the quantity of the radionuclide element contained within the sodium pool. Based on the sodium pool temperature for that timestep, the response surfaces predict the elemental equilibrium vapour fraction, which is then compared to the current vapour fraction. If the equilibrium vapour fraction is greater than the current vapour fraction, an additional quantity of the radionuclide is vaporized from the sodium pool to the cover gas region.

The thermodynamic equilibrium assumption is thought to be conservative, as equilibrium will likely maximize the number of radionuclides present in the cover gas region but typically takes an extended period of time to occur. As part of this assumption, the cover gas temperature is conservatively assumed to be at the same temperature as the sodium pool. The HSC Chemistry calculations utilized a custom thermodynamic database that was developed by Argonne as part of past SFR source term efforts [7, 17].

3.3.4 Transport within compartments

SRT assesses radionuclide behaviour within the cover gas region and the containment/confinement (a future version of the code will allow the specification of additional compartments for transport). Within these compartments, radionuclides may exist as an aerosol or a vapour/gas. Based on user-specified options, radionuclides may transition between the two classes. For example, NaI aerosols may exist within the cover gas region but may dissociate to sodium oxide aerosol and iodine gas within the containment due to the presence of oxygen. Maximum flexibility is provided to the user to explore the impact of such phenomena.

Radionuclides in the aerosol class undergo radioactive decay and also deposition. Exponential decay is utilized to model aerosol deposition, with multiple options available to the user for the determination of removal rates (decay constants). First, constant removal rates can be specified by the user, with different removal rates possible for each element modelled by the code. Second, a customizable power function can be used to calculate removal rates based on the aerosol mass concentration within the volume. Lastly, the "Henry" correlation is available,

which determines removal rates using correlations developed for sodium oxide aerosols based on the results of the ABCOVE sodium fire experiments [18, 19][2]. In addition, minimum aerosol concentrations can be specified, below which aerosol deposition is halted. For aerosols within the cover gas region, they may deposit into the sodium pool.

For the transport of radionuclides from the cover gas region to containment and from containment to the environment, the code utilizes user-specified volumetric leakage rates. As perfect mixing is assumed to occur within both the cover gas region and containment, the volumetric leakage rates directly translate to radionuclide mass leakage rates.

3.3.5 Radiological consequence analysis

SRT provides two options for the assessment of radiological consequences. First, the time-dependent radionuclide masses released to the environment are provided as outputs by SRT and can be utilized within detailed consequence codes such as MACCS [21]. In addition, SRT provides a dose calculation utilizing user-specified atmospheric dispersion factor (χ/Q) and breathing rate values. Based on this information, SRT calculates whole body dose, thyroid dose, and total effective dose equivalent (TEDE) utilizing dose conversion factors (DCFs) from U.S. Federal Guidance Reports 11 and 12 [22, 23]. In addition, the user may also specify custom DCFs.

4. EXAMPLE ANALYSIS

An example SRT analysis from Ref. [24] is presented here as a demonstration of the capabilities of the code. The examined scenario does not represent a specific SFR accident sequence and should not be interpreted as indicative of SFR performance or potential consequences. The example reactor system is described in Table 2. In this example, the core fuel is divided into four fuel batches at different burnup levels, with 217 pins per assembly. The postulated transient scenario, which is described in Table 3, is a rapid heat-up of the core fuel, which results in fuel melting and cladding failure in three of the four fuel batches. Many radionuclide transport characteristics were treated as uncertainties by the code, including the cover gas and containment leakage rates, in-pin migration fractions, fuel pin release fractions, bubble characteristics, and aerosol deposition options. For this example, the "Henry" aerosol deposition model was selected to assess aerosol deposition in the cover gas region and containment. To assess these uncertainties, 250 iterations of SRT were performed.

[2] Additional information regarding the Henry model and its performance modeling sodium aerosol environments can be found in Ref. [20].

TABLE 2. EXAMPLE SRT PROBLEM REACTOR DESCRIPTION

Parameter	**Value**
Reactor Power	500 MW(th)
Reactor Fuel	U-Pu-Zr
Core Fuel Batches and Burnup	4 Batches (60 assemblies per batch), Burnup: 2,4,6,8%
Fuel Pins Per Assembly	217
Pool Depth	~5m (Pool top to top of active core)
Cover Gas Volume	$50m^3$
Containment Volume	$1000m^3$
Sodium Pool Volume	$250m^3$

TABLE 3. EXAMPLE SRT PROBLEM TRANSIENT DESCRIPTION

Parameter	**Value or Description**
Transient	Postulated fuel failure and melting scenario (not based on a realistic event sequence)
Fuel Batch Failure Times (and Max Temperatures)	1: No Failure 2: 3.5 minutes (~1350 °C) 3: 1.5 minutes (~1250 °C) 4: 0.5 minutes (~1200 °C)
Max Pool Temperature	650°Cat time = 5 minutes
Cover Gas Leakage Rate	Normal Distribution (μ, σ): (0.1, 0.05) vol % per day
Containment Leakage Rate	Normal Distribution (μ, σ): (1.0, 0.5) vol % per day
Atm. Dispersion Factor (χ/Q)	1E-4 sec/m^3
Code iterations	250
Other input uncertainties	RN in-pin migration and release fractions, bubble characteristics, RN vaporization multipliers, aerosol deposition options, RN dissociation characteristics (physical class changes)

SRT provides multiple options to examine the output of the calculations. For example, Fig. 4 contains a cumulative distribution function (CDF) of the TEDE estimate for the 250 code iterations. The analysis resulted in a mean TEDE value of 5.2E-4 rem (5.2 micro Sv), with 5th

and 95th percentile values of 6.9E-5 and 1.2E-3 rem (0.69 and 12 micro Sv). An example of the time-dependent radionuclide inventory in the cover gas region is presented in Fig. 5, which contains both radionuclide aerosols and vapour/gases. As the plot shows, those radionuclides in the aerosol form quickly deposit back into the sodium pool or onto other structures within the cover gas region, which rapidly reduces their inventory in the cover gas region. Those radionuclides at least partially in the vapour/gas state, such as Kr, I, and Cs, remain within the cover gas region and are available for further transport to the containment through reactor head leakage.

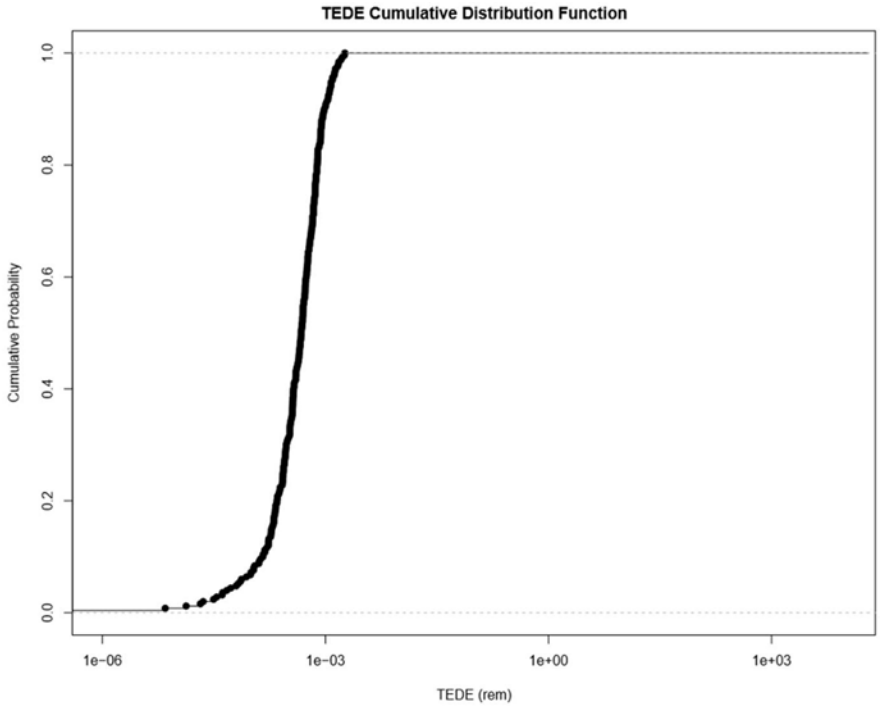

FIG. 4. Example SRT analysis – TEDE CDF.

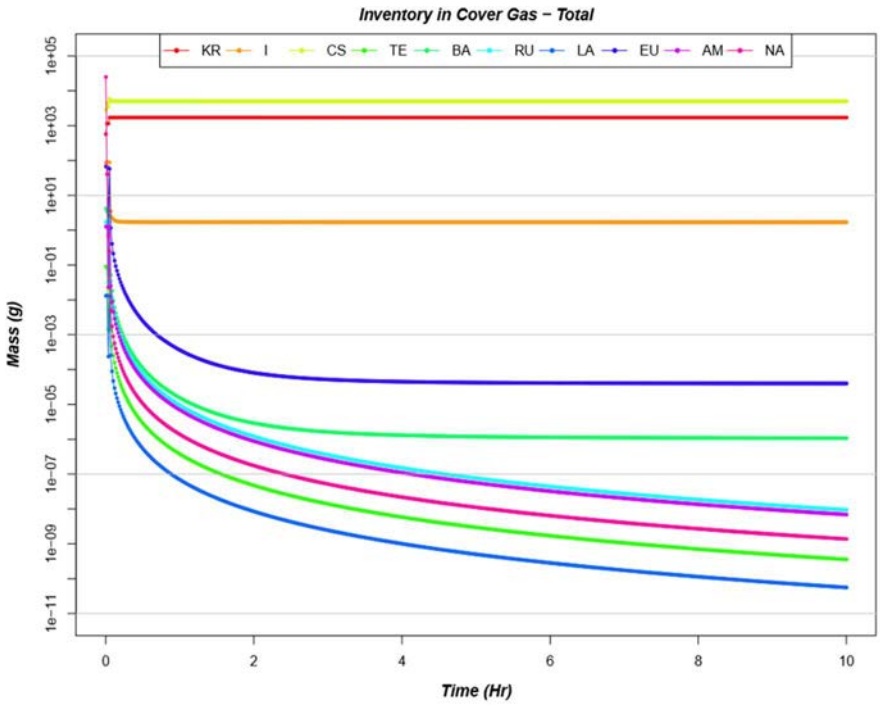

FIG. 5. Example SRT analysis – inventory in cover gas for specific iteration.

A key SRT output for each code iteration is the fractional release plot presented in Fig. 6. This plot illustrates the inventory of the radionuclide isotope available at each stage of the transport process. For this plot, surrogate TEDE values are utilized for each phase using point source χ/Q values to provide a point of comparison to the final location of interest (referenced as "offsite dose" in the figure). This information is useful for visualizing where radionuclides are retained within the reactor system. For example, a large portion of caesium is released from the fuel pin and reaches the cover gas region. However, significant retention occurs within the cover gas region and containment, likely due to deposition of caesium aerosols. This retention mechanism reduces the caesium inventory released to the environment by several orders of magnitude.

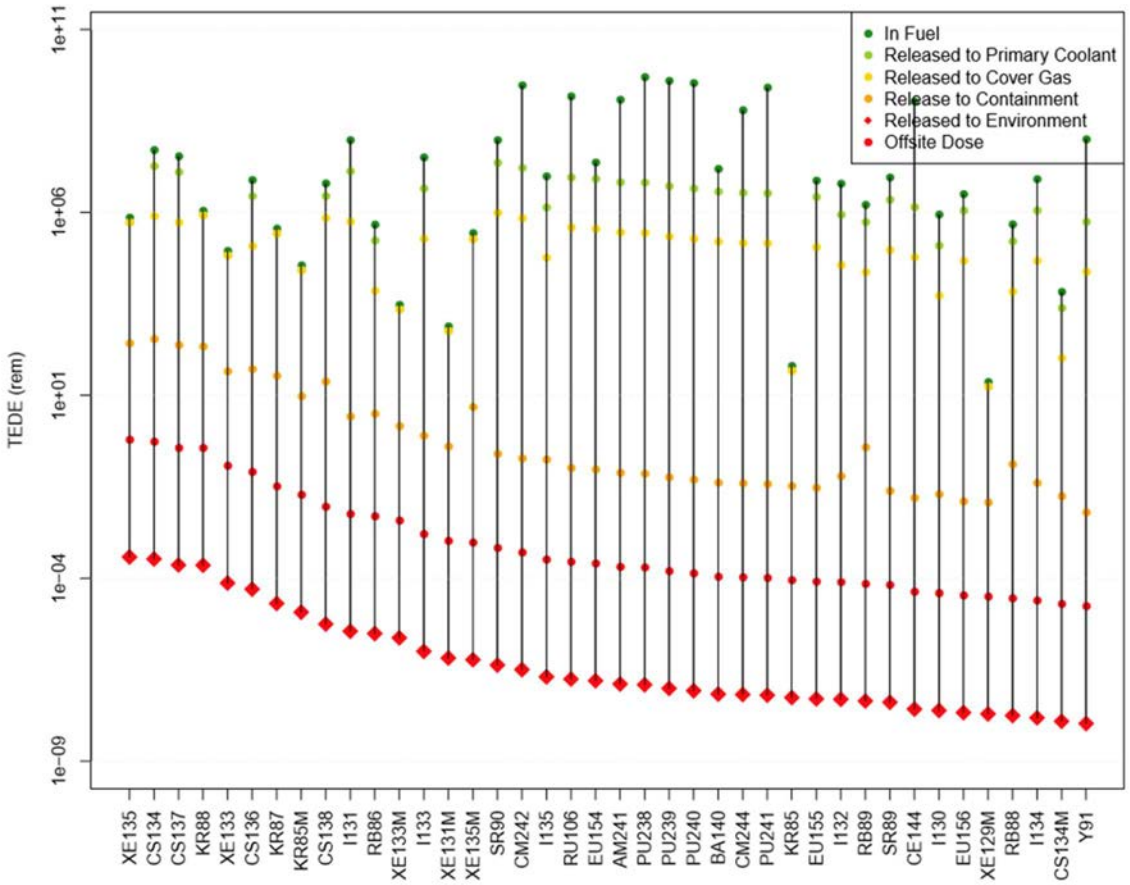

FIG. 6. Example SRT analysis – fractional release plot for specific iteration.

As mentioned in Section 3.2, SRT also provides outputs regarding the importance of specific input uncertainties. Figure 7 contains Pearson correlation coefficient raw values for each input parameter uncertainty based on the results of the 250 code iterations. As the results show, the greatest correlation was found to be with the cover gas region and containment leakage values (leakage.cg and leakage.cont). Other potentially impactful input parameters were the assumed aerosol fall height in containment (aerosol.height.cont), the aerosol particle diameter within fission product bubbles in the sodium (d.par), and fraction of caesium and rubidium that was in the vapour/gas form when entering containment (vapor.unc[Cs/Rb]). The Pearson correlation coefficient is a measure of linear correlation, with the provided Kendall rank correlation coefficients identifying non-linear correlations.

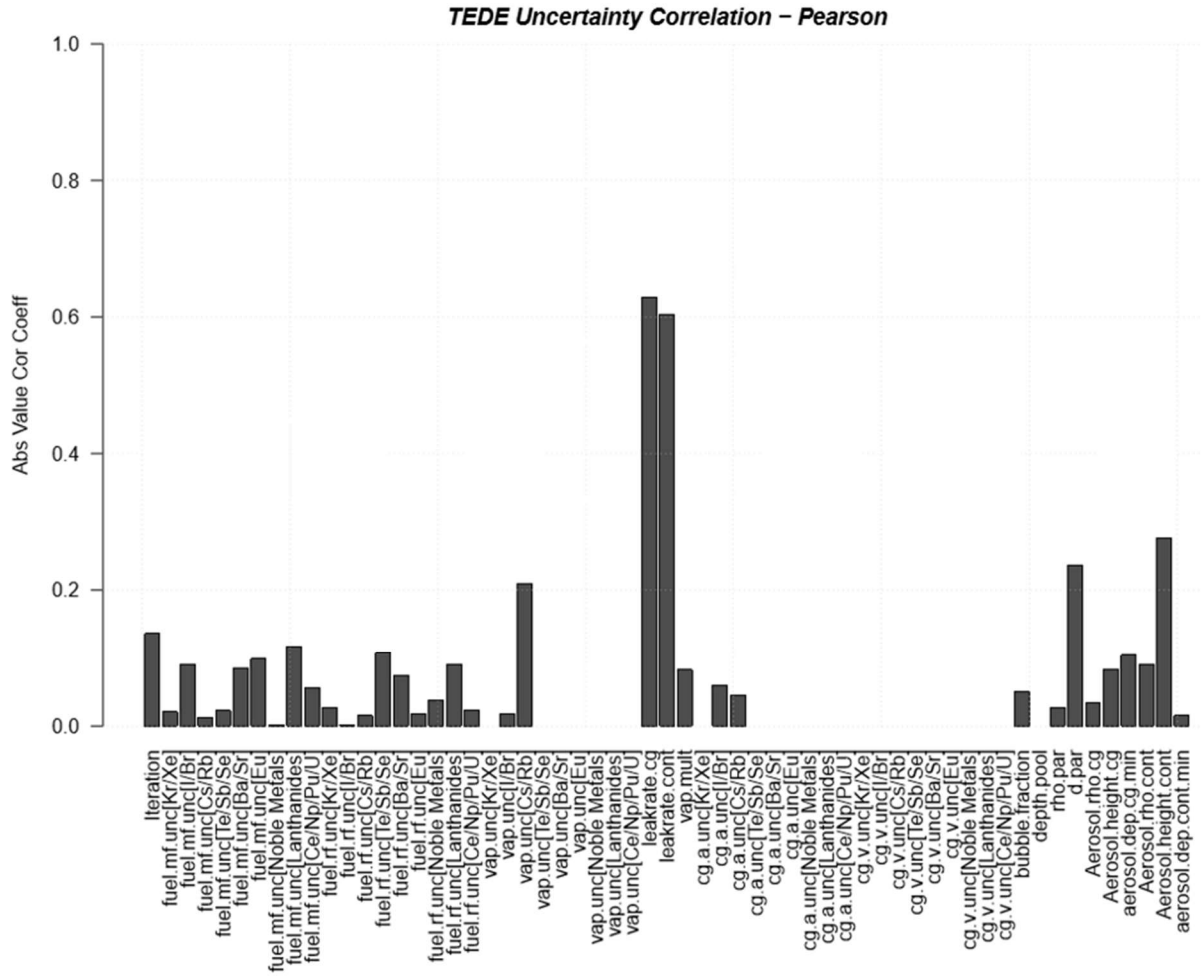

FIG. 7. Example SRT Analysis – Pearson Correlation Coefficient Raw Values[3].

5. SOFTWARE QUALITY ASSURANCE, VERIFICATION, AND VALIDATION

Given the importance of MST analysis as part of reactor design and licensing, extensive efforts are dedicated to the SRT software quality assurance (SQA) programme, including verification and validation. SRT development includes a suite of SQA documents outlining the software requirements, software design description, user manual, verification tests, and validation cases. Verification tests are developed for individual functions within the code, along with integral verification tests that evaluate the cumulative performance of the code. The verification tests compare the output of the code to hand calculations or calculations performed by alternative methods, such as comparing a numerically derived solution to one derived analytically. Many of the verification tests are provided to licensed users of the code, which can be utilized as regression tests to confirm the accurate performance of the code when installed on a new system.

The validation approach for the code varies depending on the type of model evaluated, as the models within SRT range for data-driven models dependent on user input to mechanistic evaluations based on physical or chemical models. For data-driven approaches, the evaluation focuses on validation of the underlying assumptions of the model. As an example, the model of radionuclide migration within the fuel pin during irradiation depends on burnup

[3] Input parameters with no bar on the plot were supplied as a single input value with no uncertainty distribution.

level-dependent tables supplied by the user. Therefore, validation of the model focuses on the appropriateness of the assumption regarding burnup dependence of radionuclide migration. This validation analysis is performed by examining available data on radionuclide migration within metal fuel pins and assessing the dependence on burnup level. For mechanistic models within the code, direct comparisons to experimental data are performed. As highlighted previously, the detailed bubble transport model in the code has been validated using bubble transport experiments performed in both water and sodium loops [14, 15]. Similar comparisons with experimental data are performed for the radionuclide vaporization and aerosol deposition models.

6. CONCLUSIONS

The SRT code developed by Argonne offers an integrated analysis of radionuclide transport and retention for potential severe accident scenarios at metal fuel pool-type SFRs. The code has been specifically designed to address the phenomena associated with metal fuel and pool-type layouts and was informed by multiple past studies regarding accident behaviour of such facilities. SRT is designed to provide maximum flexibility to the user, including facilitating rapid uncertainty and sensitivity analyses. A multitude of output options are available to assist the user in design and licensing calculations that are dependent on MST information. The code has been licensed by multiple U.S. SFR vendors and was also utilized for conceptual design and authorization activities for the US Department of Energy Versatile Test Reactor (VTR) project, including calculations contained within the VTR Conceptual Safety Design Report (CSDR), which was approved by the authorization body [25].

ACKNOWLEDGEMENTS

The submitted manuscript has been created by UChicago Argonne, LLC, Operator of Argonne National Laboratory (“Argonne”). Argonne, a U.S. Department of Energy Office of Science laboratory, is operated under Contract No. DE-AC02-06CH11357. Argonne National Laboratory’s work was supported by the U.S. Department of Energy, Office of Nuclear Energy under contract DE-AC02-06CH11357. This work was supported by the U.S. Department of Energy, Office of Nuclear Energy (DOE-NE) Advanced Reactor Technologies (ART) Fast Reactor Program.

REFERENCES

[1] U.S. NUCLEAR REGULATORY COMMISSION, Issues Pertaining to the Advanced Reactor (PRISM, MHTGR, PIUS) and CANDU 3 Designs and their Relationship to Current Regulatory Requirements, SECY-93-092, 1993.

[2] U.S. NUCLEAR REGULATORY COMMISSION, Policy Issues Related to Licensing Non-Light Water Reactor Designs, SECY-03-0047, 2003.

[3] U.S. NUCLEAR REGULATORY COMMISSION, Guidance for a Technology-Inclusive, Risk-Informed, and Performance-Based Methodology to Inform the Licensing Basis and Content of Applications for Licenses, Certifications, and Approvals for Non-Light-Water Reactors, RG 1.233, 2020.

[4] BAUER, T. H., WRIGHT, A., ROBINSON, W., HOLLAND, J., RHODES, E., Behavior of Modern Metallic Fuel in TREAT Transient Overpower Tests, Nuclear Technology **92** (1990).

[5] SOFU, T., A Review of Inherent Safety Characteristics of Metal Alloy Sodium-Cooled Fast Reactor Fuel Against Postulated Accidents, Nuclear Engineering and Design **47** 3 (2015) 227-239.

[6] CHANG, Y., Technical Rationale for Metal Fuel in Fast Reactors, Nuclear Engineering and Technology **39** (2007) 161-170.

[7] GRABASKAS, D. et al., Regulatory Technology Development Plan - Sodium Fast Reactor: Mechanistic Source Term Development - Trial Calculation, Argonne National Laboratory,, ANL-ART-49, 2016.

[8] GRABASKAS, D., BRUNETT, A. J., BUCKNOR, M., SIENICKI, J., SOFU, T., Regulatory Technology Development Plan - Sodium Fast Reactor: Mechanistic Source Term Development, Argonne National Laboratory, ANL-ART-3, 2015.

[9] T. H. FANNING, A. J. BRUNETT, T. SUMNER, EDS., The SAS4A/SASSYS-1 Safety Analysis Code System: User's Guide, Argonne National Laboratory, ANL/NE-16/19, 2017.

[10] GRABASKAS, D., BUCKNOR, M., JERDEN, J., STARKUS, T., SHAHBAZI, S., Simplified Radionuclide Transport (SRT) Code: Users Manual, ANL-SRT-4, Rev 2.0.1, 2020.

[11] GRABASKAS, D., BUCKNOR, M., JERDEN, J., Regulatory Technology Development Plan - Sodium Fast Reactor: Mechanistic Source Term - Metal Fuel Radionuclide Release, ANL-ART-38, 2016.

[12] BUCKNOR, M., FARMER, M. T., GRABASKAS, D., "An Assessment of Fission Product Scrubbing in Sodium Pools Following a Core Damage Event in a Sodium Cooled Fast Reactor," in International Confernce on Fast Reactors and Related Fuel Cycles: Next Generation Nuclear Systems for Sustainable Development (FR 17), Yekaterinburg, RU, 2017.

[13] KAM, D. H., GRABASKAS, D., BECKER, K., ANDERSON, M., STARKUS, T., BUCKNOR, M., Using Calibrated Water Data for Preliminary Validation of the SRT Code for Advanced Reactors, Proceedings of the IAEA International Conference on Topical Issues in Nuclear Installation Safety, 2022.

[14] BECKER, K., ANDERSON, M., Experimental Study of SRT Scrubbing Model in Water Coolant Pool, Nuclear Engineering and Design **377** (2021).

[15] BECKER, K., ANDERSON, M., Experimental Validation of Simplified Radionuclide Transport Bubble Scrubbing Code in Sodium Coolant Pool, Social Science Research Network (2022).

[16] OUTOTEC, HSC Chemistry 8 User's Guide, 2014.

[17] SHAHBAZI, S., THOMAS, S., STARKUS, T., GRABASKAS, D., Modeling Radionuclide Vaporization from Sodium Pools for SFR Mechanistic Source Term Analysis, ANL/NSE-22/69, 2023.

[18] FAUSKE & ASSOCIATES LLC, IDCOR Technical Report 11.7: FAI Aerosol Correlation, 1985.

[19] HILLIARD, R. K., MCCORMACK, J. D., POSTMA, A. K., Results and Code Predictions for ABCOVE Aerosol Code Validation -- Test AB5, HEDL-TME 83-16, 1983.

[20] STARKUS, T., GRABASKAS, D., SHAHBAZI, S., Review and Assessment of Available Data Regarding the Behavior of Sodium Aerosols, ANL/NSE-22/68, 2023.

[21] SANDIA NATIONAL LABORATORIES, WinMACCS, a MACCS2 Interface for Calculating Health and Economic Consequences from Accidental Release of Radioactive Materials into the Atmosphere - User's Guide and Reference Manual WinMACCS Version 3, 2007.

[22] U.S. ENVIRONMENTAL PROTECTION AGENCY, Limiting Value of Radionuclide Intake and Air Concentration and Dose Conversion Factors for Inhalation, Submersion, and Ingestion, EPA-520/1-88-020, Federal Guidance Report No. 11, 1988.

[23] U.S. ENVIRONMENTAL PROTECTION AGENCY, External Exposure to Radionuclides in Air, Water, and Soil, EPA-402-R-93-081, Federal Guidance Report No. 12, 1993.

[24] GRABASKAS, D., Development of the Simplified Radionuclide Transport (SRT) Code Version 2.0 for Versatile Test Reactor (VTR) Mechanistic Source Term Calculation, Proceedings of the 2022 International Conference on Fast Reactors and Related Fuel Cycles (FR21) (2022).

[25] U.S. DEPARTMENT OF ENERGY - OFFICE OF ENTERPRISE ASSESSMENTS, Conceptual Safety Design Report Assessment for the Versatile Test Reactor, 2020.

ARDECO CEA-KIT COOPERATION ON ASTRID SAFETY STUDIES AND RELATED CODE DEVELOPMENTS

A. RINEISKI
Karlsruhe Institute of Technology (KIT), Karlsruhe, Germany

L. ANDRIOLO[1,3], X.N. CHEN[1], M. FLAD[1], S. GIANFELICI[1,4], L. GUO[1,5], M. MARCHETTI[1,6], M. MASSONE[1,4], B. VEZZONI[1,6], A. BACHRATA[2], F. BERTRAND[2], T. JEANNE[2], M. ZABIEGO[2], P. GUBERNATIS[2], F. SERRE[2]

[1] Karlsruhe Institute of Technology (KIT), Karlsruhe, Germany
[2] French Alternative Energies and Atomic Energy Commission (CEA), Saint-Paul-lez-Durance, France
[3] Current address: Electricity of France (EDF), Paris, France
[4] Current address: Italian National Agency for New Technologies, Energy and Sustainable Economic Development (ENEA), Bologna, Italy
[5] Current address: Society for Plant and Reactor Safety (GRS), Garching, Germany
[6] Current address: Framatome, Paris, France

Abstract

An ARDECo CEA-KIT cooperation project on ASTRID 1500 MW(th) safety studies and related code developments was started in 2015 and planned till end of 2019, with the time for some tasks being later extended. The work programme included 4 Task Sheets (TSs), TS1 was on analyses of unprotected loss of flow (ULOF) accident, TS2 was on simulations of flow blockages in a fuel assembly, TS3 was on evaluation of sodium temperature in the lower plenum after molten fuel discharge from the core under hypothetical severe accident conditions. TS1–TS3 simulations were performed with SIMMER, a coupled fluid dynamics and neutronics code. TS4 was on development of SIMMER and its interfaces to other codes, such as fuel performance ones. The paper focuses on several TS1 tasks and particularities of the KIT approach to transient simulations with SIMMER. New SIMMER cross-section libraries, extended cross-section generation procedures, and additional reactivity feedback models addressing thermal expansion effects are applied for ARDECo studies. The preliminary results show a favourable impact of taking into account additional reactivity feedback on the ULOF accident evolution with an expected delay in power excursions that may lead to a lower level of core degradation. Moreover, thanks to new SIMMER capabilities developed at KIT, the impact of movement of absorber material into the core during the transient is also analysed. These results bring insight into the impact of a B4C fall into the core during different ULOF instants. The absorber fall is triggered by different criteria defined by CEA: hydraulic and Curie-point models determine triggering for the hydraulic and Curie-point rods, respectively, while an upper neutron protection fall is due to vapour presence in the region. Only the neutronics impact of B4C is considered in the paper, no thermo-chemistry model for simulation of B4C behaviour in the core under ULOF conditions is applied in these preliminary studies.

1. INTRODUCTION

The paper is on the ARDECo cooperation project between CEA and KIT. It was planned for 2015–2019, with some tasks extended for a longer time. The objectives were sodium fast reactor (SFR) safety studies for the ASTRID CFV v3 1500 MW(th) design [1] — CFV meaning core with a low void effect — also development of the SIMMER coupled neutronics and thermohydraulics (TH) code [2] and of related software tools for accident simulations in SFRs. The focus was on simulation of a hypothetical ULOF (unprotected loss of flow) accident and its consequences: they were studied in Task Sheet 1 (TS1) and are reported in the paper. Other activities — related to fuel assembly blockage studies (TS2), sodium behaviour in the lower plenum after molten fuel transfer to this location (TS3), and SIMMER-related developments (TS4) in continuation of those described in Refs [3, 4] — are out of scope of this paper.

CEA-KIT studies complement activities performed at CEA and in cooperation projects between CEA and other CEA partners, see in particular Refs [5, 6].

2. MODELLING APPROACH

The ASTRID CFV v3 core includes inner and outer radial parts, with different axial heights and enrichments, containing 180 and 108 fuel assemblies (SAs), respectively. Figure1 shows the radial core layout, Figure 2 shows the RZ SIMMER model, including the core, above core structures, and other in-vessel components.

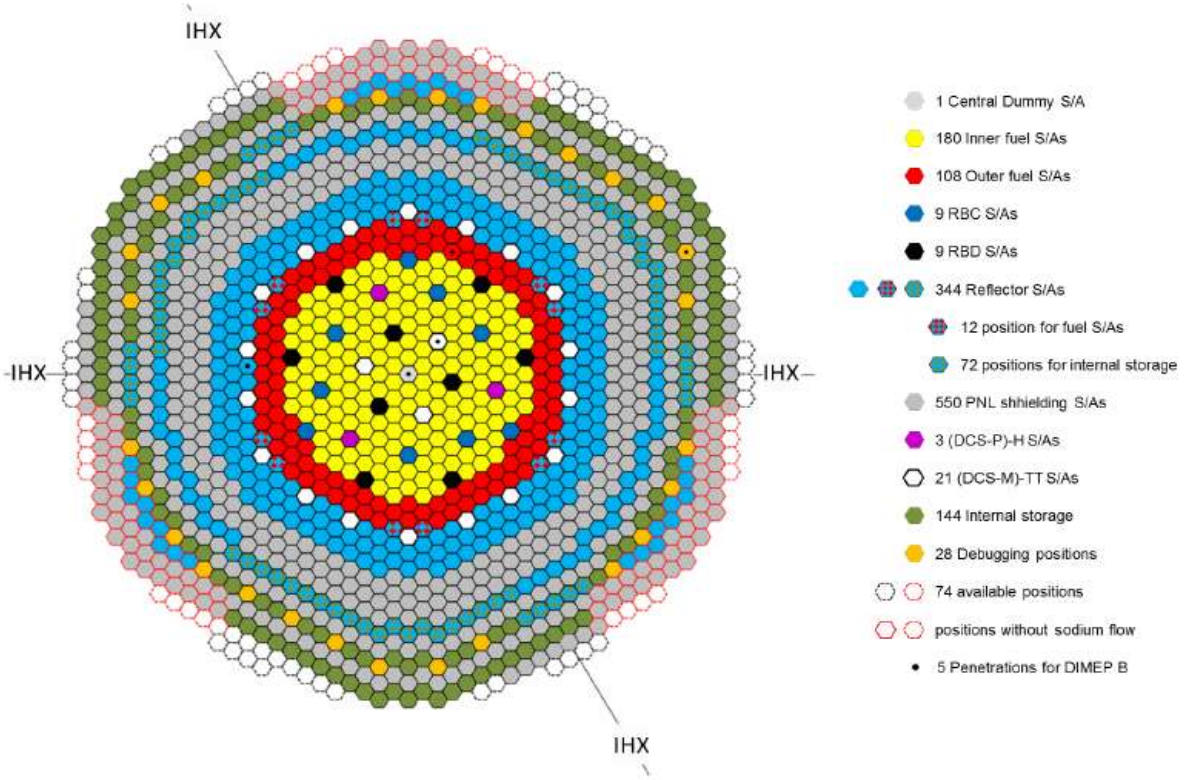

FIG. 1. Radial layout of the CFV v3 core.

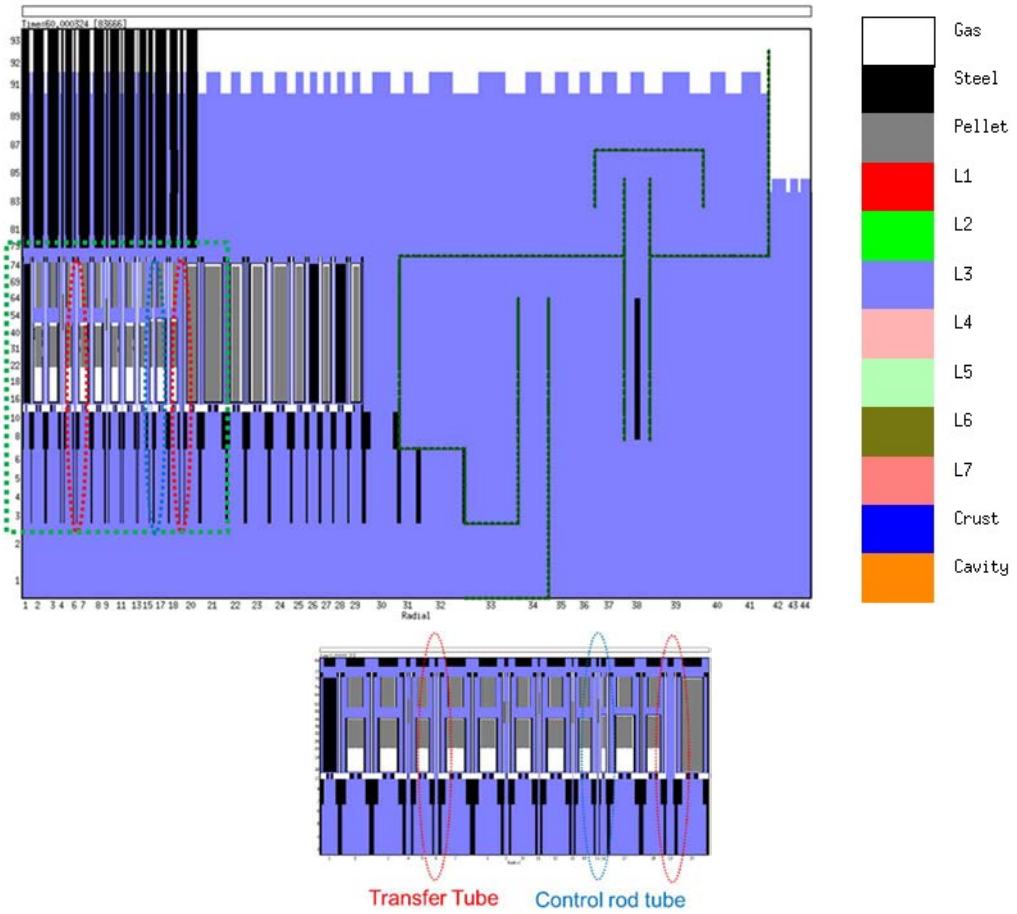

FIG. 2. Set-up of RZ model at nominal conditions.

In Fig. 2, L1, L2, L3, L4, L7 stand for liquid fuel, liquid steel, coolant, fuel particles, fuel chunks, respectively. They, except coolant, are not present at nominal conditions, but present at accident ones: see Fig. 3.

The fuel SAs contain 217 pins with MOX fuel, with a low fertile blanket, and an internal axial blanket in the inner core. The pin diameter is 9.7 mm. The core is surrounded by three rings of reflector SAs with magnesium oxide, then by three rings of shielding SAs with boron carbide. An internal assemblies storage at the core periphery is neutronically decoupled from the core.

The control and safety system are composed of nine control and shutdown devices (RBCs), nine diverse shutdown devices (RBDs), and three hydraulic prevention devices (DCS-P-Hs). The design includes 21 transfer tubes (DSC-M-TTs) referred as TTs later. TTs are dedicated for transferring molten fuel and steel, present under hypothetical accident conditions, to the core catcher below the core, to which TTs are connected. The mentioned devices and TTs are represented as rings in the 2D model shown in Fig. 2. At nominal conditions and at the beginning of ULOF, we consider the presence of TTs only above the inlet plenum, otherwise the coolant cannot enter the SAs inside the TT rings due to limitations of the RZ model. In the considered core at the beginning of life (BOL), the sodium void effect is negative due to a sodium plenum above the core and other design features.

SIMMER application to SFR ULOF simulations at KIT in the past was mainly for transient phases after the initiation one, i.e. after can wall melting. For the initiation phase, SAS4A [7] and SAS4A-like codes were applied, then their simulation results were transferred to SIMMER.

This transfer is a complex procedure introducing uncertainties in SIMMER results because of different modelling approaches in different codes.

Once-through ULOF calculations are often performed currently at KIT, so that SIMMER is applied first for nominal conditions in order to achieve a steady state, then for the initiation and later phases of the ULOF transient. To improve SIMMER applicability to the initiation phase, the code was extended at KIT so that reactivity feedback due to thermal expansion of the core and control rod drive lines (CRDLs) can be taken into account [8]. The core thermal expansion feedback extension was tested for an experimental case of EBR-II [9]. SIMMER modelling capabilities for the initiation ULOF phase may have to be extended further to match SAS4A, but for studies focused on post-initiation transient phases, the established once-through approach is often acceptable.

At KIT, using of an 11-group cross-section library [10] has been a standard option for a long time. Also, a 72-group library with more recent JEFF 3.1 data is employed [11]. A new SIMMER calculation option [12] makes possible the use of 72-group data without a significant increase in the calculation time as compared to the 11-group case. When this option is used, SIMMER computes 72-group self-shielded cross-sections and 72-group neutron flux spectra at each time step in each mesh of the neutronics domain. These calculations are quite fast because each mesh is treated independently from others as a homogeneous region. The computed 72-group self-shielded cross-sections for each mesh are condensed then to a smaller number of groups at each time step while using the mesh-wise 72-group spectra as weighting functions. The cross-sections for a smaller number of groups, e.g. 11, are then used in neutron transport and reactivity calculations performed during transient simulations. The results are usually similar to those obtained with 72-group transport and reactivity calculations, this is checked for representative cases. In ASTRID studies, both 11-group and 72-group libraries were used, while 2D neutron transport calculations in SIMMER were always performed with 11 groups, therefore the simulations took similar computer times.

The coolant void effect and Doppler constant values at BOL were computed with SIMMER for the 2D model. They are less negative than those computed with a 3D deterministic code that employs a variational nodal method for neutron transport calculations. The void/Doppler 3D deterministic values are -371/-725 pcm. With 11-group data, the 2D SIMMER values are -2/-551 pcm. With 72-group data, the values are -223/-598 pcm, in particular due to the use of more recent nuclear data. Earlier, we observed a difference between sodium void effect values obtained with the mentioned 3D deterministic code and a Monte-Carlo code for another design with a sodium plenum, the 3D Monte-Carlo results were less negative, by 74 pcm, probably due to limitations of the variational nodal method in treating low-density regions, such as the sodium plenum above the core at voided conditions. The value of 74 pcm is half of the difference between 2D/72 group and 3D void effect values. The void and Doppler effect values increase with fuel burnup, therefore the SIMMER reactivity effect values appear to be more representative for an irradiated state than for BOL.

After ULOF starts, the pump pressure head decreases rapidly from its nominal value to almost zero, leaving only a natural sodium circulation. The power decreases just after the ULOF start due to the Doppler effect, but this power reduction is not sufficient to prevent sodium boiling. Then the reactivity and power oscillate due to voiding and rewetting by sodium in the upper core part. Later, a clad break-up may occur. Then the damaged domain of the core may expand, molten core material relocation may start and lead to a reactivity increase, thus inducing a power excursion.

The most conservative KIT results were obtained with 11-group data, without taking into account thermal expansion feedback. Less conservative results were got with 72-group data and this feedback. The least conservative results were obtained with 72-group data, this feedback, and finer radial meshes in the core, including those for gaps between fuel SAs.

We do not observe a strong power excursion during a relatively long time after a ULOF start for some less conservative assumptions. As our main objective is to investigate consequences of a hypothetical core melting event, we consider in the following two simulation options: (1) the most conservative one, with 11-group data and without thermal expansion feedback, (2) a less conservative one, with 72-group data and with this feedback, but without fine radial meshes in the core. Option 1 is the basis for assessment of the mechanical energy after a ULOF as described in the next section. Option 2 is the basis for ULOF-related studies reported after the next section.

3. ASSESSMENT OF THE MECHANICAL ENERGY RELEASE AFTER ULOF

Simulations were performed first for 60 s before the ULOF start in order to approach steady state conditions. Then ULOF simulations were started. A molten core configuration, shown in Fig. 3 for part of the core, which includes radial meshes from 1 to 19 and axial meshes from 21 to 58, was obtained with 11-group nuclear data at 80.9 s after the ULOF start. In Fig. 3 the total simulation time is given, i.e. 140.9 s. As explained earlier, the molten fuel and molten steel components are shown in red and green colours, respectively, occupying fractions of meshes according to their volume fractions. At this time, the power is higher than the initial one, the core region contains the maximum amount of mobile components of fuel and steel; and the maximum core pressure is achieved after earlier narrow pressure peaks related to local FCI events.

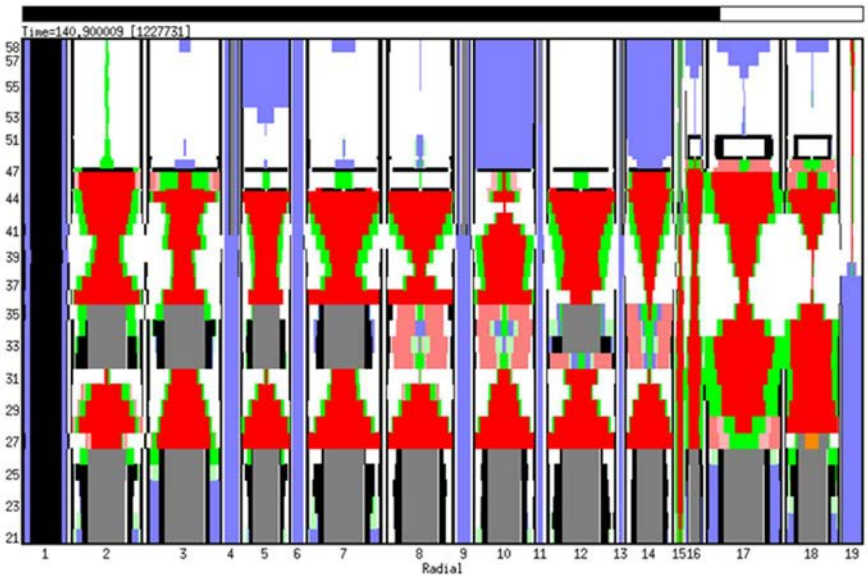

FIG.3. Core at 80.9s after ULOF start.

Starting from this “coupling” time, thermohydraulics-only (TH-only) SIMMER calculations — that simulate conversion of the internal energy into mechanical one — are performed. This is done by employing a capability, which is referred to as SIMMER-to-SIMMER coupling (S2S). This capability allows previously performed coupled neutronics and TH calculations to continue while employing a modified geometry, in particular with a more detailed mesh outside of the core. For the TH-only calculations, the increase in the internal energy due to nuclear

heating is assumed to be negligible, because this increase is very small, by about 0.025% during 0.7 s, starting from the coupling time, to the time when the power decreases from its peak value to about 0.3 GW. Two mechanical energy components are considered, to which the internal energy converts: the kinetic energy of accelerated fluids, computed from the velocity values; and the compression energy, computed from the pressure in the upper gas plenum. The results of TH-only calculations are given in Fig. 4, the upper limit of the total mechanical energy is currently about 10 MJ.

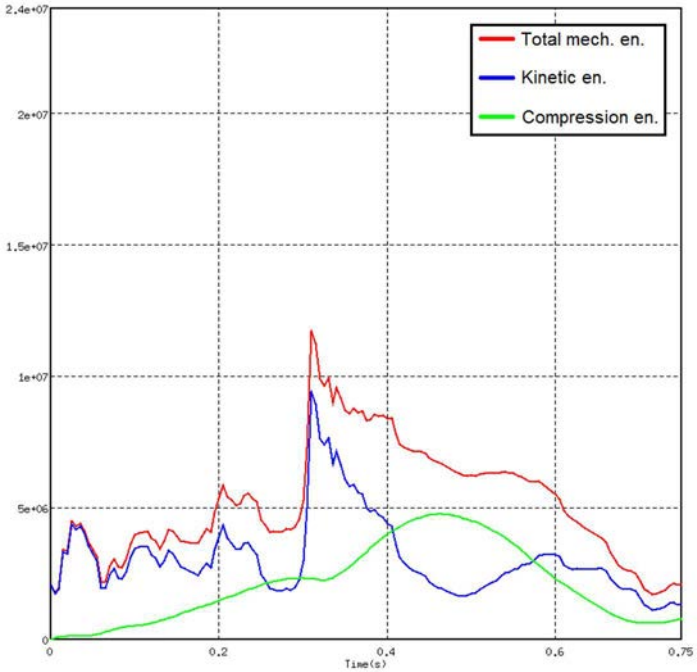

FIG. 4. Mechanical energy (J), including kinetic and compression components, after the coupling point.

With additional analyses we evaluated uncertainties in the assessed values. The melt discharge rate through the upper core structure is decisive for the energy amount added to the hot plenum, in line with earlier results [13]. With calculation options reducing the viscosity of mobile components, the mechanical energy is about two times higher as compared to the previous case. Note that SIMMER does not include structure mechanics models and applies thermal failure criteria; therefore, some structure components, such as upper plugs of fuel pins may remain in place too long. By removing the plugs and then other structures, including the above core ones, the energetic outcome increases further, but still remains quite low as compared to the internal energy.

4. ASSESSMENT OF MOLTEN MATERIAL RELOCATION FROM THE CORE AFTER ULOF

Figure 5 shows the ULOF progression starting from cladding melting, the results being obtained with 72-group nuclear data. Figure 6 shows variations in time of the mass of liquid fuel and its average temperature after ULOF.

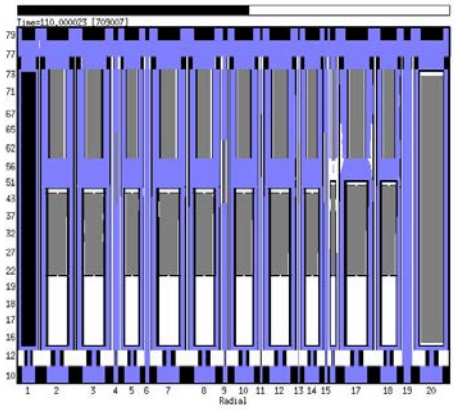

110.0 s: (cladding melting)

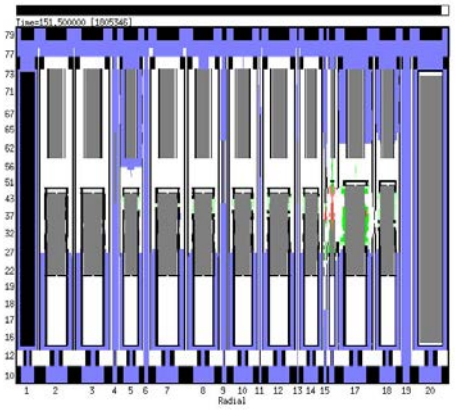

151.5: s (fuel melting)

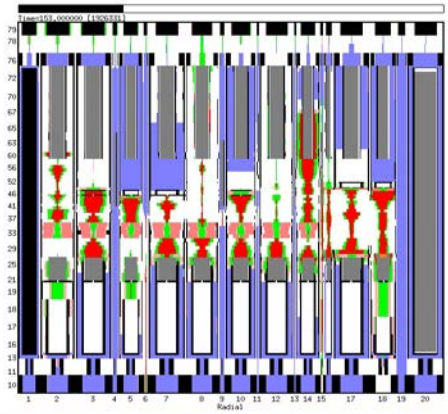

153.0 s: about 1.5s after power excursion

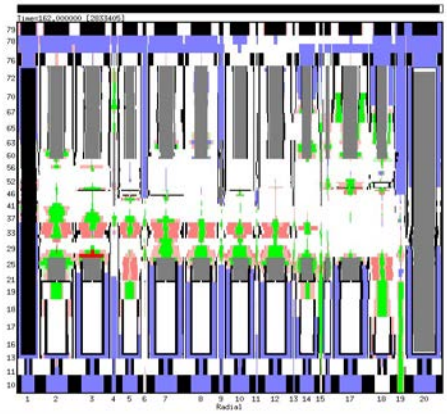

162.0 s: about 10.5 s after power excursion

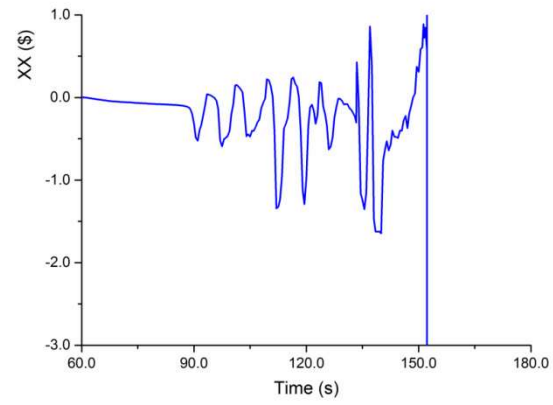

Reactivity ($)

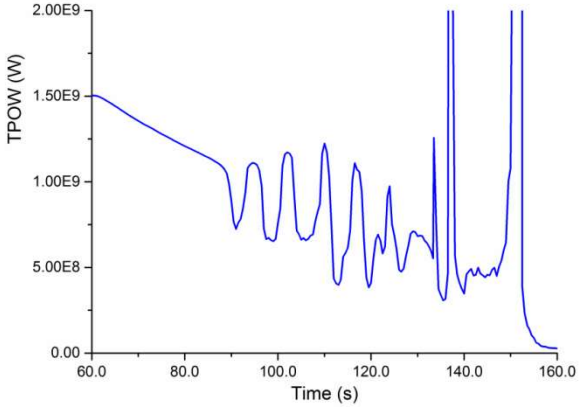

Total power (W)

FIG. 5. ULOF progression obtained with 72-group data.

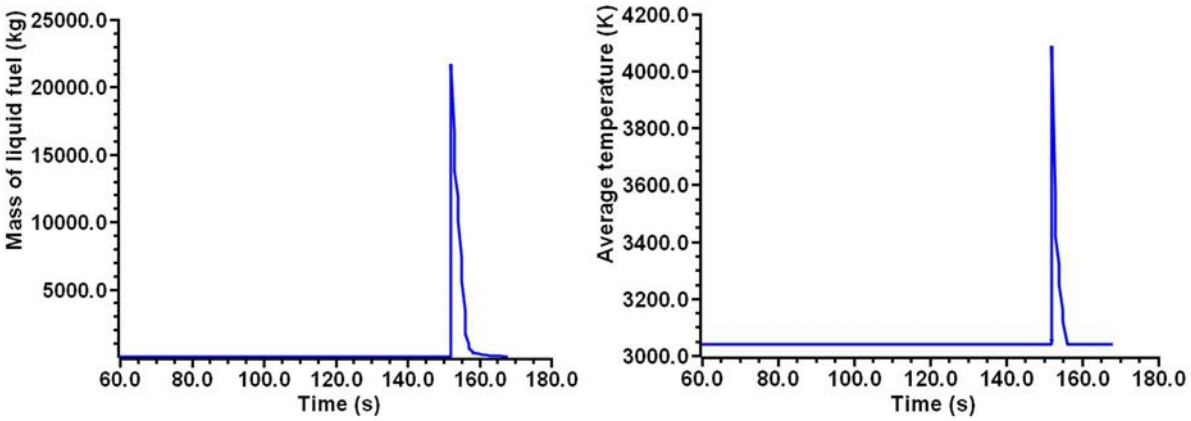

FIG. 6. Mass of liquid fuel in the core region and its average temperature after ULOF.

The core snapshots in Fig. 5 represent core configurations after the clad melting onset. Before this onset, sodium boiling occurs in the sodium plenum of the 16th ring, i.e. in the outer core, at about 90 s, i.e. about 30 s after the ULOF start. At about 2 s after the first sodium boiling event, a negative reactivity insertion — due to voiding of the sodium plenum and upper shielding of the outer core — makes the reactivity negative, about -0.5$.

As the negative reactivity insertion dominates for some time, the power decreases further, lowering the fuel temperature and inducing rewetting in/near the sodium plenum, thus augmenting the reactivity and power. Due to further boiling/rewetting cycles the reactivity and power oscillate. At about 110 s, the first cladding breakup occurs in ring 16. The fuel pellets remain intact as the thermal criterion for fuel failure has not been reached. Further power oscillations lead to voiding of almost all core rings.

The radial motion of steel becomes possible with the failure of the can walls in rings 16 and 17. Voiding of the fuel region increases the reactivity so that fuel melts at 151.5 s with the reactivity reaching the prompt criticality level. The power peaks exceed the nominal power by several times. The last material distribution shown in Fig. 5 is for the end of simulation at 162.0 s. One may see that soon after the power excursion, the fuel melting occurs, then the can walls are melting, the discharge paths through TT and control guide tubes (Rings 6, 15, 19) are opening. Fuel discharge through the mentioned paths reduces the core reactivity appreciably, then the nuclear power production is stopped except the decay heat. These conclusions are confirmed by sensitivity studies, which include two options: (1) application of a less conservative viscosity model and (2) connection of TTs to the core catcher — instead of the inlet plenum — at the beginning of melt discharge, the reason for introducing this connection during the transient being explained in Section 2.

5. INTRODUCTION OF AN ABSORBER UNDER ACCIDENT CONDITIONS

In this section, we describe studies of the impact of a B4C-material fall in the core during the ULOF transient. The SIMMER ULOF transient simulations are stopped and then continued for a modified — after an absorber fall — geometry, due to application of the S2S tool. As B4C is present in different devices, we consider cases for RBD, DCS-P-H and the absorber layer above the sodium plenum above the core. This layer is referred to as PNS in the following. Introduction of B4C is initiated by particular conditions or triggered by scenario events as explained in the following.

When absorber is introduced in the core, by using the S2S tool, the corresponding reactivity variations are also introduced. They are evaluated from static calculations.

The insertion of the DCS-P-H rods follows a coolant flow criterion: when the flow in the core decreases below a given value, the hydraulic rods start to fall into the core. The employed mesh allows to put these rods in the simulation model at three different axial locations, at distances of 0.4 m, 0.79 m and 1 m from the bottom of the fuel column (BFC). According to these locations and the outcome of the hydraulic model for the ULOF, the coupling time for the S2S coupling tool was selected at 23.5 s after ULOF start.

Two cases are reported here, simulating the insertion of 1 and 2 absorber rods, denoted as DCS1 and DCS2, respectively. The power variations for these cases are shown in Fig. 7.

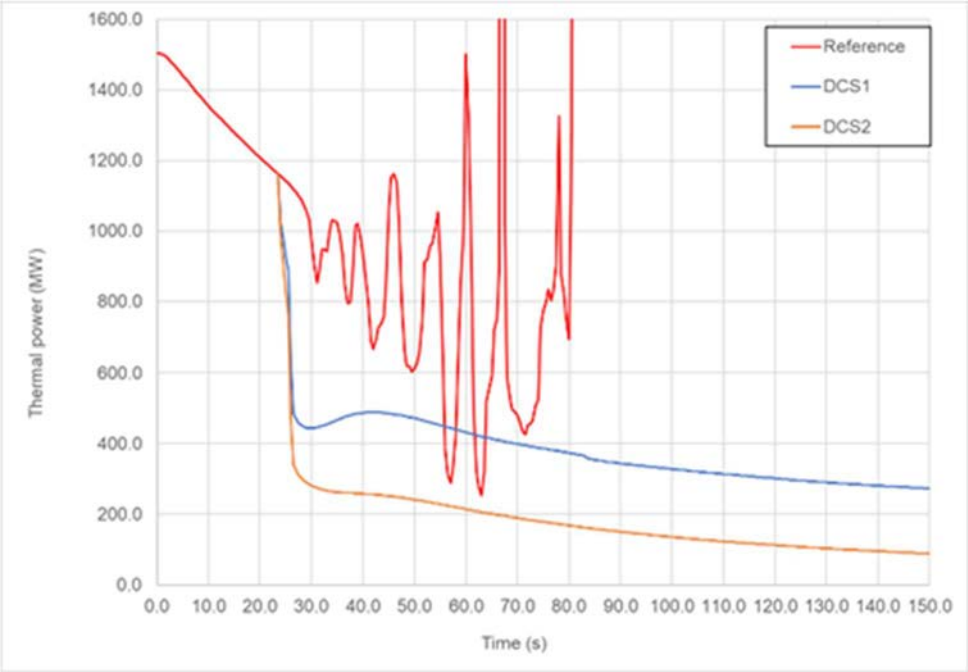

FIG. 7. Power evolution after DCS-P-H fall.

According to the simulation results, insertion of one rod with the timing provided by the hydraulic model is sufficient to prevent the degradation of the reactor during ULOF, while degradation is observed in the reference calculation procedure without rod introduction as described in Section 4. The reactivity reaches the minimum value of -1.14$ at 26.5 s with a power level of 450 MW(th). As the power goes down, the fuel temperature decreases, increasing the reactivity and the power to about 490 MW(th). The reactivity remains negative, leading to a steady decrease of the power. The power trend is similar after insertion of two control rods, with an enhanced effect at the time of the insertion, affecting the power also at later times.

The triggering events for the fall of RBD rods in different cases are selected using the Curie point approach. The average outlet sodium temperature reaches 650 °C at 24 s. This time is selected to perform the S2S coupling and to evaluate the insertion curves for the three cases: (1) 3 inner RBD rods, (2) 3 inner and 3 outer RBD rods, (3) 3 inner and 6 outer ones, i.e., all 9 RBD rods. These cases bring the reactivity effects of -700, -2000, -3500 pcm after the full insertion, respectively. The location of these rods in plane is shown in Fig. 1.

The fall of the inner 3 rods into the core is sufficient to shut down the reactor without consequences. An increase of the number of the inserted rods leads to a more rapid power decrease. All 9 RBD rods were inserted in a scenario where the fall is triggered at 10 s after the first clad rupture. The effect is strong enough to prevent the extension of the core degradation domain to the surrounding rings, limiting the pin failure to the ring with the first clad rupture.

Two PNS fall scenarios were considered. In one case, the fall is triggered by the presence of sodium vapour in the PNS region, for which a "10% volume fraction in one cell" criterion was considered. This criterion was met at 30 s after the ULOF start. In this scenario, the reactor is successfully shut down without further consequences. In a second case, the fall of the PNS into the core region is triggered when the core reactivity reaches 1$. In this case, the reactor power decreases after the absorber insertion, thus preventing further power excursions, but remains high enough to extend the pin failure domain to other rings and the transient develops further. These results are in line with those of earlier studies [14] on absorber introduction.

6. ASSESSMENT OF MECHANICAL ENERGY RELEASE FOR ASTRID IN THE CONTEXT OF OTHER STUDIES AT KIT

At KIT, assessment of the mechanical energy release was done more recently after ULOF in a large 3600 MW(th) SFR with a near-zero sodium void effect and transfer tubes. The mechanical energy components evolve with time similar to those in the ASTRID case, while the mechanical energy is larger for the larger reactor with higher power. The conversion (thermal to mechanical energy) ratio is below 1%. This is in line with earlier studies for a 300 MW(e) class reactor [13], giving the most probable ranges for the mechanical work and thermal-to-mechanical energy conversion ratio as 10–20 MJ and 0.15–0.3%, respectively.

7. CONCLUSIONS

For ASTRID safety studies, we employed the SIMMER code and extended its calculation capabilities. Old 11-group and more recent 72-group nuclear data libraries, the latter employed with cross-section condensation mesh-wise at every time step, were used in SIMMER. New reactivity feedback models for thermal expansion were applied in SIMMER calculations starting from steady state conditions to molten core configurations.

The computed mechanical energy release is limited in the most conservative case. The discharge tubes appear to be effective for all considered simulation options. Also, passive absorber introduction into the core after sodium flow rate reduction or sodium outlet temperature augmentation appears to be effective to stop the nuclear chain reaction. A fall of the PNS absorber layer into the core region, which is located above the sodium plenum, may also lead to reactor shutdown, provided that it starts not too late. If PNS falls too late, e.g. when the reactivity is about 1$, a core evolution is more complex because a large accumulated energy may enhance separation of molten fuel and other materials due to their different densities and reduce the effect of absorber introduction. Results of later studies on mechanical energy release after ULOF in a larger SFR and of earlier ones for a smaller SFR are in general consistent with those for ASTRID.

REFERENCES

[1] VENARD, C., BECK, T., BERNARDIN, B., et al. The ASTRID core at the midterm of the conceptual design phase (AVP2). Proc. International Conference ICAPP 2015, May 3-6, 2015, Nice, France.

[2] YAMANO, H., FUJITA, S., TOBITA, Y., et al., SIMMER-III: A Computer Program for LMFR Core Disruptive Accident Analysis, TN9400 2003-071, Japan Nuclear Cycle Development Institute (2003).

[3] MARCHETTI, M., GABRIELLI, F., RINEISKI, A., MASCHEK, W., The SIMMER/PARTISN Capability for Transient Analysis, Proc. International Conference PHYSOR 2014, Kyoto, Japan, Sep.28 – Oct.3, 2014.

[4] GUYOT, M., GUBERNATIS, P., LE TELLIER, R., Space–time effects in the initiating phase of sodium fast reactors and their evaluation using a three-dimensional neutron kinetics model, Ann. Nucl. Energy 85 (2015).

[5] BERTRAND, F., BACHRATA A., SEILER-MARIE, N., et al., Mitigation of severe accidents for SFR and associated event sequence assessment, Nucl. Eng. Des. 372 (2021).

[6] BACHRATA, A., BERTRAND, F., SEILER-MARIE, N., et al., Severe accident studies on the efficiency of mitigation devices in a SFR core with SIMMER code, Nucl. Eng. Des. 373 (2021).

[7] CAHALAN, J. E., WEI, T. Y. C., Modeling Developments for the SAS4A and SASSYS Computer Codes, Proc. International Fast Reactor Safety Meeting, pp. 123–132, Aug. 12–16, 1990, Snowbird, USA.

[8] ANDRIOLO, L., RINEISKI, A., VEZZONI, B., et al., An innovative methodology for evaluating core thermal expansion feedbacks in transient analyses. Proc. International Conference ICAPP 2015, May 03-06, 2015, Nice, France.

[9] VEZZONI, B., MARCHETTI, M., ANDRIOLO, L., et al., SIMMER analyses of the EBR-II shutdown heat removal tests, Proc. International Conference FR17, Yekaterinburg, Russia, June 26-29, 2017.

[10] KIEFHABER, E., Updating of an 11-groups nuclear cross section set for transmutation applications, Muehl, B. (Ed.), PNS Jahresbericht 1999, FZKA-6480, Karlsruhe, Germany (2000).

[11] RINEISKI, A., SINITSA, V., GABRIELLI, F., MASCHEK, W., C4P Cross-section Libraries for Safety Analyses with SIMMER and related studies, Proc. International Conference M&C 2011, Rio de Janeiro, Brazil, May 2-12, 2011.

[12] MASSONE, M., GABRIELLI, F., RINEISKI, A., A genetic algorithm for multigroup energy structure search. Annals of Nuclear Energy 105, 369-387 (2017).

[13] GABRIELLI, F., FLAD, M., GIANFELICI, S., et al., Probabilistic Evaluation of the Post Disassembly Energetics of a Hypothetical Core Disruptive Accident in a Sodium-Cooled SMR by using a Phenomenological Relationship Diagram, Energy Procedia 131, 222–229 (2017).

[14] RINEISKI, A., FLAD, M. GABRIELLI, F., VEZZONI, B., Fast reactor systems in the German P&T and related studies, Proc. International Conference FR17, Yekaterinburg, Russia, June 26-29, 2017.

DESIGN-ORIENTED SIMULATION TOOLS IN FRENCH SFR PROJECTS

N SEILER, J.B. DROIN, F. BERTRAND, R. CLAVIER,

CEA, DES, IRESNE Cadarache F-13108 St Paul Lez Durance France

Abstract

During the last decade, France has carried out new emerging Sodium Fast Reactor (SFR) Projects, including the advanced ASTRID project. Within this context, a significant work on SFR design has been achieved. The CEA's methodology considers the safety requirements regarding severe accidents at the earliest stage of the undergoing reactor design process. At this point, the use of mechanistic tools (like SAS4A, SIMMER codes) encompassing the whole knowledge of the severe accident phenomenology (making them capable of simulating any accidental sequence) requires an advanced knowledge of the reactor design. Also, the associated calculation costs are too high to provide the rapid feedback that the early design process demands. This motivated the development of fast running design-oriented physical tools, devoted to unprotected accidental sequences from various initiators, and mostly based on low-dimensional modelling (mostly 0D and 1D). Allowing many simulations in a reasonable computational time, they enable uncertainty propagation studies and sensitivity analyses. This approach is highly consistent with the current trend to take into account uncertainties (on input data or models) in safety studies, especially in the domain of severe accidents where many uncertainty sources remain. Various design options may be tested and their influence on the margins from the safety requirements may be rapidly characterized. Sensitivity highlight cliff edge effects which feature some major accident transient bifurcations which are of interest for safety. These design-oriented fast running simulation tools are the object of the paper. Their specificities, since each of them is dedicated to a particular accidental sequence, and main associated models are described. Their development is part of a quality process involving verification and validation steps to ensure the consistency of their results with the reality. Their validation studies on separated and integral tests versus experimental results or numerical results from mechanistic codes are summarized. Finally, illustrations of studies performed with these tools to challenge and to improve the design of the reactor cores in other versions from ASTRID are presented.

1. INTRODUCTION

Many countries actively pursue sodium cooled fast reactor (SFR) technology owing to its energy sustainability and nuclear waste management capabilities. In France, new SFR projects flourish in the context of energy transition and economic recovery. These new projects rely heavily on the R&D works achieved by the advanced ASTRID project. ASTRID (Advanced Sodium Technological Reactor for Industrial Demonstration) was initially a prototypical reactor of a 600 MW(e) sodium cooled fast breeder reactor (GEN-IV) designed from 2010 to 2017. Based on past French fast reactors (Rapsodie, Phénix and Superphénix) operating feedback, ASTRID presented breakthrough safety options such as, among others:

- A core presenting a low neutronics voiding effect in order to prevent and mitigate power excursions at the beginning of any accident [1].
- Mitigation features such as the transfer tubes (called DCS-M-TT) [2, 3]. These tubes, directly connecting the core to the core catcher, crossing the diagrid and the strong backs, were designed to rapidly reduce the amount of molten fissile material inside the core region in the case of a hypothetical accident. This would therefore decrease the likelihood and the amplitude of a core power excursion.
- Mitigation features, such as an internal core catcher to collect and cool the materials flowing from the molten parts of the core. This device safeguards the second safety barrier which is the reactor vessel, by ensuring long term cooling of these hot molten materials in order to prevent primary circuit failure and to ensure long term cooling of the core materials [4].
- A design favouring decay heat removal and an improved gas system of energy conversion based on a sodium/nitrogen exchanger and not sodium/water. The possibility of a sodium–water interaction in the power conversion system was thus eliminated.

Then to reduce costs, a smaller derived reactor of 150 MW(e) was proposed (called New-ASTRID), at the beginning with a Superphénix (SPX) type fuel to reduce the project risks and the fuel qualification.

During this period, accident simulations have been carried out at the earliest stage of the undergoing reactor design process to support it [3]. This work was performed by CEA during the CEA-JAEA collaboration [5]. At this early stage of the project, the use of mechanistic tools (such as SAS4A [6] and SIMMER [7] codes), encompassing the whole knowledge of severe accidents phenomenology and simulating any accidental sequence, is not realistic. Indeed, these simulation tools require an advanced knowledge of the reactor design and their associated calculation costs are too high to provide fast feedback that the early design process needs. This motivated the development of fast running design-oriented physical tools, devoted to unprotected accidental sequence from various initiators, and mostly based on a reduced order model (ROM) (mostly 0D, 1D or multizone). These tools allow a large number of simulations in a reasonable computational time and they enable uncertainty propagation studies and sensitivity analyses essential to reinforce the reactor design and to assess design margins. This approach is highly consistent with the current trend to take into account uncertainties (on input data or models) in safety studies, especially in the domain of severe accidents where many uncertainty sources remain. Various design options may be tested and their influence on the margins from the safety requirements may be rapidly characterized to proceed to corrective feedback. Sensitivity analyses lead to highlighting cliff edge effects that feature some major accident transient bifurcations. An example of such a bifurcation could be the fact that boiling can be restricted to the uppermost location of the core or will progress inside and induce flow redistribution leading to core degradation. Another example is the possibility to cool down a debris bed or its melting. Characterizing these bifurcations is thus of great relevance for safety. Furthermore, owing to sensitivity analyses carried out with these fast running design-oriented physical tools, the main physical parameters and design parameters causing these bifurcations are highlighted as well as the phenomena likely to govern the choices of design parameters. That allows direct feedback on the core design and may give some orientations for future R&D studies. Finally, as uncertainty propagation studies are performed, these various accidental sequences and their consequences in terms of safety may be quantitatively estimated in terms of occurrence probabilities that might be inputs for future probabilistic safety assessments (PSA).

This approach, combining mechanistic simulation tools and fast running design-oriented physical tools, has been repeatedly presented on the course of the ASTRID project [8, 9]. Complete accidental sequences are calculated by mechanistic tools with an important computation cost, considering mean values of uncertain parameters of design, the initial core state when the accident occur, parameters of the accident transient (such as the pump halving time in case of an unprotected loss of flow accident (ULOF) or time required for the delayed neutrons detector (DND) to detect the variation of neutron emission rate from transported precursors linked to an assembly failure in case of an unprotected sub-assembly fault accident (USAF)) or parameters of physical models. Although fast running design-oriented physical tools are validated on separate effects tests (SET) and integral effects tests (IET), it is then verified that their simulation results are the same as those obtained by mechanistic tools, when considering the same set of mean uncertain parameters. Following this verification, numerous simulations are carried out using fast running design-oriented physical tools, due to their low computational cost, taking into account realistic distribution laws of each uncertain parameter. This approach enables the simulation of all the possible realistic transients (of the order of thousands) of the considered accident (for example an ULOF or an UTOP) considering all the uncertainties, and obtains the distributions of the results of interest (for example, if the transient

ends to a flow redistribution and a core degradation or the final mass of molten material on the core catcher or remaining in the core, etc.). Similar approaches, considering fast running design-oriented physical tools, are not new. For decades, it has been internationally accepted that robust safety demonstrations need to take into account not only a mechanistic approach, but also a statistical approach using rapid simulation tools. This is due to the complexity of severe accidents [10]. In France, the safety demonstration of nuclear reactors such as Superphénix was based already based on 0D parametric tools. Thus the SUREX tool calculated the evolution of the core power and of the core material temperature during the primary phase of an UTOP and COMBUS evaluated the associated for the calculation of the mechanical energy release [11].

An approach using the low-dimensional tool PROCOR, combining physical event modelling with uncertainties treatment, has been developed for PWR severe accident analysis [12]. In Japan, the methodology development review of Level 2 PSA for SFRs [13] involved investigations with low-dimensional tools such as SuperCOP-D devoted to debris bed cooling on the core catcher [14]. An analogous approach, based on low dimensional design-oriented tools, is followed by IGCAR (Indira Gandhi Centre for Atomic Research) for the India fast reactors in development. So in this context, Ravi et al. [15] developed models to investigate the core damage due to the total instantaneous blockage (TIB) of an SFR fuel assembly (SA). Dubey and Sharma [16] built an effective and validated simulation tool for proceeding to informed design studies and succeeded in demonstrating the mitigating effect of in-pile molten fuel motion on the reactivity during slow UTOP (resulting from a control rod withdrawal). They derived valuable insights on top and bottom blankets design with aim of enhancing the inherent safety of SFRs [17]. Moreover, Bala Sundaram and Velusamy developed a multiphase heat transfer model for the optimization of core catcher design [18]. Finally, in Italy, an approach, based on the development of informed-design thermohydraulics and thermomechanistic tools, is also followed in the design of a Heavy Liquid Metal Cooled Reactor [19].

Thus, fast running design-oriented physical tools, part of the PROCOR-Na platform, have been developed in the framework of the French ASTRID project. These tools are continuously improved and their ability is widened and are used in ongoing and future French projects on SFRs. They are currently introduced into the PROCOR platform of CEA [12, 20], already including fast running tools dedicated to severe accidents in PWRs, which offers a more consistent development frame and facilitates the coupling of these tools.

These French design-oriented fast running simulation tools are presented in this paper. Their specificities, since each of them is dedicated to a particular accidental sequence, as well as their main associated models are described. Their development is part of a quality process involving verification and validation steps to ensure the consistency of their results. An insight of their validation on separated and integral experimental tests or on numerical results from mechanistic codes is summarized. Finally, illustrations of studies performed with these tools to challenge and improve the design of the ASTRID reactor cores are presented.

2. DESIGN-ORIENTED FAST RUNNING SIMULATION TOOLS

Currently seven designed-oriented tools, displayed in Fig.1 are used for French SFR safety studies.

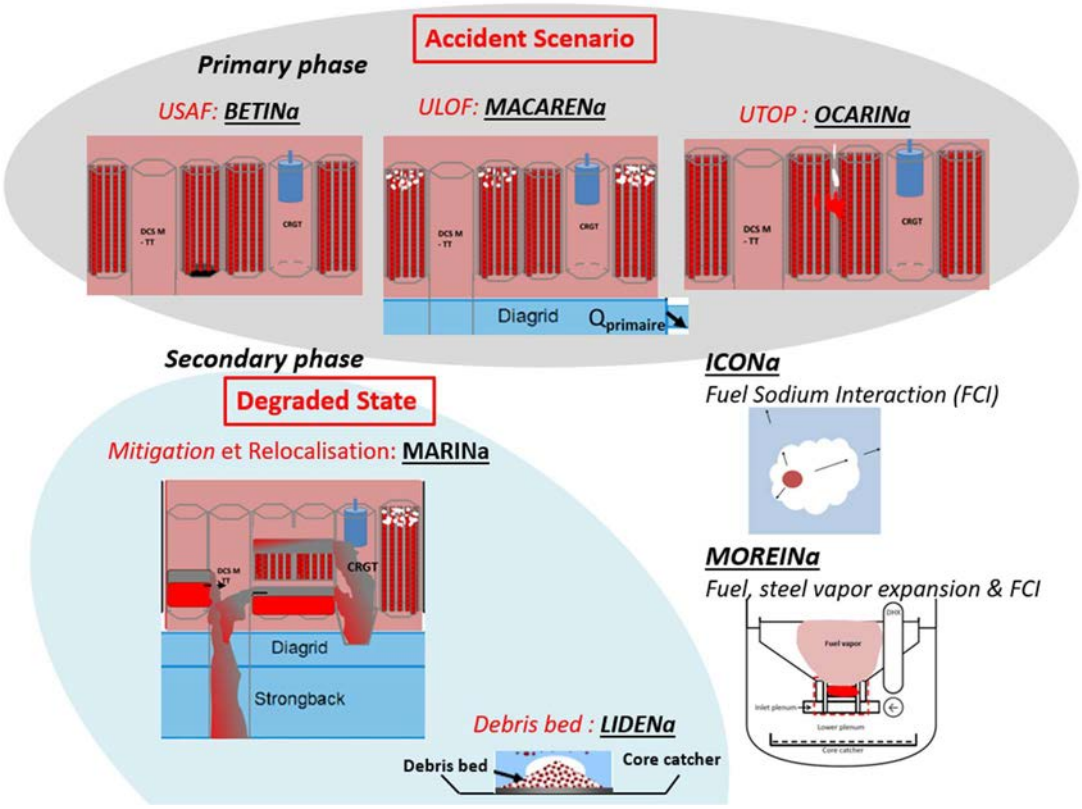

FIG. 1. Illustration of French designed-oriented tools devoted to SFR.

Some of the tools are specific to initiators of the accidental sequences and simulate the primary phase of:

- USAF transients; BETINa tool;
- ULOF transients; MACARENa tool;
- UTOP transients; OCARINa tool.

Additional designed-oriented tools are dedicated to the description of transients from a generic already degraded state situation:

- MARINa tool, which is particularly devoted to mitigation studies;
- MOREINa tool (including former ICONa, devoted to FCI and DETONa tools) treats vapour (fuel, steel, fission gas) expansion and related FCI causing vessel mechanical degradation;
- Debris Bed cooling; LIDENa tool.

These tools are coupled with each other to simulate a full accidental sequence as it is illustrated in Fig. 2 for the ULOF sequence. They are also coupled to advanced statistical methods to proceed to global sensitivity analyses [21].

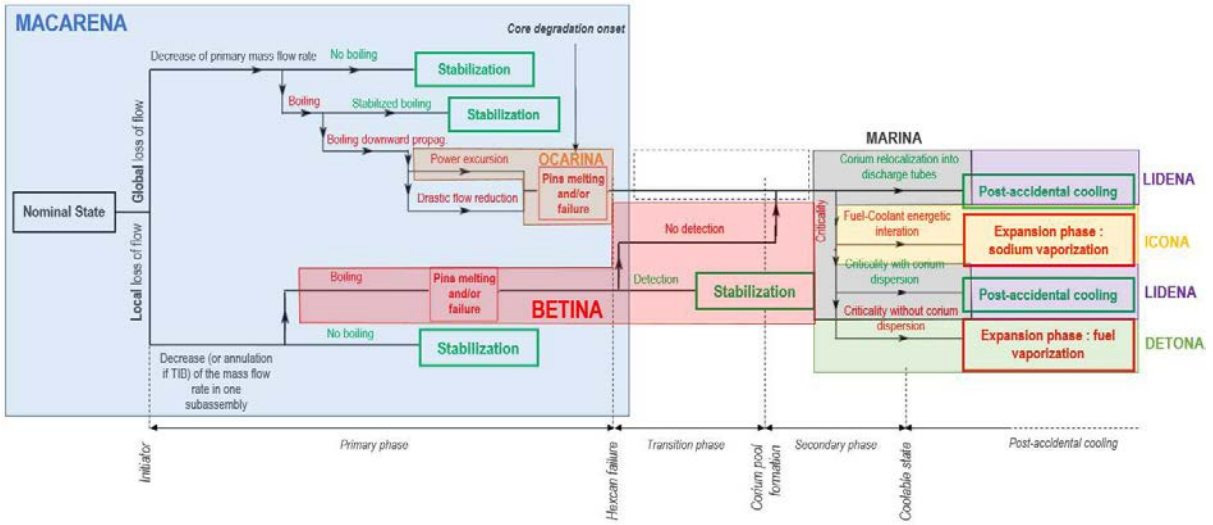

FIG. 2. Illustration of fast running tool coupling to simulate a full ULOF accidental sequence [9].

The development of these fast running tools is based on the phenomenological event tree of each major accidental sequence which is derived from a PIRT elaboration [22]. Following the PIRT methodology, the level of importance each phenomenon in the considered accidental sequences event is evaluated as well as its associated level of physical knowledge and of modelling uncertainty. This PIRT underlines the compulsory phenomena that should be modelled. A process of tool validation is carefully followed. In the following sections, main physical phenomena (issued from the PIRT), solved equations and main assumptions, validation are summarized for each fast running tool. These tools are all based on finite volume methods (to ensure the energy conservation) and time and meshing convergence are verified.

2.1 Tools devoted to primary phase

2.1.1 BETINa tool: total instantaneous blockage sequence

The TIB [23] begins with the cessation of the sodium flow at the inlet of one sub-assembly (SA). This accident is the extreme bounding case of an unprotected sub-assembly fault accidental sequence (USAF) which is a local or progressive blockage accident. A complete study and modelling is based on the sequences of events that occur during this particular accidental transient, which can be illustrated by a phenomenological event tree describing the full range of possible scenarios and their bifurcations [24]. During this transient, sodium vaporizes in the blocked SA (without renewal of the sodium mass). Then, as nuclear power continues to be released into the SA, the cladding melts at around 1700 K, followed by the fuel at around 3000 K. These molten materials are immiscible and form pools whose geometry evolves throughout the SA. Convective thermal heat transfers from these pools heat the walls of the SA, causing them to melt. This leads to the failure of the blocked SA. The molten materials may have formed a plug above this molten cavity, in which case, the pressure in the cavity may increase significantly. In this case, the propagation of molten material into neighbouring SAs is not only due to thermal effects (melting front driven propagations), but also to dynamic ones (pressure driven propagations). The BETINa tool couples 1D axial models for pins heating up before degradation and 0D models for the steel and fuel molten pools whose localisations follow their associated material melting front. Details of models and important uncertainties are given in Ref. [24].

Regarding its validation, intermediate results of the blocked assembly degradation phase have been compared to experimental various front progressions: sodium boiling and dry-out, clad

and fuel onset and end of melting fronts are consistent with results obtained in Superphénix configuration and with SCARABEE BE3+ experiment (a 37 pins bundle) [24].

2.1.2 MACARENa tool: unprotected loss of flow

MACARENa [25, 26] is a tool dedicated to the primary phase of ULOF transients. It no longer simulates the transient after the first hexagonal can failure. It provides coupled resolutions of thermohydraulics and neutronics. It couples:

- For radial heat transfer in solid materials: a two-dimensional (along the SA height and radially one mesh per material) transient heat equation in the various solids that make up the SA;
- For the axial evolution of sodium state: one-dimensional mass, momentum and energy balances resolved for sodium flow, considered as homogeneous (which can be single-phase or two-phase flow) along the assembly height.

Moreover, to distribute the sodium flow coming from the lower plenum to the various SA, a zero-dimensional momentum balance distributes the sodium mass flow rate according to pressure drop of each representative SA. This phenomenon of flow redistribution at the bottom of the core has to be well modelled, since it is of major importance in the ULOF transient. It enables flow instabilities in the various SAs to be modelled.

Finally, all these models are coupled with a neutronics point kinetics model even its validity becomes questionable in highly degraded core states. A more in-depth analysis of the validity of such a 0D neutronic model in case of large core degradation is still to be carried out and a 0D neutronic model which does not assume constant axial flux shape over time could be envisaged as done for the MARINa §2.2.4 tool.

The MACARENa results were validated on both experimental data of flow redistribution in ULOF (GR19) and on complete degradation transients (SCARABEE) and also on the results of integral degradation calculations (SIMMER-III mechanistic simulation) [25].

2.1.3 OCARINa tool: Unprotected Transient Over-Power

The UTOP transients, which are simulated by the OCARINa tool [27], are initiated by unintended insertion of reactivity.

Since radial heat conduction (with temperature-dependent conductivity) is paramount in this type of transient, OCARINa involves radial transient heat transfer modelling implicitly coupled with axial resolution of sodium thermohydraulics. In addition, at each time step, the radial resolution of the SA thermomechanics (based on analytical formulations) enables the prediction of cladding failure (modelled on von-Mises criterion) and the calculation of molten fuel mass and temperature inside the fuel pin during the transient.

To simulate the global core power evolution during the transient, these models are also coupled to a zero-dimensional neutron kinetics model.

This OCARINa physical tool was validated on the separate effects tests (characteristic of a particular phenomenon) performed on the CESAR (sodium dry-out) test loop and several CABRI integral tests. Its results have also been compared with those of SIMMER-III, with which a relative error of only 10% is exhibited [27].

2.2 Additional tools for advanced accident phases

2.2.1 MARINa: Mitigation tool

This tool [28] is dedicated to mitigation studies in the advanced accident phases. Its initial state is a generic degraded core, which could be parametrized based on the outputs of the primary phase simulations [11]. Its models are derived from experimental observations of secondary phase transient phenomenology. MARINa mainly solves zero-dimensional conservation balances. To simulate the evolution of the molten immiscible materials in the pool in the core, this 0D tool simulates the evolution of the pool geometric configuration (which evolves from mixed to stratified configurations and vice versa) and calculates the associated heat transfers to the edges, where a crust of resolidified material is deposited. These heat transfers are responsible for the radial thermal erosion of the hexagonal cans and their failure. This is followed by the discharge of molten core materials into the transfer tubes towards the core catcher. In order to obtain a realistic power evolution in the degraded geometry that evolves during the transient, these models are coupled to a global neutron evolution model of the degraded core. This special neutronic model takes into account the specific degraded core states using surrogated models derived from ERANOS simulations [29]. This physical tool was used to define the characteristics of the mitigation transfer tubes of ASTRID (number, influence of absorbers falling into the degraded core, corium mass relocated on the core catcher, etc.).

As no experimental data are still available for complex mixed materials, possibly boiling, pool behaviour and material discharge, pending the SAIGA programme [30], the results of this fast running tool has been numerically validated on 2D SIMMER-III results [28].

2.2.2 MOREINa: vapour expansion and mechanical energy, and ICONa: fuel–coolant interaction

MOREINa and ICONa tackle the issue of the mechanical energy released on the vessel, which is an important value to be calculated in order to assess the design margin of the vessel. MOREINa [31] includes ICONa, which could also be considered in stand-alone to simulate fuel–coolant interaction (FCI) [32]. MOREINa allows obtaining, from a mass of fuel overheated at a certain temperature, the mechanical energy release on the reactor vessel as well as the associated pressure impulse during the expansion phase of an energetic SFR severe accident. This mechanical energy release is due to steel, fuel, fission gas and sodium vaporization and their expansion. It implies several phases modelled in a1D multizone geometry. Thus, MOREINa models (issued on the former DETONa tool [33]) are based on dimensional analysis leading to build the balance equations with only the influent physical phenomena. In addition to various phase vaporizations, MOREINa simulates vapour and gas simultaneous expansion related to the pressure difference between the bubble containing the vaporized material and the cover gas. If this bubble expansion leads the molten materials to contact the coolant, integration of the molten material droplet into the bubble vapour is modelled as well as FCI phenomena.

Its current validation has been performed on EXCOBULLE tests [33], Cho and Wright FCI test cases [31] and it has been compared to SIMMER-III results.

2.2.3 LIDENa: debris bed cooling

The LIDENa tool is a 1D axial tool dedicated to debris bed cooling. It allows to study if saturation conditions are locally reached inside the bed. This would result in a remelting of fuel debris. Indeed to avoid further subcriticality on the core catcher, the geometry of the debris bed

should remain stable. This tool models the two-phase thermohydraulic evolution in a 1D axial representation of debris bed. It resolves a global energy balance where the equivalent fluid properties include solid debris.

3. ILLUSTRATIVE RESULTS

In this section, some illustrative results, among the numerous results that supported the ASTRID core design, are given. They were obtained with these design-oriented tools coupled to advanced statistical methods.

3.1 Results in the primary phase

3.1.1 Total instantaneous blockage sequence

Developed within the framework of the ASTRID project, the BETINa tool takes into account the specificities of its heterogeneous core, which presents a low void worth (called CFV). As the CFV core presents axially two fissile zones separated by a fertile zone, molten pool formation within each fissile zone is likely to occur during a severe accident. This formation of two molten zones cannot be simulated by mechanistic tools like SAS4A. The BETINa tool gives insight of global behaviour difference between homogeneous (SPX type) and heterogeneous (CFV type) cores submitted to a TIB through uncertainty propagation studies. Detailed analyses of the TIB scenario led to the identification of 27 uncertain input variables in the SPX core [24] and 31 in the CFV core. They are related to the core configuration and reactor features such as the power of the blocked assembly.

The second type of uncertainties is related to physical models. Their associated variable probability density functions are detailed in Ref. [24]. The propagation of input uncertainty has been performed via a Monte Carlo sampling of 1000 TIB simulations in the SPX core and 2500 simulations based on an optimized Latin hypercube sampling experimental design in the CFV case. Among others, the repartition of equivalent numbers of molten assemblies at the end of the transients is displayed in Fig. 3 and the related statistics for the SPX and the CFV cores in Table 1. Regarding the SPX core, the mean output value is 5.5 final equivalent molten SAs with a standard deviation of 7.5. From these results, it was highlighted the large variability of the predicted final numbers of molten SAs, which range from 1.02 to 37. But, despite this variability, the important result for safety is that in the great majority of realistic TIB transients, the final molten SAs number would not exceed the safety criterion of 7 molten SAs. This criterion value has been established to prevent general core melting in SPX and is reported in its safety report. Thus, thanks to this design-oriented simulation tool, the probability of exceeding this safety criterion can be estimated quantitatively to 18.1%. It could be noted that the same TIB transient (presenting same modelling assumptions and uncertainties) leads to reduced core degradation in the CFV core and shorter transients (the mean output value is 2.1 final equivalent number with a small standard deviation of 2.5). This result comes from combined effects of various design features. In the case of the heterogeneous CFV core, the empirical probability of having a final number above 3 molten SAs (taken as an illustrative value) is estimated at 16%.

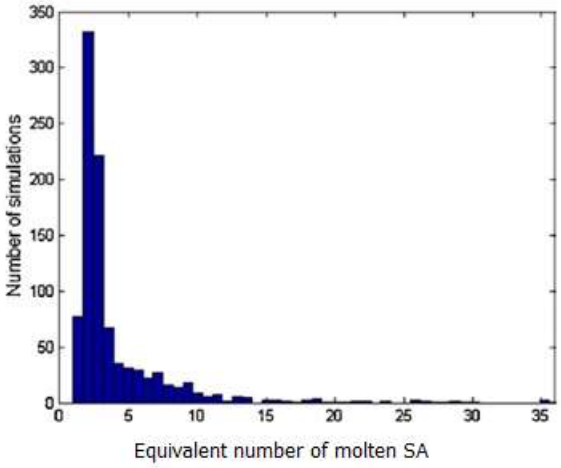

FIG. 3. Distribution of equivalent numbers of molten sub-assemblies at the end of TIB transients in a SPX core [24].

Global Sensitivity Analysis highlighted that, regarding the SPX case, the hydrodynamic propagation is the most influential variable and, in case of CFV core, it is the time delay for delayed neutron detection. This suggests R&D or design fields of research.

TABLE 1. SUMMARY STATISTICS OF EQUIVALENT NUMBERS OF MOLTEN ASSEMBLIES FOR SPX AND CFV CORES

	SPX Core	CFV core
Mean	5.5	2.1
Standard deviation	7.5	2.5
Median	2.6	1.31
Min	1.02	0.58
Max	37	21.7

BETINa is a fast running tool that is indeed highly adaptable. It has been adapted to SPX and CFV core design but also to other designs like the CADOR's core presenting a reinforced Doppler Effect.

3.3.2 Unprotected loss of flow sequence

A great deal of work has been done on ULOF sequence simulation thanks to the MACARENa tool coupled to statistical methods.

A quantified distribution of ULOF transient end states have been obtained by considering uncertainties linked to the scenario, input data and models [25]. Out of 2000 simulations, boiling is observed in most of these simulated transients (around 90%). Also, these results highlighted the paramount importance of taking into account the neutronics effect related to thermal expansion of solid material (including control rods and vessel expansion which was not modelled in SMMER-III until then) on global reactivity. When this effect is modelled (i.e. corresponding to more realistic simulations), the ULOF sequences leading to core degradation are reduced from 78% to 25%. In such cases, these ULOF transients end in stabilized boiling transients in ~70% of cases and, in only 10%, in stabilized transients without boiling.

The MACARENa tool has also been adapted to other core designs like the CADOR's core presenting a reinforced Doppler effect. Another result, illustrating the interest of these design-oriented tools, lies in the realization of flow stability maps, which present the assembly flow regime depending on the core power and on the assembly mass flow rate as illustrated in Ref. [9]. These maps, which give the flow types, summarize the results of statistical analyses carried out on the ULOF transients of the CFV and CADOR cores. The various flow types could be: either stable region of either single-phase liquid flow or stabilized boiling or even a region of unstable two-phase flow regime with risks of flow excursion. A mechanical integrity limit, related to the temperature, is also included to characterize pin loss of integrity. From these statistical studies, it has been demonstrated that the CADOR core presents a more extensive range of operating conditions with starting boiling (low-quality) and that the unstable flow region disappears when the power is under 35% of nominal power, whatever the operating conditions. In case of the CFV core, these safe operating conditions only appear for power under ~12% of nominal power. Thus, only based on this consideration, the CADOR core design seems to cope better with ULOF transients.

3.2 Results in advanced accident phases

The last illustration of the importance of these design-oriented tools is on mitigation studies. The MARINa tool had contributed to the conceptual design of mitigation devices DCS-M-TT in addition to the SIMMER code [28]. The number of such tubes, the uncertainties linked to their opening and their potential flow blockage and to the initial configuration of the molten pool (mixed or stratified steel and fuel) as well as the amount of required neutron absorber to avoid re-criticality have been assessed. Eight thousand simulations have been realized in order to cover four various initial pool configurations: either the molten materials in the upper fissile zone are initially mixed or stratified and the uppermost location could be blocked or not by a plug constituted by ejected and frozen materials. This first investigation has provided quantified results of importance to safety: a power excursion occurs in 8% of the simulated cases and material ejection in 18%.

TABLE 2. SUMMARY STATISTICS (OVER 8000 SIMULATIONS) OF FINAL DISTRIBUTION OF CORE MATERIALS RELOCATION AT THE END OF THE RELOCATION.

%	Above the core	Core-catcher	CRGT foot	Core
Fuel mass fraction	9.5	45	3.5	42
Steel mass fraction	11.5	51	3.5	34

Finally, these simulations inform the final region of core materials relocation. The results in Table 2 show that about 50% of the fuel and steel masses are on the core catcher. From these materials mass and average temperature results, MOREINa simulates the mechanical energy releases as presented in Ref. [9].

4. CONCLUSIONS

Within the framework of the Generation IV SFR R&D programme of CEA, safety requirements are already considered in the undergoing design process. Indeed, this enables an efficient design evolution towards intrinsically safe concepts. Among other methods and tools to fulfil these studies, several design-oriented tools are used. These fast running tools have been developed as a complement to more complex mechanistic tool which require high computational costs.

These tools allow a large number of simulations in a reasonable computational time and they enable uncertainty propagation studies and sensitivity analyses essential to achieve a satisfactory reactor design. These design-oriented physical tools are devoted to a dedicated unprotected accidental sequence, compared to the mechanistic tools which encompass the physical models enabling the simulation of any accidental sequence. They are mostly based on ROM (mostly 0D, 1D or multizone). Currently, seven designed-oriented tools are available for French SFR safety studies. Three of them are dedicated to the primary phase of each accidental sequence: ULOF, UTOP and USAF. Additional tools are dedicated to the mitigation studies from a generic already degraded state and specific situations; vapour (fuel, steel, fission gas) expansion and related FCI causing vessel mechanical degradation and debris bed cooling. The physical models of these tools and their validation have been summarized. Finally, example of obtained results has been presented highlighting the great interest of these fast running tools in the ASTRID design process. The integration of those tools into the PROCOR platform is under progress.

ACKNOWLEDGEMENTS

The authors would like to thank the Generation IV programme of the industrial nuclear support and innovation Division of CEA which supports this work as well as the SFR R&D Project.

REFERENCES

[1] P. Sciora, D. Blanchet, L. Buiron, B. Fontaine, M. Vanier, F. Varaine, C. Venard, S. Massara, A.C. Scholer, D. Verrier., 2011, Low void effect core design applied on 2400 MWth SFR reactor, proceedings of ICAPP 2011, Nice, France.

[2] A. Bachrata, F. Bertrand, N. Marie, A. Edeline, R. Kubota, K. Kamiyama, S. Kubo, Severe accident studies on the efficiency of mitigation devices in a SFR core with SIMMER code, Nuclear Engineering and Design, 373 (2021).

[3] F. Bertrand, N. Marie, A. Bachrata, V. Brun-Magaud, J.B. Droin, X. Manchon, K. Herbreteau, B. Farges, B. Carluec, S. Poumerouly, D. Lemasson, Status of severe accident studies at the end of the conceptual design of ASTRID: Feedback on mitigation features, Nuclear Engineering and Design, 326, pp. 55-64 (2018).

[4] A. Bachrata et al., Code simulation of quenching of a high temperature debris bed: Model improvement and validation with experimental results, International Conference on Nuclear Engineering, Proceedings, ICONE, 5 (1), pp. 77-85 (2012).

[5] F. Serre, F. Bertrand, A. Bachrata, N. Marie, S. Kubo, K. Kamiyama, B. Carluec, B. Farges, K. Koyama, (2017), France-Japan Collaboration on the Severe Accident Studies for ASTRID: Outcomes and future work program, ICAPP 2017 April 24-28, Fukui & Kyoto, Japan (2017).

[6] J.C Carter, G.J. Fischer, T.J. Heames, D.R. MacFarlane, N.A. McNeal, W.T. Sha, C.K. Sanathanan, C.K Youngdahl, SAS1A, A Computer Code for the Analysis of Fast-Reactor Power and Flow Transients, ANL-7607 (1970).

[7] S. Kondo, K. Morita, Y. Tobita, K. Kamiyama, D.J. Brear, E.A. Fischer, SIMMER-III: computer program for LMFR core disruptive accident analysis. O-arai Engineering Center, Power Reactor and Nuclear Fuel Development Corporation (1996).

[8] F. Bertrand, A. Bachrata, N. Marie, S. Kubo, Y. Onoda, A. Shibata, R. Kubota, B. Carluec, Mitigation of severe accidents for SFR and associated event sequence assessment, Nuclear Engineering and Design. 372 (2021).

[9] J.B Droin, N Seiler, F. Bertrand, X. Manchon, Safety-oriented SFR core design: methodology and application to transient bifurcations and stability maps analyses, Annals of Nuclear Energy 187, 109790 (2023).

[10] L. Luck, C. Bell, The case of integral core – disruptive accident analysis. ANS/ENS Fast Reactor Safety Meeting, Knoxville, TN, USA (1985).

[11] F. Bertrand, N. Marie, G. Prulhière, J. Lecerf, JM. Seiler, Comparison of the behaviour of two core designs for ASTRID in case of severe accidents, Nuclear Engineering and Design, 297, 327–342 (2016).

[12] R. Le Tellier, R., Saas, L., Payot, F., Phenomenological analyses of corium propagation in LWRs: the PROCOR software platform, The 7th European Review Meeting on Severe Accident Research ERMSAR-2015, Marseille, France (2015).

[13] R. Nakai, T. Suzuki, H. Yamano, H. Seino, H. Ishikawa, Development of severe accident evaluation technology (Level 2 PSA) for Sodium-cooled Fast Reactor (1) Overview of evaluation methodology development, ICAPP'09, Tokyo, Japan (2009).

[14] J. Sogabe, et al., Validation analyses of a debris bed heat removal model using D series experiments, Proc. of 2013 Fall Meeting of the Atomic Energy Society of Japan (2013).

[15] L. Ravi, K. Velusamy, P. Chellapandi, A robust thermal model to investigate radial propagation of core damage due to total instantaneous blockage in SFR fuel assembly. Ann. Nucl. Energy 62, 342–356 (2013).

[16] A. Dubey, A.K. Sharma, Melting and multi-phase flow modelling of nuclear fuel in fast reactor fuel rod, International Journal of Thermal Sciences, 125, 256-272 (2018).

[17] T. Sathiyasheela, R. John, A. Dubey, K. Devan, Comparisons of Reactivity Feedbacks Under UTOPA in Fast Reactors. Nuclear Engineering and Design, *384*, 111443 (2021).

[18] G Bala Sundaram, K. Velusamy, Development of a robust multi-phase heat transfer model and optimization of multi-layer core catcher for future Indian sodium cooled fast reactor, Annals of Nuclear Energy, 136 (2020).

[19] F. Lodi et al. ANTEO+: a subchannel code for thermal-hydraulic analysis of liquid metal coolant systems. Nuclear Engineering and Design, 301:128–152 (2016).

[20] R. Clavier, M. Johnson, B. Bigot. Corium pool behaviour in the core catcher of a sodium-cooled fast reactor. Nuclear Engineering and Design, 412, 112439 (2023).

[21] A. Marrel, N. Marie, M. De Lozzo. Advanced Surrogate model and sensitivity analysis methods for SFR accident assessment, Reliability Engineering and System Safety, 138, 232–241 (2014).

[22] G.E Wilson, B.E. Boyack, The role of PIRT in experiments, code development and code applications associated with reactor safety assessment. Nuclear Engineering and Design 186, 23–37 (1998).

[23] J. Papin,, Behaviour of Fast Reactor Fuel During Transient and Accident Conditions. Comprehensive Nuclear Materials. Elsevier Ltd (2012).

[24] N. Marie, A. Marrel, J.M. Seiler, F. Bertrand, Physico-statistical approach to assess the core damage variability due to a total instantaneous blockage of SFR fuel sub-assembly, Nuclear Engineering and Design 297, 343–353 (2016).

[25] J.B. Droin, N. Marie, A. Bachrata, F. Bertrand, E. Merle, J.M. Seiler, Physical tool for unprotected loss of flow transient simulations in a sodium fast reactor. Ann. Nucl. Energy 106, 195–210 (2017).

[26] J.B. Droin, N. Marie, A. Marrel, F. Bertrand, A. Bachrata, Design-oriented tool for Unprotected Loss Of Flow simulations in a Sodium Fast Reactor: Validation and application to stability analyses, Nuclear Engineering and Design, 361, 110550 (2020).

[27] K. Herbreteau, N. Marie, F. Bertrand, J.M. Seiler, P. Rubiolo, Sodium-cooled fast reactor pin model for predicting pin failure during a power excursion. Nuclear Engineering and Design 335, 279–290 (2018).

[28] N. Marie, A. Bachrata, J.M. Seiler, F. Barjot, A. Marrel, S. Gossé, F. Bertrand, A physical tool for severe accident mitigation, Nuclear Engineering and Design 309 224–235 (2016).

[29] J.M. Ruggieri, J. Tommasi, J.F. Lebrat, C. Suteau, D. Plisson-Rieunier, C. De Saint Jean G. Rimpault, J.C. Sublet, ERANOS 2.1: International Code System for GEN IV Fast Reactor. ICAPP 2006, Reno, USA (2006).

[30] F. Payot, F. Serre, A. Bassi, C. Suteau, E. Batyrbekov, A. Vurim, A. Pakhnits, V. Vityuk, The SAIGA experimental program to support the ASTRID Core Assessment in Severe Accident Conditions. In: Proceedings of the Fast Reactor conference (FR17). Yekaterinburg, Russia, June 26-29 (2017).

[31] A. Mouly, N. Seiler, F. Bertrand, M. Gradeck, Modelling of the expansion phase of sodium fast reactor severe accident, Annals of Nuclear Energy 186: 109717 (2023).

[32] D. Caraghiaur, N. Marie, F. Bertrand, P. Kudinov, Simplified models dedicated to vapour explosion applicable for ASTRID pre-conceptual design, the 13th International Conference on Multiphase Flow in Industrial Plants, Sestri Levante (Genova), Italy, 17-19 September (2014).

[33] X. Manchon, F. Bertrand, N. Marie, M. Lance, D. Schmitt, Modelling and analysis of molten fuel vaporization and expansion for a sodium fast reactor severe accident. Nuclear Engineering and Design, 322:522 535 (2017).

CEA EXPERIMENTAL ROADMAP FOR SODIUM FAST REACTOR SEVERE ACCIDENT R&D

C. JOURNEAU[1], A. BACHRATA[1], E. PLUYETTE[1], F. CHAROLLAIS[1], R. CLAVIER[1], A. LECOANET[1], N. SEILER[1], J. DELACROIX[1], A. QUAINI[2], C. GUENEAU[2], F. DERASSE[3], F. PAYOT[4],

[1]CEA, DES, IRESNE, DTN, Cadarache, France
[2]University of Paris-Saclay, Corrosion and Material Behavior Research Service, Gif sur Yvette, France
[3]CEA, DES, DIMP, Cadarache, France
[4]CEA, DES, IRESNE, DER, Cadarache, France

Abstract

After the end of ASTRID conceptual design studies, CEA has launched a long term R&D effort on several generic Sodium Fast Reactor (SFR) issues including severe accidents. In support of modelling and expertise, an experimental roadmap is being carried out on SFR severe accidents including in-pile integral tests, out-of-pile integral and separate effects experiments with prototype materials and analytical experiments with simulant materials. In support of modelling and expertise, an experimental roadmap is being constructed on SFR severe accidents. The main issues under study are the efficiency of corium transfer tubes to mitigate energetic power surges in the core region, interactions between materials, relocation from core region to lower plenum, fuel–coolant interaction (FCI), short and long term behaviours of an in-vessel core catcher. An in-pile experiment, SAIGA, is being prepared at NNC-RK Impulse Graphite Reactor (IGR) to study unprotected loss of flow with a transfer tube. Concerning FCI, a separate effect experiment, SERUA, is to start in 2023–2024 at the CEA/IRESNE Cadarache site to study the transition from film to nucleate boiling in sodium around a corium droplet. CEA is carrying out an updated conceptual design of the newPLINIUS facility in order to be able to run experiments with 100-kg scale prototypic corium mixture. The first test section that will be installed in newPLINIUS sodium hall will be devoted to the study of jet fragmentation in gas and in sodium. Later, other test sections are planned for newPLINIUS, one to deal with melt relocation in a transfer tube and one to study energetic FCI at significant scale. Another important topic, jet ablation of core catcher structures is being studied in collaboration with LEMTA owing to European projects. Furthermore, interactions of B_4C absorbers with stainless steel and/or oxidic fuel is being studied at CEA. Experimental programmes have started at the CEA/IRESNE VITI facility in Cadarache and the CEA/ISAS high temperature mass spectrometer furnace at Saclay. These experimental programmes have been constructed in order to provide the necessary data to validate the calculation tools under development for SFR severe accident modelling and to inform the design of severe accident mitigation devices. They will also concur to maintaining CEA knowledge and knowhow on SFR technology in view of its future developments.

1. INTRODUCTION

After the end of ASTRID conceptual design studies, CEA has launched a long term R&D effort on generic sodium fast reactor (SFR) issues including the severe accident field. In support of SFR severe accident modelling and expertise, an experimental roadmap is being carried out including in-pile integral tests, out-of-pile integral and separate effects experiments with prototypic or simulant materials. The main issues under study are the efficiency of corium transfer tubes to mitigate energetic power surges in the core region, interactions between materials, fuel–coolant interaction (FCI), short and long term behaviour of an in-vessel core catcher.

The SAIGA in-pile test programme simulating corium transfer tubes will be described. Then the FCI experimental programme will be described. Finally, the experiments related to core catcher issues and those for thermochemistry will be presented.

2. IN-PILE EXPERIMENTS: SAIGA EXPERIMENT

The SAIGA in-pile experiment [1] is being prepared at NNC-RK in the Impulse Graphite Reactor (IGR) to study the degradation of two 16-fuel pins bundles having different power densities and the propagation of a molten pool called corium from one fuel assembly to its neighbour (assembly, transfer tube) in an unprotected loss of flow (ULOF) transient.

The test device consists of three assemblies in a hexagonal tube (see Fig. 1): Two fuel assemblies with a bundle of 16 homogeneous annular fuel pins and one transfer tube assembly. Each argon-filled pin consists of a 0.8 m high column of 5.9 mm diameter pellets wrapped with a 1 mm spacer wire. The test section is to be installed in the central channel of IGR.

The enrichment in ^{235}U of the two assemblies leads to different power densities (120 W/g vs. 93 W/g in each fuel assembly respectively) representative of SFR fuels with different burnups [2]. A 1.8 kg/s sodium flow rate (inlet temperature ~400 °C) will be provided into each assembly in the initial 'steady state' phase of the test. The sodium circulation is indicated by arrows in Fig. 1 left. Sodium in the transfer tube is quasi static.

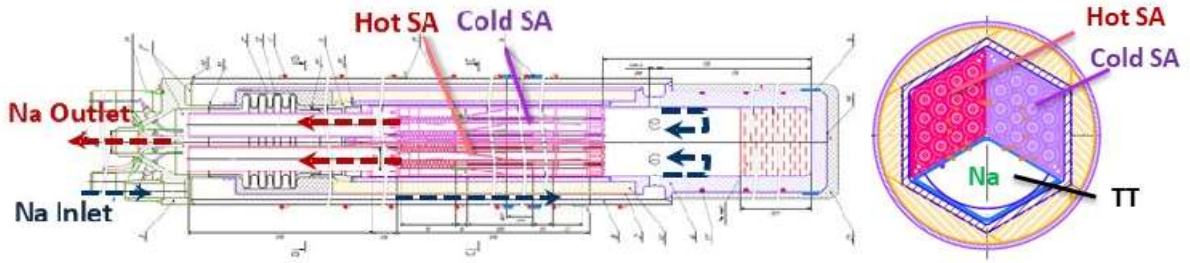

FIG. 1. Cross-sectional schematic view of the SAIGA multiassembly test: axial (on the left) and radial (on the right) views [3].

The SAIGA test sequence will start by a thermalization phase by 400°C sodium without any neutronic power. Then IGR will provide power to reach a steady state with a 150°C temperature increase in the hot assembly. Keeping the reactor power constant, ULOF will be started by cutting sodium flow over a 5 s period and the accident progression will be recorded.

The aim of this test is to qualify SIMMER-V calculations of transfer tubes operation [3]. In this view, pre-calculations have already been carried out, indicating a cladding wall melting about 31 s after the start of the steady state, leaving more than 10 s of available reactor power before the end of the test [3].

3. FUEL COOLANT INTERACTION EXPERIMENTAL PROGRAMME

CEA is developing the SCONE (**S**oftware for COrium-Na interaction Evaluation) software [4] in view of having a validated fast transient multiphase multicomponent simulation tool. Even though there is a large legacy of FCI experiments, some data are still missing and require dedicated experimental programmes, as follows:

- SERUA, a small scale facility to give an insight on the transition from film to nucleate boiling in sodium around a corium droplet;
- newPLINIUS (formerly PLINIUS2) to study jet fragmentation and explosion at larger scales (30-100 kg).

3.1 SERUA

During FCI, the film boiling regime plays a major role in the vapour production, energetic phase initiation and pressure buildup. Knowledge gaps in the understanding of this regime (and then in the sodium boiling curve) have been clearly identified at CEA [5]. The SERUA facility aims at filling these gaps by a careful assessment of the film boiling regime based upon a new experimental programme for which a sodium quenching facility has to be built.

This quenching set-up will be very similar to the Farahat experiment [6], the only available sodium film boiling experiment. Farahat investigated film boiling heat transfer over a hot tantalum sphere (1800 K < sphere temperature < 2633 K with a sphere diameter of 25.4 mm) immersed into a stagnant sodium pool close to saturation (natural convection, 6.4 K < sodium subcooling < 31.4 K). The detailed re-analysis of the Farahat results led us to suspect the occurrence of two film boiling regimes: a low-flux stable film regime and a high-flux unstable film (with contacts) regime. However, the Farahat experimental results were not precise enough, due to some experimental limitations, nor representative enough of a FCI for CEA to validate our first theoretical approach [7].

An illustration of the SERUA facility with the instrumented tantalum sphere is given in Fig. 2. It gives a schematic representation of the various components of the SERUA facility:

- An instrumented tantalum sphere;
- An induction furnace in which the tantalum sphere will be heated;
- A sodium volume, capable of dealing with low subcooling.
- A pneumatic transfer system to relocate the sphere from the furnace to the sodium.

In the first phase of the programme, the facility needs to enable a hot sphere to be quenched in sodium, and the data obtained will enable comparison with the experimental data published by Farahat et al. [6]. New instrumentation based on Coef h™ sensors [8] will be used to measure and monitor the heat fluxes and temperatures of the heating element in the sodium film. Comparing our data with the previous experimental data will enable us to assess the reliability of the facility. In the second phase, we will carry out quenching experiments with small hot spheres, applying experimental conditions to assess the effects of the relevant parameters (e.g. sodium temperature, flow around the sphere, size of the sphere). Lastly, providing experimental data that is sufficiently reliable is the key to developing a heat transfer model of the boiling behaviour of sodium in FCI conditions.

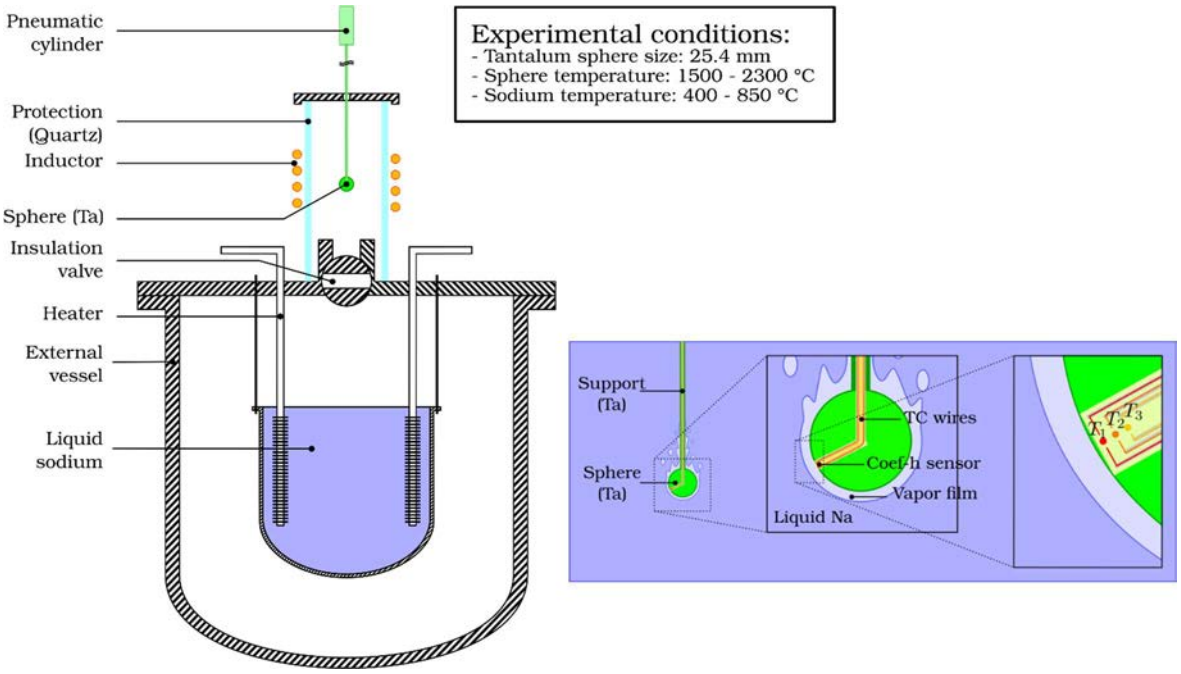

FIG. 2. Sketch of the SERUA facility.

The induction furnace design has been experimentally validated by tests conducted in the VITI facility at Cadarache (France) [9]. In parallel, tests have been carried out to validate the heating

procedures for sodium close to boiling temperature. The facility is planned to be constructed in 2023 so that it can be commissioned in 2024, starting with the comparison with Farahat's data.

3.2 NewPLINIUS – LARGE EXPERIMENTAL PROGRAMME

CEA is carrying out an updated conceptual design of the newPLINIUS facility in order to be able to run experiments with 100-kg scale prototypic corium mixture (depleted uranium oxide based melts with, if needed, metallic melt). This facility is based on the large experience gained from running the current PLINIUS experimental platform [9] and on the design phase of the terminated PLINIUS-2 project [10].

The newPLINIUS versatile facility will be devoted to both water and sodium cooled reactor severe accident experimental simulation. It will mainly be composed of:

- A furnace, called FOURNAISE (Furnace for Oxides of URanium melting in New Advanced Infrastructure for Safety Experiments), able to melt 100 kg of corium including nuclear fuel (depleted UO_2);
- An experimental hall devoted to FCI tests with high energy X ray imaging [11];
- A sodium circuit supporting experiments with corium and sodium;
- A second experimental hall, including a steam quenching system, in which experiments can be carried out with up to 500 kg of uranium thermite;
- A corium load preparation workshop, storage and service rooms;
- Small scale facilities to study thermo-physical properties of corium and material interactions.

Figure 3 presents the current layout of the newPLINIUS platform design with FOURNAISE and the large scale interaction hall at ground level and the FCI hall underground.

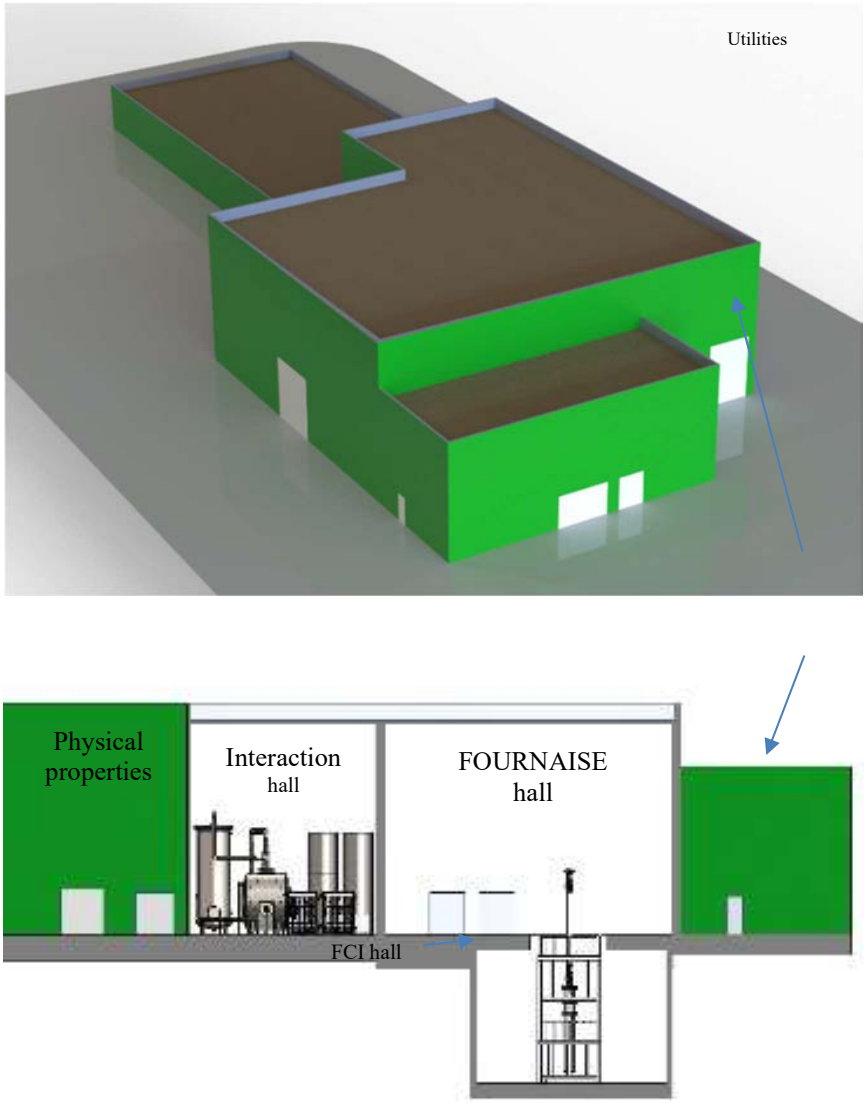

FIG. 3. General Layout of newPLINIUS (provisional design) Top: 3D view, bottom: cut view.

Two test sections will be needed to study FCI for the sodium programme. An X ray imaging system with a very rapid image acquisition system (coupled with accurate image processing software) makes it possible to better understand the phenomena involved in the fragmentation of corium and the phase distribution (liquid sodium, sodium vapour and corium) in the system. However, implementation of the image acquisition system raised a number of issues with respect to the design of only one test section. It therefore became necessary to design two different test sections:

- A small test section (FR: fragmentation test section) in which an X ray image acquisition system could be installed, while meeting all technical specifications (Fig. 4 left);
- A large test section (EXPLO: explosion test section) that can withstand more energetic events but is too thick to be instrumented with X ray devices (Fig. 4 right).

The main difference between the two test sections is their size, as FR will only employ between 30 and 50 kg of corium interacting with 141 litres (Ø0.3 m x 2m) of sodium while EXPLO could use corium masses up to 300 kg (assuming an upgrade of FOURNAISE) interacting with 1500 litres (Ø1 m x 2m) of sodium.

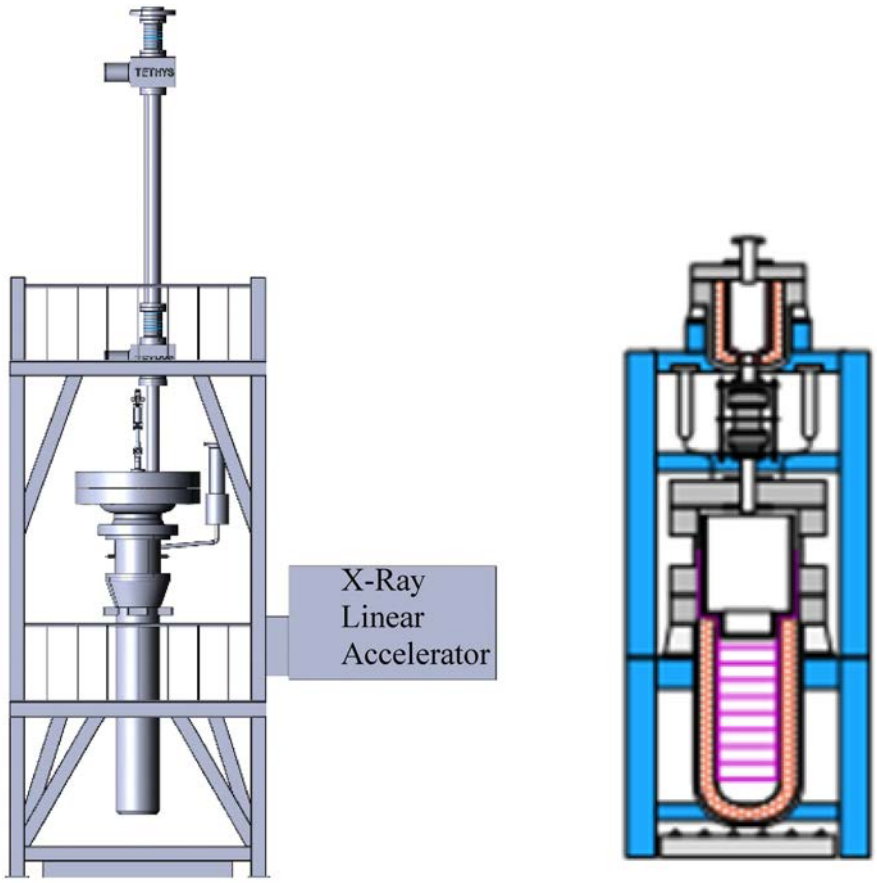

FIG. 4. Sketches of the FR[augmentation] (left) and EXPLO[sion] (right) test sections.

The FR test section is scheduled at the beginning of the newPLINIUS platform commissioning. After the operation of this FR test section, the design studies and fabrication of the EXPLO test section will be initiated. The test section commissioning will be made step by step to overcome technical hurdles and to take advantage of the lessons learned from the future FR test series. The phenomena that will be investigated are:

1. Corium fragmentation mechanisms in subcooled sodium: In this case, we will focus on the first corium flows (UO_2 at T~3100 K or steel at T~2000 K) exiting the discharge tubes into the sodium at the bottom of the reactor vessel at a temperature of about 670 K. Though past experiments have shown that a coherent flow of UO_2 could not penetrate subcooled sodium, we still have limited knowledge about the physics involved in the first contact between these substances under such conditions.

2. Corium fragmentation mechanisms in sodium close to saturation point: Even though successive and/or extended flows of corium will take place through the discharge tubes, the sodium will be reheated — locally at least — and the corium is expected to penetrate the sodium in a more coherent manner. The fragmentation mechanisms occurring at the top and in the cylindrical part of the corium jet where the vapour flows counter-current, are expected to be similar to phenomena involved in corium–water interactions, though this remains to be confirmed. We should also be able to identify a break-up length in the jet.

3. Physical conditions during which fragmentation phenomena evolve: We need to understand the temperature (for sodium in particular) and pressure conditions during which the fragmentation phenomena will take place (transition from mechanism 1 to mechanism 2).

4. Formation and changes of sodium vapour, and general phase distribution (liquid sodium, sodium vapour and corium) in the system: We are looking to understand how pockets of sodium vapour form and how they can be hindered by structures, considering that these pockets are likely to promote the penetration of a coherent jet of corium in the sodium.

5. Physical conditions leading to an explosive situation (fine fragmentation of corium):
   - In subcooled sodium;
   - In hot sodium, in particular, we need to understand why the pressure reached 60 bar in the sodium pool during the FARO-TERMOS-T2 experiment [12].

6. Delayed interactions: This refers to the time between the moment the corium comes into contact with the sodium and the development of the first pressure peak. It is assumed that heat transfers between the fuel and the sodium during this time are insignificant since the heat exchange surface between the two substances is insufficient. Past experimental results do not reveal any clear trend between the duration of the delay and the initial sodium temperature, though this point remains to be clarified.

7. Morphology of the debris bed: Regardless of the pressure levels reached during interactions and the mechanical energy released, past experiments have always shown significant fragmentation in the corium with a clear difference in morphology between the oxide debris (irregular, fractured and average sized fragments of about several hundred microns in size and massed together) and metallic debris (rounder in shape and average sizes of about a millimetre). The characteristics of the debris bed (size and porosity as a function of axial and radial extensions) will control its coolability during post-accident management.

4. CORE CATCHER EXPERIMENTAL PROGRAMME

This experimental programme is devoted to gaining relevant data for the simulation of the phenomena occurring on an in-vessel core catcher and in particular the interaction between corium and the core catcher material.

4.1 Jet ablation

A first issue lies with the ablation of the core catcher by a molten jet. This configuration is more likely if a vapour bubble at the exit of the corium transfer tube prevents significant fragmentation by liquid sodium.

Prototype experiments have been carried out with a metallic jet at the JIMEC facility [13] in the Karlsruhe Institute of Technology. In this test, one ton of liquid steel is prepared using an alumino-thermite reaction. The melt is then poured on a thick steel block (Fig. 5 left), the ablation of which is monitored by thermocouples. It has to be noted that during both tests carried out within the ESFR SMART European project, the 40 cm thick steel block has been ablated and ablation rate shows that a pool effect has been reached.

It is planned to complement these metallic jet tests with tests dealing with prototypic oxide tests and mixed oxide–metal jets. This new programme could start with FR facility commissioning tests before filling the vessel with sodium in the newPLINIUS platform.

In parallel to these large scale tests with high temperature prototypic materials, a separate-effect test series is being carried out in the HAnSoLO facility (Fig. 5 right) at LEMTA, University of Lorraine, using water and transparent ice as simulant materials [14]. A first series of tests have been carried out within ESFR SMART European project to study the cavity shape and the pool

effect [15]. A new test series is planned within the new ESFR SIMPLE European project to study the effect of mitigation systems on ablation processes.

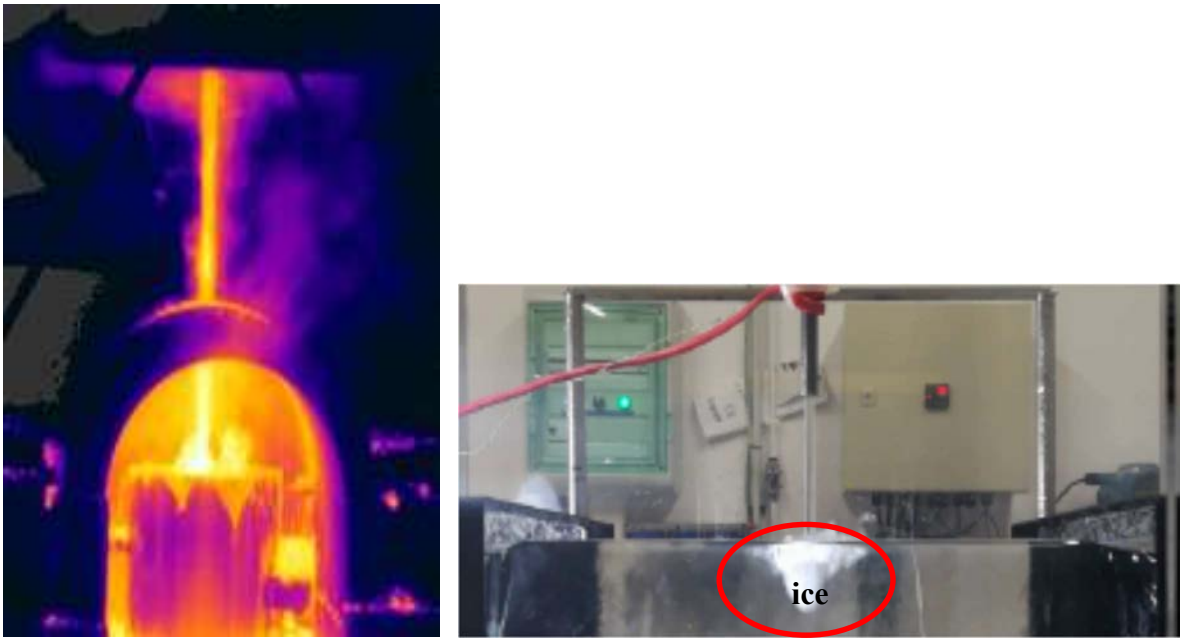

FIG. 5. Left: Thermographic image of steel jet in JIMEC ©KIT, 2019 – Right: View of HAnSoLO experiment with water jet on an ice block ©Université de Lorraine, 2021.

4.2 Long term interaction of corium met with core catcher material

In the longer term of an accident scenario, a molten pool can interact with the core catcher. The LIVE-CC vessel [16] has been installed in the LIVE facility at KIT Karlsruhe (Fig. 6). It has a truncated cone geometry in its bottom and is cylindrical above, as are most SFR core catcher designs. It is cooled from outside and can be cooled from the top. Two experiments have been carried out in which the heating power and the pool geometry have been varied. The measured temperature fields compared favourably with DNS calculations [16]. In a new programme, within ESFR SIMPLE with pre and post calculations by CEA, more complex geometries will be considered to simulate the effect of an ablation hole or the presence of a protective block below the exhaust of the corium transfer tube.

In the future, the newPLINIUS interaction hall could be used to carry out experiments similar to LIVE CC tests but using prototypic melts instead of molten salt simulant.

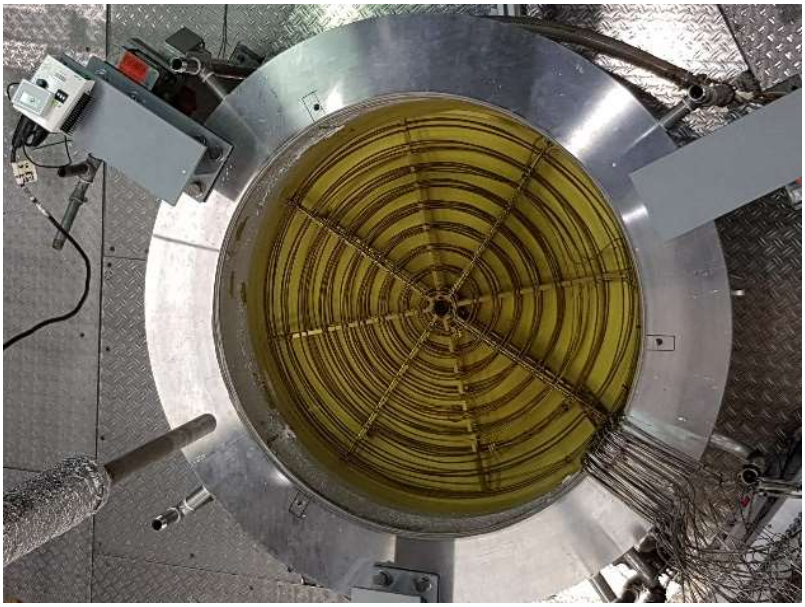

FIG. 6. Top-view of the LIVE-CC facility filled with molten salt and heated by several layers of resistors.

5. THERMOCHEMISTRY PROGRAMME

Although most SFR codes do not currently deal with chemical evolution of melts during an accident, there can be some thermochemical effects of importance. This is particularly the case for interactions with B_4C neutron absorbing material.

A first experimental programme is devoted to the study of the UO_2-Fe-B_4C system (as the major subsystem of the UO_2-Stainless Steel-B_4C system of interest). Heat treatments are carried out at Saclay in a high temperature tungsten furnace coupled with a mass spectrometer. Figure 7 left presents a view of the high vacuum vessel of this furnace. A series of five compositions is to be studied at 1900°C to identify the relevant physico-chemical interactions between a mixture of SS/B_4C and UO_2 [17]. The first heat treatments have been carried out in 2022 showing a strong effect of B and O content on the kinetic release of non-condensable gases (e.g. $CO_{(g)}$) driven by a carbo-reduction reaction.

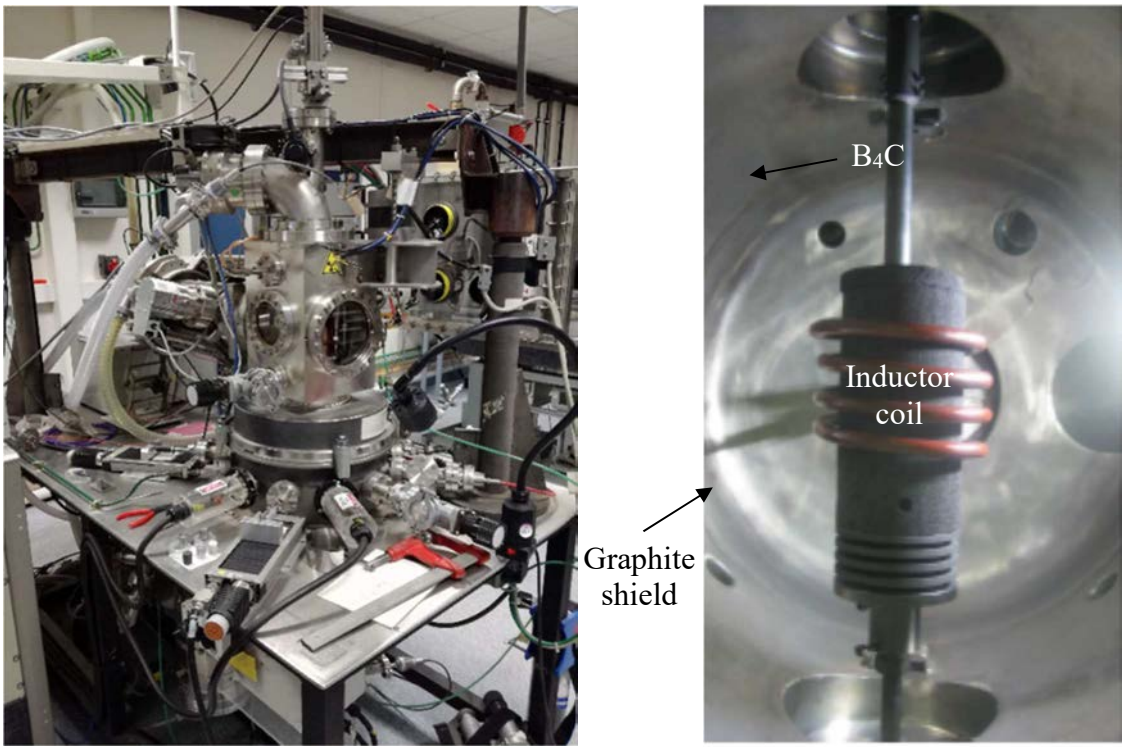

FIG. 7. Left: High vacuum vessel of the Nabertherm® furnace. Right: View of the VITI facility with a movable B_4C rod.

A second point of interest lies with the interaction between B_4C and molten fuel that may lead to the vaporization of boron oxide, reducing the availability of boron as a neutron absorber. After a first series of tests on the kinetics of the UO_2-B_4C interaction at UJV and CVR Řež [18], a series of experiments in the VITI facility [9] has been launched. In these tests, B_4C will be introduced in an UO_2-CeO_2 molten pool simulating molten MOX. Tests are planned with and without stainless steel cladding.

In support of these tests, a series of characterizations have started on the UO_2-CeO_2 mixture: determination of liquidus temperature using visual polythermal analysis [19]; measurement of the melt density and surface tension by maximum bubble pressure technique [19]. Similar characterizations are also planned on UO_2-CeO_2-fission product prototypes mixtures, UO_2-CeO_2 melt including dissolved boron and steel containing dissolved boron and uranium.

Finally, specific interaction tests are also conducted at Saclay in a furnace with B_4C crucibles in which a SS316L disk is installed. In some of these tests, an UO_2 pellet is installed on top of the stainless steel disk. This 'sandwich' configuration is representative of the possible interaction of cladded pellets interacting with boron carbide. This test programme comprises interactions at five different temperatures and has started in 2022.

6. SUMMARY

CEA has started a comprehensive experimental programme in support of its renewed SFR severe accident R&D programme. This programme comprises experiments that are carried out in facilities operated by our partners either through dedicated contracts such as the SAIGA test at IGR or thanks to European projects (at JIMEC, LIVE and HaNSoLO facilities). Other experimental programmes have been launched at existing CEA facilities: VITI at Cadarache and the high temperature mass spectrometer furnace at Saclay. Finally, the SERUA facility is

being built at Cadarache and a new conceptual design of newPLINIUS facility has been launched.

These experimental programmes have been constructed in order to provide the necessary data to validate the calculation tools] under development for SFR severe accident modelling and to inform the design of severe accident mitigation devices. They will also help to maintain CEA knowledge and knowhow on SFR technology in view of its future development.

ACKNOWLEDGEMENTS

The authors would like to thank the “Generation IV Reactors” programme of CEA Energy Program Division which supports this work as well as the SFR R&D Project. Some of the work described in this paper are carried out with the ESFR SMART Horizon 2020 (EURATOM) project and the ESFR SIMPLE Horizon Europe (EURATOM) project.

REFERENCES

[1] PAYOT, F. et al., The SAIGA in-pile experimental program to qualify the SIMMER calculation tool in SFR severe accident conditions, FR22 IAEA conference, IAEA-CN-291/ID155, Vienna, Austria (2022).

[2] PAYOT, F., CHAROLLAIS F., DUFOUR, E., LEJEAIL, Y., BLEVIN, G., TROTIGNON, L., DE IZARRA, G., MICHEL, F., DUPONT, V., CHIKHI, N., CLAVIER, R. The SAIGA in-pile experimental test to study the degradation of a SFR core with mitigation devices in Severe Accident Conditions, NURETH, Washington DC, USA (2023).

[3] BACHRATA, A., BERTRAND, F., MARIE, N., EDELINE, A., KUBOTA, R., KAMIYAMA, K., KUBO, S., Severe accident studies on the efficiency of mitigation devices in a SFR core with SIMMER code, Nucl. Eng. Des., 373, 111037 (2021).

[4] ZABIÉGO M., FOCHESATO C., Corium-sodium interaction: the development of the SCONE software, Accepted for 17th Nuclear Reactor Thermal Hydraulics Conference, NURETH-17, Xi’an, China (2017).

[5] BERTHOUD G., LE BELGUET A., ZABIÉGO M., The Farahat sodium natural convection film boiling experiment revisited, Exp. Therm. Fluid Sci., 91, 117-125 (2018).

[6] FARAHAT M.M.K., Transient Boiling Heat Transfer from spheres to sodium, Report ANL-7909, Argonne Nat. Lab. (1972).

[7] LE BELGUET A., BERTHOUD G., ZABIÉGO M., Analysis of Film Boiling Heat Transfer on a High Temperature Sphere Immersed into Liquid Sodium, J. Energ. Power Eng., 8, 628-635 (2014).

[8] BRAILLARD, O., PINQUIER, J-M., Capteur de mesure du coefficient de transfert de chaleur entre l'action d'un fluide sur une paroi, ASTELAB thermique 2016, Toulouse, France (2016).

[9] JOURNEAU, C., BOUYER, V., CHAROLLAIS, F., CHIKHI, N., DELACROIX, J., DENOIX, A., LAFFOLLEY, H., MATTASSOGLIO, C., MOLINA, D., PILUSO, P., SAUVECANE, P., THILLIEZ, S., TURQUAIS, B., SUTEAU, C., Upgrading the

PLINIUS platform toward smarter prototypic-corium experimental R&D, Nucl. Eng. Des. 386, 111511 (2022).

[10] JOURNEAU, C., AUFORE, L., BERGE, L., BRAYER, C., CASSIAUT-LOUIS, N., ESTRE, N., PAYOT, F., PILUSO, P., PRELE, J.-C., SINGH, S., ZABIEGO, M., PLUYETTE, E., SERRE, F., TEISSEIRE, B., Corium-Sodium and Corium-Water Fuel-Coolant-Interaction Experimental Programs for the PLINIUS2 Prototypic Corium Platform, Nucl. Technol. 205, 239-247 (2019).

[11] BERGE, L., ESTRE, N., TISSEUR, D., PAYAN, E., ECK, E., BOUYER, V., CASSIAUT-LOUIS, N., JOURNEAU, C., LE TELLIER, R., SINGH, S., PLUYETTE, E., Fast high-energy X-ray imaging for Severe Accidents experiments on the future PLINIUS-2 platform, IEEE Trans. Nucl. Sci., 65 9 2573-2581 (2018).

[12] MAGALLON, D., HOHMANN, H., SCHINS, H., Pouring of 100-kg-scale molten UO2 into sodium, Nucl. Technol., 98. 79-90 (1992).

[13] TROMM.W., GAUS-LIU, X., KIT-JIMEC Experiments to Investigate Jet Impingement on the Ablation of Core Catcher Bottom, Proc. Nucl. Ener. New Europe, Bled, Slovenia (2021).

[14] LECOANNET, A., PAYOT, F., JOURNEAU, C., RIMBERT, GRADECK, M., Study of the ablation consecutive to jet impingement on a meltable solid – Application to SFR core-catcher, Nucl. Eng. Des., 377, 111147 (2021).

[15] LECOANET, A., PAYOT, F., JOURNEAU, C., RIMBERT, N., GRADECK, M., Classification of ablation mode during impact of hot liquid jet on a solid, Int. J. Heat Mass Transf., 181, 121883 (2021).

[16] BIGOT, B., GAUS-LIU, X., CLAVIER, R., JOURNEAU, C., PAYOT, F., CRON, T., ANGELI, P.E., PEYBERNES, M., FLUHRER, B. Experiment and Numerical Simulations on SFR Core-Catcher Safety Analysis after Relocation of Corium, 10th European Review Meeting on Severe Accident Research (ERMSAR2022), Karlsruhe, Germany (2022).

[17] GARRIGUE, M., QUAINI, A., ALPETTAZ, T., BONNET, C., BRACKX, E., DOMENGER, R., TOUZIN, M., TOUGAIT, O., GUENEAU, C., Chemical interaction between uranium dioxide, boron carbide and stainless steel at 1900 °C — Application to a severe accident scenario in sodium cooled fast reactors, J. Nucl. Mater. 557, 153266 (2021).

[18] JOURNEAU, C., KISELOVÁ, M., POZNIAK, I., BEZDIČKA, P., SVORA, P., ŠUBRT, J., BECHTA, S., Transient Interactions of Boron Carbide with Molten Uranium Oxide, Nucl. Mater. Ener. 29, 101078 (2021).

[19] DELACROIX, J., JOURNEAU, C., PILUSO, P., High-Temperature Characterization of Melted Nuclear Core Materials: Investigating Corium Properties through the Case Studies of In-Vessel and Ex-Vessel Retention, Front. Energy Res. 10, 883972 (2022).

SESSION II

PRIMARY AND TRANSITION PHASES OF SEVERE ACCIDENTS FOR SODIUM COOLED FAST REACTORS

Chairpersons

T. SATHIYASHEELA
India

M. BUCKNOR
United States of America

T. ISHIZU
Japan

STATUS OF THE SAS4A/SASSYS-1 CODE METALLIC FUEL MODELS FOR THE SIMULATION OF POSTULATED SEVERE ACCIDENTS IN LIQUID METAL COOLED FAST REACTORS

A.M. TENTNER
Argonne National Laboratory
Argonne, Illinois, United States of America

Abstract

The SAS4A/SASSYS-1 (SAS) safety analysis code was developed for the analysis of postulated severe accidents in both oxide and metal fuel sodium cooled fast reactors (SFR). These are unlikely events, with extremely low probability well below the beyond design basis limits. Advanced metal fuel models describing the behaviour of metal fuel cores during such accidents have been implemented in the research version of SAS, named SAS-RES. The SAS-RES metal fuel models simulate the metal fuel thermo-mechanical and chemical behaviour and track the evolution and redistribution of the fuel constituents during the pre-transient irradiation. During postulated severe accidents leading to fuel melting and pin disruption the SAS-RES metal fuel models continue to track the relocation and interactions of the metal fuel constituents, allowing a physics-based description of the core behaviour during the postulated accidents. The paper describes recent extensions of the SAS-RES metal fuel relocation module LEVITATE-M to allow the simulation of inter-assembly interactions, including the inter-assembly heat transfer (IAHT) and post-assembly failure inter-assembly material contact and physical interactions. The implementation of the post-assembly failure LEVITATE-M models significantly extends the ability of the SAS-RES code to analyse the extended initiating phase of postulated severe accident sequences. Instead of terminating the SAS-RES calculations at the time of the assembly wall failure, we can now continue the simulation of subsequent events in the framework of SAS-RES. The simulation of a reference severe unprotected loss of flow (ULOF) which did not consider the inter-assembly heat transfer shows that even if a failure of the lead assembly wall occurs, the damage to the neighbouring assemblies remains limited and the assembly failure does not propagate to the neighbouring assemblies. When the inter-assembly heat transfer is considered, the coolability of the damaged assembly is restored without failure of the assembly wall. Initial results of a simulation of an assembly blockage (ASBL) accident are also presented. The IAHT provides an important mechanism for removing heat from the blocked assembly and can prevent the fuel pin damage in the blocked assembly from extending to the neighbouring assemblies.

1. INTRODUCTION

SAS4A/SASSYS-1 (SAS) is a reactor dynamics and safety analysis code developed at Argonne National Laboratory (ANL) for the safety analysis of sodium cooled fast reactors (SFRs). While the initial development and validation effort begun in the early 1960s was focused on SFRs fuelled by oxide fuel [1], around 1985 a SAS4A metal fuel model development effort began [2]. The development and upgrading of the SAS code continued at Argonne National Laboratory with a focus on the analysis of inherently safe SFR designs. The latest distribution version of the code SAS4A/SASSYS-1 Version 5.6 [3] was released in 2022.

Starting in 2014, the interest in the analysis of severe accidents in SFRs fuelled by metal fuel has led to renewed emphasis on the development and validation of the SAS metal fuel models that describe the accident sequence of events. A significant metal fuel model development and validation effort has been undertaken at Argonne National Laboratory as part of the collaboration with Korea Atomic Energy Research Institute on the Prototype Gen-IV sodium cooled fast reactor [4–6]. The new metal fuel models were implemented in the research version of SAS referred to as SAS-RES. They will be gradually integrated in the distribution version of the SAS code. An overview of the SAS-RES metal fuel models is presented in Section 2. The results presented in this paper are obtained with the SAS-RES version of SAS.

Recent work has extended the SAS-RES metal fuel relocation module LEVITATE-M to allow the simulation of inter-assembly interactions, including inter-assembly heat transfer, assembly wall failure, and post-assembly failure inter-assembly material contact and physical interactions. The SAS code has been developed initially for the analysis of the initiating phase of postulated severe accidents in liquid metal fast reactors (LMFRs). The initiating phase is traditionally defined as the sequence of events that occur before the failure of an assembly wall,

when the transition phase of the accident begins. The implementation of the post-assembly failure models significantly extends the ability of the SAS-RES code to analyse extended severe accident sequences. Instead of terminating the SAS-RES calculations at the time of the assembly wall failure, we can now continue the simulation of subsequent events in the framework of SAS-RES. These are unlikely events, with extremely low probability well below the beyond design basis limits. The new models describing the inter-assembly interactions are presented in Sections 3 and 4. Results of extended simulations of a postulated loss of flow (LOF) accident and a severe assembly blockage accident in a generic metal fuel core using the new SAS-RES modelling capabilities are also presented and discussed in these sections.

2. OVERVIEW OF METAL FUEL PHENOMENA MODELLED IN SAS-RES

The response of the metal fuel reactor core during an accident is affected by several important phenomena that occur in metal fuel pins but are not present in the oxide fuel pins: a) the migration of the U-Zr and U-Pu-Zr fuel components during irradiation, which leads to the formation of radial fuel regions with different composition and thus different thermo-physical properties, b) the formation of fuel–cladding eutectic at the interface between the fuel and cladding, which leads to changes in the local composition of both fuel and cladding, c) the formation of fuel–cladding eutectic at the outer cladding surface and at the inner assembly wall surface after the cladding failure and fuel ejection in the coolant channel, which affects fuel freezing and cladding and assembly wall ablation, d) the presence of the in-pin sodium in the molten fuel cavity which can affect the cavity pressure and molten fuel relocation both prior and after the cladding failure, and e) the in-pin molten fuel relocation to the pin plenum prior to cladding failure and re-entry from plenum into the pin cavity after the cladding failure. The changes in the local composition of the metal fuel and cladding during irradiation can significantly affect the local thermophysical properties of the fuel and cladding, including the melting and freezing temperatures. These changes in turn can affect the timing and magnitude of cladding failure and material relocation events, and therefore the reactivity feedback that determines the core response. Mechanistic models describing these important metal fuel phenomena have been developed and included in the SAS-RES code metal fuel modules: a) SSCOMP-A: pre-transient metal fuel characterization, b) DEFORM5-A: transient metal fuel pin mechanics, c) PINACLE-M: pre-failure in-pin metal fuel relocation, d) LEVITATE-M: post-failure metal fuel relocation.

To allow an accurate description of the local fuel composition, the new metal fuel modules track multiple fuel components, including uranium, plutonium, actinides, fission products, lanthanides, zirconium, and iron. The in-pin sodium and fission gas are also tracked. The changes in the local composition of the fuel can lead to significant changes in the fuel thermos-physical properties and can also affect the reactivity feedback calculation. The reactivity feedback is now calculated by considering the axial distribution of each fuel component and its corresponding reactivity worth, while in the previous SAS version the fuel composition was assumed to remain unchanged and only one fuel component distribution was used to calculate the reactivity feedback. The impact of the variable fuel composition on reactivity becomes relevant after the onset of fuel melting and in-pin fuel relocation and can be more pronounced after the cladding failure because the relocating molten fuel tends to have a composition different from the stationary still-solid fuel. The integral validation of the SAS-RES metal fuel models was performed through analyses of eight TREAT M-Series Transient Over Power experiments [4]. In these analyses all the new SAS-RES metal fuel models were used to calculate the fuel behaviour during the test and good agreement of the calculated cladding failure and fuel relocation results with the observed corresponding

experimental data was obtained. The new metal fuel models are part of the research version of the code SAS-RES and are not included yet in the distribution version.

2.1 SSCOMP-A: the pre-transient metal fuel characterization models

The SSCOMP-A pre-transient models describe the metal fuel behaviour during the pre-transient irradiation. The model captures essential physical phenomena taking place during normal operation. The main processes simulated are redistribution of fuel constituents, fuel swelling, porosity evolution, fission gas release, plenum pressurization, solid fission product swelling, radial and axial stresses, strains, and displacements for the fuel and cladding, formation of the fuel phases, lanthanide migration to the cladding and formation of brittle layer at the clad inner surface, iron migration to the fuel surface and formation of complex iron bearing layers, sodium infiltration to the fuel, burnup dependent formation of various nuclide groups and corresponding reactivity feedback coefficients, and clad failure margin assessment. Some of these processes are depicted in Fig. 1. The SSCOMP-A pre-transient models were validated against EBR-II normal operation database using the real irradiation histories [4] up to 19 % peak burnup. The module predicted satisfactorily essential parameters such as fuel swelling, fission gas release behaviour, fuel axial elongation, fuel constituent redistribution, clad wastage formation due to lanthanide attack, clad strain, and clad failure margin.

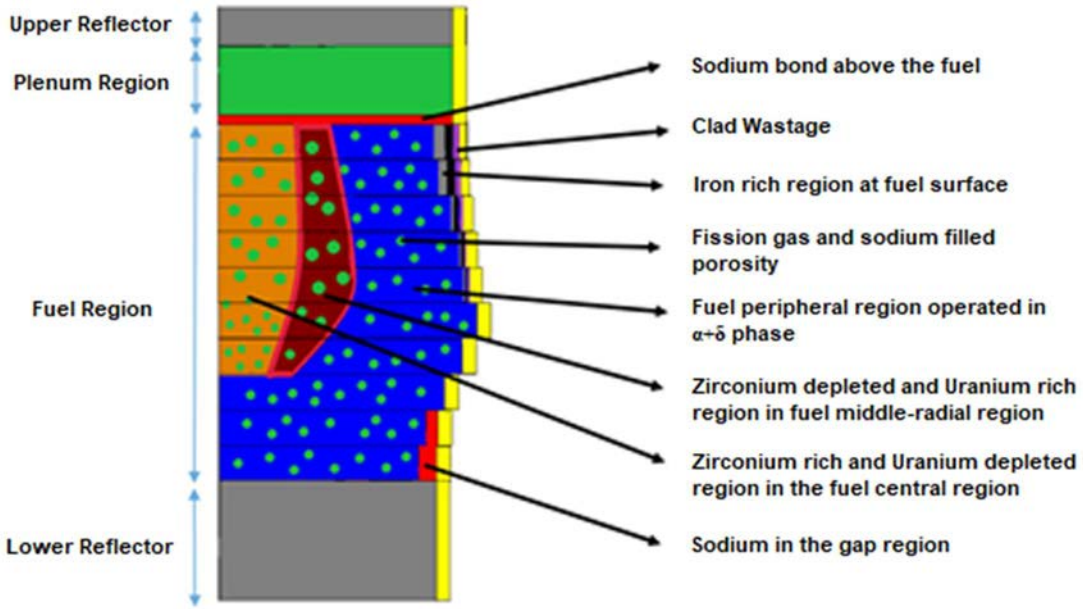

FIG. 1. Metallic fuel phenomena modelled in SSCOMP-A.

2.2 DEFORM5-A: the transient metal fuel pin mechanics models

The α+δDEFORM5-A transient models are an extension of the pre-transient models, addressing transient-related issues such as rapid changing conditions during the transient, eutectic formation between fuel and cladding, gas bubble behaviour, creep of the soft fuel and clad failure. Several important models related to transient fuel modelling include:

- Fuel mechanics: During the transients, occurrence of fuel liquefaction at the fuel cladding interface and formation of single gamma phase leads to frictionless and soft metallic fuel, which is prone to expansion or contraction. The mechanical analysis model captures these phenomena by allowing creep of the fuel driven mainly by the

fission gas swelling and thermal expansion. This is an important axial relocation mode for the metallic fuels.

- Fuel swelling and fission gas behaviour: The evolution of the fission gas bubbles is captured by modelling three different groups of bubbles: small, medium, and large bubbles are based on their atom number and phases present. The large bubble formation takes place during the transient at elevated temperatures or upon the fuel liquefaction.
- Fuel–clad chemical interaction: Upon eutectic formation between fuel and cladding the eutectic penetration of the clad is driven by iron dissolution and actinide diffusion. The models are validated using the results of furnace tests [7].
- Clad failure models: The failure margin for HT9 cladding is modelled using: 1) combined cumulative damage fraction (CDF) and 2) mechanistic creep fracture (MCF) models. The combined CDF is an empirical model, covering a wide range of data. MCF is a constrained diffusion cavity growth model, tracking the nucleation, growth, coalescence of the cladding grain boundary cavities. It is validated using the HT9 failure database.

2.3 PINACLE-M: the pre-failure metal fuel in-pin fuel relocation module

PINACLE-M is a Eulerian, two-phase, transient hydrodynamic model describing the pre-failure in-pin relocation of the molten fuel. PINACLE-M retains all the physical models of the earlier oxide-fuel PINACLE model [8] but extends them to allow the mechanistic modelling of metallic fuel specific phenomena. It describes the melting and relocation of the multiple fuel components tracked by SSCOMP-A and uses the composition-dependent, thermo-physical properties at each axial location. During a postulated severe accident, the fuel pin begins to melt leading to the formation of an internal cavity. PINACLE-M uses the fuel composition provided by the SSCOMP-A model to dynamically determine the geometry and growth of the molten fuel cavity. This pressurized cavity is filled with a mixture of molten fuel, fission gas and sodium and expands both radially and axially, due to continued fuel melting. As the cavity continues to expand there is a competition between two effects:

1) The radial extension of the cavity and cladding melting which can cause fuel pin cladding failure. The fuel ejection into the coolant channel and subsequent axial relocation that occurs after cladding failure are modelled by the post-failure fuel relocation model LEVITATE-M.
2) The axial extension of the cavity, which can cause the cavity to reach the top of the fuel pin. When the fuel pin top is breached the pressurized molten fuel in the cavity is connected to the lower pressure upper plenum and can relocate suddenly, leading to a potentially significant insertion of negative reactivity. The rapid in-pin molten fuel relocation prior to cladding failure is modelled by the PINACLE-M module.

2.4 LEVITATE-M: the post-failure metal fuel relocation model

The LEVITATE-M model describes the phenomena that occur in a metal fuel assembly after the cladding failure and fuel ejection into the coolant channel. LEVITATE-M retains all the physical models of the oxide fuel LEVITATE model [9] but extends them to allow the modelling of metallic fuel specific phenomena. It describes the post-failure relocation of the multiple fuel components tracked by SSCOMP-A and PINACLE-M, both in the coolant channel and in the pin cavities, and uses the composition-dependent, thermo-physical properties

at each axial location to determine the fuel phase transitions (melting and freezing) and the corresponding mass exchanges between various LEVITATE-M fields. LEVITATE-M has also been extended to model the metal fuel ejection into non-empty coolant channels replacing the PLUTO-2 model still used in the oxide fuel version of SAS to simulate TOP accident conditions. LEVITATE-M continues the PINACLE-M calculations after the cladding failure but extends them to model the phenomena that occur in the coolant channel. As the accident proceeds, molten fuel ejected in the coolant channel can relocate axially and freeze in the colder regions of the channel, leading to the formation of blockages or/and solid fuel particles, depending on the local conditions. LEVITATE-M describes a large spectrum of physical phenomena which depend on the metal fuel composition and properties, including fuel pin melting and disruption, cladding ablation due to melting or eutectic formation, multiple fuel and steel flow regimes, fuel fragmentation and freezing, and channel blockage formation due to freezing fuel or/and cladding. The local composition of the moving and stationary fuel fields (molten fuel, fuel chunks/particles, frozen crust on cladding and structure) is carefully tracked, allowing an accurate calculation of the time-dependent reactivity changes.

3. POST-ASSEMBLY FAILURE LEVITATE-M MODELS

The SAS code has been developed for the analysis of the initiating phase of postulated severe accidents in LMFRs. These are unlikely events, with extremely low probability well below the beyond design basis limits. The initiating phase is traditionally defined as the sequence of events that occur before the failure of an assembly wall, when the so-called transition phase of the accident begins. Thus, the LEVITATE code was designed to monitor the assembly wall conditions and stop the SAS simulations with an appropriate warning when the failure of the assembly wall was predicted. The transition phase is analysed with codes such as SIMMER [10] which use a different core representation and less detailed thermo-physical models to represent the fuel assembly phenomena. It was recognized for some time that terminating the SAS calculations at the time of the first assembly wall failure may be too pessimistic, as the effect of the failure may be limited, and the accident could still terminate with limited core damage to the neighbouring assemblies. In this case the use of the transition phase codes may not be necessary. Recent work has extended the capabilities of the SAS-RES code to the simulation of events that occur after the assembly wall breach, during a period that we will refer to as the pre-transition phase [11].

3.1 Post-assembly failure model implementation

In the initial implementation, the failure of the assembly wall is assumed to lead to local expansion of the assembly and direct contact of the molten fuel and other components in the coolant channel of the failed assembly with the outer surface of the neighbouring assembly wall. The sodium in the inter-assembly gap is displaced by the walls of the failed assembly and does not contact the coolant channel materials. The expanding assembly walls and/or local freezing of the molten fuel/steel mixture due to contact with the colder neighbouring assembly prevent the axial relocation of the molten fuel and other components in the inter-assembly space.

The post-assembly failure (PAF) model is designed for the simulation of a SAS-RES lead channel consisting of a single fuel assembly, surrounded by six identical fuel assemblies that form another is assumed. The model requires that the SAS-RES lead channel contains only one fuel assembly, surrounded by six identical fuel assemblies that belong to the neighbouring SAS-RES channel. These restrictive conditions are necessary because the modelling of the PAF conditions require the definition of physically neighbouring assemblies, as opposed to the

conceptual channels previously used in SAS, which can contain assemblies that are not physical neighbours.

The LEVITATE-M routines were extended to allow the continuation of calculations beyond the breach of the assembly wall which traditionally marked the end of the initiating phase of the accident and caused the termination of LEVITATE-M calculations. If the breach of the assembly wall is predicted the accident simulation is allowed to continue. When the first breach of the assembly wall occurs in a LEVITATE-M channel the following phenomena are modelled: a) the inter-assembly heat transfer (IAHT) due to direct contact between the molten fuel in the failed assembly and the neighbouring assembly wall is calculated; b) the assembly wall temperatures in the neighbouring channel are calculated, considering the IAHT for the assembly sides that face the failed assembly. The temperatures of the sides in contact with the failed assembly are initially the same at those of the other sides of the neighbouring channel but will start to increase faster than the other sides due to the IAHT; c) the wall penetration for the neighbouring assembly walls in contact with the failed lead assembly is tracked. This penetration occurs at the outside of the neighbouring assembly wall, for the sides that face the failed assembly cells.

The penetration rate of the assembly wall is determined by the temperature of the fuel that contacts the wall [11]. This is initially the temperature of the molten fuel ejected from the pin cavity into the coolant channel. However, in the extended accident simulations performed to study the assembly-wall failure, freezing of the molten fuel can lead to assembly conditions where the amount of frozen fuel particles/chunks is significantly larger than the amount of molten fuel. To capture the effect of the changing ratio between the molten and frozen fuel components on wall penetration, the fuel temperature used to calculate the assembly wall penetration has been modified to be a volume-weighted average of the molten and frozen fuel components.

The selection of the appropriate temperature for the penetration rate has a significant effect on the predicted assembly wall ablation and timing of the assembly-wall failure and the penetration model will be further evaluated and enhanced in future work. It is also noted that the rate correlation is based on fuel dipping tests where only one fuel species was in contact with the cladding material, and all previous integral validation of this correlation was based on analyses of the cladding failure in multiple metal fuel TREAT test analyses. However, the assembly wall is in contact with multiple fuel components (molten fuel, frozen mobile fuel particles/chunks, frozen stationary fuel crusts) which have different temperatures and contact areas with the assembly wall. Validation analyses of this complex assembly wall penetration process have not been performed yet but will be needed to ensure the correct simulation of the assembly-wall failure and subsequent events. Initial data for such validation analyses is already available from the initial MUSE metal fuel tests [12, 13] conducted at Argonne National Laboratory, and additional enhanced validation data could be provided by future MUSE tests properly designed for this purpose.

The accident simulation continues after failure of the assembly wall in the lead channel, with LEVITATE-M tracking the penetration of the neighbouring assembly wall. Failure of the assembly wall can occur in other axial cells, usually neighbours of the first axial cells to fail. If full penetration of the neighbouring assembly wall is predicted the simulation stops with a message from the LEPENE-M routine indicating that the models have to be further extended. However, as the results in Section 3.2 illustrate, the temperatures of the fuel in the leading channel continue to decrease after the assembly wall failure due to the decreasing power, and the penetration rate of the neighbouring assembly wall decreases to low values approaching

zero. The sodium coolant re-entry into the damaged lead assembly continues, and failure of the neighbouring assemblies does not occur. This is an important result of the SAS-RES accident analysis, indicating that even if failure of the lead assembly wall is predicted, the assembly failure does not necessarily propagate to other assemblies and the accident can still terminate with limited core damage.

3.2 Post-assembly-failure simulation results

To evaluate the post-failure simulation capabilities implemented in SAS-RES we performed an extended simulation of a postulated unprotected loss of flow (ULOF) accident with a flow rate halving-time of ~5 s, in a generic 600 MW(e) SFR metallic fuel core. The fuel pins consist of U-10Zr metallic fuel with HT9 cladding. The core was initially modelled by dividing the fuel assemblies into 14 SAS-RES fuel channels, with 7 channels containing a single fuel assembly while the remaining 7 channels contained multiple fuel assemblies assumed to behave identically. The fuel pin failure was found to occur first in Channel 11 which was assumed to be the 'hot' or 'peak' channel in these calculations. To evaluate the effect of inter-assembly interactions an additional channel 15 was defined consisting of 6 identical fuel assemblies taken from channel 4. The number of assemblies in channel 4, which was previously 29, was reduced by 6 so that the channel 4 now contains 23 assemblies and the total number of assemblies is unchanged. The 6 assemblies of channel 15 were defined as neighbours of the peak channel 11, as illustrated in Fig. 2. This 15-channel core model was used to evaluate the effect of the inter-assembly interactions after the assembly wall failure in channel 11.

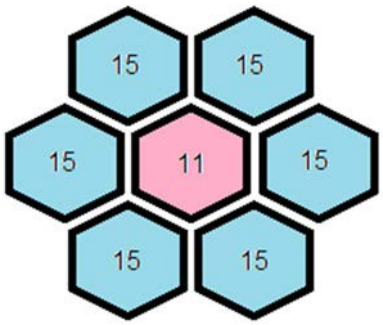

FIG. 2. The lead channel 11 and six neighbouring assemblies of channel 15.

The simulation was performed using the new structure penetration model described in Section 3.1 which accounts for the presence of fuel chunks and reduces the effect of the molten fuel while increasing the effect of fuel chunks depending on the local volume fraction. To help understand the simulation results the LEVITATE-M visualization program has been extended to allow the visualization of post-assembly failure events. In addition to the traditional LEVITATE geometry pictures that show the fuel pin, cladding assembly wall and the moving material in the coolant channel at selected accident times, the picture now includes the assembly wall failures, the neighbouring assembly wall, and the penetration of the neighbouring assembly wall at the failure locations, as seen in Figs 3 and 4.

The fuel pin failure in the lead channel 11 and the initiation of the LEVITATE-M fuel relocation module occur at ~32 s after the initiation of the ULOF accident. At this time the power is P = 0.47 P0 and the net reactivity is ρ_{net}=-0.31\$. The negative reactivity is due mainly to the fuel axial expansion, radial core expansion, and Doppler contributions. The assembly wall failure is predicted at ~18 s after pin failure. At this time the power has decreased to P = 0.23 P0 and ρ_{net}=-0.62\$. The reactivity due to the fuel relocation is ρ_{fuel}=-0.32\$. One axial cell of the

assembly wall has failed, and a foamy molten fuel pool is present in the axial region where the failure is located.

The channel 11 conditions at 14 s after the failure of the assembly wall (32 s after pin failure) are illustrated in Fig. 3. Some of the fuel is now frozen in the form of particles/chunks that are seen moving upward. Three axial cells of the assembly wall have failed at this time. The penetration of the neighbouring assembly wall has advanced but remains less than 25% of the wall thickness. Significant steel freezing is observed to occur at the location of the channel 11 assembly wall failure. The presence of this frozen steel was not yet included in the wall penetration model and could significantly delay the failure of the assembly wall in the neighbouring channel 15. In this simulation it was assumed that the frozen steel leaves a path for the molten fuel to reach the neighbouring assembly wall.

Figure 4 shows the results of the extended simulation at 26.5 s after assembly wall failure (44.5 s after pin failure) in channel 11. The penetration of the neighbouring assembly wall has reached over 50% of the wall thickness, but the penetration rate is zero at this time due to decreased fuel temperatures in channel 11. All the fuel in channel 11 is now frozen, either as solid chunks/particles or frozen crust on the walls. Sodium coolant re-entry continues at the channel inlet. Penetration of the fuel debris bed by the liquid sodium is slow but continues monotonically. The power has decreased to P = 0.12 P0 and ρ_{net}=-0.75$. The reactivity due to the fuel relocation is ρ_{fuel}=-0.58$.

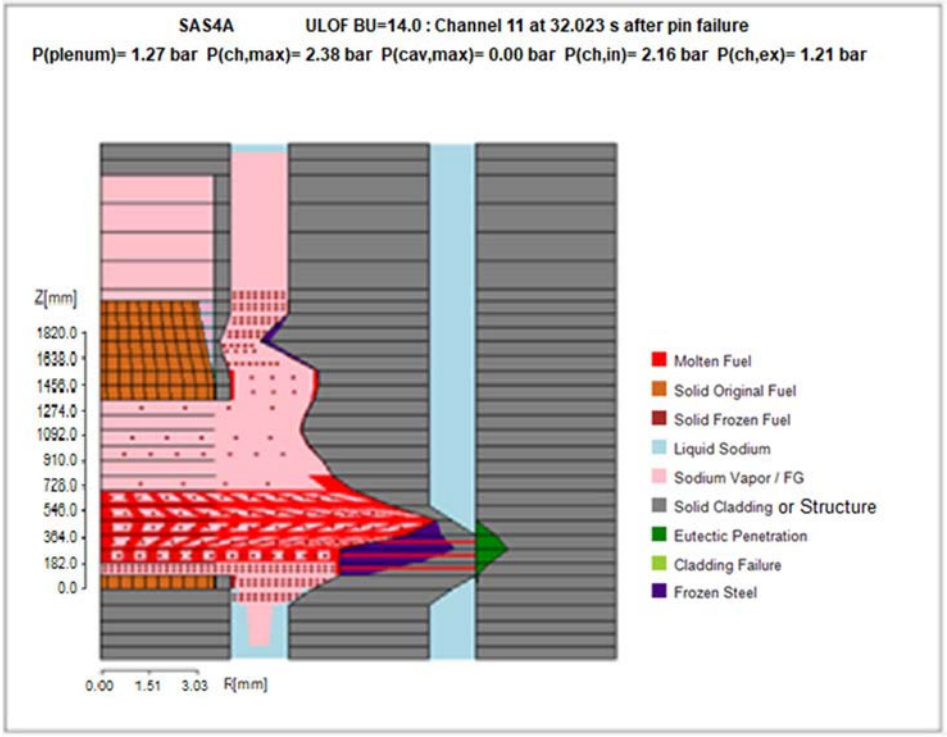

FIG. 3. LEVITATE-M results at 14s after assembly wall failure in channel 11(32s after pin failure in channel 11) (No IAHT considered).

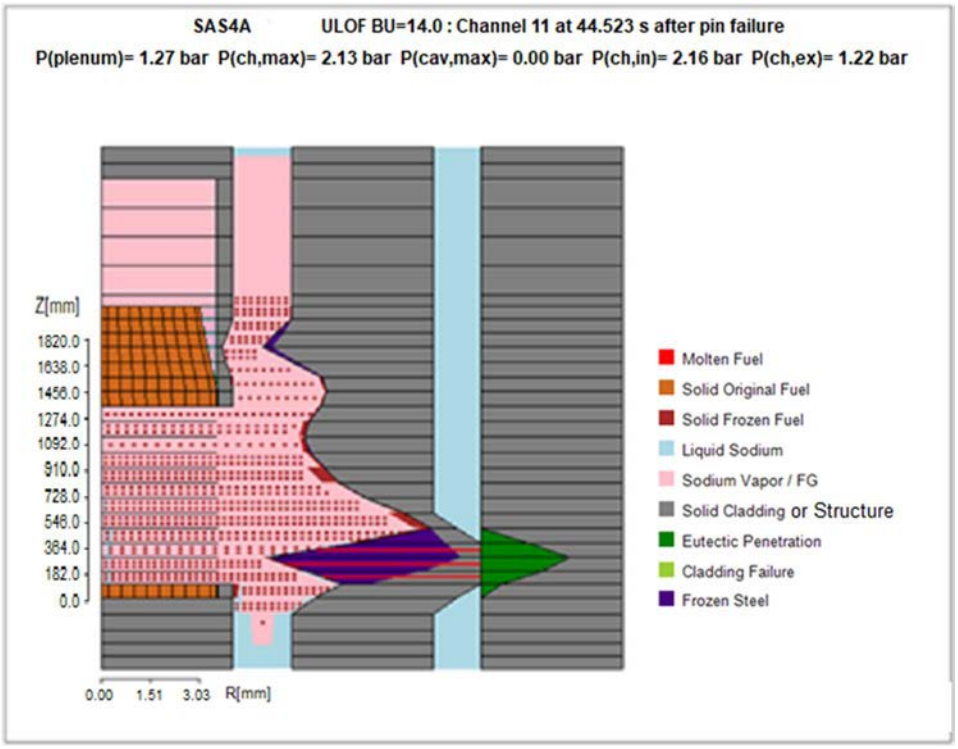

FIG. 4. LEVITATE-M results at 26.5s after assembly wall failure in channel 11 (44.5s after pin failure in channel 11) (No IAHT considered).

The simulation was extended for another 10s to observe the behaviour of fuel, assembly wall penetration, and sodium coolant re-entry. At 37 s after assembly wall failure (55 s after pin failure) the penetration of the neighbouring assembly wall has remained stationary, as the penetration rate is zero. Sodium re-entry in the channel from the bottom plenum has continued and increasing amounts of liquid sodium can be observed in the frozen fuel debris region.

These results show that even if failure of the lead assembly wall occurs, the damage to the neighbouring assemblies can remain limited and the assembly failure will not propagate to other parts of the core. As the reactor power is already low and still decreasing and liquid sodium continues to re-enter the damaged lead assembly the postulated ULOF accident is expected to terminate with only limited core damage.

4. INTER-ASSEMBLY HEAT TRANSFER MODELS IN SAS-RES

The ULOF accident simulations described above did not consider the IAHT through the inter-assembly gap. Only the direct contact heat transfer which occurs after the assembly wall failure was considered, as an inter-assembly gap heat transfer model was not available for the analysis of postulated severe accidents. The SAS channels were assumed to be thermally isolated from their neighbours prior to the assembly wall failure and an adiabatic boundary condition was applied at the outer surface of the assembly walls. As the SAS-RES models for the simulation of postulated severe accidents are extended, it was recognized that IAHT can play a significant role during certain accidents, transferring heat from the hotter assemblies to the colder neighbouring assemblies and mitigating the accident consequences. An example is the assembly blockage accident, where the temperatures of the blocked assembly increase rapidly after the blockage formation, leading to large temperature differences between the blocked assembly and its neighbours even before the occurrence of boiling and fuel failure in the blocked assembly. In other accidents such as the ULOF accident described in Section 3.2, the temperature differences between the lead assemblies and their neighbours become

significant after the fuel pin failure in the lead assembly if fuel failure did not occur yet in the neighbouring assemblies with lower power.

An effort to extend the SAS-RES models to account for the heat transfer through the inter-assembly gap throughout the entire accident sequence has been undertaken recently and is described in Section 4.1. The new IAHT models are developed for the simulation of a postulated assembly blockage accident, and preliminary results are presented in Section 4.2. However, the new IAHT models will also help improve the accuracy of SAS-RES simulations of other postulated severe accidents.

4.1 Inter-assembly heat transfer model implementation

The recent implementation of the IAHT models in the SAS-RES code allows the definition of the physical neighbouring assemblies of the lead assembly studied. The sidewalls of the neighbouring assemblies that face the lead assembly are also identified, and their temperature is tracked independently of the other sidewalls which are not facing the lead assembly (Fig. 2). Previously the SAS models assumed that all sidewalls of an assembly have the same temperature. It is noted that the SAS-RES accident simulation can be divided into several phases: a) the pre-boiling phase, b) the boiling phase, and c) the fuel relocation phase. Each phase of the accident is simulated by a different code module, and each module includes its own heat transfer models. The new IAHT models have been implemented gradually for all three phases, starting with the fuel relocation phase, continuing with the boiling module, and completed recently for the pre-boiling module.

The IAHT between the blocked assembly and the neighbouring assemblies is considered for all the axial cells in the reactor core during the assembly blockage accident simulation. For each axial cell a heat flux boundary condition is applied to calculate the temperature of the outer cell of the assembly wall of the lead assembly and that of the assembly wall of the neighbouring assembly. The heat flux boundary condition replaces the previous adiabatic boundary condition used in the SAS heat transfer models for these assembly wall cells. The heat flux between assemblies is calculated as:

$$H_{(i,sr,nc)} = h_{(i,sr,nc)} \times \left(T_{(i,sr,xx)} - T_{(i,sr,nc)}\right) \quad (1)$$

Where:

$H_{(i,sr,nc)}$= heat flux in W/m^2

$h_{(i,sr,nc)}$= heat transfer coefficient in W/m^2/K; it includes the heat resistance of the assembly wall for both channels and the heat resistance of the inter-assembly space; currently a fixed inter-assembly space is used, and it is assumed filled with liquid sodium. Only the heat conduction through liquid sodium was considered for the results presented in Section 4.2, and the sodium is assumed stagnant. The IAHT model has been recently enhanced to check for the occurrence of boiling in the inter-assembly gap and modify the heat transfer coefficient accordingly.

$T_{(i,sr,xx)}$= the temperature of the lead assembly wall outer cell (facing the neighbouring assembly).

$T_{(i,sr,nc)}$= the temperature of the neighbouring assembly wall outer cell.

The heat flux $H_{(i,sr,nc)}$ is used to calculate the enthalpy removed from the outermost radial cell of the assembly wall in the blocked channel axial cell I, and the reduced cell enthalpy is used to obtain the reduced temperature of the wall cell in the blocked assembly. The enthalpy removed from the blocked assembly wall cell is then added to the outermost cell of the neighbouring assembly wall, leading to an increase of the temperature of that wall cell.

As the temperature of the neighbouring assembly wall that faces the blocked assembly can be significantly higher than the temperature of the other assembly wall faces, the heat transfer models for all three SAS-RES modules mentioned above have also been modified to account for the presence assembly wall faces with different temperatures. The heat transfer between the coolant in the neighbouring assemblies and the assembly wall faces and is based on the actual temperature of each assembly face.

4.2 Assembly blockage accident simulation using the inter-assembly heat transfer model

To evaluate the assembly blockage capabilities of the SAS-RES models and the effect of the IAHT models we simulated an assembly blockage (ASBL) accident in a generic 100 MW(e) pool-type SFR with a metal fuel core at the beginning of life (BOL). The SAS-RES core model consisted initially of 11 channels. Two additional SAS-RES channels were defined: channel 12, which contains the blocked assembly, and channel 13, which contains 6 identical assemblies that surround the blocked assembly, in an arrangement similar to that shown in Fig. 2. The assemblies used for channels 12 and 13 were removed from some of the original 11 channels. The inlet blockage in channel 12 is imposed by increasing the inlet coolant flow pressure drop at the beginning of the accident simulation. For the case presented the original pressure drop coefficient was multiplied by a blockage factor KBL=260. The initial simulation was performed without considering the effect of the IAHT.

The coolant boiling begins at ~18 s after blockage initiation when the coolant flow rate was reduced to W= 0.15*W0. As boiling continues the flow rate becomes zero W=0.0 at 31 s and displays small oscillations around zero afterwards. The first cladding failure occurs at 37.6 s after blockage initiation, prior to fuel melting and triggering the plenum fission gas ejection into the coolant channel. The post-pin-failure fuel relocation module LEVITATE-M is initiated at 47.47 s. The assembly blockage simulation was extended to ~30 s after pin failure. The status of the blocked assembly at 28.5 s after pin failure is illustrated in Fig. 5.

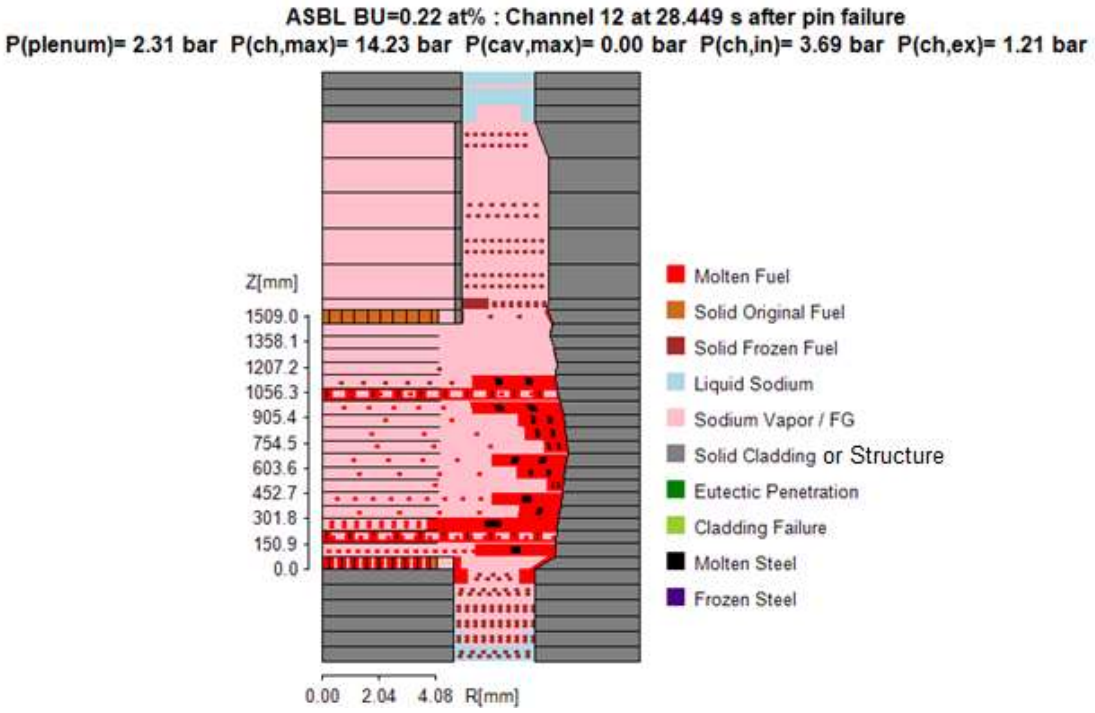

FIG. 5. Status of the blocked assembly at 28.5s after pin failure (No IAHT considered).

The fuel pins are largely disrupted, and molten fuel is present in the core region. A fraction of the fuel in the form of frozen particles is seen both below and above the active fuel region. Ablation of the assembly wall can also be observed. The maximum ablation at this time is 0.716 mm, or ~24% of the assembly wall. Based on the current penetration rate, assembly wall failure would occur after another ~44 s. The fuel relocation in the blocked assembly leads to a negative fuel reactivity contribution of -0.23$ at the end of the simulation. The core net reactivity at the same time is -0.13$ and the relative power has decreased to P_{rel}=0.64 P0. At the end of the simulation, the maximum temperature difference between the wall of the blocked assembly and its neighbouring assemblies is 1061 K, suggesting that the IAHT is likely to have a significant effect on the accident sequence of events.

The assembly blockage accident simulation presented above was repeated after the implementation of the IAHT models for the post-pin-failure phase. The simulation was extended to ~45 s after pin failure. The status of the blocked assembly at 41.5s after pin failure is illustrated in Fig. 6.

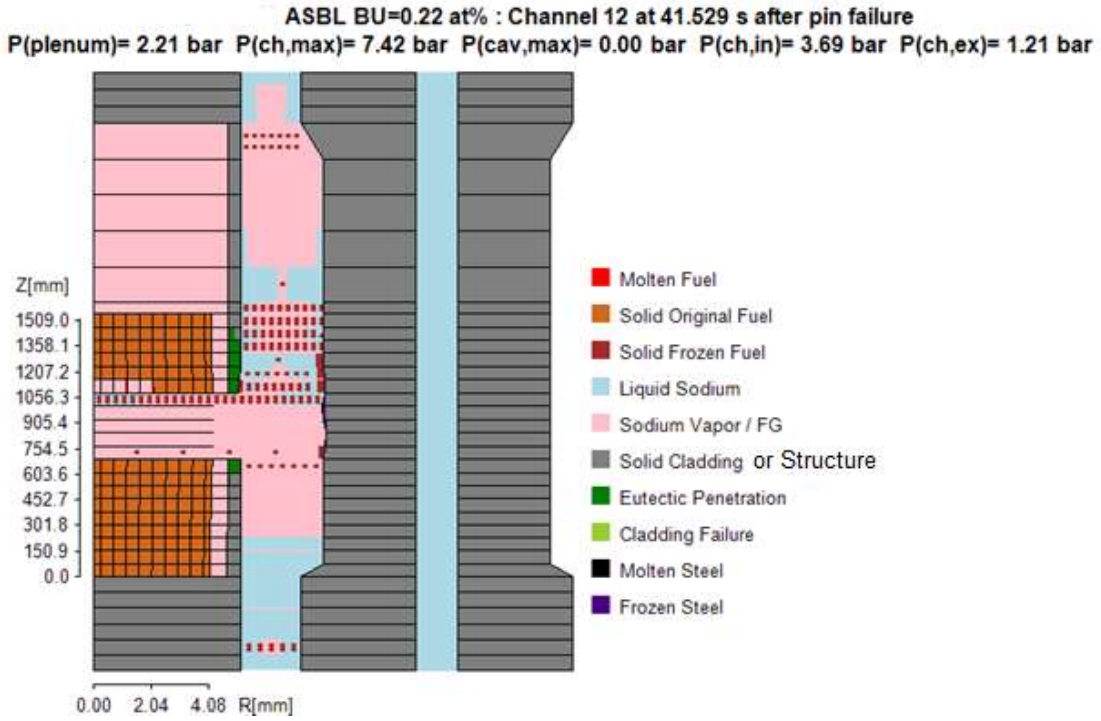

FIG. 6. Status of the blocked assembly at 41.5s after pin failure (IAHT considered after pin failure).

The fuel pin disruption region is smaller than calculated in the case without IAHT, and little molten fuel is present in the core region. Most of the relocated fuel is in the form of frozen particles seen both below and above the active fuel region. Ablation of the assembly wall is limited and significantly smaller than calculated in the case without IAHT. The fuel relocation in the blocked assembly leads to a negative fuel reactivity contribution of -0.10$ at the end of the simulation at 92.3 s after blockage initiation and 44.8s after pin failure. The core net reactivity at the same time is -0.02$ and the relative power has decreased to P_{rel}=0.78 P0.

Recent simulations have examined the effect a more sever blockage with inlet pressure loss multiplying constant KBL=520 and included the effect of the IAHT during the boiling and pre-boiling phases of the accident. These simulations were extended to 73 s after the blockage occurrence. At this time all the mobile fuel is frozen, only little ablation of the assembly wall is predicted, and liquid sodium is re-flooding the damaged blocked assembly.

These initial results of the ASBL simulation including IAHT show that the IAHT can significantly affect the accident outcome providing an effective path for removing heat from the blocked assembly in the absence of the sodium coolant flow in the blocked assembly.

5. CONCLUSIONS

The paper reviews the status of the SAS-RES metal fuel models and describes two recent model extensions focused on the simulation of the inter-assembly interactions during a postulated severe accident: the post-assembly failure models and the IAHT models. The implementation of the post-assembly failure LEVITATE-M models significantly extends the ability of the SAS-RES code to analyse the extended initiating phase of postulated severe accident sequences. These are unlikely events, with extremely low probability well below the beyond design basis limits. Advanced metal fuel models describing the behaviour of metal fuel cores during such accidents have been implemented in the research version of SAS, named SAS-RES. These SAS-RES models will be gradually integrated in the distribution version of the SAS code.

The implementation of the post-assembly failure models described in Section 3 allows the SAS-RES code to explore the accident events that could occur after a potential assembly wall failure. The preliminary results of a postulated severe ULOF accident show that even if a failure of the lead assembly wall occurs, the damage to the neighbouring assemblies can be limited and the assembly failure will not necessarily propagate to other parts of the core. As the reactor power is already low and continues to decrease, the liquid sodium continues to re-enter the damaged lead assembly and the postulated ULOF accident is expected to terminate with only limited core damage. The use of a transition phase code which uses a coarser core description to model large scale core disruption is not necessary in this case and the accident termination can be simulated using the more detailed metal fuel models available in SAS-RES.

The IAHT models described in Section 4 are essential for the correct simulation of postulated assembly blockage accidents where significant temperature differences between the blocked assembly and its neighbours. These models will also help improve the accuracy of SAS-RES simulations of other severe accidents such as the ULOF accident described in Section 3.2. Initial results of assembly blockage simulation including the IAHT models show that the IAHT can provide an effective path for removing heat from the blocked assembly in the absence of the sodium coolant flow in the blocked assembly allowing the blocked assembly to reach a stable coolable configuration, limiting the damage to the blocked assembly and preventing it from extending to the neighbouring assemblies.

ACKNOWLEDGEMENTS

The submitted paper has been created by uChicago Argonne, LLC, Operator of Argonne National Laboratory. Argonne, a U.S. Department of Energy Office of Science laboratory is operated under Contract No. DE-AC02-06CH11357. The U.S. Government retains for itself, and others acting on its behalf, a paid-up nonexclusive, irrevocable worldwide license in said article to reproduce, prepare derivative works, distribute copies to the public, and perform publicly and display publicly, by or on behalf of the Government. The Department of Energy will provide public access to these results of federally sponsored research in accordance with the DOE Public Access Plan (http://energy.gov/downloads/doe-public-access-plan). Argonne National Laboratory's work was supported by the U.S. Department of Energy, Office of Nuclear Energy.

REFERENCES

[1] A. Tentner et al., The SAS4A LMFBR Whole Core Accident Analysis Code, International Meeting on Fast Reactor Safety, Knoxville, TN (1985).

[2] A. Tentner et al., Analyzing Unprotected Transients in Metal Fuel Cores with the SAS4A Accident Analysis Code, Int'l Topical Meeting on Safety of Next Generation Power Reactors, Seattle, Washington, May (1988).

[3] T. Fanning, A. Brunett, L. Ibarra, et al., The SAS4A/SASSYS-1 Version 5.6 Safety Analysis Code System, Argonne National Laboratory ANL/NSE-SAS/5.6 (2022).

[4] A. Karahan and A. Tentner, Validation of Advanced Metallic Fuel Models of SAS4A using TREAT M-Series Overpower Test Simulations, International Conference on Fast Reactors and Related Fuel Cycles (FR-17), Yekaterinburg, Russian Federation, June, (2017).

[5] A. M. Tentner, S.H. Kang, A. Karahan, Advances in the Development of the SAS4A Code Metallic Fuel Models for the Analysis of PGSFR Postulated Severe Accidents, International Conference on Fast Reactors and Related Fuel Cycles, Yekaterinburg, Russian Federation (2017).

[6] A. M. Tentner, S.H. Kang, A. Karahan, Overview of the SAS4A Metallic Fuel Models and extended Analysis of a Postulated Severe Accident in the Prototype Gen-IV Sodium-cooled Fast Reactor, Advanced Thermal-Hydraulics Symposium, American Nuclear Society Winter Meeting, Orlando, Florida, November (2018).

[7] A. Karahan, Mechanistic Modeling of Metallic Fuel/Cladding Metallurgical Interactions, Transactions of American Nuclear Society, Vol. 110, pp. 747-750 (2014).

[8] A. M. Tentner and D. J. Hill, PINACLE – A mechanistic Model for the Analysis of In-Pin Fuel Relocation for SAS4A, Transactions of American Nuclear Society, Boston, MA (1985).

[9] A. M. Tentner and H. U. Wider, LEVITATE – A mechanistic Model for the Analysis of Fuel and Cladding Dynamics under LOF Conditions, Intl. Meeting on Fast Reactor Safety Technology, Seattle, WA (1979).

[10] S. Kondo et. al., Current Status and Validation of the SIMMER-III LMFR Safety Analysis Code, International Conference on Nuclear Engineering ICONE-7, Tokyo, Japan (1999).

[11] A. M. Tentner and A. Karahan, Extension of the SAS4A Code Metallic Fuel Relocation Module LEVITATE-M to the Simulation of inter-assembly Interactions, International Topical Meeting on Nuclear Reactor Thermal Hydraulics (NURETH-19) (2021).

[12] T. Kim, D. Harbaruk, C. Gerardi, M. Farmer, Y. I. Chang, Experimental studies on metallic fuel relocation in a single-pin core structure of a sodium-cooled fast reactor, Nuclear Engineering and Design, 322 (2017).

[13] T. Kim, D. Harbaruk, D. Lisowski, N. Bremer, M. Farmer, C. Grandy, Y. I. Chang, Experimental Studies on Metallic Fuel Relocation in a Pin Bundle Core Structure of a Sodium-Cooled Fast Reactor, Nuclear Engineering and Design, 365 (2020).

STATUS OF NUMERICAL TOOL DEVELOPMENT FOR THE INITIATING PHASE IN SEVERE ACCIDENTS OF SFR IN JAPAN

Y. FUKANO, S. ISHIDA, S. KUBO
JAEA
O-arai/Ibaraki, Japan

Abstract

The SAS4A code has been developed and used for the analyses of the initiating phase in severe accidents including those for licensing of sodium cooled fast reactors (SFRs) in Japan. The SAS4A code had been originally developed in the Argonne National Laboratory (ANL) in U.S. for thermal, hydraulic, and neutronic analysis of power and flow transients in liquid metal cooled nuclear and flow reactors. It was further developed and improved for analysis of initiating phase during severe accident in reactor core with oxide fuels in cooperation with the Japan Atomic Energy Agency (JAEA) and European research institutes, including the addition of new models based on the findings from the in-pile CABRI test. In recent years, the phenomena identification and ranking table (PIRT) method has been applied to select important phenomena to be verified for unprotected loss-of-flow (ULOF) and unprotected transient over power (UTOP) in a medium-sized SFR. Through these studies, 16 and 14 physical phenomena were extracted for ULOF and UTOP, respectively. Then 10 and 8 respective key important phenomena were identified through the ranking of extracted phenomena. Furthermore, a validation test matrix was created for the extracted important phenomena, and validation was conducted according to the validation test matrix. These studies further improved the validity and reliability of the SAS4A code. The SAS4A code has been used in a lot of severe accident analyses and for licensing of SFRs. Examples of the evaluation of ULOF event for a medium-sized SFR showed that prompt criticality was avoided in the initiating phase, and net reactivity remained negative at the time of the wrapper tube melting, which is the application limit of SAS4A. Compared to previous evaluations, the present SAS4A calculations show that the elimination of mechanical energy release due to prompt criticality during initiating phase is possible even under conservative conditions due to the reduction of excess uncertainty. The paper describes the status of development and application of SAS4A code in JAEA and the future research plan.

1. INTRODUCTION

Since the core of a sodium cooled fast reactor (SFR) is not in the most reactive configuration, positive reactivity can be inserted due to coolant boiling or concentration of degraded fuel. Therefore, research and development of evaluation methods for severe accidents has been conducted in the field of safety research for SFR. Unprotected loss of flow (ULOF) and unprotected transient over power (UTOP) have historically been evaluated in licensing as representative severe accidents in SFRs.

Figure 1 shows the analysis codes used for ULOF and UTOP evaluations in the Japan Atomic Energy Agency (JAEA). After initiation of ULOF, fuel starts melting due to loss of coolant. The SAS4A code [1–5] is used from steady state operation to fuel pin melting within the wrapper tube. This phase is called the initiating phase. Then, the SIMMER code [6] is used for the phase of core melt to the whole core scale. In this phase, molten material can be moved laterally. This phase is called transition phase or early discharge phase. Although the design goal of SFR is to apply design measures for non-energetics, evaluation methods for the core expansion phase is also being developed since energetics were evaluated in the safety analysis of Monju and Joyo. In the case of re-criticality and energetics in the transition phase or initiating phase, mechanical energy and subsequent structure response are analysed. The SIMMER code is used for the mechanical energy analysis, and based on this analysis, the structural response of the reactor vessel is analysed by the AUTODYN code [7]. Sodium ejection through the rotation plugs is also calculated by the PLUG code in this phase. In the non-energetic case in the transition phase or after the core expansion phase, it moves to the material relocation phase and heat removal phase. For these phases, Super-COPD [8] and FLUENT code [9] are used for the analyses of cooling of residual core material in the core and relocated core material in the bottom and upper plenum of the reactor vessel by coolant circulation.

The status of development and application of SAS4A code in JAEA and the future research plan in initiating phase are described in the following sections.

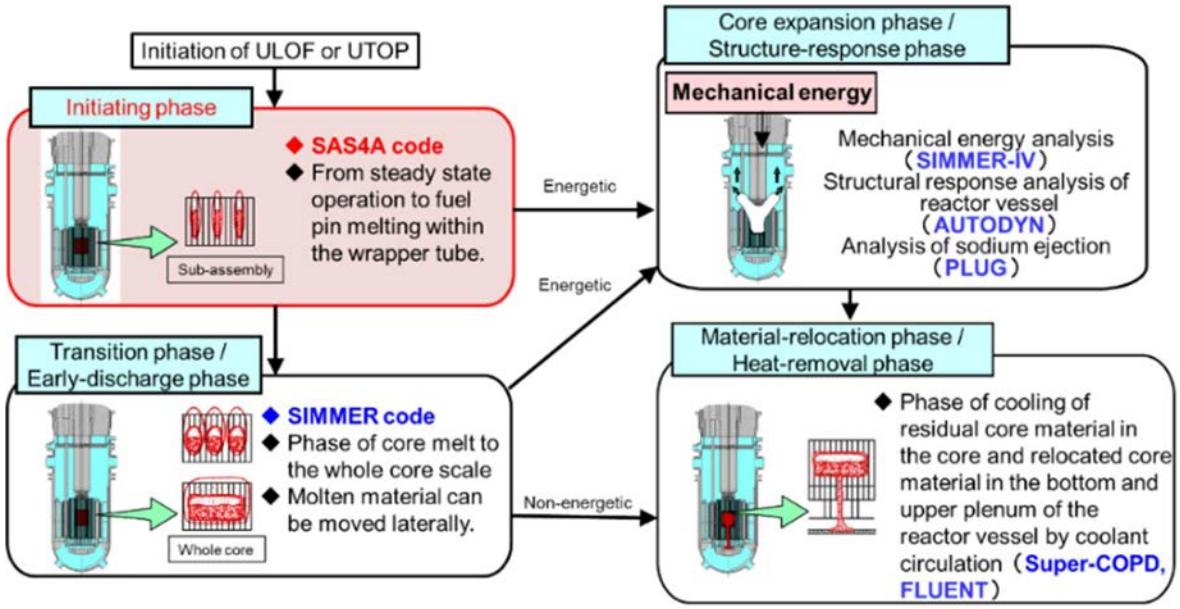

FIG. 1. Analysis codes used for CDA evaluation in JAEA.

2. BASIC MODEL DESCRIPTION OF THE SAS4A CODE

SAS4A is a calculation code developed at Argonne National Laboratory (ANL) in the United States as a next-generation improvement of SAS3D [10, 11], which was used in the safety analysis of the prototype fast breeder reactor "Monju". It was further developed and improved for oxide fuels in cooperation with European research institutes and JAEA, including the addition of new models based on the findings from the in-pile CABRI test [11].

The following phenomena are modelled and incorporated in the SAS4A code: 1) thermal and mechanical behaviour of fuel pin at a steady state and transient; 2) behaviour of coolant boiling and cladding dry out; 3) failure prediction of cladding and subsequent behaviours; 4) fuel disruption and relocation; 5) cladding melting and subsequent cladding motion. The reactivity changes owing to fuel and cladding axial expansion, coolant density change and coolant boiling, fuel and molten steel motion, etc. can be analysed based on a reactivity-worth map which is given in advance as an input. Figure 2 shows a conceptual image of the modelling.

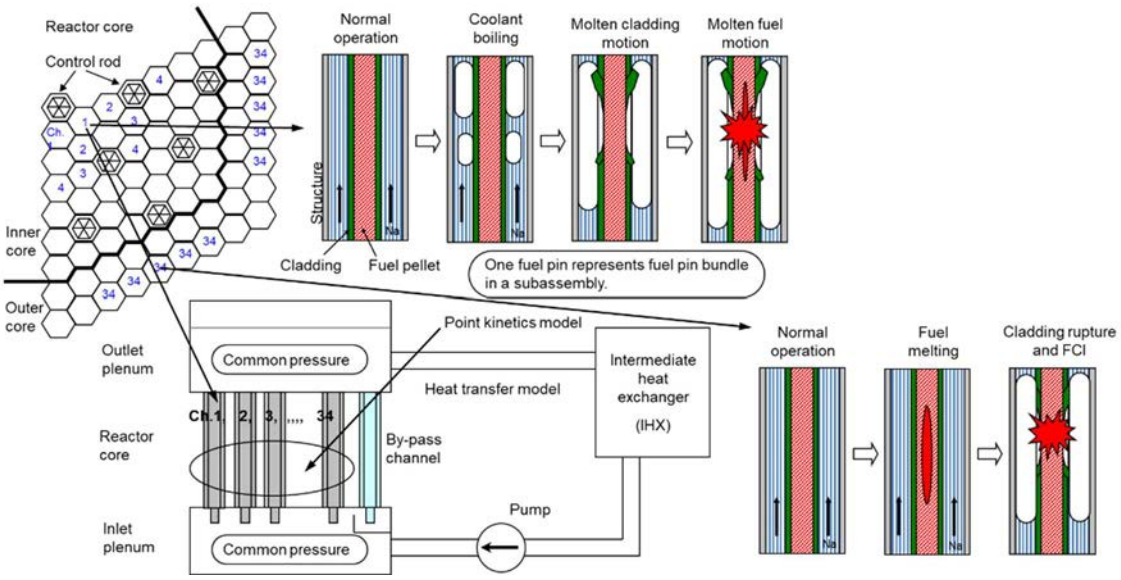

FIG. 2. Conceptual image of SAS4A code.

In the SAS4A code, hundreds of fuel assemblies constituting the reactor core are grouped to SAS channels according to their power-to-flow ratio, burnup, etc., and the entire reactor core is represented by up to about 30 SAS channels. Each SAS channel is hydraulically coupled in the upper and lower plenums and coupled by the point kinetics and reactivity coefficients in each mesh to analyse the accident propagation behaviour of the entire core. One SAS channel consists of a single fuel element heat transfer model divided in radial and axial directions. Fuel pellets, fuel-to-cladding gap, cladding, coolant, and wrapper tubes are coupled by the radial heat transfer model and axially via coolant thermohydraulics. The behaviour of molten fuel and other materials after fuel failure in the coolant channels is modelled by solving the axial one-dimensional mass, momentum, and energy conservation equations. In non-voided or partially voided channels, the fuel–coolant interaction (FCI) behaviour and the fuel relocation behaviour are calculated.

3. APPLICATION OF PIRT TO THE SAS4A CODE VALIDATION

The phenomena identification and ranking table (PIRT) method [12] has been applied to the SAS4A code in order to select important phenomena to be validated for ULOF and UTOP in a medium-sized SFR.

3.1 Steps of the validation process

The steps of the validation process are illustrated in Fig. 3 which are based on the generic PIRT process. (1) Issue was obviously the SAS4A code. (2) The PIRT objective was defined as extensive validation of the SAS4A code for severe accident analyses. (3) Monju was selected as a typical medium-sized SFR plant design. (4) ULOF and UTOP were selected as representative scenarios due to rapid event progression and potential of large energy release. (5) The importance of the physical phenomena is determined by the figure of merit (FOM) and each physical phenomenon is ranked based on the magnitude of its influence on the FOM. In vessel retention (IVR) is important in SFR, so it is necessary to evaluate whether mechanical energy is released that may affect the integrity of the reactor vessel in the evaluation of the initiating phase. Since the mechanical energy was converted from the thermal energy which could be represented by average core fuel temperature, the average core fuel temperature was selected as the FOM. (6) As shown in the introduction and Fig. 1, the event scenario was divided

into several time phases, and evaluation methods were developed for each time phases. (7) The range where the influence of ULOF and UTOP is limited to the reactor core region. Therefore, only the core region was set as the physical region in this study. The remaining steps of the validation process are described in the following sections.

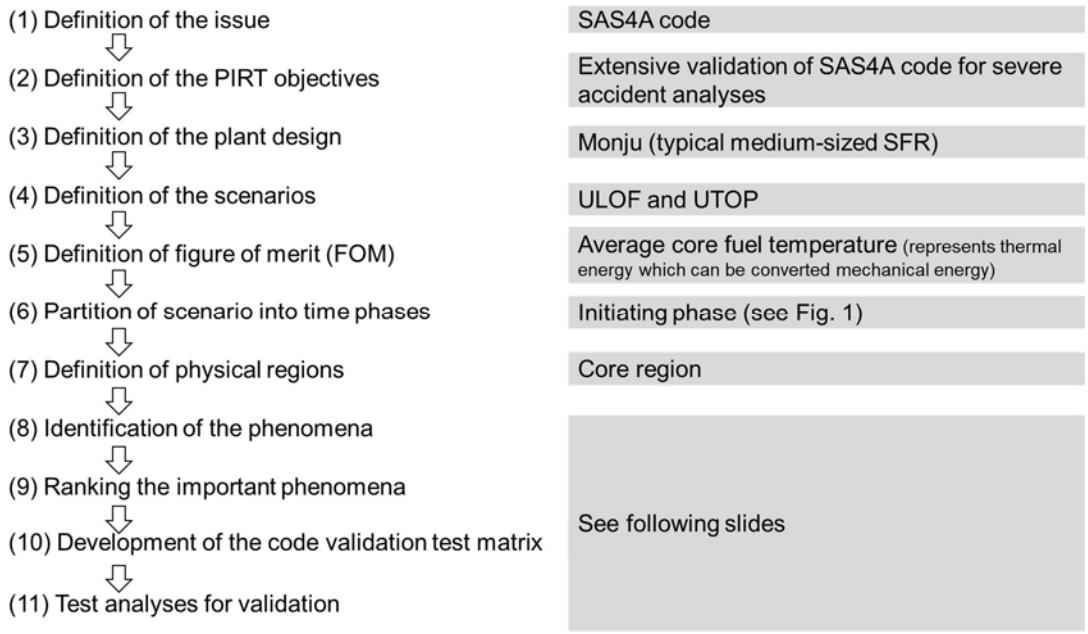

FIG. 3. Steps of the validation process.

3.2 Identification of the phenomena

Figure 4 shows event progression of ULOF and UTOP. Based on this figure and hierarchical architecture [13] for the system which comprehensively covered the phenomena in the defined core region, 16 and 14 physical phenomena were extracted for ULOF and UTOP, respectively.

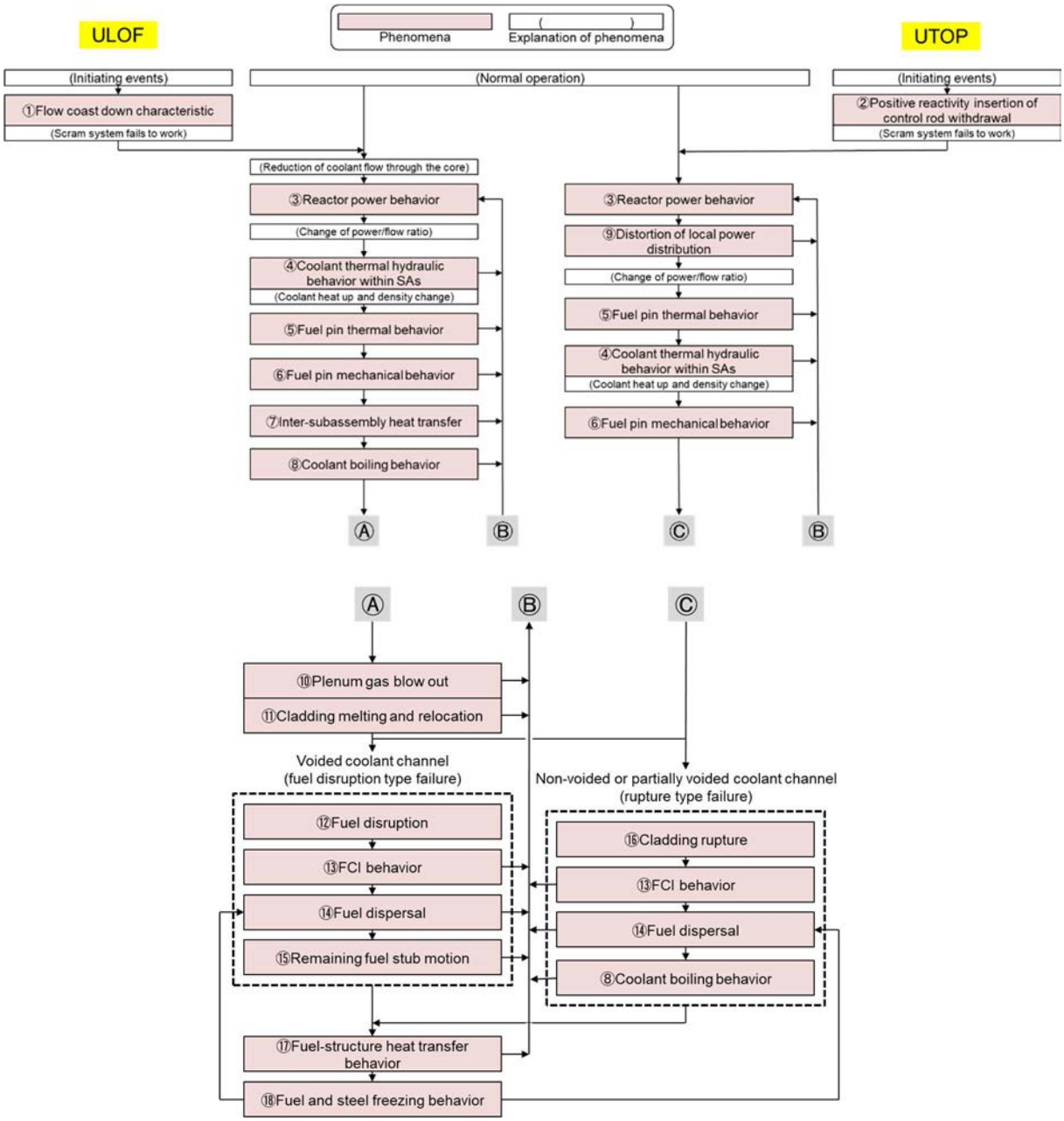

FIG. 4. Event progression of ULOF and UTOP.

3.3 Ranking the important phenomena

The 16 and 14 extracted physical phenomena for ULOF and UTOP were ranked in terms of importance. The ranks were defined as High (H), Medium (M), and Low (L) in descending order of importance. The importance of each physical phenomenon was determined by its influence on the FOM, which was the average core fuel temperature. Since the reactivity of the reactor, the energy release, and the average core fuel temperature are highly related, the importance of each physical phenomenon was determined and ranked by examining its influence on these. As shown the results of the ranking in Fig. 5, following 10 key important phenomena for ULOF were identified:

- Flow coast down characteristics;
- Reactor power behaviour;
- Coolant thermohydraulic behaviour within SAS;

- Fuel pin thermal behaviour;
- Fuel pin mechanical behaviour;
- Coolant boiling behaviour;
- Fuel disruption;
- FCI behaviour;
- Fuel dispersal;
- Cladding rupture.

The following key important phenomena for UTOP were identified:

- Positive reactivity insertion of control rod withdrawal;
- Reactor power behaviour;
- Fuel pin thermal behaviour;
- Fuel pin mechanical behaviour;
- Fuel disruption;
- FCI behaviour;
- Fuel dispersal;
- Cladding rupture.

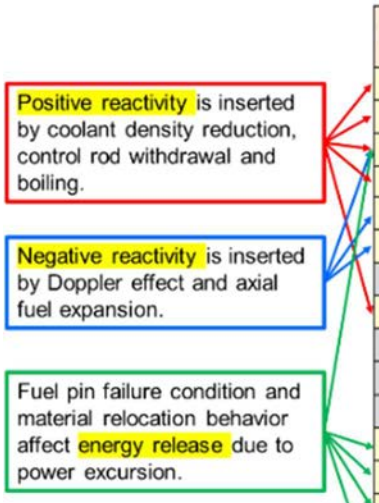

No.	Phenomena	Ranking*	
		ULOF	UTOP
①	Flow coast down characteristic	H	-
②	Positive reactivity insertion of control rod withdrawal	-	H
③	Reactor power behavior	H	H
④	Coolant thermal hydraulic behavior within SAs	H	M
⑤	Fuel pin thermal behavior	H	H
⑥	Fuel pin mechanical behavior	H	H
⑦	Inter-subassembly heat transfer	L	-
⑧	Coolant boiling behavior	H	M
⑨	Distortion of local power distribution	-	L
⑩	Plenum gas blow out	L	-
⑪	Cladding melting and relocation	L	-
⑫	Fuel disruption	H	H
⑬	FCI behavior	H	H
⑭	Fuel dispersal	H	H
⑮	Remaining fuel stub motion	L	L
⑯	Cladding rupture	H	H
⑰	Fuel-structure heat transfer behavior	L	L
⑱	Fuel and steel freezing behavior	L	L

* The rank is defined as High (H), Medium(M) and Low (L).

FIG. 5. Ranking table of ULOF and UTOP.

3.4 Code validation test matrix

An evaluation matrix was created for the important phenomena identified by ranking the physical phenomena as shown in Fig. 6. The evaluation matrix describes the analytical models corresponding to the important phenomena and the validation methods of the models in a matrix form and confirms that the physical phenomena required for the evaluation of the targeted accident scenario have been modelled without any deficiencies.

CABRI tests are invaluable for the validation of the SAS4A code. In the AI3 test, which was a transient overpower (TOP) type test, the cladding rupture and subsequent ejection of large

amount of molten fuel were observed. On one hand, cladding rupture took place in a partially voided coolant channel before cladding melting in the BI4 test which was transient undercooled overpower (TUCOP) type test. On the other hand, the power transient was triggered after cladding melting in the BI3 test which was also TUCOP type test. Therefore, all test data were used for the models related to coolant thermohydraulic behaviour, fuel pin thermal behaviour and fuel dispersal. The models of fuel pin mechanical behaviour and FCI behaviour were validated with AI3 and BI4 test data. The models related to coolant boiling behaviour and fuel disruption were validated with BI3 test data. It is unnecessary to validate flow coast-down characteristic and positive reactivity insertion of control rod withdrawal because they are provided by inputs. It is also unnecessary to validate reactor power behaviour because the point reactor kinetics equation is a general theory formula and material reactivity worth map is given by input.

No.	Important phenomena	Related SAS4A models	CABRI tests		
			TOP	TUCOP	
			AI3	BI4	BI3
①	Flow coast down characteristic	Boundary condition	-	-	-
②	Positive reactivity insertion of control rod withdrawal	Boundary condition	-	-	-
③	Reactor power behavior	Material reactivity worth map Point reactor kinetics equation	-	-	-
④	Coolant thermal hydraulic behavior within SAs	Fuel pin heat transfer model	✓	✓	✓
⑤	Fuel pin thermal behavior	Fuel pin heat transfer model	✓	✓	✓
⑥	Fuel pin mechanical behavior	Fission product model Fuel swelling model Stress strain model Molten cavity model	✓	✓	-
⑧	Coolant boiling behavior	Multiple-bubble slug ejection boiling model	-	-	✓
⑫	Fuel disruption	Failure criteria (Fuel disruption) Voided channel material motion model	-	-	✓
⑬	FCI behavior	Non-voided channel material motion model	✓	✓	-
⑭	Fuel dispersal	Non-voided channel material motion model Voided channel material motion model	✓	✓	✓
⑯	Cladding rupture	Failure criteria (Cladding rupture) Non-voided channel material motion model	✓	✓	-

FIG. 6. Code validation test matrix.

3.5 Test analyses for validation

Analyses of the above-mentioned three tests were performed for the validation of the SAS4A code. Figure 7 shows a comparison between the analytical result and the BI3 test data.

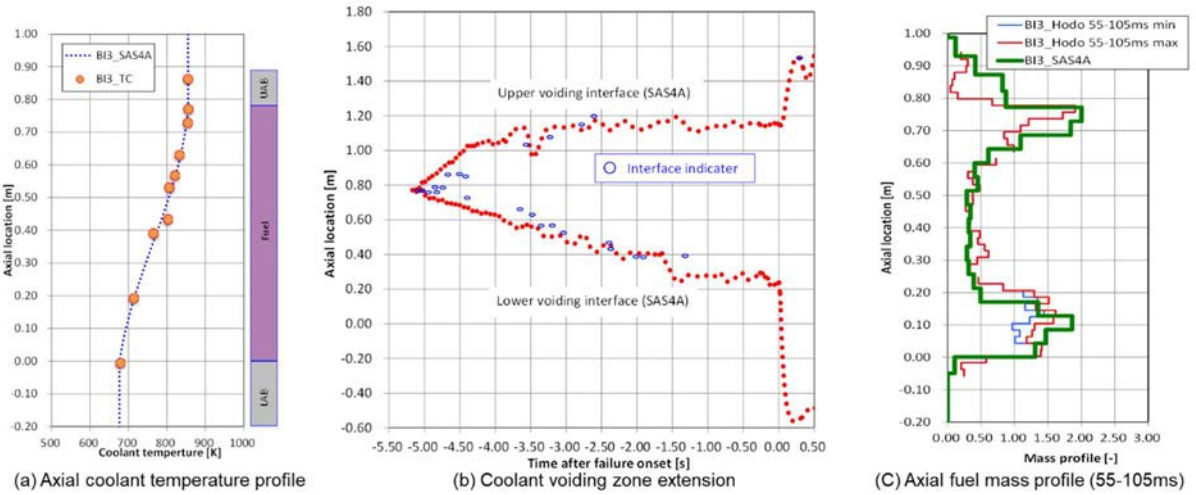

FIG. 7. Comparison between analytical result and BI3 test data.

Concerning the coolant thermal behaviour and fuel pin thermal behaviour, the fuel pin heat transfer model was validated by the coolant temperature profile because the radial temperature distribution was obtained by the solving the one-dimensional heat conduction equation and the axial power distribution was given by the input data obtained in the CABRI experiment. Figure 7(a) shows axial coolant temperature profile of the BI3 test, in which a blue dotted line indicates the analytical result and orange plots indicate experimental data of thermocouple. Based on such comparisons, the validity of the fuel pin thermal behaviour model was confirmed.

Coolant boiling model was validated with BI3 data. Figure 7(b) shows the coolant voiding zone extension of the BI3 test, in which a red dotted line indicates the analytical result and blue plots indicate experimental data. The good agreement between the analysis and the experiment confirms the validity of the boiling model of the SAS4A code.

The fuel dispersal model was validated using the AI3, BI4, and BI3 tests based on the matrix. This model is validated by the axial distribution of fuel mass after the fuel pin failure. Figure 7(c) shows the axial fuel mass profile of the BI3 test, in which a green solid line indicates the analytical result and red and blue lines indicate experimental data of neutron hodoscope. Based on such comparisons [14], the validity of the fuel dispersal model is confirmed.

The physical mechanism of fuel pin failure differs between UTOP and ULOF, and UTOP has a more complex mechanism. Using the relationship between fuel smear density and fuel areal melt fraction at failure obtained by CABRI in-pile tests [15], setting a small areal melt fraction for determining fuel pin failure results in a conservative evaluation. From the above points, it was found that the use of the areal melt fraction model as a fuel failure prediction model for SAS4A enables a conservative evaluation of the event progression of UTOP. The other models were also compared with AI3, BI4 and BI3 test data in the same way. The test data and the results of the analysis based on the code validation test matrix were in good agreement, indicating that the SAS4A model was sufficiently validated for the evaluation of the initiating phase.

4. EVALUATION OF A ULOF EVENT FOR A MEDIUM-SIZED SFR

With regard to the licensing of Monju, SAS3D, the former version of SAS4A, was used to analyse the initiating phase. As a result, a conservative evaluation showed that the prompt criticality was exceeded and 330 MJ of mechanical energy was released [16].

Figure 8 shows histories of reactor power and reactivity under reference condition evaluated by SAS4A. The net reactivity increased due to the increase of void reactivity caused by coolant boiling, but after fuel disruption, the net reactivity decreased and remains below 0$ due to negative reactivity feedback mainly caused by fuel dispersal. About 27 s after the onset of ULOF, the net reactivity was almost stable, at which point the core region consists almost entirely of coolant voids, and the transition phase takes over thereafter. Therefore, according to the analysis results of SAS4A under the reference conditions, the prompt criticality was avoided in initiating phase.

Figure 9 shows maximum net reactivity for various coolant void and Doppler reactivities under conservative conditions. Even in any combinations of conservative void and Doppler reactivities, the prompt criticality was avoided in SAS4A analyses.

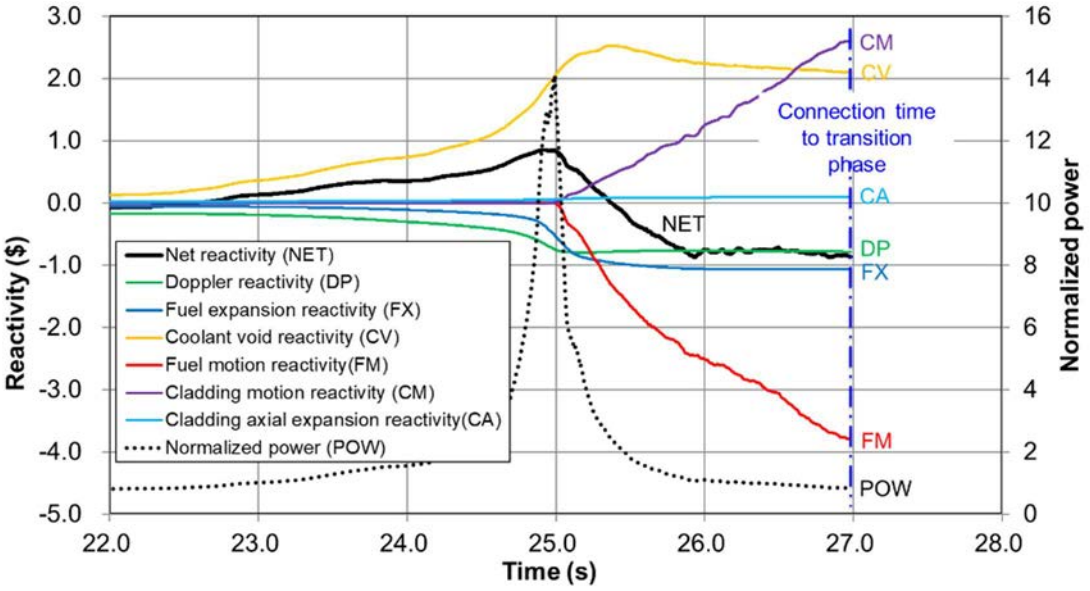

FIG. 8. Histories of reactor power and reactivity under reference condition.

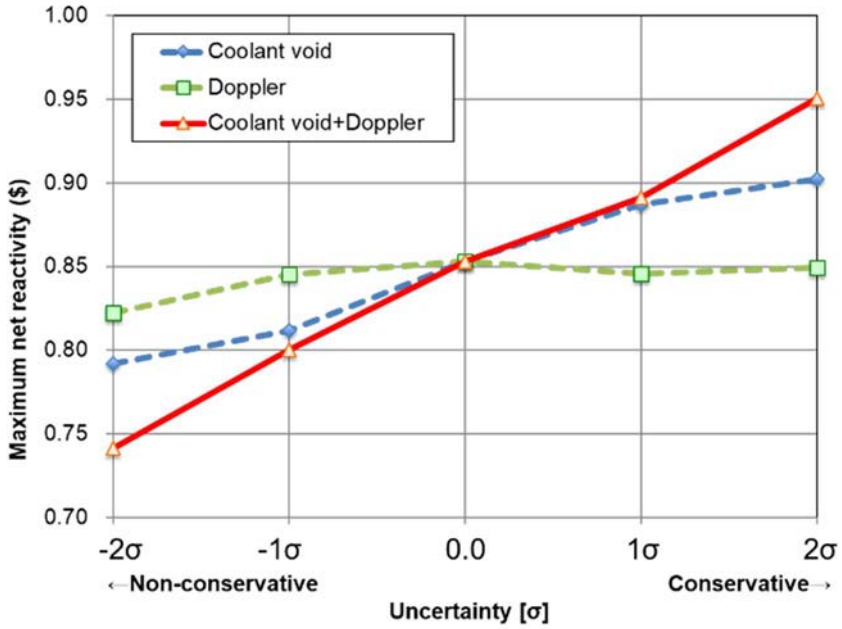

FIG. 9. Maximum net reactivity for various coolant void and Doppler reactivities under conservative conditions.

5. FUTURE RESEARCH PLAN

Different analysis codes have been applied to the initiating and transition phase as shown in Fig. 1. In order to enable consistent analysis of these phases for various core designs, SIMMER-V is being developed in cooperation with France. As part of this development, a detailed fuel pin model (DPIN3) is being developed to simulate the failure behaviour of fuel pins in detail during the initiating phase.

Figure 10 shows a conceptual image of the DPIN3 model in the SIMMER code. In this model, the fuel assembly is modelled as a single fuel pin, which consists of fuel pellets, cladding, fuel-cladding gap and other gases. In order to simulate the failure behaviour of the fuel pins, the thermal behaviour, deformation behaviour and fission product gas behaviour are modelled. In addition, the thermohydraulic behaviour in the centre hole and in the molten cavity formed by the fuel melting is also modelled. This makes it possible to simulate the behaviour of the molten fuel as it is released into the coolant channels due to fuel pin failure. This model can be applied to axially heterogeneous core and can be used for various core designs.

A prototype of DPIN3 was developed and a verification and validation plan was formulated. Based on this plan, we will proceed with model verification, validation, and applicability to actual reactor core, and plan to develop DPIN3 as a tool that can be used for safety evaluation of SFRs.

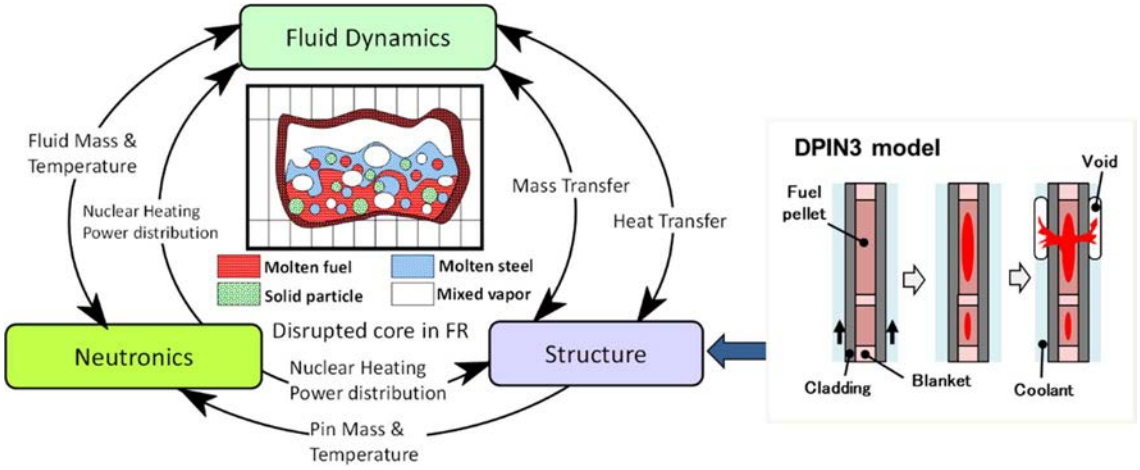

FIG. 10. Conceptual image of DPIN3 model in SIMMER code.

6. CONCLUSIONS

The status of development and application of the SAS4A code in JAEA and the future research plan have been described.

The PIRT method has been applied for ULOF and UTOP in a medium-sized SFR. Through these studies, 16 and 14 physical phenomena were extracted for ULOF and UTOP, respectively. Then, 10 and 8 key important phenomena respectively were identified through the ranking of extracted phenomena. Furthermore, a validation test matrix was created for the important phenomena extracted, and validation was conducted according to the validation test matrix. These studies further improved the validity and reliability of the SAS4A code.

Examples of the evaluation of ULOF event for a medium-sized SFR showed that prompt criticality was avoided in the initiating phase and net reactivity remained negative at the time of the wrapper tube melting, which was the application limit of SAS4A. Compared to previous evaluations, the present SAS4A calculations show that the elimination of mechanical energy release due to prompt criticality during the initiating phase is possible even under conservative conditions due to the reduction of excess uncertainty.

As part of the SIMMER-V development, a prototype of DPIN3 was developed. Based on verification and validation plan, model verification, validation, and applicability to actual reactor core are underway.

ACKNOWLEDGEMENTS

The authors would like to express their gratitude to K. Takahashi of NESI Inc. who assisted in analyses using the SAS4A code.

REFERENCES

[1] Tentner, A.M., Weber, D.P., Birgersson, G., Bordner, G.L., Briggs, L.L., Cahalan, J.E., Dunn, F.E., Kalimullah, Miles, K.J., Prohammer, F.G., The SAS4A LMFBR whole core accident analysis code (Proc. Int. Mtg. on Fast Reactor Safety, 1984), Knoxville, TN (1984).

[2] Miles, K.J., Hill, D.J., DEFORM-4: fuel pin characterization and transient response in the SAS4A accident analysis code system (Proceedings of International Topical Meeting on Fast Reactor Safety, 1985), Guernsey, UK (1985).

[3] Tentner, A.M., Miles, K.J., Kalimullah, Hill, D.J., Fuel relocation modeling in the SAS4A accident analysis code system (Proceedings of International Topical Meeting on Fast Reactor Safety, 1985), Guernsey, UK (1985).

[4] Cahalan, J.E., Wei, T.Y.C., Modeling developments for the SAS4A and SASSYS computer codes (Proceedings of Int. Fast Reactor Safety Mtg.,1990), Snowbird, UT (1990).

[5] Fukano, Y., SAS4A analysis on hypothetical total instantaneous flow blockage in SFRs based on in-pile experiments, Annals of Nuclear Energy, 77, 376–392 (2015).

[6] Kondo, S., Morita, K., Tobita, Y., Shirakawa, N., SIMMER-III: An advanced computer program for LMFBR severe accident analysis (Proc.'ANP'92, 1992) Tokyo, Japan (1992).

[7] Ansys, Ansys Autodyn, https://www.ansys.com/products/structures/ansys-autodyn. (2023).

[8] YAMADA, F., FUKANO, Y., NISHI, H., KONOMURA, M., Development of natural circulation analytical model in Super-COPD code and evaluation of core cooling capability in Monju during a station blackout, Nucl. Technol., 188, 292-321 (2014).

[9] Ansys, Ansys Fluent, https://www.ansys.com/products/fluids/ansys-fluent. (2023).

[10] Nonaka, N., Kasahara, F., Niwa, H., Sato, I., In-pile experiment analyses relevant to initiating-phase energetics (Proceedings of International Topical Meeting on Fast Reactor Safety, 1985), Guernsey, UK (1985).

[11] Nonaka, N., Sato, I., Improvement of evaluation method for initiating-phase energetics based on CABRI-1 in-pile experiments, Nucl. Technol., 98, 54-69 (1992).

[12] Wilson, G.E, Boyack, B.E., The role of the PIRT process in experiments, code development and code applications associated with reactor safety analysis, Nuclear Engineering and Design, 186, 23-37(1998).

[13] Ishida, S., Kawada, K. and Fukano, Y., Validation study of SAS4A code for the unprotected loss-of-flow accident in an SFR, Mechanical Engineering Journal, 7 1-17 (2020).

[14] Kussmaul, G., Vath, W., Wolff, J., Dadillon, J., Haessler, M., Sabathier, F., The CABRI project — Overall status and achievements (Proceedings of International Topical Meeting on Fast Reactor Safety, 1985), Guernsey, UK (1985).

[15] FUKANO, Y, ONODA, Y., SATO, I., CHARPENEL, J., Fuel pin behavior under slow ramp-type transient-overpower conditions in the CABRI-FAST experiments, J.Nucl.Sci.Technol. 1049-1058 (2009).

[16] Sato, I., Tobita, Y., Suzuki, T., Kawada, K., Fukano, Y., Fujita, S., Kamiyama, K., Nonaka, N., Ishikawa, M., Usami, S., Analysis of ULOF accident in Monju reflecting the knowledge from CABRI In-pile experiments and others, JAEA-Research 2007-055, Japan Atomic Energy Agency, Japan (2007).

RECENT DEVELOPMENTS IN MODELLING OF SEVERE ACCIDENT ANALYSIS CODE PREDIS

V. L. ANURAJ, T. SATHIYASHEELA. K. DEVAN

Indira Gandhi Centre for Atomic Research
Kalpakkam, India

Abstract

Severe accident analysis is carried out in three phases namely 1) pre-disassembly phase 2) disassembly phase 3) mechanical energy release phase. The pre-disassembly phase calculations are carried out using the point kinetics-based safety analysis code PREDIS, and the VENUS-II code is used for disassembly calculations. Recently, these computer codes have been modified by adding improved models such as a clad relocation model, an in-pin fuel motion model, a post-disassembly fuel expansion model, etc. One possible event that can lead to a severe accident is the unprotected loss of flow accident (ULOFA). The accident is initiated when the power supply to coolant circulating pump fails, resulting in flow coast-down. This leads to coolant voiding, and clad melting will soon be initiated. A single channel model for molten clad relocation based on Ishii's model has been developed and integrated with the safety analysis code PREDIS. The modified code is then used for the ULOFA analysis of a prototype fast breeder reactor. A computer code called FEXPAN is used to model the time-dependent fuel expansion following disassembly and to calculate the resultant work potential. The code calculates the dynamic behaviour of the reactor during the hydrodynamic expansion based on the von Neumann-Richtmyer pseudo-viscous pressure method with the assumption of a homogeneous fluid medium. An unprotected transient over power accident (UTOPA) can also lead to severe accident condition in a fast reactor. In a UTOPA, fuel melts before initiation of clad melting. UTOPA analyses has been carried out for a 600 MW(e) SFR core using a newly developed in-pin fuel motion module called MITRA, which is incorporated in the code PREDIS. Recently the PREDIS code has been benchmarked against loss of flow without scram (LOFWOS) tests conducted in the Fast Flux Test Facility; the results of the benchmark exercise are also discussed in the paper.

1. INTRODUCTION

Fast spectrum reactors can undergo core disruptive accidents (CDA) since they are not in the most reactive configuration. Changes in core geometry or core collapse under a meltdown accident can make the reactor highly supercritical and the consequences to such an event can be severe. A proper analysis of such events is an important part of safety analysis. Sophisticated computer codes are used for simulating such accidents and to study the consequences. The recent advances in the safety analysis code PREDIS [1] are discussed in the paper. A clad relocation model and in-pin fuel motion model have been incorporated in the PREDIS code and the effect of those phenomena on the severe accident evolution has been studied. The fuel expansion after core disassembly has been analysed using the FEXPAN model. The code was then validated against results from literature. Finally, the benchmark analysis of PREDIS using the loss of flow without scram test results from the Fast Flux Test Facility is also discussed.

2. ULOFA ANALYSIS WITH CLAD RELOCATION FEEDBACK

The unprotected loss of flow accident (ULOFA) is initiated when power supply to the coolant circulating pump fails, resulting in flow coast-down along with failure of the plant protection system. This leads to coolant voiding, and clad melting will be initiated soon after sodium voiding. The molten clad may get displaced during the transient and cause reactivity feedback. A lot of theoretical studies and some experiments have been performed to understand the overall implications of clad relocation and sweep out in CDA. The STAR series of experiments, CABRI-1 in-pile experiment and R4 and R5 TREAT in-pile tests are a few examples of the experiments carried out [2–4]. A lot of theoretical models have been developed to study clad relocation phenomenon and they are used to verify experimental results. The CLAZAS model in SAS2A and the CLAP model used in SAS3A are the two important ones used for clad relocation dynamics analysis [5, 6]. A one-dimensional cladding relocation model, based on a continuous film flow with flooding and de-flooding mechanisms, was developed by Ishii et al [7, 8]. This is simpler compared to CLAZAS and CLAP and assumes uniform film thickness

for the entire length of the film. In the present study, a single channel clad relocation model based on Ishii's method was developed and integrated with the existing transient analysis code PREDIS.

Ishii's model is based on a single channel film flow model and a simple thermal transient model for fuel pins. In this model it was assumed that the coolant channel was voided prior to the initiation of the molten clad motion, which is the case for ULOFA. During the initiation phase of ULOFA, the sodium vapour phase is assumed to be incompressible, and no source of gas either due to fission gas release or steel vaporization is included. The molten clad is assumed to be moving as a film under the influence of gravity, the channel pressure gradient, the frictional drag due to streaming sodium vapour and friction between moving cladding and the fuel pin. Because of the high upward sodium vapour flow there will be an initial upward motion of molten clad and it is possible that the molten steel reaches the blanket region and freezes. This frozen layer of steel can block the vapour flow completely or partially. The reduction in sodium vapour velocity due to the blockage can cause a clad film flow reversal, the film drains down the channel and eventually it slumps into the cold liquid sodium. The necessary input data for the calculation are the properties of sodium and cladding materials, geometry of the fuel pins and flow channels, and the initial and boundary conditions. The initial and boundary conditions consist of the information on the locations of the upper and lower ends of the melted cladding section and the total pressure drop over the coolant channel. A new subroutine RELOCS has been developed and integrated with the PREDIS code for the calculation. The code is then used for the ULOFA analysis of 500 MW prototype fast breeder reactor (PFBR).

In PREDIS, the PFBR core is divided into 10 radial channels based on coolant flow rate. A representative fuel pin is considered from each radial channel for heat transfer calculations. The 100 cm fuel region of the pin is divided into 10 axial meshes. The 30 cm long upper and lower blanket regions are divided into two 15 cm long meshes. That is the core is divided into 10 radial and 14 axial meshes. Ishii's model uses a simple heat transfer model for temperature calculations which assumes a fuel pin with no division into axial meshes (continuous along z-axis). The model has been modified to suit the mesh wise calculations in PREDIS. The large meshes are not suitable for simulation of clad relocation using the model and therefore finer meshes are to be used. For clad melting and relocation simulation a mesh size of 1 cm is used. The 14 axial meshes in a fuel pin is further divided into 160 meshes in the RELOCS subroutine. The heat transfer equations are solved in PREDIS at 14 axial locations and clad temperatures are available at those locations. To estimate the clad temperatures at the 160 mesh points from the known 14 values a linear interpolation technique is used. Once the clad temperature at any particular mesh (out of 160) reaches melting point that mesh is assumed to be melted. The one-dimensional equation of motion for the sodium vapour and the molten clad are given by:

$$\frac{\partial}{\partial t}\left(\alpha_g v_g\right) + \frac{\partial}{\partial Z}\left(\alpha_g v_g^2\right) = -\frac{\alpha_g}{\rho_g}\frac{\partial p}{\partial Z} - \alpha_g g - \frac{\tau_g P_g}{\rho_g\left(A_g + A_{cm}\right)} \qquad (1)$$

$$\frac{\partial}{\partial t}\left[\left(1-\alpha_g\right)v_c\right] + \frac{\partial}{\partial Z}\left[\left(1-\alpha_g\right)v_c^2\right] = -\frac{\left(1-\alpha_g\right)}{\rho_c}\frac{\partial p}{\partial Z} + \frac{P_g\tau_g + P_c\tau_c}{\rho_c\left(A_g + A_{cm}\right)} - \left(1-\alpha_g\right)g \qquad (2)$$

To determine the molten clad velocity, it is necessary to solve Eqs (1) and (2) simultaneously. The one-dimensional vapour continuity equation is:

$$\frac{\partial}{\partial t}\left(\alpha_g \rho_g\right) + \frac{\partial}{\partial Z}\left(\alpha_g \rho_g v_g\right) = \Gamma_g - \alpha_g \rho_g v_g \frac{\partial}{\partial Z}\left[\ln\left(A_g + A_{cm}\right)\right] \qquad (3)$$

Where, α is the void fraction, v is the velocity, ρ is the density, P is the pressure, and A is the flow area per channel. The suffix g denotes sodium vapour and c denotes clad. The momentum and continuity equations are solved by a simple Euler method to get the clad film velocity. The net displacement of molten clad and the associated reactivity changes are estimated.

The clad removal worth in the core region of a PFBR is positive, while it is negative for the blanket region. Therefore, clad relocated from core and freezing in the upper axial blanket will add a considerable amount of positive reactivity into the system. The net positive reactivity added to the system due to clad relocation is to be calculated to obtain an accurate prediction of the transient propagation in such an accident case. The relative steel volume change in each mesh is calculated from the clad thickness in each mesh and the film length and position in each channel. The removal worth of each mesh is multiplied with the relative volume change in the corresponding mesh and then added for all the meshes to find the net positive feedback added to the system.

In a ULOFA, the drop in coolant flow leads to coolant boiling followed by melting of fuel and clad. Once the fuel melts, slumping of molten fuel cause large reactivity addition, resulting in a surge in power. Pre-disassembly simulation is terminated when the fuel temperature in the highest rated mesh crosses the boiling point. The pressure due to fuel vapour expansion disassemble the core and make it subcritical, terminating the accident. The disassembly phase calculations were done using the VENUS II code [9]. Without a clad relocation model, the duration of pre-disassembly phase was 78.84 s and at the end the reactor is at a power level of 14.59×10^9 W. The positive reactivity addition rate due to fuel slumping was 11\$/s. The disassembly phase calculations carried out considering the reactivity addition rate of 11\$/s resulted in a mechanical energy release of 0.02 MJ. Even though the mechanical energy release was less than 1 MJ, the main vessel of the reactor is designed to withstand an energy excursion of 100 MJ, which corresponds to an input reactivity addition rate of 65.6\$/s for the disassembly phase calculations.

The analysis was repeated using a modified version of PREDIS that contains the clad relocation model. The important change was the inclusion of feedback due to clad relocation. Even if the time duration from clad melting to end of pre-disassembly phase is much less, the positive reactivity addition due to steel removal from the core region and its freezing in the upper axial blanket affects the course of the transient. The positive reactivity addition due to clad motion was found to be 1.46\$ at the end of pre-disassembly phase. The duration of pre-disassembly phase was reduced to 76.17 s with the clad relocation feedback. The reactor power at the end of pre-disassembly phase was found to be significantly higher (93.42×10^9 W) compared to the nominal analysis. The mechanical work potential depends on the temperature and pressure distribution across the core. A closer look into the pressure and temperature at various meshes revealed that, a greater number of meshes were at an elevated temperature with clad relocation feedback. The thermal to mechanical energy conversion is more efficient in that case. The net reactivity at the end of the transient was also relatively higher with the clad relocation model. The results are compared in Table 1.

TABLE 1. COMPARISON OF RESULTS OF ULOFA WITH AND WITHOUT CLAD RELOCATION FEEDBACK

Parameter	Without clad relocation feedback		With clad relocation feedback	
At the end of pre-disassembly phase				
Reactor power (W)	14.56×10^9		93.42×10^9	
Net reactivity ($)	0.881		0.993	
Phase duration (s)	78.84		76.17	
Reactivity addition rate ($/s)	10.5		21	
At the end of disassembly phase				
Reactivity addition rate	Calculated	Hypothetical	Calculated	Hypothetical
Input reactivity addition rate ($/s)	10.5	65.6*	21	65.6*
Phase duration (ms)	42.2	10.81	21.7	8.15
Fuel vapour fraction (%)	0.11	39.8	5.24	34.9
Thermal energy release (MJ)	298.8	5544	1495	5107
Mechanical energy release (MJ)	0.02	100	2.09	103

**65.6$/s is the reactivity addition rate corresponds to 100 MJ of energy release for which the vessel is designed for.*

Clad melting and relocation were observed in the first three radial channels (a total of 55 fuel assemblies out of 181). The status of clad melting and relocation at the end of pre-disassembly phase is depicted in Fig. 1, seven radial channels in the fuel region are represented by seven pins. Clad melting in the first, second and third channel were initiated at 73.56 s, 75.73 s and 76.16 s, respectively. In the first radial channel 47 cm long portion of clad was found to be molten at the end of pre-disassembly. Molten steel was moved upward and reached upper axial blanket where it froze. In the second channel (30 FSAs) the clad was melted by 31 cm and for the third channel (24 FSAs) the extend of clad melting was 20 cm. As in the R-4 and R-5 tests there was an initial upward motion of clad and freezing observed but there was no draining down of molten clad since the pre-disassembly phase ended before the molten clad flow reversal. Reactor power and net reactivity change with and without the clad motion model are compared in Figs 2 and 3.

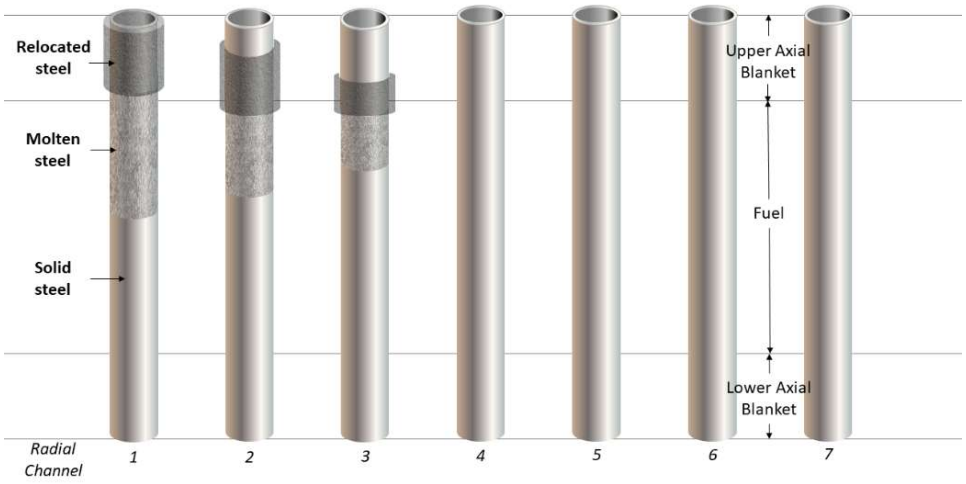

FIG. 1. Clad melting and relocation at the end of pre-disassembly phase.

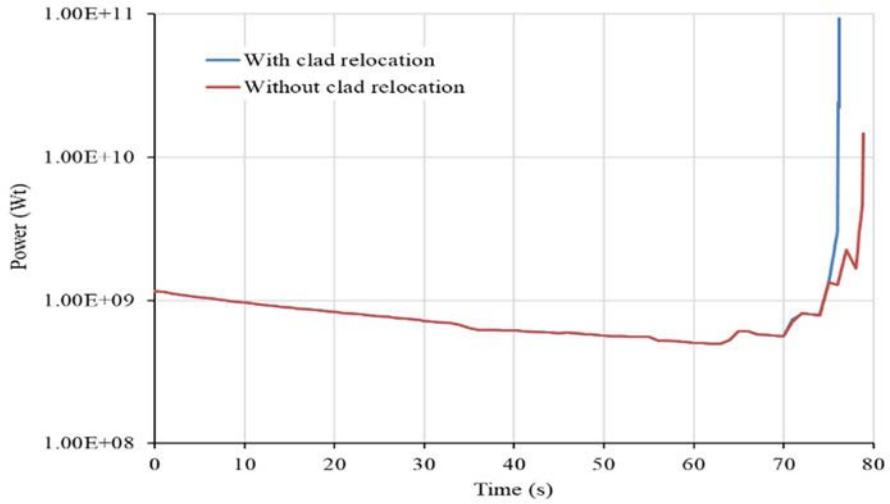

FIG. 2. Reactor power evolution with and without clad relocation feedback.

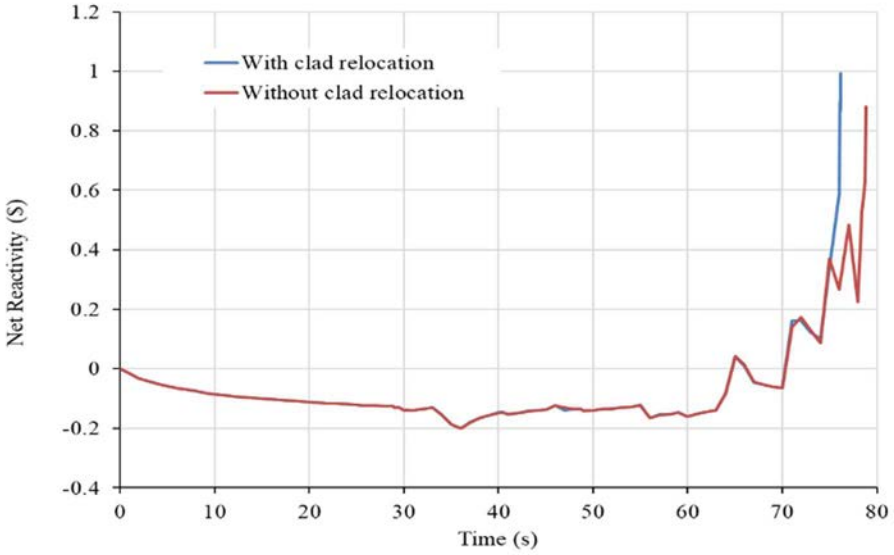

FIG. 3. Net reactivity evolution with and without clad relocation feedback.

The positive reactivity addition rate due to both fuel slumping and clad motion makes the net reactivity close to 1$. The time evolution of clad relocation feedback and other important feedback are shown in Fig. 4. The large power and lower heat removal cause initiation of fuel boiling and the fuel vapour thus produced causes disassembly of the core. During the disassembly phase no heat transfer is assumed from fuel to coolant. The positive reactivity addition due to fuel slumping and clad motion results in power rise leading to further fuel boiling. The negative feedback from Doppler and fuel displacement brings the net reactivity below zero and the power drops rapidly. The whole duration of this disassembly phase is a few tens of millisecond. The mechanical work potential of the core at the end of disassembly phase is calculated to be 2.098 MJ which is more than the value obtained without clad relocation model. The two cases are compared in Table 1. Compared to the reference case the fuel melt fraction and vapour fraction were also more in the present analysis. An energy release of 100 MJ is considered for the design of PFBR main vessel. To get such a high energy release the reactivity addition rate during disassembly phase needs to be 65.6$/s. The disassembly phase calculations were repeated with an input reactivity addition rate of 65.6$/s and the results compared with the case without clad relocation feedback. As shown in Table 1 the duration of the phase and fuel melt and vapour fractions are close to each other.

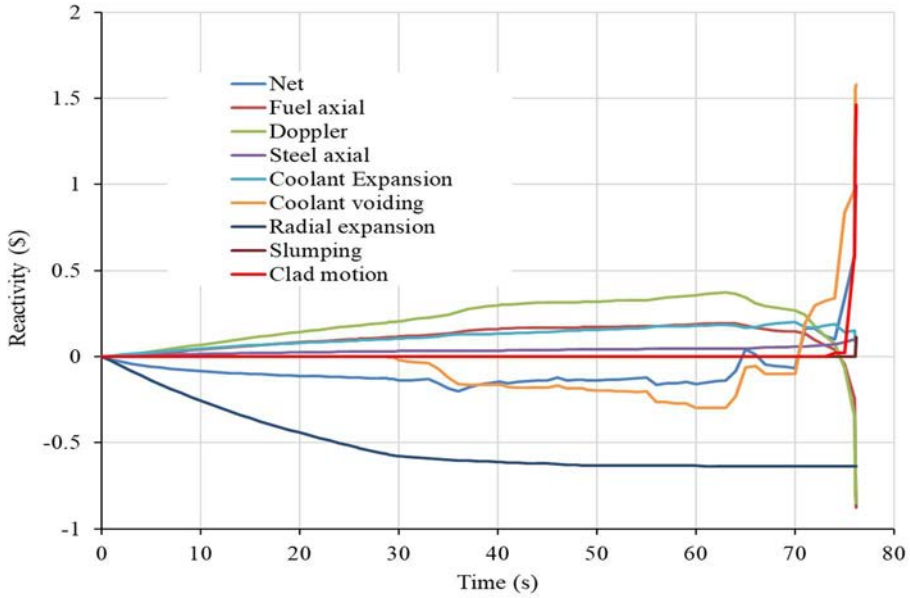

FIG. 4. Total reactivity and feedback reactivity components.

3. FUEL EXPANSION MODULE IN THE DISASSEMBLY PHASE

The behaviour of the core in the disassembly phase depends on reactor parameters such as power, net reactivity, reactivity addition rate, temperature distribution and the volume fractions of vapour, liquid and solid phases of core materials at the end of the pre-disassembly phase. The energy available from fuel expansion in a core disassembly accident in an LMFR has been studied extensively. At the end of disassembly, i.e. when the neutronic excursion ends, the core is left at a very high temperature and pressure. This condition is the beginning of core disintegration. The core expansion due to pressure gradients and the work done by expanding fuel were calculated by assuming isentropic expansion of the fuel to low pressure. The work done by whole core expansion to a final pressure is the sum of the work produced by each zone as the fuel in each zone expands independently of the final pressure. This is a time-independent technique [10] for estimating fuel expansion work.

FEXPAN [11, 12] models a time-dependent hydrodynamic expansion of a homogeneous fluid medium in a spherical geometry. The model calculates the core expansion surrounded by a compressible medium. The high fuel pressures compress the surrounding medium. Shock waves generate in such conditions, which are treated using a pseudo-viscous pressure method developed by von Neumann and Ritchmyer [13].

The FEXPAN model was adapted in the present analysis and a study of post disassembly hydrodynamic expansion for FFTF geometry was performed. The study is performed for complete sodium out case. The calculations were carried out up to the time of impact of the sodium column upon the cover. The calculations were carried out without a reflector. The time history of work is compared in Fig. 5. The FEXPAN output provides the temporal and spatial pressure distribution in the fuel bubble following disassembly. The spatial pressure distributions at four times are shown in Fig. 6. The results show that the results of the developed FEXPAN model agree with the results given in Ref. [12]. The new model is planned to be used for the PFBR work calculations.

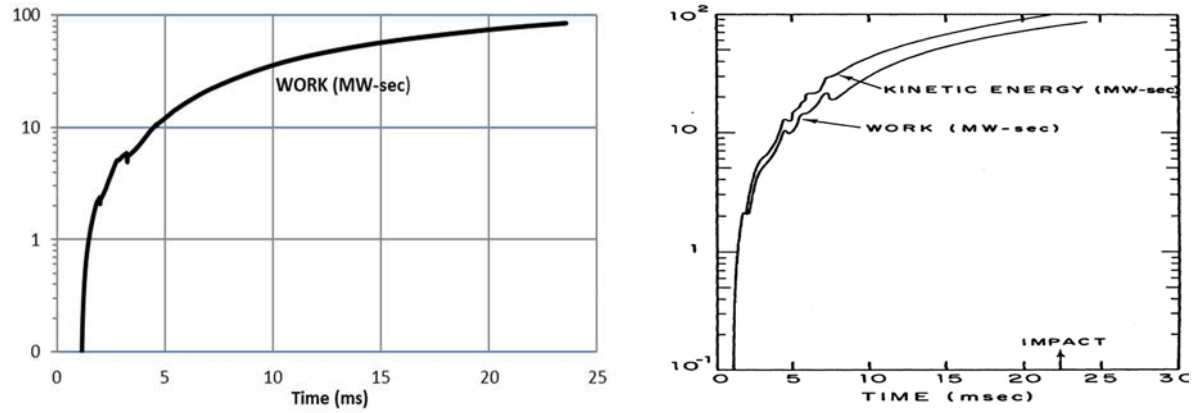

(a) (b)

FIG. 5. Cumulative work- time history, (a) calculated and (b) reference.

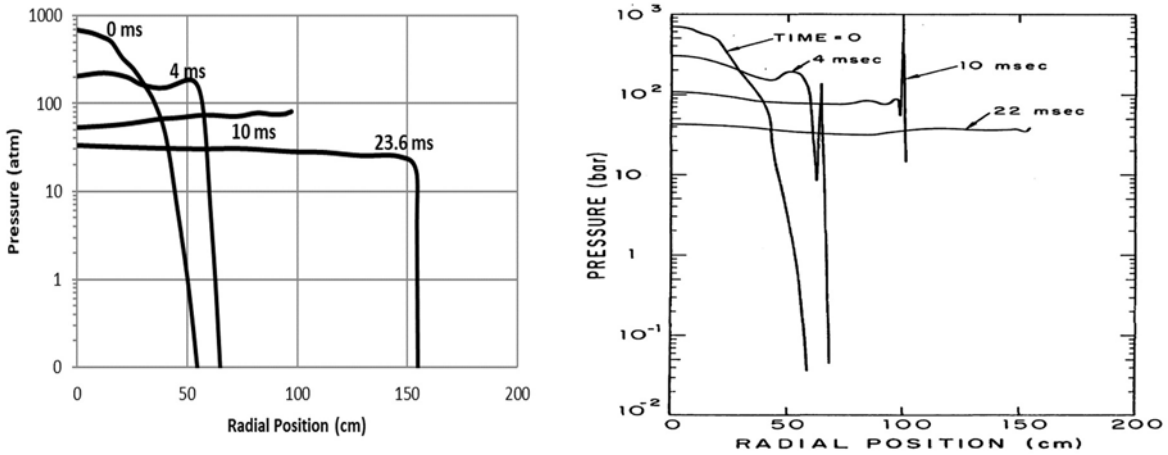

(a) (b)

FIG. 6. Spatial pressure distribution at various times for the present FEXPAN model, (a) calculated and (b) reference.

4. UTOPA ANALYSIS IN-PIN FUEL MOTION MODEL

Unlike ULOFA, in an unprotected transient over power accident (UTOPA), fuel melts before initiation of clad melting. Based on international experimental results [14, 15], the use of annular oxide pin is expected to provide an inherent shutdown mechanism during the hypothetical LMFBR accidents by providing a pathway for molten fuel to be ejected from the active core region to the top and bottom blanket. In-pin fuel motion is a multiphase hydrodynamic movement of molten fuel inside the fuel pins of a fast reactor during a UTOPA. The UTOPA analyses were carried out for a 600 MW(e) SFR core using a recently developed in-pin fuel motion module called MITRA [16], which is incorporated in the code PREDIS.

The reactivity feedback due to in-pin fuel motion and its effect on the transient progression were studied. It was deduced that in slow overpower, molten fuel hydrodynamics is dominated by gravity and solidification blockage. The module goes through important sub-programs such as: a heat transfer program to calculate temperature; a fission gas module to calculate the fission gas release and cavity pressure; multiphase fluid dynamics to calculate fuel melt fraction, changes in cavity radius due to melting, vapour and liquid density of fuel, vapour and liquid velocity of fuel in the central hole; and a program to calculate the fuel motion feedback.

The UTOPA analysis of a medium sized MOX fuelled fast reactor of rated power 600 MW was carried out and it was found that the accident does not lead to CDA. However, transient studies were revised in the present study to consider the effects of fuel melting and its feedback due to in-pin fuel motion. Based on the UTOPA studies, it is understood that the reactor stabilised at 41 % overpower and initiation of fuel melting was observed. Fuel melting took place in four axial nodes and four radial nodes up to the time of complete withdrawal of control rods. However, the feedback due to in-pin fuel motion of molten fuel was ignored. UTOPA analyses were revised with in-pin fuel motion feedback.

The external reactivity insertion due to uncontrolled withdrawal of control rod was 432.27 pcm (1.198$) with a peak addition rate of 2.77 pcm/s. With the positive external reactivity, the reactor power and the reactor material temperatures started increasing. With the change in power and temperature, feedback contribution becomes effective. The negative reactivity contributions are from the Doppler feedback, fuel axial expansion and core radial expansion. The coolant expansion gives positive reactivity contribution, which is very small, as there is no coolant boiling. Reactivity feedback due to control rod driveline expansion and vessel expansion were also considered. Under UTOPA, thermal expansion of the vessel was calculated based on the difference in inlet temperature at any instant and the initial steady state cold pool temperature. Feedback reactivities could balance the external reactivity and make the net reactivity almost close to zero. Before melting the annular fuel cavity radius was 0.08 cm. With melting the melt radius increased and the molten fuel was relocated to the central hole as shown in Fig. 7. Once relocated, the molten fuel drops due to gravity, and when it reaches the lower portion it solidifies, as the temperature in that location is much less than that of the fuel melting temperature. Even though there was melting, outer part of the fuel was found to be in solid state. Hence, it can be concluded that, there was no fuel pin failure. The peak clad temperature was 758^0C as compared to 819^0C without a fuel dynamics module, Similarly, the peak coolant temperature was 756^0C as compared to 817^0C without a fuel dynamics module, which is smaller than its boiling point. From the above analyses it was learnt that, considering in-pin fuel motion feedback not only reduces the power at the end of the transient it also reduces the hot spot clad, coolant temperature and also the number of radial channels undergo melting. At the end of the transient it introduced reactivity feedback of about -0.432$. Various reactor parameters at 500 s

after the initiation of the transient are compared in Table 2. The normalised power variation with time is compared in Fig. 8.

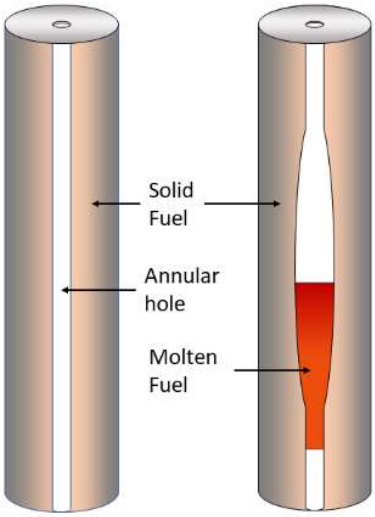

FIG. 7. Schematic representation of in-pin fuel motion.

TABLE 2. COMPARISON OF RESULTS OF UTOPA WITH AND WITHOUT IN-PIN FUEL MOTION FEEDBACK

Parameter (at 500 s)	UTOPA without IPFM	UTOPA with IPFM
Power (%)	150	131
Peak clad temperature (^{0}C)	819	758
Peak coolant temperature (^{0}C)	817	756
Clad hotspot temperature (^{0}C)	863	796
Coolant hotspot temperature (^{0}C)	855	789
Inlet coolant temperature (^{0}C)	492	471

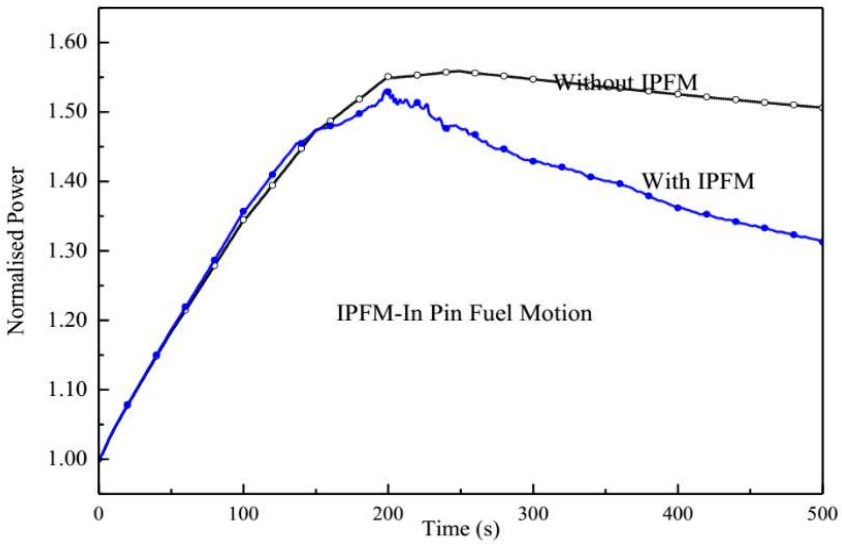

FIG. 8. Comparisons of Results of UTOPA with and Without Fuel Dynamics Module MITRA.

5. PREDIS CODE BENCHMARKING AGAINST FFTF LOFWOS TEST

The PREDIS code has been validated with many experimental results; recently the code was benchmarked against The Fast Flux Test Facility (FFTF) loss of flow without scram (LOFWOS) test [17]. FFTF is a 400 MW(th), oxide-fuelled, liquid sodium cooled test reactor. In July 1986, a series of unprotected transients were performed in FFTF as part of the passive safety demonstration programme. Among these were the series of LOFWOS tests. These tests were useful in demonstrating the inherent and passive safety benefits of specific reactor designs and also in confirming the safety margins and providing data for computer code validation.

LOFWOS Test #13 was initiated at 50% power and 100% flow and all three primary sodium pumps were tripped simultaneously. With the loss of flow, the normalized flow falls. Code PREDIS was used to analyse this transient. The core was divided into various radial and axial meshes for temperature and reactivity feedback calculations. A point kinetics model was used for the neutron kinetics. The axial and radial power distribution and the perturbation worths for fuel, clad and steel were estimated and given as input to the safety analysis code PREDIS. Gas expansion modules (GEM) were introduced for the LOFWOS tests to demonstrate their ability to mitigate the consequences of unprotected loss of flow transients. Each GEM was inserted into an assembly position within the inner row of the radial reflector region. Argon gas was trapped by a plug at the top of the module and exposed to sodium at the bottom of the module. At nominal full flow conditions, the pressure of the sodium compressed the gas to a level above the top of the active fuel column. Due to loss of flow, the pressure exerted on the gas by the sodium is decreased, allowing the gas to expand in GEM assemblies. The displaced sodium at the periphery of the core led to increased neutron leakage and hence, there is negative reactivity feedback, which takes the reactor to a substantially subcritical condition. The net reactivity becomes negative and thus there is a drop in power. Transient analyses were carried out with the PREDIS code and the net reactivity in the core is compared with the ANL result in Fig. 9. The evolution of power is compared in Fig. 10. FFTF has a core restraint mechanism, which is expected to give core radial motion during power transients, and result in an overall negative reactivity feedback. In the PREDIS simulation, the negative feedback reactivity contribution from radial expansion is neglected. This is the primary reason for the observed discrepancy between calculated and measured values of power and reactivity.

With the drop in power, there was a drop in fuel temperature. However, temperature of coolant and clad increased for some time due to the drop in flow, then ultimately also falls due to the drop in fuel temperature to a very low value, as shown in Fig. 11. Important reactivity feedback contributing to the transients are: the Doppler, fuel axial expansion, GEM reactivity, clad and coolant expansion, control rod drive mechanism (CRDM) and vessel expansion feedback. Since FFTF is a small test reactor, the control rod worth at the banking is slightly high (7.8 pcm/mm). With this control rod worth, there is a rise in contribution of CRDM feedback to a considerable amount with all the six CRDM. However, with the dominating GEM feedback, the net reactivity finally follows the GEM reactivity feedback. CRDM feedback through hot pool temperature determination is small and hence, GEM reactivity feedback is the only controlling reactivity. The net reactivity feedback and its components are plotted in Fig. 12. The peak clad temperature is much less than 700°C and the coolant temperature is far away from its saturation temperature which demonstrate that there is no concern for these under LOFWOS condition.

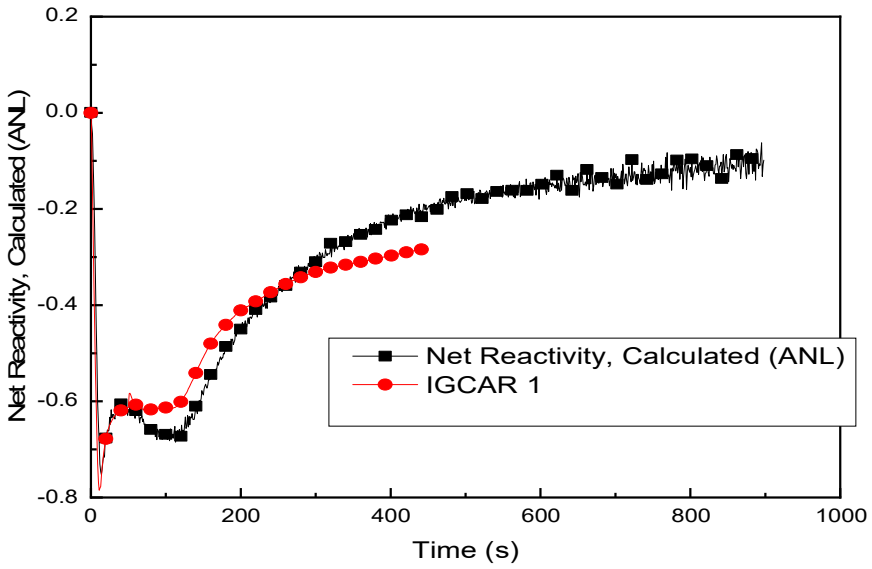

FIG. 9. Reactivity variation comparison.

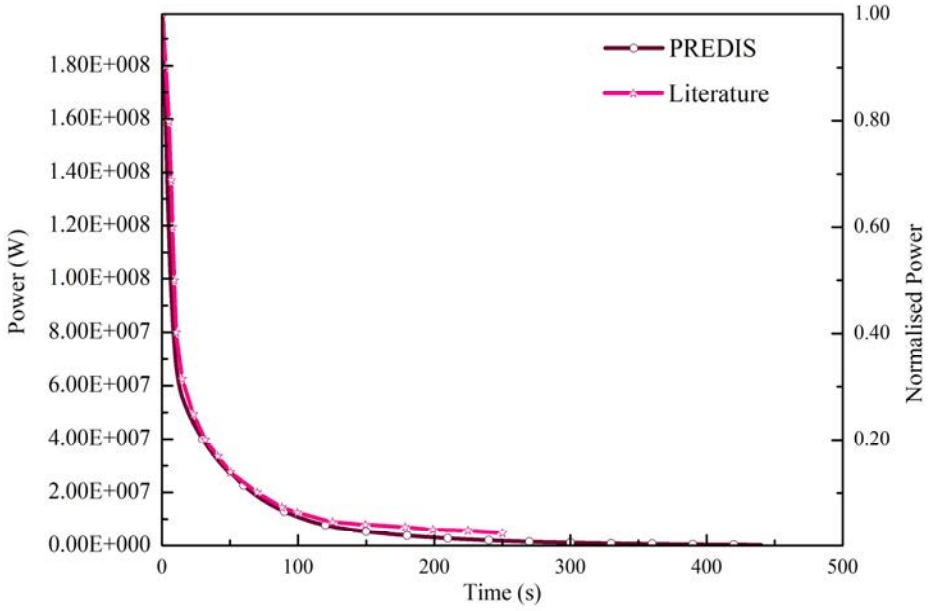

FIG. 10. Power profile of FFTF under LOFWOS test #13.

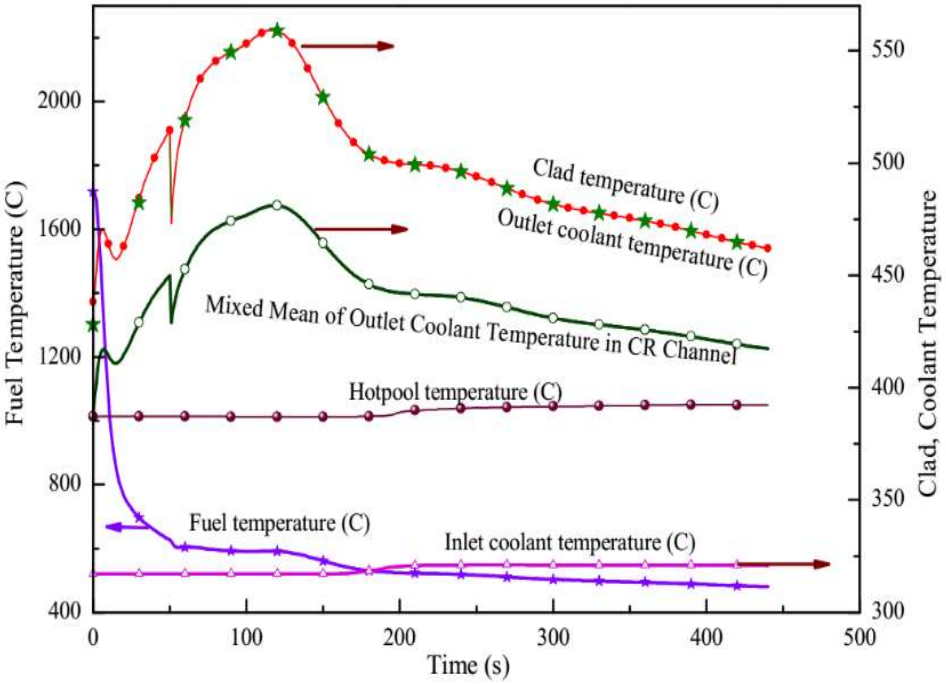

FIG. 11. Peak fuel, clad, coolant inlet and outlet temperature profile obtained using PREDIS.

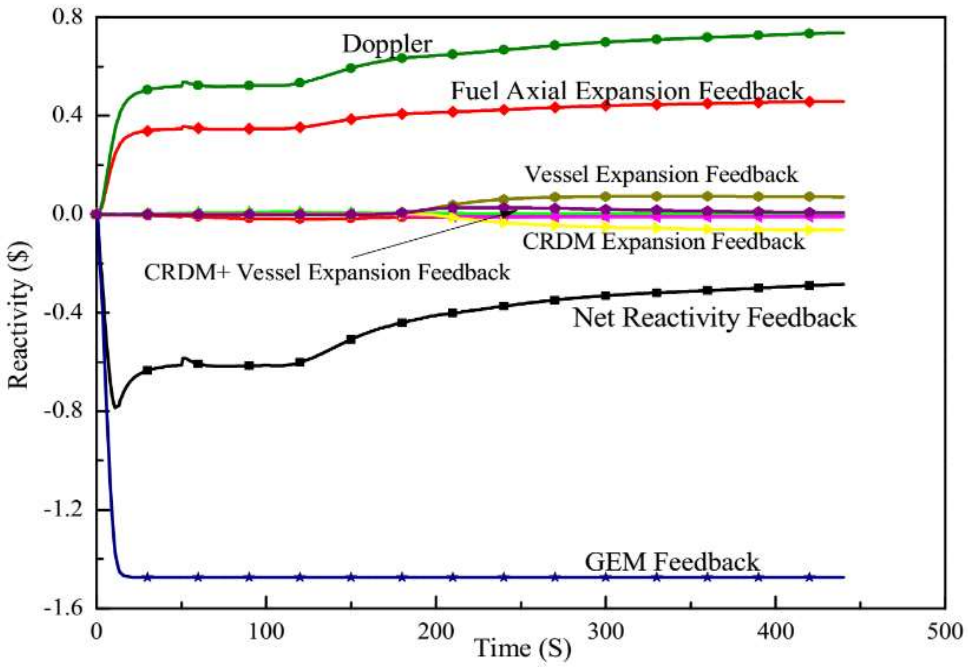

FIG. 12. Net reactivity feedback and its components calculated using PREDIS.

6. CONCLUSIONS

A clad relocation model and in-pin fuel motion models were implemented in the safety analysis code PREDIS and the effect of those phenomena in the severe accident characteristics of fast reactors were studied. The ULOFA analysis for PFBR was carried out considering clad motion feedback and the results compared against the reference case without a clad relocation model. The mechanical energy release was found to be comparable in both cases. The UTOPA analysis of a medium sized LMFBR was carried out with an in-pin fuel motion model and it was found, that the in-pin fuel motion feedback reduced the total reactor power at the end of the transient. It also reduced the hot spot clad, coolant temperature and also the amount of melting. Finally, a benchmark analysis for the PREDIS code was carried out against the FFTF LOFWOS test #13. The code could predict the net reactivity change and power evolution fairly well. Hence the newly added models on clad relocation, in-pin fuel motion and the fuel expansion helped in simulating fast reactor severe accidents in more detail. With these new capabilities the code can simulate the accident more realistically removing conservative assumptions.

REFERENCES

[1] HARISH, R., et al., KALDIS: A computer code system for core disruptive accident analysis in fast reactors, Internal report IGC-208, IGCAR, Kalpakkam (1999).

[2] WRIGHT, et al., In pile observations of fuel and clad relocation during LMFBR initiation phase accident experiments – the STAR experiments, Proc. International topical meeting on fast reactor safety, 439, Guernsey, UK (1986).

[3] STRUWE, D., et al., Two phase flow, clad melting and transient materials relocation in the CABRI-I experiments, Proc. International fast reactor safety meeting, 431, Snowbird, USA (1990).

[4] GROLMES, M. A., HOLTZ, R. E., SPENCER, B. W., MILLER, C. E., KRAMER, N. A., R-series loss-of-flow safety experiment in TREAT, Proc. Fast Reactor Safety Mtg., Beverly Hills, California, 1, 297 (1974).

[5] BOHL, W. R., CLAP: A cladding action program for LMFBR HCDA LOF analysis, T-ANS, 23, 346 (1976).

[6] Cladding Motion Model – CLAP, The SAS4A/SASSYS-1 Safety Analysis Code System, ANL/NE-12/4, Nuclear Engineering Division, Argonne National Laboratory (2012).

[7] ISHII, M., CHEN, W. L., GROLMES M. A., Molten Clad Motion for Fast Reactor Loss-of-Flow Accidents, Nucl. Sci. Eng. 60, 435–451 (1976).

[8] ISHII, M., CHEN, W. L., GROLMES M. A., multichannel model for relocation of molten fuel cladding in unprotected loss-of-flow accidents in liquid-metal fast breeder reactors, Nucl. Sci. Eng. 69, 297-318 (1979).

[9] JACKSON, J. F., NICHOLSON, R. B., VENUS-II: A LMFBR Disassembly Program, ANL - 7951, ANL, USA (1972).

[10] WALTER, A. E., REYNOLD, A. B., Fast Breeder Reactors, Pergamon Press, New York (1981).

[11] KIRBIYIK, M., GARNER, P. L., REFLING, J. G., REYNOLDS, A. B., Hydrodynamics of post-disassembly fuel expansion, Nucl. Eng. Des. 35, 441-460 (1975).

[12] KIRBIYIK, M., Fuel Vapour Generation in LMFBR Core Disruptive Accidents, Ph. D. dissertation, Nuclear Engineering Department, University of Virginia (1975).

[13] VON NEUMANN, J., RICHTMYER, R.D., A method for the numerical calculation of hydrodynamic shocks, J. Appl. Phys. 21, 232 (1951).

[14] PORTEN, D. R., PADILLA Jr., A., BAARS, R.E., Concept Verification of an Inherent Shutdown Mechanism for HCDA's. HEDL-SA-1737 FP (1979).

[15] SMITH, D.E., Comparative Analysis of Internal Fuel Motion in Annular Fuel Design. HEDL-SA-2934-FP (1983).

[16] DUBEY, A., SATHIYASHEELA, T., SHARMA, A. K., Reactor dynamics of in-pin fuel motion in fast breeder reactors, Nucl. Eng. Des. 340, 431–446 (2018).

[17] SUMNER, T., et al., Benchmark Specification for FFTF LOFWOS Test #13, ANL-ART-102, USA (2017).

DEVELOPMENT OF FUEL DEFORMATION MODULE IN TRAN-SCORE CODE DURING POWER AND FLOW TRANSIENT IN SFR

Amandeep Singh
Atomic Energy Regulatory Board, Nuclear Safety Analysis Division
Mumbai, India

K. Obaidurrahman, S. C. Utkarsh
Atomic Energy Regulatory Board, Nuclear Safety Analysis Division
Mumbai, India

Abstract

A hypothetical uncontrolled reactivity insertion or flow blockage in a fast neutron reactor may lead to a core disruptive accident. A thorough understanding of the progression of core disruptive accident and estimation of core energy released during the accident is necessary to find out the consequences of this event. TRAN-SCORE, a computer code, was developed specifically to evaluate the pre-disassembly phase of sodium cooled fast breeder reactors that use MOX as fuel. The code includes the modelling of neutronic, thermal hydrodynamic and simplified fuel deformation behaviour. The capability of code was demonstrated by simulating a few test problems and comparing against SAS 1A results. The fuel deformation module has been recently improved in TRAN-SCORE for the thermoelastic mechanical estimation for fuel and clad. Axial and radial deformations from thermal expansion and mechanical stresses can be estimated using this module with and without cracking. The paper presents the basic phenomena of the stress–strain equation, with and without a crack in a fuel pin. The code can be used to analyse a spectrum of events involving flow and reactivity transients with more precise modelling of fuel deformation following a core disruptive accident.

1. INTRODUCTION

Uncontrolled reactivity excursions or flow blockage in fast neutron reactors could lead to a core disruptive accident (CDA), specifically if there is significant mismatch between the rate of heat generation and the rate of heat removal from the core. This could be on account of a transient overpower (TOP) event initiated by reactivity addition, such as uncontrolled withdrawal of control and protection rods resulting in heat generation greater than heat removal, or by deficient cooling transients initiated by loss of flow (LOF) or loss of heat sink (LOHS) events resulting in a lower heat removal rate than the rate of heat generation. These accidents may lead to core melting and consequent core disruption. For fast reactor systems, understanding of the progression of a CDA and estimation of core energy released during the accident is crucial for evaluating the actual damage caused to the main vessel and top shield, and the amount of sodium that can come out into the reactor containment building. The extreme complexity of modelling various underlying physical phenomena during a CDA poses a challenge for safety analysis. In general, progression of a fast reactor CDA is modelled in three phases: accident initiation (pre-disassembly phase), disassembly phase and post-disassembly phase. This article presents modelling of fuel deformation phenomenon during the pre-disassembly phase of a CDA.

The simulation of the pre-disassembly phase includes coupled modelling of core neutronics, fuel heat transfer, coolant dynamics, sodium boiling, fuel deformation and dynamic behaviour of the molten fuel during slumping. An in-house computer code (TRAN-SCORE) [1–3] has been developed for analysing flow and power transient for the pre-disassembly phase in sodium cooled fast breeder reactors that use MOX as fuel. The TRAN-SCORE code has different models for analysing the pre-disassembly phase. It includes multichannel core descriptions for realistic thermohydraulic simulation for different flow zone fuel assemblies. Different reactivity feedback like fuel, clad and coolant temperature feedback are calculated using the temperature obtained by solving heat transfer equations and two-phase coolant dynamic equations. A deformation module has been recently incorporated into the code to find out the stresses and strains for fuel and clad consistent with respective temperatures.

The Doppler coefficient in a fast reactor becomes less dominant due to the neutron spectrum being shifted with respect to absorption resonances. Additionally, fuel expansion also contributes to the negative fuel temperature coefficient inside the core. The radial temperature distribution inside the fuel pin also depends on the magnitude of gap conductance, which in turn depends on radial expansion of fuel and clad. For realistic assessment of the accident consequences, it is important to predict the fuel expansion and its integrity. The fuel deformation module has been recently incorporated into the code to find out the radial and axial stresses and strains for solid and cracked fuel. The governing equations for the fuel deformation model for solid and cracked fuel are presented here and the computational approach is also discussed. Sample problems from the SAS-1A test [4] have been solved and analytical results are discussed.

2. MATHEMATICAL MODEL

The fuel deformation module developed in the TRAN-SCORE code estimates fuel pin stresses and deformations occurring during transients and treats both elastic and plastic deformation of the cladding. Mechanical deformations of the fuel and cladding are estimated in the elastic as well as in plastic regime. The gap width τ is calculated as a function of time, and when it predicts that the fuel and cladding have come into contact, the thermal conductance of the bond, gap conductance (h_b) is set equal to a maximum value $h_{b,max}$. The value of h_b can be estimated as a function of pressure as required during the transient.

Thermo-elastic deformation of the fuel and the elastic-plastic deformation of the cladding is estimated using the fuel and cladding temperature profiles obtained from the heat transfer module. Fuel and cladding stresses and deformations are calculated by assuming a stress-free configuration at normal operating conditions. This assumption is justified if the stresses produced by the change from room temperature to operating conditions are annealed out. Therefore, in the following description, the temperature at a point is the difference between the actual temperature and the temperature corresponding to the steady state operating conditions.

The fuel element is divided into axial segments as in the heat transfer module. Since the radial temperature variations for a reactor fuel rod are significantly higher than the axial ones, the field equations [5] of elasticity with the appropriate boundary conditions are solved exactly in closed form with respect to radial variations. The fuel pin in an axial segment is divided into different radial zones as required, i.e. the central void, the solid continuous fuel zone, the cracked fuel zone, the fuel–cladding gap, and the fuel pin cladding. These zones are illustrated in Fig. 1. Three deformation cases are considered in this module which refer to the elastic deformation where solid fuel is presents, elastic plastic deformation where solid and cracked fuel is present and plastic deformation where only cracked fuel is presents inside the fuel pin.

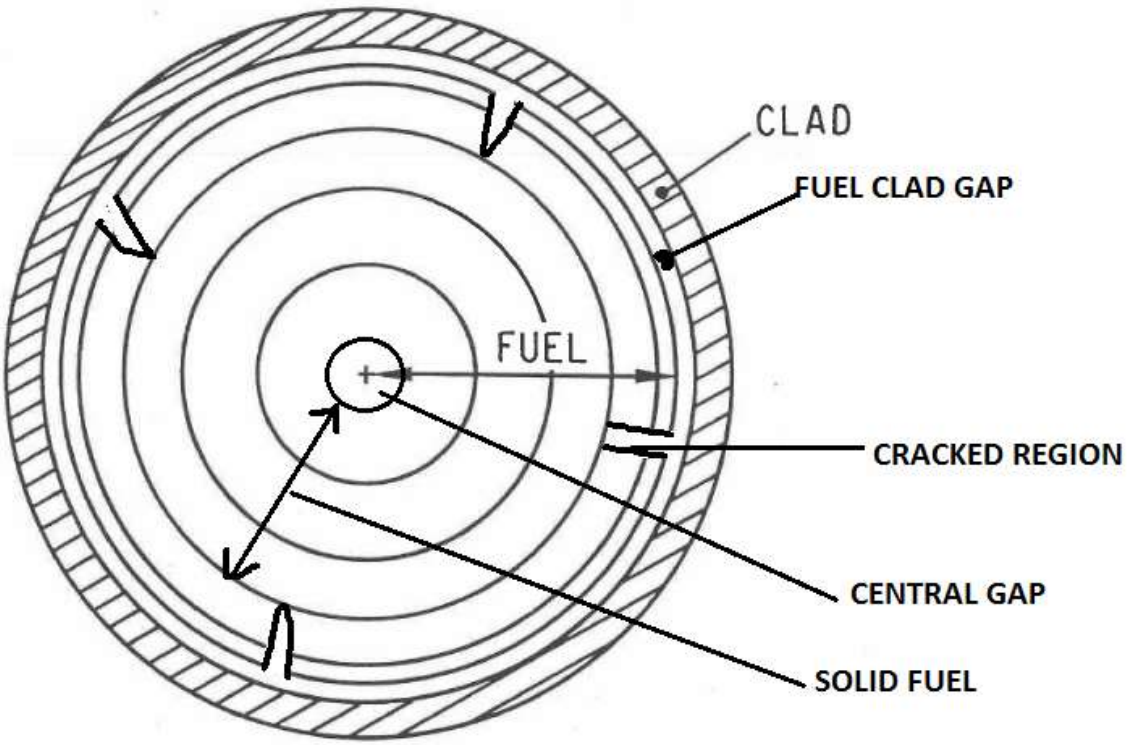

FIG. 1. Pin geometry in r-direction with the presence of crack.

2.1 Elastics deformation (solid fuel)

The strain displacement equations for axisymmetric problems are as follows:

$$\epsilon_r = \frac{\partial u_r}{\partial r}$$

$$\epsilon_\theta = \frac{u_r}{r} + \frac{1}{r}\frac{\partial u_\theta}{\partial \theta} \tag{1}$$

$$_z = \frac{\partial u_z}{\partial z}$$

Hooke's Law in Polar Coordinates can be written as follows:

$$\epsilon_r = \frac{1}{E}[\sigma_r - \nu(\sigma_\theta + \sigma_z)] + \Delta(\alpha T)$$

$$\epsilon_\theta = \frac{1}{E}[\sigma_\theta - \nu(\sigma_r + \sigma_z)] + \Delta(\alpha T) \tag{2}$$

$$\epsilon_z = \frac{1}{E}[\sigma_z - \nu(\sigma_\theta + \sigma_r)] + \Delta(\alpha T)$$

$$\Delta(\alpha T) = \alpha(T_2)(T_2 - T_r) - \alpha(T_1)(T_1 - T_r)$$

Where:

σ_r= radial normal stress,

$\sigma_{r,f}$= radial normal stress from externally applied stress,

$\sigma_{r,th}$= radial normal stress due to thermal expansion,

σ_θ = circumferential (hoop) stress,

$\sigma_{\theta,r}$ = circumferential (hoop) stress from externally applied stress,

$\sigma_{\theta,th}$ = circumferential (hoop) stress due to thermal expansion,

σ_z = axial normal stress,

$\sigma_{z,r}$ = axial normal stress from externally applied stress,

$\sigma_{z,th}$ = axial normal stress due to thermal expansion,

σ_{rz} =shearing stress on z planes,

u_r = radial displacement,

u_f = radial displacement from externally applied stress,

u_{th} = radial displacement due to thermal expansion,

u_z = axial displacement,

u_θ = circumferential displacement,

ϵ_r=radial strain,

ϵ_θ= circumferential (hoop) strain,

ϵ_z=axial strain,

ϵ_z=axial strain from externally applied stress,

ϵ_z=axial strain due to thermal expansion,

ϵ_{rz}=shearing strain,

E=Modulus of elasticity,

ν= Poisson's ratio,

P_g= Plenum Pressure,

T_r=Reference temperature,

T_2, T_1=Temperature at the final and initial states

In this approach, the stress equation is solved in the radial direction taking axially average properties over the node.

The equilibrium equation will be:

$$\frac{\partial \sigma_r}{\partial r} + \frac{\sigma_r - \sigma_\theta}{r} = 0 \tag{3}$$

The analytical solution of Eqs (1) and (3) will give radial and circumstantial stress and radial strain as follows:

$$\sigma_r = \frac{E}{(1+\nu)(1-2\nu)}\left[\frac{\partial u_r}{\partial r}(1-\nu) + \frac{u_r}{r}\nu + \nu\epsilon_z - (1+\nu)\Delta(\alpha T)\right] \tag{4}$$

$$\sigma_{\theta\theta} = \frac{E}{(1+\nu)(1-2\nu)}\left[\frac{u_r}{r}(1-\nu) + \frac{\partial u_r}{\partial r}\nu + \nu\epsilon_z - (1+\nu)\Delta(\alpha T)\right]$$

$$I(r) = \frac{1}{r^2}\int_a^r dr\, r\, \Delta(\alpha T(r))$$

$$u_r = u_f + u_{th} \tag{5}$$

$$\frac{u_f}{r} = \frac{(1+\nu)}{(b^2-a^2)E}\left[b^2\sigma_r(b)\left\{(1-2\nu) + \frac{a^2}{r^2}\right\} - a^2\sigma_r(a)\left\{(1-2\nu) + \frac{b^2}{r^2}\right\}\right] - \nu\epsilon_{z,f} \tag{6}$$

$$\frac{u_{th}}{r} = \frac{(1+\nu)}{(1-\nu)}\left[I(r) + \frac{I(b)b^2}{b^2-a^2}\left\{(1-2\nu) + \frac{a^2}{r^2}\right\}\right] - \nu\epsilon_{z,th} \tag{7}$$

$$\sigma_r = \sigma_{r,f} + \sigma_{r,th} \tag{8}$$

$$\sigma_{r,f} = \frac{1}{(b^2-a^2)}\left[b^2\sigma_r(b)\left\{1 - \frac{a^2}{r^2}\right\} - a^2\sigma_r(a)\left\{1 - \frac{b^2}{r^2}\right\}\right] \tag{9}$$

$$\sigma_{r,th} = \frac{E}{(1-\nu)}\left[-I(r) + \frac{I(b)b^2}{b^2-a^2}\left\{1 - \frac{a^2}{r^2}\right\}\right] \tag{10}$$

$$\sigma_\theta = \sigma_{\theta,f} + \sigma_{\theta,th} \tag{11}$$

$$\sigma_{\theta,f} = \frac{1}{(b^2-a^2)}\left[b^2\sigma_r(b)\left\{1 + \frac{a^2}{r^2}\right\} - a^2\sigma_r(a)\left\{1 + \frac{b^2}{r^2}\right\}\right] \tag{12}$$

$$\sigma_{\theta,th} = \frac{E}{(1-\nu)}\left[I(r) + \frac{I(b)b^2}{b^2-a^2}\left\{1 + \frac{a^2}{r^2}\right\} - \Delta(\alpha T)\right] \tag{13}$$

Where:

α= linear thermal expansion coefficient

a= inner radius of fuel

b= outer radius of fuel

η= outer radius of solid fuel which is not cracked

Eqs (5) and (8) have been solved to find out the radial displacement and radial and circumstantial stresses.

2.2 Plastic deformation (partially cracked fuel)

When circumstantial stress inside the fuel or clad exceeds the fracture strength of the fuel or clad, a crack tends to begin inside fuel or clad. The stable boundary of the crack is estimated by checking the value of circumstantial stress at different radial nodes. During this phase, there will be two regions; a solid zone and a cracked zone, and the elastic deformation calculation is performed for the solid zone. In the cracked zone, circumstantial and axial stresses will be equal to negative plenum pressure and circumstantial stresses at the solid zone boundary will be also same.

$$\sigma_\theta = \sigma_z = -P_g \tag{14}$$

With these conditions, radial stresses for cracked region can be estimated by integrating Eq. (3) from the outer boundary (R_{out}) of fuel as:

$$\sigma_r = -P_g + \frac{\eta}{r}(P_g + \sigma_\eta) \tag{15}$$

$$\text{where } \sigma_\eta = -P_g + \frac{R_{out}}{\eta}(P_g + \sigma_{FC})$$

σ_{FC} and σ_η are stresses at fuel cladding interface and outer boundary of solid fuel respectively. The radial displacement, u_r is obtained by solving stress equation. The final solution will be:

$$u_r = u_\eta + (2\nu - 1)(r - \eta)\frac{P_g}{E_c} + \frac{(P_g + \sigma_\eta)}{E_c}\eta\, ln\frac{r}{\eta} + \int_\eta^r dr\ \ \Delta(\alpha T) \tag{16}$$

2.3 Fully cracked fuel

As a crack progresses during a transient, solid fuel may achieve a fully cracked condition where the stresses are governed by central cavity pressure and fuel cladding interface pressure. The maximum fuel cladding interface pressure will be equivalent to the plenum pressure if there is no fuel melting inside the fuel cavity. If there is melting, due to pressure of the molten cavity, radial relocation of fuel will take place up to the cladding surface in the gap. The interface pressure can be found using Eq. (15) with the assumption that cracked fuel will remain at plenum pressure.

$$\sigma_{FC} = -P_g + \frac{R_{in}}{R_f}(P_g + \sigma_{in}) \tag{17}$$

where σ_{in} is molten cavity pressure at the inner radius of the crack. The radial displacement will be calculated using Eq. (16) and radial stresses.

The radial expansion due to thermal stress of the fuel is estimated using Eqs (16)(15), (*5*), (17) according to the crack inside the fuel.

2.4 Fuel axial expansion

Stress strain equations are evaluated by rearranging Eq. (2) assuming the axial strain ϵ_z is uniform all along the axial segments. The axial stress can be estimated by substituting Eq. (8) into Eq. (2) which will give:

$$\sigma_z = \frac{2\nu E}{(b^2 - a^2)}\left[\frac{I(b)b^2}{1-\nu} - \frac{b^2\sigma_r(b) - a^2\sigma_r(a)}{E}\right] - \frac{E\Delta(\alpha T)}{1-\nu} + E\epsilon_z \quad (18)$$

The axial force in any axial node can be estimated by integrating the axial stress over radial nodes:

$$F_f = -2\pi E a^2 I(a) + 2\pi\nu\left(b^2\sigma_r(b) - a^2\sigma_r(a)\right) + \pi E\epsilon_z(b^2 - a^2) \quad (19)$$

To determine the axial stress, the axial force is calculated from the cavity force F_{cav}, the axial force due to plenum gas pressure F_{ax} and the force from cladding F_c.

$F_{cav} = \pi a^2 P_{cav}$ where P_{cav} is molten cavity pressure and a is central void radius

$F_{ax} = \pi r_p^2 P_{gas}$ where P_{gas} is Fission gas plenum pressure and r_p is plenum radius

The force from the cladding will be zero with free axial expansion. The uniform axial strain can be finally found with the help of above equation as:

$$\epsilon_z = (\epsilon_z^f + \epsilon_z^{th})A_f \quad (20)$$

Where:

$$\epsilon_z^f = \frac{-2\nu}{(b^2 - a^2)}\left[\frac{b^2\sigma_r(b) - a^2\sigma_r(a)}{E}\right] - \frac{a^2 P_{cav} + r_p^2 P_{gas}}{E(b^2 - a^2)} \quad (21)$$

$$\epsilon_z^{th} = \frac{2I(b)b^2}{(b^2 - a^2)} \quad (22)$$

Where: A_f is fraction of axial expansion to be used in the model.

3. RESULTS

Analysis of a reactivity transient has been done using the TRAN-SCORE code for an SFR. The fuel pin has been divided into 10 radial nodes and 16 axial nodes for analysis. Normalised power and feedback reactivity have been calculated with TRAN-SCORE code for a 2.5$/s reactivity insertion (the value is taken from the SAS-1A test problem) as shown in Fig. 2. The coolant temperature and pressure distribution at a steady state at 0.5 s have been estimated and are shown in Fig. 3. The estimated steady state radial fuel temperature is shown in Fig. 4.

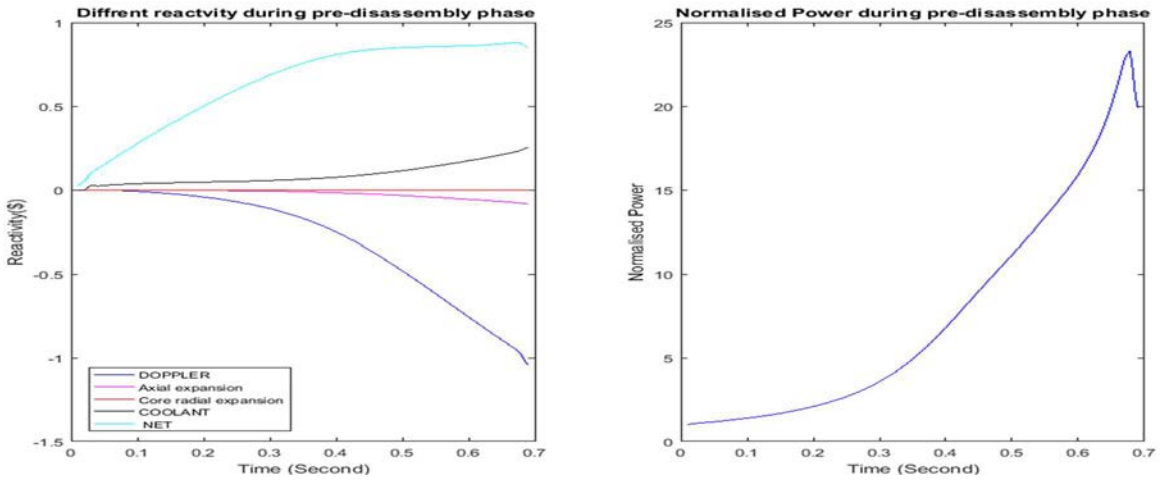

FIG. 2. Normalised power and different reactivity feedback at a 2.5$/sec reactivity insertion.

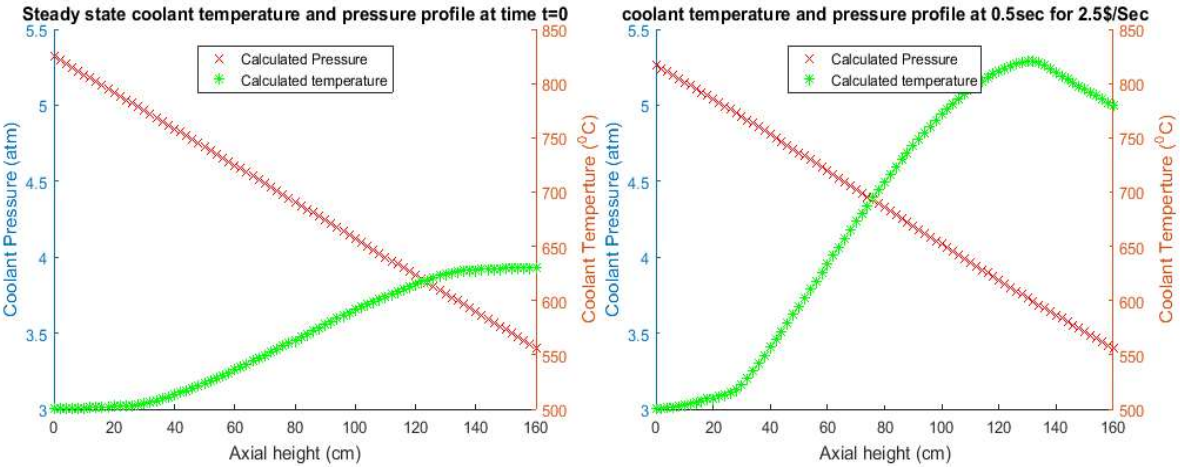

FIG. 3. Coolant temperature and pressure profile along the axial direction at a steady state at 0.5 s.

The radial mesh stress distribution for the fuel and clad are estimated using the deformation module for different axial nodes. The radial and circumstantial stresses for the fuel and clad have also been determined using the model developed. With increases in power, circumstantial stress increases and exceeds the fracture strength value at a point where the crack will be generated. The crack inside the fuel pin can be seen in the results. The radial crack progression in fuel is presented in Fig. 5 for two axial nodes. The results are also given in Table 1 and it can be seen that the crack inside the fuel is progressing from the outer radius to the fuel centre region. At time t = 0, the fuel is in solid region and circumstantial stresses are lower than fracture strength. When the normalized power is ~3.6 at 0.3 s, the crack in the outer radial fuel meshes can be clearly visible. After including this model, a crack in the fuel and clad can be estimated and stress and strain for solid and cracked fuel can be found. Figure 6 illustrates the progression of maximum fuel and clad temperature, as well as axial expansion feedback reactivity, with and without the deformation module. Figure 6 shows that the deformation module can produce a more realistic estimation of both the distribution of fuel mesh and the feedback reactivity caused by axial expansion.

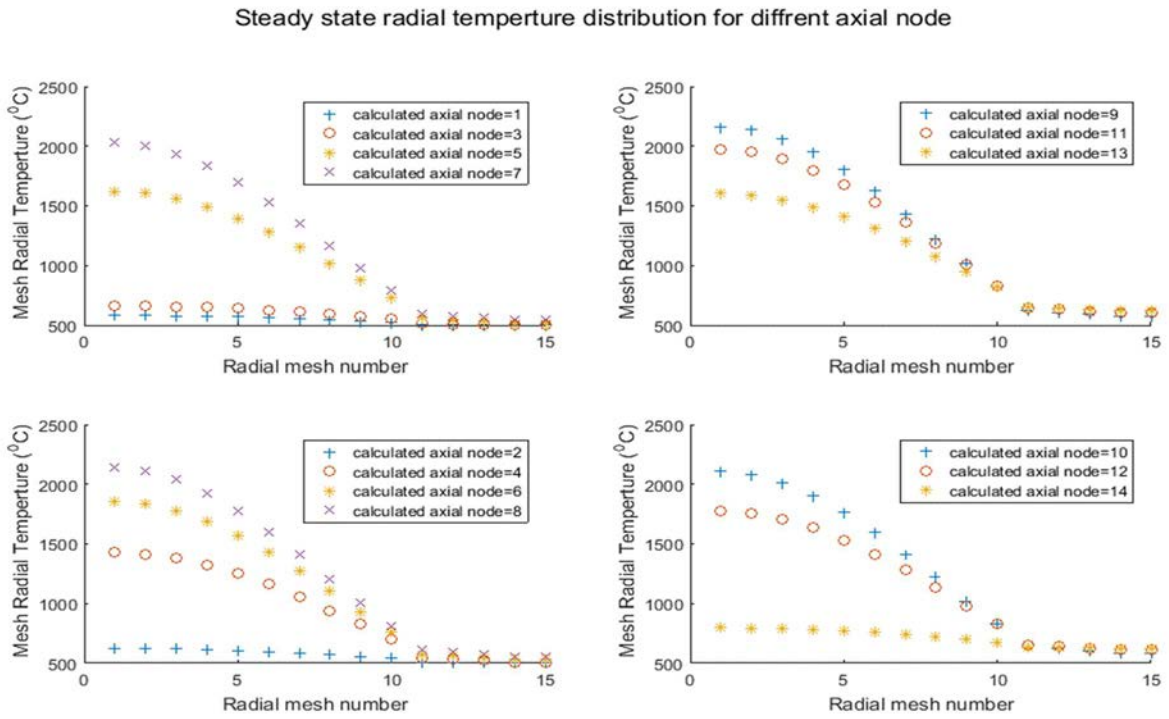

FIG. 4. Fuel temperature distribution along the radial node for different axial node at steady state.

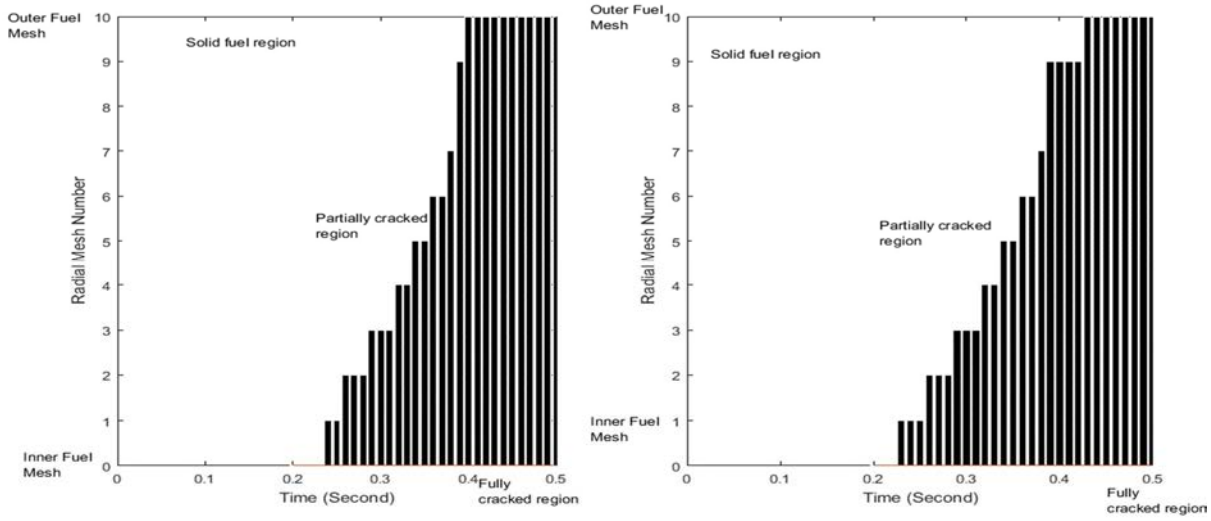

FIG. 5. Radially crack progression inside fuel pin for two different axial node.

The normalised power and temperature distribution across the fuel, clad and coolant can be estimated with the TRAN-SCORE code. With the inclusion of the new deformation module, analysis with TRAN-SCORE is more realistic in term of fuel mesh distribution which is very important to find out axial expansion feedback reactivity and fuel temperature distribution.

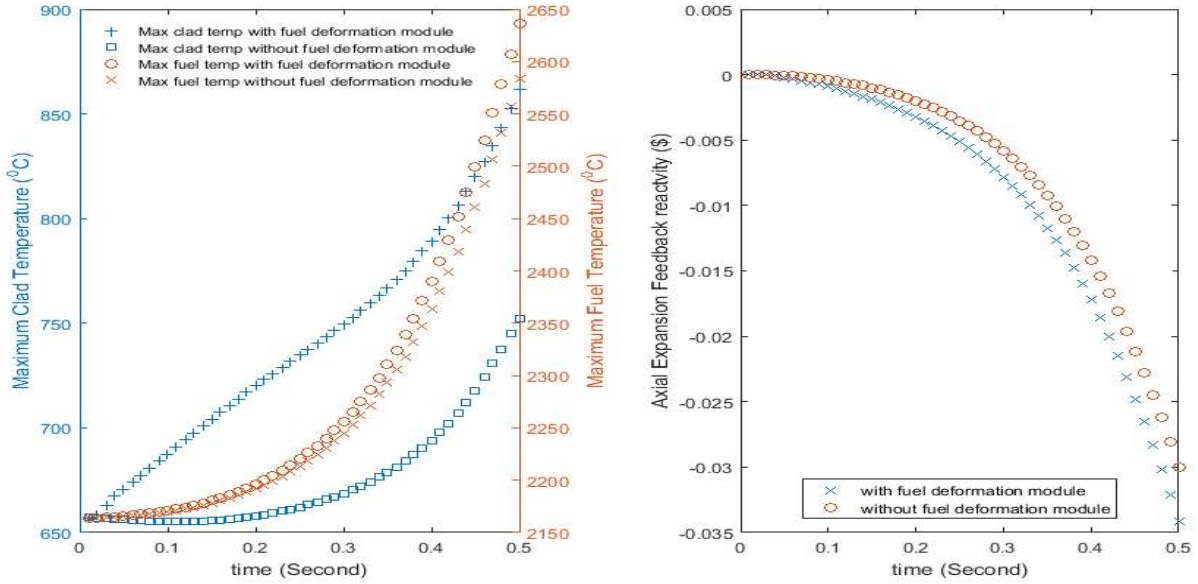

FIG. 6. Maximum Fuel, clad temperature, and axial expansion feedback reactivity progression with and without deformation module.

4. SUMMARY

A core dynamic code, TRAN-SCORE, has been developed for pre-disassembly analysis of CDA in sodium cooled fast reactors which has been augmented with a fuel deformation module. The realistic fuel deformation module, incorporated in the code solves stress and strain equations for solid and cracked fuel. Radial and axial meshes have been found for solid and cracked fuel regions using this module. This module can be used for solving stress and strain equations for solid and cracked fuel pins. The efficacy of the improved TRAN-SCORE code has been demonstrated through a sample test problem. Incorporation of more realistic modules, such as fuel swelling due to fission products, clad swelling, fission gas plenum pressure, molten fuel cavity pressure estimation, and modification in fuel cladding gap conductance, for a realistic solution is in progress.

ACKNOWLEDGMENT

We would like to express our sincere gratitude to Dr H. P. Gupta, Ex BARC, and Shri S. A. Bhardwaj, former chairman, AERB for their invaluable contributions to this work. Dr H. P. Gupta provided critical insights and understanding of the problem that helped shape the direction of our research and provided valuable feedback throughout the process. Shri S. A. Bhardwaj played a crucial role in the development of this work by assigning us the task that led to the development of the ideas presented in this paper.

REFERENCES

[1] Amandeep Singh and H. P. Gupta, Pre-disassembly phase analysis for Sodium cooled Fast breeder reactor, AERB/NSARG/TR/2019, Mumbai (2019).

[2] Amandeep Singh¸ Obaidurrahman K. and H. P. Gupta, Development of a Power and Flow Transient Model for Sodium Cooled Fast Reactor Core, Proceedings of Advances in Reactor Physics, Mumbai, 18–21 May 2022 (2022)

[3] Amandeep Singh¸ Obaidurrahman K. and H. P. Gupta, Development of a coolant dynamic model for Sodium Cooled Fast Reactor Core, Proceedings of Advances in Reactor Physics, Mumbai, 18 – 21 May 2022 (2022).

[4] J. C. Carter, G. J. Fischer, T. J. Heames, D. R. MacFarlane, N. A. McNeal, W. T. Sha, C. K. Santhanan and C. K. Youngdahl, SAS1A, A computer code for the analysis of Fast Reactor power and flow transients, Argonne National Laboratory (1970).

[5] K. J. Miles, Chapter 8: Deform 4: Steady State and Transient Pre-Failure Pin Behaviour, Nuclear Engineering Division, Argonne National Laboratory (2017).

Table 1: Radial, circumferential stress for fuel and clad with its cracked region for sample time Case

NORMALIZED POWER = 1.025 time = 0.01000 sec

			DEFORMATION PARAMETERS							
			********** FUEL **********				*** CLAD ***		CRACKED	
AXIAL FUEL NODE	AXIAL FUEL LOCATION	FREE RADIUS OF MELTED FUEL	RADIAL STRESSES STRESSES (DYNES/CM**2) INNER SOLID	OUTER SOLID	CIRCUMFERENTIAL (DYNES/CM**2) INNER SOLID	OUTER SOLID	RADIAL STRESSES (DYNES/CM**2) INNER CLAD	OUTER CLAD	REGION (MESH NUMBER) INNER	OUTER
1	5.045	0.000e+00	-3.127e+06	-3.000e+06	-2.865e+06	1.446e+07	-3.000e+06	-5.330e+06	0	0
2	15.136	0.000e+00	-3.262e+06	-3.000e+06	-2.731e+06	1.446e+07	-3.000e+06	-5.199e+06	0	0
3	25.232	0.000e+00	-3.384e+06	-3.000e+06	-2.611e+06	1.446e+07	-3.000e+06	-5.079e+06	0	0
4	35.366	0.000e+00	-5.867e+06	-3.000e+06	-4.206e+05	1.417e+07	-3.000e+06	-4.959e+06	0	0
5	45.544	0.000e+00	-6.348e+06	-3.000e+06	-2.477e+04	1.408e+07	-3.000e+06	-4.837e+06	0	0
6	55.740	0.000e+00	-7.154e+06	-3.000e+06	6.838e+05	1.398e+07	-3.000e+06	-4.716e+06	0	0
7	65.953	0.000e+00	-7.414e+06	-3.000e+06	8.734e+05	1.391e+07	-3.000e+06	-4.593e+06	0	0
8	76.179	0.000e+00	-7.719e+06	-3.000e+06	1.161e+06	1.389e+07	-3.000e+06	-4.471e+06	0	0
9	86.410	0.000e+00	-7.792e+06	-3.000e+06	1.233e+06	1.390e+07	-3.000e+06	-4.348e+06	0	0
10	96.641	0.000e+00	-7.370e+06	-3.000e+06	8.441e+05	1.393e+07	-3.000e+06	-4.226e+06	0	0
11	106.867	0.000e+00	-6.861e+06	-3.000e+06	4.081e+05	1.400e+07	-3.000e+06	-4.103e+06	0	0
12	117.081	0.000e+00	-6.304e+06	-3.000e+06	-5.610e+04	1.409e+07	-3.000e+06	-3.968e+06	0	0
13	127.281	0.000e+00	-5.575e+06	-3.000e+06	-7.045e+05	1.417e+07	-3.000e+06	-3.834e+06	0	0
14	137.438	0.000e+00	-3.486e+06	-3.000e+06	-2.528e+06	1.444e+07	-3.000e+06	-3.713e+06	0	0
15	147.556	0.000e+00	-3.374e+06	-3.000e+06	-2.634e+06	1.445e+07	-3.000e+06	-3.593e+06	0	0
16	157.670	0.000e+00	-3.234e+06	-3.000e+06	-2.769e+06	1.445e+07	-3.000e+06	-3.485e+06	0	0

NORMALIZED POWER = 3.657 time = 0.30000 sec

DEFORMATION PARAMETERS

AXIAL FUEL NODE	AXIAL FUEL LOCATION	FREE RADIUS OF MELTED FUEL	********** FUEL ********** RADIAL STRESSES STRESSES (DYNES/CM**2) INNER SOLID	OUTER SOLID	CIRCUMFERENTIAL (DYNES/CM**2) INNER SOLID	OUTER SOLID	*** CLAD *** RADIAL STRESSES (DYNES/CM**2) INNER CLAD	OUTER CLAD	CRACKED REGION (MESH NUMBER) INNER	OUTER
1	5.045	0.000e+00	-2.851e+07	-3.000e+06	3.709e+07	2.903e+07	-3.000e+06	-5.307e+06	0	0
2	15.136	0.000e+00	-3.570e+07	-3.000e+06	5.227e+07	3.702e+07	-3.000e+06	-5.178e+06	0	0
3	25.232	0.000e+00	-3.573e+07	-3.000e+06	5.925e+07	4.397e+07	-3.000e+06	-5.061e+06	0	0
4	35.366	0.000e+00	-1.543e+07	-3.000e+06	1.204e+08	1.254e+08	-3.000e+06	-4.942e+06	9	11
5	45.544	0.000e+00	4.291e+07	-3.000e+06	7.883e+07	1.422e+08	-3.000e+06	-4.821e+06	8	11
6	55.740	0.000e+00	1.003e+08	-3.000e+06	3.862e+07	1.593e+08	-3.000e+06	-4.699e+06	8	11
7	65.953	0.000e+00	1.523e+08	-3.000e+06	-8.048e+05	1.720e+08	-3.000e+06	-4.577e+06	8	11
8	76.179	0.000e+00	1.941e+08	-3.000e+06	-3.456e+07	1.800e+08	-3.000e+06	-4.454e+06	8	11
9	86.410	0.000e+00	2.183e+08	-3.000e+06	-5.593e+07	1.828e+08	-3.000e+06	-4.331e+06	8	11
10	96.641	0.000e+00	2.267e+08	-3.000e+06	-6.668e+07	1.805e+08	-3.000e+06	-4.209e+06	8	11
11	106.867	0.000e+00	2.181e+08	-3.000e+06	-6.545e+07	1.731e+08	-3.000e+06	-4.087e+06	8	11
12	117.081	0.000e+00	2.015e+08	-3.000e+06	-6.115e+07	1.608e+08	-3.000e+06	-3.953e+06	8	11
13	127.281	0.000e+00	1.848e+08	-3.000e+06	-5.681e+07	1.484e+08	-3.000e+06	-3.821e+06	9	11
14	137.438	0.000e+00	1.631e+08	-3.000e+06	-1.107e+08	7.289e+07	-3.000e+06	-3.702e+06	0	0
15	147.556	0.000e+00	1.454e+08	-3.000e+06	-1.021e+08	6.381e+07	-3.000e+06	-3.586e+06	0	0
16	157.670	0.000e+00	1.345e+08	-3.000e+06	-1.011e+08	5.382e+07	-3.000e+06	-3.482e+06	0	0

SESSION III

EXPANSION PHASE AND LONG TERM BEHAVIOUR FOR SODIUM COOLED FAST REACTORS

Chairpersons

A. RINEISKI
India

C. JOURNEAU
France

ANALYSIS OF THE REMAINING CORE MATERIAL COOLABILITY IN AN SFR CORE

J. SOGABE, K. KAMIYAMA, Y. OKANO, Y. TOBITA
Japan Atomic Energy Agency
Oarai-machi/Ibaraki, JAPAN

Abstract

The achievement of in-vessel retention (IVR) against severe accidents caused by an anticipated transient without scram is an effective and rational approach to enhance the safety characteristics of a sodium cooled fast reactor. After the termination of the transition phase, in which the molten core pool which consists of the mixture of molten fuel and molten steel would be formed and expand, the molten fuel in the core region would be solidified due to the heat transfer to the molten steel and surrounding structures, and the remaining core material, which consists of the solid fuel and the molten steel, would be formed: this is the initial state of the post-accident material relocation/post-accident heat removal (PAMR/PAHR) phase. To ensure that IVR is possible, it is necessary to confirm that the disrupted core materials could be stably cooled over a long period in the PAMR/PAHR phase, and the coolability of the remaining core material is one of the main evaluation items. The paper is concerned with the case without sodium flow from the lower region. In this case, the decay heat generated from the fuel is transferred to the surrounding structures through the molten steel, and the transferred heat is eventually transported to a heat sink. Thus, it is necessary to solve the heat balance between the decay heat generated from the fuel and the heat transport. Then, the effective thermal conductivity of the remaining core material, which is the main contributor to the heat transfer from the remaining core material to the surrounding structures, is one of the dominant physical quantities. In the paper, the effective thermal conductivity of the remaining core material is estimated based on the data of the ID3 test of the EAGLE experimental series, in which the mixture pool of nuclear-heated solid fuel and molten steel is formed.

1. INTRODUCTION

A sodium cooled fast reactor (SFR) uses liquid sodium as a coolant with high thermal conductivity and high natural circulation capability, which makes it stable against off normal operating conditions and core damage can be prevented in a design basis accident. Despite this, hypothetical core disruptive accidents (CDAs) beyond design basis accidents have been assumed and evaluated as accidents with a large energy release [1, 2], including an anticipated transient without scram (ATWS). One of the typical event sequences to lead to core damage is an unprotected loss of flow (ULOF).

A typical core damage sequence of ULOF is shown in Fig. 1. The entire sequence is divided into several phases: initiating, transition, and post-accident material relocation/post-accident heat removal (PAMR/PAHR). One of the objectives of the CDA evaluation of the SFR is to pursue the prospect of in-vessel retention (IVR), which is an effective and rational approach to enhance safety characteristics. The following two points should be confirmed for the achievement of IVR: 1) the absence of significant mechanical energy release, and 2) the stable removal of decay heat generated from relocated fuels. Assessment of the initiating and transition phases for a small scale SFR showed the absence of significant mechanical energy release [3, 4]. For a large scale SFR, the introduction of the so-called FAIDUS (Fuel Assembly with Inner-Duct Structure) as a design feature prevents re-criticality potential due to large scale fuel compaction by realizing fuel discharge before the formation of a large scale molten core pool [1]. The paper is to focus on the stable removal of decay heat generated from the relocated fuels, especially a remaining core material, in the PAMR/PAHR phase.

The event progression in the PAMR/PAHR phase is shown in Fig. 2. A typical and probable scenario in the transition phase is as follows. The core degrades gradually, a molten-core pool which consists of a mixture of molten fuel and molten steel would be formed and expand due to the failure of assembly (SA) walls, and then due to pressure increase in the core region, a part of the molten fuel would be discharged outside the disrupted core region, e.g. a control rod guide tube (CRGT) and/or the gaps of the assembly walls, resulting in the achievement of a

subcritical state and the termination of the transition phase. After that, the molten fuel in the core region would be solidified due to the heat transfer to the molten steel and surrounding structures, and the remaining core material which consists of the solid fuel and the molten steel would be formed, which is the initial state of the PAMR/PAHR phase. To ensure the possibility of IVR, it is necessary to confirm that the disrupted core materials could be stably cooled over a long period in the PAMR/PAHR phase, and the coolability of the remaining core material is one of the main evaluation items.

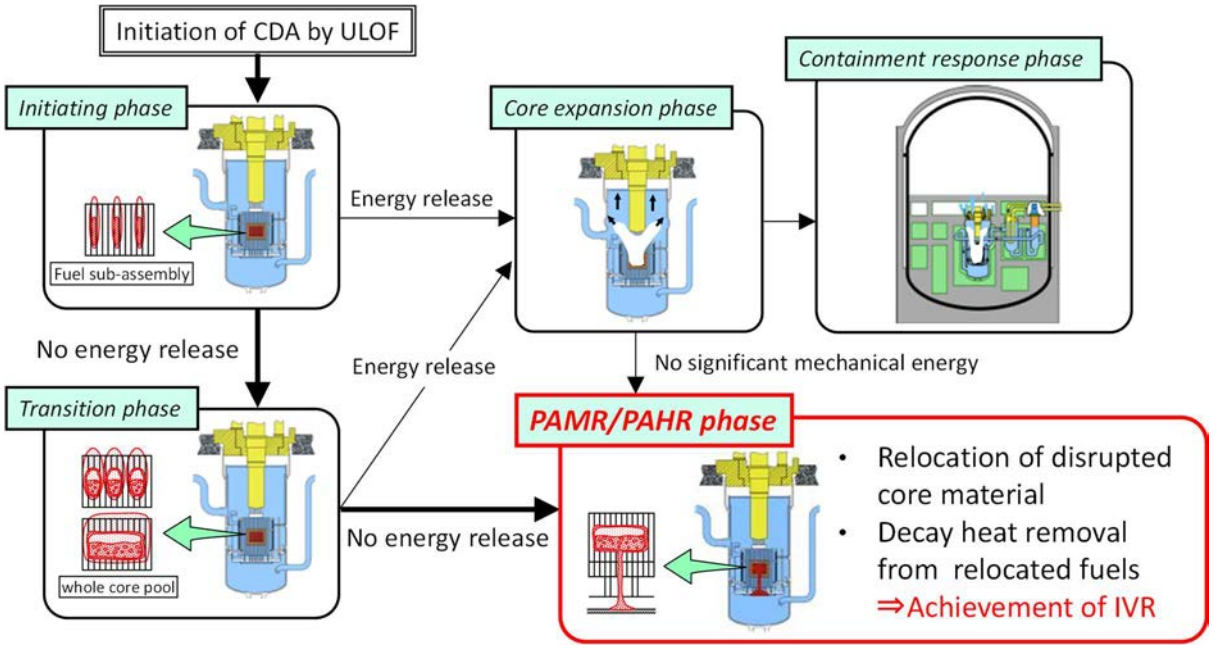

FIG. 1. Typical ULOF core damage sequences.

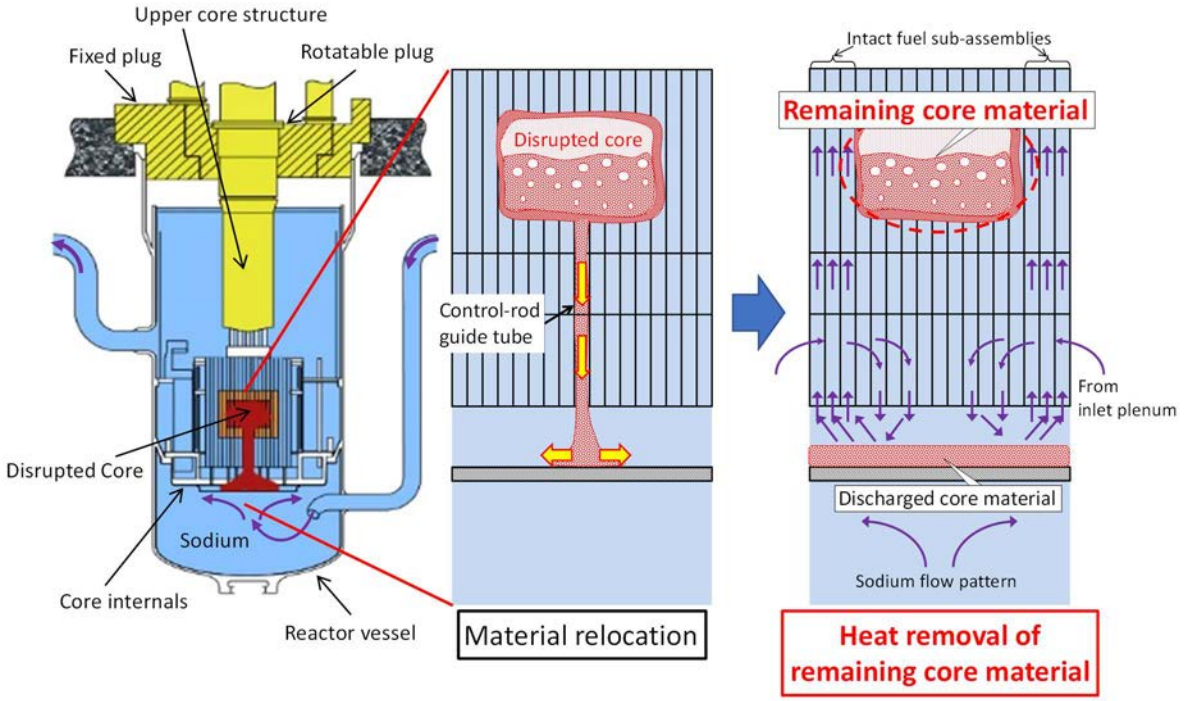

FIG. 2. Event progression in PAMR/PAHR phase.

The coolability of the remaining core material is assumed to occur in two cases based on the disrupted core state: with or without sodium flow into the remaining core material from the lower region. The paper is concerned with the case without sodium flow from the lower region. In this case, the mechanism of heat transfer from the remaining core material to the surrounding structures is shown in Fig. 3. The decay heat generated from the fuel is transferred to the surrounding structures through the molten steel, and the transferred heat is eventually transported to the heat sink by (1) the coolant inflowing from the upper region of the SAs, (2) the coolant flowing inside non-destructive neighbouring the SAs, and (3) the coolant flowing in inter-assembly gaps between the assembly walls. That is, it is necessary to solve the heat balance between the decay heat generated from the fuel and the heat transport. Then, the effective thermal conductivity of the remaining core material, which is the main contributor to the heat transfer from the remaining core material to the surrounding structures, is one of the dominant physical quantities.

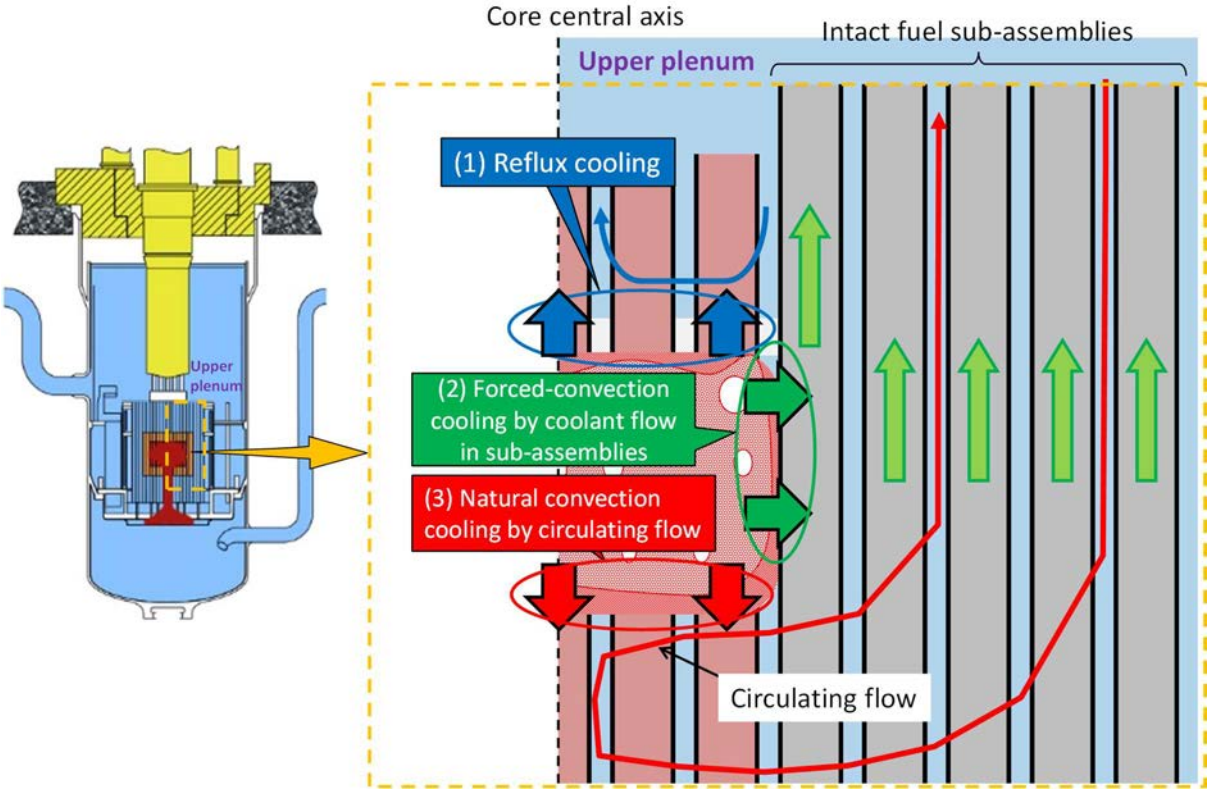

FIG. 3. Mechanism of heat transfer from remaining core material to surrounding structures.

The typical range of the uncertainty of the effective thermal conductivity of a mixture is from the harmonic mean to the arithmetic mean. In the previous study, for the lack of experimental knowledge, the coolability of the remaining core material was evaluated using conservative conditions for the subsequent event progression [5]. In the evaluation in the PAMR/PAHR phase, it was difficult to set the best estimate conditions, and the conservative evaluations considering the uncertainty had been commonly performed. To establish the best conditions for the effective thermal conductivity of the remaining core material, it is estimated based on the data of the ID3 test of the EAGLE experimental series [6], in which the mixture pool of nuclear-heated solid fuel and molten steel is formed.

2. TEST OVERVIEW

The ID3 test of the EAGLE experimental series [6] was selected to evaluate the effective thermal conductivity of a mixture which consists of solid fuel and molten steel. This test was selected because data on heat transfer from the disrupted core (solid fuel/molten steel mixture) to a duct simulating the CRGT was obtained.

The description of the ID3 test is shown in Fig. 4. The ID3 test is an in-pile test using the Impulse Graphite Reactor (IGR), which is an experimental facility at National Nuclear Center of the Republic of Kazakhstan. The fuel assembly, which simulates the core region, consists of approximately 6.0 kg of uranium dioxide (88 fuel pin bundles; 22 pin bundles arranged in a four-ring configuration) and approximately 6.6 kg of a steel block. In the test, the steel block was melted by fuel nuclear heating, generating the mixture of the solid fuel and the molten steel, which simulates the disrupted core materials in the initial state of the PAMR/PAHR phase. Then, data on heat transfer from the disrupted core materials to the duct was obtained by thermocouple responses installed in the experimental facility. A schematic of the core simulating vessel and the temperature transients measured by the thermocouples installed at the

mid-height position in the core are shown in Fig. 4. The duct failure would take place by thermal load from the disrupted core approximately 80 s after the test start. The effective thermal conductivity in the disrupted core region is estimated using the test data on the amount of heat transfer to the duct and the sodium, the temperature of the core region, and the temperature of the duct surface on the core region side, as discussed in Section 3.

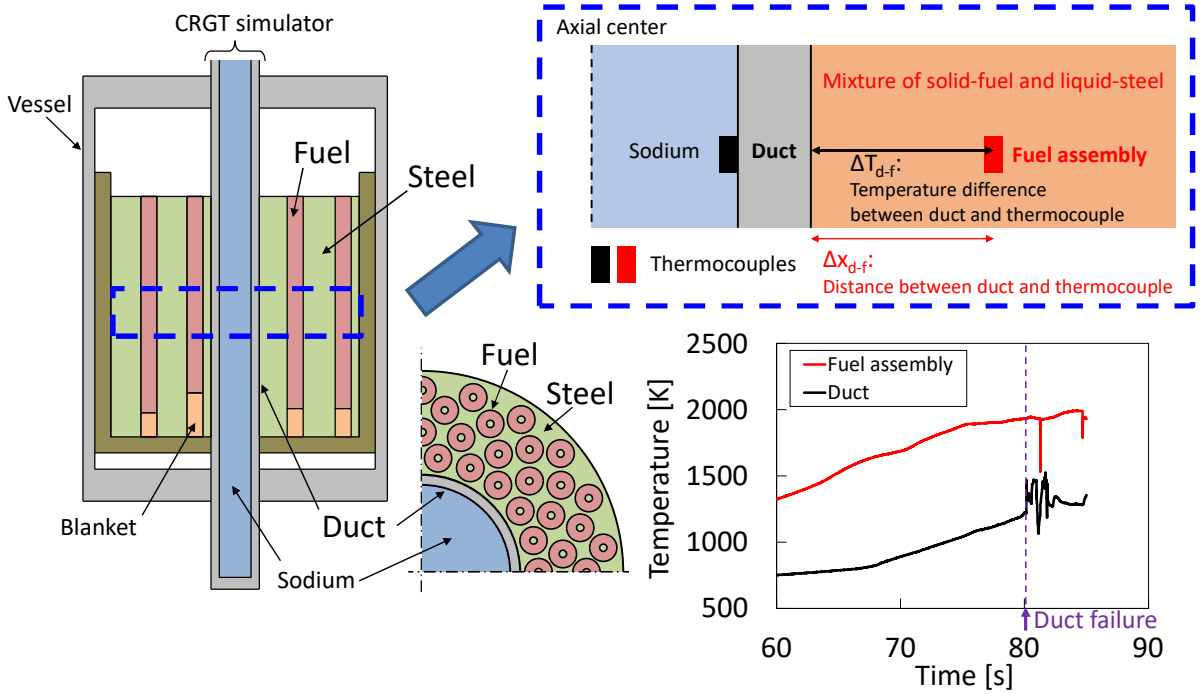

FIG. 4. Description of ID3 test of EAGLE experimental series.

3. ANALYSIS OF EXPERIMENTAL RESULTS

The effective thermal conductivity in the disrupted core region is estimated by the following three steps, as shown in Fig. 5.

(a) Calculate the average heat flux q to the duct using the amount of the heat transfer to the duct and the sodium per unit area, which is derived from the change of temperature measured by the thermocouple installed on the duct;
(b) Substitute q obtained in (a), Δx, and ΔT into the heat flux formula $q=\lambda\cdot\Delta T/\Delta x$ to estimate the effective thermal conductivity λ, where Δx and ΔT mean the distance between the duct and the fuel assembly and the temperature difference between the duct and the fuel assembly;
(c) Confirm that the thermal conductivity developed in (b) is valid by a thermal conductivity calculation in a one-dimensional cylindrical coordinate system.

Calculate the average heat flux to the duct:

The following equation is used to calculate the heat flux q from the disrupted core material to the duct using the test data, as in Ref. [6]:

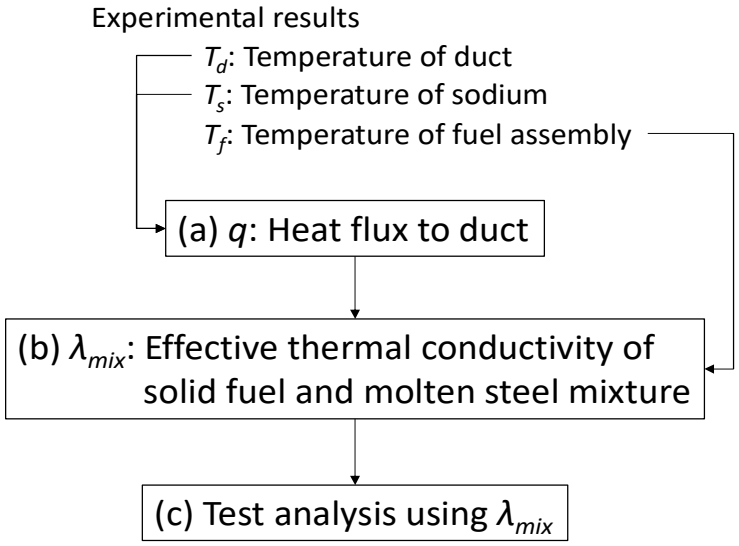

FIG. 5. Process for estimation of effective thermal conductivity.

$$q = \frac{1}{\Delta t_{HT}} \cdot \frac{\rho_d \left[\left(D_d + 2\delta_d \right)^2 - {D_d}^2 \right] \Delta i_d + \rho_s {D_d}^2 \Delta i_s}{4\left(D_d + 2\delta_d \right)} \tag{1}$$

where Δt_{HT} is the heating time, ρ is the density, D_d is the duct inner diameter (35 mm), δ_d is the duct thickness (5 mm), and Δi is the change of internal energy. The subscript d stands for duct and s for sodium. The internal energies at each temperature are calculated by using the equation of state adopted in the SIMMER code [7]. The time range to be considered is from approximately 67 s when the rate of temperature increases in the duct and sodium is constant, to approximately 80 s when just before the duct fails.

On the other hand, from the heat flux formula in the duct:

$$T_d^{\,t} = T_d^{\,m} + \frac{\delta_d}{2\lambda_d} q \tag{2}$$

where the superscript t is the radial centre of the duct and m is the sodium side surface of the duct. $T_d^{\,m}$ is the temperature measured by the thermocouple. Equations (1) and (2) are repeated to obtain a heat flux of approximately 1.1 MW/m^2.

Estimate the effective thermal conductivity of the mixture:

The effective thermal conductivity λ_{mix} of the solid fuel and molten steel mixture is estimated by substituting q obtained at (a) into the following equation.

$$q = \lambda_{mix} \frac{\Delta T_{d-f}}{\Delta x_{d-f}} \tag{3}$$

where $\Delta T_{d\text{-}f}$ is the temperature difference between the duct and the thermocouple installed at the fuel assembly, and $\Delta x_{d\text{-}f}$ is the distance between the duct and the thermocouple installed at the fuel assembly. The effective thermal conductivity is estimated at 87 W/(m·K).

Confirm the developed thermal conductivity model:

The thermal conductivity calculation in the one-dimensional cylindrical coordinate system was performed to confirm whether the temperature response of the ID3 test can be reproduced under the condition of the developed effective thermal conductivity of 87 W/(m·K) for the mixture of solid fuel and molten steel. The calculation geometry is shown in the upper right corner of Fig. 4, with 1 mesh for the sodium in the CRGT simulator, 5 meshes for the duct, and 20 meshes for the solid fuel and molten steel mixture (5 meshes per one ring of the fuel assembly). The calculation starts at about 72 s when the measured fuel assembly temperature is above the steel liquidus temperature of 1753 K. The calculation ends at about 80 s when just before the duct fails (the same as the endpoint in the effective thermal conductivity estimation). The initial temperatures of the sodium, the duct, and the solid fuel and molten steel mixture elements are set based on the thermocouple measurements at about 72 s, respectively. The comparison of the temperature changes of the fuel assembly and the duct by the experiment and the calculation with the developed thermal conductivity model is shown in Fig. 6. The thermal conductivity calculation results as shown by the dashed line, in which the effective thermal conductivity was set to 87 W/(m·K), are confirmed to be in general agreement with the test results shown by the solid line. Therefore, 87 W/(m·K) is obtained as the effective thermal conductivity of the mixture of solid fuel and molten steel.

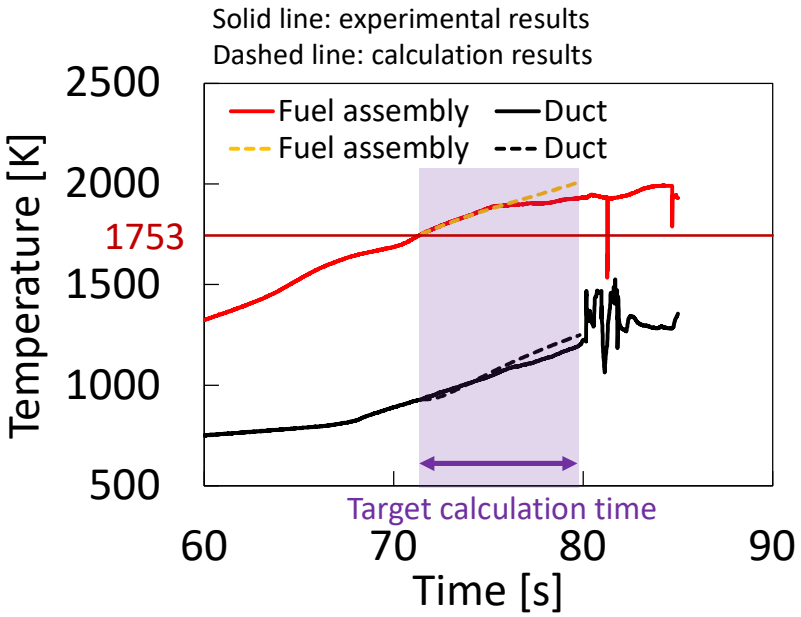

FIG. 6. Comparison of temperature changes of fuel assembly and duct by experiment and calculation with developed thermal conductivity model.

4. DISCUSSION

Using the developed thermal conductivity model in Section 3, quantitative evaluations were performed for the impact on the range of phenomena in an actual reactor. For the calculation for the ID3 test shown in Fig. 6, sensitivity calculations were performed with the following parameters used as the effective thermal conductivities of the mixture of solid fuel and molten steel.

- **Case 1:** λmix = 87 W/(m·K), which is the same calculation shown in Fig. 6.

- **Case 2:** λmix = 17 W/(m·K), which is equivalent to the thermal conductivity of molten steel [8, 9] (value at 1850 K, the average of the temperature range of the mixture in the ID3 test).
- **Case 3:** λmix = 2.2 W/(m·K), which is equivalent to the thermal conductivity of solid MOX fuel [8, 9] (value at 1850 K).

The effective thermal conductivities of the mixture calculated by the arithmetic mean and the harmonic mean are 8.1 W/(m·K) and 3.4 W/(m·K), respectively, under the fuel-to-steel volume ratio of 6:4, which is equivalent to that of the actual reactor. The uncertainty range from Case 2 to Case 3 is set to account for larger than the typical uncertainty ranges from the harmonic mean to the arithmetic mean.

The comparison of the temperature changes of the fuel assembly and the duct by the calculations with developed thermal conductivity (Case 1) and liquid steel thermal conductivity (Case 2) is shown in Fig. 7. The temperatures of the fuel assembly and the duct at the end of the calculations are shown in Table 1. Because the heat transfer from the fuel assembly to the duct is more enhanced in Case 1 than in Case 2, at the end of the calculations, the fuel assembly temperature in Case 1 is about 50 K lower than that in Case 2 (Case 1: about 2010 K, Case 2: about 2060 K) and the duct temperature on the fuel assembly side in Case 1 is about 90 K higher than that in Case 2 (Case 1: about 1370K, Case 2: about 1280K).

The comparison of the temperature changes of the fuel assembly and the duct by calculations with developed thermal conductivity (Case 1), liquid steel thermal conductivity (Case 2), and solid fuel thermal conductivity (Case 3) is shown in Fig. 8, in which is added the results of Case 3 to Fig. 7. Table 1 also includes the results of Case 3. Comparing temperatures at the end of the calculations in Case 2 and Case 3, the fuel assembly temperature is almost the same (Case 3: about 2060 K) and the duct temperature on the fuel assembly side in Case 2 is about 30 K higher than that in Case 3 (Case 3: about 1250 K). Therefore, the impact on the subsequent event progression of Case 1 which is based on the developed thermal conductivity model described in this paper is greater than that of Case 2 and Case 3, which are examples of the effective thermal conductivity of the mixture estimated by conventional ways.

The effective thermal conductivity of 87 W/(m·K) is about five times greater than the thermal conductivity of molten steel, which is about 17 W/(m·K). One possible physical reason for this is the convection of molten steel in the solid fuel at low velocity. A further physical reason for this, and the impact on the subsequent event progression due to the several-fold increase in heat transfer from the disrupted core material to the surrounding structures, should be considered.

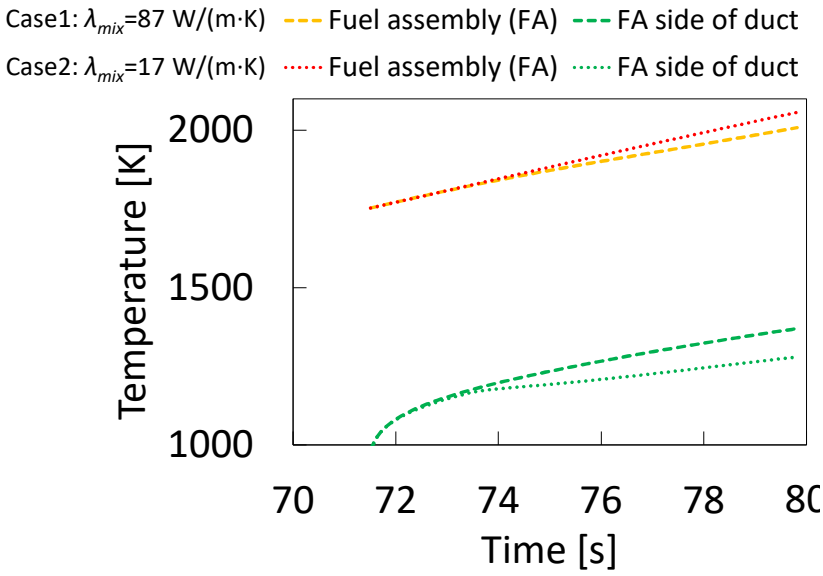

FIG. 7. Comparison of temperature changes of fuel assembly and duct by calculations with developed thermal conductivity and liquid steel thermal conductivity.

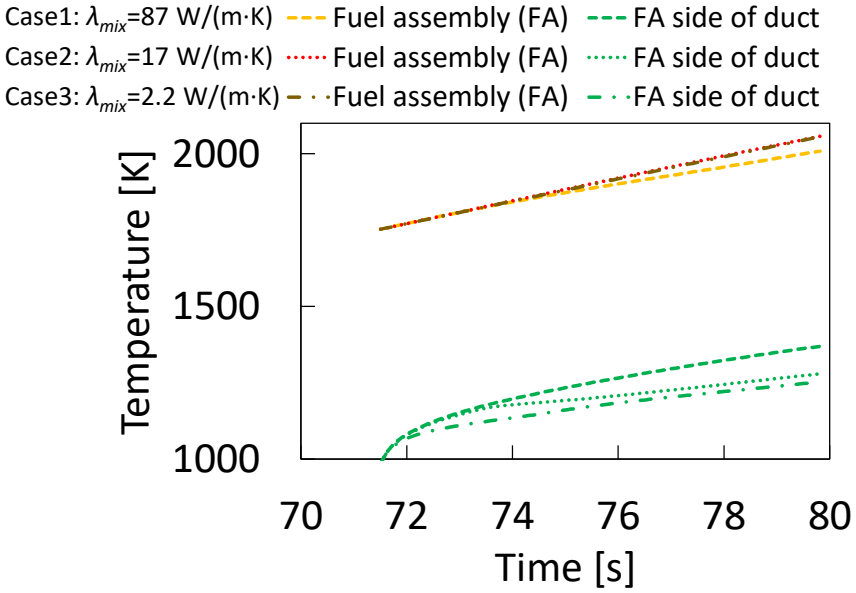

FIG. 8. Comparison of temperature changes of fuel assembly and duct by calculations with developed thermal conductivity, liquid steel thermal conductivity, and solid fuel thermal conductivity.

TABLE 1. COMPARISON OF TEMPERATURES OF FUEL ASSEMBLY AND DUCT BY CALCULATIONS WITH THERMAL CONDUCTIVITIES

	Thermal conductivity λ_{mix}	Temperature of fuel assembly (FA)	Temperature of FA side of duct
Case 1	87 W/(m·K)	2010 K	1370 K
Case 2	17 W/(m·K)	2060 K	1280 K
Case 3	2.2 W/(m·K)	2060 K	1250 K

5. CONCLUSION

The effective thermal conductivity of the mixture of solid fuel and molten steel, one of the dominant physical quantities which is the main contributor to the heat transfer from the remaining core material to the surrounding structures, was estimated at 87 W(m·K) based on the data of the ID3 test of the EAGLE experimental series, in which the mixture pool of nuclear-heated solid fuel and molten steel is formed. The results of the sensitivity calculations using the effective thermal conductivity of the mixture as a parameter showed that the impact of the thermal conductivity developed in this paper was greater than that of the uncertainty of the effective thermal conductivity of the mixture developed by conventional ways. The effective thermal conductivity of 87 W/(m·K) is about five times greater than the thermal conductivity of molten steel. In the future, it is necessary to consider the physical meaning of this value and the impact of the several-fold increase in heat transfer from the disrupted core material to the surrounding structures on the subsequent event progression.

REFERENCES

[1] SUZUKI, T., KAMIYAMA, K., YAMANO, H., KUBO, S., TOBITA, Y., NAKAI, R., KOYAMA, K., A scenario of core disruptive accident for Japan sodium-cooled fast reactor to achieve in-vessel retention, Journal of Nuclear Science and Technology, 51 4, 493–513 (2014).

[2] SUZUKI, T., TOBITA, Y., NAKAI, R., Evaluation of recriticality behavior in the material-relocation phase for Japan sodium-cooled fast reactor, Journal of Nuclear Science and Technology, 52 11, 1448–1459 (2015).

[3] SUZUKI, T., TOBITA, Y., KAWADA, K., TAGAMI, H., SOGABE, J., MATSUBA, K., ITO, K., OHSHIMA, H., A Preliminary Evaluation of Unprotected Loss-of-Flow Accident for a Prototype Fast-Breeder Reactor, Journal of Nuclear Engineering and Technology, 47 3, 240–252 (2015).

[4] SUZUKI, T., SOGABE, J., TOBITA, Y., SAKAI, K., NAKAI, R., "Study on In-Vessel Retention (IVR) of unprotected accident for fast reactor, 1; Overview of IVR evaluation in Anticipated Transient without Scram (ATWS)", Transactions of the JSME (in Japanese), 83 848, 16-00395 (2017).

[5] SOGABE, J., SUZUKI, T., WADA, Y., TOBITA, Y., "Study on In-Vessel Retention (IVR) of unprotected accident for fast reactor, 2; Assessment of PAMR/PAHR phase in ULOF", Transactions of the JSME (in Japanese), 83 848, 16-00393 (2017).

[6] KAMIYAMA, K., KONISHI, K., SATO, I., TOYOOKA, J., MATSUBA, K., SUZUKI, T., TOBITA, Y., PAKHNITS, A. V., VITYUK, V. A., VURIM, D. A., GAIDAICHUK, V. A., KOLODESHNIKOV, A. A., VASSILIEV, Y. S., "An Experimental Study on Heat Transfer from a Mixture of Solid-Fuel and Liquid-Steel during Core Disruptive Accidents in Sodium-Cooled Fast Reactors", Proc. NUTHOS-10 (the 10th International Topical Meeting on Nuclear Thermal Hydraulics, Operation and Safety), NUTHOS10-1050, Okinawa, Japan (2017).

[7] MORITA, K., FISCHER, E.A., Thermodynamic properties and equations of state for fast reactor safety analysis Part I: Analytic equation of state model, Nuclear Engineering and Design 183 3, 177–191 (1998).

[8] MORITA, K., FISCHER, E.A., THURNAY, K., Thermodynamic properties and equations of state for fast reactor safety analysis Part II: Properties of fast reactor materials, Nuclear Engineering and Design 183 3, 193–211 (1998).

[9] MORITA, K., TOBITA, Y., KONDO, Sa., FISCHER, E. A., THURNAY, K., SIMMER-III Analytic Thermophysical Property Model, JNC Report, JNC TN9400 2000-004 (1999).

ANALYSIS METHODOLOGIES FOR THE EVALUATION OF ATWS ACCIDENT ON SFR IN JAEA – MECHANICAL CONSEQUENCES DURING EXPANSION PHASE OF THE ACCIDENT

Y. ONODA
Japan Atomic Energy Agency
Oarai/Ibaraki, Japan

Y. TOBITA, Y. OKANO
Japan Atomic Energy Agency
Oarai/Ibaraki, Japan

Abstract

The paper describes the analysis methodologies for the evaluation of an unprotected loss of flow accident in a sodium cooled fast reactor of the Japan Atomic Energy Agency (JAEA), focusing on the mechanical consequences that would arise during the expansion phase of the accident. The analyses of the expansion phase examine two major consequences of the energetics: mechanical loads on the primary boundary including the reactor vessel (RV); and sodium and radioactive material ejection onto the top shield through the gaps between shield plugs, which causes sodium combustion and damages the containment vessel. Analytical evaluation of the process of such energetics is important for checking the capability of the containment vessel against the source term release under a severe accident condition of a fast reactor. JAEA developed the analysis methodologies for the evaluation of energetics and divided the analysis process into three: 1) using the SIMMER code, analysis of heat conversion into the mechanical energy during core melt due to re-criticality, 2) using the AUTODYN code, analysis of the structural response of the RV, and 3) using the PLUG code, analysis of the amount of sodium ejected onto the top shield through the gaps between shield plugs. The pressure–volume relationship of a CDA bubble, which is a mixture of gases (fuel vapour, steel vapour, and fission gas) and molten core materials, obtained by SIMMER calculation is used as the input to structural response analysis that uses AUTODYN. The history of pressure exerted on the lower surface of the top shield obtained by SIMMER calculations is used as the input to PLUG. These analysis codes are validated by simulating the dominant phenomena that significantly affect the results of each calculation. These analysis methodologies developed by JAEA were applied to reactor case analyses, which confirmed their applicability.

1. INTRODUCTION

Severe accidents in a sodium cooled fast reactor (SFR) can be divided into two: anticipated transient without scram (ATWS), and loss of heat removal systems (LOHRS). ATWS, which are unprotected accidents, are characterized by a short period of time from accident initiation to core damage, whereas LOHRS, protected accidents, provides operators with a sufficient period of time to implement core damage preventive measures. Core disruption involving mechanical energy release is of particular concern in ATWS, and unprotected loss of flow (ULOF) is the representative accident among ATWS for SFRs regarding its contribution to core damage frequency [1].

Figure 1 shows the typical event progression of ULOF by connecting the accident phases commonly used in safety evaluations. The first accident phase is the initiating phase, from normal reactor operation to core damage. The path from the initiating phase is divided into two: an energetic sequence leading to the expansion phase, and a non-energetic sequence leading to the transition phase. If re-criticality occurs, the transition phase also may lead to the expansion phase. In the analysis of the energetic sequence, structural integrity is evaluated using the value of mechanical energy obtained by the expansion phase analysis. After the transition phase and expansion phase, post-accident material relocation and heat removal are of concern. To bring the effects of the accident under control, both decay heat removal and to withstand the mechanical impact of the generated mechanical energy are crucial. Although the non-energetic accident sequence is dominant using most probable parameter settings in the analyses, the consequence of an energetic accident have been conservatively evaluated in Japan in order to understand how much the plant can tolerate energetics.

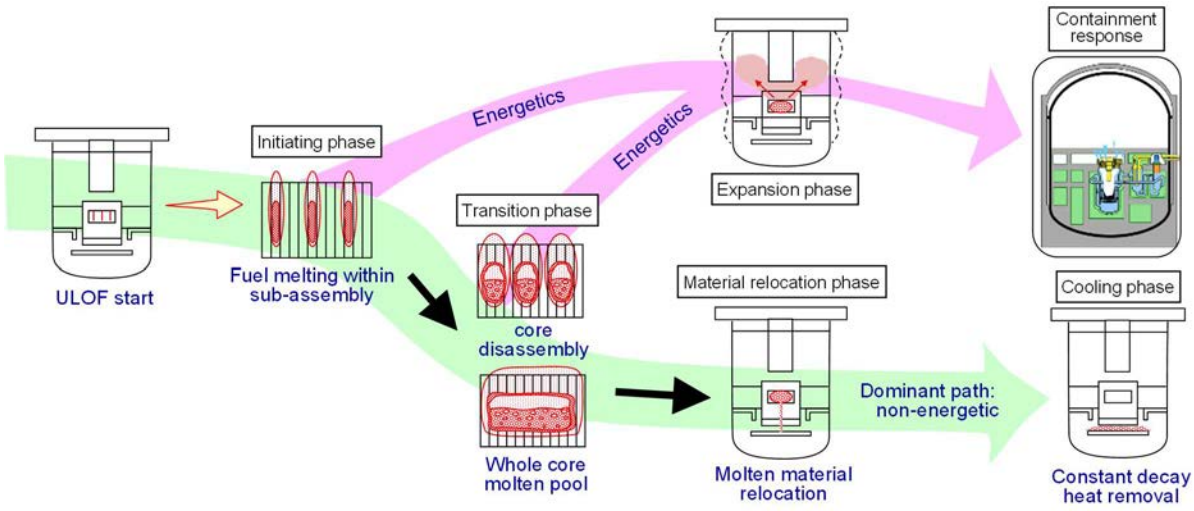

FIG. 1. Typical event progression of a ULOF core damage accident in an SFR.

Typical phenomena in the expansion phase are presented in Fig. 2. Fuel vapour and steel vapour are generated due to heat generated in the transition phase. Then a CDA bubble, which is a mixture of gases, fuel vapour and steel vapour, fission gas, and molten core materials, expands into the upper plenum via the upper core structure. After that, sodium vapour is generated due to fuel–coolant interaction (FCI) in the upper plenum. If the mechanical energy released by the FCI is significant, a sodium slug impacts the lower surface of the top shield. One of the consequences of energetics is that the reactor vessel (RV) will be mechanically loaded and deformed. The other is that sodium and radioactive material are ejected onto the top shield through the gaps between the shield plugs, causing sodium combustion and damaging the containment vessel. These events may lead to a large scale source term release.

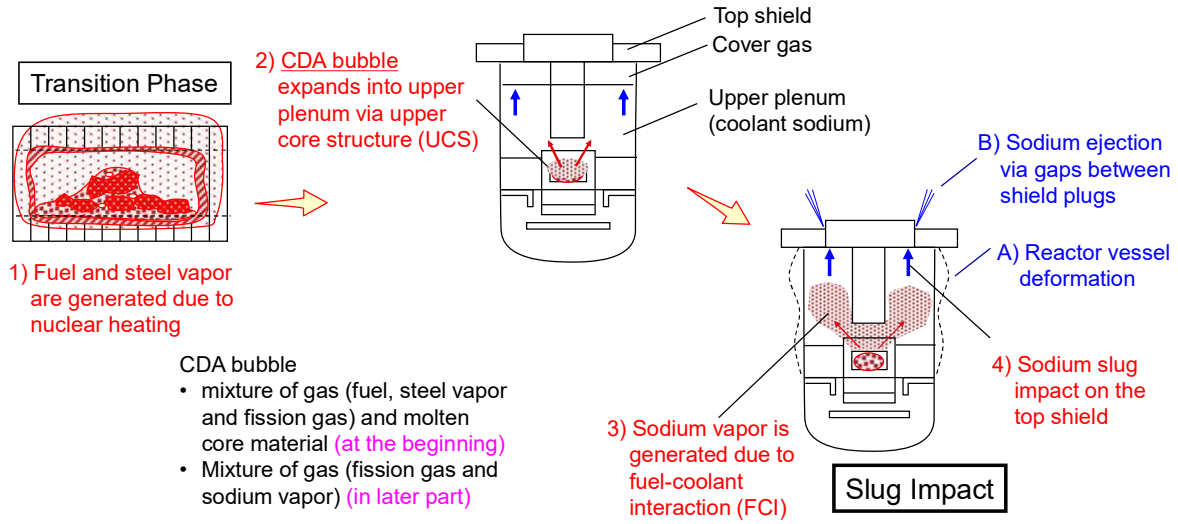

FIG. 2. Typical phenomena in the expansion phase.

Development of methods for safety evaluation of the expansion phase and experiments supporting it have been carried out in many parts of the world since the early stage of fast reactor development. In Japan, evaluation methods have been developed and maintained through safety evaluations against severe accidents for the experimental fast reactor Joyo, the prototype fast reactor Monju, and a demonstration fast breeder reactor, and this is still ongoing.

2. ANALYSIS METHODOLOGIES

2.1 Process of the analysis on mechanical consequence

JAEA developed the analysis methodologies for the evaluation of the energetics and divided the analysis process into three: 1) using the SIMMER code, analysis of heat conversion into the mechanical energy during core melts due to re-criticality [2], 2) using the AUTODYN code, analysis of the structural response of the RV, and 3) using the PLUG code, analysis of the amount of sodium ejected onto the top shield through the gaps between shield plugs (Fig. 3).

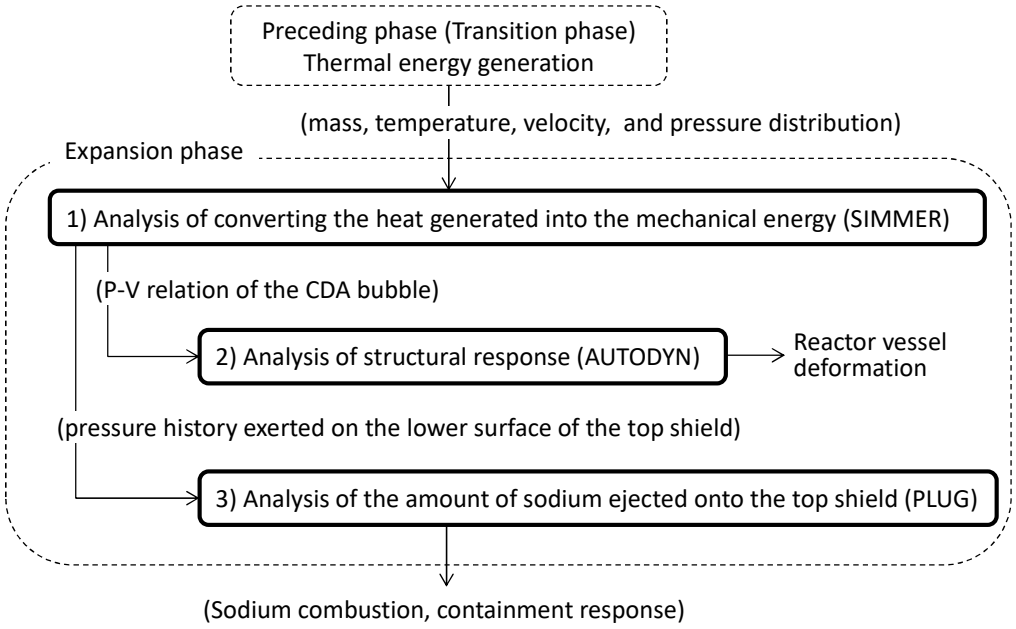

FIG. 3. Process of the analysis on mechanical consequence.

First, analysis of heat conversion into mechanical energy is performed with SIMMER, which is a code capable of coupling nuclear reactions and thermohydraulics including FCI. In this analysis, the thermal energy produced by nuclear reaction is converted to mechanical energy, which is represented by a pressure–volume relation (P–V relation) of the CDA bubble, through the calculation of FCI. The input of the first analysis is the mass, temperature, velocity, and pressure distribution in the core, which were calculated in the preceding phase (transition phase) with SIMMER. Transition phase analysis and mechanical energy analysis are intentionally divided, although analyses for both phases are conducted using SIMMER, because the calculation cost accumulates much more in transition phase analysis which uses neutronic modelling. In the mechanical energy calculation in the expansion phase, neutronic modelling is no longer necessary because the FCI is the most important phenomenon in this phase and neutronic reaction no longer occurs due to fuel dispersion into the upper sodium pool.

Next, structural response analysis of the RV is performed using AUTODYN, a commercial code that enables analysis of the interaction between fluid flow and structural deformation. The P–V relation obtained by the SIMMER calculation is used as the input to structural response analysis.

Finally, analysis of the amount of sodium ejected is performed using PLUG, which calculates the dynamic response of the shield plugs and the amount of sodium ejected onto the top shield. The pressure history under the shield plugs is obtained by the SIMMER calculation and is used as the input to the PLUG calculation.

These methodologies have developed through the licensing application of the Japanese experimental reactor Joyo and the Japanese prototype reactor Monju. In their licensing, safety analyses against hypothetical severe accident were required in the past, even it was before the accident at Fukushima Daiichi nuclear power plant. In the licensing, structural integrity of the primary boundary and tolerability of the containment vessel against sodium combustion due to sodium ejection onto the operating floor were evaluated.

2.2 SIMMER

SIMMER [3] has been developed by JAEA to evaluate the energy generated by a severe reactivity insertion accident in SFRs. This code can calculate material relocation during the accident together with the reactivity change due to the material relocation. The SIMMER code consists of major three models: a fluid dynamics model, a structure model, and a neutronics model.

In the fluid dynamics model, momentum and energy conservation equations use six velocity fields at a maximum. SIMMER models the five basic SFR core materials: fuel, steel, sodium, control materials and fission gas. The materials can exist as different physical states: For example, fuel needs to be represented by fabricated pin fuel, molten liquid fuel, a crust refrozen on the structure, solid particles, and fuel vapour. Thus, the material mass distributions are modelled by 38 density components in the current version of SIMMER. The mobile components, which include liquids, solid particles, and vapours, are applied to one of six velocity fields so that the relative motions of different fluid components can be simulated.

The structure model represents the configuration, and time-dependent degradation of the fuel pins and assembly can walls. The can walls at a cell boundary prevent radial fluid convection and provide a surface on which fuel can freeze or vapour can condense. The break-up of structure components depends on thermal conditions and temperature and the wall thickness threshold for mechanical break-up.

The space-time-dependent neutron kinetics model in SIMMER is based on an improved quasi-static method with a diffusion acceleration technique where the flux shape is calculated by a standard Sn neutron transport theory based on THREEDANT [4]. Since the changes in material number densities and temperatures are crucial, a cross-section model is included in the code to perform self-shielding operations. By doing so, effective macroscopic cross-sections can be determined whenever the reactivity is updated.

2.3 AUTODYN

AUTODYN [5] is a commercially available code for structural response analysis of nonlinear problems such as explosion/impact problems. This code simultaneously handles a Eulerian-type computational grid suitable for fluid (gas and liquid) flow analysis and a grid using Lagrange-type and shell-type elements suitable for deformation analysis of structures and can deal with interactions between these computational grids. This enables FCI analysis. The strain and displacement of the structure can be obtained based on the geometry and material properties of the structure, and the properties of the pressure source acting on it.

2.4 PLUG

PLUG, also developed by JAEA, models the dynamic movement of shield plugs and their connecting bolts, and evaluates the amount of sodium ejected onto the top shield through the gaps between the shield plugs. The code models shield plugs as point mass and their connecting

bolts as elastoplastic elements and calculates their dynamic responses including the collisions between shield plugs in a one dimensional coordinate. The amount of sodium ejected from the gaps caused by the relative displacement between the plugs is calculated based on the modified Bernoulli's equation using the pressure difference above and below the shield plugs. The major inputs are the geometry and weight of the plugs, the geometry and material properties of the bolts, and the history of pressure acting on the lower surface of the plugs. Vertical flow paths are modelled as concentric rings, horizontal flow paths are modelled as a path with a rectangular cross-section, and pressure loss in the flow paths and bends are considered. Based on these, the dynamic response of the plugs and bolts and the sodium ejection rate are calculated.

3. VALIDATION OF THE METHODOLOGIES

3.1 SIMMER

SIMMER has already been validated in several papers. The FCI behaviour and the resultant pressure development are of concern when hot molten core materials are released into the coolant plenum in the expansion phase. The expansion phase analysis from this point of view has been validated by Kondo [6], Morita [7], and Yamano [8].

3.2 AUTODYN

AUTODYN, a highly versatile calculation code, is widely applied to shock response analysis and explosion analysis. Its validity and high reliability have been proven by many past records in the industrial world and research institutes. AUTODYN has been used for the integrity evaluations of a pressurized water reactor (PWR) containment vessel against a hydrogen explosion [9], of the concrete structure of a PWR reactor cavity against a steam explosion [10], and of the RV of a fast demonstration reactor under a severe accident [11].

To confirm the applicability and validity of AUTODYN, experimental analysis of the FV102 test [12] was conducted using a 1/30 scale test vessel of US Clinch River Breeder Reactor. The FV102 test has been adopted as an international benchmark for structural response analysis codes [13] and is widely analysed in Europe and the United States. In the analysis of the FV102 test by AUTODYN, the test rig was modelled in a two-dimensional cylindrical coordinate system, and the expansion behaviour of the pressure source was given by the GASBAG model [14]. The results show that the impulse acting on the cylindrical vessel and residual strain are accurately reproduced, and that AUTODYN is applicable to the structural response analysis of the RV under mechanical loads.

3.3 PLUG

Seven sample calculations were conducted to validate PLUG, which is used to analyse plug response and sodium ejection. In this analysis, a simplified system was used to confirm its basic functions.

- Dynamic response analysis of bolts and plugs
    - **Case-1:** Bolt elasticity analysis
    - **Case-2:** Bolt elastoplastic analysis
- The analysis of the amount of sodium ejection

- **Case-3:** Sodium flowing through the vertical flow path
- **Case-4:** Sodium flowing through the horizontal flow path
- **Case-5:** Sodium flowing through the inlet and bend

- Plug collision analysis
  - **Case-6:** Collision analysis between mutually independent plugs
  - **Case-7:** Collision analysis of the integrated plugs

For Cases 1–5, the dynamic responses of the plugs fixed by the bolts were analysed by applying increasing pressure. For Cases 6 and 7, the dynamic responses of the plugs and the behaviour of their collision were analysed by giving an initial constant velocity. The theoretical solution and the calculation results for all the calculation cases are in good agreement, validating the code.

4. REACTOR APPLICATION

In this section, SIMMER and PLUG simulations are presented for a 500 MW(e) reactor, and an AUTODYN calculation is presented for a 280 MW(e) reactor.

4.1 Conversion from thermal energy to mechanical energy

Figure 4 shows a sample result of the SIMMER code calculation for heat conversion into mechanical energy [14]. The version of the SIMMER code used in this calculation is SIMMER-IV Ver.2.G (CSF19) (AFF09). The target reactor is a 500 MW(e) pool-type SFR and is modelled in a x-y-z three-dimensional mesh from the bottom of active fuel to the lower surface of the top shield in a vertical direction. Components such as radial blanket assemblies, radial shied assemblies, control plug (all in green in Fig. 4) were treated as rigid structures and excluded from thermohydraulic calculation. The boundary of the calculation geometry as well as the inner vessel were also treated as rigid structures. Initial fuel temperature and pressure distribution in the core region were given as input values, the averages of which are 3530 K and 2.5 MPa, and the process of thermal energy conversion into mechanical energy was calculated. This initial condition was given as the benchmark condition in a Coordinated Research Project [14] assuming a conservative condition that the middle one-third of the core slumps and occupies the bottom one-third, and the top one-third slumps and occupies the middle one-third. However, in this calculation, fuel and steel are homogeneously distributed in the original core region, because the volume fraction of the fuel and steel in the bottom one-third of the core exceeds unity if the material motion mentioned above is adopted. The steel temperature is assumed to be 3000 K as a parameter. This varies based on the power transient before the expansion phase. The longer the power transient, the higher the steel temperature.

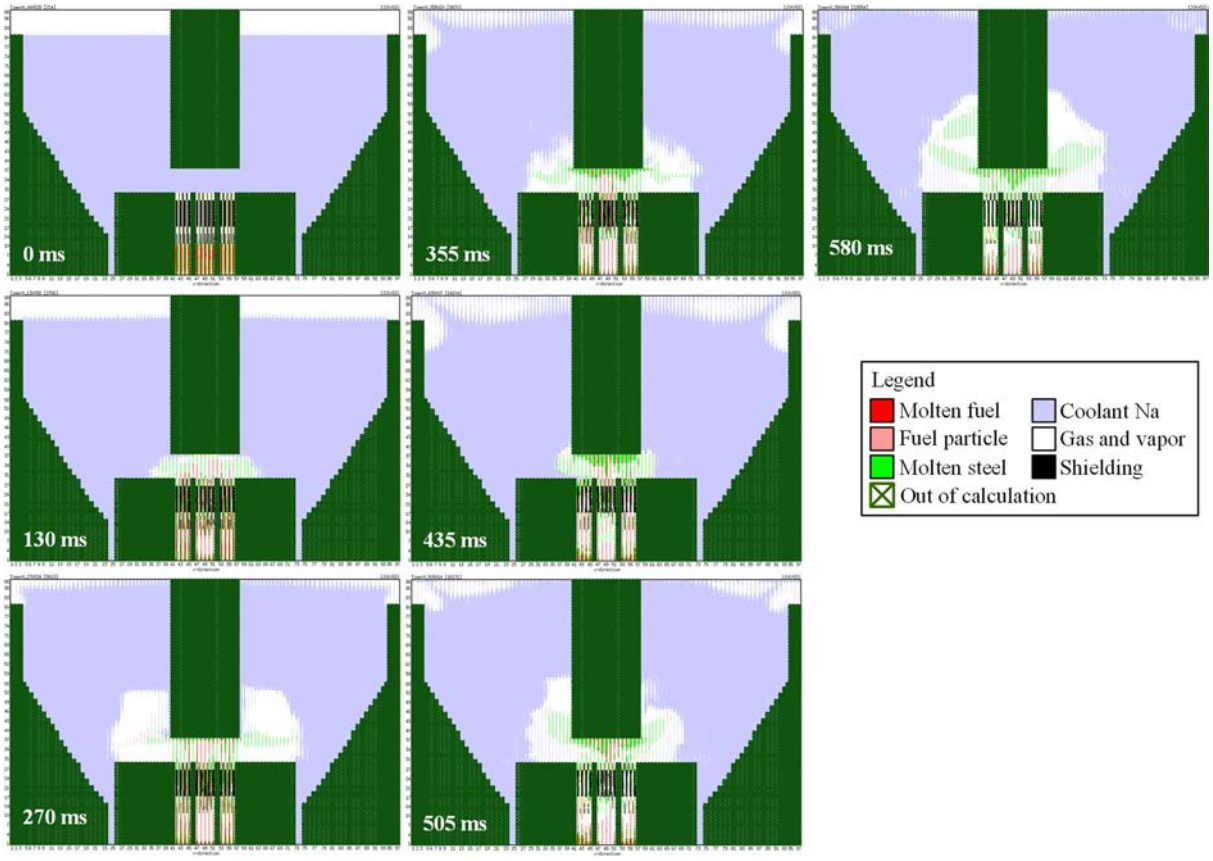

FIG. 4. Material distribution during molten core material ejection into the upper plenum (reproduced from Ref. [14] with permission of the IAEA).

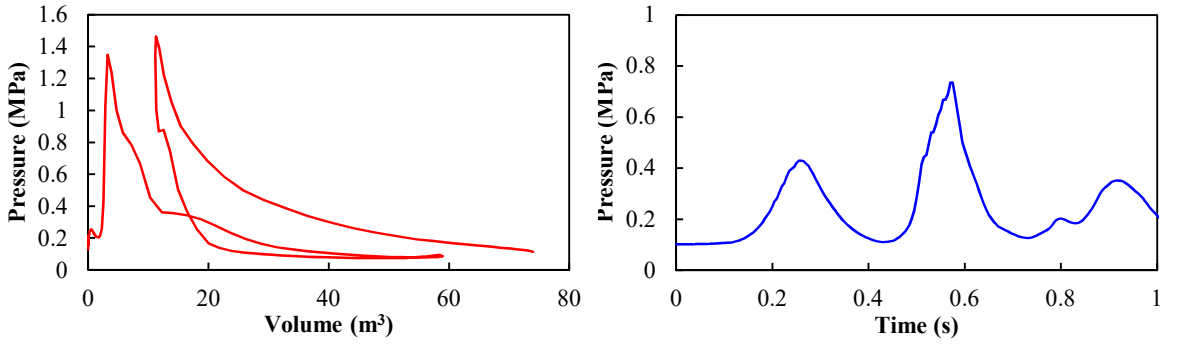

(a) P-V relation of CDA bubble (b) Pressure at the lower surface of the top shield

FIG. 5. Obtained P–V relation and pressure exerted on the lower surface of the top shield (reproduced from Ref. [14] with permission of the IAEA).

Molten fuel and steel, together with fission gas, were ejected from the core region to the hot pool through the upper core structure, which includes the upper blanket and upper shielding. Then, hot molten core materials mix with the sodium at the lower surface of the control plug, generating sodium vapour due to FCI. A CDA bubble expands until 270 ms at which its maximum volume is attained, and a sodium slug impacts the lower surface of the shield plug (but the impact is insignificant). After the first slug impact, the CDA bubble volume starts to decrease, and at 430 ms, it increases again due to subsequent FCI starting from around 380 ms. Then, the second slug impact occurs at around 580 ms. This volume expansion and contraction continue in a repetitive manner.

Figure 5 plots the obtained P–V relation up to the second slug impact, and the history of pressure exerted on the lower surface of the top shield. The former is used as the input to the structural response analysis of the RV and the latter to the plug response and sodium ejection analysis.

4.2 Structural response analysis of the reactor vessel

Figure 6 shows a sample result of the AUTODYN calculation for the structural response analysis of the RV. The target reactor is a 280 MW(e) Japanese prototype SFR (loop-type) and is modelled in an r-z two-dimensional mesh from the bottom of the RV to the lower surface of the top shield in a vertical direction. Note that the target reactor is different from that adopted in Sections 4.1 and 4.3. The upper sodium plenum is modelled with a Eulerian grid, and the structure including the RV is modelled with shell elements. The pressure source is given with a GASBAG model, for which a mechanical energy of 42 MJ at the maximum expansion is given assuming hypothetical conditions. Coolant sodium impacts the lower surface of the top shield at around 180 ms and the evaluated residual strain (effective plastic strain) at the upper cylindrical part of the RV amounts to 1.5% at a maximum. Supported by other calculation cases with varying mechanical energy values, this analysis shows that plastic strain remains if the mechanical energy exceeds 30 MJ in this geometry.

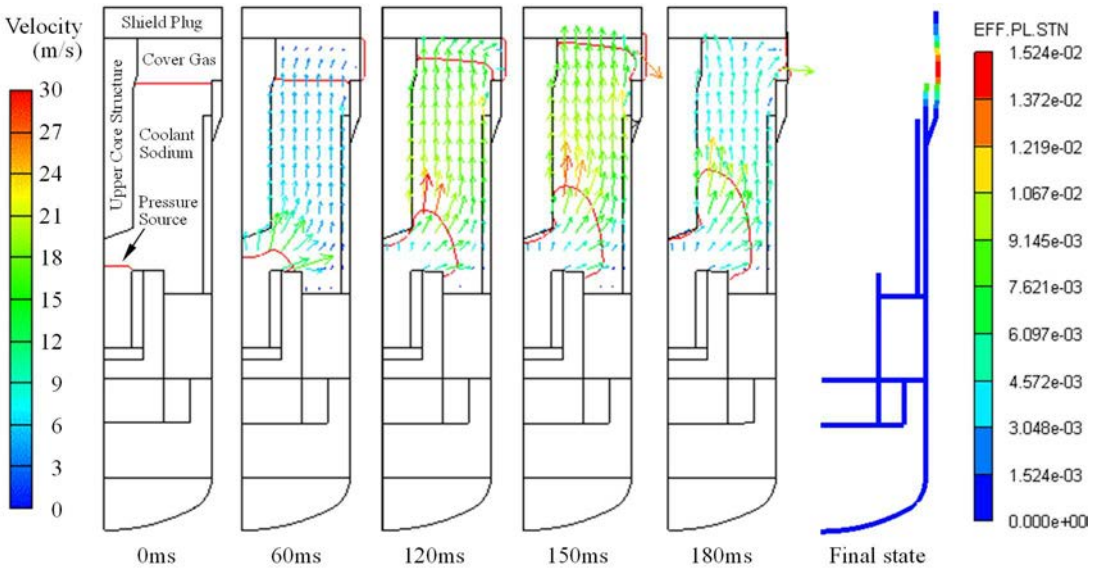

FIG. 6. A sample result of AUTODYN calculation for the structural response analysis of the reactor vessel.

4.3 Analysis of sodium ejection through the top shield

Figure 7 shows a sample result of the PLUG calculation for the analysis of sodium ejection through the top shield [14]. The target reactor is again a 500 MW(e) pool-type SFR. This reactor has 16 flow paths on its top shield. Figure 7 plots the calculation results of sodium flow in a flow path between the roof slab and large rotating plug (RS–LRP), together with the pressure exerted on the lower surface of the top shield. This pressure history was obtained by SIMMER in the calculation of thermal energy conversion into the mechanical energy.

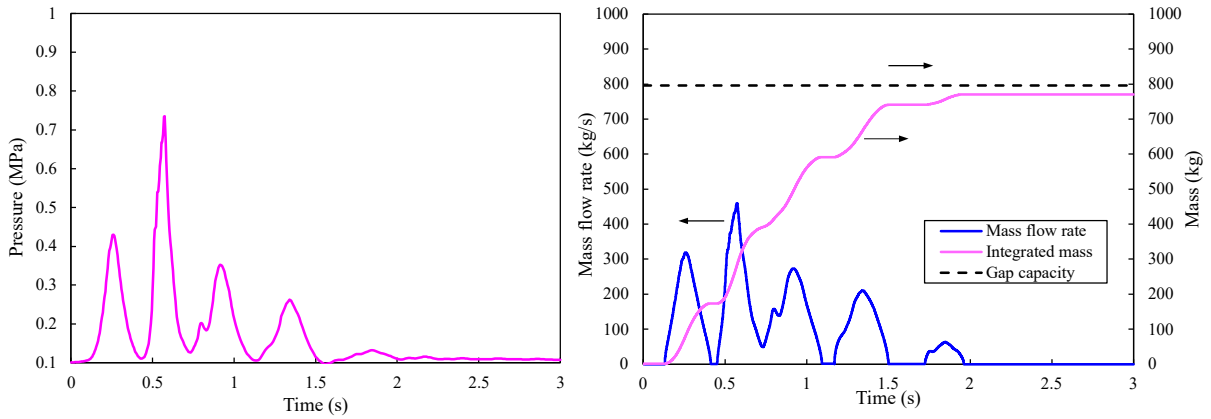

(a) Pressure history (b) Mass flow rate and integrated mass

FIG. 7. A sample result of the PLUG calculation for the analysis of sodium ejection through the top shield. Fig.7(a) is reproduced from Ref. [14] with permission of the IAEA.

Figure 8 illustrates the flow path of the RS–LRP divided into several parts in the PLUG calculation. The calculated mass flow rate amounts to 460 kg/s at a maximum at flow path 1 (from AB1 to RB2 in Fig. 8), and the amount of sodium that flowed into flow path 1 is 770 kg. No sodium ejection onto the top shield via path 1 nor path 2 is evaluated because the gap capacity of the path 1 in RS–LRP, which amounts to 796 kg, is greater than that the amount of sodium that flowed into flow path 1 In this calculation, it was assumed that the flow path opened at a certain width in advance (1 mm for path 1) as the calculation condition, and the width was not changed during the calculation. In reality, though, the plugs including a roof slab are fixed with their connecting bolts to prevent them from being missiles, and there is no open flow path through the top shield. In order to calculate the opening or closing behaviour of the flow paths, the dynamic movement of the plugs should be calculated with proper modelling of the shield plugs and their connecting bolts.

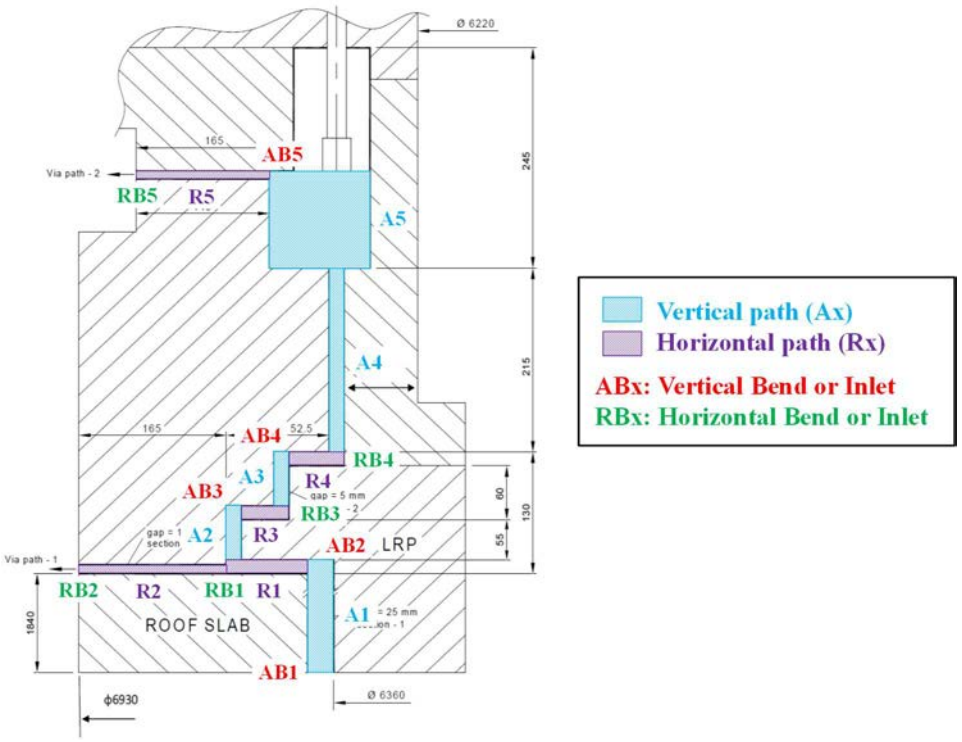

FIG. 8. Flow path model between the roof slab and large rotating plug (RS–LRP) adopted in PLUG. This figure is reproduced from Ref. [14] with permission of the IAEA.

5. CONCLUSION

The analysis methodologies for the evaluation of an unprotected loss of flow accident in a JAEA SFR have been described, focusing on the mechanical consequences that would arise during the expansion phase of the accident. JAEA developed the analysis methodologies for the evaluation of energetics and divided the analysis process into three: 1) using the SIMMER code, analysis of heat conversion into the mechanical energy during core melt due to re-criticality, 2) using the AUTODYN code, analysis of the structural response of the RV, and 3) using the PLUG code, analysis of the amount of sodium ejected onto the top shield through the gaps between shield plugs. The P–V relation of a CDA bubble, which is a mixture of gases (fuel vapour, steel vapour, and fission gas) and molten core materials, obtained by the SIMMER calculation is used as the input to structural response analysis that uses AUTODYN. The history of pressure exerted on the lower surface of the top shield obtained by the SIMMER calculation is used as the input to PLUG. These analysis codes are validated by simulating the dominant phenomena that significantly affect the results of each calculation. These analysis methodologies developed by JAEA were applied to reactor case analyses and confirmed their applicability.

ACKNOWLEDGEMENTS

The authors express their great appreciation to Masahiro Mizuno and Junichiro Kanaiwa of NESI Inc. for technical assistance in calculations using SIMMER, AUTODYN, and PLUG codes.

REFERENCES

[1] ONODA, Y., KURISAKA, K., SAKAI, T., Fundamental safety strategy against severe accidents on prototype sodium-cooled fast reactor, Journal of Nuclear Science and Technology, Vol.53, No.11, pp.1774–1786 (2016).

[2] ONODA, Y., MATSUBA, K., TOBITA, Y., SUZUKI, T., Preliminary analysis of the post-disassembly expansion phase and structural response under unprotected loss of flow accident in prototype sodium cooled fast reactor, Mechanical Engineering Journal, Volume 4, No. 3 (2017).

[3] YAMANO, H., FUJITA, S., TOBITA, Y., SATO, I., NIWA, H., Development of a three-dimensional CDA analysis code: SIMMER-IV and its first application to reactor case, Nucl. Eng. and Des., vol. 238, pp. 66-73 (2008).

[4] BUCKEL, G., HESSELSCHWERDT, E., KIEFHABER, E., KLEINHEINS, S., MASCHEK, W., A New SIMMER-III Version with Improved Neutronics Solution Algorithms, FZKA-6290, Karlsruhe, Germany (1999).

[5] ANSYS, Inc., ANSYS AUTODYN user's manual: release 15.0, Pennsylvania, USA (2013).

[6] KONDO, Sa., YAMANO, H., TOBITA, Y., FUJITA, S., KAMIYAMA, K., MASCHEK, W., COSTE, P., PIGNY, S., and LOUVET, J., Phase 2 Code Assessment of SIMMER-III, A Computer Program for LMFR Core Disruptive Accident Analysis, JNC TN9400 2000-105, O-arai, Japan (2000).

[7] MORITA, K., KONDO, Sa., TOBITA, Y., BREAR, D.J., SIMMER-III applications to fuel-coolant interactions, Nuclear Engineering and Design, Vol.189, pp.337–357 (1999).

[8] YAMANO, H., TOBITA, Y., "SIMMER-III code assessment for material expansion dynamics during core disruptive accident in sodium-cooled fast reactors", Proc. 22nd International Conference on Nuclear Engineering (ICONE22), July 7-11, Prague, Czech Republic (2014).

[9] KAWABATA, O., KAJIMOTO, M., TANAKA, N., "Hydrogen detonation and dynamic structural response analysis for large dry containment vessels of steel and pre-stressed concrete types", Proc. 8th International Conference on Nuclear Engineering (ICONE 8), Apr. 2-6, Baltimore, MD USA (2000).

[10] KAWABATA, O., "Analyses of ex-vessel steam explosion and its structural dynamic response for a typical PWR plant," Proc. 12th International Conference on Nuclear Engineering (ICONE 12), Apr. 25-29, Arlington, Virginia USA (2004).

[11] NAKAMURA, T., KAGUCHI, H., IKARIMOTO, I., KAMISHIMA, Y., KOYAMA, K., KUBO, S., KOTAKE, S., Evaluation method for structural integrity assessment in core disruptive accident of fast reactor, Nuclear Engineering and Design, Vol.227, pp97-123 (2004).

[12] WANG, C.Y., Comparison of ICECO code predictions with flexible vessel experiments, Nuclear Engineering and Design, Vol.49, pp.145-154 (1978).

[13] Results of Phase 2 of The APRICOT Program Final Report, DOE/SF/01112-T2 (DE82007965), work performed under contract No. AC03-76SF01112, Science Applications, Incorporated (1981).

[14] INTERNATIONAL ATOMIC ENERGY AGENCY, Modelling and Simulation of the Source Term for a Sodium Cooled Fast Reactor Under Hypothetical Severe Accident Conditions, IAEA-TECDOC-2006, IAEA, Vienna (2022).

ABBREVIATIONS

ATWS	Anticipated transient without scram
P–V relation	Pressure–volume relation
RS–LRP	Representing the gap between the roof slab and the large rotating plug
FCI	Fuel–coolant interaction
RV	Reactor vessel
JAEA	Japan Atomic Energy Agency
SFR	Sodium cooled fast reactor
LOHRS	Loss of heat removal systems
ULOF	Unprotected loss of flow

CEA RESEARCH PROGRAMMES RELATED TO THE SEVERE ACCIDENT PHENOMENOLOGY IN THE LOWER PLENUM OF AN SFR

R. CLAVIER[1], N. SEILER[1], A. LECOANET[1], B. BIGOT[1], C. BRAYER[1], J. FRANCESCATO[1], R. CHAUVIN[1], C. TREOL[1], A. AVRIT[1], P. SCIORA[2], V. PETITEAU[2]

[1] CEA, DES, IRESNE, DTN, Cadarache, F-13108, Saint-Paul-lez-Durance, France
[2] CEA, DES, IRESNE, DER, Cadarache, F-13108, Saint-Paul-lez-Durance, France

Abstract

The French approach concerning the safety demonstration of a fourth generation sodium cooled fast reactor (SFR) demands the resilience of new designed reactors to postulated severe accident (SA) sequences. The most severe situations come from an unprotected degradation of the nuclear core, resulting in a molten mixture of fuel and core structures commonly referred to as "corium". For the ASTRID design developed in France before 2019, the safety demonstration relied on innovative reactor designs exhibiting a low neutron void effect (CFV in French), along with specific safety devices dedicated to SA prevention and mitigation, namely the transfer tubes and the core catcher, whose major role is to promote and accelerate the relocation of the corium into the lower plenum of the primary vessel. This strategy enhances the interest in the modelling of the behaviour of the corium in the lower plenum. The associated phenomenology is complex and involves i) fuel–coolant interaction (FCI), which provokes a fragmentation of the jet and potentially violent vaporization of the sodium; ii) jet impingement on the core catcher if the fragmentation is not total, which provokes a local ablation; iii) formation of a debris bed by sedimentation whose coolability is not guaranteed; and iv) the formation of a liquid corium pool on the core catcher leading to severe thermal loads on its structures.

FCI has been the subject of a continuous interest at CEA for the last decades, and motivates the development of the new SCONE (Software for Corium Na Evaluation) calculation tool, dedicated to the evaluation of the consequences of FCI with a fine level of description (compressible, transient, multiphase, multimaterial and multidimensional flows), associated with experimental programmes at both integral (PLINIUS2-FR, PLINIUS2-EXPLO) and local (SERUA) scales. The study of jet impingement on the core catcher combines small scale experiments with simulant system (ice/water) to access local ablation phenomenology, and foreseen large scale prototypical experiments (PLINIUS2-FR) to study the scale transposition of this phenomenology and CFD simulations to support the experimental work and derive accurate models at reactor scale.

An appropriate representation of the corium debris bed on the core catcher requires a dynamic model able to capture the changes in its configuration over time: sedimentation of the debris resulting in a globally conic-shaped debris bed; potential re-melting of the corium; possible neutron re-criticality; and intense convection and boiling into the debris bed that provokes the so-called 'self-levelling', which is of particular interest to prevent the re-melting of the debris and neutron re-criticality. A new model to describe the main aspects of the self-levelling phase is under development in the framework of a Ph.D. thesis at CEA, with a focus on the granular flow of debris. In parallel, the neutron criticality of postulated configurations of debris beds are under evaluation. The promotion of corium transfer to the lower section of the reactor vessel increases the importance of the core catcher, the increased corium inventory and thermal loads compared to past reactors. Therefore, the modelling of large corium pools on the core catcher is the subject of renewed interest and the CEA is performing numerical simulations using Trio-CFD to better characterize the turbulent flow structures and heat transfers in the corium pool.

1. INTRODUCTION

The French approach concerning the safety demonstration of a fourth generation sodium cooled fast reactor (SFR) demands the resilience of new designed reactors to postulated severe accident (SA) sequences. Among the many possible scenarios, the most severe situations occur in case of unprotected degradation of the nuclear core, resulting in a molten mixture of fuel and core structures commonly referred to as the corium. For the ASTRID design developed in France before 2019, the safety demonstration relied on innovative reactor designs exhibiting a low neutron void effect (CFV in French), along with specific safety devices dedicated to SA prevention and mitigation, namely the transfer tubes and the core catcher, whose major role is to promote and accelerate the relocation of the corium into the lower plenum of the primary vessel. This strategy enhances the interest in the modelling of the behaviour of the corium in the lower plenum. The associated phenomenology (Fig. 1) is complex. Immediately after the arrival of the corium from the transfer tube, the fuel–coolant interaction (FCI) provokes a more or less intense fragmentation of the jet and potentially violent vaporization of the sodium (steam

explosion). In case of incomplete fragmentation, the corium jet may directly impact the core catcher, the so-called 'jet impingement', leading to a local ablation of its structures at the point of impact. The fragmented corium solidifies into fine particles, which settle down on the core catcher and form a so-called 'debris bed' that exhibits a very complex behaviour involving self-levelling and possible re-melting if the internal sodium flow is ineffective in extracting all the decay heat from the debris. Ultimately, the formation of a liquid corium pool on the core catcher, leading to severe thermal loads on its structures, appears as the worst case final state of interest to demonstrate that the primary vessel is not damaged by the corium.

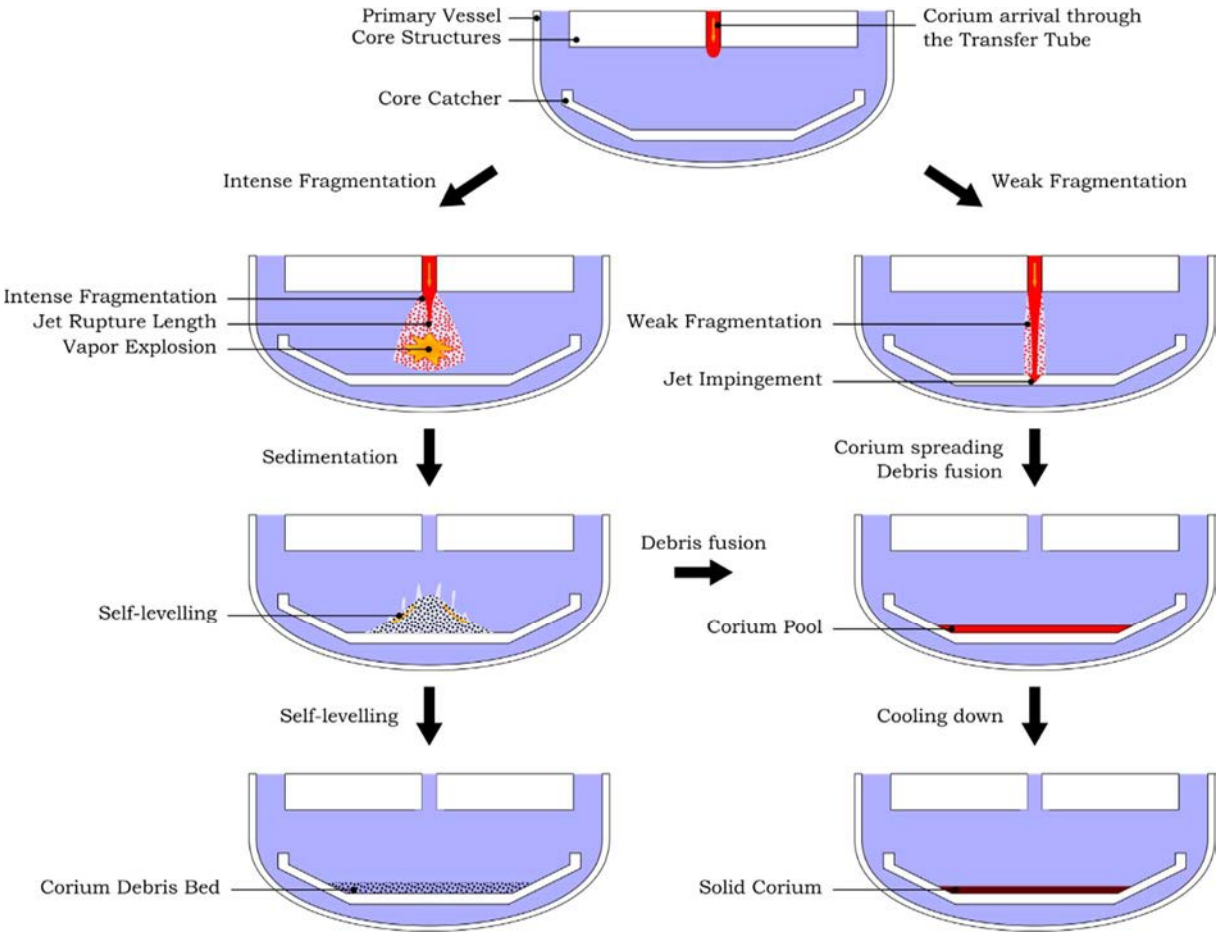

FIG. 1. Overview of the states of interest describe the possible evolutions of the corium in the lower plenum of a SFR.

The CEA is currently pursuing consistent research programmes dedicated to each situation described in Fig. 1, including theoretical modelling, code developments and experiments. This paper gives an overview of these programmes. Section 2 presents the actions on the modelling of the FCI, while Section 3 focuses on the jet impingement. Section 4 gives an insight on the current state of the modelling of debris beds on the core catcher, and Section 5 is dedicated to the modelling of corium pools on the core catcher.

2. FUEL–COOLANT INTERACTION

2.1 Context

FCI has a significant impact on the safety of reactors. Indeed, it may generate a violent release of mechanical energy, compromising the integrity of the vessel.

For some years now, the CEA has been building a CFD tool, called SCONE (Software for Corium Na Evaluation co-development at CEA Saclay and Cadarache), in order to finely evaluate the consequences of a corium–sodium interaction (i.e. FCI) [1]. Since 2022, SCONE has been linked to the TRUST multiphase digital platform developed at CEA in Saclay [2]. The TRUST platform provides services and software tools used by dedicated applications (designated as BALTIK in the platform terminology) to perform numerical simulations (see Fig. 2). Five BALTIK currently exist, basically dedicated to multiphase flow simulation at different scales: TrioIJK performs two-phase flows DNS with front-tracking methods, and is optimized for Cartesian meshing; TrioCFD performs CFD-scale multiphase flow simulations with subgrid models, typically LES or RANS modelling of turbulence; FLICA5, TrioMC and GENEPI+ perform simulations at the scale of a technological component, which is respectively the LWR core, SFR core and steam generator. The new BALTIK SCONE will be a multiphase, multicomponent simulation tool that aims at representing the main phenomena associated with FCI as accurately as possible, relying on experimental results (past and future) to develop and validate the necessary models.

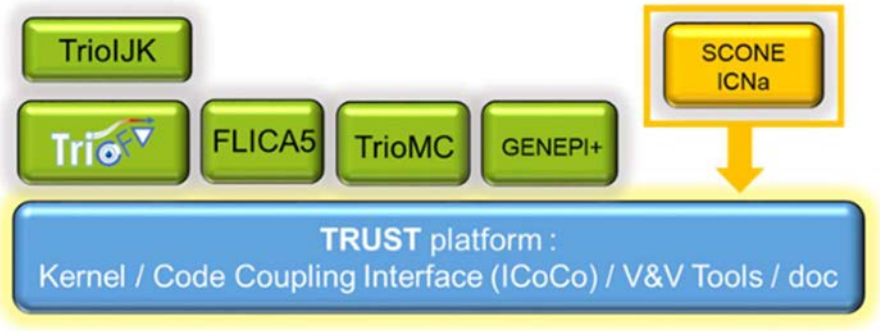

FIG. 2. General organization of the TRUST numerical platform and its physical applications, including SCONE.

In parallel to this simulation tool development, CEA is conducting experimental programmes to feed the software with physical models and to validate it. Full scale tests are planned in the SAFETy platform (initially called PLINIUS2 platform), to be constructed after 2026 [3]. Inside the SAFETy platform, the PLINIUS2-FR programme will study the fragmentation of the corium jet and PLINIUS2-EXPLO will study the steam explosion. Another local-scale experimental facility, SERUA, is being designed at CEA-Cadarache. This experiment will characterise the heat exchange in the film boiling regime between a hot sphere, representing a corium droplet, and the liquid sodium, with a special focus on the stability of the sodium vapour film. The first tests are planned for 2024. The MELT tests carried out by the JAEA and interpreted with the SPECTRA tool [4] developed at CEA Cadarache will also be a source of data for understanding the physics of FCI. All these tests will then serve as a basis for the validation of the SCONE-TRUST simulation platform.

2.2 Preliminary results

At this early point of the developments of SCONE, the capabilities of the TRUST platform have been tested to evaluate which developments are specifically required to extend its applicability to the simulation of FCI (SCONE application). For example, the phase separation problem, proposed by Coquel et al. (1997) [5], focuses on the separation of two phases with different densities that are initially mixed under the effect of gravity. This test case serves as a stiff and yet useful benchmark for testing numerical schemes of simulating problems with phase appearance and disappearance. In the case of FCI, it is of interest to evaluate the ability of the

platform to treat phase mixtures, as the fragmenting jet will be described as a mixture of particles, liquid jet, liquid sodium and sodium vapour.

Starting from a homogeneous mixture, the liquid fraction and liquid velocity profiles at $t = 0.5$ s obtained with the Bestion model (the pressure correction term in CATHARE [6]) are compared in Fig. 3 with the analytical solution, and exhibit a satisfactory agreement. This is an encouraging indication concerning the relevance of the TRUST platform to support the simulation of FCI by the SCONE application.

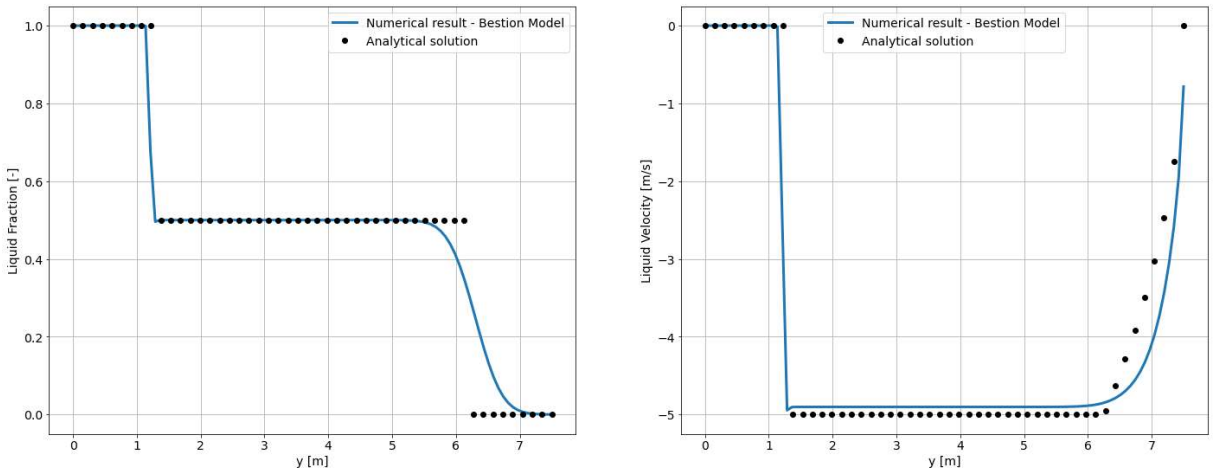

FIG. 3. Phase separation problem with TRUST. Comparison between simulation and the analytical solution.

3. JET IMPINGEMENT ON THE CORE CATCHER

3.1 Research strategy

As described in the introduction, the worst jet configuration regarding core catcher ablation is a coherent jet undergoing no fragmentation surrounded by a gaseous phase. Furthermore, past studies, summarized in Ref. [7], highlighted that the core catcher ablation is faster when the jet and the core catcher are of similar composition [8] (metal/metal or oxide/oxide). Indeed, in case of oxide jet and metallic core catcher, a protective crust at the ablation surface reduces the ablation [9]. Furthermore, correlations for the heat transfer at the jet impingement, in close configurations of those encountered in ASTRID, exist [8, 9] but are not valid for a pool regime. This regime corresponds to the collapse of the liquid film in the cavity formed by ablation. The heat transfers at the jet impingement are thus reduced because the cavity is filled. This effect is thus of great importance to realistically predict the core catcher ablation. In order to better understand this phenomenology and model it, a research programme has been launched [10] and continued which aims to go from the experiments to modelling and finally to numerical simulations. The first simulation (water/ice) experiments have been carried out after having estimated their representativeness, and advanced models were derived. Also, to transpose this work to the issue of metallic jet impinging on metallic core catcher, CFD simulations are being set. First, the CFD simulations are calibrated using the simulant experiments. Then calculations will be conducted on the low Prandtl number system, trying to reproduce available experimental data [8, 11]. When the CFD is fully validated using these experiments, CFD simulations of steel jet impinging a steel core catcher will be assured.

3.2 Experimental results and advanced models

The first step of the research programme on the ablation of a core catcher by a corium jet was to improve physical knowledge on the ablation when both the jet and the solid are of the same nature, which is considered to be the most penalizing case [7]. To do so, an experimental set up called HAnSoLO has been built [7], to study the water/ice system. This system delivers turbulent water jets on a block of transparent ice [11] allowing for real-time tracking of the cavity produced by ablation within the solid, as well as the recording ablation from new points of view [7]. Figure 4 shows examples of shadowgraphy observations of a cavity in the film ablation regime (left) and the pool regime (right). Note that only the projection of the cavity shape is visible using this technique. In particular, the water film cannot be observed directly in the left picture, but it is clearly identified due to the irregularities in the ablation front that indicate the laminar to turbulent transition in the film flow regime. Experiments performed with this setup provided information on the ablation: the shape of the cavity was revealed and explained, the pool regime was directly studied and measured, a new type of correlation was proposed, and improved modelling of the pool regime was achieved [7, 12].

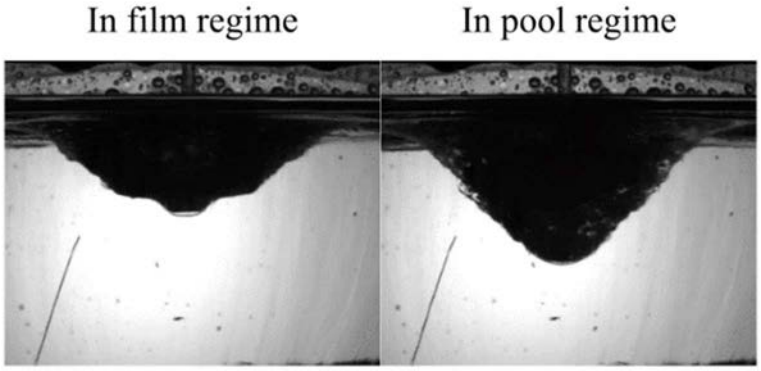

FIG. 4. Examples of cavity visualization with HAnSoLO in the film ablation regime (left) and in the pool regime (right).

From there, numerical simulation work was started. To support an incremental logic for the research project, the setup was modified to study the ablation of transparent ice by a water jet when the system is submerged in water. This is an important first step for CFD code validation as the effect of the gas/liquid interface is removed. Validations on such cases give a strong basis for further validation on cases for which the jet is surrounded by gas.

3.3 Preliminary simulation results in water/ice

As stated above, the simplified case of an immersed jet of water impinging an ice block is studied to validate the melting model in the code.

The code used is OpenFOAM®. A large eddy simulation (LES) approach is used, with a wall adapting local eddy-viscosity (WALE) [13] model for the turbulence. Turbulence is already simulated at the inlet of the jet with a synthetic turbulence method called the divergence-free synthetic eddy method (DF-SEM) [14]. An enthalpy method [15, 16], based on a penalization method, is used for the simulation of solid melting.

The case without melting was first studied and compared to results in the literature to determine meshing requirements in order to solve correctly the heat transfers at the solid–fluid interface. The case with melting is now under investigation and is giving encouraging results. Fig. 5 compares the evolutions of the molten depth of ice, scaled by the jet diameter, in the simulation

and in HAnSoLO experiments. The effect of mesh refinement is showed, but further analysis is needed to assess the validity of the calculations.

In the longer term, the models developed in the framework of this exploratory research will be integrated into a CEA software platform.

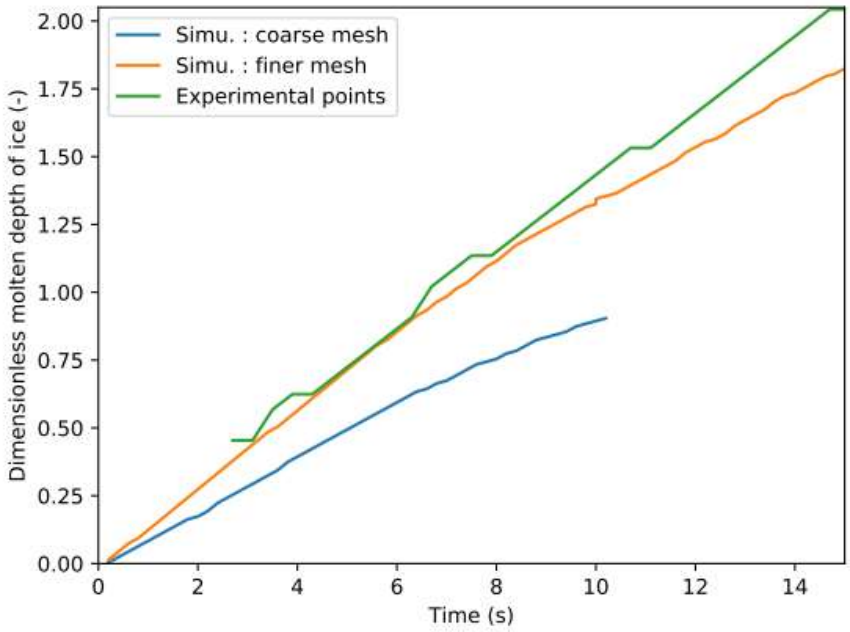

FIG. 5. Dimensionless depth of molten ice versus time for an experiment and corresponding numerical simulations.

4. DEBRIS BEDS ON THE CORE CATCHER

4.1 Context

At its arrival in the lower plenum, the corium undergoes a more or less intense fragmentation into solid particles due to the FCI. After sedimentation, these fragments then form a so-called debris bed, which includes fuel and steel particles. The extraction by the sodium of the heat due to the decay of fission products is essential to avoid the re-melting of the debris bed, which would result in a liquid corium pool interacting with the core catcher structures (see Section 5 for further details). Another important issue concerning the debris bed is to evaluate its neutron reactivity. A positive neutron reactivity would certainly result in a brief but violent power excursion, implying partial re-melting of the debris, dispersion of the corium beyond the core catcher, and possible mechanical loads on the structures.

The coolability of the debris bed (i.e. the capacity of the sodium to evacuate all the decay heat from the debris bed), and the neutron reactivity of the debris bed present common dependencies on several coupled aspects. The sodium thermohydraulics inside the debris bed directly impacts its coolability, because the amount of sodium that penetrates into the centre of the bed drives the amount of energy that can be extracted from it, and indirectly influences the neutron reactivity, through the void effect due to sodium vaporization and the Doppler effect induced by the variation of temperature. In addition, the particles close to the surface of the debris bed are moved by the sodium flow, producing self-levelling, i.e. progressively flattening of the debris bed from a globally conical shape. The self-levelling of the debris bed has a positive impact, from the safety point of view, on both its coolability and its neutron reactivity, because of the induced increase of the surface to volume ratio, but it may be counterbalanced by the

effect of late corium discharges, in case of several corium relocation phases, which increase the mass of corium in a non-levelled configuration in the lower plenum, and therefore bring the debris bed closer to neutron criticality.

These considerations enlighten the need for a simulation tool able to quantitatively characterize the behaviour of the debris bed and its evolution in terms of temperature, internal configuration (sodium void fraction, material repartition) and shape, and to evaluate the neutron reactivity of the debris bed. Those axes are both explored at CEA and the corresponding actions are described in the next paragraphs.

4.2 Development of a new CFD model for the debris bed coolability and preliminary results

Historically, coolability assessments have been performed at CEA with use of integral fast calculation tools. LIDEB [17] then LIDENa implement 1-D modelling approaches to evaluate the temperatures, void fraction and eventually re-melting in a fully levelled debris bed. They appear inadequate to describe the phenomenology presented in the previous paragraph, which requires at least a multidimensional and multiphase transient approach.

A new modelling is being developed in the framework of a Ph.D. thesis to reach this objective. Considering the debris bed as an unconsolidated granular medium with an internal heat source exchanging with an internal boiling flow of sodium, homogenized equations are derived from the micro-scale boundary-value 3-phases problem by using the volume averaging method [18], taking advantage of its successful applications to various similar (and simpler) problems: single-phase viscous and inertial flows in porous media [19], multiphase viscous [20] and inertial [21] flows in porous media, heat and mass transfers in porous media [22], and dense particle flows in single phase viscous flows [23]. The implementation of the macroscopic equations is under progress in the OpenFOAM® platform.

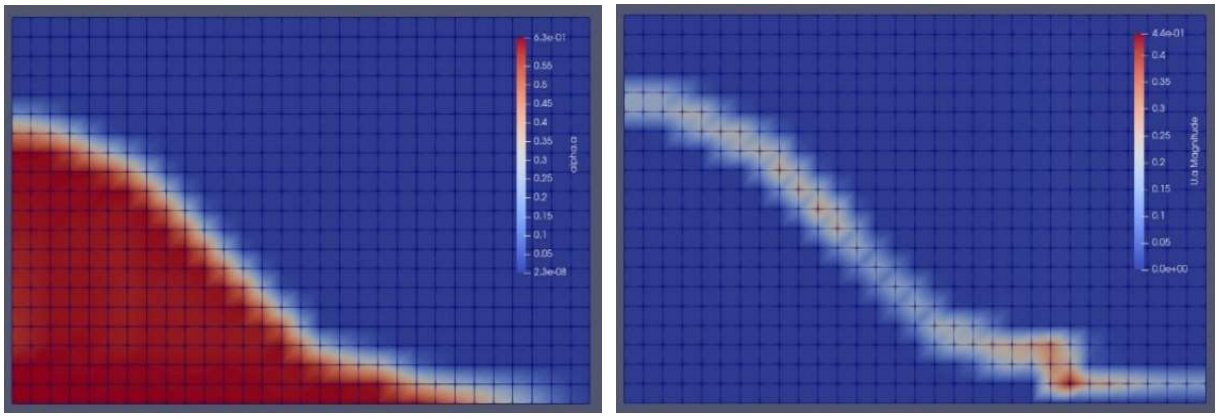

(a) *(b)*

FIG. 6. Preliminary test of debris bed gravity collapse in water. Volume fraction of debris (a); Debris velocity (b).

Figure 6 shows the results of a preliminary verification test of a partial implementation of the model where an isothermal debris bed collapses into air under the action of gravity. The debris bed phase macroscopic viscosity is considered to follow Mohr-Coulomb rheology [24]. Figure 6(a) shows the volume fraction of debris. It does not exceed 63 % (37 % porosity), which is consistent with the implemented viscosity law where the equivalent viscosity increases when the volume fraction of debris approaches a maximal value (63 %). Figure 6(b) shows the

corresponding velocity field (norm). Only the surface of the bed is moving, which is consistent with expectations because this is where the volume fraction of particles falls below the maximum occupation rate, and so where the viscosity of the particle phase reduces.

As for the developments for the jet impingement simulation, the physical models assessed in the framework of this programme are intended to be integrated into a CEA software platform in the future.

4.3 Characterization of the debris bed reactivity

Monte Carlo evaluations of the neutron reactivity of the debris bed are performed using Tripoli 4 [25] on postulated configurations. The effect of the bed geometry, temperature, material masses (fuel, steel, sodium, neutron absorbers) and internal repartition (stratification, mixture, local compaction) have been investigated. Neutron criticality may be reached on some cases, underlying the importance of its evaluation for a safety demonstration.

As an illustration, Fig. 7 compares the evolution of the effective multiplication factor k_{eff} with fuel mass for a debris bed globally homogeneous and with a cylindrical shape with various diameters. The four curves figure the evolution of the k_{eff} factors with the mass of the bed for four different bed diameters: 150 cm (yellow), 200 cm (red), 250 cm (blue) and 300 cm (green). For a given diameter, the increase of mass results in a higher and higher bed and brings the system closer and closer to neutron criticality, which is obtained when $k_{eff} = 1$ (critical mass). For a given mass of the debris bed, an increase in diameter results in a flatter and flatter debris bed, which increases the surface to volume ratio, and therefore reduces the k_{eff} factor. For example, Fig. 7 shows that the critical mass of the 150 cm bed is ~7500 kg, while the critical mass of the 300 cm debris bed is ~25 000 kg. Therefore, in this configuration, increasing by a factor 2 of the diameter of the bed leads to increase its critical mass by a factor of ~3.3.

These calculations are intended to form the validation basis of a faster calculation module, which will have to be coupled to a thermohydraulic module based on the work described in the previous paragraph. Ultimately, the objective is to integrate those models into the PROCOR platform.

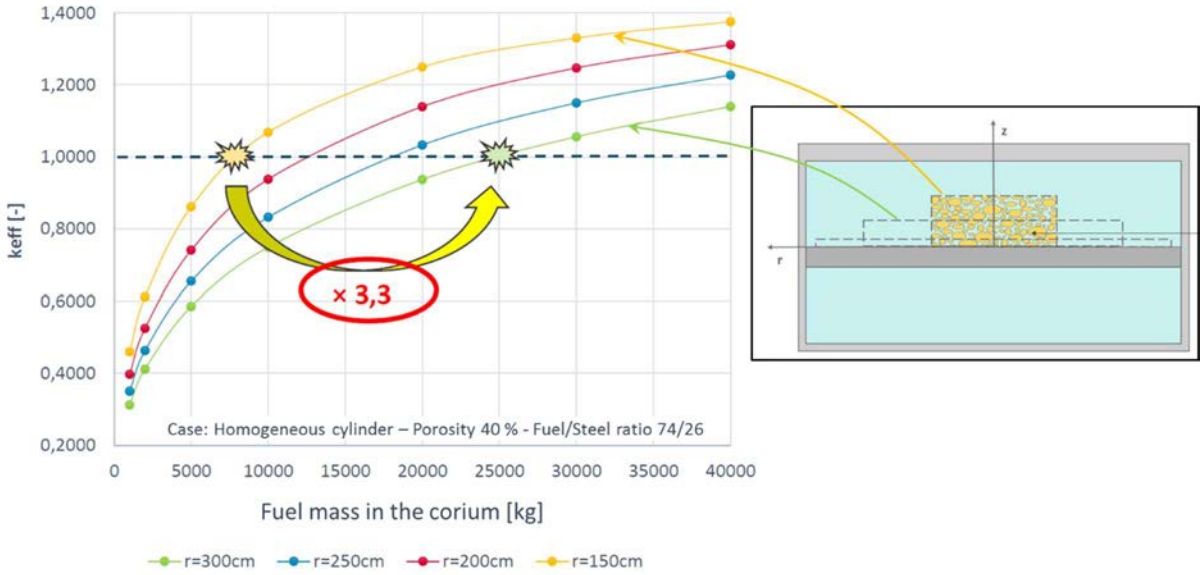

FIG. 7. Example of k_{eff} calculations as a function of the corium mass for a postulated debris bed configurations on the core catcher: cylindrical bed with variable diameter and height, porosity 40 % and fuel/steel ratio 74%/26%.

5. CORIUM POOLS ON THE CORE CATCHER

5.1 Context

The modelling of large corium pools on the core catcher is a subject of interest in order to guarantee the long term safety criteria. The important related safety issues concern the turbulent flow structures and heat transfers within the corium pool, and the potential melting of thermal structures of the core catcher which has to resist to the heat transfer from the corium. In this context, the CEA is performing numerical simulations using Trio-CFD [26] to characterize the turbulence and heat transfers in the liquid corium pool. In addition to the numerical simulations, experiment tests (with a KNO_3–$NaNO_3$ eutectic mixture as simulant material for the corium, and a metal plate for core catcher) are performed on the ESFR-LIVE facility at KIT (with a length scale of 1:6 of a large scale prototype reactor), in order to study the interaction between the simulant material and the core catcher [27, 28]. The pool thermohydraulics, the heat transfers and the dissolution kinetics by ablation of the refractory material of the core catcher have started to be investigated.

To evaluate the thermal load distribution on the core catcher walls and the temperature wall resistance, dimensionless correlations for the convective heat transfer are usually used. Several types of dimensionless correlation are provided in the literature [29, 30] for different geometries and ranges of the similitude criteria (internal Rayleigh (Ra_i) and Prandtl (Pr) numbers) but none of them is fully adapted to the expected conditions: the specificities of the corium captured in the core catcher are the large aspect ratio, which is expected to decrease the downwards and lateral thermal loads on the core catcher while favouring the upward loads, and the pitched lateral wall, which has not been considered in previous works. The new experiments, associated with numerical studies, are expected to provide new adapted correlations for the convective heat transfers.

5.2 Preliminary results and perspectives

Preliminary numerical simulations have been performed to calculate the ESFR-LIVE experiments with a KNO_3-$NaNO_3$ eutectic mixture. Figure 8 shows a snapshot of the horizontal and vertical slices of the temperature field obtained from a direct numerical simulation under a partial geometry of the ESFRLIVE facility (1:2 of scale with a- $\pi/6$ angle) performed with the code Trio-CFD and with use of the HPC resources of the CEA's Very Large Computing Centre (TGCC). The physical properties of the eutectic mixture are used. The temperature is imposed at all boundaries at the fusion temperature of the material, figuring a liquid pool surrounded by its crusts which are not explicitly represented. Internal Rayleigh and Prandtl numbers are respectively 10^8 and 10.

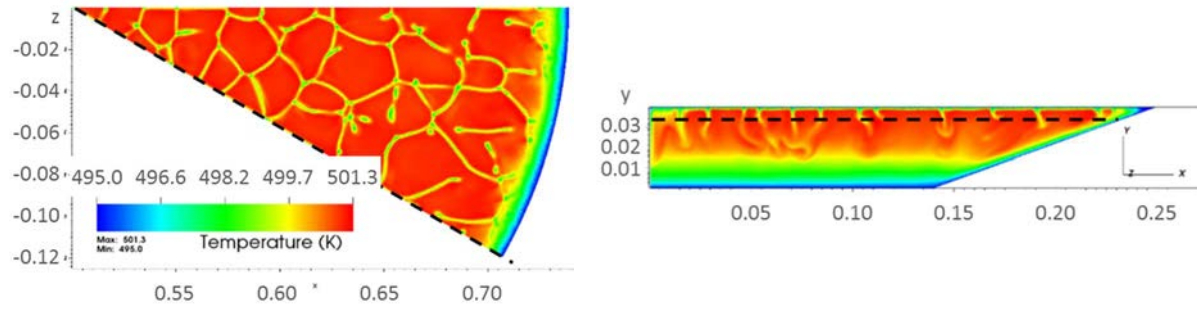

(a) (b)

FIG. 8. DNS simulation of a liquid pool of $NaNO_3$-KNO_3 eutectic mixture with $Ra_i = 10^8$ and Pr = 10 using Trio-CFD. Snapshot of the temperature field.

In Fig. 8(a), the flow exhibits convective vortices of a natural Rayleigh-Bénard convection sustained by an internal 'in volume' power density and the external wall cooling (imposed temperature). The fluid properties are representative of the KNO_3–$NaNO_3$ eutectic mixture used in the LIVE-ESFR experiments. The observed structures are transient, but the average behaviour corresponds to a steady state. Figure 8(b) shows the stratification of the temperature field with two distinct zones: a lower region of thermal conduction (corresponding to the low velocity region) with a temperature stratification and an upper region with uniform temperature (corresponding to the convective region). The fluid in contact with the lateral pitched surface is cooled and due to a buoyancy effect quickly falls down to the lower region.

The short term perspectives of this work focus on extending these results to the case of a prototypical corium, whose physical properties differ from the eutectic mixtures, in particular concerning the Prandtl number (0.5 instead of 10), which has an impact on the hydrodynamic and thermal flows [31].

In the longer term, the efforts will be dedicated to the realization of simulations with higher Rayleigh numbers, closer to the expected prototypical conditions (~10^{14}, which is strongly turbulent). This requires a modelling of the turbulence (LES and RANS approaches) within homogeneous natural convection flows.

6. CONCLUSIONS

This paper gives an overview of the research programmes pursued by CEA to characterize the behaviour of the corium in the lower plenum of a SFR during the late phase of a severe accident. These programmes concern the FCI, jet impingement, the debris beds, and the corium pools on the core catcher. They include both code development and dedicated experiments.

Experiments dedicated to FCI are included in the PLINIUS2 experimental programme, and the SERUA analytical experiments for film boiling in liquid sodium. The programme for the simulation of FCI mainly consists of the development of SCONE. Since 2022, SCONE has been linked to the TRUST multiphase digital platform developed at the CEA.

The jet impingement has been studied both experimentally, with the HAnSoLO analytical experiments, and numerically, with use of an OpenFOAM® solver. An LES approach using a WALE model for the turbulence and coupled with an enthalpy method for the simulation of solid melting is giving encouraging results compared to HAnSoLO experimental data.

Another OpenFOAM® solver has been developed at CEA to characterize the thermohydraulic behaviour of subcritical debris beds on the core catcher. In parallel, the neutron criticality of debris beds is also studied numerically with TRIPOLI4 simulations on postulated configurations. Both axes require further developments in the short term. In the longer term, the coupling of those aspects will be investigated. In the future, when primary and exploratory research will be completed, all these developments will be integrated into CEA software.

The behaviour of a corium liquid pool on the core catcher has been studied numerically with the TRUST platform. A comparison between DNS simulations and small scale experiments with a simulant fluid is under progress. In the longer term, efforts will be devoted to larger scale simulations with more representative conditions, notably in terms of turbulence intensity, which requires specific developments of new LES and RANS models.

ACKNOWLEDGEMENTS

The authors would like to thank the Generation IV programme of the industrial nuclear support and innovation Division of CEA which supports this work as well as the SFR R&D Project. The numerical work was granted access to the HPC resources of the CEA's Very Large Computing Centre (TGCC) under the allocation 2022 A0092A07691 made by GENCI. ESFR-LIVE facility of the KIT research centre was used in the frame of the ESFR-SMART project and is partially funded by the ESFR-SMART project funded by the Euratom research and training programme 2014-2018 under grant agreement No 754501.

REFERENCES

[1] M. Zabiego and C. Fochesato. Corium-sodium interaction the development of the SCONE software', Proceedings of NURETH-17 Conference, Xi'an, Shaanxi, China, (2017).

[2] P.-E. Angeli, U. Bieder, G. Fauchet. Overview of the TrioCFD code: Main features, VetV procedures and typical applications to nuclear engineering. NURETH 16 - 16th International Topical Meeting on Nuclear Reactor Thermalhydraulics, Chicago, United States (2015).

[3] C. Journeau et al. Corium-Sodium and Corium-Water Fuel-Coolant-Interaction Experimental Programs for the PLINIUS2 Prototypic Corium Platform. Nucl. Technol., vol. 205, no. 1–2, pp. 239–247 (2019).

[4] M. Johnson, C. Journeau, K. Matsuba, Y. Emura, and K. Kamiyama, Characterization of high-temperature nuclear fuel-coolant interactions through X-ray visualization and image processing. Ann. Nucl. Energy, vol. 151, p. 107881 (2021).

[5] Coquel, F., El Amine, K., Godlewski, E., Perthame, B., Rascle, P., A numerical method using upwind schemes for the resolution of two-phase flows. J. Comput. Phys. 136 (2), 272–288 (1997).

[6] D. Bestion. The physical closure laws in the CATHARE code. Nuclear Engineering and Design, vol. 124 (1990).

[7] A. Lecoanet, F. Payot, C. Journeau, N. Rimbert, M. Gradeck. Study of the ablation consecutive to jet impingement on a meltable solid – Application to SFR core-catcher. Nuclear Engineering and Design 377, 111147 (2021).

[8] K. Sato, A. Furutani, M. Saito, M. Isozaki, K. Suganuma, S. Imahori. Melting attack of solid plates by a high-temperature liquid jet [ii] – erosion behavior by a molten metal jet. Nuclear Engineering and Design 132 (2), 171186 (1991).

[9] M. Saito, K. Sato, A. Furutani, M. Isozaki, S. Imahori, Y. Hattori. Melting attack of solid plates by a high temperature liquid jet – effect of crust formation. Nuclear Engineering and Design 121 (1), 1123 (1990).

[10] F. Payot, C. Journeau, C. Suteau, F. Serre, M. Gradeck, N. Rimbert, A. Lecoanet, A. Miassoedov. A new experimental R&D program associated with the corium jet impingement on the ASTRID core catcher sacrificial material. Proc. of ICAPP 2018, ANS, Charlotte, NC, USA, pp. 657-666 (2018).

[11] A. Lecoanet, M. Gradeck, X. Gaus-Liu, T. Cron, B. Fluhrer, F. Payot, C. Journeau, N. Rimbert. Ablation of a Solid Material by High-Temperature Liquid Jet Impingement: An Application to Corium Jet Impingement on a Sodium Fast Reactor Core-Catcher. ASME J of Nuclear Rad Sci, 8(1) (2022).

[12] A. Lecoanet, F. Payot, C. Journeau, N. Rimbert, M. Gradeck. Classification of ablation mode during impact of hot liquid jet on a solid. Int. J. Heat Mass Transf., 181 (2021).

[13] F. Nicoud, F. Ducros. Subgrid-scale stress modelling based on the square of the velocity gradient tensor. Flow, Turbulence and Combustion 62(3), pp 183–200 (1999).

[14] R. Poletto, T. Craft, A. Revell. A New Divergence Free Synthetic Eddy Method for the Reproduction of Inlet Flow Conditions for LES. Flow Turbulence and Combustion 91(3), pp 519–539 (2013).

[15] V. Voller, C. Prakash. A fixed grid numerical modelling methodology for convection-diffusion mushy region phase-change problems. International Journal of Heat and Mass Transfer 30(8), pp 1709–1719 (1987).

[16] A. Brent, V. Voller, K. Reid. Enthalpy-porosity technique for modeling convection-diffusion phase change: application to the melting of a pure metal. Numerical Heat Transfer 13(3), pp 297–318 (1988).

[17] G. Geroudet, F. Balard. Modélisation de l'évolution thermique d'un lit de débris de combustible fissile sous puissance résiduelle. NT/SERA/LAPE/89/2035/LIDEB/RPA, (1989).

[18] M. Quintard, S. Whitaker. Transport in ordered and disordered porous media 2: generalized volume averaging. Transport in Porous Media, vol. 14, pp. 179-206 (1994).

[19] S. Whitaker. Flow in porous media I: A theoretical derivation of Darcy's Law. Transport in Porous Media, vol. 1, pp. 3–25 (1986).

[20] D. Lasseux, M. Quintard, S. Whitaker. Determination of Permeability Tensors for Two-Phase Flow in Homogeneous Porous Media: Theory. Transport in Porous Media, vol. 24, pp. 107-137 (1996).

[21] D. Lasseux, A. Ahmadi and A. A. A. Arani. Two-phase inertial flow in homogeneous porous media: A theoretical derivation of a macroscopic model. Transport in Porous Media, vol. 75, pp. 371-400 (2008).

[22] F. Duval, F. Fichot, M. Quintard. A local thermal non-equilibrium model for two-phase flows with phase-change in porous media. International Journal of Heat and Mass Transfert, vol. 47, pp.613-639 (2004).

[23] J. Ni, C. Beckermann. A Volume-Averaged Two-Phase Model for Transport Phenomena during Solidification. Metallurgical Transactions B, vol. 22, pp. 349-361 (1991).

[24] GDR MiDi. On dense granular flows. Eur. Phys. J. E 14, 341-365 (2004).

[25] J. P. Both, H. Derriennic, B. Morillon, J. C. Nimal. A Survey of TRIPOLI-4. Proceedings of the 8th International Conference on Radiation Shielding (ICRS), April, 24-28 1994, Arlington, TX (1994).

[26] Trio-CFD code, CEA. Available from: https://triocfd.cea.fr/Pages/Presentation/TRUST_plateform.aspx.

[27] X. Gaus-Liu, B. Bigot, C. Journeau, F. Payot, T. Cron, R. Clavier, M. Peybernes, P.-E.. Angeli, B. Fluhrer, Experimental and Numerical Simulations on SFR Core-Catcher Safety Analysis After Relocation of Corium. Proceedings of the International Conference on Fasts Reactors and Related Fuel Cycles FR22 (2022).

[28] B. Bigot, X. Gaus-Liu, R. Clavier, C. journeau, F. Payot, T. Cron, P-E. Angeli, M. Peybernes, B. Fluhrer, Experimental and Numerical Simulations on the SFR Core-Catcher Safety Analysis After Relocation of Corium. Proceedings of the 10th European Review Meeting on Severe Accident Research (ERMSAR 2022) (2022).

[29] J.M. Bonnet, and J.M. Seiler. Thermal Hydraulic Phenonena in Corium Pools: the BALI Experiment. ICONE-7. Tokyo, Japan. p. ICONE-7057 (1999).

[30] U. Steinberner and H.-H. Reinecke. Turbulent buoyancy convection heat transfer with internal heat sources. 6th International Hear Transfer Conference, Toronto, Canada (1978).

[31] R.R. Nourgaliev, T.N. Dinh, and B.R. Sehgal. Effect of fluid Prandtl number on heat transfer characteristics in internally heated liquid pools with Rayleigh numbers up to 1012. Nuclear Engineering and Design, 169(1), pp. 165–184 (1997).

SESSION IV

ACCIDENT ANALYSIS AND EXPERIMENTAL PROGRAMS FOR LEAD COOLED FAST REACTORS

Chairpersons

G. SCHEVENEELS
Belgium

S. GIANFELICI
Italy

DEVELOPMENT OF EXPERIMENTAL INFRASTRUCTURE FOR SEVERE ACCIDENTS INVESTIGATIONS IN SUPPORT OF ALFRED LICENSING PROCESS IN ROMANIA

M.CONSTANTIN[1], M. TARANTINO[2], G. GRASSO[3], D. GUGIU[1], D. DIAMANTI[2], I. DI PIAZZA[2] M. CARAMELLO[4], M. FRIGNANI[4], F. LODI[3], A. VALCU[1]

[1]RATEN ICN, Institute for Nuclear Research, Pitesti, Romania
[2]ENEA, FSN, Brasimone, Italy
[3]ENEA, FSN, Bologna, Italy
[4]ANSALDO Nucleare, Genova, Italy

Abstract

Lead fast reactor (LFR) technology is considered as the key option in Romania. The demonstrator of this technology, ALFRED (Advanced Lead Fast Reactor European Demonstrator) will be hosted by the country. Currently the project is in the preparation phase, including the pre-licensing activities aimed to create good conditions for the authorization phase. The pre-licensing phase was started in 2017. An important effort was dedicated to the improvement and enlargement of experimental facilities for LFRs in order to create the conditions for an extensive demonstration and authorization programme. Six large facilities were identified as necessary to be built on the reference site of ALFRED in Romania: ATHENA, ChemLab, HELENA-2, ELF, Hands-ON, and Meltin'Pot. ATHENA and ChemLab are in the construction phase, supported by a project funded by European structural funds (22 million Euro), and will be operational at the beginning of 2024. The other four facilities are approved to be funded and the implementation period is 2023–2026. For severe accident conditions, the analysis has concluded it is important to address, experimentally and analytically, the following issues: (1) fuel fragmentation and re-distribution in the melt, (2) fuel–coolant interaction, (3) fission products retention in lead, migration in the cover gas, gas and steam stripping phenomena, investigating the risk of release of radiotoxicity in the cover gas and potentially in the environment. The paper is focused on the experimental facilities and scientific programme devoted to the investigation of the phenomena associated with severe accident in pure lead environment, including the preparation of the conceptual design for the facilities grouped into the Meltin'Pot research infrastructure.

1. INTRODUCTION

The development of a nuclear power sector includes cutting-edge advanced reactor designs with high performance in terms of safety, economics, minimization of radioactive waste, resistance to proliferation, and adaptability to the new energy markets. Generation IV nuclear reactors includes six technologies: Sodium cooled fast reactor (SFR), Lead cooled fast reactor (LFR), gas cooled fast reactor (GFR), supercritical water reactor (SCWR), very high temperature reactor (VHTR), and molten salt reactor (MSR). In the Europe Union, the three first technologies are currently supported by ESNII (European Sustainable Nuclear Industry Initiative) [1]. After the conceptual design stage, a demonstrating phase is followed. The lead fast reactor (LFR) is very promising due to the properties of the lead coolant and the development of passive system solutions.

To demonstrate the technical and economic viability of LFRs, a demonstrator of 125 MW(e), ALFRED (Advanced Lead Fast Reactor European Demonstrator) was designed [2, 3]. In 2011, Romania expressed, by a government decision, the availability to host ALFRED. In 2013 an international consortium, FALCON, was set-up to coordinate the implementation in Romania. The existing nuclear platform in Mioveni is considered as the reference site due to some important advantages, such as the existing networks, proximity of specialists, use of existing nuclear facilities.

The envisaged financing scheme is based on a mix of European structural funds, national funds and contribution from industry. The implementation was structured into four phases: viability (dedicated to investigating the feasibility of implementation in Romania), preparatory,

construction, and operation [4]. The project is currently in the preparatory phase, with starting of the pre-licensing in 2017.

Based on the efforts of the FALCON consortium and of the ARCADIA project [5], a detailed investigation on the needs for the licensing process was performed. Additionally, the identification of the experimental activities to support the development of solutions for the open issues of LFR technology was considered. As a main outcome of these efforts, the definition of a set of new experimental facilities was done. These facilities are grouped into the LFR experimental infrastructure of the nuclear platform at Mioveni. The platform is in the construction process and will serve as the main experimental basis for the licensing of ALFRED.

2. LFR MAIN FEATURES

LFRs and the ALFRED demonstrator use a pure lead coolant, and pool configuration. Based on the inertness of the lead in relation with water and air, a very compact design is possible due to the elimination of the intermediate loop. The steam generators are directly installed inside the reactor vessel with a great reduction of the complexity of the primary system (Fig. 1). Consequently, there are no primary pipes to be considered in a LOCA type accident [6, 7].

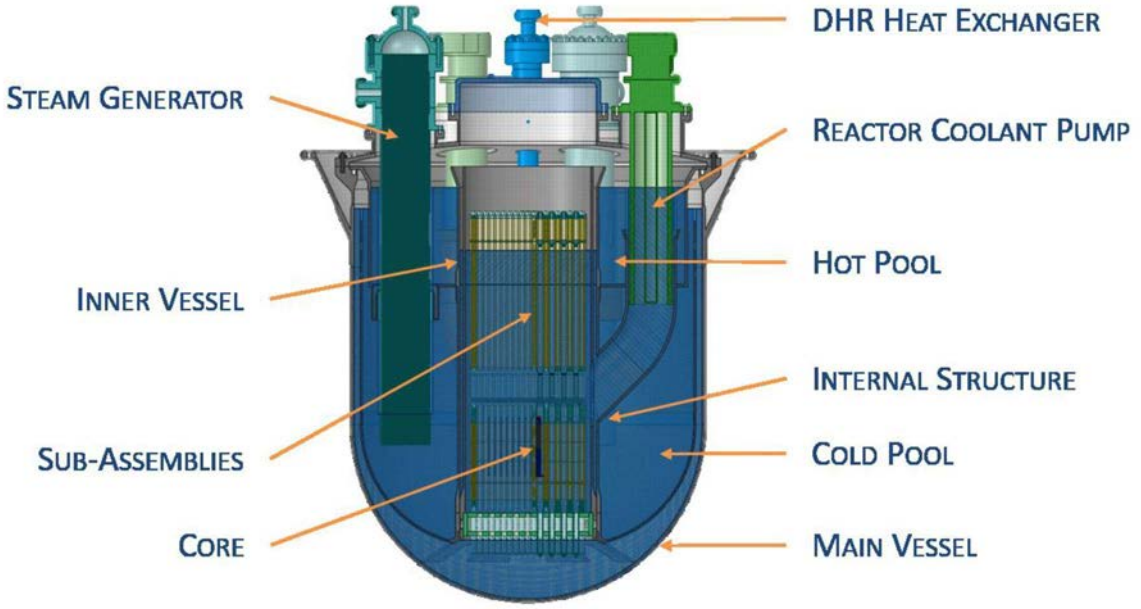

FIG. 1. Geometrical configuration of the ALFRED demonstrator.

Due to the absence of water in the primary system, in LFRs there are no hydrogen generation challenges (such as flammability, explosion or acceleration, or reaching the threshold pressure for containment failure). The primary system cannot affect the design pressure of the containment system.

In contrast to other coolants used for fast reactors, lead has a very low moderating power allowing a hard neutron spectrum and better conditions for circulation of the coolant, i.e.: (i) large flowrate at low velocity, (ii) low pressure drop, and (iii) effective natural convection. In addition, lead has low absorption cross-section, and the activation is highly reduced in

comparison with other coolants. As a consequence of the low moderating the fuel assemblies can have fuel rods spaced large apart.

With regard to postulated accidents, the good properties of lead in the retention of different fission products acts as a powerful component of the primary system barrier. In this way, the large amount of lead in the pool will prevent the dispersion of radionuclides in the containment. As a result, even in the case of a severe accident, the LFR is expected to have no impact on the environment outside the containment building.

Lead has a higher density than the oxide fuel (for example UO_2, 10.97 g/cm^3, lead, 11.34 g/cm^3). In accident conditions, any fuel fragments from fuel–coolant interaction, will be driven by a complex balance between buoyancy and transport forces, resulting in specific parts being collected in the upper part of the pool. Some simplifications appear, such as: no needs for a core catcher to deal with core melt, and no risk of re-criticality in the case of core melt. However, some complexity is introduced at the level of the control and safety rods handling system. In the ALFRED reactor, two independent systems are designed: (1) control rods (CRs) with injection from the bottom (CRs are extracted downward and rise up by buoyancy in case of scram), (2) safety rods (SRs) extracted upward and inserted downward against the buoyancy force. The absorber gets inserted by the actuation of a pneumatic system. In case of loss of this system, a tungsten ballast will force the absorber down by gravity in a slow insertion.

Lead has a high boiling point (1745^0C) and low vapour pressure ($3 \cdot 10^{-5}$ Pa, at 400°C) creating better conditions to avoid a severe accident. However, the melting point (327.5°C) of lead may introduce concerns in relation to the possibility of freezing of the coolant in conditions of an excess of heat extracted from the primary system by an abnormal functioning of the secondary system. However, such concerns are more connected to economics, not safety.

For LFR technology, one of the most important concerns is related to the formation of polonium by activation. The effect is important in the case of the use of lead-bismuth eutectic (referred as LBE technology) as coolant. It is not the case for ALFRED, but it should be noted that bismuth remains as an impurity in pure lead and may produce ^{210}Po. Even if bismuth-free lead is used, the formation of polonium remains possible. It may be produced (in a very reduced amount) after an extended operation time of the reactor because of the bismuth generation by the (n, gamma) reaction with ^{208}Pb (52.3% abundance).

Finally, it should be noted that lead has an chemical toxicity. It can accumulate in the body and cause serious health problems. Lead and its compounds are toxic and are retained by the body, accumulating over a long period of time (cumulative poisoning, until a lethal quantity is reached). There are narrow limits already established for the maximum allowed concentrations in the bodies of adults and children [8].

3. EXPERIMENTAL INFRASTRUCTURE FOR ALFRED AND LFR

An important experimental effort is planned for the licensing process of ALFRED, consisting of testing of materials, components and equipment, demonstration of full control of the phenomena, qualification activities, validation and verification of computer codes. Additionally, the infrastructure will support R&D efforts addressing open issues of LFR technology, including studies on materials, corrosion, erosion and degradation of structural materials, pool thermohydraulics, fuel assembly thermohydraulics in normal and postulated accident conditions, chemistry of the coolant and of the cover gas. A very stringent issue for the nuclear community of fast reactors is the need to investigate irradiated structural materials.

The siting of ALFRED at the Mioveni nuclear platform will allow the efficient use of the existing facilities, such as the research reactors and post-irradiation laboratories, and the LFR experimental facilities and the demonstrator itself.

The LFR experimental infrastructure consists of the following facilities: (1) ATHENA, a large pool to test the main components in different thermohydraulic regimes; (2) ChemLab, a chemistry laboratory coupled with ATHENA to investigate lead and cover gas chemistry; (3) HELENA2, a loop type facility to test components and equipment in relevant thermohydraulic conditions, in particular, the ALFRED hottest fuel assembly; (4) ELF, a large scale pool-type facility, to test the endurance and reliability under both forced circulation and natural circulation regimes; (5) HandsOn, a pool-type experimental facility, to demonstrate the fuel handling of fuel assemblies; and (6) Meltin'Pot, a set of facilities to investigate severe accident phenomena.

The experimental infrastructure and, at a later stage, the ALFRED demonstrator itself, will be highly valuable to the scientific and technological communities due to the expected valuable and representative experimental data. From this perspective, there is a crucial need for the management of the information associated with the experimental data. This need is not only expressed by the FALCON consortium, but also by the international R&D organizations that will be involved in the cooperation programmes stemming from the availability of the ALFRED infrastructure. In such context, the appropriate solution is to build a coordination centre (entitled Hub) to support of the scientific management of the experimental infrastructure. The Hub will ensure centralized services for the management of all the experimental data resulting from the operation of the LFR experimental infrastructure, including the hosting of the related logistics. The LFR experimental facility will be operated in the option of open access allowing the participation of international projects and scientists based on their applications.

The selection of the appropriate site for these experimental facilities was based on the following criteria: (1) proximity of the existing networks, (2) grouping in a cluster for all the installations using common services, (3) using of existing buildings and facilities of the platform. A siting with four experimental facilities grouped in a cluster and two in existing buildings was the result. The cluster is formed by ATHENA, ChemLab, HELENA2, and ELF, together with an auxiliary building to supply common services. Meltin'Pot will be hosted by the hot cells of the Post-Irradiation Laboratory. HandsON will use the existing tower of the out-of-pile testing department (see Fig. 2).

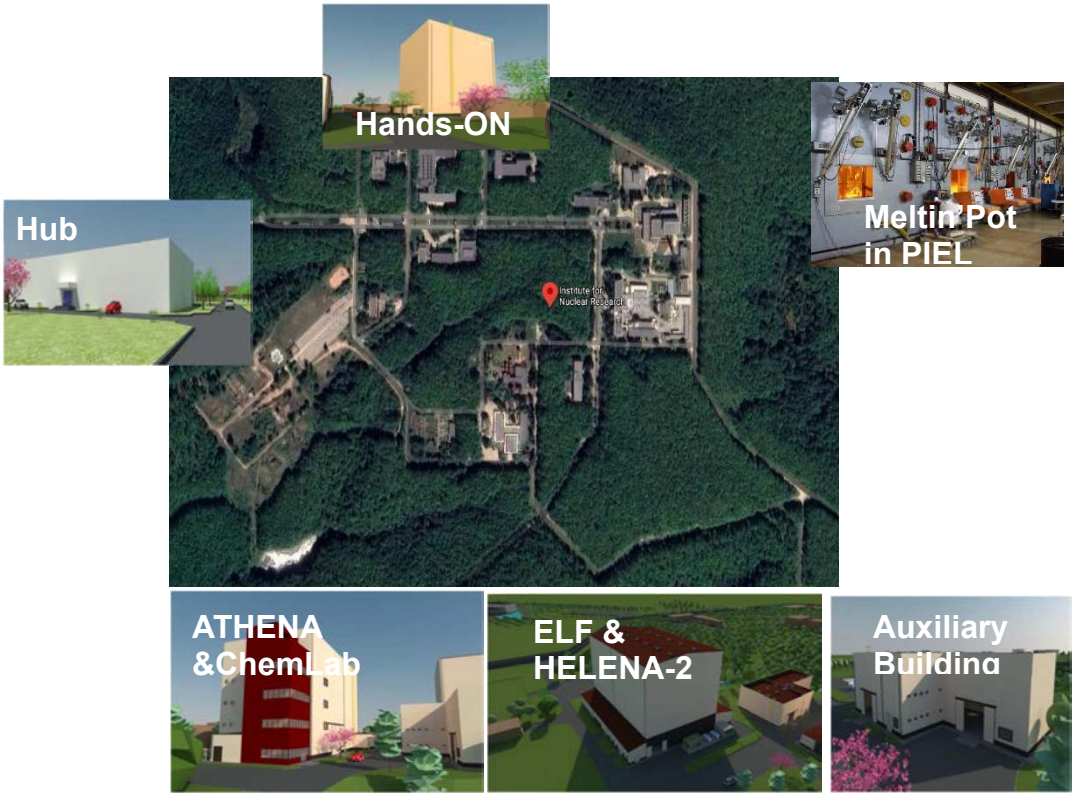

FIG. 2. Siting of the components of the LFR experimental infrastructure.

ATHENA and ChemLab are in the construction phase, based on a European structural funds project (22 MEuro). The facilities are planned to be operational mid-2024. For the other four facilities, an important effort was performed by the national support (PRO-ALFRED project, supported by Ministry of Education and Research, approx. 2.5 MEuro) with the main outcome the achievement of the conceptual design and supporting documentation for future applications. In 2022 the four facilities were accepted to be financed by the European programme POCIDIF (Operational Program Smart Growth, Digitization and Financial Instruments), with a total sum of 105 MEuro. According with the planning the facilities will be operational at the end of 2027.

4. SOME CONSIDERATION ON SEVERE ACCIDENTS IN THE LFR SYSTEMS

According with the provisional System Steering Committee of GIF [9], LFR technology can demonstrate excellent safety features to avoid a set of severe accident scenarios. However, even if the probabilities are very low, any licensing process will consider them in the analysis. Demonstrations should be performed to understand the different phenomena, their interconnections, and to collect experimental data to build the necessary knowledge.

Form the point of view of the relevant scenarios for severe accidents it should be noted:

(1) LFR is very resilient to an extended blackout condition; this capability is offered by the natural circulation capabilities in primary configuration, and by the passively operated Decay Heat Removal (DHR) system with long grace; in such circumstances, LFR does not need backup power.

(2) The loss of primary coolant (LOCA) is very improbable in an LFR due to the low operating pressures, and the pool configuration with double structure vessels (Fig. 3). Even in the event

of a failure of the reactor vessel, the guard vessel will keep the lead inside. The solidification of lead below 327°C facilitates the stopping of any leakage.

(3) The oxidation of the cladding by steam, an important phenomenon with high impact in the acceleration of severe accidents in water cooled reactors, is not present in LFR; hydrogen generation does not occur in the LFR containment.

(4) A steam generator tube rupture (SGTR) introduces some concerns and needs investigating. The entrance of the high pressure steam in the primary circuits may produce pressure waves and bubbles with consequences that need to be clarified by experiments [10].

(5) Special attention should be devoted to possible coolant flow blockage, generated mainly by corrosion and erosion of the materials. Such a situation may produce hot spots and the issue has to be clearly documented and the impacts determined. Presently, the approach was a drastic reduction of the corrosion by limiting the cold coolant temperature to below 450°C, and the use of coatings for sensitive components exposed at high temperature. The issue of erosion is approached by limiting the lead velocity to a maximum of 2.0 m/s.

(6) Similar concerns to those for water cooled reactors remain for severe accidents connected with the spent fuel pool (SFP), such as the loss of cooling.

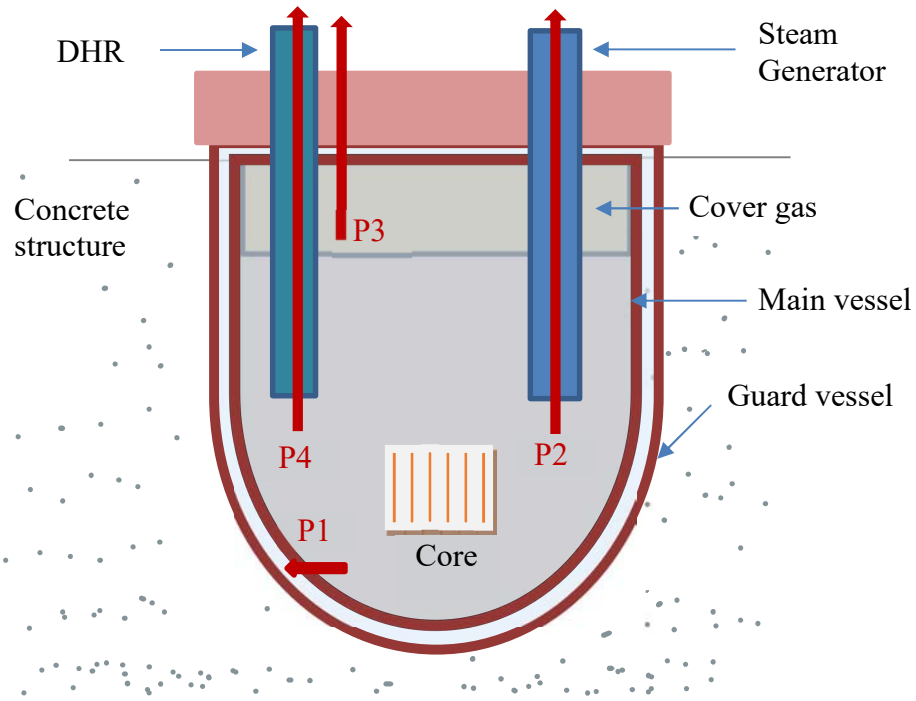

FIG. 3. Main hypothetical release paths in LFR systems.

(P1) main vessel rupture, (P2) SG tube rupture, (P3) top vessel penetrations failure, (P4) DHR rupture

(7) in Fig. 3 the hypothetical paths for the release are presented; the first path consists of the failure of the main vessel and transfer of lead and a part of source term in the gap between the reactor vessel and guard vessel; the second consists of the rupture of the tubes of the steam generator; the third is the rupture of the DHR; the fourth consists of the accidental opening of

top vessel penetrations. Even low probable all of the paths should be considered in the future analysis.

The high boiling point of pure lead (1780°C) makes voiding of the core, through coolant boiling, very unlikely. Also, the low operating pressures contribute to a reduction of the risk of a LOCA. On the other hand, the natural circulation capacity of pure lead and configuration is excellent [11], offering enough capacity to evacuate the heat during a loss of forced pumping power.

The numerical simulations [11] of the entire spectrum of accidents under design extension conditions performed by using RELAP5, CATHARE, SIM-LFR, TRACE, and SPECTRA computer codes didn't predict any clad failure excepting "the unprotected fuel assembly flow area blockage greater than ~85%, which might be excluded by design (many orifices at the FA inlet)". On the other hand, for all the investigated accidents, the simulations show enough grace time for corrective operator actions, and it was concluded that for "all analysed unprotected transients there is no risk for significant core damage and then for transient evolution towards severe accidents" [11].

However, there are uncertainties concerning: (1) the materials (including existing coatings) behaviour under corrosion and erosion phenomena at higher temperatures higher than 600°C and lead velocity greater than 2.5 m/s, (2) consequences of steam generator tube rupture with pressure waves induced in the lead and steam bubbles movement, (3) severe blockage of the cooling producing local damage of the cladding and initiating the interaction between lead and fuel.

Since the fast reactors are not designed in the most reactive configuration, re-criticality is a significant issue, and any fuel relocation should be evaluated. Due to the great differences in the melting temperatures of lead, clad material and fuel the release of solid fuel fragments is possible before lead boiling. It introduces the need for re-criticality evaluation. The blockage of an assembly is considered the reference scenario initiating the core degradation [12].

Considering the previous elements and the discussions generated by the pre-licensing process, some needs for experimental activities are defined as following: (1) fuel fragmentation due to interaction with the lead coolant, (2) the resulting typical configuration of fragments released into the lead pool, (3) retention in a large pool of lead, deposition and transport of fission products (FP) to the cover gas, (4) chemistry of FP in the lead pool and cover gas, and transport of different species, (5) polonium formation in the large pure lead pool and the transport to cover gas, and (6) interaction between stem and lead.

The next section is devoted to present the experimental configurations aimed to cover the identified needs.

5. CONCEPTUAL DESIGN OF LFR FACILITIES FOR SEVERE ACCIDENTS INVESTIGATION

Even if it is challenging to imagine severe accident scenarios for the ALFRED design, some demonstrations for the licensing process are compulsory to prove there are no paths to severe accidents, or that passive systems can prevent such accidents. At the same time, experimental data for the supposed dangerous situations should be collected to be used in the computational models for severe accident simulation.

Taking into consideration the main phenomena that appear in accident conditions and hypothetical severe accident scenarios, a set of facilities are defined, called Meltin'Pot. The main objective of Meltin'Pot is to provide a suitable experimental configurations to investigate: (1) fuel–coolant interaction, (2) fuel dispersion and relocation in a severe accident scenario, (3) retention of fission products (PF) in lead and/or migration in the cover gases, (4) retention of polonium isotopes in molten lead, (5) interaction of FP with water vapour and cover gas, (6) stripping of polonium in the cover gas.

Meltin'Pot consists of four experimental modules that operate independently of each other aimed to investigate:

- (M1) Fuel–coolant interaction;
- (M2) Fuel fragmentation and relocation;
- (M3) Fission products transport and retention;
- (M4) Polonium retention and dispersion.

The modules will be designed to be hosted inside dedicated post-irradiation cells (among those existing in the Post Irradiation Examination Laboratory (PIEL) of RATEN ICN) or to be operated in a glovebox located in a non-nuclear area. The experimental modules can be introduced into the cell after irradiation with the help of the crane and by placing/mounting in the cell with the help of the remote handling system, which is part of the cell. Also, the existing cell penetrations will be used for the cables of the required sensors. Some initial constraints were defined based on the existing configuration of the hot cells and their possibilities for instrumentation and manipulation.

All of the modules will operate with nuclear-grade lead to investigate the main phenomena associated with severe accidents, such as the fragmentation and dispersion of the fuel, deposition and transfer of FP. The target is to obtain the experimental data needed to be used in the qualification of simulation tools for severe accidents and also for the correct understanding of phenomena and the development of reports for the regulator.

In addition to the four installations, two storage tanks will be located inside the hot cell: (1) the lead storage tank that supplies the experiments, (2) the drain and storage tank that will collect the contaminated lead resulting from experiments.

The tanks are permanently installed in the hot cell and are connected hydraulically, at different times, to the modules, by means of quick connection/disconnection systems. A shield for radiation protection is provided for the exhaust tank. The operating conditions will cover the applicable operating modes of the ALFRED demonstration reactor.

The main challenge is connected with the complexity of severe accident phenomena. During such accidents, different phenomena occur. Moreover, the phenomena are strongly interconnected. Therefore, suitable solutions are to be developed to reduce the complexity (separate effect facilities), but without diminishing the value of experimental data for the characterization of a real accident. From this perspective, the modular solution (four independent modules/small facilities) was chosen. The second challenge is the work in a radioactive environment. For this purpose, three modules will be placed in hot cells of the post irradiation laboratory. The third challenge is the experimental acquisition of data and the

experimental configuration, by adequate sensors/detectors and signals, together with their transfer from hot cells to the computers placed outside.

5.1 M1, Fuel–coolant interaction

The first module is devoted to investigating the chemical interaction between the fuel and the lead coolant. The experimental facility consists of a main vessel containing 10 l of pure lead, operating in a temperature range of 400–750°C, having a cover gas (argon) system (Fig. 4). The small size was chosen due to the contamination of the lead and the need to replace it after each experiment, while being large enough to accommodate the device for the injection of irradiated MOX fuel pellets.

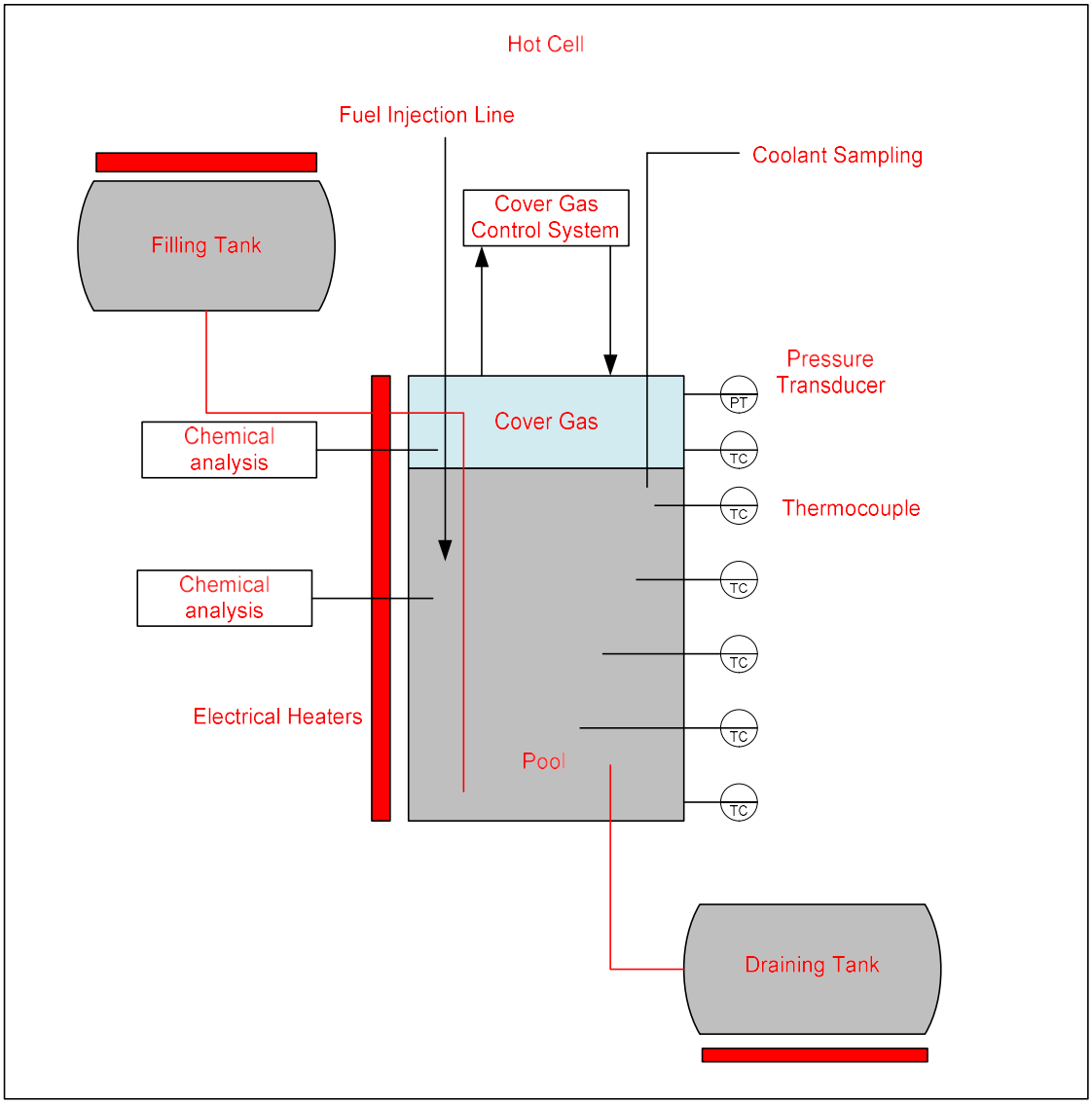

FIG. 4. Meltin'Pot Module 1, Fuel–coolant interaction.

Two storage tanks are used for operational purposes, the first one for filling, and the second for the storage of the contaminated lead from the experiments. A heating system of the main vessel is used to reach the lead temperature range required for the experiments. The facility has dedicated systems for the injection of fuel pellets inside the main vessel device and to keep them in fixed positions and a system to control the oxygen concentration in the lead between 10^{-7} and 10^{-8} %w.

The main vessel, the two storage tanks and the filling and draining lines (i.e. piping and valves) are thermally insulated to minimize the heat losses to the environment and equipped with electrical heating cables, installed on the bottom and lateral surfaces, in order to avoid cold points for the freezing of the lead.

Instrumentation will be installed to allow the control of the operational parameters: (1) bulk thermocouples for monitoring the temperature in the lead and cover gas, (2) wall thermocouples for the temperature on the vessel, storage tanks and walls of the pipes, (3) pressure transducers for the pressure inside the cover gas. Various instrumentation is added to collect the experimental data to characterize the interaction between fuel and coolant such as: X ray diffraction, optical microscopy, scanning electron microscopy, gas chromatography, inductively coupled plasma mass spectrometry (for lead samples), quadrupole-mass spectrometer gas analyser (for gas chemical composition), energy dispersive X ray spectroscopy.

5.2 M2, Fuel fragmentation and relocation

The second module is dedicated to the investigation of fuel fragmentation and relocation of the fragments in the coolant. Since the objective is to work both with fresh and irradiated fuel, M2 is placed in hot cells.

The main part of the facility consists of a slab representing a slice of the vessel, filled with lead, in which the reactions of interest take place (Fig. 5). The volume of lead is about 5 l. A cover gas (argon) system is used controlling the pressure and the composition for the gas. The temperature range for the experiments (400–750°C) is obtained and controlled by electrical heating cables.

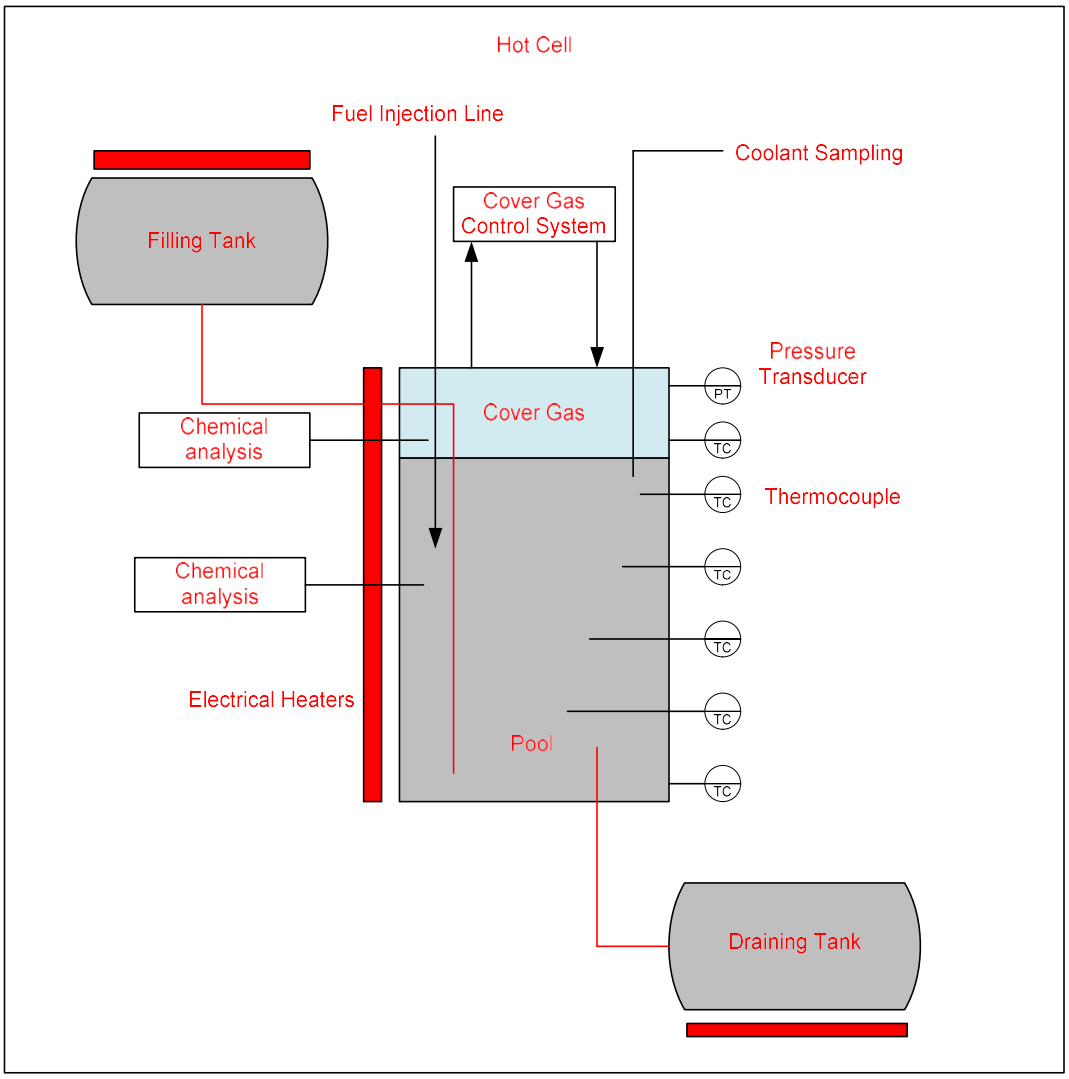

FIG. 5. Meltin'Pot Module 2, Fuel fragmentation and relocation.

Two storage tanks, one for filling the main volume with pure lead, the other for the draining of contaminated lead, are used. The slab, the two storage tanks and the filling and draining lines are thermally insulated to minimize the heat losses to the environment.

A dedicated system is used to inject the fuel inside the slab.

Instrumentation will be installed to allow the control of the operational parameters: (1) bulk thermocouples for monitoring the temperature in the lead and cover gas, (2) wall thermocouples for the temperature on the slab, storage tanks and walls of the pipes, (3) pressure transducers for the pressure inside the cover gas. Various instrumentation is used for the experimental data acquisition such as gamma scanning for monitoring the fuel concentration and deposition along the slab and/or dispersed in the lead.

5.3 M3, Fission products transport and retention

The third module is devoted to experimental investigation of FP retention in the lead, deposition on the structures, and transport to the cover gas. The use of stable isotopes, representing the

radioactive FP, is foreseen. In such conditions the module can be hosted in a glovebox, outside of the hot cell.

The main part of the facility (Fig. 6) consists of a small vessel (about 5 l) filled with lead and covered by a cover gas system (argon) able to control the pressure and its chemical composition. The facility will work in the temperature range of 400–750°C with the aid of an electrical system consisting of heating cables.

Similar with the other modules, two storage tanks, one for filling the main volume with pure lead, the other for the draining of contaminated lead, are used. A dedicated system is responsible with for the injection of isotopes inside the vessel.

For the control of operational parameters the facility will use: (1) bulk and wall thermocouples for monitoring the temperature in the lead and cover gas, and the temperature on the vessel, storage tanks and piping walls, (2) pressure transducers for monitoring pressure inside the cover gas. Scanning electron microscopy (SEM), gas chromatography, X ray powder diffraction (XRD), mass spectrometry, differential scanning calorimetry (DSC) will be used to obtain the envisaged experimental data.

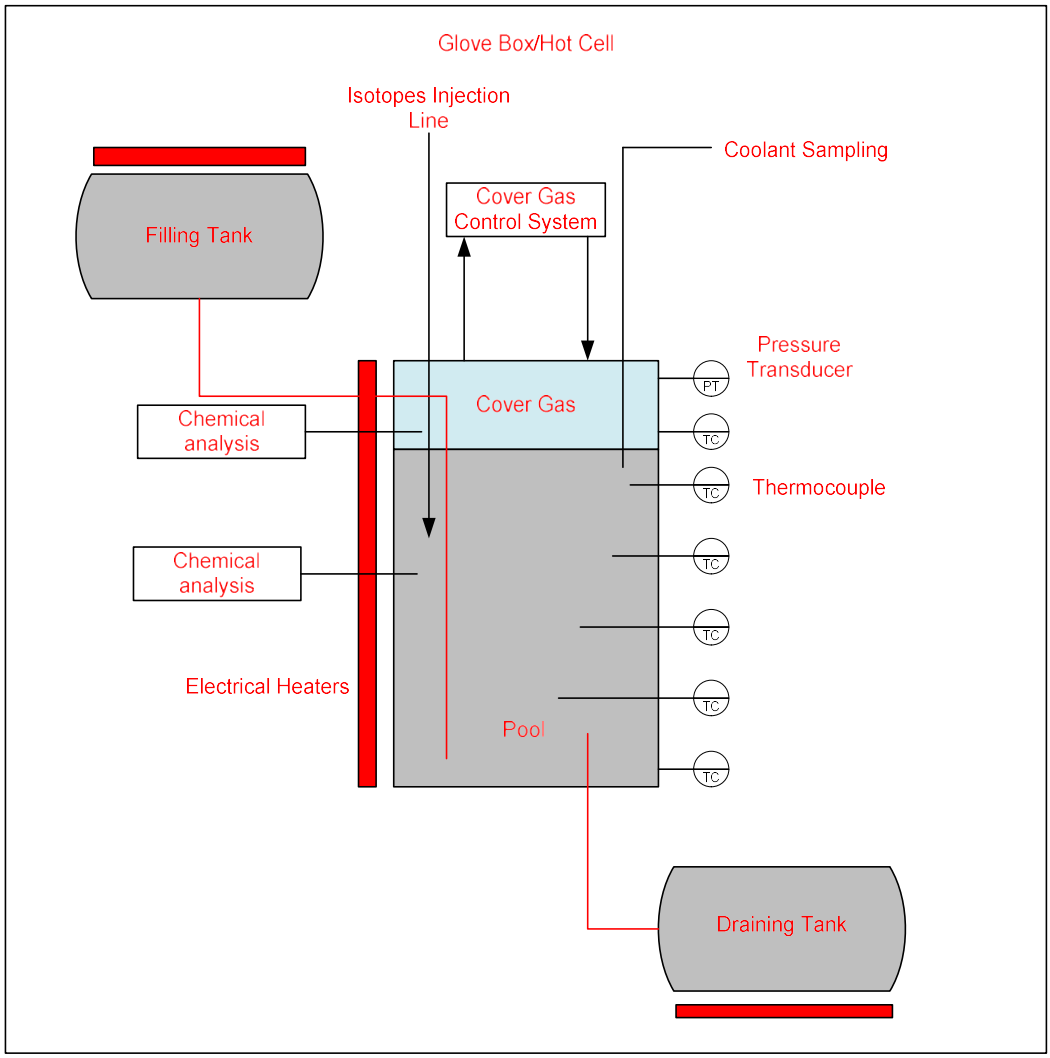

FIG. 6. Meltin'Pot Module 3, Fission products transport and retention.

5.4 M4, Polonium retention and dispersion

The fourth facility is designed for polonium formation, its retention in lead, and the transport to the cover gas. The volatility at different Po concentrations in lead will be investigated in order to obtain the necessary knowledge for the behaviour of Po in the ALFRED configuration. A water loop and a gas loop will be available to be connected to the lead pool in order to investigate the influence of water (steam) and gas (Ar) on the volatilization of Po isotopes in lead by stripping.

The facility (Fig. 7) has a main vessel of small volume, about 5 l, filled with pure lead and covered by a gas system (Argon). The range of operational temperatures is 400–750°C. A heating system consisting of electrical cables is used. Similar with the configuration of the other modules, two tanks will ensure the filling, respectively the storage of contaminated lead.

A dedicated system is used for the injection of the Po inside the lead of the main vessel. For the control of operational parameters, bulk and wall thermocouples will be used for monitoring the temperature (lead, cover, tanks, walls of pipes) and transducers for monitoring pressure inside the cover gas. Various instrumentation for chemical analysis of the lead and of the cover gas, e.g. scanning electron microscopy (SEM), gas chromatography, X ray powder diffraction (XRD), mass spectrometry, differential scanning calorimetry (DSC), thermochromatography (TC), will be used, together with instrumentation for the dose measurement to take into account the capability of lead to shield polonium decay.

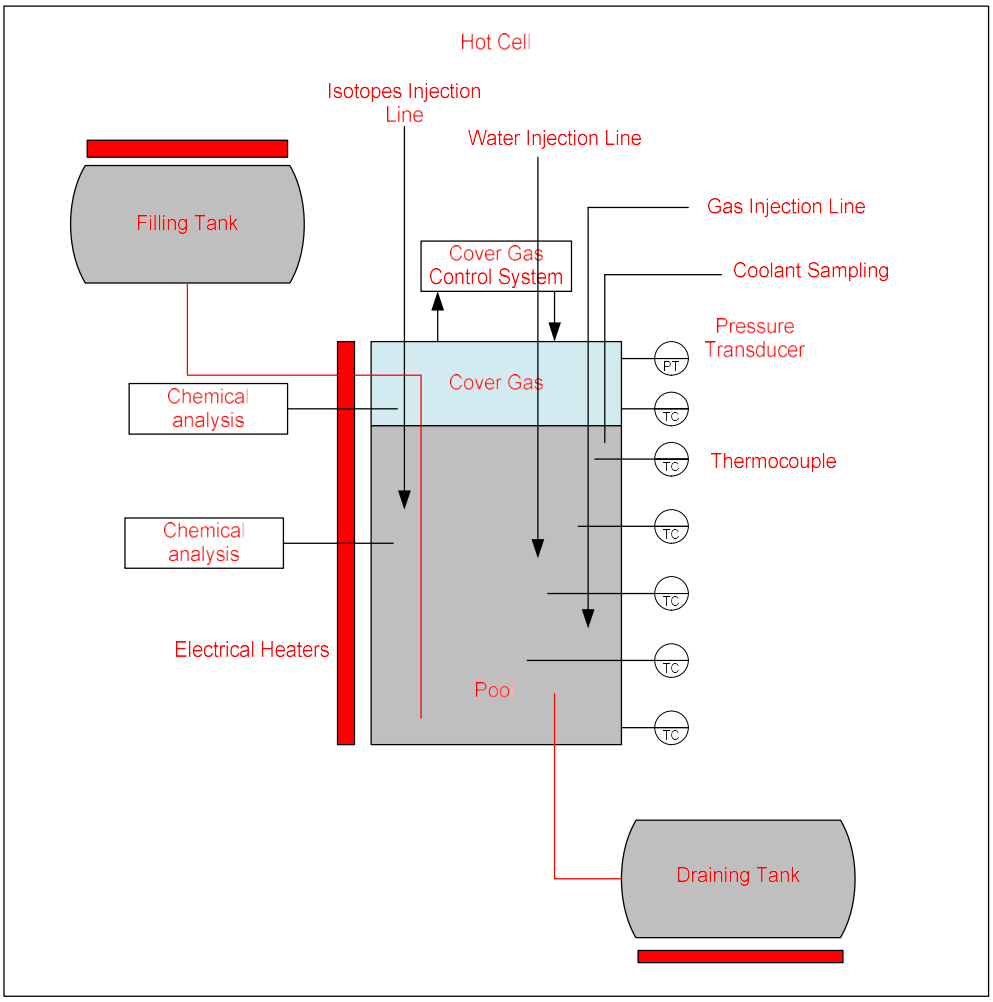

FIG. 7. Meltin'Pot Module 4, Polonium retention and dispersion.

6. EXPERIMENTAL PROGRAMME

The design and construction of all the four modules of the Meltin'Pot facility will provide suitable experimental configurations to investigate:

(1) Fuel–coolant interaction (Module 1) – to obtain experimental data on: the fuel integrity, the interaction compounds formed and their quantities, how the fuel and cladding microstructures are affected by interaction as well information about fuel composition after its interaction with the molten lead.

(2) Fuel dispersion and relocation in a severe accident scenario (Module 2) – to obtain experimental data on: the distribution of fresh MOX fuel fragments in lead as well as on irradiated fuel fragments dispersion in lead (for various burnup levels) to understand the fuel dispersion behaviour which may lead to re-criticality and the influence on the heat removal under core damage conditions.

(3) Fission products (FP) dispersion/retention in lead and/or their migration in the cover gas (Module 3) - to obtain data on: the retention of fission/activation products in lead, on the migration of volatile elements in the cover gas, the chemical form of the volatile elements in lead and/or cover gas, the kinetics of the fission/activation products in liquid lead as well as

data on the solubility of other elements that form different species (e.g. Fe, oxides of the structural materials, etc.).

(4) Polonium isotopes' retention/dispersion in molten lead (Module 4)– to obtain experimental data on: the retention of Po in lead, on its volatilisation in the cover gas, on the kinetics of different Po forms in liquid lead as well as data on the volatilisation of Po isotopes in lead by steam stripping and by Ar gas stripping.

It is planned that the four facilities will be operational at the end of 2026. A preliminary scientific programme was defined in 2022. It will be detailed and harmonized with the evolution from the conceptual to the detailed design.

The preliminary scientific programme supposes a stepwise approach. The experiments will start by using fresh fuel (uranium oxide and MOX) and, in a second stage, irradiated fuel, at different burnup levels (from 10 MWd/kg to 100 MWd/kg). The different phenomena will be investigated at different temperatures (at least 5) relevant for the ALFRED demonstrator in the range 400–750^{0}C.

The fuel fragmentation and the resulting configurations of fragments are planned to elucidate the re-criticality issue. Later the compatibility of lead coolant with advanced fuels (for example uranium nitride) will be investigated to understand the potential for the development of future LFRs.

The experimental data on the retention capabilities of lead are crucial for the construction of realistic simulation computer codes to be used in further investigations on severe accidents. The existing theoretical evaluations should be completed by the use of more accurate experimental data on the retention of the radionuclides in pure lead under representative temperature and oxygen concentration. Special attention will be given to the toxicity of the lead produced by the retention process, and in this context to the development of appropriate techniques for the cleaning of components extracted from the coolant.

The analysis of the existing codes and models will provide the necessary support to decide which is the most suitable. Additionally, the discussions with code developers will be important in making a final decision.

7. CONCLUSIONS

(1) Based on an extensive analysis for the expected needs of ALFRED licencing process and for the estimated R&D activities devoted to the open issues of LFR technology, looking to the capabilities of the existing experimental facilities and also to their availability, a set of six large experimental installations was defined to be built at the Mioveni nuclear platform, the reference site for the LFR demonstrator. The installations are grouped in the LFR experimental infrastructure and will be served by a Hub for the coordination of the activities.

(2) Special attention was given to the identification of the phenomena relevant to the hypothetical conditions of severe accidents. A dedicated facility, Meltin'Pot, consisting of four modules, was defined with the role to create the necessary knowledge to be integrated in the analysis and in the computer codes. The modules are dedicated to the investigation of fuel-coolant interaction, fragmentation of fuel and configurations of fragments in the lead pool, retention and transport of radionuclides in pure lead, and polonium formation, chemistry and transport in the lead environment and cover gas.

(3) The construction of experimental infrastructure was started in 2020 with the ATHENA large pool facility and the coupled chemistry laboratory, ChemLab based on a project supported by European structural fund programme. The facilities will be operational in 2024. The other four facilities, including the modules of Meltin'Pot are grouped in a second project approved to be financed by structural funds (POCIDIF), with 2026 as the planned operational stage. In 2027 the first set of experiments will be supported by POCIDIF.

(4) The conceptual design of facilities ELF, HELENA2, HandsOn, and Meltin'Pot was produced based on the national PRO-ALFRED project. The technical design is a part of the POCIDIF project. A preliminary experimental programme was drafted in support of the clarifications for the instrumentation and data acquisition. This programme will evolve with the progressing of the design. It is expected to be finalised at the end of 2025.

(5) Meltin'Pot will offer significant possibilities to improve existing knowledge on some relevant phenomena associated with severe accident conditions in a pure lead environment. The experimental data will be complementary with the data collected for a lead-bismuth environment.

REFERENCES

[1] ESNII, European Sustainable Nuclear Industrial Initiative, ESNII Vision paper (2021).

[2] LEADER: Lead-cooled European Advanced DEmonstration Reactor. FP7 Project 249668, www.leader-fp7.eu.

[3] ALEMBERTI, A., et al, The European Lead Fast Reactor Strategy and the Roadmap for ALFRED Demonstrator, Int. Conference on Fast Reactors and Related Fuel Cycles (FR13), Paris (2013).

[4] FALCON Consortium, The Action Plan (2016).

[5] ARCADIA (Assessment of Regional Capabilities for New Reactors Development through an Integrated Approach) Euratom-FP7 project, arcadiaproject.eu.

[6] ALEMBERTI, A., et al, ALFRED reactor coolant system design, Nuclear Engineering and Design (2020).

[7] GRASSO, G., et al, An improved design for the ALFRED core. In International Congress on Advances in Nuclear Power Plants (ICAPP 2019), Juan-les-pins, France, May 12-15, 2019 (2019).

[8] LATIF WANI, A., et al, Lead toxicity: a review, Interdisciplinary Toxicology, 8(2): 55–64, (2015).

[9] ALEMBERTI, A., et al., Lead-cooled Fast Reactor (LFR) Risk and Safety Assessment White Paper, GIF, LFR-provisional System Steering Committee (pSSC) (2014).

[10] CARLSSON J, TUCEK K, WIDER H. Severe Accident Considerations for the Lead-Cooled Fast Reactor. In Conference Proceedings: Proceeding of ANS Winter Meeting 2007. La Grange Park (United States of America): American Nuclear Society – ANS, p. 1-2. JRC43300 (2007).

[11] BANDINI G. et al, Safety Analysis Results of Representative DEC Accidental Transients for the ALFRED Reactor, International Conference on Fast Reactors and Related Fuel Cycles: Safe Technologies and Sustainable Scenarios (FR13) (2013).

[12] WANG Z. et al, Preliminary simulation of fuel dispersion in a Lead-Bismuth Eutectic (LBE)-cooled research reactor, Progress in Nuclear Energy, Volume 85, pp 337-343 (2015).

MODELLING OF THE LEAD COOLED FAST REACTOR ACCIDENTS WITH THE EUCLID/V2 MULTIPHYSICS CODE

D.P. VEPREV

Nuclear Safety Institute of the Russian Academy of Sciences (IBRAE RAN)
Moscow, Russian Federation

Ya.V. GRUDTSYN, N.A. MOSUNOVA
Nuclear Safety Institute of the Russian Academy of Sciences (IBRAE RAN)
Moscow, Russian Federation

Abstract

The EUCLID/V2 multiphysics computer code is designed for the safety analysis and justification of the new generation NPPs with liquid metal cooled (with sodium, lead or lead-bismuth coolant) fast reactors under normal operating conditions, anticipated operational occurrences, design basis and beyond design basis accidents, including severe accidents. BREST-OD-300 is the Russian project of the test and demonstration lead cooled fast reactor facility. The BREST-OD-300 high pressure steam drum depressurization with additional failures in the safety system of the primary and secondary loops has been modelled by means of the EUCLID/V2 code. In this beyond design basis accident the high pressure steam drum depressurizes, which results in an increase of steam flow and consequently an increase of heat removal from the primary loop with the lead coolant freezing in the steam generators. It has been shown that at the beginning of the scenario the lead coolant temperature in the steam generators decreases to the lead coolant freezing point and the solid lead formation starts on the heat exchange tube surfaces. After a while the solid lead occupies most of the flow area at some axial sections in the steam generators. When scram happens and the reactor pumps shutdown the core outlet temperature falls but then begins to rise. The peak cladding temperature increases by 109 K but does not exceed design limits and radiological consequences are absent.

1. INTRODUCTION

The Russian development strategy for nuclear power engineering proposes a transition to a two-component nuclear power structure including thermal and fast reactors with a closed nuclear fuel cycle [1]. The key milestones of the development of two-component nuclear power are:

- Completion of research work on the BN-1200M reactor;
- Development of the pilot demonstration energy complex including the BREST-OD-300 reactor facility, the fuel fabrication/refabrication facility and the reprocessing facility.

For mathematical modelling of the BREST-OD-300 and BN-1200M innovative fast reactor facilities with liquid metal coolants, the EUCLID multiphysics code is being developed under the project “Codes of a new generation” [2]. The code has two versions: the first (EUCLID/V1) and the second (EUCLID/V2). EUCLID/V1 is designed to simulate normal operating conditions, anticipated operational occurrences and the initial stages of accidents. EUCLID/V2 is aimed at modelling of severe accidents with disruption of the core and release of radioactivity into the environment.

The paper presents the results of simulation of the BREST-OD-300 high pressure steam drum depressurization accident with additional failures in the safety system of the primary and secondary loops by means of the EUCLID/V2 multiphysics code.

2. EUCLID/V2 MULTIPHYSICS CODE

The EUCLID/V2 multiphysics computer code is designed for the safety analysis and justification of the new generation NPPs with liquid metal cooled (with sodium, lead or lead-bismuth coolant) fast reactors under normal operating conditions, anticipated operational

occurrences, design basis and beyond design basis accidents, including severe accidents [3, 4]. The EUCLID/V2 code includes the modules responsible for modelling of:

- Thermohydraulics, including steam generator tube rupture of a reactor facility with lead coolant, lead freezing (HYDRA-IBRAE/LM and CELSIST);
- Neutronics (DN3D/CORNER);
- Processes in fuel rods (BERKUT);
- Burnup and decay heat (BPSD);
- Fission, activation and corrosion products transport in the primary loop and gas system of a reactor facility (AEROSOL-LM);
- Tritium migration (TRITIUM);
- Solid phase impurities transport in the primary loop of a reactor facility with the heavy liquid metal coolant (OXID);
- Lead melt–concrete and corium–concrete interaction (CORCONIT);
- Fission product source in the primary loop (BERKUT);
- Fuel rod and core disruption including nitride fuel dissociation (SAFR);
- Secondary criticality (SECRIT);
- Corium in-vessel retention (HEFEST-FR);
- Mass transfer and fission product transport in the reactor containment compartments (HYDRA-IBRAE/LM with AEROSOL-LM);
- Offsite radiological situation (ROM).

The verification and validation of the above modules have been carried out using analytical and numerical tests and experimental results.

The EUCLID/V2 multiphysics code structure is presented in Fig. 1.

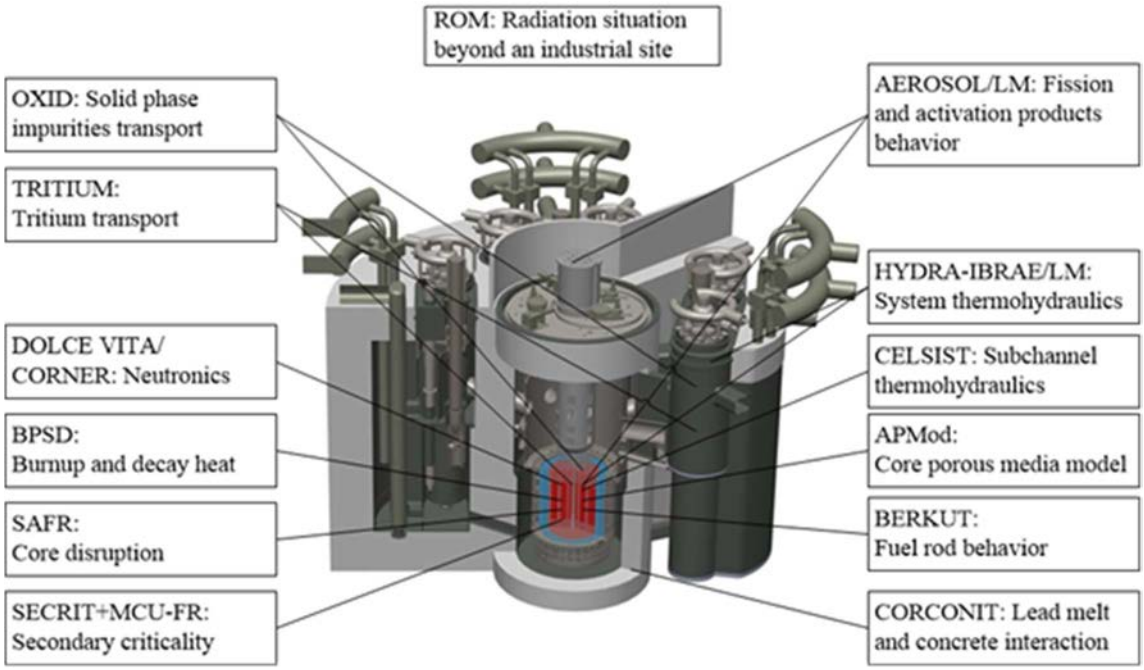

FIG. 1. EUCLID/V2 multiphysics code structure.

3. BREST-OD-300 REACTOR FACILITY

BREST-OD-300 is the Russian project of the test and demonstration lead cooled fast reactor facility [5]. BREST-OD-300 has an integral layout: the primary circuit equipment is located in the central and four peripheral cavities of the metal–concrete vessel. The primary circuit has four hydraulically identical loops. The central cavity contains the core with the side reflector, the control and protection system elements, the storage of spent fuel assemblies, and the core barrel. Steam generators, reactor pumps, heat exchangers of the emergency heat removal system, and other auxiliary equipment are situated in the peripheral cavities. The circulation of lead coolant is performed due to the difference of lead levels in the central and peripheral cavities created by the reactor pumps. Mixed uranium-plutonium nitride is used as nuclear fuel. Fuel rod claddings are made of low-swelling ferrite-martensitic steel. Fuel rods are bundled in jacketless fuel assemblies.

4. BREST-OD-300 SIMULATION MODEL

The EUCLID/V2 multiphysics code model has been developed for the BREST-OD-300 reactor. The BREST-OD-300 core model consists of 169 fuel assemblies, including the central and peripheral zones, and the lead and steel baffle blocks.

The model of the coolant circuit has four independent loops and all the key reactor elements such as the central and peripheral cavities of the reactor, the steam generators, the reactor coolant pumps, the heat exchangers of the emergency heat removal system. The lead coolant flows from the core to the steam generators, flowing out of them it goes into the pump suction and then through the downflow part of the central cavity comes to the core inlet chamber.

5. ACCIDENT SCENARIO

In the initial state, the BREST-OD-300 reactor facility is in full power operation. The high pressure steam drum depressurization is postulated. A complete failure of the shut-off and control valves of all steam generators sensitive to the pressure drop in the steam pipelines and

feedwater mixing heater is postulated, that leads to continuation of the feedwater supply and additional cooling of the lead coolant. It is also postulated that the normal heat removal system and two of the four loops of the emergency heat removal system failed. The scenario is presented in Table 1.

TABLE 1. ACCIDENT KEY EVENTS

Time, s	Event	Result
0	High pressure steam drum depressurization	Increase in the flow rate of the coolant of the second circuit, lead freezing in steam generators
72	Steam generators shutdown for steam and water, steam discharge into the atmosphere	Lead freezing stops
73	Reactor pump shutdown, reduction of reactor power	Transition to the natural circulation mode
6500	Activation of the emergency heat removal system	Reactor cooling

6. CALCULATION RESULTS

The steam generator cross-section is blocked 80 s after high pressure steam drum depressurization; at the end, the cause of freezing is the mass of solid lead cooled below the melting point (Fig. 2).

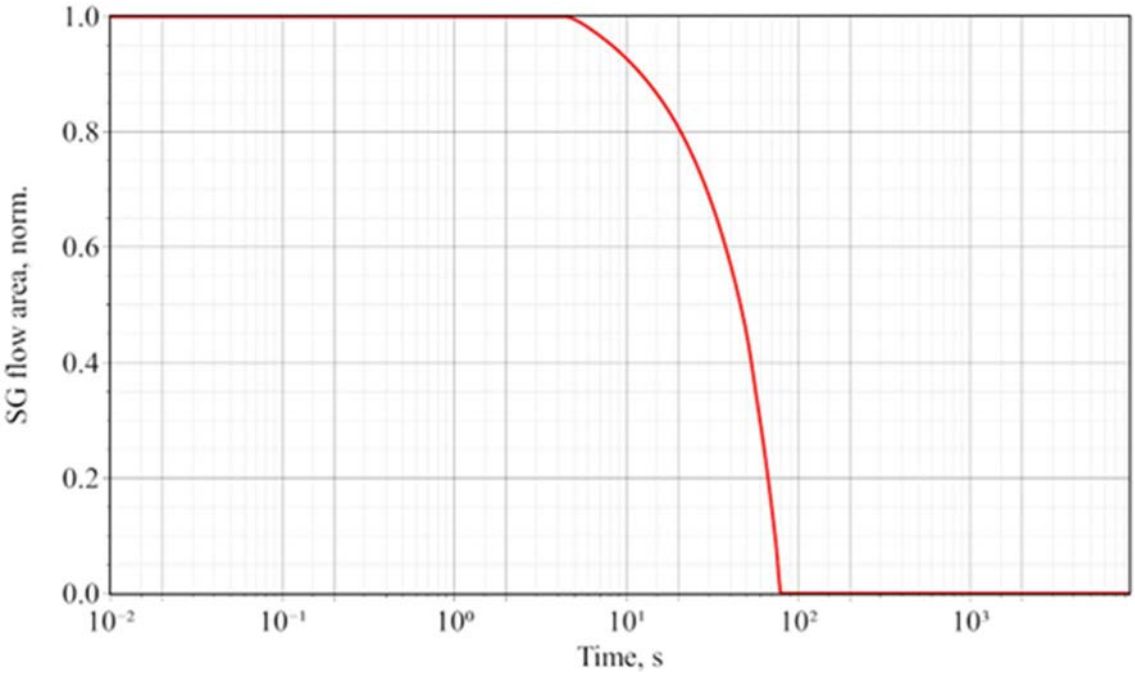

FIG. 2. Normalized steam generator flow area versus time.

As lead freezes, the hydraulic resistance of the circuit increases, as a result of which the flow rate through the core drops even before the pumps shutdown (Fig. 3).

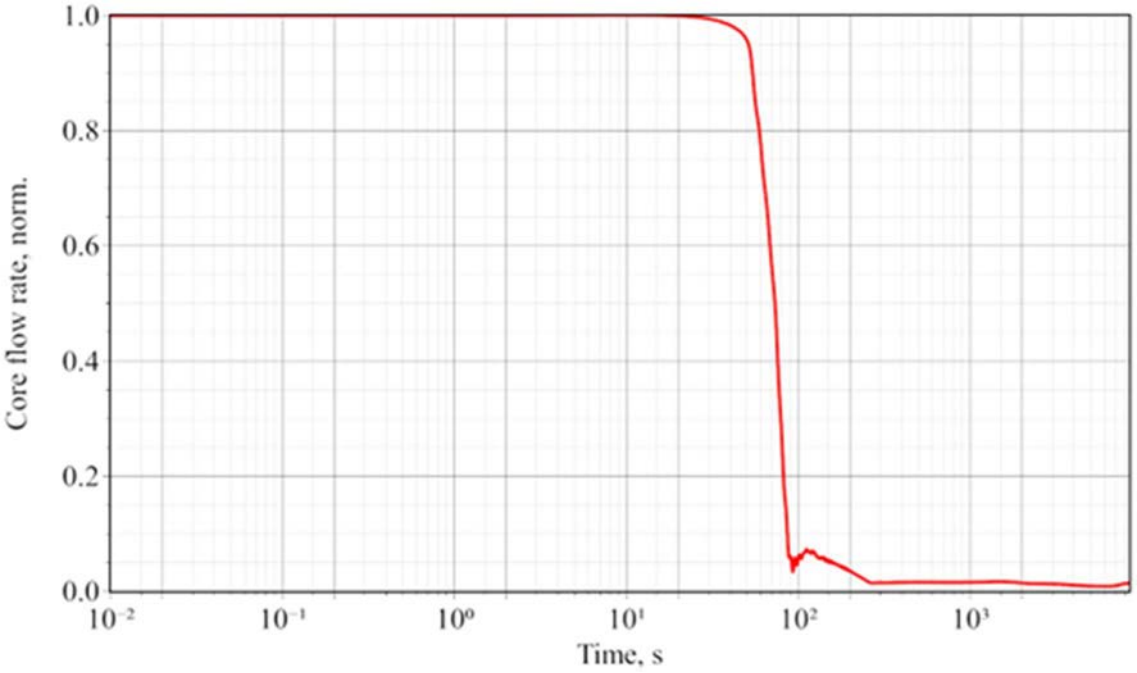

FIG. 3. Normalized core flow rate versus time.

The temperature at the core outlet behaves as follows: first, due to a decrease in coolant flow rate it increases, then, it decreases because of the rapid power reduction; after the forced circulation stops, it increases due to residual heat, which causes natural circulation (Fig. 4). The circuit gradually warms up, which leads to the start of the emergency heat removal system.

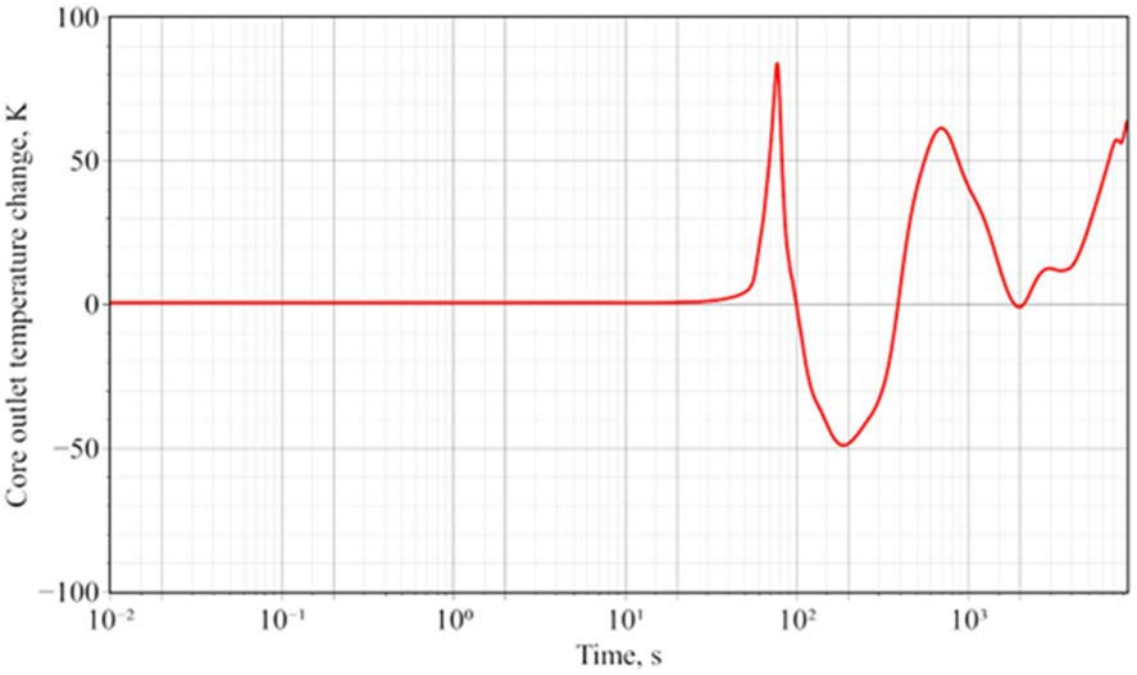

FIG. 4. Core outlet temperature change versus time.

The peak cladding temperature increases by 109 K but does not exceed design limits (Fig. 5).

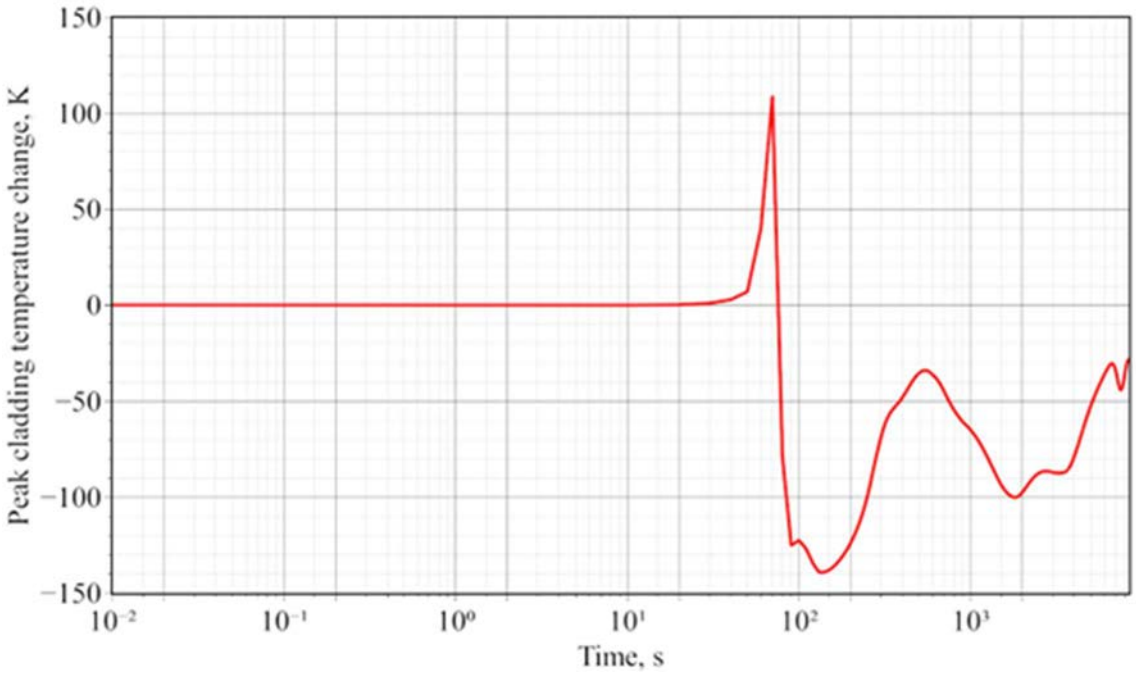

FIG. 5. Peak cladding temperature change versus time.

7. CONCLUSION

The BREST-OD-300 reactor facility is a key element of the pilot demonstration energy complex developed under the "PRORYV" project in the Russian Federation. The BREST-OD-300 high pressure steam drum depressurization with additional failures in the safety system of the primary and secondary loops has been modelled by means of the EUCLID/V2 multiphysics code. It has been shown that the core outlet temperature and the peak cladding temperature increase by 84 and 109 K, respectively, but does not exceed design limits and radiological consequences are absent.

ACKNOWLEDGEMENTS

The work was carried out with the financial support of the State Corporation "Rosatom" (under the State Contract No. H.4o.241.19.21.1068 dated April 14, 2021).

REFERENCES

[1] ADAMOV, E., Closed fuel cycle technologies based on fast reactors as the corner stone for sustainable development of nuclear power, International Conference on Fast Reactors and Related Fuel Cycles: Next Generation Nuclear Systems for Sustainable Development FR17 (Proc. Int. Conf. Yekaterinburg, Russian Federation, 26–29 June 2017), IAEA, Vienna (2018).

[2] BOLSHOV, L., Strizhov, V., Mosunova, N., Codes of new generation for safety justification of power units with a closed nuclear fuel cycle developed for the "PRORYV" project, NUCET 6 3 (2020) 203–214.

[3] ALIPCHENKOV, V., et al., Models of the integral EUCLID/V2 code for numerical modeling of different regimes of lead-cooled fast reactor, International Conference on Fast Reactors and Related Fuel Cycles: Next Generation Nuclear Systems for Sustainable Development FR22 (Proc. Int. Conf. Vienna, Austria, 19–22 April 2022).

[4] ALIPCHENKOV, V., et al., Models of the integral EUCLID/V2 code for numerical simulation of severe accidents in a sodium-cooled fast reactor with MOX and MNUP fuels, International Conference on Fast Reactors and Related Fuel Cycles: Next Generation Nuclear Systems for Sustainable Development FR22 (Proc. Int. Conf. Vienna, Austria, 19–22 April 2022).
[5] ADAMOV, E., et al., Pilot Demonstrational Fast Reactor with Lead Coolant BREST-OD-300, International Conference on Fast Reactors and Related Fuel Cycles: Next Generation Nuclear Systems for Sustainable Development FR22 (Proc. Int. Conf. Vienna, Austria, 19–22 April 2022).

MODELLING OF SEVERE ACCIDENTS FOR SODIUM AND LEAD COOLED REACTORS

I.A. Danicheva, S.N. Senatorova
SEC NRS
Moscow, Russian Federation

Abstract

The paper contains a description of calculation models for fast neutron reactors with sodium and lead coolant, the results of cross-verification of the calculated values of the main parameters of reactors with sodium and lead coolant in a steady state with the design values of the BN-800 and BREST reactors. An analysis of a design basis accident of the BN-800 reactor with complete blocking of the flow in fuel assembly (FA), including failure of the emergency protection system, was performed using the developed calculation model of core melting. Calculation of reactivity effects and the analysis of accidents with a decrease of flow rate, freezing of the coolant and boiling of the lead coolant were performed using the developed calculation model of the BREST reactor.

1. INTRODUCTION

In accordance with the federal rules and regulations in the field of the use of atomic energy, when justifying the safety of nuclear power plants, the operating organization analyses severe accidents, i.e. beyond design basis accidents. Based on its results the planning of emergency response measures is carried out and manuals for accident management are developed.

SEC NRS is a TSO of Rostechnadzor, and performs expert assessments of safety justifications submitted by the operating utilities.

To conduct expert assessments of safety justifications, models are developed, in particular, for fast neutron reactors with sodium and lead coolants the recommendations of the IAEA Safety Standards Series No. GSG-13, Functions and Processes of the Regulatory Body for Safety [1] are taken into account. Models developed by SEC NRS are used for independent analysis of severe accidents.

When developing models, domestic and foreign software tools are used (SOCRAT-BN [2], SERPENT [3], ATHLET [4]). SOCRAT-BN was developed at IBRAE RAN for simulation of neutron-physical and thermohydraulic processes in sodium cooled fast neutron reactors during abnormal operation, including design and beyond design accidents and accidents with fuel melting. The SOCRAT-BN was certified by Rostechnadzor in 2019. SERPENT and ATHLET have been successfully applied to sodium cooled fast neutron reactors. In this work an attempt is made to use previously tested codes for calculating the neutron-physical and thermohydraulic characteristics of sodium cooled reactors (BN-800) to lead cooled reactors (BREST).

2. MODELING OF SEVERE ACCIDENTS FOR SODIUM COOLED REACTOR

2.1 Reactor BN-800 with sodium coolant model

The development of calculation models for an independent analysis of the safety justification of a fast sodium reactor was carried out taking into account the design features of the BN-800 reactor. At the first stage of development of calculation model of BN-800 reactor, a thermohydraulic model of the core (with partial loading of MOX fuel), the primary, second and

third circuits of the reactor were prepared and subsequent verification of the calculation results obtained using the program SOCRAT-BN with design data [5, 6] was done.

According to Refs [5, 6], the core of the BN-800 reactor with a partial load of MOX fuel contains the following types of fuel assembly:

- FA with enriched uranium dioxide pellets and depleted uranium dioxide pellets in the upper and lower breeding zones (FA UTT);
- FA with vibrocompacted MOX fuel and depleted uranium dioxide pellets in the upper and lower breeding zones (FA SVUT);
- FA with pellet MOX fuel and pellets of depleted uranium dioxide in the lower breeding zone (FA STT).

Models of fuel elements of fuel assemblies of the core for the code SOCRAT-BN are shown in Fig. 1. In the calculation, model thermal elements (fuel rods) were divided in 13 layers along the height of the core. The height of the layers was chosen in accordance with the axial profile of the energy release in the reactor. The fuel part of the core in the calculation model was divided into 8 axial segments.

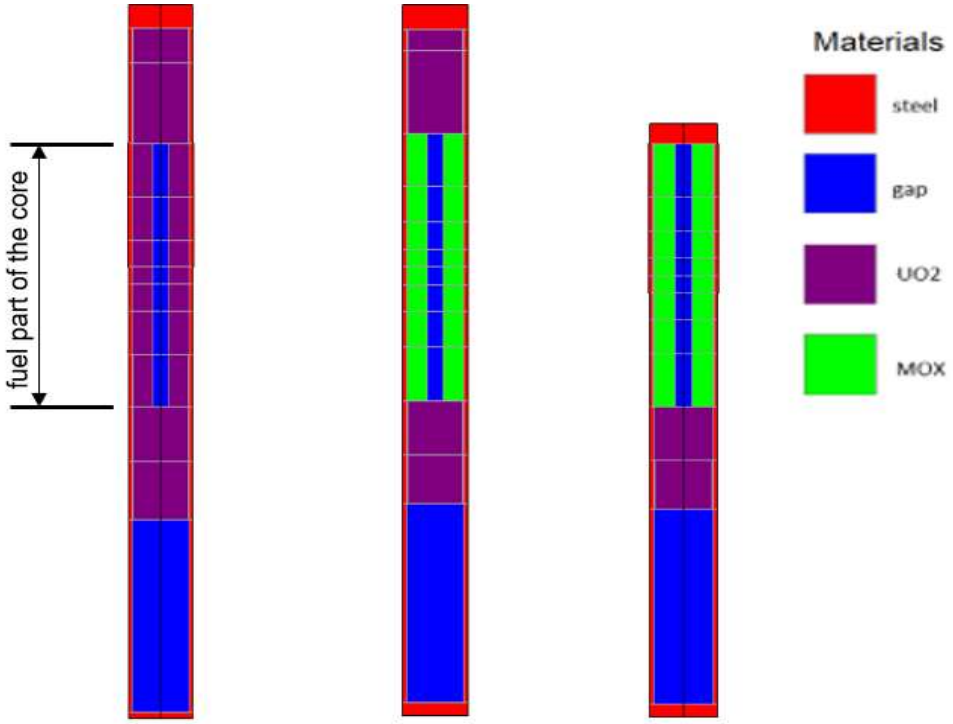

a) fuel rod of FA UTT b) fuel rod of FA SVUT c) fuel rod of FA STT

FIG. 1. Models of fuel elements for fuel assemblies of the core of BN-800 reactor plant.

The SOCRAT-BN program provides for the possibility of using both point and three-dimensional neutron kinetics in the calculation of severe accidents [7]. A decision was made to use the point kinetics model at the stage of testing and verification of the thermohydraulic model of the reactor.

To calculate the characteristics of the steady state of the BN-800 reactor, nodalization schemes of the core, primary, second and third circuits were prepared. The core nodalization scheme is shown in Fig. 2.

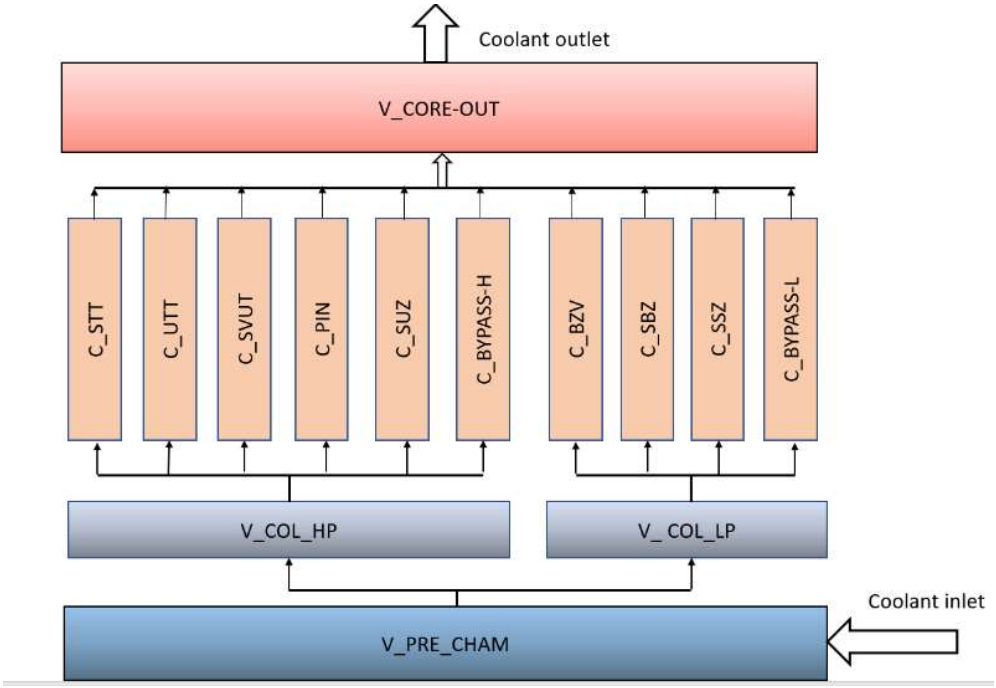

V_PRE_CHAM - pressure chamber; V_COL_HP, V_COL_LP - high and low pressure collectors; C_STT - channels of fuel assemblies with mixed pelletized MOX fuel, C_UTT - channels of fuel assemblies with uranium pellet fuel, C_SVUT - channels of fuel assemblies with mixed vibrocompacted MOX fuel, C_BZV - channels of fuel assemblies of the side breeding zone; C_BZV – fuel assemblies of the side breeding zone; C_SUZ, C_PIN – CPS and trigger neutron source cooling channels; C_BYPASS-H, C_BYPASS-L - leaks in the space between cassettes and steel and boron protection assemblies; C_SBZ - boron protection assemblies; C_SSZ - steel protection assemblies; V_CORE-OUT - upper drain cavity.

FIG. 2. Nodalization scheme of the BN-800 reactor core.

The mathematical model for calculation of the thermohydraulic characteristics during reactor normal operation in SOCRAT-BN is based on solving a system of heat and mass transfer equations at a one-dimensional approximation.

When developing the model, the dimensions and hydraulic characteristics of the core, main equipment and pipelines, flow pressure characteristics of MCP-1, MCP-2 (main circulation pump) were used; thermophysical properties of BN-800 design materials and fuel were also used [5, 6, 8].

To confirm the correctness of the developed calculation model for the analysis of severe accidents, test calculations of the BN-800 parameters were performed when the reactor was operating at the nominal power level. The fitting of the hydraulic parameters of the calculation model was carried out by changing the reactor parameters (in particular, the values of the coolant flow rate and the hydraulic resistances of the core elements) within allowable operating ranges. When fitting of the hydraulic parameters of the secondary and third circuits, the flow rates and temperatures at the outlet of the intermediate heat exchanger were changing.

The following parameters were calculated: for the first reactor circuit – the total sodium flow through the core, average sodium temperature at the outlet of the fuel assembly, and the average sodium temperature at the inlet and outlet of the intermediate heat exchanger (Fig. 3); for the second reactor circuit – the total sodium flow through the section of the steam generator, average sodium temperature at the outlet of the intermediate heat exchanger, and the average

sodium temperature at the outlet of the steam generator sections (Fig. 4); for the third reactor circuit – the flow of feedwater in the steam generator, average temperature of the feedwater at the inlet to the steam generator, average steam temperature at the outlet of the steam generator, and the feedwater pressure at the inlet to the steam generator (Fig. 5).

According to the calculation results, the maximum deviations from the design values were: for the coolant temperatures of the first circuit - 1.4%; for the second circuit - 3.7%, for feedwater temperature in the third circuit - 0.5%; for sodium flow in the first circuit - 0.7%, in the second circuit - 4.5%, for feedwater flow in the third circuit - 5.1% (Figs 3–5). The results of the calculations confirm the correctness of the developed calculation model for the stationary states of the BN-800 reactor.

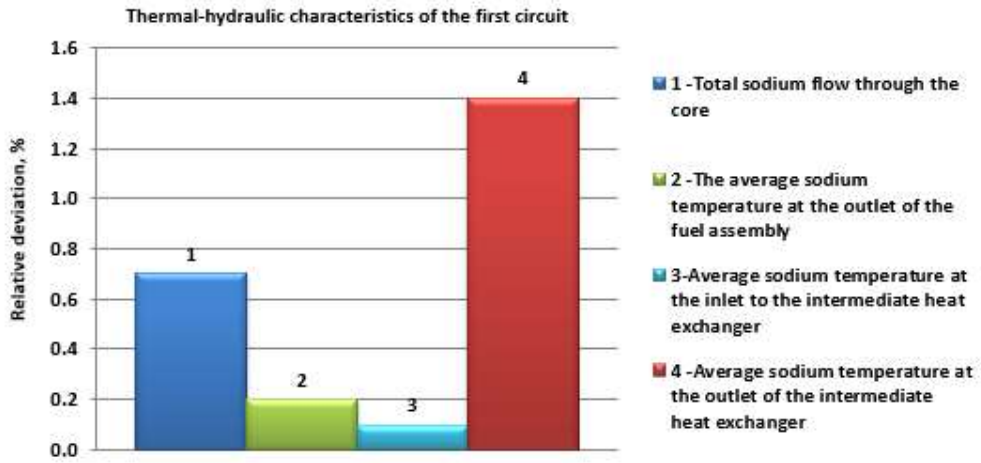

FIG. 3. Relative deviations of the results of calculating the thermohydraulic characteristics of the first circuit between SOCRAT-BN and design data.

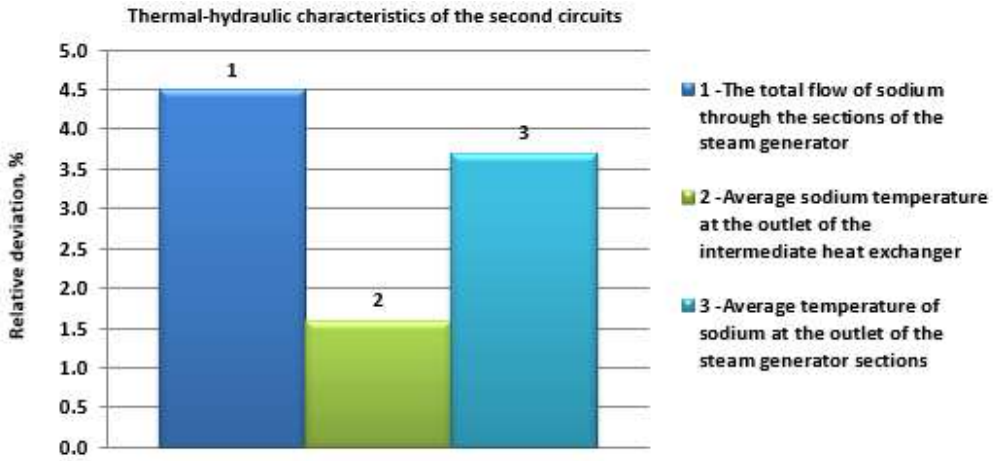

FIG. 4. Relative deviations of the results of calculating the thermohydraulic characteristics of the second circuit between SOCRAT-BN and design data.

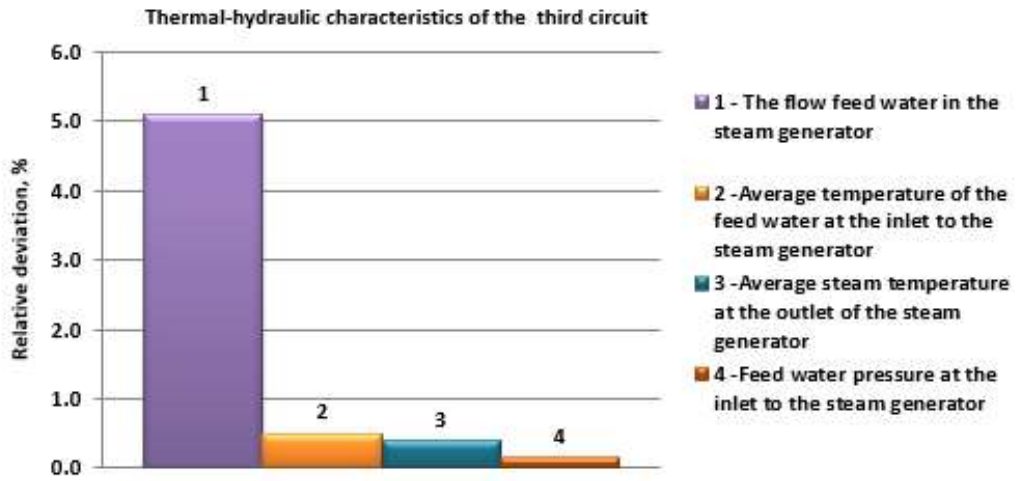

FIG. 5. Relative deviations of the results of calculating the thermohydraulic characteristics of the third circuit between SOCRAT-BN and design data.

An attempt was made to use the calculation model developed by the authors to analyse the accidents involving failure of heat removal from the core of the BN-800 reactor. If heat removal is finished, the temperature rises and the sodium coolant boils, and a positive sodium void reactivity effect in the BN-800 reactor leads to a power surge and the probability of destruction and melting of the core.

The model developed for analysis of accidents takes into account the possibility of destruction and melting of the core, as well as the possibility of moving part of the melt upward due to the high speed of sodium vapour. The model of melt displacement along the fuel rod axis is used, which considers melt friction in drop and film flow with an upward flow of sodium vapour, implemented in SOCRAT-BN.

2.2 Calculation of a severe accident with core elements melting in a sodium cooled reactor

Using the developed thermohydraulic model and the core melting model, the calculation of the characteristics of the core for a design basis accident with blocking of the flow pass section of one FA when the reactor is operating at the nominal power level was performed.

The BN-800 reactor project provides for the conversion to full scale loading with tablet MOX fuel (FA STT). So, for the analysis of the accident, just such a fuel assembly was chosen, located in the area of maximum energy release by the reactor.

To simulate the blocking of the flow section at the inlet to the FA, a valve is modelled in the region of the FA shank. It is postulated that the blocking of the flow pass section of the FA starts from 118 s from the start of the calculation. Complete blocking of the flow pass section of the FA occurs for 120 s. The FA characteristics before and during the accident are presented in Figs 6–8. These characteristics are presented in relative units.

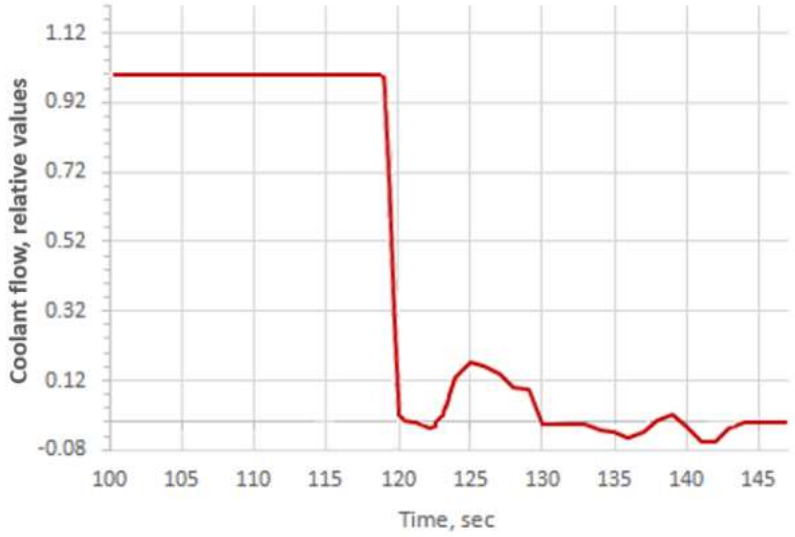

FIG. 6. Coolant flow rate at the outlet of the emergency fuel assembly.

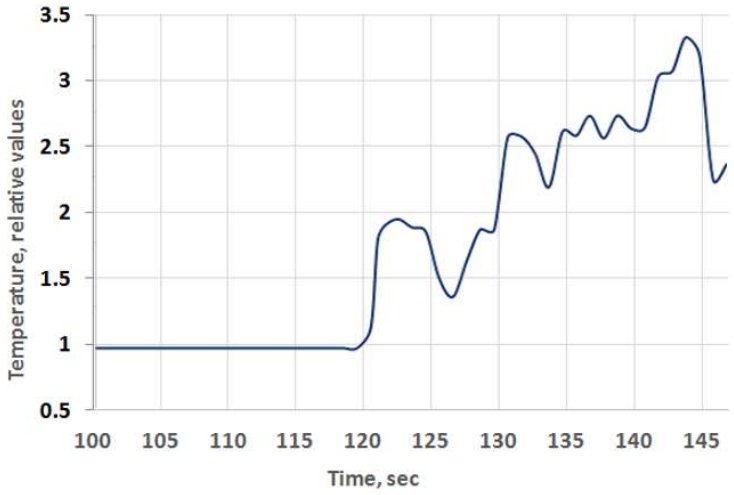

FIG. 7. Coolant temperature at the outlet of the emergency fuel assembly.

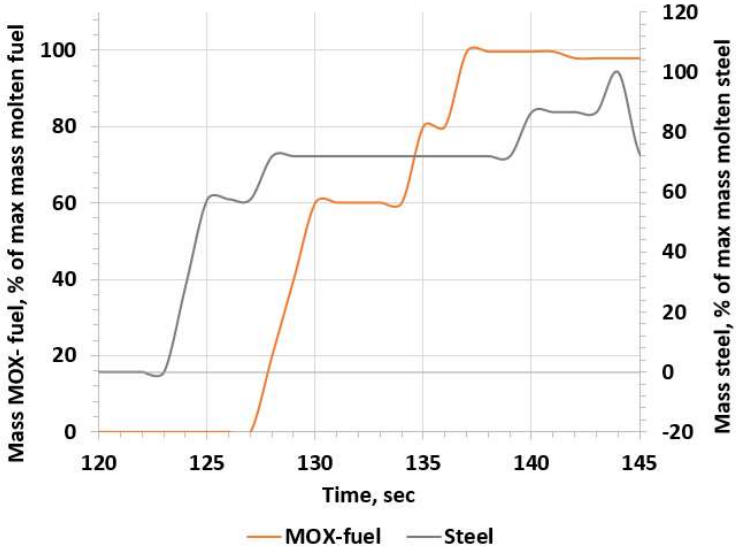

FIG. 8. Mass of molten fuel and molten steel.

As follows from the analysis of Figs 6–8, boiling of sodium in the inter fuel rod space of the FA as a result of blocking the flow pass section occurs in 1.78 s after the complete blocking of the flow pass section of the FA (121.78 s from the beginning of the calculation). After that, for three seconds, there is an intense release of sodium from the FA. As the inter fuel rod space dries, sodium films shed from the surface of the fuel rods, which leads to a fast increase of the fuel rod cladding temperature and their melting. Fuel melting begins in the central part of the fuel element along the height corresponding for the maximum fuel energy release, then 7 seconds later after the complete blocking of the flow pass section of the FA.

The change in the mass of the molten fuel and steel of the fuel cladding (Fig. 8) during the accident occurs due to the moving and transfer of part of the melt by the sodium flow on the fuel rod sections with lower temperatures. The change in the configuration of FA STT fuel rods during the accident is shown in Fig. 9.

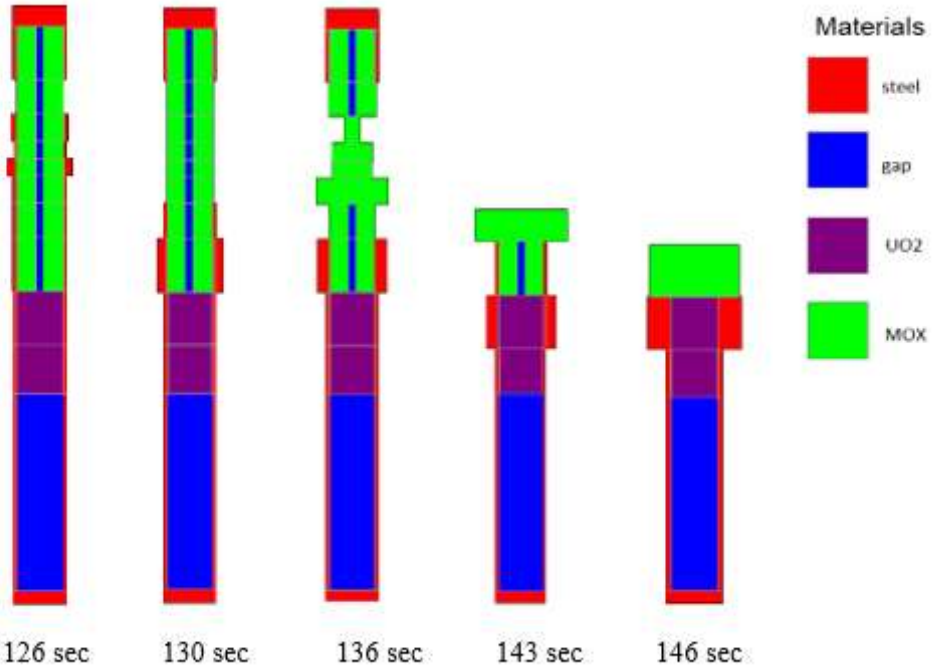

FIG. 9. Distribution of materials in the fuel rods of emergency fuel assemblies with MOX pellet fuel.

According to Fig. 9, the collapse of the upper layer of the fuel part due to the runoff of fuel and fuel cladding steel occurs at 143 s, when the fuel and fuel cladding temperatures reach melting points. In this case, the collapse occurs in the region with the highest energy release in height.

3. MODELING OF SEVERE ACCIDENTS FOR LEAD COOLED REACTOR

3.1 Lead cooled reactor core model (BREST)

To carry out calculations of the neutron-physical characteristics and reactivity effects of the BREST reactor, calculation models were prepared for modelling a core loaded with mixed uranium-plutonium nitride fuel. Calculations included sequential thermohydraulic and neutron-physical calculations.

To carry out neutron-physical calculations in three-dimensional geometry by the Monte Carlo method we used the code SERPENT v2.32 [3] developed at VTT (Finland). The

thermohydraulic calculation was performed using the ATHLET v3.2 program as part of the AC2 code [4] developed at GRS (Germany).

The initial load of the BREST reactor core was taken from Refs [9–11] and includes: FA of the central zone (CZ); FA of the peripheral zone (PZ); the rods of the control and protection system (CPS rod); reflector channels (RC); reflector channels with a passive feedback system (RC with PFS); steel channels of radiation protection (PC). Assemblies of reflector channels with a passive feedback system are designed to control the leakage of neutrons from the core and are filled with lead coolant and argon. With a decrease in the level of lead in the core, the amount of argon in this assembly increases. This increases the leakage of neutrons from the core.

Initial data has been prepared for two design states of the core of a lead cooled reactor:

- "Cold" state, corresponding to a shutdown reactor with a constant temperature of the fuel, coolant, structural elements (the state with the maximum reactivity margin). The coolant level in reflector channels with a passive feedback system is set at the minimum level (the rest space is filled with argon). Thermohydraulic calculation for this state was not carried out.
- Operating ("hot") state corresponding to the operation of the reactor at the nominal power level. The critical state is provided by the position of the automatic CPS rods. The other CPS rods were fully removed from the core. The temperature distribution of the fuel, coolant and structural materials, as well as the density of the coolant in the fuel assemblies, was determined from the results of thermohydraulic calculation. The FA placement step was determined taking into account the thermal expansion of the header pressure chamber due to a change in temperature at the core inlet.

The cartogram of the initial load of the BREST reactor core is shown in Fig. 10.

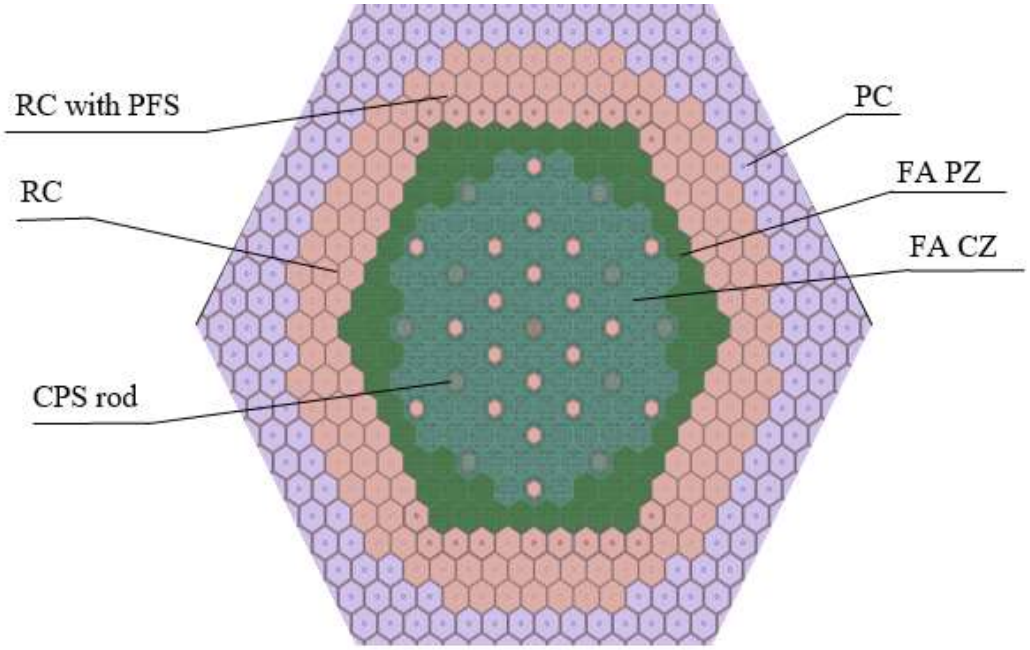

a) Section along the XY plane through the core centre.

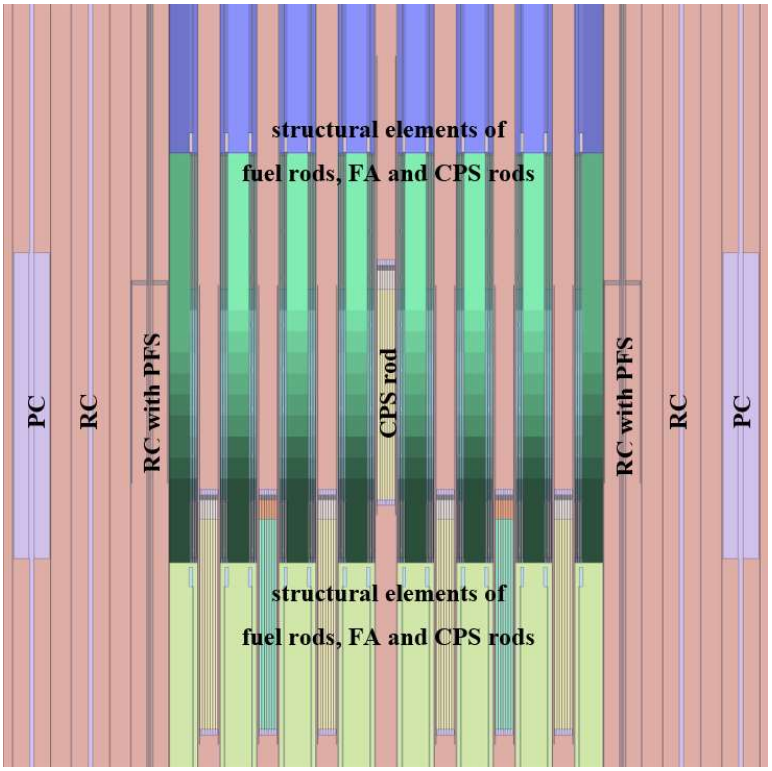

b) Section along the YZ plane through the core centre

FA PZ - FA of the peripheral zone; FA CZ- FA of the central zone; CPS rod - the rod of the control and protection system; RC - reflector channel; RC with PFS - reflector channel with a passive feedback system; PC - protection channel.

FIG. 10. Calculation neutron-physical model of the BREST reactor core in operating state.

The geometry of the core elements basically corresponds to the design. For some structural elements (in particular, elements of fuel rods and spacer grids), the following simplifications were used: homogenization with maintaining of the mass ratio of materials; modelling of equivalent volumes of structural elements with maintaining of the volume fractions of materials.

To assess the correctness of the results obtained when modelling the core using the SERPENT/ATHLET programs [3, 4], a cross-verification of the calculated values of the reactor characteristics with the design values of the same characteristics, which were obtained using the certified MCU-BR program [12], implementing the Monte Carlo method. Cross-verification carried out showed that the deviations of the calculation results obtained using the SERPENT/ATHLET programs and the certified MCU-BR program do not exceed the errors specified in the MCU-BR certificate [12].

Deviations of the efficiencies of the shutdown system[1] and of the heat resulting from the decay of fission products are not more than 7% and 4%, respectively. The results obtained demonstrate the correctness of the application of the models developed using the codes SERPENT/ATHLET in assessing the safety of the BREST reactor.

[1] The efficiency of the shutdown system is calculated as the change in reactivity due to rods insertion in the core.

3.2 Calculation of the states of the core of a lead cooled reactor under conditions of possible accidents

To demonstrate the application of the calculation model for the BREST reactor, reactivity effects were calculated for "cold" and "hot" states of the initial core load under conditions of possible accidents. The selection and subsequent analysis of these states were carried out taking into account the hypothetical possibility of:

- Core cooling followed by coolant freezing;
- Changes in the coolant level in the core;
- Removal (floating) of fuel rods structural materials from the core.

3.2.1 Cooling of the core with subsequent freezing of the coolant

The "cold" state of the reactor with CPS rods fully inserted into the core was used to evaluate the reactivity effects upon freezing of the coolant in the core. Coolant freezing can occur mainly during the reactor commissioning stage, because in a core with fresh nuclear fuel the source of heat is only external. For example, this can be due to a long term electrical blackout. The reactivity effect in this case is associated with a change in the density of the lead coolant when it freezes and a decrease in the temperature in the core (a decrease to 20°C is conservatively assumed in the calculations). The SERPENT calculation of the corresponding state of the reactor showed that the introduced positive reactivity reduces the subcriticality of the shutdown reactor by 6.81% from the initial level; however, the efficiency of the CPS rods is sufficient to ensure the subcriticality of the reactor.

3.2.2 Change in coolant level in the reactor and core

The "cold" state of the reactor with the CPS rods fully inserted into the core was used to evaluate the reactivity effect upon changes in the coolant level in the core. This choice of the placement of the CPS rods is based on the assumption that the possible transient process associated with loss of coolant is realized for a long time, sufficient to shut down the reactor.

The effect of reactivity due to the coolant level in the reactor changing, was assessed taking into account the possibility of complete or partial exposure of the fuel part of the core. Despite the fact that, in accordance with the safety concept adopted in the design of the BREST reactor, the loss of such an amount of coolant is practically eliminated, the analysis of the state of the reactor with a change in the level of lead coolant in the core is of interest due to, in particular, the fact that sodium cooled reactors are characterized by a positive effect on reactivity from the removal of coolant. The dependence of injected reactivity from the level of lead in the core calculated using SERPENT is shown in Fig. 11.

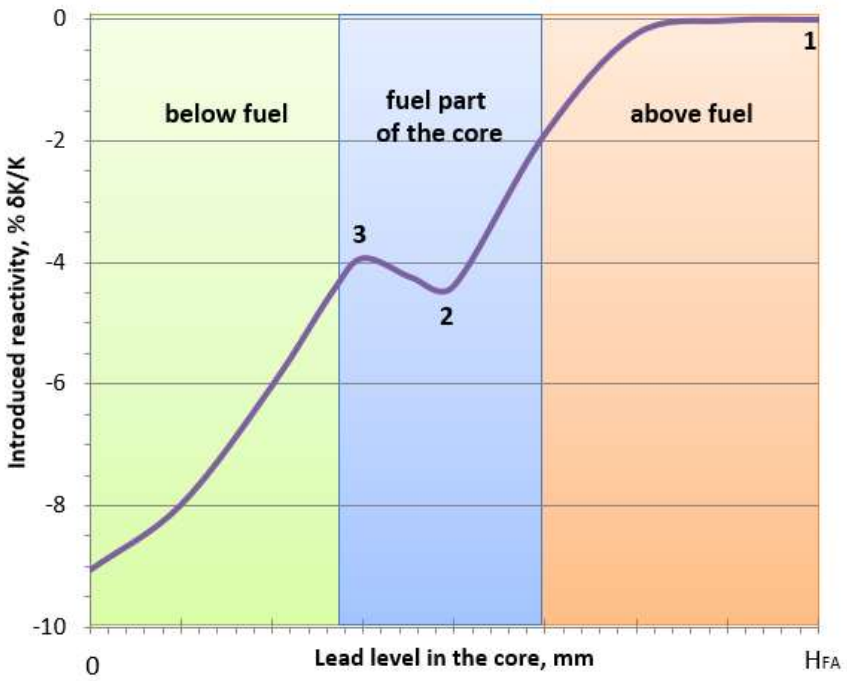

FIG. 11. Dependence of injected reactivity from the level of lead in the core.

An analysis of the calculation results showed that the reactivity introduced during the loss of coolant has a variable nature. When the coolant level decreases from mark 1 to mark 2, negative reactivity is introduced, which is associated with an increase in neutron leakage through the upper of the core. When the coolant level decreases from 2 to 3, the positive component of reactivity prevails, associated with a decrease in the absorption of neutrons in the core during a decrease the amount of lead coolant. A further decrease in the coolant level leads to leakage of neutrons through the lower of the core and an increase in the subcriticality value. The efficiency of CPS rods is sufficient to maintain the reactor subcriticality in all states associated with the loss of coolant without changing the configuration of the core.

3.2.3 Removal (floating) of structural materials of fuel rods from the core

In the case of initiating events associated with the loss of heat removal or the introduction of positive reactivity, the temperature of the lead coolant can reach the melting temperature of fuel cladding steel (1400–1500°C) [8]. For reactors with a lead coolant, its boiling point (1745°C) exceeds the melting point of fuel claddings [8]. Thus, the melting of structural materials begins before the boiling of the coolant. Due to the fact that the density of structural materials is lower than the density of the lead coolant, and also due to the fact that during forced and natural circulation the lead coolant moves from bottom to top of the core, conditions can be created for floating of the fuel rod structural materials during their melting.

Using the SERPENT program, calculations of the reactivity effect associated with the removal (floating) of cladding steel from the core were made:

- During floating of the fuel claddings of the seven central FAs (2.26% of the total fuel rods);
- During floating of the fuel claddings of all FAs in the central zone, including FAs with CPS rods (61.97% of the total fuel rods).

The calculation of the neutron-physical characteristics of the core showed:

- When fuel claddings float, the reactivity effect is positive.
- The positive reactivity introduced during the melting and floating of the fuel claddings of all FA of the central zone reduces the reactor subcriticality by 37% of the initial value; however the design requirements for the minimum subcriticality value are met.

Due to the fact that the value of the subcriticality of the reactor decreases by a significant amount, it can be concluded that the amount of structural materials in the core has a significant impact to the course of such accidents as ULOF (accident with loss of coolant flow in the core) and UTOP (accident with uncontrolled injection of positive reactivity).

4. CONCLUSIONS

Calculation models were developed for fast neutron reactors with sodium and lead coolants. The results of cross-verification of the calculated values of the main parameters of the reactors with sodium and lead coolants in the steady state with the design values of the BN-800 and BREST reactors indicate the correctness of the developed models.

Using the developed calculation model of core melting, an analysis of the course of a design accident of the BN-800 reactor with the blocking of the passage section of one fuel assembly, including without operating of the CPS was performed.

The characteristics of the core of the BREST lead cooled reactor were calculated using the codes SERPENT/ATHLET. The cross-verification carried out for stationary neutronic characteristics of the BREST reactor showed that the differences between the calculation results obtained using the SERPENT/ATHLET programs and the certified MCU-BR program do not exceed the calculation errors indicated in the MCU-BR certificate. The results obtained indicate the correctness of the use of codes SERPENT/ATHLET for assessing the safety of the BREST reactor.

REFERENCES

[1] INTERNATIONAL ATOMIC ENERGY AGENCY, Functions and Processes of the Regulatory Body for Safety, IAEA Safety Standards Series No. GSG-13, IAEA, Vienna (2018).

[2] Certification Passport of the Software No. 472 dated 20.11.2019 “SOKRAT-BN/V2”. (in Russian) (2019).

[3] LEPPÄNEN, J., The Serpent Monte Carlo code: Status, development and applications in 2013, Annals of Nuclear Energy (2015).

[4] WIELENBERG, A., Recent improvements in the system code package AC2 2019 for the safety analysis of nuclear reactors, Nuclear Engineering and Design (2019).

[5] ZVEREV, D., Mastering the technology of fast sodium reactors. Creation of BN-800, Nuclear energy (2011).

[6] VASILIEV, B., FARAKSHIN, M., BELOV, S., KUZNETSOV, A., Prospects of development of BN-800 reactor core, 10th International Scientific and Technical Conference, Moscow (2016).

[7] USER MANUAL, SOCRAT-BN, IBRAE RAN (2016).

[8] KIRILLOV, P., Reference book on thermal-hydraulic calculations in nuclear power engineering, Atomizdat, Moscow (2010).

[9] ADAMOV, E., KAPLIENKO, A., ORLOV, V., SMIRNOV, V., LOPATKIN, A., LEMEKHOV, V., MOISEEV, A., Lead-Cooled Fast Reactor BREST: From Concept to Technology Implementation, Atomic Energy, Moscow (2020).

[10] BALOVNEV, A., DAVYDOV, V., ZHIRNOV, A., KALUGINA, K., MOISEEV, A., UMANSKY, A., SMIRNOV, V., Analysis of reactivity effects in emergency situations with steam entering the core of a lead-cooled fast reactor, Conference of young professionals. Innovations in nuclear energy, JSC "NIKIET", Moscow (2019).

[11] LEMEKHOV, V., SMIRNOV, V., UMANSKY, A., BREST Reactor Core: State of the Art and Prospects, Problems of mechanical engineering and automation, Moscow (2013).

[12] Certification Passport of the Software No. 405 dated 08.12.2016 “MCU-BR with MDBBR50 Constant Library”. (in Russian) (2016).

OVERVIEW OF ENEA EXPERIMENTAL CAMPAIGN CONCERNING LFR PROJECTS

A. BELLOMO [1], P. FERRONI [2], S. J. LEE [3], M. TARANTINO [4]

[1] University of Pisa, Pisa, Italy
[2] Westinghouse Electric Company LLC, Pittsburgh, United States of America
[3] Fauske & Associates Inc., Burr Ridge, United States of America
[4] Italian Agency for New Technologies, Energy and Sustainable Economic Development (ENEA), Bologna, Italy

Abstract

ENEA Brasimone Research Centre hosts different experimental infrastructures for research on severe accident initiators in Generation IV lead cooled fast reactors (LFRs), in particular regarding steam generator tube rupture (SGTR) events and flow blockages. The experimental activities are performed in the framework of the EU Euratom H2020 projects: PATRICIA, PASCAL, ANSELMUS, INNUMAT. In the context of the collaborations of ENEA with third parties, as universities, research institutes and industries, the paper contains an overview of the ALFRED (Advanced Lead Cooled Fast Reactor European Demonstrator) project and the FALCON consortium (Fostering ALFRED Construction). In addition, the pre-test analyses for the LEWIN facility, performed with the SIMMER-III (S-III) code, are reported; LEWIN is a separate effect test facility built by Westinghouse Electric Company (WEC) under the supervision of ENEA Brasimone. The collaboration between UNIPI and ENEA has led to a modification of the S-III code for the simulation of the lead–water interaction. The S-III LEWIN simulation shows that the code represents the phenomena characterizing the high pressure water injection into molten lead pool: pressure wave generation and propagation; water flashing; two-phase critical flow blowdown; displacement of the liquid lead as the vapour bubble keeps growing; sloshing motions of the lead; solidification of lead particles.

1. INTRODUCTION

Since 2000, ENEA has been actively involved in supporting the design, safety evaluation, and technological advancement of innovative nuclear systems cooled by heavy liquid metals (HLMs), with a recent focus on lead cooled fast reactors (LFRs). ENEA is building expertise in fast spectrum core design and operates one of the largest arrays of experimental facilities in Europe, dedicated to studying HLM thermohydraulics, coolant chemistry control, structural material corrosion behaviour, and material properties in HLM environments. Additionally, ENEA is involved in the development of corrosion resistant coatings, components, instrumentation, and innovative systems. The organization also focuses on developing, validating, and integrating numerical tools specific to these applications, including neutronics codes, system and core thermohydraulic codes, computational fluid dynamics (CFD), and fuel pin performance codes.

2. ENEA Brasimone Research Centre experimental facilities

CIRCE (CIRColazione Eutettico) is a lead-bismuth eutectic (LBE)-cooled pool type facility, in operation since the early 2000s. The large scale of the plant makes it suitable to perform integral experiments. CIRCE comprises a cylindrical main vessel filled with LBE, with a total capacity of approximately 70 tons. The facility includes LBE heating and cooling systems, a storage tank, a transfer tank, and auxiliary systems for LBE circulation and gas recirculation. The main vessel is designed to accommodate prototypical test sections (TS), which are customized for each experimental requirement. In particular, the THETIS (Thermal-hydraulic HElical Tubes Innovative System) TS [1] (Fig. 1) is currently under development: it will be composed of a fuel pin simulator (FPS), a main circulation pump and a helical coil steam generator (HCSG). Despite the HCSG concept being promising, its application in HLMs is still prototypical: dedicated R&D activity is mandatory to test the suitability for Gen-IV nuclear power plants. The experimental campaign foreseen in CIRCE-THETIS aims to investigate the thermohydraulic behaviour of the system in steady state operation (forced circulation regime)

during operational and accidental transients (postulated scenarios) and in the natural circulation regime.

The HERO (Heavy liquid mEtal – pRessurized water cOoled tube) TS [2] differs from THETIS in that it has a steam generator bayonet tube as the main cooler (mock-up 1:1 in length); it has been designed and implemented to perform integral effect tests to study steam generator tube rupture (SGTR) and protected loss of flow accidents. A large scale test section (TS) has been designed specifically to experimentally investigate postulated SGTR events, using a configuration relevant to the primary heat exchanger (HX) of the MYRRHA reactor. The post-test analysis has been performed by the SIMMER code in 3D version (SIMMER-IV). The code can estimate the right timing and amplitude of the pressure oscillations in the cover gas due to sloshing in the main LBE pool. SIMMER-IV can also predict the steam flow path in the tube bundle, separator, and main pool.

Also regarding SGTR initiators, LIFUS 5/Mod2 [3] is a separate effect test facility which is focused on HLM/water interaction investigations (i.e. PbLi, LBE, Pb), designed to study dynamic effects of energy release on tubes and shell structures relevant in SGTR scenarios (e.g. pressure wave generation and propagation and lead sloshing). SIMMER-III and SIMMER-IV, RELAP5/Mod3.3 and FEM codes have been largely used for validation purposes.

Concerning flow blockage initiator studies, the NACIE-UP (NAtural CIrculation Experiment Upgraded) facility [4] (Fig. 2) is designed to characterize the thermohydraulic behaviour of an HLM cooled fuel assembly during transition from forced to natural circulation. NACIE-UP is a rectangular loop cooled by LBE; a prototypical wire-spaced fuel pin bundle simulator is installed in the bottom part of the riser, while a shell and tubes HX is placed in the right descending vertical branch. The blockage FPS test section installed into the NACIE-UP loop facility aims to fully investigate the different flow blockage regimes in a 19-fuel pin bundle. An experiment has been designed to analyse the thermohydraulic behaviour of a simplified version of a fuel assembly (FA) during an internal flow blockage accident. This was achieved by intentionally closing some holes in the first spacer grid, located at the beginning of the heated length.

CFD models and simulations of the ALFRED FA, both in its nominal configuration and with various types of internal blockage, were developed and executed. Specifically, different blockage scenarios at the spacer grids were examined using CFD RANS simulations. Currently an IAEA benchmark activity is ongoing since NACIE loop tests provide an excellent opportunity for validation of the physical and mathematical models and numerical simulation codes. The overall objective of the Coordinated Research Project is to improve the member states' analytical capabilities in the field of simulation of fast reactors cooled by HLMs.

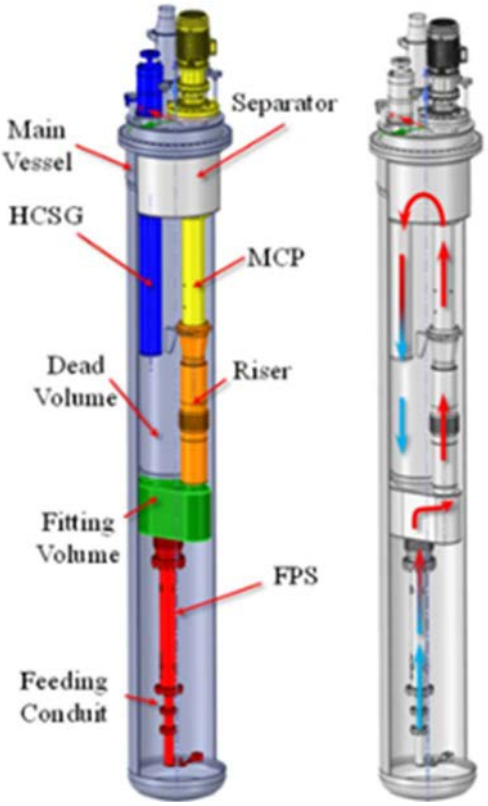

FIG. 1. CIRCE-THETIS schematic view.

FIG. 2. NACIE-UP facility.

3. WEC LEWIN FACILITY

The LEad-to-Water INteraction (LEWIN) facility is designed to assess the effects potentially resulting from failure of a primary HX in the Westinghouse LFR [5]. The SGTR is of substantial interest for the safety assessment of the Gen-IV LFRs design, as both a design basis accident and severe accident (SA) precursor. The main phenomena to be studied are the pressure wave generation and propagation, the lead sloshing and the pool level variation. The physical quantities to be assessed are the subcooled and supercritical water blowdown flow rates, and the lead and steam jet impingement loads on the vessel walls.

3.1 SIMMER-III pre-test analysis

With respect to the original version of the code, SIMMER-III Ver. F [6] has been modified in such a way that the liquid lead can be used as a coolant simultaneously with water. Then, a model of the LEWIN interaction vessel has been set up (Fig. 3), including the following geometries (with associated initial conditions) into the nodalization grid: the injection line, filled by high pressure subcooled water at 190 bar and 303°C; the lead pool, filled with lead at 415°C and 1.1 bar; the cover gas region with argon at 1.1 bar.

The 23 s transient simulation shows the water flashing as it enters the molten lead, the growing of the steam bubble, the displacement of the lead and the variation of the pool level. The mass flow rate of the choked flow characterizing the water injection is predicted consistently with the Henry-Fauske Subcooled Model. The first pressure peak due to the pressure wave generation soon after the injection is correctly simulated.

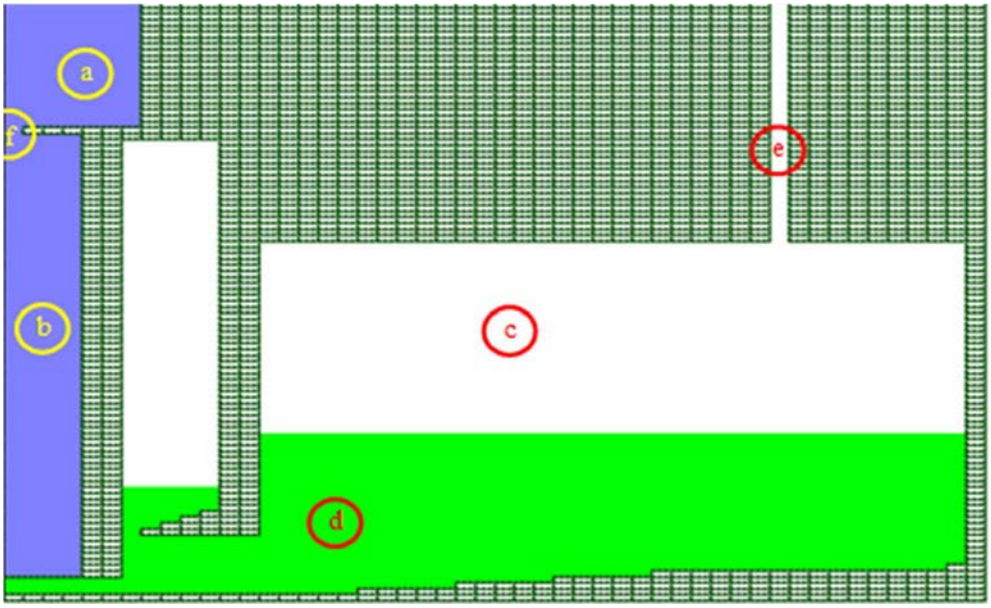

FIG. 3. S-III fluid model nodalization view (note: the real proportions are not preserved): a) Water volume, b) Long Capillary Tube, c) Cover gas region, d) Lead pool, e) Dump line, f) Orifice.

4. CONCLUSIONS AND PERSPECTIVES

The Experimental Engineering Division (FSN-ING) of the ENEA Brasimone Research Centre has decades of scientific expertise in experimental and numerical research activities in supporting LFR technology development. The SGTR and the coolant flow blockage should be taken into consideration for SA scenarios in LFRs. CIRCE, LIFUS5 and LEWIN are the facilities designed to investigate phenomena related to SGTR, while NACIE-UP is designed to study the coolant flow blockage. In parallel with the experimental activities, Validation and verification (V&V) activities are ongoing on the SIMMER code, with the perspective of using it as a SA safety analysis tool. The experiments described above are intended to support the deterministic approach required for the licensing of an LFR. Additionally, they aim to establish an experimental database that can be used for code validation. The design of each experiment needs to consider these specific objectives, enabling a faster licensing process and aiding in the overall design and development of LFR systems.

REFERENCES

[1] P. Lorusso, I. Di Piazza, D. Martelli, A. Musolesi, M. Tarantino, Preliminary design of THETIS test section for the CIRCE facility, ENEA report for MYRTE, Ref CI-I-R353 (2021).

[2] Pesetti A., Forgione N., Narcisi V., Lorusso P., Giannetti F., Tarantino M., ENEA CIRCE-HERO test facility: geometry and instrumentation description, ENEA report for Project H2020 SESAME WP5.2, Ref CI-I-R-343 (2018).

[3] M. Tarantino et al., Fusion technologies development at ENEA Brasimone research centre: status and perspectives, in 14th International Symposium on Fusion Nuclear Technologies, Budapest (2019).

[4] Lorusso P., Di Piazza I., Martelli D., Musolesi A., Tarantino M., NACIE-UP: An Heavy Liquid Metal Loop for Mixed Convection Experiments with Instrumented Pin Bundle, in HLMC-2013, IPPE, Obninsk, Russian Federation (2013).

[5] P. Ferroni, Westinghouse Lead Fast Reactor Design and Safety, in Proceedings of ICAPP 2021 (2021).

[6] Kondo Sa., Tobita Y., Morita K., Shirakawa, "SIMMER-III: an advanced computer program for LMFBR severe accident analysis.," in Int. Conf. on Design and Safety of Advanced Nuclear Power Plant, Tokyo, Japan (1992).

HEAT TRANSFER CHARACTERISTICS OF LIQUID METAL FAST REACTORS

A. ALI
Egyptian Atomic Energy Authority, Reactor Department, Nuclear Research Center Cairo, Egypt

Abstract

The heat transfer characteristics in the reactor core are of significance importance for the proper design and safety assessment of all types of reactor including liquid metal cooled fast reactors. The heat transfer characteristics of liquid metal are different from other fluids due to the extremely low Prandtl number. In the early studies, thermohydraulics calculations with respect to heat transport in the core of a liquid metal fast reactor (LMFR) were dependent on one-dimensional codes and based on experimental data. With the increased computational resources, three-dimensional computational fluid dynamics (CFD) simulations allow adequate details about the heat transfer characteristics of liquid metals. In the present work, a full three-dimensional CFD study is conducted for 5x5 vertical rods bundle cooled with liquid lead as coolant. The wire wrap spacer in LMFR acts as a momentum exchange promoter in addition to its main function for keeping the inter-rods spacing for the fuel bundle. A wire wrap spacer with twisting pitches ratios of 5, 10, 20, 30, and 40 of the rod diameters is considered in this work. A wide range of turbulence models is tested to better reflect the results of the available experimental work. The effect of rods wire wrap spacer on heat transfer characteristics is reported. A slight increase of temperature in the wake regions of the wire is detected and reported.

1. INTRODUCTION

Nuclear energy production in the world is one of the lowest CO_2 emitting energy sources [1]. The current ability of nuclear energy to meet the global demand for electricity depend mainly on the resources of natural uranium and U-235 as nuclear fuel. The relatively low percentage of this fissile isotope in natural uranium is a restriction on the progress of nuclear power when only depend on the current light water reactors (LWR) which, with its low conversion ratio, cannot make use of more than 2% of the energy available in natural uranium. Therefore, the fundamental value of nuclear energy in the long term may not be fully employed unless more reserves of natural uranium are found or until significant progress is conducted for effective using of uranium [2]. Fast breeder reactors provide an opportunity of dealing with this issue in the near future.

Many of the present issues for fast reactors require extended and reliable knowledge of the characteristics of turbulent flow and heat transfer in liquid metals; Among these issues are, in particular, the thermohydraulic design of liquid metal cooled fast reactors (LMFRs). The research gaps and modelling challenges in LMFRs are mainly related to two points. Firstly, the heat transfer characteristic of liquid metal is clearly different from that of the conventional fluids (air and water) because of its very low value of Prandtl number. The low value of the Prandtl number makes the conventional turbulence models invalid under certain conditions [3]. Secondly, the pool-type design causes thermohydraulic phenomena like natural circulation and stratification to have a great impact on LMFRs. In addition, there is no adequate benchmarking data because of the difficulties associated with measuring the fluid velocity and temperature fields in liquid metal. The high boiling point of lead as a liquid metal is of significant safety importance for effective cooling of the reactor even at a very high temperature above normal operating conditions. The thermohydraulic characteristics of liquid metal are an important area of research because it's the main working fluid for breeder reactors, i.e. reactors that produce more fissionable material than they consume to generate nuclear energy [4]. This special type of reactor is constructed to prolong the nuclear fuel supply for electric power production.

This study presents the results of three-dimensional parametric computations of turbulent flow and heat transfer of liquid metal for longitudinal flow through a fuel bundle with a wire wrap spacer at different twisting pitches. The wire twisting pitch plays a significant role in the heat

transfer characteristics for LMFRs. The low momentum diffusivity of liquid metal makes it inevitable to use turbulent and momentum mixing capabilities. The wire wrap spacer enhances the heat transfer characteristics but increases the pressure drop The calculations were carried out based on the Reynolds equations (the RANS method) using the ANSYS Fluent computational fluid dynamics software.

2. MATHEMATICAL MODELING

The geometry of the physical model is illustrated in Fig. 1. The thermal and flow fields are calculated numerically with commercial CFD software ANSYS FLUENT 19 R3. The flow is assumed steady state, turbulent, and the effect of thermal radiation is included.

The equations in the present model are:

$$\frac{\partial}{\partial x_i}(\rho v_i) = 0.0 \tag{1}$$

$$\frac{\partial}{\partial x_j}\left(\rho V_i V_j\right) = -\frac{\partial P}{\partial x_i} + \rho g + \frac{\partial \tau_{ij}}{\partial x_j} \tag{2}$$

$$\frac{\partial}{\partial x_i}(V_i(\rho E + P) = -\frac{\partial}{\partial x_i}\left(K\frac{\partial T}{\partial x_i}\right) \tag{3}$$

where $k, \rho, V,$ and P are the fluid thermal conductivity, density, velocity, and pressure respectively.

The SST (shear-stress-transport) $k-\omega$ turbulence model (Menter, 1994) [5, 6] has been adopted for turbulence modelling. The SST model combines the $k-\omega$ turbulence model near the wall and $k-\varepsilon$ away from the wall as a unified two equation turbulence model. The simulated domain boundary conditions are reported in Table 1

TABLE 1. SIMULATION DOMAIN PARAMETERS AND BOUNDARY CONDITIONS [7]

Physical domain boundary conditions	• Mass flow inlet boundary condition at inlet to the bundle • Pressure outlet at bundle outlet • Wall (No slip conditions) at all other boundary of the simulation domain.
Wire wrap spacer pitch	5d, 10 d, 20 d, 30 d, and 40 d. where d is the rod diameter
Bundle power	16 KW, chopped cosine shape distribution
Inlet mass flow rate	5.6 kg/s
Liquid lead inlet temperature	693 K

The study was conducted for wire wrap spacer pitches of 5d, 10d, 20d, 30d and 40d. where d is the rod diameter.

For liquid regions (the lead coolant), the following material properties are required over the range of temperatures encountered in the analysis:

- Thermal conductivity
- Specific heat

- Density
- Dynamic viscosity, as shown in Table 2

TABLE 2. LIQUID LEAD THERMOPHYSICAL PROPERTIES USED IN THE MODEL

Property	Correlation	Applicable range
ρ	$11441 - 1.2795T$	$600 < T < 1500$
C_p	$176.2 - 4.923x10^{-2}T + 1.544x10^{-5}T^2 - 1.524x10^{-6}T^{-2}$	$600 < T < 1500$
k	$9.2 + 0.011T$	$600 < T < 1300$
μ	$4.55x\ 10^{-4}e^{1069/T}$	$600 < T < 1473$

The average heat transfer coefficient of the rods bundle is calculated as follows:

$$h = \frac{q}{A(T_{ave} - T_{in})} \tag{4}$$

where q is the bundle power, T_{ave} is the average rods bundle temperature computed from the simulation results.

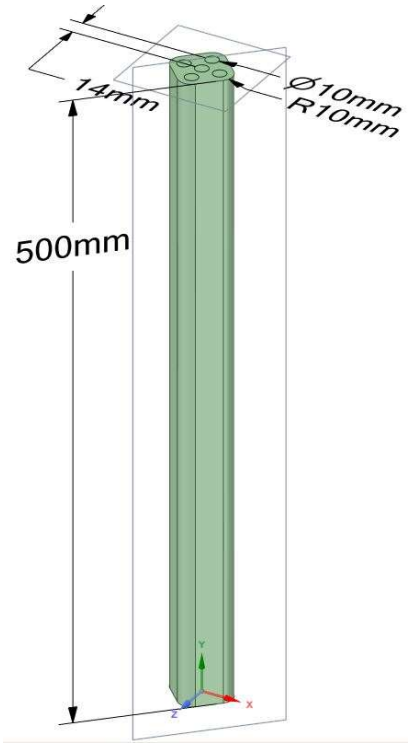

a) 3D view of the test section

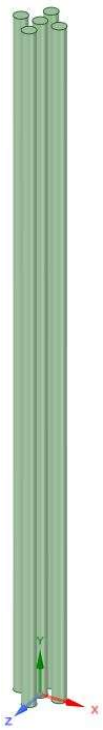

b) Smooth rods

c) Wire wrap pitch of 5d

d) Wire wrap pitch of 10d

e) Wire wrap pitch of 20d

f) Wire wrap pitch of 30d

g) Wire wrap pitch of 40d

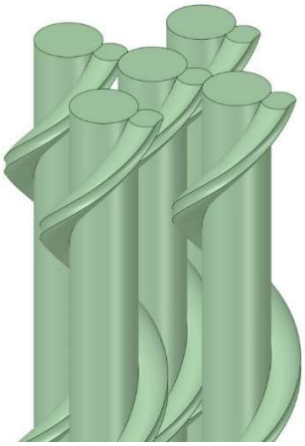

h) Zoom view of the rods bundle

FIG. 1. Physical domain of the model.

2.1 Sensitivity to the mesh

In this work to get numerical results that are independent of the grid density, the numerical study was conducted with different mesh densities. When the number of nodes increased from 1898572 to 2747858 a deviation of about 1 % in bundle maximum temperature was obtained. Whereas, when the number of nodes increased from 2747858 to 3702215, only 0.01% variation in bundle maximum temperatures was obtained. The case with node numbers of 3875496 was found to be within Y+ of the order of 1 to accommodate the flow and temperature fine gradients in the vicinity of the rods' surface. A polyhedral mesh was generated with inflation layers on the rods surface for all cases. Starting with course mesh, the simulation was conducted in FLUENT. Then, the Y+ values on the clad surfaces were checked. If the Y+ values were greater than 1, a new fine mesh was generated and solved in ANSYS FLUENT and Y+ was checked again. This cycle was repeated until the final acceptable mesh was approved. The generated mesh is demonstrated in Fig. 2

a) 3D mesh view of the smooth bundle

b) Cross-sectional elevation mesh view of the bundle pitch 5d

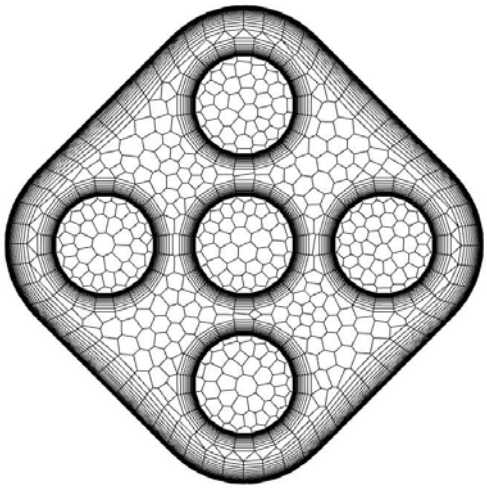

c) Plane sectional mesh view of the smooth bundle

FIG. 2. Generated mesh characteristics.

3. RESULTS AND DISCUSSION

The results of the CFD model are postprocessed and presented in this section. Figure 3 shows the temperature profile for the tested bundle without the wire wrap effect. All temperature values are in K.

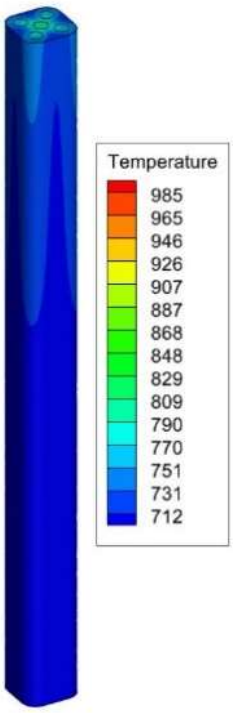

a) 3D temperature contour for smooth bundle

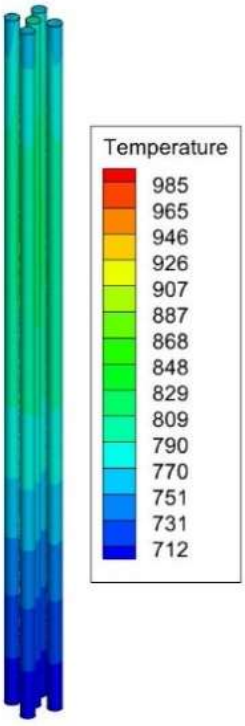

b) 3D temperature contour for smooth rods

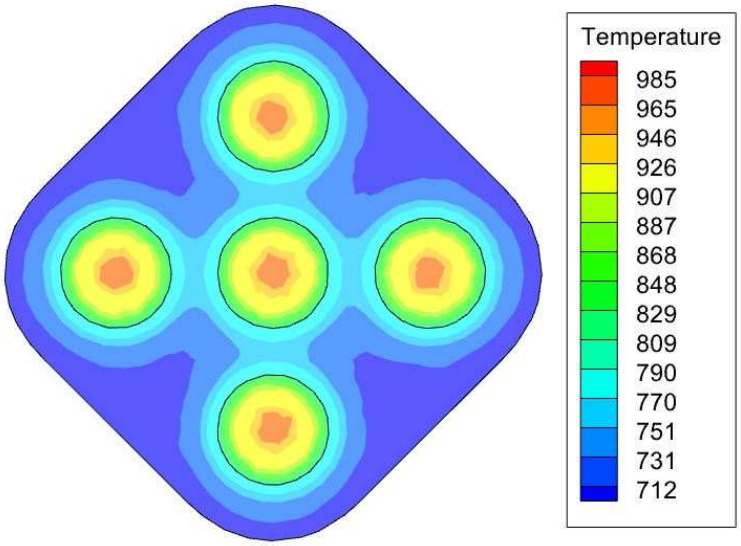

c) Plane sectional temperature contour at mid-height of the smooth bundle

FIG. 3. Temperature distribution for bundle without wire wrap effect.

Figure 4 illustrates the temperature profile for the central rod for different wire wrap pitching. Decreasing the wire wrap pitching results in a decrease in the rods maximum temperature as demonstrated in Fig. 4.

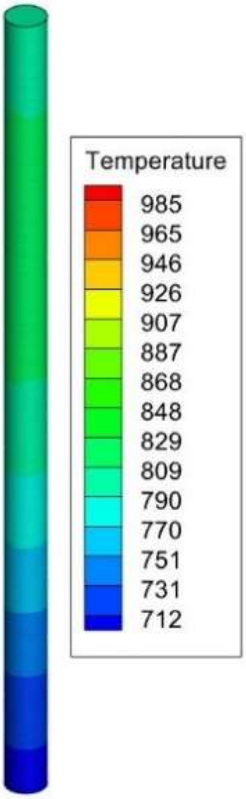

a) Smooth rod

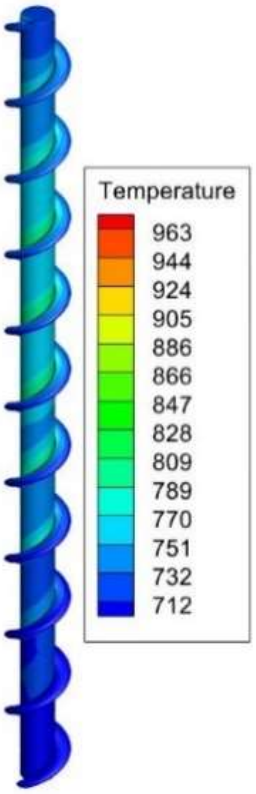

b) Wire wrap pitch of 5d

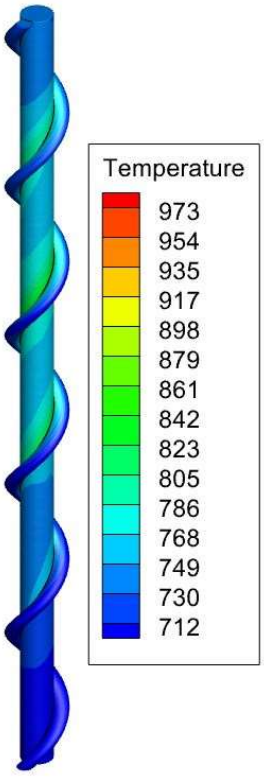

c) Wire wrap pitch of 10d

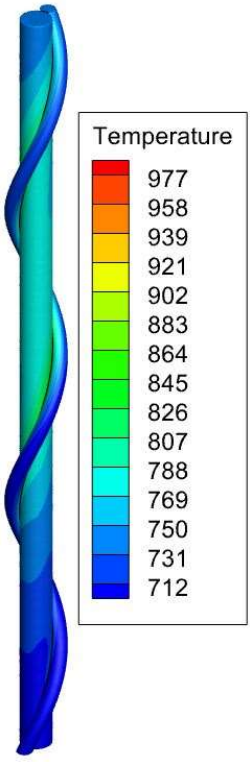

d) Wire wrap pitch 20d

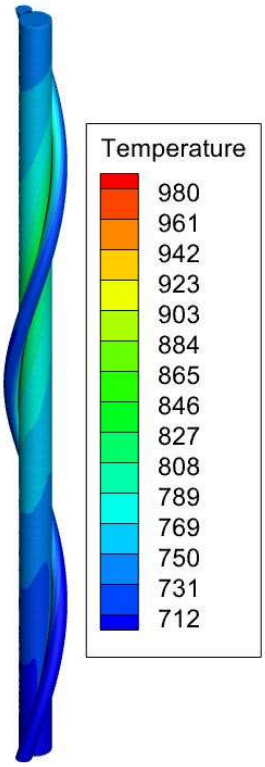

e) Wire wrap pitch 30d

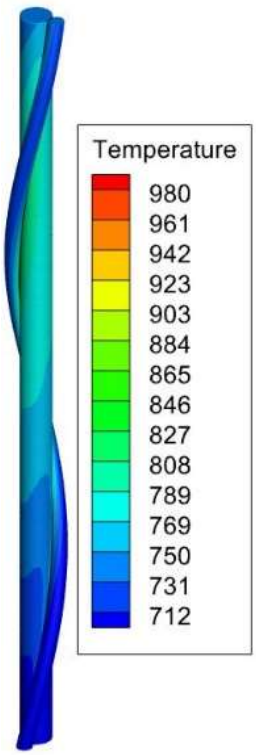

f) Wire wrap pitch 40d

FIG. 4. Temperature contour for central rod for different wire wrap pitching.

Figure 5 shows the temperature profiles at the surface of the central rod for different wire wrap pitching. The average rod surface temperature decreases with decreasing the wire wrap pitching as depicted in Fig. 5. This is attributed to the fact that the heat transfer coefficient increases with decreasing the wire wrap pitching as shown in Fig. 6. The wires act as a momentum exchange promoter in addition to its main function for keeping the inter rod spacing for the bundle.

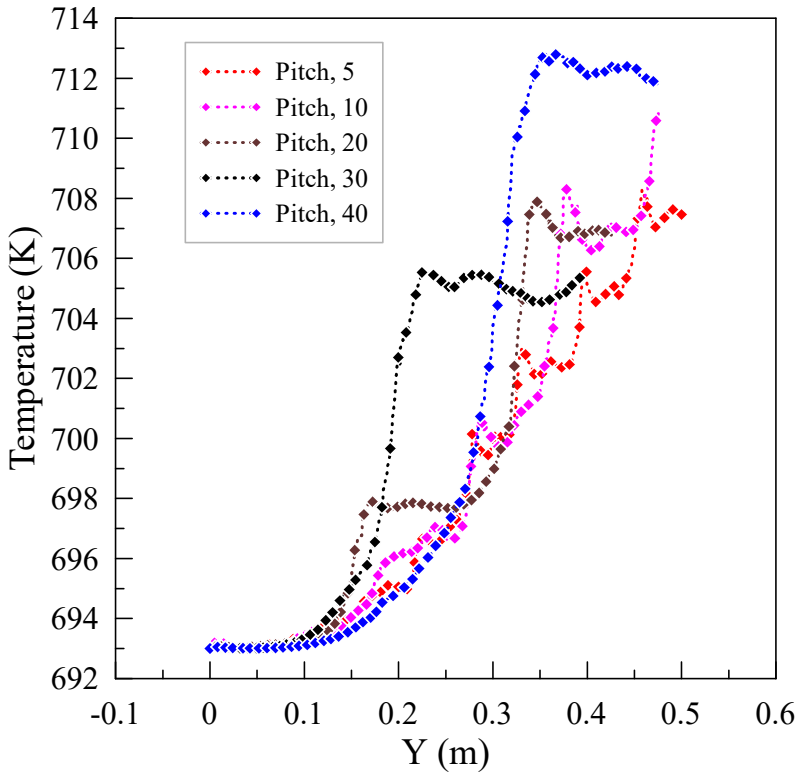

FIG. 5. Rod surface temperature for central bundle rod at different wire wrap pitching.

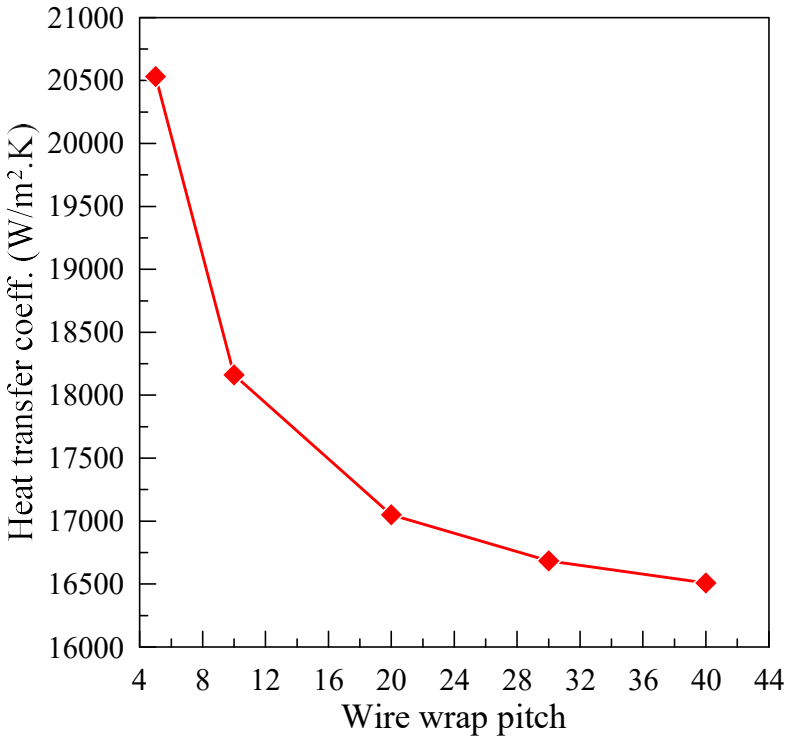

FIG. 6. Variation of average Nusselt number for different wire wrap pitching.

Figures 7 and 8 show the temperature in the middle coolant gap of the central rod in the bundle. These two figures show the effect of wire wrapping in enhancing the process of heat transfer from the rods. The wires act to increase the momentum diffusivity of the liquid lead. Liquid lead has a relatively low Prandtl due to its low momentum diffusivity. The wire wrap spacer leads to an increase in the momentum exchange of the liquid metals.

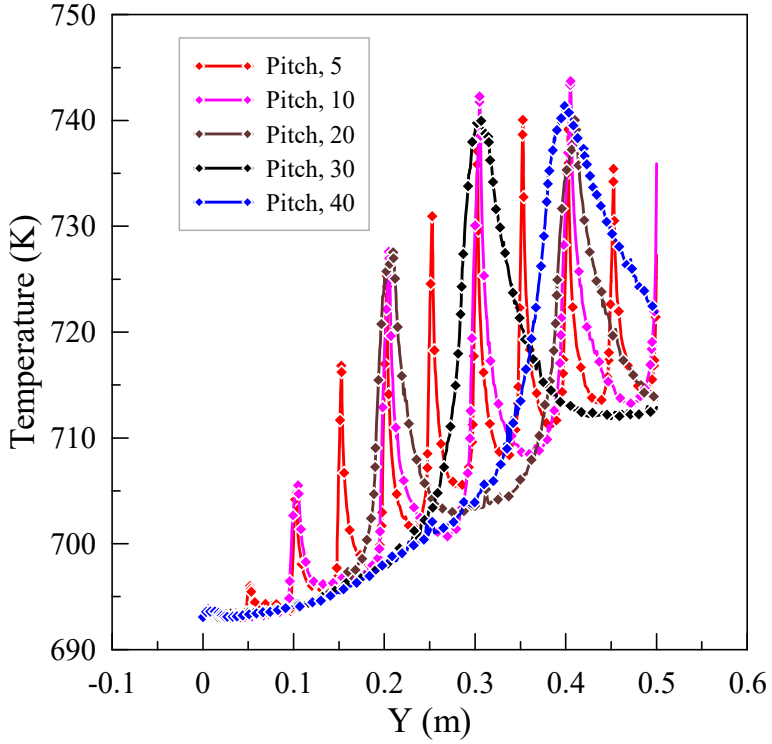

FIG. 7. Variation coolant temperature in the middle coolant gap of the central rod of the bundle.

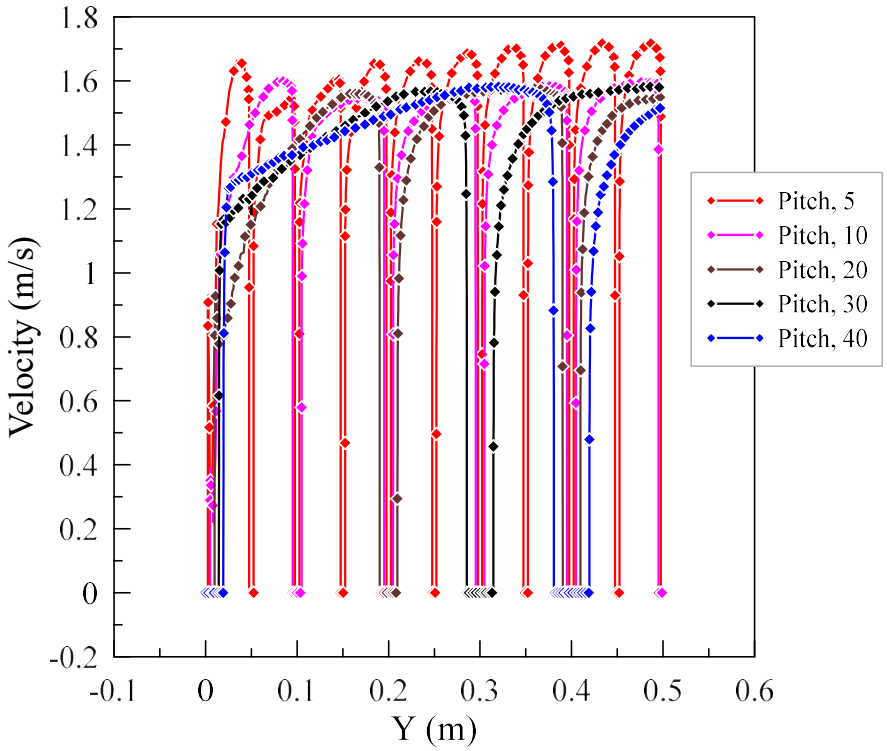

FIG. 8. Variation coolant velocity in the middle coolant gap of the central rod of the bundle for different wire wrap pitching.

4. CONCLUSION

This study presents the results of three-dimensional parametric computations of turbulent flow and heat transfer of liquid metal for longitudinal flow through bundle with wire wrap spacer at different twisting pitches. The wire twisting pitch plays a significant role on the heat transfer

characteristics of LMFRs. The low momentum diffusivity of liquid metal makes it inevitable to use turbulent and momentum mixing capabilities. The effect of decreasing the wire twist pitch is to increase the momentum exchange between the boundary layer flow of the liquid lead and the bulk flow and therefore the heat transfer coefficient increases. Therefore, the rods' pitch acts in the same way to the enhance the overall heat transfer coefficient. A slight increase of temperature in wake region of the wire is detected and reported. So, the wires act as a momentum exchange promoter in addition to their main function of keeping the inter rod spacing for the bundle.

REFERENCES

[1] Roelofs, F., et al., Core thermal hydraulic CFD support for liquid metal reactors. Nucl. Eng. Des. 355, 110322 (2019).

[2] Roelofs, F., et al., Review of fuel assembly and pool thermal hydraulics for fast reactors, Nucl. Eng. Des. 265, 1205–1222 (2013).

[3] Fricano, J. and E. Baglietto, A quantitative CFD benchmark for Sodium Fast Reactor fuel assembly modeling, Ann. Nucl. Energy 64 32–42 (2014).

[4] Vasil'ev, A.Y., et al., Turbulent convective heat transfer in an inclined tube filled with sodium, Tech. Phys. 60, 1305–1309 (2015).

[5] Menter, F.R., 1994. Two-equation eddy-viscosity turbulence models for engineering applications, AIA A J. 32 8, 1598e1605 (1994).

[6] Abramov, A.G., et al., Numerical simulation of liquid metal turbulent heat transfer from an inline tube bundle in cross-flow, St. Petersbg. State Polytech. Univ. J.: Phys. Math 1 4 356–363 (2015).

[7] Kolesnichenko, I., et al., "On boundary conditions in liquid sodium convective experiments", J. Phys.: Conf. Ser. 891 (2017), IOP Publishing, Proc. Int. Conf. Problems of thermal physics and power engineering, Moscow, Russian Federation, 9-11 October (2017).

LIST OF CONTRIBUTORS TO DRAFTING AND REVIEW

Abdelfattah, A.	Egyptian Atomic Energy Authority, Egypt
Bachrata Kubic, A.	French Alternative Energies and Atomic Energy Commission, France
Barbarino, A.	NEWCLEO SRL, Italy
Barbe, V.	Électricité de France, France
Baudrand, O.	Institute for Radioprotection and Nuclear Safety, France
Bellomo, A.	University of Pisa, Italy
Bertrand, F.	French Alternative Energies and Atomic Energy Commission, France
Bucknor, M.	Argonne National Laboratory, United States of America
Carluec, B.	Independent consultant, France
Chalyy, R.	Nuclear Safety Institute of the Russian Academy of Sciences, Russian Federation
Choi, G.	International Atomic Energy Agency
Clavier, R.	French Alternative Energies and Atomic Energy Commission, France
Constantin, M.	Institute for Nuclear Research – Pitesti; Romanian Authority for Nuclear Activities, Romania
Coyne, K.	United States Nuclear Regulatory Commission, United States of America
Danicheva, I.	Scientific and Engineering Centre for Nuclear and Radiation Safety, Russian Federation
DeMerchant, M.	ARC Clean Technology, Canada
Dufour, E.	French Alternative Energies and Atomic Energy Commission, France
El-Morshedy, S.	Egyptian Atomic Energy Authority, Egypt
Everett, P.	Oklo, Inc., United States of America
Ferroni, P.	Westinghouse Electric Company, United States of America
Flood, J.	New Brunswick Power Corporation, Canada
Fukano, Y.	Japan Atomic Energy Agency, Japan

Gianfelici, S.	Italian National Agency for New Technologies Energy and Sustainable Economic Development, Italy
Girault, N.	Institute for Radioprotection and Nuclear Safety, France
Gomez Cobo, A.	International Atomic Energy Agency
Grabaskas, D.	Argonne National Laboratory, United States of America
Gubernatis, P.	French Alternative Energies and Atomic Energy Commission, France
Hamburger, K.	Nuclear Regulatory Commission, United States of America
Ibrahim, M.	Egyptian Atomic Energy Authority, Egypt
Imaizumi, Y.	Japan Atomic Energy Agency, Japan
Ishizu, T.	Nuclear Regulation Authority, Japan
Journeau, C.	French Alternative Energies and Atomic Energy Commission, France
Kang, S.	TerraPower LLC, United States of America
Kriventsev, V.	International Atomic Energy Agency
Kubo, S.	Japan Atomic Energy Agency, Japan
Lee, S.	Fauske & Associates, LLC, United States of America
Liao, J.	Westinghouse Electric Company, United States of America
Liu, F.	Nuclear and Radiation Safety Centre Ministry of Ecology and Environment, China
Martelli, D.	National Agency for New Technologies, Energy and Sustainable Economic Development, Italy
Martin Lopez, E.	French Alternative Energies and Atomic Energy Commission, France
Massara, S.	International Atomic Energy Agency
Massone, M.	National Agency for New Technologies, Energy and Sustainable Economic Development, Italy
McTiernan, N.	ARC Clean Technology, Canada
Mohamed, A.	Nuclear Power Plants Authority, Egypt
Mohanty, A.	Atomic Energy Regulatory Board, India
Momkus, A.	Oklo, Inc., United States of America

Morelova, N.	International Atomic Energy Agency
Morita, K.	Institute of Environmental Systems, Japan
Onoda, Y.	Japan Atomic Energy Agency, Japan
Payot, F.	French Alternative Energies and Atomic Energy Commission, France
Peguero, L.	International Atomic Energy Agency
Petrosyan, A.	Armenian Scientific-Research Institute for NPP Operation, Armenia
Power, M.	New Brunswick Power Corporation, Canada
Renner, A.	Oklo, Inc., United States of America
Rineiski, A.	Karlsruhe Institute of Technology Institute for Neutron Physics and Reactor Technology, Germany
Ryzhov, N.	Nuclear Safety Institute of the Russian Academy of Sciences, Russian Federation
Sanda, I.	Belgian Nuclear Research Centre, Belgium
Sanna, A.	Électricité de France, France
Sathiyaheela, T.	Indira Gandhi Centre for Atomic Research, India
Scheveneels, G.	Belgian Nuclear Research Centre, Belgium
Seiler, N.	French Alternative Energies and Atomic Energy Commission, France
Settimo, D.	Electricity of France, France
Singh, A.	Atomic Energy Regulatory Board, India
Sogabe, J.	Japan Atomic Energy Agency, Japan
Song, W.	Nuclear and Radiation Safety Centre Ministry of Ecology and Environment, China
Stanislava, S.	Scientific and Engineering Centre for Nuclear and Radiation Safety, Russian Federation
Stone, Z.	International Atomic Energy Agency
Swalwell, G.	NEWCLEO, United Kingdom
Tentner, A.	Argonne National Laboratory, United States of America
Tiberi, V.	International Atomic Energy Agency

Tobita, Y.	Japan Atomic Energy Agency, Japan
Trotignon, L.	French Alternative Energies and Atomic Energy Commission, France
Usov, E.	Nuclear Safety Institute of the Russian Academy of Sciences, Russian Federation
Veprev, D.	Nuclear Safety Institute of the Russian Academy of Sciences, Russian Federation
Vijayan Leela, A.	Indira Gandhi Centre for Atomic Research, India
Wang, D.	China Nuclear Power Technology Research Institute Co., Ltd., China
Wekking, T.	Society for Plant and Reactor Safety, Germany
Xue, F.	China Institute of Atomic Energy, China
Yamano, H.	Japan Atomic Energy Agency, Japan
Zhang, X.	China Institute of Atomic Energy, China
Zhang, D.	Xi'an Jiaotong University School of Nuclear Science and Technology, China
Zhou, L.	Permanent Mission of China to the UN and other International Organization in Vienna, China

IAEA
International Atomic Energy Agency

No. 27

ORDERING LOCALLY

IAEA priced publications may be purchased from the sources listed below or from major local booksellers.

Orders for unpriced publications should be made directly to the IAEA. The contact details are given at the end of this list.

NORTH AMERICA

Bernan / Rowman & Littlefield

15250 NBN Way, Blue Ridge Summit, PA 17214, USA
Telephone: +1 800 462 6420 • Fax: +1 800 338 4550
Email: orders@rowman.com • Web site: www.rowman.com/bernan

REST OF WORLD

Please contact your preferred local supplier, or our lead distributor:

Eurospan

1 Bedford Row
London
WC1R 4BU
United Kingdom

Trade Orders and Enquiries:

Tel: +44 (0)1235 465576
Email: trade.orders@marston.co.uk

Individual Customers:

Tel: +44 (0)1235 465577
Email: direct.orders@marston.co.uk
www.eurospanbookstore.com/iaea

For further information:

Tel. +44 (0) 207 240 0856
Email: info@eurospan.co.uk
www.eurospan.co.uk

Orders for both priced and unpriced publications may be addressed directly to:

Marketing and Sales Unit
International Atomic Energy Agency
Vienna International Centre, PO Box 100, 1400 Vienna, Austria
Telephone: +43 1 2600 22529 or 22530 • Fax: +43 1 26007 22529
Email: sales.publications@iaea.org • Web site: www.iaea.org/publications

International Atomic Energy Agency
Vienna
www.iaea.org